

TECHNICAL REPORTS SERIES NO. 459

# Labelling of Small Biomolecules Using Novel Technetium-99m Cores



**IAEA**

International Atomic Energy Agency

**LABELLING OF SMALL BIOMOLECULES  
USING NOVEL TECHNETIUM-99m CORES**

The following States are Members of the International Atomic Energy Agency:

AFGHANISTAN	GREECE	NORWAY
ALBANIA	GUATEMALA	PAKISTAN
ALGERIA	HAITI	PALAU
ANGOLA	HOLY SEE	PANAMA
ARGENTINA	HONDURAS	PARAGUAY
ARMENIA	HUNGARY	PERU
AUSTRALIA	ICELAND	PHILIPPINES
AUSTRIA	INDIA	POLAND
AZERBAIJAN	INDONESIA	PORTUGAL
BANGLADESH	IRAN, ISLAMIC REPUBLIC OF	QATAR
BELARUS	IRAQ	REPUBLIC OF MOLDOVA
BELGIUM	IRELAND	ROMANIA
BELIZE	ISRAEL	RUSSIAN FEDERATION
BENIN	ITALY	SAUDI ARABIA
BOLIVIA	JAMAICA	SENEGAL
BOSNIA AND HERZEGOVINA	JAPAN	SERBIA
BOTSWANA	JORDAN	SEYCHELLES
BRAZIL	KAZAKHSTAN	SIERRA LEONE
BULGARIA	KENYA	SINGAPORE
BURKINA FASO	KOREA, REPUBLIC OF	SLOVAKIA
CAMEROON	KUWAIT	SLOVENIA
CANADA	KYRGYZSTAN	SOUTH AFRICA
CENTRAL AFRICAN REPUBLIC	LATVIA	SPAIN
CHAD	LEBANON	SRI LANKA
CHILE	LIBERIA	SUDAN
CHINA	LIBYAN ARAB JAMAHIRIYA	SWEDEN
COLOMBIA	LIECHTENSTEIN	SWITZERLAND
COSTA RICA	LITHUANIA	SYRIAN ARAB REPUBLIC
CÔTE D'IVOIRE	LUXEMBOURG	TAJIKISTAN
CROATIA	MADAGASCAR	THAILAND
CUBA	MALAWI	THE FORMER YUGOSLAV REPUBLIC OF MACEDONIA
CYPRUS	MALAYSIA	TUNISIA
CZECH REPUBLIC	MALI	TURKEY
DEMOCRATIC REPUBLIC OF THE CONGO	MALTA	UGANDA
DENMARK	MARSHALL ISLANDS	UKRAINE
DOMINICAN REPUBLIC	MAURITANIA	UNITED ARAB EMIRATES
ECUADOR	MAURITIUS	UNITED KINGDOM OF GREAT BRITAIN AND NORTHERN IRELAND
EGYPT	MEXICO	UNITED REPUBLIC OF TANZANIA
EL SALVADOR	MONACO	UNITED STATES OF AMERICA
ERITREA	MONGOLIA	URUGUAY
ESTONIA	MONTENEGRO	UZBEKISTAN
ETHIOPIA	MOROCCO	VENEZUELA
FINLAND	MOZAMBIQUE	VIETNAM
FRANCE	MYANMAR	YEMEN
GABON	NAMIBIA	ZAMBIA
GEORGIA	NETHERLANDS	ZIMBABWE
GERMANY	NEW ZEALAND	
GHANA	NICARAGUA	
	NIGER	
	NIGERIA	

The Agency's Statute was approved on 23 October 1956 by the Conference on the Statute of the IAEA held at United Nations Headquarters, New York; it entered into force on 29 July 1957. The Headquarters of the Agency are situated in Vienna. Its principal objective is "to accelerate and enlarge the contribution of atomic energy to peace, health and prosperity throughout the world".

TECHNICAL REPORTS SERIES No. 459

LABELLING OF  
SMALL BIOMOLECULES  
USING NOVEL  
TECHNETIUM-99m CORES

INTERNATIONAL ATOMIC ENERGY AGENCY  
VIENNA, 2007

## COPYRIGHT NOTICE

All IAEA scientific and technical publications are protected by the terms of the Universal Copyright Convention as adopted in 1952 (Berne) and as revised in 1972 (Paris). The copyright has since been extended by the World Intellectual Property Organization (Geneva) to include electronic and virtual intellectual property. Permission to use whole or parts of texts contained in IAEA publications in printed or electronic form must be obtained and is usually subject to royalty agreements. Proposals for non-commercial reproductions and translations are welcomed and considered on a case-by-case basis. Enquiries should be addressed to the IAEA Publishing Section at:

Sales and Promotion, Publishing Section  
International Atomic Energy Agency  
Wagramer Strasse 5  
P.O. Box 100  
1400 Vienna, Austria  
fax: +43 1 2600 29302  
tel.: +43 1 2600 22417  
email: [sales.publications@iaea.org](mailto:sales.publications@iaea.org)  
<http://www.iaea.org/books>

© IAEA, 2007

Printed by the IAEA in Austria  
November 2007  
STI/DOC/010/459

### **IAEA Library Cataloguing in Publication Data**

Labelling of small biomolecules using novel technetium-99m cores. —

Vienna : International Atomic Energy Agency, 2007.

p. ; 24 cm. (Technical reports series, ISSN 0074-1914 ; no. 459)

STI/DOC/010/459

ISBN 92-0-101607-7

Includes bibliographical references.

1. Biomolecules. 2. Technetium. 3. Radiolabeling. 4. Radio-pharmaceuticals. I. International Atomic Energy Agency. II. Series: Technical reports series (International Atomic Energy Agency) ; 459.

IAEAL

07-00495

## FOREWORD

Technetium-99m radiopharmaceuticals, which were introduced in the mid-1960s, account for nearly 80% of all diagnostic studies performed in nuclear medicine. The ability to determine the exact molecular structure of coordination compounds by using modern powerful analytical tools such as nuclear magnetic resonance, mass spectroscopy and X ray diffraction helped in understanding the structure–activity relationships underlying the biological behaviour of  $^{99m}\text{Tc}$  agents. Consequently, careful design of new ligands and their  $^{99m}\text{Tc}$  complexes led to the discovery of imaging agents for perfusion in the myocardium and the brain. These developments significantly extended the scope of present day diagnostic imaging using  $^{99m}\text{Tc}$  radiopharmaceuticals.

The in vivo behaviour of new tracers is determined by their molecular properties, such as charge, lipophilicity and the reactivity of biologically active functional groups. Conversely, the current design of new generations of imaging agents is based on careful selection of suitable biomolecules that may function as effective vectors for in vivo delivery of activity to more specific biological targets such as receptors and transporters. This strategy implies that the labelling approach employed for introducing a radionuclide into the structure of a biomolecule should not lead to any distortion of that part of the molecule responsible for its biological activity. Thus the preparation of novel  $^{99m}\text{Tc}$  imaging agents targeting selected biomolecular substrates would require the development of more sophisticated labelling approaches going beyond previous technologies.

The IAEA organized a Consultants Meeting in 2002 at the University of Zurich, Switzerland, to assess the new developments in  $^{99m}\text{Tc}$  labelling methodologies and the opportunities they might provide. The consultants suggested that the low valent  $[\text{Tc}(\text{CO})_3]^+$  metal core and the  $[\text{Tc}(\text{N})(\text{PNP})]^{2+}$  (PNP = heterodiphosphane) metal fragment offer new avenues for  $^{99m}\text{Tc}$  radiolabelling of biologically active compounds. It was also identified that the  $^{99m}\text{Tc}-(4 + 1)$  and  $^{99m}\text{Tc}$ -HYNIC cores are versatile for developing new radiopharmaceuticals. The above four  $^{99m}\text{Tc}$  cores offer the possibility to make  $^{99m}\text{Tc}$  labelled small biomolecules with exceptionally high specific activity and with minimum alteration of the bioactivity of the ligand molecule.

The coordinated research project (CRP) on Development of  $^{99m}\text{Tc}$  Based Small Biomolecules Using Novel  $^{99m}\text{Tc}$  Cores was started during 2003 with the specific objective to develop  $^{99m}\text{Tc}$  labelled biomolecules with the above four novel  $^{99m}\text{Tc}$  metal cores. Development of a few promising  $^{99m}\text{Tc}$  labelled small biomolecules of high purity and stability for further investigation as potential radiopharmaceuticals was also expected as the outcome of this CRP. The first research coordination meeting (RCM) of the CRP was held in Ferrara, Italy, in

May 2003, during which the participants made an overall workplan of the CRP based on the above objectives. The second RCM was held during November 2004 at IAEA Headquarters in Vienna, in which the participants reviewed the results obtained in the first part of the CRP and decided on the future directions. The final RCM was held in May 2006 in Budapest, in which the participants presented the results obtained by each participating laboratory and reviewed the overall achievements of the CRP.

All the participants reported significant achievements in the application of the new labelling technologies based on the  $^{99m}\text{Tc}$ -carbonyl,  $^{99m}\text{Tc}$ -nitrido,  $^{99m}\text{Tc}$ -(4 + 1) and  $^{99m}\text{Tc}$ -HYNIC cores during the course of the CRP. The preparation, quality assessment and biological evaluation of a large number of  $^{99m}\text{Tc}$  complexes with biomolecules such as RGD peptides, annexin derived peptides, fatty acid derivatives, quinazoline derivatives and glucose analogues were achieved. The biological evaluations of the different radiotracers were conducted in several laboratories, some with promising but most with negative biological uptakes. One notable development was the synthesis of  $^{99m}\text{Tc}(\text{N})(\text{Cys}2\text{-Anx}13)$  through a collaborative effort between Izotop, Hungary, and the Bhabha Atomic Research Centre, India. This  $^{99m}\text{Tc}$ -nitrido complex showed specific binding to cultured apoptotic cells. Further investigations on this compound may enlighten the mechanism underlying this specific uptake and provide an opportunity for developing a novel radiopharmaceutical targeting apoptotic tissues. The participants were also successful in publishing a large number of scientific papers in peer reviewed journals.

The results obtained by various laboratories during the course of the CRP are summarized in this report. The work reported is the culmination of the efforts of participants from Austria, Brazil, China, Germany, Greece, Hungary, Italy, India, Portugal, the Russian Federation, Switzerland, the United States of America and Uruguay. The IAEA thanks all the participants in the CRP for their valuable contributions and A. Duatti for his help in compiling and editing this document. The IAEA officer responsible for this publication was M.R.A. Pillai of the Division of Physical and Chemical Sciences.

#### EDITORIAL NOTE

*The use of particular designations of countries or territories does not imply any judgement by the publisher, the IAEA, as to the legal status of such countries or territories, of their authorities and institutions or of the delimitation of their boundaries.*

*The mention of names of specific companies or products (whether or not indicated as registered) does not imply any intention to infringe proprietary rights, nor should it be construed as an endorsement or recommendation on the part of the IAEA.*

# CONTENTS

## PART I: OVERVIEW OF THE COORDINATED RESEARCH PROJECT

CHAPTER 1. OVERVIEW OF THE COORDINATED RESEARCH PROJECT .....	3
1.1. Introduction .....	3
1.1.1. Background .....	3
1.1.2. Objectives of the coordinated research project .....	4
1.1.3. Work plan of the coordinated research project .....	4
1.2. Scientific background on technetium-99m cores .....	6
1.2.1. [ <sup>99m</sup> Tc(CO) <sub>3</sub> ] <sup>+</sup> -carbonyl core .....	6
1.2.1.1. Tridentate chelators .....	6
1.2.1.2. Combination of bidentate and monodentate chelators (2 + 1 approach) .....	7
1.2.1.3. Higher technetium-carbonyls .....	8
1.2.2. [ <sup>99m</sup> Tc≡N] <sup>2+</sup> -nitrido core .....	8
1.2.3. Technetium-99m-HYNIC core .....	10
1.2.4. <sup>99m</sup> Tc(III)/Re(III)-(4 + 1) core .....	12
1.3. Summary of scientific work .....	14
1.3.1. Chart 1: Technetium-99m labelling of RGD peptides targeting $\alpha_v\beta_3$ integrin receptors .....	14
1.3.1.1. Radiolabelling .....	14
1.3.1.2. Biological characterization .....	17
1.3.1.3. Conclusion (chart 1) .....	19
1.3.2. Chart 2: Labelling of annexin V fragments .....	20
1.3.2.1. Radiolabelling .....	21
1.3.2.2. Biological characterization .....	23
1.3.2.3. Conclusion (chart 2) .....	24
1.3.3. Chart 3: Labelling of fatty acids using the <sup>99m</sup> Tc-tricarbonyl core .....	24
1.3.4. Chart 4: Technetium-99m labelling of quinazoline derivatives .....	26
1.3.5. Chart 5: Development of technetium-99m glucose analogues .....	27
1.4. Achievements of the coordinated research project .....	30
1.5. Intergroup collaborations .....	31
1.5.1. Exchanges of reagents and precursors .....	31
1.5.2. Exchange visits .....	32
1.6. Conclusion .....	33

## PART II: REPORTS BY THE PARTICIPANTS IN THE COORDINATED RESEARCH PROJECT

CHAPTER 2. TECHNETIUM-99m LABELLING OF RGD PEPTIDES TARGETING INTEGRIN RECEPTORS: COMPARISON OF DIFFERENT CONJUGATES OF cRGDyK UTILIZING DIFFERENT TECHNETIUM-99m CORES .....	37
<i>C. Decristoforo, R. Haubner, M. Rupprich, E. von Guggenberg</i>	
2.1. Introduction .....	38
2.2. Peptide synthesis and distribution .....	39
2.3. Experimental methods .....	40
2.3.1. Analytical methods .....	40
2.3.1.1. HPLC .....	40
2.3.1.2. Purification by solid phase extraction .....	41
2.3.2. Technetium-99m labelling .....	41
2.3.2.1. HYNIC-cRGDyK .....	41
2.3.2.2. Labelling with $[^{99m}\text{Tc}(\text{OH}_2)_3(\text{CO})_3]^+$ .....	43
2.3.2.3. 4 + 1 approach .....	43
2.3.2.4. Labelling of Cys-RGD with the $^{99m}\text{Tc}$ -nitrido fragment .....	44
2.3.3. In vitro evaluation of radiolabelled peptides .....	44
2.3.3.1. Stability .....	44
2.3.3.2. Protein binding .....	44
2.3.3.3. Log $P$ values .....	45
2.3.4. Internalization and binding studies in $\alpha_v\beta_3$ positive and $\alpha_v\beta_3$ negative cells .....	45
2.3.5. In vivo evaluation of radiolabelled peptides .....	45
2.4. Results .....	46
2.4.1. Characterization of cold peptides .....	46
2.4.2. Labelling experiments .....	46
2.4.3. Stability experiments, log $P$ and protein binding .....	48
2.4.4. Internalization studies .....	48
2.4.5. In vivo tumour model .....	50
2.5. Discussion and outlook .....	52
References .....	52

CHAPTER 3. RADIOLABELLING ANGIOGENIC AND APOPTOTIC AGENT WITH DIFFERENT TECHNETIUM-99m TECHNIQUES .....	55
<i>B. Linkowski Faintuch, R.L.S. Ribeiro Santos, R. Teodoro, E. Muramoto, L. Morganti, I.V. Da Silva Nunes, M.R.Y. Okamoto</i>	
3.1. Introduction .....	56
3.1.1. Angiogenesis markers .....	56
3.1.2. Investigation of apoptosis .....	56
3.1.3. Labelling procedures .....	57
3.2. Materials .....	58
3.3. Methods .....	59
3.3.1. Labelling of HYNIC-RGD and HYNIC-annexin with technetium-99m using EDDA/tricine as exchange products .....	59
3.3.2. Preparation of <sup>99m</sup> Tc-nitrido precursor .....	59
3.3.3. Labelling of Cys-RGD and Cys-annexin using the <sup>99m</sup> Tc-nitrido precursor .....	59
3.3.4. Radiochemical stability, transchelation towards cysteine and partition coefficient .....	60
3.3.5. Synthesis of <sup>99m</sup> Tc-carbonyl .....	60
3.3.6. Labelling of Ter-Cys-RGD, PZ1-RGD, His-RGD and His-annexin with the precursor <sup>99m</sup> Tc(CO) <sub>3</sub> .....	60
3.3.7. Quality control .....	60
3.3.7.1. <sup>99m</sup> Tc-HYNIC peptide complexes .....	60
3.3.7.2. <sup>99m</sup> Tc(CO) <sub>3</sub> peptide complexes .....	61
3.3.7.3. <sup>99m</sup> TcN(PNP6) peptide complexes .....	61
3.3.8. Purification .....	61
3.3.9. Biodistribution studies in healthy animals .....	61
3.3.10. Animal model with tumour cells .....	61
3.3.11. Animal model for annexin studies .....	62
3.3.12. Imaging of tumour .....	62
3.4. Results and discussion .....	62
3.4.1. Labelling of HYNIC-RGD and HYNIC-annexin with technetium-99m using EDDA/tricine as exchange products .....	62
3.4.2. Preparation of <sup>99m</sup> Tc-nitrido and labelling of Cys-RGD and Cys-annexin .....	63
3.4.3. Radiochemical stability, transchelation towards cysteine and partition coefficient .....	64

3.4.4. Synthesis of $^{99m}\text{Tc}$ -carbonyl and labelling of Ter-Cys-RGD, PZ1-RGD, His-RGD and His-annexin .....	65
3.4.5. Biodistribution studies in normal and tumour bearing animals .....	66
3.4.6. Animal model with tumour cells .....	66
3.4.7. Animal model for annexin studies .....	69
3.4.8. Imaging of tumour uptake .....	69
3.5. Conclusions .....	70
Acknowledgements .....	72
References .....	72

**CHAPTER 4. RADIOLABELLING OF RGD PEPTIDES  
USING NOVEL TECHNETIUM-99m CORES .....** 75

*Ji Hu, Baojun Chen, Jixin Liang, Lianzhe Luo, Hongyu Li,  
Yang Chen, Langtao Shen, Zhifu Luo*

4.1. Introduction .....	75
4.2. Materials and methods .....	76
4.2.1. Radiolabelling .....	78
4.2.1.1. Radiolabelling of Cys-RGD with the $[\text{}^{99m}\text{Tc}(\text{N})]^{2+}$ core .....	78
4.2.1.2. Radiolabelling of HYNIC-RGD with $^{99m}\text{Tc}$ .....	78
4.2.1.3. Radiolabelling of His-RGD and Cys(X)-RGD with $[\text{}^{99m}\text{Tc}(\text{H}_2\text{O})_3(\text{CO})_3]^+$ .....	78
4.2.1.4. Purification of radiolabelled RGD peptides .....	79
4.2.1.5. In vitro stability .....	79
4.2.2. In vivo animal experiment .....	79
4.2.2.1. Tumour xenograft .....	79
4.2.2.2. Biodistribution studies .....	80
4.2.2.3. Blocking studies .....	80
4.2.2.4. Gamma camera imaging .....	80
4.3. Results and discussion .....	80
4.3.1. Radiolabelling of RGD peptides .....	80
4.3.1.1. In vitro stability .....	82
4.3.2. Biodistribution studies .....	83
4.4. Conclusion .....	85
References .....	86

CHAPTER 5. <sup>99m</sup>Tc-HYNIC-Anx13: PREPARATION,  
STABILITY, BIODISTRIBUTION AND  
IMAGING OF APOPTOSIS ..... 89

*Hongyu Li, Ji Hu, Jixin Liang, Baojun Chen, Ja Lu, Lianzhe Luo,  
Yang Chen, Zhifu Luo*

5.1. Introduction .....	89
5.2. Materials and methods .....	90
5.2.1. Radiolabelling of technetium-99m .....	90
5.2.1.1. Tricine as a coligand .....	90
5.2.1.2. EDDA as a coligand .....	90
5.2.1.3. Tricine/EDDA as coligands .....	90
5.2.2. Quality control .....	91
5.2.2.1. Thin layer chromatography .....	91
5.2.2.2. HPLC .....	91
5.2.2.3. Sep-Pak purification procedure .....	91
5.2.3. Stability of radiolabelled peptides .....	92
5.2.4. Biodistribution in normal mice .....	92
5.2.5. Imaging and biodistribution in apoptotic model animals ....	92
5.3. Results and discussion .....	93
5.3.1. Preparation of <sup>99m</sup> Tc-tricine-HYNIC-Anx13 using tricine as a coligand .....	93
5.3.2. Preparation of <sup>99m</sup> Tc-EDDA-HYNIC-Anx13 using EDDA as a coligand .....	93
5.3.3. Technetium-99m labelling of HYNIC-Anx13 using EDDA/tricine as coligands .....	94
5.3.4. Stability in vivo and in vitro .....	96
5.3.5. Biodistribution in normal mice .....	97
5.3.6. Biodistribution and radionuclide imaging in model animals .....	98
5.4. Conclusion .....	101
References .....	101

CHAPTER 6. PREPARATION AND COMPARATIVE  
EVALUATION OF TECHNETIUM-99m  
LABELLED FATTY ACIDS ..... 103

*Ji Hu, Jixin Liang, Baojun Chen, Lianzhe Luo, Hongyu Li,  
Langtao Shen, Zhifu Luo*

6.1. Introduction .....	103
6.2. Materials .....	104

6.3. Methods .....	104
6.3.1. Preparation of $[^{99m}\text{Tc}(\text{CO})_3(\text{H}_2\text{O})_3]^+$ intermediate .....	104
6.3.2. Labelling of CYST FAC11 and IDA FAC11 .....	105
6.3.3. Purification of radiolabelled products by the SPE method ...	105
6.3.4. In vitro stability .....	105
6.3.5. Biodistribution studies in normal mice .....	106
6.4. Results and discussion .....	106
6.4.1. Radiolabelling .....	106
6.4.2. In vitro stability .....	107
6.4.3. Biodistribution .....	108
6.5. Conclusions .....	110
References .....	112

CHAPTER 7. TECHNETIUM-99m LABELLING OF AN ANNEXIN  
FRAGMENT USING THE 4 + 1 MIXED LIGAND  
CHELATE SYSTEM .....

*J.-U. Küntler, B. Pawelke, A. Duatti, J. Környei, H.-J. Pietzsch*

7.1. Introduction .....	113
7.2. Materials and methods .....	114
7.2.1. General .....	114
7.2.2. L1-AF, L2-AF, $\text{Re}(\text{NS}_3)(\text{L1-AF})$ and $\text{Re}(\text{NS}_3)(\text{L2-AF})$ .....	114
7.2.3. $^{99m}\text{Tc}(\text{NS}_3)(\text{L1-AF})$ and $^{99m}\text{Tc}(\text{NS}_3)(\text{L2-AF})$ .....	115
7.2.4. In vivo stability .....	115
7.2.5. Cell binding assay .....	116
7.2.5.1. Binding studies.....	116
7.3. Results and discussion .....	116
7.4. Conclusions .....	119
References .....	120

CHAPTER 8. TECHNETIUM-99m LABELLING OF A  
QUINAZOLINE DERIVATIVE USING THE  
4 + 1 MIXED LIGAND CHELATE SYSTEM .....

*J.-U. Küntler, I. Santos, I. Pirmettis, H.-J. Pietzsch*

8.1. Introduction .....	121
8.2. Results and discussion .....	122
8.2.1. In vitro evaluation .....	124
8.2.1.1. Inhibition of cell proliferation .....	124
8.2.1.2. Inhibition of EGFR-TK .....	126

8.3. Conclusions .....	126
References .....	127

CHAPTER 9. TECHNETIUM-99m LABELLING OF THE RGD  
 PEPTIDE c(RGDyK) USING THE 4 + 1 MIXED  
 LIGAND APPROACH ..... 129

*J.-U. Küntler, P. Ansorge, R. Bergmann, E. Gniazdowska,  
 C. Decristoforo, A. Rey, H. Stephan, H.-J. Pietzsch*

9.1. Introduction .....	130
9.2. Materials and methods .....	130
9.2.1. General .....	130
9.2.2. L1-c(RGDyK), L2-c(RGDyK), Re(NS <sub>3</sub> )(L1-c(RGDyK)) and Re(NS <sub>3</sub> )(L2-c(RGDyK)) .....	131
9.2.3. Re(NS <sub>3</sub> (COOH) <sub>3</sub> )(L2-c(RGDyK)) .....	131
9.2.4. Technetium-99m labelling .....	132
9.2.5. Analytical data .....	132
9.2.6. Distribution ratio (log <i>D</i> , octanol/PBS, pH7.4) .....	132
9.2.7. Biodistribution studies .....	133
9.3. Results and discussion .....	133
9.3.1. Biodistribution studies in mice .....	136
9.4. Conclusions .....	136
References .....	140

CHAPTER 10. DEVELOPMENT OF TECHNETIUM-99m  
 LABELLED ANNEXIN V FRAGMENTS  
 USING THE Tc-TRICARBONYL CORE ..... 141

*D. Psimadas, C. Zikos, M. Fani, E. Livaniou, M. Papadopoulos,  
 I. Pirmettis*

10.1. Introduction .....	141
10.2. Materials and methods .....	141
10.2.1. General .....	141
10.2.2. Derivatization of CAQVLRGTVTDFPG×2TFA with vinyl pyridine.....	142
10.2.3. Preparation of the precursor [ <sup>99m</sup> Tc(H <sub>2</sub> O) <sub>3</sub> (CO) ] <sup>+</sup> .....	142
10.2.4. Radiolabelling of peptides .....	142
10.2.5. Cysteine and histidine challenge of technetium-99m labelled peptides .....	143
10.2.6. Biodistribution studies in mice .....	143

10.3. Results and discussion .....	143
10.4. Conclusion .....	145

CHAPTER 11. DEVELOPMENT OF TECHNETIUM-99m LABELLED BIOMARKERS FOR HEART METABOLISM USING THE Tc-TRICARBONYL CORE .....	147
---	-----

*A. Papadopoulou, C. Tsoukalas, A. Panagiotopoulou, M. Pelecanou,  
M. Papadopoulos, I. Pirmettis*

11.1. Introduction .....	147
11.2. Materials and methods .....	148
11.2.1. General .....	148
11.2.2. Synthesis of ligands.....	148
11.2.2.1. Synthesis of 11-[bis(carboxymethyl)amino] undecanoic acid (IDA-FA11) .....	148
11.2.2.2. Synthesis of 11-(S-cysteine)undecanoic acid Cyst-FA11.....	149
11.2.2.3. Synthesis of 16-(S-cysteine)hexadecanoic acid Cyst-FA16 .....	149
11.2.2.4. Synthesis of 16-(S-cysteine)hexadecanoic acid dimethylester, Cyst-FA16 dimethylester .....	150
11.2.2.5. Synthesis of N-undecanoicdithiocarbamate sodium salt CS2-FA11 .....	150
11.2.2.6. Synthesis of 16-(N-(pyridine-2-yl-methyl)-N- aminoethyl acetate)hexadecanoic ethylester PAM-FA16 .....	150
11.2.2.7. Synthesis of NSC-FA11 .....	150
11.2.3. Synthesis of rhenium complexes .....	151
11.2.3.1. Synthesis of Re(CO) <sub>3</sub> (IDA-FA11) .....	151
11.2.3.2. Synthesis of the complex Re(CO) <sub>3</sub> (Cyst-FA11)...	151
11.2.3.3. Synthesis of the complex Re(CO) <sub>3</sub> (NSC-FA11) ...	152
11.2.3.4. Synthesis of the complex Re(CO) <sub>3</sub> PAM-FA16 ....	152
11.2.4. Labelling with technetium-99m .....	152
11.2.4.1. Preparation of the precursor [ <sup>99m</sup> Tc(H <sub>2</sub> O) <sub>3</sub> (CO)] <sup>+</sup> .....	152
11.2.4.2. General method for the preparation of the technetium-99m labelled fatty acids with [ <sup>99m</sup> Tc(CO) <sub>3</sub> ] <sup>+</sup> .....	153
11.2.4.3. Synthesis of the technetium-99m complex with 11-[bis(carboxymethyl)amino]undecanoic acid... ..	153

11.2.4.4. Synthesis of the complex $^{99m}\text{Tc}(\text{CO})_3$ (Cyst-FA11) .....	153
11.2.4.5. Synthesis of the complex $^{99m}\text{Tc}(\text{CO})_3$ (NSC-FA11) .....	153
11.3. Results and discussion .....	153
11.4. Conclusions .....	156
References .....	156

CHAPTER 12. DEVELOPMENT OF TECHNETIUM-99m LABELLED BIOMARKERS FOR EGFR-TK USING THE Tc-TRICARBONYL CORE .....	157
<i>N. Margaritis, N. Bourkoula, M. Paravatou, E. Livaniou, A. Papadopoulos, A. Panagiotopoulou, C. Tsoukalas, M. Pelecanou, M. Papadopoulos, I. Pirmettis</i>	

12.1. Introduction .....	157
12.2. Materials and methods .....	158
12.2.1. General .....	158
12.2.2. Synthesis .....	158
12.2.2.1. 6-nitroquinazoline (1) .....	158
12.2.2.2. 4-chloro-6-nitroquinazoline (2) .....	159
12.2.2.3. 4-[(3-bromophenyl)amino]-6-nitro- quinazoline (3) .....	159
12.2.2.4. 6-amino-4-[(3-bromophenyl)amino]- quinazoline (4) .....	159
12.2.2.5. 6-(pyridine-2-methylimin)-4-[(3-bromophenyl) amino]-quinazoline (5) .....	160
12.2.2.6. N-{4-[(3-bromophenyl)amino]-quinazoline-6-yl}- 2-chloroacetamide (6) .....	160
12.2.3. Synthesis of rhenium complexes, general method .....	160
12.2.4. Labelling with technetium-99m .....	161
12.2.4.1. Preparation of the precursor $[\text{}^{99m}\text{Tc}(\text{H}_2\text{O})_3(\text{CO})]^+$ .....	161
12.2.4.2. General method for the preparation of the $^{99m}\text{Tc}$ labelled quinazolines $[\text{}^{99m}\text{Tc}(\text{CO})_3]^+$ .....	161
12.2.4.3. In vitro evaluation of quinazoline analogues .....	161
12.3. Results and discussion .....	162
12.4. Conclusions .....	164
References .....	164

CHAPTER 13. DEVELOPMENT OF ANNEXIN V FRAGMENTS  
FOR LABELLING WITH TECHNETIUM-99m ..... 167  
*J. Környei, F. Tóth, E. Szemenyei, A. Duatti*

13.1. Introduction .....	167
13.2. Materials and methods .....	168
13.2.1. Synthesis of annexin V fragments .....	168
13.2.2. Stability studies .....	168
13.2.3. <sup>99m</sup> Tc-nitrido labelling .....	169
13.2.4. Determination of the radiochemical purity .....	169
13.3. Results and discussion .....	169
13.3.1. Peptide synthesis and stability .....	169
13.3.2. <sup>99m</sup> Tc-nitrido labelling .....	172
13.3.3. Other studies with derivatized Anx13 fragments .....	174
13.4. Conclusions .....	175
References .....	175

CHAPTER 14. DEVELOPMENT OF TECHNETIUM-99m  
BASED SMALL BIOMOLECULES USING  
NOVEL TECHNETIUM-99m CORES:  
<sup>99m</sup>Tc-TRICARBONYL, <sup>99m</sup>Tc-HYNIC AND  
<sup>99m</sup>Tc-NITRIDO CHEMICAL APPROACHES ..... 177  
*K. Kothari, A. Mukherjee, D. Satpati, A. Korde, S. Joshi,  
H.D. Sarma, A. Mathur, M. Mallia, S. Banerjee, M. Venkatesh*

14.1. Introduction .....	178
14.2. Materials .....	180
14.3. Methods .....	181
14.3.1. Synthesis and characterization of <sup>99m</sup> Tc(CO) <sub>3</sub> -RGD, <sup>99m</sup> Tc(N)-RGD and <sup>99m</sup> Tc-HYNIC-RGD complexes for tumour targeting .....	181
14.3.1.1. Synthesis of <sup>99m</sup> Tc-tricarbonyl complexes of RGD .....	181
14.3.1.2. Preparation of <sup>99m</sup> Tc-nitrido complexes of RGD ...	182
14.3.1.3. Synthesis of <sup>99m</sup> Tc-HYNIC-RGD .....	182
14.3.1.4. Quality control .....	183
14.3.1.5. In vitro studies .....	183
14.3.1.6. In vivo studies .....	184
14.3.2. Synthesis and evaluation of <sup>99m</sup> Tc(N)-Anx13 and <sup>99m</sup> Tc(CO) <sub>3</sub> -Anx13 as apoptosis marker .....	184

14.3.2.1. Preparation and characterization of technetium-99m Anx13. ....	185
14.3.2.2. In vitro studies . . . . .	185
14.3.2.3. In vivo studies . . . . .	186
14.3.3. Synthesis and characterization of technetium-99m fatty acid analogues for myocardial imaging . . . . .	187
14.3.3.1. Radiolabelling studies. . . . .	187
14.3.3.2. Quality control . . . . .	188
14.3.3.3. In vitro studies . . . . .	188
14.3.3.4. In vivo studies . . . . .	188
14.4. Results . . . . .	189
14.4.1. Synthesis and characterization of $^{99m}\text{Tc}(\text{CO})_3\text{-RGD}$ and $^{99m}\text{Tc}(\text{N})\text{-RGD}$ for tumour targeting . . . . .	189
14.4.1.1. $^{99m}\text{Tc}$ -tricarbonyl complexes of RGD . . . . .	189
14.4.1.2. $^{99m}\text{Tc}(\text{N})\text{Cys-RGD}$ (symmetric complexes) . . . . .	189
14.4.1.3. $^{99m}\text{Tc}(\text{N})(\text{PNP})\text{-Cys-RGD}$ (asymmetric complex) . . . . .	190
14.4.1.4. Preparation of $^{99m}\text{Tc-HYNIC-RGD}$ . . . . .	190
14.4.1.5. In vitro studies . . . . .	190
14.4.1.6. In vivo studies . . . . .	191
14.4.2. Synthesis and evaluation of $^{99m}\text{Tc}(\text{N})\text{-Anx13}$ and $^{99m}\text{Tc}(\text{CO})_3\text{-Anx13}$ as an apoptosis marker . . . . .	191
14.4.2.1. Radiolabelling of Anx13 analogues . . . . .	191
14.4.2.2. In vitro studies . . . . .	192
14.4.2.3. In vivo studies . . . . .	195
14.4.3. Synthesis and characterization of $^{99m}\text{Tc}(\text{CO})_3$ undeconic acid for myocardial imaging . . . . .	197
14.4.3.1. $^{99m}\text{Tc}(\text{CO})_3\text{-CYSFA11}$ . . . . .	197
14.4.3.2. $^{99m}\text{Tc}(\text{CO})_3\text{-CYSFA16}$ . . . . .	198
14.4.3.3. $^{99m}\text{Tc}(\text{N})\text{-CS2FA11}$ . . . . .	198
14.5. Conclusion . . . . .	200
Acknowledgements . . . . .	200
References . . . . .	201

## CHAPTER 15. LABELLING OF SMALL MOLECULES

WITH THE  $^{99m}\text{Tc}$ -NITRIDO CORE . . . . . 203

*M. Pasquali, L. Uccelli, A. Boschi, A. Duatti*

15.1. Introduction . . . . .	203
15.2. Labelling methods . . . . .	204
15.2.1. Symmetrical complexes . . . . .	204

15.2.2.	Asymmetrical complexes .....	204
15.3.	Results and discussion .....	206
15.3.1.	Development of $^{99m}\text{Tc}$ glucose analogues .....	206
15.3.2.	Labelling of bioactive peptides .....	207
15.3.2.1.	RGD peptides .....	208
15.3.2.2.	Annexin V .....	210
15.3.2.3.	Quinazoline ligands.....	211
15.4.	Experimental procedures .....	215
15.4.1.	Symmetrical complexes .....	215
15.4.1.1.	Bis(dithiocarbamate) nitrido $^{99m}\text{Tc}$ complexes ...	215
15.4.2.	Asymmetrical complexes .....	215
15.4.2.1.	Mixed $[\text{}^{99m}\text{Tc}(\text{N})(\text{PNP})(\text{XY})]^{0/+}$ (PNP = amino-bis-phosphino ligand; XY = monoanionic or dianionic bidentate ligand) complexes .....	215
15.4.2.2.	Mixed $[\text{}^{99m}\text{Tc}(\text{N})(\text{PS})(\text{DTC})]$ (PS = phosphino-thiol ligand; DTC = monoanionic dithiocarbamate ligand) complexes .....	217
References	.....	218

CHAPTER 16. LABELLING OF QUINAZOLINE AND RGD PEPTIDES WITH THE  $[\text{}^{99m}\text{Tc}(\text{CO})_3]^+$  CORE: SYNTHESIS, CHARACTERIZATION AND BIOLOGICAL EVALUATION ..... 219

*I. Santos, C. Fernandes, S. Alves, J. Galamba, L. Gano, I. Pirmettis, C. Decristoforo, C.J. Smith, R. Alberto*

16.1.	Introduction .....	220
16.2.	Results .....	221
16.2.1.	Synthesis and characterization of quinazoline derivatives to be coupled to different chelators and synthesis of a novel chelator for tricarbonyl .....	221
16.2.2.	Evaluation of $\text{L}^1$ as a new ligand for the $[\text{}^{99m}\text{Tc}(\text{CO})_3]^+$ core .....	222
16.2.3.	Conjugation of a quinazoline fragment to $\text{L}^1$ and labelling of the conjugate with the $[\text{}^{99m}\text{Tc}(\text{CO})_3]^+$ core .....	223
16.2.4.	Cell growth and EGFR-TK inhibition .....	225
16.2.5.	Labelling of an RGD peptide with the <i>fac</i> - $[\text{}^{99m}\text{Tc}(\text{CO})_3]^+$ moiety .....	227
16.2.6.	Internalization and binding studies in $\alpha_v\beta_3$ positive and $\alpha_v\beta_3$ negative cells .....	227
16.2.7.	Biodistribution in healthy and in nu/nu mice .....	228

16.3. Summary and conclusions .....	229
References .....	230

CHAPTER 17. LIGANDS OF LOW DENTICITY AS COORDINATION  
 UNITS FOR TETHERING THE  $^{99m}\text{Tc}$ -CARBONYL  
 CORE TO BIOMOLECULES ..... 233

*N.I. Gorshkov, E.M. Levitskaya, A.A. Lumpov, A.E. Miroslavov,  
 G.V. Sidorenko, D.N. Suglobov*

17.1. Introduction .....	233
17.2. Experimental .....	234
17.3. 2 + 1 ligand systems for binding Tc-tricarbonyl core .....	235
17.3.1. Complexation with bidentate ligands .....	235
17.3.2. 2 + 1 systems with dithiocarbamates .....	236
17.3.3. 2 + 1 systems with bidentate nitrogen bases .....	237
17.3.4. Biodistribution studies of 2 + 1 systems with bipyridine and related compounds .....	238
17.4. Derivatives of higher technetium-carbonyls .....	240
17.4.1. Preparation of higher technetium-carbonyls at the non-carrier added level .....	241
17.4.2. Tetracarbonyltechnetium diethyldithiocarbamate .....	243
17.4.3. Pentacarbonyltechnetium phosphine and isonitrile complexes .....	243
17.4.4. Hexacarbonyltechnetium(I) cation .....	244
17.5. Conclusion .....	247
Acknowledgements .....	247
References .....	247

CHAPTER 18. SMALL MOLECULE LABELLING WITH  
 $^{99m}\text{Tc}(\text{OH}_2)_3(\text{CO})_3^+$ : LIGANDS, AMINO ACIDS  
 AND INTERCALATORS ..... 249

*R. Alberto, Y. Liu, N. Agorastos, I. Santos, P. Raposinho, H. Knight,  
 J. Mertens, M. Bauwens*

18.1. Introduction .....	250
18.2. Results .....	251
18.2.1. New ligands for the $[\text{Tc}(\text{CO})_3]^+$ core .....	251
18.2.2. Labelling of amino acids .....	252
18.2.3. Targeting the nucleus: intercalators .....	254
18.2.4. Kit preparation of $^{188/186}\text{Re}(\text{OH}_2)_3(\text{CO})_3^+$ .....	256
18.3. Summary and conclusions .....	257

18.4. Experimental .....	258
18.4.1. Triethyl 1,6-diacetamido-6-cyanoheptane-1,1,6-tricarboxylate (II) .....	258
18.4.2. Triethyl 1,6-diacetamido-7-(tert-butoxycarbonylamino)heptane-1,1,6-tricarboxylate (III) .....	259
18.4.3. Preparation of V .....	259
Acknowledgements .....	260
References .....	260

CHAPTER 19. DESIGN AND EVALUATION OF POTENTIAL <sup>99m</sup>Tc RADIOPHARMACEUTICALS BASED ON THE Tc-CARBONYL, 4 + 1 MIXED LIGAND CHELATE SYSTEM AND Tc-NITRIDO APPROACHES .....

*J. Giglio, A. Muslera, M. Incerti, R. Fernández, E. León, A. Paolino, A. Brugnini, E. Manta, A. Chabalgoity, A. León, A. Rey*

19.1. Introduction .....	262
19.2. Materials .....	263
19.3. Methods .....	263
19.3.1. Synthesis of glucose derivatives .....	263
19.3.1.1. N-(3,4,6-tri-O-acetyl-β-D-glucopyranosyl)piperidine (1) .....	263
19.3.1.2. N-[3,4,6-tri-O-acetyl-2-O-(6-bromohexyl)β-D-glucopyranosyl]piperidine (2) .....	264
19.3.1.3. N-[3,4,6-tri-O-acetyl-2-O-(6-bromobutyl)β-D-glucopyranosyl]piperidine (2') .....	264
19.3.1.4. (2R,3S,4R,5R)-2-(acetoxymethyl)-5-(4-azidobutyl)-6-(piperidin-1-yl)-tetrahydro-2H-pyran-3,4-diyl diacetate (3) .....	265
19.3.1.5. (2R,3S,4R,5R)-2-(acetoxymethyl)-5-(4-azidobutyl)-6-(piperidin-1-yl)-tetrahydro-2H-pyran-3,4-diyl diacetate (4) .....	265
19.3.1.6. (2-aminoethylamino)acetic acid (5) .....	265
19.3.2. Preparation and evaluation of technetium-99m labelled RGD peptides .....	266
19.3.2.1. Technetium-99m labelling .....	266
19.3.2.2. In vitro evaluation .....	267
19.3.2.3. in vivo evaluation .....	268

19.3.3.	Preparation and evaluation of technetium-99m labelled annexin 13 peptides .....	268
19.3.3.1.	Biodistribution in animals treated with doxorubicin.....	269
19.4.	Results and discussion .....	269
19.4.1.	Glucose derivatives .....	269
19.4.2.	RGD peptides .....	270
19.4.2.1.	Labelling of RGD peptides with HYNIC.....	271
19.4.2.2.	Labelling of RGD peptides with tricarbonyl.....	274
19.4.2.3.	Labelling of RGD peptides with 4 + 1 chemistry.....	277
19.4.2.4.	Labelling of RGD peptides with nitrido chemistry .....	279
19.4.3.	Annexin .....	280
19.4.3.1.	Labelling of annexin peptides with HYNIC and carbonyl .....	281
19.5.	Conclusions .....	283
	Acknowledgements .....	284
	References .....	284

## CHAPTER 20. IN VITRO AND IN VIVO EVALUATION OF

$[^{99m}\text{Tc}(\text{CO})_3\text{-CYCLO}[\text{Arg-Gly-Asp-D-Tyr-Lys}(\text{PZ1})]] \dots$  287

*S. Alves, J.D.G. Correia, I. Santos, C. Decristoforo, R. Alberto, C.J. Smith*

20.1.	Introduction .....	287
20.2.	Materials .....	290
20.3.	Methods .....	290
20.3.1.	Synthesis of PZ1 (3,5Me <sub>2</sub> -PZ(CH <sub>2</sub> ) <sub>2</sub> N((CH <sub>2</sub> ) <sub>3</sub> COOH)(CH <sub>2</sub> ) <sub>2</sub> NH-BOC) .....	290
20.3.2.	Peptide synthesis .....	291
20.3.3.	Radiolabelling of PZ1-RGD conjugate cyclo[Arg-Gly-Asp-D-Tyr-Lys(PZ1)] .....	292
20.3.4.	In vitro serum stability .....	292
20.3.5.	In vitro internalization analysis .....	292
20.3.6.	In vivo evaluation of $[^{99m}\text{Tc}(\text{CO})_3\text{-cyclo}[\text{Arg-Gly-Asp-D-Tyr-Lys}(\text{PZ1})]]$ in normal mouse models .....	293
20.4.	Results .....	294
20.5.	Conclusion .....	300
	References .....	301

PAPERS PUBLISHED BY THE PARTICIPANTS RELATED TO THE COORDINATED RESEARCH PROJECT .....	305
PARTICIPANTS IN THE COORDINATED RESEARCH PROJECT .....	311

Part I

OVERVIEW OF THE  
COORDINATED RESEARCH PROJECT



# Chapter 1

## OVERVIEW OF THE COORDINATED RESEARCH PROJECT

### 1.1. INTRODUCTION

#### 1.1.1. Background

Technetium-99m radiopharmaceuticals account for nearly 80% of diagnostic studies in nuclear medicine. These agents are available for imaging almost all the important organs of the body and are routinely used worldwide due to the favourable logistics of having a transportable  $^{99}\text{Mo}$ – $^{99\text{m}}\text{Tc}$  generator in the hospital radiopharmacy.

Technetium-99m radiopharmaceuticals were introduced in the mid-1960s, when static cameras were the standard nuclear medicine imaging equipment and other imaging modalities such as magnetic resonance imaging, computed tomography or ultrasound were not available. Introduction of these competing imaging modalities has influenced nuclear medicine to focus more on dynamic and functional studies. Functional imaging involving *in vivo* biochemistry is unique to nuclear medicine, and its clinical usefulness has been established using positron emission tomography (PET) together with small bioactive molecules labelled with positron emitting radionuclides such as  $^{11}\text{C}$ ,  $^{13}\text{N}$ ,  $^{15}\text{O}$  and  $^{18}\text{F}$  produced in cyclotrons. Using cyclotron produced  $^{123}\text{I}$  and single photon emission computed tomography (SPECT) for labelling bioactive molecules, functional imaging has been extended to other nuclear medicine centres not having PET/cyclotron facilities.

Production of both positron emitting and  $^{123}\text{I}$  radiopharmaceuticals has limitations in terms of high cost and logistics of distribution. Hence, there have been demands for development of suitable  $^{99\text{m}}\text{Tc}$  labelled substitutes that can be used more conveniently, economically and universally. In particular, in the past two decades efforts have been focused on the design of new categories of  $^{99\text{m}}\text{Tc}$  labelled imaging agents incorporating organic and biologically active molecules that can be used for targeting specific receptor sites or metabolic processes. Unlike  $^{11}\text{C}$ ,  $^{18}\text{F}$  or  $^{123}\text{I}$ ,  $^{99\text{m}}\text{Tc}$  cannot be introduced into small bioactive molecules readily and without the risk of losing its bioactivity. Many organic and bioactive molecules can be attached to  $^{99\text{m}}\text{Tc}$  in a reduced oxidation state by complex formation, but the *in vivo* behaviour of the resulting  $^{99\text{m}}\text{Tc}$  compounds is often different and unpredictable compared with the original molecule. These difficulties include inability of penetration through

cellular membranes and the blood–brain barrier, lack of recognition by receptor sites of the ‘foreign’  $^{99m}\text{Tc}$  complexes and absence of adequate clearance from non-target tissues. Therefore, design of  $^{99m}\text{Tc}$  complexes that are recognized by target sites in vivo requires sophisticated and difficult coordination chemical approaches in order to achieve their utility.

The most common approach for designing a target specific  $^{99m}\text{Tc}$  agent has been to attach a chelating group to a bioactive molecule, resulting in a combined ligand that can form a complex with  $^{99m}\text{Tc}$  in a reduced oxidation state. This procedure is commonly known as a bifunctional approach and the specific ligands employed as bifunctional chelating agents (BFCAs). The conventional technetium chemistry of using the  $\text{Tc(V)}\text{-oxo}$  core and BFCAs such as  $\text{N}_2\text{S}_2$  or  $\text{N}_3\text{S}$  chelating systems has been investigated for radiolabelling bioactive molecules such as antibodies and peptides. A major limitation of such an approach was the inability to yield high specific activity tracers that can be utilized for mapping the peptide receptors, which are present in relatively small concentrations.

Introduction of novel  $^{99m}\text{Tc}$  moieties such as  $^{99m}\text{Tc}$ -tricarbonyl,  $^{99m}\text{Tc}$ -nitrido,  $^{99m}\text{Tc}$ -HYNIC and  $^{99m}\text{Tc}$ -(4 + 1) cores has revived interest in  $^{99m}\text{Tc}$  labelling of several small biomolecules, and considerable work is already in progress in several laboratories. These novel cores have opened new avenues for  $^{99m}\text{Tc}$  radiolabelling of biologically active compounds that could yield high specific activity tracers with potential new applications in oncology, infection imaging and improving the efficacy of conventional  $^{99m}\text{Tc}$  radiopharmaceuticals for organ imaging.

### 1.1.2. Objectives of the coordinated research project

The overall objective of the CRP was to generate know-how and expertise favouring the development of reproducible and simple methodologies for preparing small  $^{99m}\text{Tc}$  labelled biomolecules using the novel chemistries introduced in the recent past. Consequently,  $^{99m}\text{Tc}$ -carbonyl,  $^{99m}\text{Tc}$ -nitrido,  $^{99m}\text{Tc}$ -(4 + 1) and  $^{99m}\text{Tc}$ -HYNIC cores were identified to be used for labelling of small molecules with  $^{99m}\text{Tc}$ . The CRP also aimed to develop a few promising  $^{99m}\text{Tc}$  radiopharmaceuticals of high purity and stability based on the above chemistries for further investigation and evaluation as potential diagnostic imaging agents.

### 1.1.3. Work plan of the coordinated research project

In the first research coordination meeting (RCM) of the CRP held in Ferrara, Italy, in May 2003, the participants deliberated on the need for

## CHAPTER 1

diagnostic radiopharmaceuticals for clinically useful targets, and small molecules for targeting some specific biological substrates were selected. These were:

- (a) RGD bioactive peptides;
- (b) Short chain, annexin derived peptides;
- (c) Glucose analogues;
- (d) Fatty acid derivatives;
- (e) Quinazoline derivatives.

The participants initiated work on the radiolabelling of these biomolecules with the novel  $^{99m}\text{Tc}$  cores discussed above with the aim of developing potential diagnostic radiopharmaceuticals.

The second RCM was held during November 2004 at IAEA Headquarters in Vienna, and reviewed the results of the first part of the CRP. Participants reported significant achievements on the application of the new labelling technologies based on the  $^{99m}\text{Tc}$ -carbonyl,  $^{99m}\text{Tc}$ -nitrido,  $^{99m}\text{Tc}$ -(4 + 1) and  $^{99m}\text{Tc}$ -HYNIC cores. In particular, the various groups involved in the study were able to reproduce successfully the different chemical procedures in their laboratories and thus achieve a high standard of experience with these cores. Based on a careful analysis of the first experimental results, the participants decided to focus the different subprojects on the labelling of biologically active molecules carrying a more selected set of chelating systems. In particular, histidine functionalized biomolecules were selected for optimal labelling with the  $^{99m}\text{Tc}$ -carbonyl core. Similarly, dithiocarbamate and cysteine derived biomolecules proved to be highly reactive chelating groups for the  $^{99m}\text{Tc}$ -nitrido core. Finally, isocyanide linked biomolecules showed the most promising coordinating ability towards the  $^{99m}\text{Tc}$ -(4 + 1) core. Hence, efforts during the second part of the CRP were directed towards synthesizing new ligands preferably containing the above chelating groups.

The final RCM of this CRP was held in Budapest during May 2006, at which the results of the research carried out by each laboratory were presented. The following sections describe the results obtained by the various groups during the CRP. The essential features of the chemical methods employed with the four different metallic fragments and the results obtained by application of the four new technologies to the labelling of five different categories of bioactive molecules are given in Section 1.3. Based on analysis of the experimental work reported here, the main achievements of this CRP are described in Section 1.4. Finally, conclusions are reported in Section 1.6.

## 1.2. SCIENTIFIC BACKGROUND ON TECHNETIUM-99m CORES

As the main focus of the CRP was on the preparation and biological evaluation of  $^{99m}\text{Tc}$  complexes formed through the conjugation of small bioactive molecules to the novel  $^{99m}\text{Tc}$  cores  $^{99m}\text{Tc}$ -carbonyl,  $^{99m}\text{Tc}$ -nitrido,  $^{99m}\text{Tc}$ -(4 + 1) and  $^{99m}\text{Tc}$ -HYNIC, the basic chemical properties of these metallic fragments are briefly reviewed below.

1.2.1.  $[\text{}^{99m}\text{Tc}(\text{CO})_3]^+$ -carbonyl core

Three possible types of ligand arrangement can be considered for coordination to the  $[\text{}^{99m}\text{Tc}(\text{CO})_3]^+$  moiety, namely:

- $^{99m}\text{Tc}$ -tricarbonyl core with tridentate chelators;
- $^{99m}\text{Tc}$ -tricarbonyl core with combinations of bidentate and monodentate ligands;
- Higher (tetracarbonyl and pentacarbonyl)  $^{99m}\text{Tc}$ -carbonyl containing cores with bidentate and monodentate ligands, respectively.

## 1.2.1.1. Tridentate chelators

Studies performed on the chemistry of the  $^{99m}\text{Tc}$ -tricarbonyl core, at the macroscopic and tracer levels, have shown that bis- or tris-scorpionates act similarly as tridentate ligands (Fig. 1.1). However, in terms of both stability in aqueous solution and formation of well defined species, soft scorpionates appear to be the most convenient choice for radiopharmaceutical applications.

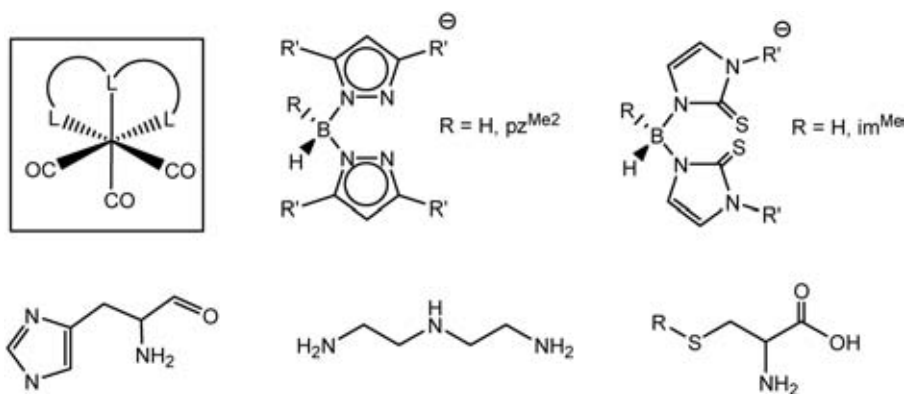


FIG. 1.1. Examples of tridentate ligands for the  $^{99m}\text{Tc}$ -carbonyl core.

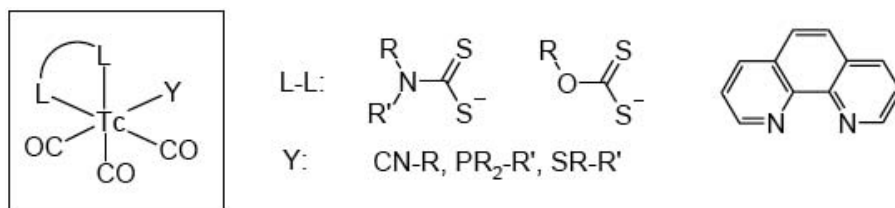


FIG. 1.2. Examples of combinations of bidentate and monodentate ligands for the 2 + 1 approach with the  $^{99m}\text{Tc}$ -carbonyl core.

It has also been shown that these lipophilic building blocks can be easily functionalized at different positions in the molecule.

Other tridentate chelators, such as diethylenetriamine, trispyrazolylmethane and N-[2-(1-pyrazolyl)ethyl]ethylenediamine (Fig. 1.1) also form stable hydrophilic building blocks by coordination to the  $^{99m}\text{Tc}$ -carbonyl group at both the macroscopic and tracer levels. All of these ligands can be efficiently coupled to different biomolecules. Histidine and alkylated cysteine also have very good chelating properties and high stability. Derivatization has also been possible for these two chelators through different positions.

#### 1.2.1.2. Combination of bidentate and monodentate chelators (2 + 1 approach)

Reactions of the  $^{99m}\text{Tc}$ -tricarbonyl core with charged or neutral bidentate chelators such as beta-diketonates, xanthates, dithiocarbamates and neutral bidentate nitrogen bases have been explored (Fig. 1.2). As monodentate ligands amines, imidazoles, phosphines, thiols, thioethers and isocyanides were also tested.

Dithiocarbamate ligands, which are very good anionic bidentate ligands, provide efficient 2 + 1 complexation in combination with isocyanides. Biomolecules can be linked via both monodentate and bidentate components. Phenanthroline and bipyridine provided efficient complexation in combination with imidazoles and isonitriles. The complexes  $[\text{}^{99m}\text{Tc}(\text{CO})_3(\text{N}^{\wedge}\text{N})\text{L}]^+$  themselves ( $\text{N}^{\wedge}\text{N}$  = phenanthroline, bipyridine; L = imidazole, isocyanide) showed selective heart uptake in rats, comparable with that of  $^{99m}\text{Tc}$ -sestamibi and  $^{99m}\text{Tc}$ -tetrafosmin. The arrangement formed by a  $^{99m}\text{Tc}$ -carbonyl core and a bidentate  $\text{N}^{\wedge}\text{N}$  ligand is suitable for linking of biomolecules via imidazole or isocyanide groups and seems particularly promising for biomolecules intended for heart imaging.

In another (2 + 1)-like approach, picolinic acid was used as bidentate ligand in combination with an isocyanide group linked to an intercalator and acting as monodentate ligand. These neutral complexes might be suitable as nuclear targeting agents.

### 1.2.1.3. Higher technetium-carbonyls

A procedure and a device for high pressure synthesis of pentacarbonyltechnetium-99m halides were developed by the Russian participants of the CRP. These compounds can be transferred through the gas phase without accompanying impurities or reagents into required media for subsequent transformations.  $[\text{}^{99\text{m}}\text{TcI}(\text{CO})_5]$  showed selective, rapid and persistent lung uptake in rats and rabbits. Reaction of  $[\text{TcI}(\text{CO})_5]$  (with both  $^{99}\text{Tc}$  and  $^{99\text{m}}\text{Tc}$ ) with dithiocarbamates ( $\text{S}_2\text{CNR}_2$ ) yields the kinetically stable complex  $[\text{Tc}(\text{S}_2\text{CNR}_2)(\text{CO})_4]$ . The dithiocarbamate group can be introduced into biomolecules through either primary or secondary amino groups. Dithiocarbamates derived from secondary amino groups are more stable than those derived from primary amino groups.

Complexes of the type  $[\text{Tc}(\text{CO})_5\text{L}]^+[\text{X}]^-$  with monodentate ligands  $\text{L} = \text{Ph}_3\text{P}$  ( $\text{CH}_3$ )<sub>3</sub>CNC;  $\text{X} = \text{ClO}_4$ ,  $\text{CF}_3\text{SO}_3$  were prepared in non-aqueous medium from  $[\text{TcI}(\text{CO})_5]$  after replacement of  $\text{I}^-$  with a non-coordinating anion. The complexes are kinetically stable. Their preparation opens prospects for linking of biomolecules to the  $[\text{Tc}(\text{CO})_5]^+$  core via the isocyanide group. This approach is expected to reduce the disturbing effect of the coordination core on biomolecules.

The hexacarbonyltechnetium(I) cation,  $[\text{Tc}(\text{CO})_6]^+$ , was reportedly prepared in aqueous solutions under conditions similar to those employed in radiopharmaceutical preparations. This complex may exhibit interesting biodistribution properties, as it appears as the simplest structural analogue of the cationic heart imaging agent  $^{99\text{m}}\text{Tc}$ -MIBI.

### 1.2.2. $[\text{}^{99\text{m}}\text{Tc}\equiv\text{N}]^{2+}$ -nitrido core

In a formal chemical picture, the formation of a terminal  $^{99\text{m}}\text{Tc}\equiv\text{N}$  triple bond can be viewed as derived from the bonding interaction between a  $^{99\text{m}}\text{Tc}^{+5}$  ion and a  $\text{N}^{3-}$ -nitrido nitrogen atom. The resulting metallic group behaves as a true inorganic functional moiety exhibiting high stability and peculiar chemical properties. Generally,  $^{99\text{m}}\text{Tc}$ -nitrido complexes assume a five-coordination arrangement, in which one position is always occupied by a nitrido nitrogen atom and the other remaining positions are available for coordination of four additional donor atoms. Molecular structures for these complexes range between the two ideal limits of square pyramidal and trigonal bipyramidal geometries.

Bidentate chelating ligands constitute the most important class of coordinating agents for the  $[\text{}^{99\text{m}}\text{Tc}\equiv\text{N}]^{2+}$  core. Two main categories of  $^{99\text{m}}\text{Tc}$ -nitrido complexes can be formed with bidentate ligands, namely symmetrical and

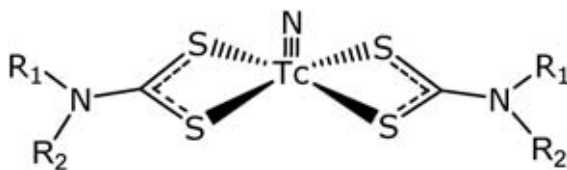


FIG. 1.3. Schematic drawing of the structure of symmetrical bis(dithiocarbamate) nitrido  $^{99m}\text{Tc}$  complexes.

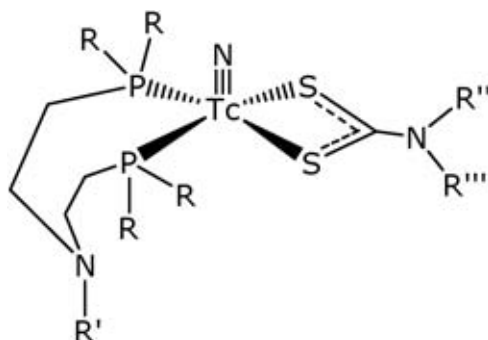


FIG. 1.4. Schematic drawing of the structure of asymmetrical bis(dithiocarbamate) nitrido  $^{99m}\text{Tc}$  complexes.

asymmetrical complexes. Symmetrical complexes,  $[\text{}^{99m}\text{Tc}(\text{N})(\text{L})_2]$ , are composed of two identical bidentate ligands (L) coordinated to the same  $^{99m}\text{Tc}\equiv\text{N}$  group. Conversely, asymmetrical complexes,  $[\text{}^{99m}\text{Tc}(\text{N})(\text{L})(\text{L}')] ]$ , are formed by two different bidentate ligands (L, L') bound to the same  $^{99m}\text{Tc}\equiv\text{N}$  group. The formation of these two types of nitrido  $^{99m}\text{Tc}$  complexes is completely determined by the nature of the coordinating atoms surrounding the metallic centre. Symmetrical complexes are easily produced when bidentate ligands possessing a pair of two  $\pi$  donor coordinating atoms are used. A representative example of symmetrical  $^{99m}\text{Tc}$ -nitrido compounds is given by the class of bis(dithiocarbamate) nitrido  $^{99m}\text{Tc}$  complexes (Fig. 1.3), in which two identical  $\pi$  donor bidentate  $[\text{R}(\text{R}')\text{-N-C(=S)S}]^-$  (R, R' = organic functional group) ligands are coordinated to the same  $[\text{}^{99m}\text{Tc}\equiv\text{N}]^{2+}$  core.

Conversely, asymmetrical complexes are obtained when a combination of  $\pi$  acceptor and  $\pi$  donor bidentate ligands is employed. A representative example of the category of asymmetrical  $^{99m}\text{Tc}$ -nitrido coordination complexes is given by the class of compounds formed by one bidentate heterodiphosphane  $\pi$  acceptor ligand (PNP) and one bidentate dithiocarbamate  $\pi$  donor ligand bound to the same  $[\text{}^{99m}\text{Tc}\equiv\text{N}]^{2+}$  core (Fig. 1.4).

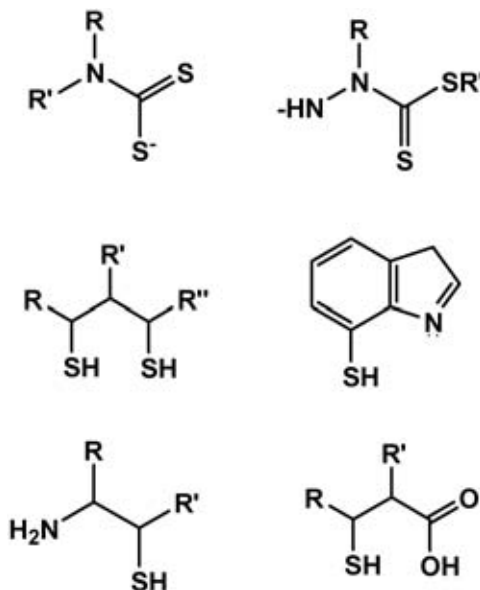


FIG. 1.5. Bidentate chelating ligands for the preparation of asymmetrical <sup>99m</sup>Tc-nitrido complexes.

In these preparations, the simultaneous interaction of the  $\pi$  acceptor ancillary PNP ligand in the presence of the nucleophilic  $\pi$  donor ligand always favours the quantitative formation of the asymmetrical product. These results can be nicely interpreted by assuming that these reactions always lead to the transient formation of the intermediate metal fragment  $[\text{}^{99\text{m}}\text{Tc}(\text{N})(\text{PNP})]^{2+}$ , composed of a  $\text{Tc}\equiv\text{N}$  group coordinated to a chelating heterodiphosphane ligand PNP. It turns out that this arrangement of atoms behaves as a strong electrophilic moiety, which selectively reacts with incoming monoanionic or dianionic  $\pi$  donor ligands (L) to afford asymmetrical complexes of the type  $[\text{}^{99\text{m}}\text{Tc}(\text{N})(\text{PNP})(\text{L})]^{0/+}$ . Thus the metal synthon  $[\text{}^{99\text{m}}\text{Tc}(\text{N})(\text{PNP})]^{2+}$  could be conveniently utilized to obtain a very broad class of asymmetrical nitrido Tc(V) complexes with a variety of bidentate ligands. Figure 1.5 is an illustration of other possible  $\pi$  donor bidentate chelating systems for the preparation of asymmetrical nitrido <sup>99m</sup>Tc complexes.

### 1.2.3. Technetium-99m-HYNIC core

The compound 2-hydrazino-nicotinic acid (HYNIC) can be considered a bifunctional coupling agent, especially suitable for <sup>99m</sup>Tc labelling of peptides.

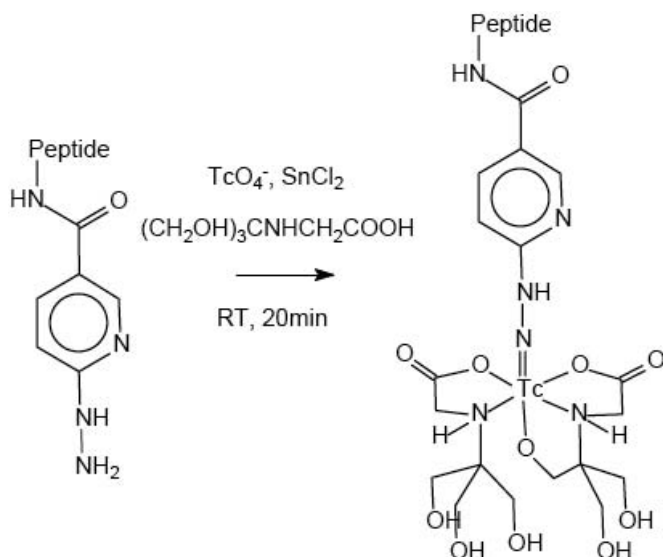


FIG. 1.6. Schematic drawing of the general structure of  $^{99m}\text{Tc}$ -HYNIC/tricine coordination complexes incorporating a peptide chain.

It can be coupled via the carboxylic function to free amines forming a bridge between the biomolecule and the technetium centre. The HYNIC conjugated molecules react as monodentate ligands, while coligands such as tricine are required to complete the coordination sphere around the metal. A typical HYNIC/tricine labelling coordination system is illustrated in Fig. 1.6.

The choice of a coligand has a decisive influence on the stability and biological behaviour of the resulting complex. Whereas tricine allows labelling at very high specific activities at room temperature, complex stability is suboptimal. A considerably higher stability is achieved by using ternary coligand systems including tricine and a monodentate ligand such as triphenylphosphine or pyridine derivatives such as nicotinic acid. Ethylenediamine-diacetic acid (EDDA) has also been employed as a coligand for labelling a number of biomolecules because it imparts high stability and hydrophilicity to the resulting complexes.

The HYNIC approach ensures mild labelling conditions, thus avoiding the risk of reduction of the -S-S- disulphide bridges of cysteine-containing peptides. In this manner,  $^{99m}\text{Tc}$ -somatostatin derivatives can be easily prepared. The most interesting version of these derivatives is the  $^{99m}\text{Tc}$ -EDDA-HYNIC-TOC complex, in which the modified peptide octreotide (TOC), containing tyrosine in place of phenylalanine in the amino acid chain and EDDA as

a coligand, are incorporated in the molecule.  $^{99m}\text{Tc}$ -EDDA-HYNIC-TOC is considered a useful diagnostic tool for imaging tumours and metastatic tissues expressing somatostatin receptors.

The HYNIC system was used successfully in the labelling of annexin V, a specific protein for targeting phosphatidylserine residues expressed on the surface of apoptotic cells, and is currently employed for *in vivo* imaging of programmed cell death (apoptosis). The HYNIC method was also utilized for the labelling with  $^{99m}\text{Tc}$  of various bioactive molecules involved in infections and inflammation processes, such as the antimicrobial peptide UBI 29-41, interleukin-8, LTB(4) receptor antagonists, the RP-463 chemotactic peptide, human IgGs and leptosomes. HYNIC coupled antisense DNAs are currently considered promising imaging tools for the application of  $^{99m}\text{Tc}$  labelled oligonucleotides to biomedical research.

#### 1.2.4. $^{99m}\text{Tc(III)/Re(III)-(4 + 1)}$ core

A novel type of metal chelating system is formed when the tripodal tetradentate chelator 2,2',2''-nitrilotris(ethanethiol) ( $\text{NS}_3$ ) in combination with a monodentate tertiary phosphine ( $\text{PR}_3$ ), or alternatively an isocyanide derivative ( $\text{CNR}'$ ), as a coligand, binds to the metallic ions  $\text{Tc(III)}$  or  $\text{Re(III)}$ . This moiety contains sterically well shielded, oxo free  $\text{Tc(III)/Re(III)}$  centres embedded in a trigonal bipyramidal arrangement (Fig. 1.7). The resulting complexes, of general formula  $[\text{M}^{\text{III}}(\text{L}^{\text{n}})(\text{L}^{\text{m}})]$  ( $\text{M} = \text{Tc, Re}$ ;  $\text{L}^{\text{n}} = \text{NS}_3$  or its derivatives;  $\text{L}^{\text{m}} = \text{PR}_3, \text{CNR}'$ ), are stable against ligand exchange with cysteine or glutathione, *in vitro* incubation with both plasma and whole blood of rats, and *in vivo*.

The class of 4 + 1 complexes belongs to the family of 'n + 1' mixed ligand  $\text{Tc/Re}$  species, and offers the advantage of high versatility in providing different sites for conjugation of a biomolecule. In fact, biomolecules can be coupled either to the  $\text{NS}_3$  tripodal ligand (Fig. 1.7a) or to the isocyanide or phosphino coligands (Fig. 1.7b) through the introduction of lateral carboxylic groups. For example, coupling of bioactive groups to the monodentate linkers  $\text{PR}_3$  or  $\text{CNR}'$  can be easily obtained using activated esters. Furthermore, a new hydrophilic  $\text{NS}_3$  chelator,  $\text{NS}_3(\text{COOH})_3$ , bearing three lateral carboxylic groups, has been introduced and evaluated in labelling reactions. These methods enable both the stable incorporation of a biomolecule into the final metallic complex and a careful control of its lipophilic character.

Improved methods for the production of  $^{99m}\text{Tc}$ - and  $^{188}\text{Re}$ -(4 + 1) complexes at the tracer level have been developed. In particular, only micromolar amounts of the appropriate monodentate ligand are required in radiopharmaceutical preparations resulting in high specific activity labelling of

CHAPTER 1

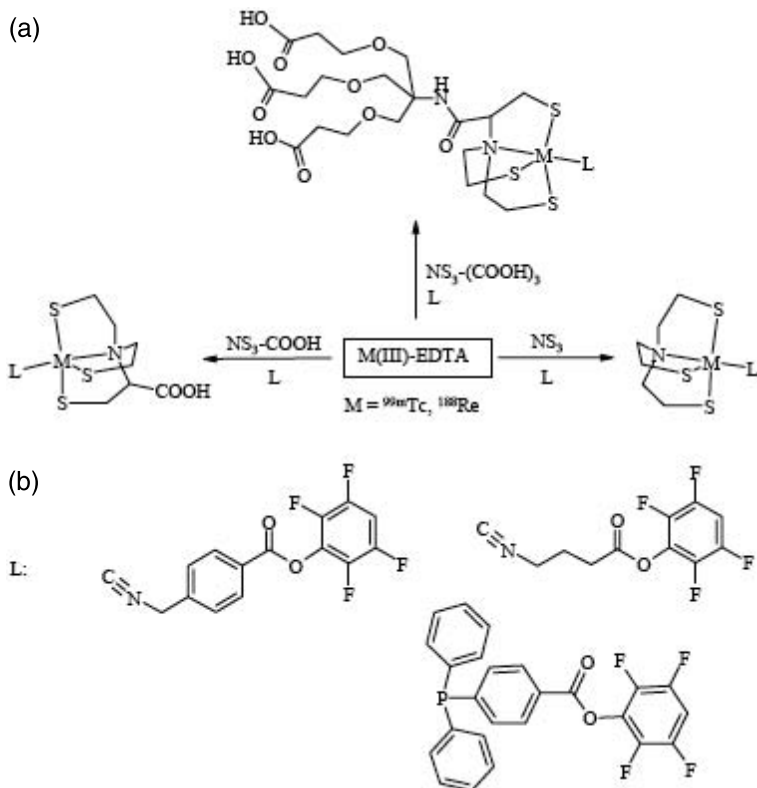


FIG. 1.7. Reaction diagram showing the formation of trigonal bipyramidal  $M-(4 + 1)$  ( $M = Tc, Re$ ) complexes. Some representative examples of a bioactive molecule appended either to the tripodal  $NS_3$  ligand (a) or to a monodentate coligand (b) are also reported.

interesting bioactive molecules. To avoid production of reduced hydrolysed metallic species, all preparations are performed through a two-step procedure involving the preliminary formation of the complexes  $Tc(III)$ -/ $Re(III)$ -EDTA (EDTA = ethylenediaminetetraacetic acid) as reaction intermediates. In the second step, these species further react with mixtures of the appropriate tripodal and monodentate ligands to afford the final  $4 + 1$  complexes (Fig. 1.7).

Isocyanide ligands can be used in the form of their  $Cu(I)$  complexes. This improves their stability and facilitates storage, thus allowing the development of suitable kit formulations. Moreover, the use of a stabilized form of isocyanides enables the formation of  $^{188}Re$  complexes in acidic solution.

## 1.3. SUMMARY OF SCIENTIFIC WORK

The work carried out by the participants is divided into five different charts. Each chart represents a group of biomolecules radiolabelled with one or more of the novel chemistries described above. Summaries of the studies carried out in different laboratories are described below.

### 1.3.1. Chart 1: Technetium-99m labelling of RGD peptides targeting $\alpha_v\beta_3$ integrin receptors

Integrins are cell surface transmembrane glycoproteins that are found as  $\alpha\beta$  heterodimers. The  $\alpha_v\beta_3$  integrin is known to be overexpressed in many tumour types and in sprouting blood vessels in the tumour, but is expressed at lower levels in normal tissues. Peptides containing the arginine-glycine-aspartate (RGD) sequence bind with high affinity to  $\alpha_v\beta_3$  receptors, and have attracted increasing interest in the search for a new class of diagnostic agents for targeting  $\alpha_v\beta_3$  receptors and in vivo imaging of angiogenesis. Recently, by using a  $^{18}\text{F}$  labelled galacto-RGD peptide and PET, it was demonstrated that monitoring of  $\alpha_v\beta_3$  receptors is possible in animal models as well as in humans.

In this CRP a small cyclic peptide, RGDyK (cyclo[Arg-Gly-Asp-D-Tyr-Lys]), was selected for radiolabelling with  $^{99\text{m}}\text{Tc}$ . This peptide has been shown to target  $\alpha_v\beta_3$  integrins with high affinity. It can be easily derivatized to yield a bifunctional ligand with various chelating moieties. However, because of its small size, some influence on the in vitro and in vivo properties of the resulting radioconjugate may come from the type of labelling approach utilized.

Seven different peptide derivatives formed from the RGDyK basic sequence (RGDyK = cyclo[Arg-Gly-Asp-D-Tyr-Lys]) were selected for  $^{99\text{m}}\text{Tc}$  labelling conjugation via the novel  $^{99\text{m}}\text{Tc}$  cores. Specifically, the following peptide derivatives were synthesized: X-RGDyK, X = 5-Me<sub>2</sub>-pyrazol-1-yl-ethylidiamine (PZ1-RGDyK), DTPA (DTPA-RGDyK), 2-hydrazinonicotinic acid (HYNIC-RGDyK), cysteine (Cys-RGDyK), aromatic and aliphatic isocyanides (L1-RGDyK, L2-RGDyK), tridentate amino acid derivatives (t-Cys-RGDyK, t-His-RGDyK). These bifunctional peptidic ligands were distributed to nine different participating laboratories. Selected structures are shown in Fig. 1.8. Details of the underlying chemistry, synthesis and biological evaluation can be found in Chapter 2.

#### 1.3.1.1. Radiolabelling

Analytical characterization, radiolabelling and in vitro/in vivo investigations were performed using all RGD derivatives cited above and employing

each of the four different  $^{99m}\text{Tc}$  cores proposed in this study. Concerning the HYNIC approach, experiments using different coligands were performed at the Universitätsklinik für Nuklearmedizin, Innsbruck, Universidad de la República, Montevideo, China Institute of Atomic Energy (CIAE), Beijing, Bhabha Atomic Research Centre, Mumbai, and Nuclear and Energy Research Institute (IPEN), São Paulo. Consistent results between the various research institutions were obtained, which showed that labelling yields were always  $\geq 90\%$ , yielding very high specific activity products. High in vitro stability for these conjugates was observed only when EDDA was employed as a coligand.

Radiolabelling with the  $^{99m}\text{Tc}$ -carbonyl core was performed using DTPA-, Cys-, HYNIC-, t-Cys, t-His-RGDyK as bifunctional ligands. Preparations were conducted in different participating laboratories. High specific activity labelling was achieved by reacting the *fac*- $[\text{}^{99m}\text{Tc}(\text{CO})_3(\text{H}_2\text{O})_3]^+$  synthon at high temperatures. However, chromatographic characterization demonstrated the formation of multiple species in the reaction solution, a result that reflects the suboptimal complexing characteristics of these peptide ligands for the  $^{99m}\text{Tc}$ -carbonyl core. Moreover, the observed lower stability in solution and higher protein binding values in human blood may partially be attributed to the presence of such a mixture of complexes. In a collaboration between the University of Missouri-Columbia and the Institute of Nuclear Technology, Portugal, it was shown that the peptidic ligand PZ1-RGDyK could be efficiently radiolabelled, with a very high yield, upon simple heating with the *fac*- $[\text{}^{99m}\text{Tc}(\text{CO})_3(\text{H}_2\text{O})_3]^+$  precursor. A single radiolabelled conjugate was formed that was found to be stable in solution and in human serum. These results were subsequently confirmed also by laboratories in Austria, Uruguay, India and Brazil.

At the Institute of Radiopharmacy, Forschungszentrum Dresden-Rossendorf, Germany, a two-step procedure was developed for the high specific activity  $^{99m}\text{Tc}$  labelling of the isocyanide peptidic derivatives L1- and L2-RGDyK. This method requires the preliminary preparation of the compound  $^{99m}\text{Tc}$ -EDTA as a precursor complex from which the desired  $^{99m}\text{Tc}$ -(4 + 1) conjugate is produced by a ligand exchange reaction. The final product consists of a Tc(III) ion coordinated to a monodentate isocyanide ligand and the tetradentate tripodal ligand 2,2',2''-nitriлотris(ethanethiol) ( $\text{NS}_3$ ) (Fig. 1.8). This labelling technology was experimentally well tested and the results were confirmed by the laboratories in Innsbruck and Montevideo, where biological characterization of the resulting complexes was also carried out. Lipophilicity of these conjugates results from the combination of the hydrophobic nature of the bifunctional ligand employed (L1-RGDyK > L2-RGDyK) as well as on the hydrophilic/hydrophobic character of the coligand employed.

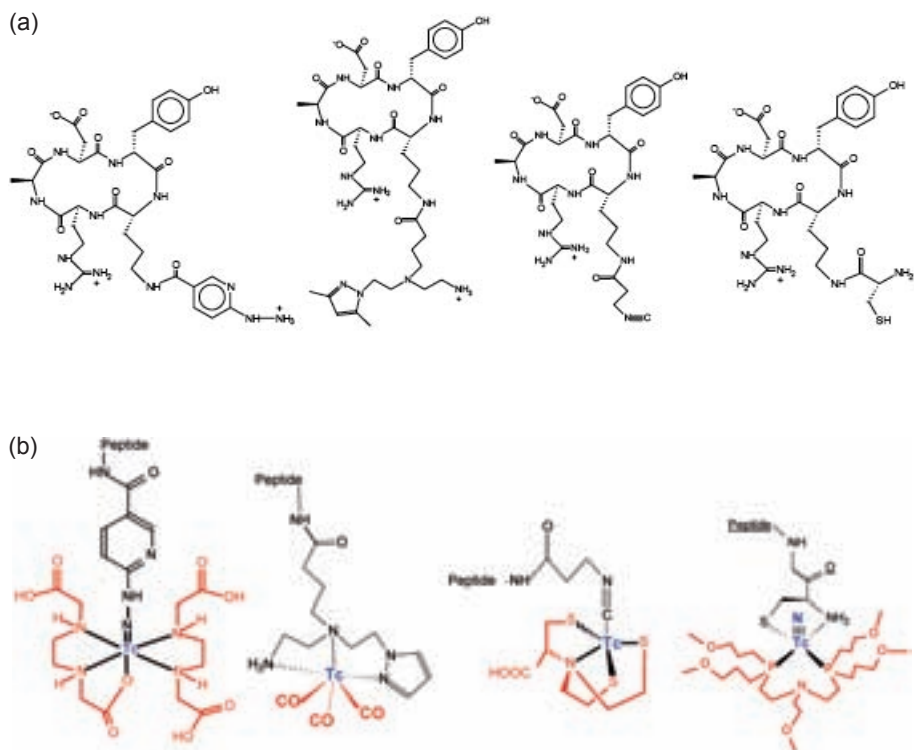


FIG. 1.8. (a) Selected structures of the derivatized RGD peptides used in this study: from left to right, HYNIC-RGDyK, PZI-RGDyK, L2-RGDyK and Cys-RGDyK. (b) Structures of the respective  $^{99m}\text{Tc}$  conjugate complexes after labelling with the different  $^{99m}\text{Tc}$  cores: from left to right,  $^{99m}\text{Tc}(\text{EDDA})_2(\text{HYNIC-RGDyK})$ ,  $^{99m}\text{Tc}(\text{CO})_3(\text{PZI-RGDyK})$ ,  $^{99m}\text{Tc}(\text{NS}_3)(\text{L2-RGDyK})$  and  $^{99m}\text{Tc}(\text{N})(\text{Cys-RGDyK})(\text{PNP})$ .

At the University of Ferrara, Italy, complexes incorporating the Cys-RGDyK ligand coordinated to a  $[\text{}^{99m}\text{Tc}\equiv\text{N}]^{2+}$  group were prepared at high specific activities and with very high yields using the asymmetrical approach based on the reactivity of the  $[\text{}^{99m}\text{Tc}(\text{N})(\text{PNP})]^{2+}$  metal fragment (PNP = heterodiphosphane coligand) towards peptide sequences having a terminal cysteine residue (Fig. 1.8). Two diastereomers were formed and analytically characterized. Labelling yields were quantitative and high solution stability was observed. These results were experimentally verified and confirmed by various laboratories in Austria, Brazil, China, India and Uruguay, where further biological characterization was carried out.

1.3.1.2. *Biological characterization*

The lipophilic character of the radiolabelled conjugates with RGD derivatives was determined by high performance liquid chromatography (HPLC). Log *P* values (ranging between -0.92 and -3.57) and binding to serum proteins (in the range 2–32%) varied considerably. The lowest protein binding and lipophilicity, determined by various laboratories, was assigned to the conjugate complex  $^{99m}\text{Tc}(\text{EDDA})_2(\text{HYNIC-RGDyK})$ .

The  $^{99m}\text{Tc}$  peptide conjugates showed specific uptake in  $\alpha_v\beta_3$  positive M21 melanoma cells, with values comparable for all compounds (approximately 1% of total/mg protein content). Only the complexes  $^{99m}\text{Tc}(\text{NS}_3)(\text{L1-RGDyK})$  and  $^{99m}\text{Tc}(\text{NS}_3)(\text{L3-RGDyK})$  showed low uptake values of less than 0.5%. Experiments with other cell lines were conducted in different laboratories. In particular, ovarian cancer cells (OVCAR-3 cells) were employed by the group at the University of Columbia, whereas HT29 human colon carcinoma cells were used by the group in India. A broad variation of uptake values was observed and no evidence of receptor mediated binding or internalization was clearly established.

A number of *in vivo* studies were carried out with the various  $^{99m}\text{Tc}$  labelled conjugates. Biodistribution and pharmacokinetic behaviour in normal mice were studied in Brazil, China, India, the USA and Uruguay. High variability in both distribution and excretion patterns was found, ranging from predominant renal excretion to predominant hepatobiliary elimination.

A variety of tumour models were used to investigate targeting properties *in vivo*. The group in Uruguay found tumour uptake of approximately 1.5% of injected dose per gram (ID/g) at 1 h post-injection for the complexes  $^{99m}\text{Tc}(\text{EDDA})_2(\text{HYNIC-RGDyK})$ ,  $^{99m}\text{Tc}(\text{CO})_3(\text{PZ1-RGDyK})$  and  $^{99m}\text{Tc}[\text{NS}_3(\text{COOH})_3](\text{L2-RGDyK})$  using a B16-F1 murine melanoma cell mouse model. At IPEN a nude mouse model employing A549 human non-small-cell lung carcinoma cells was used for evaluating three RGD conjugates labelled via the  $[\text{}^{99m}\text{Tc}(\text{CO})_3]^+$  core (i.e. PZ1-, t-Cys- and t-His-RGDyK) as well as the complexes  $^{99m}\text{Tc}(\text{EDDA})_2(\text{HYNIC-RGDyK})$  and  $^{99m}\text{Tc}(\text{N})(\text{PNP6})(\text{Cys-RGDyK})$  {PNP6 = bis[(diethoxypropylphosphanyl)ethyl]ethoxyethyl amine}. These studies showed variable tumour uptakes ranging from 1.54% to 5.73% ID/g at 4 h post-injection. However, receptor specificity was not experimentally verified. Imaging studies (Fig. 1.9a) did indicate significant reduction of tumour uptake after blocking of  $\alpha_v\beta_3$  receptors with excess of free peptide. At the Bhabha Atomic Research Centre, uptake of 1.1% ID/g was measured in the xenografted tumour tissue of a murine fibrosarcoma model for the complex

## CHAPTER 1

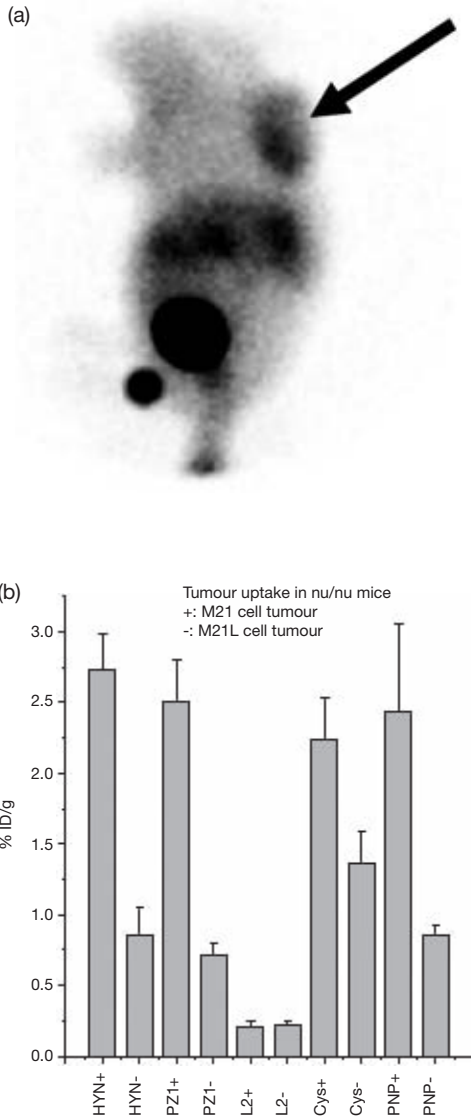


FIG. 1.9. Planar gamma camera images of  $^{99m}\text{Tc}(\text{EDDA})_2(\text{HYNIC-RGDyK})$  in an A549 tumour bearing mouse 4 h post-injection. The tumour is clearly delineated in the left upper quadrant of the back. Uptake, as calculated from an ROI technique, was determined to be 4.92%. Excretion patterns are dominated by renal washout, as shown by high activity in the bladder (a). The graph shows tumour uptake values of various  $^{99m}\text{Tc}$  labelled RGD derivatives in an  $\alpha_v\beta_3$  receptor positive (+) and negative (-) melanoma tumour model (b).

$^{99m}\text{Tc}(\text{EDDA})_2(\text{HYNIC-RGDyK})$ . Conversely, no reduction in tumour uptake was observed by coinjection with excess of free peptide. Tumour uptake studies in nude mice bearing FWK-1 pancreatic tumour xenografts were performed in China. Tumour uptake was 1.34% ID/g for  $^{99m}\text{Tc}(\text{EDDA})_2(\text{HYNIC-RGDyK})$ , and 2.92% ID/g for  $^{99m}\text{Tc}(\text{N})(\text{PNP6})(\text{Cys-RGDyK})$  at 1 h post-injection. These values significantly decreased after coinjection of excess of free RGDyK. At the Universitätsklinik für Nuklearmedizin, Innsbruck, all labelling cores were tested in a nude mouse model employing  $\alpha_v\beta_3$  receptor positive M21 and  $\alpha_v\beta_3$  receptor negative M21L tumour models (Fig. 1.9b). Tumour uptake at 1 h post-injection varied between 0.2 and 2.7% ID/g. The highest specific tumour uptake values and tumour to background ratios were found for the compounds  $^{99m}\text{Tc}(\text{EDDA})_2(\text{HYNIC-RGDyK})$ ,  $^{99m}\text{Tc}(\text{N})(\text{PNP5})(\text{Cys-RGDyK})$  (PNP5 = bis[(dimethoxypropyl phosphanyl)ethyl]ethoxyethylamine) and  $^{99m}\text{Tc}(\text{CO})_3(\text{PZ1-cRGDy})$ . Uptake values were approximately 2.5% ID/g in M21 receptor positive tumours and less than 1% in receptor negative M21L tumours. Biodistribution studies also indicated lower intestinal excretion for the  $^{99m}\text{Tc}(\text{EDDA})_2(\text{HYNIC-RGDyK})$  conjugate.

### 1.3.1.3. Conclusion (chart 1)

Seven different RGDyK derivatives were synthesized by the Austrian participant and distributed to nine laboratories participating in this subproject. All groups were able to radiolabel successfully specific bifunctional peptide ligands using the  $^{99m}\text{Tc}$ -HYNIC,  $^{99m}\text{Tc}$ -carbonyl,  $^{99m}\text{Tc}$ -nitrido- or  $^{99m}\text{Tc}$ -(4 + 1) approaches yielding  $^{99m}\text{Tc}$  products with high specific activity and with comparable outcomes.

Data on tumour uptake obtained from the various biodistribution studies showed concordant results with acceptable interlaboratory variability. They showed that the specific labelling approach had a profound effect on the biological properties of these  $^{99m}\text{Tc}$  labelled receptor specific model peptides in terms of distribution, excretion pathways (renal to hepatobiliary) and receptor mediated tumour uptake. These investigations demonstrated that in the labelling of bioactive peptides with  $^{99m}\text{Tc}$ , labelling strategies have to be properly selected and optimized. Different in vitro assays are necessary in order to predict in vivo targeting properties of the final radiolabelled conjugates. If peptide radiopharmaceuticals have to be used as diagnostic tracers, high stability, increasing hydrophilic properties and low plasma protein binding conjoined with retention of biological activity are critical features enabling the identification of the most promising candidates for sensitive in vivo detection of specific receptors in oncology and potentially in other diseases.

## CHAPTER 1

In conclusion, the results obtained within this CRP will form the basis for a subsequent development of new radiopharmaceuticals targeting  $\alpha_v\beta_3$  receptors. Moreover, this scientific knowledge may provide a valuable and unique set of experimental data in fundamental technetium chemistry, which could be conveniently utilized for pursuing a further optimization of the targeting properties of  $^{99m}\text{Tc}$  tracers derived from highly specific bioactive peptides.

### 1.3.2. Chart 2: Labelling of annexin V fragments

Imaging of programmed cell death (apoptosis) is one of the most interesting challenges in radiopharmaceutical chemistry, and this modality is of high interest in oncology, cardiology and the study of atherosclerosis. Cell damage is usually sensed by various cellular mechanisms and leads to the disruption at system that causes expression of phosphatidylserine. This phospholipid is normally maintained on the inner surface of the cell membrane in a healthy cell, but in programmed cell death it appears on the outer surface of the membrane, giving the earliest signs of apoptosis.

Annexin V is a 36 kDa protein consisting of 320 amino acids that binds specifically to phosphatidylserine groups with high affinity. Recently, annexin V has been labelled with  $^{99m}\text{Tc}$ , and this diagnostic agent is currently considered a useful tool for apoptosis detection, although it has many disadvantages from the point of view of radiopharmaceutical kit formulation. Hence, this CRP subproject focused on the development of phosphatidylserine specific small  $^{99m}\text{Tc}$  labelled molecules for in vivo imaging of the apoptotic process.

As annexin type proteins generally exhibit their biospecific sequences at the N-terminal, it would be reasonable to assume that the phosphatidylserine specific sequence might be attributed to a chain at the N-terminal. Based on this concept, a peptide has been developed consisting of 13 amino acids bearing the identical sequence of the N-terminal of annexin V. This 13 amino acid peptide, abbreviated Anx13, was derivatized by attaching to its amino acidic chain various functional groups so that different novel  $^{99m}\text{Tc}$  labelling methods could be attempted. The following peptide sequences and their BFCA conjugates were synthesized at the Institute of Isotopes Co. Ltd in Budapest:

- (a) Anx13:  $\text{H}_2\text{N}$ -[Ala-Glu-Val-Leu-Arg-Gly-Thr-Val-Thr-Asp-Phe-Pro-Gly]-OH.
- (b) Cys-Anx13:  $\text{H}_2\text{N}$ -Cys-[Ala-Glu-Val-Leu-Arg-Gly-Thr-Val-Thr-Asp-Phe-Pro-Gly]-OH.
- (c) Cys2-Anx13:  $\text{H}_2\text{N}$ -Cys-Gly-[Ala-Glu-Val-Leu-Arg-Gly-Thr-Val-Thr-Asp-Phe-Pro-Gly]-OH.

- (d) His-Anx13:  $\text{H}_2\text{N-Hys-[Ala-Glu-Val-Leu-Arg-Gly-Thr-Val-Thr-Asp-Phe-Pro-Gly]-OH}$ .
- (e) HYNIC-Anx13:  $\text{HYNIC-[Ala-Glu-Val-Leu-Arg-Gly-Thr-Val-Thr-Asp-Phe-Pro-Gly]-OH}$ .

An additional derivatization of Anx13 was carried out at the Institute of Radiopharmacy, Forschungszentrum Dresden–Rossendorf, Germany:

- (f) CN-Anx13:  $\text{C}\equiv\text{N}\text{---[Ala-Glu-Val-Leu-Arg-Gly-Thr-Val-Thr-Asp-Phe-Pro-Gly]-OH}$ .

The Anx13 peptide and its derivatives exhibited a rather good long run chemical stability when stored in a refrigerator at  $-18^\circ\text{C}$  or at  $+5 \pm 3^\circ\text{C}$ .

### 1.3.2.1. Radiolabelling

All the four novel methods based on the new  $^{99\text{m}}\text{Tc}$  cores were used for labelling the different derivatives of the Anx13 sequence. The results are discussed below.

*Labelling with the  $^{99\text{m}}\text{Tc}$ -nitrido core.* Labelling of the peptide Cys2-Anx13 with the  $^{99\text{m}}\text{Tc}$ -nitrido core was carried out at the University of Ferrara, Italy, using the asymmetric approach and the heterodiphosphane bis[(dimethoxypropylphosphanyl)ethyl]methoxyethylamine (PNP3) as an ancillary coligand. The resulting  $^{99\text{m}}\text{Tc}$  labelled compound was obtained with high radiochemical purity. Two main peaks were observed in the HPLC chromatogram at 35.21 and 36.10 min, indicating the presence of *syn* and *anti* stereoisomers. The proposed chemical structures are shown in Fig. 1.10. Stability studies showed that the radiochemical purity of the asymmetrical complex  $^{99\text{m}}\text{Tc}(\text{N})(\text{Cys2-Anx13})(\text{PNP3})$  decreased to 73% of the initial activity 2 h after labelling. Similar results were obtained by groups in Brazil and India. In particular, in Brazil the coligand PNP6 was utilized in the application of the asymmetrical approach, resulting in a final radiochemical yield of 92.6%. The labelled complex was found to be relatively inert to transchelation in solutions containing excess of free cysteine, the decrease in radiochemical purity being approximately 4.7% after 6 h.

Labelling studies with the  $^{99\text{m}}\text{Tc}$ -nitrido core and the peptide Cys2-Anx13 following the symmetrical approach were performed in India, Italy and Hungary. This procedure involved the interaction of the peptidic ligand with the metal  $[\text{}^{99\text{m}}\text{Tc}\equiv\text{N}]^{2+}$  group in the absence of the ancillary diphosphane coligand. Although the structure of this product was not exactly determined, the relatively short retention time of the resulting labelled species (HPLC

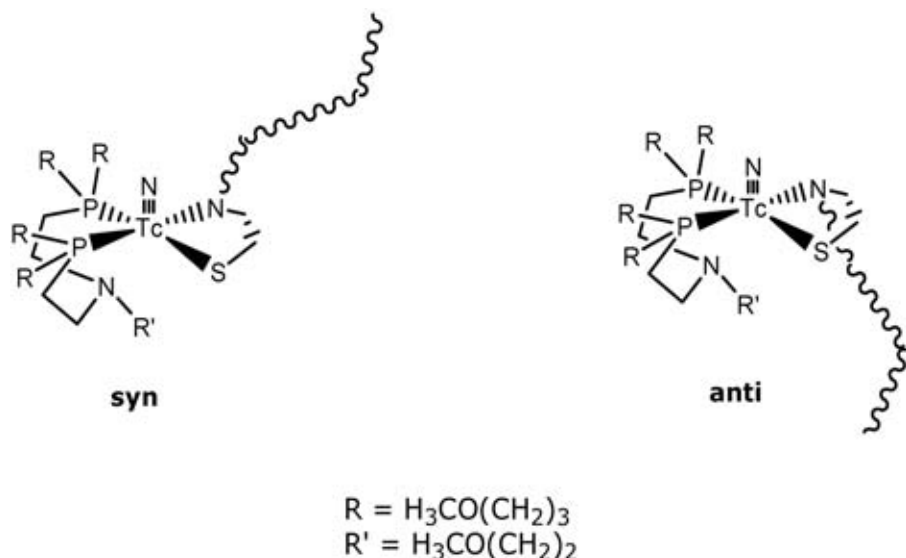


FIG. 1.10. Chemical structure of *syn* and *anti* stereoisomers obtained in asymmetrical  $^{99\text{m}}\text{Tc}$ -nitrido labelling of Cys2-Anx13.

peaks at 13.2 and 16.9 min) suggested the formation of two isomers of a single  $^{99\text{m}}\text{Tc}$ -nitrido complex incorporating the peptide moiety. Radiochemical purity was higher than 90% and was maintained almost constant over time.

*Labelling with the  $^{99\text{m}}\text{Tc}$ -carbonyl core.* Labelling of the His-Anx13 peptide derivative with the  $^{99\text{m}}\text{Tc}$ -carbonyl core was performed in Brazil, Greece, India and Uruguay. In experiments carried out at IPEN, radiochemical yields varying from 82.6% to 91.3% were observed. The group in India reported a radiochemical yield of 95% for the same complex, which also appeared highly stable in solution and almost completely inert towards transchelation with cysteine or histidine. Similar results were attained in Uruguay. At the Demokritos National Centre of Scientific Research in Greece, labelling of both His-Anx13 and of the modified peptide pyridine-ethyl-Cys-Anx13 with the  $^{99\text{m}}\text{Tc}$ -carbonyl core was accomplished with high yields. The resulting peptide complexes were found to be resistant to transchelation when incubated with excess of histidine and cysteine.

*Labelling with the  $^{99\text{m}}\text{Tc}$ -HYNIC core.* Labelling of the peptide derivative HYNIC-Anx13 was performed in laboratories in China, Brazil and Uruguay. In China, three different labelling procedures based on the  $^{99\text{m}}\text{Tc}$ -HYNIC approach were applied using tricine, EDDA and a combination of tricine + EDDA as coligands. Yields higher than 90% were obtained when complexes

were prepared with tricine as a coligand at pH range pH6.1–7.2. When EDDA was used as a coligand, labelling yield was mainly influenced by the concentration of stannous chloride. An average yield of approximately 72% was obtained when 5–20  $\mu\text{g}$  of this reducing agent was employed. With the addition of a tricine + EDDA mixture, a radiochemical yield of 98% was attained in the presence of 10  $\mu\text{g}$  of stannous chloride. In Brazil, radiochemical yields up to 78.5% were obtained when tricine + EDDA were used as coligands. In Uruguay, the standard labelling procedure was applied using the EDDA as a coligand. High specific activity (7000 Ci/mmol) and high radiochemical yields (90–95%) for the final  $^{99\text{m}}\text{Tc}(\text{EDDA})_2(\text{HYNIC-Anx13})$  peptide complex were obtained.

*Labelling with the  $^{99\text{m}}\text{Tc}-(4 + 1)$  core.* Attachment of a terminal isocyanide group to the Anx13 peptide sequence was accomplished at the Institute of Radiopharmacy, Forschungszentrum Dresden–Rossendorf, Germany. The resulting monodentate bifunctional ligand CN-Anx13 was labelled with the  $^{99\text{m}}\text{Tc}-(4 + 1)$  core using  $^{99\text{m}}\text{Tc-EDTA}$  as an intermediate precursor and tri(mercaptoethyl)amine ( $\text{NS}_3$ ) as a tetradentate coligand. The radiochemical yield was approximately 60%. However, after chromatographic purification, a high radiochemical purity of about 95% was attained. This value decreased to 90% when the labelled peptide was left to stand in the recovered HPLC eluate at room temperature for 24 h.

### 1.3.2.2. *Biological characterization*

Normal biodistribution of the different  $^{99\text{m}}\text{Tc}$  labelled Anx13 derivatives was studied in mice in Brazil, Greece and Uruguay. It was found that the common excretion route for these complexes occurs via the kidneys and bladder. In Uruguay, His-Anx13 labelled with the  $^{99\text{m}}\text{Tc}$ -carbonyl core was also observed to be partly taken up in the liver and intestine. Similarly, the laboratory in São Paulo, Brazil, reported that the complex  $^{99\text{m}}\text{Tc}-(\text{N})(\text{Cys-Anx13})(\text{PNP6})$  accumulated to a significant extent in the liver and intestine. An animal model of cardiac apoptosis induced by doxorubicin was developed in Uruguay, but no specific uptake of  $^{99\text{m}}\text{Tc}$  Anx13 complexes was observed in apoptotic tissues. Likewise, negative results were obtained in Brazil when tumour apoptosis was investigated in nude mice. In China, low in vivo stability of the  $^{99\text{m}}\text{Tc}(\text{tricine/EDDA})(\text{HYNIC-Anx13})$  complex was observed in rats subjected to intramedullary apoptosis induced by cyclophosphamide treatment. In Germany, low in vivo stability of the derivative  $^{99\text{m}}\text{Tc}(\text{CN-Anx13})(\text{NS}_3)$  was also measured by detecting the formation of five different  $^{99\text{m}}\text{Tc}$  labelled metabolites identified in protein free plasma samples of rats. In

Italy, investigations carried out on apoptotic cell cultures led to similar negative results.

Despite the above negative results, an interesting positive observation was found in biological studies carried out in India, where it was proved that approximately 6.5% of the administered activity of the  $^{99m}\text{Tc}$ -nitrido complex  $^{99m}\text{Tc}(\text{N})(\text{Cys}2\text{-Anx}13)$ , prepared through the application of the symmetrical labelling approach, was specifically taken up by apoptotic HL-60 cells. In this model, the apoptotic process was induced by camptotecin treatment.

### 1.3.2.3. Conclusion (chart 2)

Anx13 fragment and its bifunctional derivatives exhibited rather good long run stability when stored at low temperatures. The novel  $^{99m}\text{Tc}$  labelling approaches utilized in this study usually afforded complexes with high radio-chemical yields, thus indicating that highly efficient coordination systems appended to the derivatized biomolecule were employed. Conversely, biological evaluations in different laboratories showed poor affinity of the labelled compounds for phosphatidylserine groups, except for the complex  $^{99m}\text{Tc}(\text{N})(\text{Cys}2\text{-Anx}13)$ , which binds specifically to cultured apoptotic cells, as demonstrated by the results at the Bhabha Atomic Research Centre. Further investigations on this compound may enlighten the mechanism underlying this specific uptake and provide an opportunity to develop a novel radiopharmaceutical targeting apoptotic tissues.

### 1.3.3. Chart 3: Labelling of fatty acids using the $^{99m}\text{Tc}$ -tricarbonyl core

Long chain fatty acids are the major source of energy for heart muscle and are rapidly metabolized by beta oxidation under normal conditions. Regional alterations in the myocardial fatty acid oxidation may indicate ischaemic heart disease and cardiomyopathy at an early stage, and therefore fatty acids possess a remarkable diagnostic potential in nuclear medicine. Many fatty acids or their analogues have been labelled with positron and gamma emitting radionuclides in order to non-invasively assess changes in fatty acid metabolism. Over the past 30 years, various research groups have explored the possibility of incorporating  $^{99m}\text{Tc}$  into fatty acid carrier molecules using a variety of ligands. Even though neutral and lipophilic  $^{99m}\text{Tc}$  complexes were formed, the myocardial profiles of these agents were not adequate.

In the framework of this CRP, the synthesis and evaluation of new fatty acid derivatives labelled with  $^{99m}\text{Tc}$  were undertaken. At the Demokritos National Centre of Scientific Research, Greece, four derivatives of undecanoic acid and two derivatives of hexadecanoic acid were synthesized and their

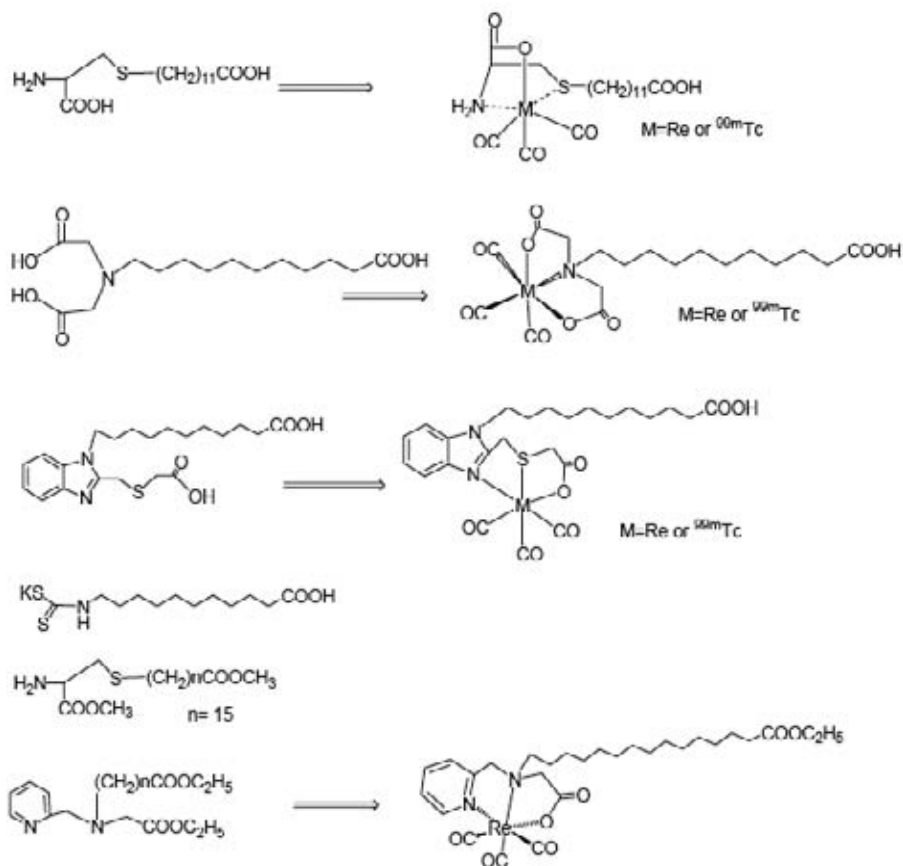


FIG. 1.11. Schematic representation of the reactions between the  $^{99m}\text{Tc}$ -carbonyl core with functionalized fatty acid derivatives.

coordination chemistry towards the  $^{99m}\text{Tc}$ -carbonyl core and the corresponding rhenium analogue was investigated. Figure 1.11 shows a schematic illustration of these reactions.

All four derivatives were also provided to groups in China, India and the Russian Federation, and in these laboratories the influence of reaction parameters such as pH, concentration, reaction time and temperature were investigated. HPLC analysis demonstrated that in all preparations a single complex was produced with a radiochemical yield higher than 93%. These species remained unchanged in solution 6 h from preparation. The molecular structure of the  $^{99m}\text{Tc}$  complex was tested by comparative HPLC studies using well characterized Re(I) complexes having the same chemical composition as a reference.

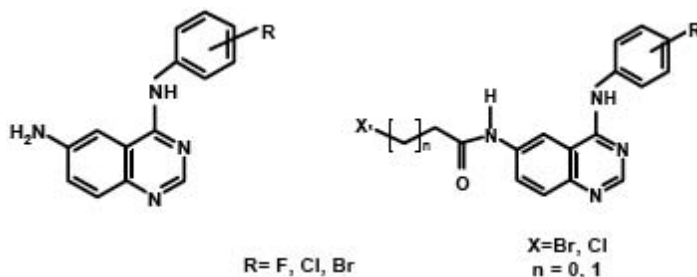


FIG. 1.12. Quinazoline derivatives utilized in this study.

Studies of the biodistribution of these  $^{99m}\text{Tc}$  complexes in mice revealed a rather low heart uptake.

#### 1.3.4. Chart 4: Technetium-99m labelling of quinazoline derivatives

The epidermal growth factor receptor (EGFR) is known to be over-expressed in several solid tumour types. Several therapeutic agents have been developed for targeting EGFR, namely small molecules such as quinazoline derivatives, which exhibit high affinity for the EGFR associated tyrosine kinase (EGFR-TK), competing with ATP (adenosine triphosphate) for binding to the intracellular tyrosine kinase region. A bioprobe to help on cancer diagnosis and predict the efficacy of a given class of EGFR-tk inhibitors is needed to optimize the therapeutic potential of EGFR inhibitors.

The two quinazoline derivatives reported in Fig. 1.12 have been designed and synthesized as a starting material for the preparation of a series of bifunctional ligands specifically tailored for conjugation to the new cores considered in this CRP.

After reaction with the different  $^{99m}\text{Tc}$  cores, the resulting quinazoline derived ligands afforded a new set of  $^{99m}\text{Tc}$  complexes, which are schematically illustrated in Fig. 1.13. In particular, a quinazoline derived ligand (CN-Qz) having a terminal isocyanide coordinating group was employed in reactions with the  $^{99m}\text{Tc}$ -(4 + 1) core to yield the complex  $^{99m}\text{Tc}(\text{CN-Qz})(\text{NS}_3)$  (Fig. 1.13, part 1). Furthermore, a quinazoline-dithiocarbamate derivative (CS2-Qz) was employed for the preparation of a series of  $^{99m}\text{Tc}$ -nitrido compounds, including the symmetrical bis substituted complex  $^{99m}\text{Tc}(\text{N})(\text{CS2-Qz})_2$  (Fig. 1.13, part 2), the asymmetrical complex  $^{99m}\text{Tc}(\text{N})(\text{CS2-Qz})(\text{PNP3})$  (Fig. 1.13, part 3) and a novel type of asymmetrical complex,  $^{99m}\text{Tc}(\text{N})(\text{PS})(\text{CS2-Qz})$  [PS = 2-(diisopropylphosphino)ethanethiol], composed of a  $[\text{N}^{99m}\text{Tc}\equiv\text{N}]^{2+}$  group bound to one dithiocarbamate ligand and one phosphino-thiol ligand (Fig. 1.13, part 4) (for details see Chapter 15). Finally, two tridentate quinazoline derived ligands

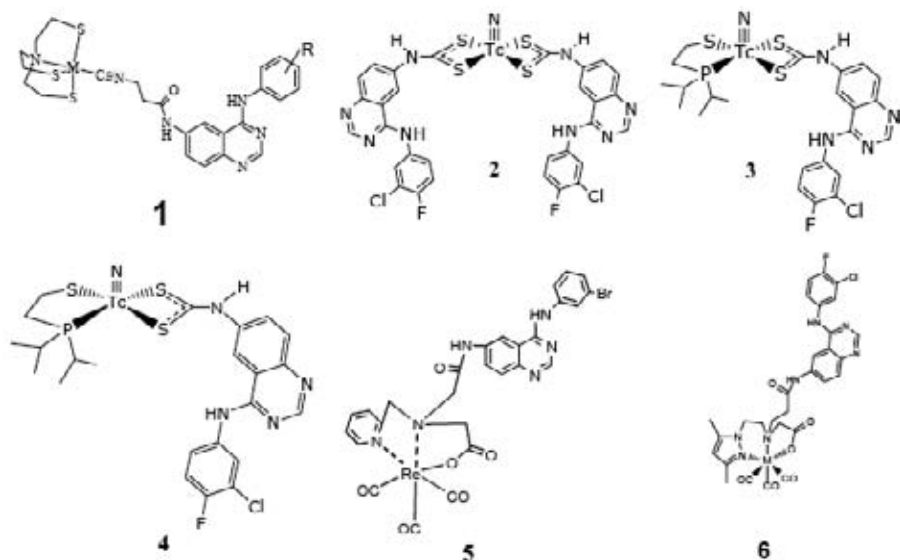


FIG. 1.13. The new  $^{99m}\text{Tc}$  complexes bearing an appended quinazoline moiety.

suitable for coordination to the  $^{99m}\text{Tc}$ -carbonyl core were prepared and utilized in the synthesis of the corresponding monosubstituted complexes (Fig. 1.13, parts 5 and 6). The new  $^{99m}\text{Tc}$  compounds were obtained with a high radiochemical yield and were characterized by comparison with the corresponding rhenium analogues as shown in Fig. 1.13. They were found to possess a remarkable stability both *in vitro* and *in vivo*.

When mixed with A431 cells, the new  $^{99m}\text{Tc}$  conjugates were able to significantly inhibit cellular growth, with  $\text{IC}_{50}$  values being in the micromolar range. At the lowest concentration of  $1.0\mu\text{M}$ , all compounds also inhibited cellular phosphorylation. A representative example is reported in Fig. 1.14, in which results obtained with some  $^{99m}\text{Tc}$  complexes are compared with standard inhibition carried out in the presence of EGF (+) and without addition of EGF (-).

### 1.3.5. Chart 5: Development of technetium-99m glucose analogues

Glucose is considered a key molecule for metabolism, and therefore availability of a  $^{99m}\text{Tc}$  labelled glucose derivative as a SPECT analogue of the well established PET tracer  $^{18}\text{F}$ FDG is considered to be of great interest.

The labelling of bioactive small molecules of any nature is always a difficult task, since subtle structural changes may affect to a significant extent

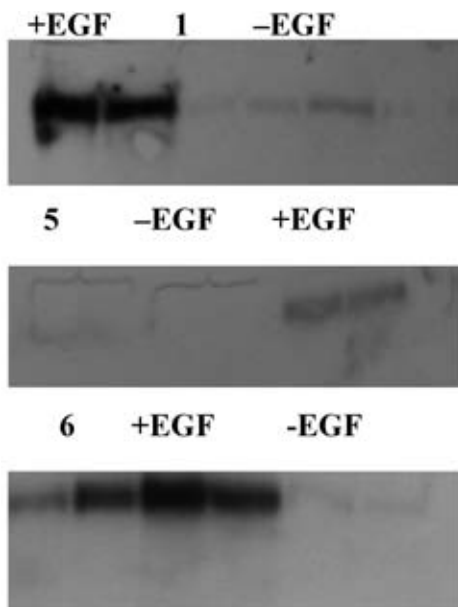


FIG. 1.14. A representative example of phosphorylation inhibition induced by the new quinazoline-derived  $^{99m}\text{Tc}$  complexes as compared with standard EGF inhibition.

recognition by the corresponding biological substrate. In particular, with glucose analogues a difficult challenge is to preserve recognition by GLUT1, the essential glucose transporter. This highly specific transport system does not tolerate much variation in the substrate basic structure, a fact that easily explains why the preparation of a  $^{99m}\text{Tc}$  glucose surrogate is considered highly challenging.

As a first step of this investigation, the synthesis of glucose derived bifunctional ligands containing adequate donor groups for coordination to the various cores utilized here was pursued. The design of these ligands was restricted to glucose derivatives modified at the 2' position, as this was thought to be the most suitable site to tolerate some structural change. Using  $\beta$ -D-pentaacetyl glucose as the starting material, a linker containing either six or four carbon atoms was introduced at position 2' by a two-step procedure as illustrated in Fig. 1.15. The role of this linker in the final bifunctional ligand would be in connecting the glucose moiety to an appropriate chelating system for the metal. Organic synthesis was carried out at the Universidad de la República, Montevideo, following a synthetic pathway elaborated at the University of Zurich.

## CHAPTER 1

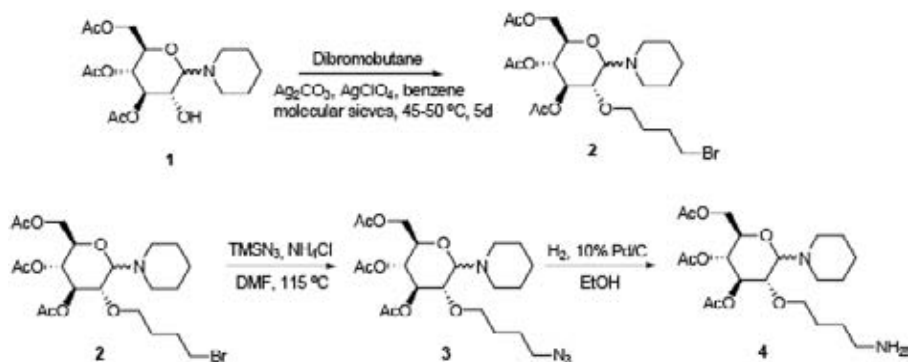


FIG. 1.15. Synthetic pathway for introducing a terminal nucleophilic leaving group to a carbon side chain attached to the 2'-OH group of glucose followed by its conversion to an electrophilic amino group.

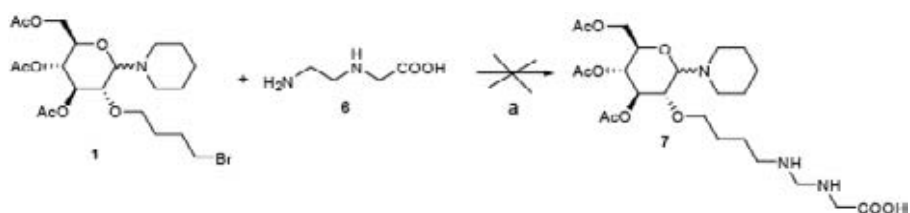


FIG. 1.16. Attempted coupling of a tridentate  $\text{N}_2\text{O}$  type ligand to the 2'-OH group of glucose.

The O-hexyl and O-butylbromide (Fig. 1.15) glucose derivatives were successfully prepared with a good yield and with high purity. Compound **2** (Fig. 1.15) constitutes an essential starting material as it may open the possibility of obtaining a series of glucose based bifunctional ligands suitable for coordination to the various metallic cores. Preliminary attempts to introduce an  $\text{N}_2\text{O}$  donor type chelating group failed due to the strong difference in solubility properties between parts **2** and **6** (Figs 1.15 and 1.16). In spite of this, it was planned to follow up this approach after the termination of the actual CRP with more suitable ligands.

According to the reaction diagram reported in Fig. 1.15, compound **2** was further converted into compound **3** by reaction with trimethylsilyl-azide. Compound **3** was isolated with a good yield and fully characterized. Then, reduction of the azido group to the corresponding amino-glucose (part **4**) was conveniently accomplished with 70% yield. The possibility to achieve

## CHAPTER 1

subsequent conversion of compound 4 to a final dithiocarbamate ligand suitable for application with the  $^{99m}\text{Tc}$ -nitrido technology was not verified because of some intrinsic difficulties and complexity in the underlying carbohydrate chemistry.

Although the encountered synthetic difficulties did not allow significant results to be obtained within the present subproject of this CRP, experimental procedures designed here for preparing a number of appropriate bifunctional chelating agents for the different  $^{99m}\text{Tc}$  cores starting from carbohydrate precursors may provide an important basis for promoting further developments in the field of  $^{99m}\text{Tc}$  radiopharmaceuticals mimicking the biological behaviour of glucose.

### 1.4. ACHIEVEMENTS OF THE COORDINATED RESEARCH PROJECT

The following was achieved by the CRP:

- (a) In accordance with the objectives, the fundamental chemical methods required for the preparation of the different  $^{99m}\text{Tc}$  cores were efficiently transferred to the various laboratories involved in the CRP.
- (b) Transfer of basic knowledge, labelling technologies and protocols was highly successful and the various groups were able to achieve a correct use of the different labelling techniques within a very short time. This process of scientific communication and exchange proved to be much more efficient and reliable than reading the same information in a scientific publication.
- (c) Chemical reagents required for the production of the different  $^{99m}\text{Tc}$  cores were shared with various laboratories.
- (d) Similarly, a considerable number of ligands were prepared through the application of chemical methods ranging from peptide chemistry to organic synthesis. These ligands were then distributed among the various laboratories.
- (e) Scientific relevance of all arguments included in the CRP greatly stimulated interaction and collaboration between the various groups.
- (f) The most appropriate experimental conditions for obtaining high specific activity labelling with the various cores and biomolecules were correctly identified. This knowledge will be of much utility for the various laboratories for planning and conducting future work on these systems.
- (g) The CRP was effective in increasing the technological level of the various laboratories. This allowed reliable experimental data to be obtained and

## CHAPTER 1

led to a number of interesting scientific publications. Further, the various laboratories have been very efficient in assimilating the new technologies and improving their ability in these fields. Data reported by the various laboratories were similar and consistent, thus indicating correct application of the various methodologies.

- (h) The various groups were also able to go further on with the experimental work and perform a preliminary biological evaluation of the novel radiopharmaceutical products by using in vitro cell experiments and biodistribution studies in animal models.
- (i) Analysis of the results of the CRP revealed that the new labelling technologies have been fully incorporated into the scientific background of the various laboratories, and therefore they could be conveniently utilized for pursuing the design and preparation of novel classes of radiopharmaceuticals other than those considered in this CRP.
- (j) The CRP was also helpful to the participants in expanding their scientific relationships and identifying research collaborations, which may allow them to enter scientific projects funded by others sources.
- (k) A large number of publications and communications to scientific meetings were presented and accepted during the CRP.

### 1.5. INTERGROUP COLLABORATIONS

During this CRP the participants undertook several joint programmes and researcher exchanges. Special intermediate compounds and ligands were synthesized in different specialized laboratories and distributed to the other members of the CRP. Details of these collaborations are given below.

#### 1.5.1. Exchanges of reagents and precursors

- (a) Cooperation was established between the University of Zurich and the Universidad de la República in Montevideo for pursuing the synthesis of a glucose derived bifunctional ligand. Peptide ligands suitable for labelling with the  $^{99m}\text{Tc}$ -carbonyl core were synthesized at the University of Zurich and distributed to interested groups and to the company producing the RGD peptides.
- (b) Heterodiphosphane ligands (PNP) employed in the asymmetrical labelling approach with the  $^{99m}\text{Tc}$ -nitrido core were prepared at the University of Ferrara, Italy, and distributed to groups in Brazil, China, Hungary, India and Uruguay.

## CHAPTER 1

- (c) Freeze dried kits for the preparation of the  $[^{99m}\text{Tc}\equiv\text{N}]^{2+}$  core were obtained as a gift courtesy of CIS Biointernational and distributed by the University of Ferrara to groups in Brazil, China, Greece, Hungary, India and Uruguay.
- (d) At the Demokritos centre in Greece long chain fatty acids were synthesized and distributed to groups in China, India and the Russian Federation.
- (e) RGD peptide analogues were synthesized at the Universitätsklinik für Nuklearmedizin, Innsbruck, and distributed to participants from Brazil, China, Germany, India, Italy, Uruguay and the USA.
- (f) RGD-isocyanide derivatives were prepared at the Institute of Radiopharmacy, Forschungszentrum Dresden–Rossendorf, Germany, and sent to the group in Uruguay together with coligands and protocols for labelling using the  $^{99m}\text{Tc}$ -(4 + 1) mixed ligand approach.
- (g) The 13 amino acid annexin V fragment, Anx13, was synthesized at the Biological Research Centre of the Hungarian Academy of Sciences and distributed to participant laboratories in Brazil, China, Germany, Greece, India, Italy, Portugal, Switzerland, Uruguay and the USA.

### 1.5.2. Exchange visits

- (a) A PhD student from the Institute of Nuclear Technology, Portugal, visited the University of Missouri-Columbia for a six month research period.
- (b) A. Rey, from the Universidad de la República, Montevideo, visited the Universitätsklinik für Nuklearmedizin, Innsbruck, in September 2004 and the University of Ferrara, Italy, in October 2005 with the purpose of applying radiolabelling methods based on the  $^{99m}\text{Tc}$ -HYNIC,  $^{99m}\text{Tc}$ -carbonyl and  $^{99m}\text{Tc}$ -nitrido cores to RGD peptides.
- (c) J.U. Künstler, from the Institute of Radiopharmacy, Forschungszentrum Dresden–Rossendorf, Germany, visited the Universitätsklinik für Nuklearmedizin, Innsbruck, in November 2005 to develop labelling methods for RGD peptides based on the  $^{99m}\text{Tc}$ -(4 + 1) approach and to initiate biological evaluation of the resulting  $^{99m}\text{Tc}$  labelled compounds.
- (d) M. Pasquali, from the University of Ferrara, Italy, visited the Universitätsklinik für Nuklearmedizin, Innsbruck, in April 2006 to develop labelling methods for RGD peptides based on the  $^{99m}\text{Tc}$ -nitrido core and to initiate biological evaluation of the resulting  $^{99m}\text{Tc}$  labelled compounds.
- (e) B. Linkowski Faintuch, from IPEN, São Paulo, visited the University of Missouri-Columbia with the purpose of applying the  $^{99m}\text{Tc}$ -HYNIC technology to labelling bioactive peptides.

## CHAPTER 1

- (f) Hu Ji, from the CIAE, visited the Universitätsklinik für Nuklearmedizin, Innsbruck, to apply the labelling methods based on the new  $^{99m}\text{Tc}$  cores to RGD peptides.
- (g) A. Rey, from the Universidad de la República, Montevideo, visited the Institute of Radiopharmacy, Forschungszentrum Dresden–Rossendorf, Germany, to evaluate cell uptake, tumour uptake and biodistribution behaviour of RGD peptides labelled with the  $^{99m}\text{Tc}$ -(4 + 1) core.
- (h) A PhD student exchange was established between the University of Missouri-Columbia and the Institute of Radiopharmacy, Forschungszentrum Dresden–Rossendorf, Germany, to evaluate cell uptake, tumour uptake and biodistribution behaviour of bombesin derivatives labelled with the  $^{99m}\text{Tc}$ -(4 + 1) core.
- (i) A research exchange was established between the Institute of Nuclear Technology, Portugal, the Demokritos National Centre of Scientific Research, Greece, and the Universidad de la República, Montevideo, to undertake the synthesis, radiolabelling and biological evaluation of quinazolines derivatives labelled with the  $^{99m}\text{Tc}$ -(4 + 1) core.
- (j) A research exchange was established between the Institute of Isotopes Co. Ltd, Budapest, the Universidad de la República, Montevideo, and the University of Ferrara, Italy, to undertake radiolabelling and biological evaluation of annexin V fragments labelled with the  $^{99m}\text{Tc}$ -nitrido core.

### 1.6. CONCLUSION

Technetium-99m based radiopharmaceuticals still remain among the most convenient diagnostic agents for developing countries. This fact strongly supports the need to continue the search for novel and the most effective  $^{99m}\text{Tc}$  radiopharmaceuticals able to offer a true alternative to PET tracers.

The CRP was very successful in expanding the investigation on novel  $^{99m}\text{Tc}$  cores and in supporting the transfer of these advanced labelling technologies to all participant laboratories. As a consequence, these novel techniques are currently available for all research groups and could be efficiently employed for developing new and more effective  $^{99m}\text{Tc}$  radiopharmaceuticals. In particular, through these powerful chemical tools, it would be possible to explore new strategies for approaching the design of unprecedented categories of  $^{99m}\text{Tc}$  imaging agents that may overcome problems related to conventional  $^{99m}\text{Tc}$  labelling methods mostly based on the application of the so called bifunctional approach. The use of these categories of  $^{99m}\text{Tc}$  complexes would appear of utmost importance for the production of a new generation of highly specific diagnostic tracers targeting selected biological substrates and for improving the

## CHAPTER 1

biological properties of  $^{99m}\text{Tc}$  imaging agents currently employed in clinical nuclear medicine, particularly in the field of nuclear oncology.

The above considerations strongly support the view that the results of the present CRP may provide the basis for a further development of the field related to the novel  $^{99m}\text{Tc}$  cores that might be mostly focused on the preparation of a new generation of  $^{99m}\text{Tc}$  radiopharmaceuticals potentially exhibiting a more complex and useful biodistribution behaviour. In principle, these new biological properties may allow the new agents to monitor in vivo some fundamental biomolecular pathways relevant to the detection of the early stages of a disease. These novel characteristics may originate from a different approach to the design of the molecular structure of the new tracers mostly founded on the chemistry of the  $^{99m}\text{Tc}$  cores investigated in this CRP.

Part II

REPORTS BY THE PARTICIPANTS  
IN THE COORDINATED RESEARCH PROJECT



## Chapter 2

### **TECHNETIUM-99m LABELLING OF RGD PEPTIDES TARGETING INTEGRIN RECEPTORS: COMPARISON OF DIFFERENT CONJUGATES OF cRGDyK UTILIZING DIFFERENT TECHNETIUM-99m CORES**

C. DECRISTOFORO, R. HAUBNER, M. RUPPRICH,  
E. VON GUGGENBERG  
Universitätsklinik für Nuklearmedizin, Innsbruck, Austria

#### **Abstract**

One working group within the coordinated research project on Development of  $^{99m}\text{Tc}$  Based Small Biomolecules Using Novel  $^{99m}\text{Tc}$  Cores dealt with labelling of RGD peptides with  $^{99m}\text{Tc}$ . These peptides target the  $\alpha_v\beta_3$  integrin receptor expressed on tumour cells and neoangiogenesis during metastasis. Seven different peptide conjugates based on the cRGDyK sequence were prepared and characterized (HYNIC-, DTPA-, Cys-, tert-Cys, His, L2 and PZ1-cRGDyK) and distributed. Radiolabelling experiments using different coligands for HYNIC, the  $^{99m}\text{Tc}(\text{CO})_3$  metal fragment, the Tc-nitrido core and the 4 + 1 concept were performed and showed labelling yields >90% at high specific activities. A high in vitro stability was observed for the resultant products; however, the plasma protein binding and lipophilicity varied considerably between different radiolabelled RGD conjugates. Experiments on the biological activity of the radiolabelled peptides using  $\alpha_v\beta_3$  positive (M21) and negative (M21L) tumour cells did show specific uptake of various conjugates. Studies in tumour bearing animals revealed significant differences between different conjugates in pharmacokinetic behaviour as well as tumour uptake (0.2–2.7% injected dose (ID)/g). The highest specific tumour uptake and tumour/background values were found for  $^{99m}\text{Tc}$ -EDDA/HYNIC-cRGDyK,  $^{99m}\text{Tc}$ -nitrido-PNP-Cys-cRGDyK and  $^{99m}\text{Tc}(\text{CO})_3$ -PZ1-cRGDyK. In conclusion, using novel technetium cores such as the  $^{99m}\text{Tc}(\text{CO})_3$  metal fragment, Tc-nitrido and the 4 + 1 concept peptides could be labelled with  $^{99m}\text{Tc}$  at high specific activities, resulting in complexes with high stability, but binding moieties have to be optimized, especially concerning hydrophilicity resulting in renal rather than hepatobiliary excretion. This comparative study underlines that for labelling of peptides with  $^{99m}\text{Tc}$ , labelling strategies have to be properly selected and optimized. Different in vitro assays are necessary to predict targeting properties in vivo.

## 2.1. INTRODUCTION

Tumours depend on sufficient blood supply for their growth. They are able to promote new blood vessel formation (neoangiogenesis) via angiogenic factors. Among these factors, integrin receptors have attracted interest for in vivo tumour targeting [2.1]. The integrin receptor subtype  $\alpha_v\beta_3$ , which is a receptor for vitronectin, fibronectin and the latency associated peptide (LAP) of tumour growth factor beta (TGF $\beta$ ), occurs at very low or undetectable levels in only a subset of epithelial cells in normal adults, but it is consistently over-expressed in carcinomas, especially at the invasive edge and in a stage where metastatic processes are initiated. Inhibition of this receptor results in tumour involution or necrosis. Peptides targeting the  $\alpha_v\beta_3$  receptor contain the RGD sequence (Arg-Gly-Asp) [2.2] and are reported to antagonize neoangiogenesis, for example by binding to  $\alpha_v\beta_3$  receptors on blood vessels [2.3]. They may be linear [2.4] or cyclic peptides, and dimeric and polymeric forms have been shown to have high affinity for the receptor [2.5]. Radiolabelled RGD peptides have been suggested to visualize neoangiogenesis in tumours in vivo [2.6], and a number of different labelling approaches have been described employing radionuclides such as  $^{111}\text{In}$ ,  $^{99\text{m}}\text{Tc}$ ,  $^{123}\text{I}$  and  $^{18}\text{F}$  [2.7–2.10]. As a model peptide for labelling with the new technetium cores, a cyclic analogue ([c(Arg-Gly-Asp-D-Tyr-Lys)]) or cRGDyK, see Fig. 2.1) was chosen for several reasons:

- (a) This peptide has been derivatized with DTPA for labelling with  $^{111}\text{In}$ , showing promising in vitro and in vivo properties [2.11].

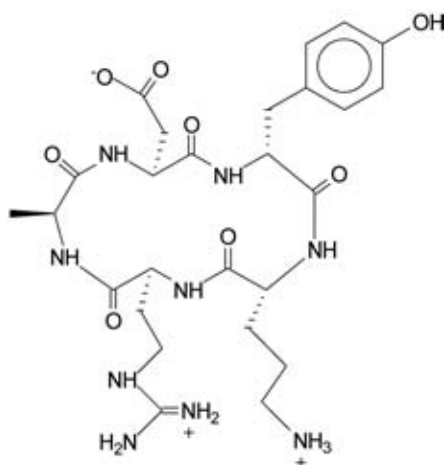


FIG. 2.1. Structure of cRGDyK.

## CHAPTER 2

- (b) It can be easily derivatized with anchors for  $^{99m}\text{Tc}$  labelling appended on the free amino group of the Lys residue.
- (c) It does not contain amino acid residues that may cause problems in the derivatization or radiolabelling processes (e.g. Cys or additional Lys).
- (d) It contains a Tyr residue that can be used for radioiodination [2.12] for binding assays.
- (e) It is a very small peptide, and therefore any changes introduced during derivatization or radiolabelling should have considerable impact on the overall chemical and biological properties [2.13], making comparison between different labelling approaches easier.

### 2.2. PEPTIDE SYNTHESIS AND DISTRIBUTION

A variety of derivatizations of the peptide were selected for labelling approaches based on the novel technetium cores. Peptide synthesis was carried out at Biosynthan, Berlin, by applying standard f-moc chemical approaches. Analytical characterization included high performance liquid chromatography (HPLC) and mass spectrometry (MS). Table 2.1 shows the derivatives of cRGDyK that were prepared (see also Figs 2.2 and 2.3).

The first synthesis was finished in February 2004, distribution was performed in March 2004 and a second synthesis was carried out in April 2005. Each group participating in this project received a certain amount of several conjugates as well as underivatized peptide for analytical tests and blocking experiments in biological assays. The amounts were chosen in such a way as to allow evaluation of selected derivatives labelled with  $^{99m}\text{Tc}$  via carbonyl,

TABLE 2.1. LIST OF RGD DERIVATIZED PEPTIDES SYNTHESIZED AS PART OF THE COORDINATED RESEARCH PROJECT

Peptide structure	Code	Total in the first synthesis (mg)
C(Arg-Gly-Asp-D-Tyr-Lys)	1	28.0
C(Arg-Gly-Asp-D-Tyr-Lys)-DTPA	2	4.9
C(Arg-Gly-Asp-D-Tyr-Lys)-Cys	3	13.8
C(Arg-Gly-Asp-D-Tyr-Lys)-HYNIC	4	14.0
C(Arg-Gly-Asp-D-Tyr-Lys)-PZ1	5	14.4
C(Arg-Gly-Asp-D-Tyr-Lys)-tert-Cys	7	9.1
C(Arg-Gly-Asp-D-Tyr-Lys)-HIS	8	6.6

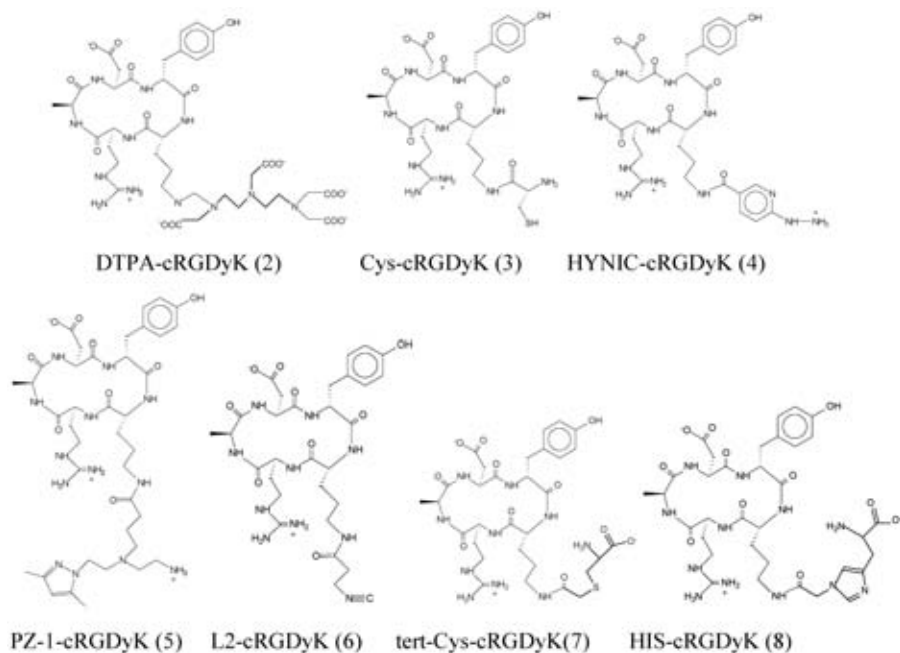


FIG. 2.2. Structures of peptide conjugates (cyclic RGDyK-derivatives).

HYNIC or nitrido technology. The Rossendorf group accomplished derivatization in their own laboratory for labelling with the Tc-(4 + 1) approach. The exact amounts and groups for distribution are summarized in Table 2.2.

## 2.3. EXPERIMENTAL METHODS

### 2.3.1. Analytical methods

#### 2.3.1.1. HPLC

A Dionex P680 low pressure gradient pump with a Spectra Physics, Spectra Chrom 100, variable ultraviolet (UV) detector and Bioscan radiometric detection were used for reverse phase HPLC analysis. A Macherey & Nagl Nucleosil 120-5, C18, 250 × 4.6 mm column with flow rates of 1 mL/min and UV detection at 220 nm were employed with the following gradients:

- (a) Method 1: CH<sub>3</sub>CN/0.1% TFA(H<sub>2</sub>O), 0–1.5 min 0% CH<sub>3</sub>CN, 1.5–18 min 0–30% CH<sub>3</sub>CN, 18–21 min 30–60% CH<sub>3</sub>CN, 21–24 min 60% CH<sub>3</sub>CN.

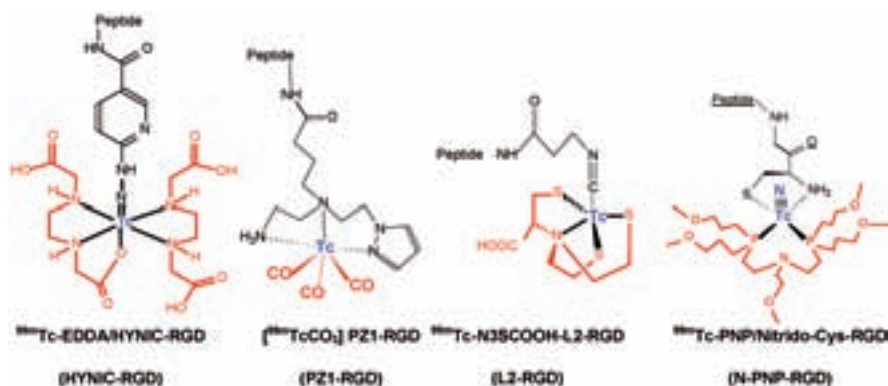


FIG. 2.3. Selected structures of  $^{99m}\text{Tc}$  labelled RGD peptide conjugates included in this study.

- (b) Method 2:  $\text{CH}_3\text{CN}/0.1\% \text{TFA}(\text{H}_2\text{O})$ , 0–1.5 min 0%  $\text{CH}_3\text{CN}$ , 1.5–16.5 min 0–18%  $\text{CH}_3\text{CN}$ , 16.5–21.5 min 18–60%  $\text{CH}_3\text{CN}$ , 21.5–23 min 60%  $\text{CH}_3\text{CN}$ .

### 2.3.1.2. Purification by solid phase extraction

For purification of the radiolabelled peptide for stability studies, a solid phase extraction (SPE) method was used. The radiolabelling mixture was passed through a C18 Sep-Pak Mini cartridge (Water). The cartridge was washed with 5 mL physiological solution and the radiolabelled peptide was eluted with 70% ethanol. This method efficiently removed all hydrophilic, non-peptide bound impurities (mainly  $^{99m}\text{TcO}_4^-$ ,  $^{99m}\text{Tc}$  coligands).

## 2.3.2. Technetium-99m labelling

### 2.3.2.1. HYNIC-cRGDyK

*Tricine as a coligand.* In a rubber sealed vial, 5  $\mu\text{g}$  of HYNIC-RGDyK was incubated with 0.5 mL of tricine solution (70 mg/mL in water), 0.5 mL of  $^{99m}\text{TcO}_4^-$  solution (>200 MBq) and 20  $\mu\text{L}$  of Sn(II) solution (10 mg of  $\text{SnCl}_2 \cdot 2\text{H}_2\text{O}$  in 10 mL of nitrogen purged 0.1N HCl) for 20 min at room temperature or 75°C.

*Tricine/EDDA exchange labelling.* In a rubber sealed vial, 10  $\mu\text{g}$  of HYNIC-cRGDyK was incubated with 1 mL of EDDA/tricine solution (20 mg/mL tricine, 10 mg/mL EDDA in pH6–7), 1 mL of  $^{99m}\text{TcO}_4^-$  solution (800 MBq) and 20  $\mu\text{L}$  of tin(II) solution (10 mg of  $\text{SnCl}_2 \cdot 2\text{H}_2\text{O}$  in 10 mL of nitrogen purged 0.1N HCl) for 10 min in a boiling water bath.

TABLE 2.2. AMOUNTS OF PEPTIDES DISTRIBUTED AMONG THE VARIOUS LABORATORIES

Reference laboratories	Code	Amount (mg)
	1	7
C. Decristoforo	2	1
Universitätsklinik für Nuklearmedizin,	3	2
Innsbruck, Austria	4	3
(Total 18 mg)	5	2
	7	2
	8	1.3
	1	2
J. Smith	2	1
University of Missouri-Columbia, Department of Radiology,	3	1
Columbia, MO, USA	4	1
(Total 8.3 mg)	5	2
	8	1.3
Participating laboratories		
A. Duatti		
Laboratory of Nuclear Medicine, University of Ferrara, Ferrara,	1	3
Italy	3	4
(Total 7 mg)		
H.-J. Pietzsch		
Forschungszentrum Dresden-Rossendorf, Germany	1	4
(Total 4 mg)		
I. Santos		
Department of Chemistry, Institute of Nuclear Technology, Portugal	1	2
(Total 9 mg)	5	7
	1	3
B. Linkowski Faintuch	2	1
Radiopharmacy Centre, Nuclear and Energy Research Institute,	3	2
São Paulo, Brazil	4	1
(Total 11.2 mg)	5	1.2
	7	2
	8	1

## CHAPTER 2

TABLE 2.2. AMOUNTS OF PEPTIDES DISTRIBUTED AMONG THE VARIOUS LABORATORIES (cont.)

Reference laboratories	Code	Amount (mg)
	1	2
	2	1
K. Kothari	3	1.7
Bhabha Atomic Research Centre, Mumbai, India	4	3.4
(Total 12.3 mg)	5	1.2
	7	2
	8	1
	1	3
	2	1
Ji Hu	3	2.5
China Institute of Atomic Energy, Beijing, China	4	2
(Total 11.5 mg)	7	2
	8	1
	1	3
	2	2.5
A. Rey	3	2.5
Faculty of Chemistry, Universidad de la República,	4	2
Montevideo, Uruguay	5	1
(Total 13.1 mg)	7	1.1
	8	1

### 2.3.2.2. Labelling with $[^{99m}\text{Tc}(\text{OH}_2)_3(\text{CO})_3]^+$

Carbonyl aquaion  $[^{99m}\text{Tc}(\text{OH}_2)_3(\text{CO})_3]^+$  was prepared as described above from a commercial kit (Isolink) in accordance with the manufacturer's instructions (1 mL volume, 200–1000 MBq  $^{99m}\text{Tc}$ ). Five or 20  $\mu\text{g}$  of peptide (Cys-cRGDyK, DTPA-cRGDyK, PZ1-cRGDyK, HYNIC-cRGDyK) was incubated with 100  $\mu\text{L}$  of carbonyl precursor to a specific activity between 0.5 and 2 Ci/ $\mu\text{mol}$ .

### 2.3.2.3. 4 + 1 approach

1 mg  $\text{Na}_2\text{EDTA}$ , 5 mg mannitol, 100  $\mu\text{g}$   $\text{SnCl}_2$ , were incubated with 500 MBq  $^{99m}\text{TcO}_4^-$  solution in a total volume of 0.8 mL at room temperature for 15 min. Then 0.3 mg coligand ( $\text{NS}_3$ -oxalate or  $\text{NS}_3$ -COOH) freshly dissolved in 300  $\mu\text{L}$  methanol was added, and this solution was transferred to a vial

containing the isocyanide derivatized peptide (L1, L2) and incubated at 75°C for 1 h.

#### 2.3.2.4. Labelling of Cys-RGD with the $^{99m}\text{Tc}$ -nitrido fragment

5 mg succinic hydrazide, 0.05 mg  $\text{SnCl}_2$ , were incubated with 1500–2000 MBq  $^{99m}\text{TcO}_4^-$  solution in a total volume of 1.1 mL. After 15 min at room temperature, 0.125 mg PNP3 ligand  $[\text{N}(\text{CH}_2\text{CH}_2\text{OCH}_3)(\text{CH}_2\text{CH}_2\text{P}(\text{CH}_2\text{CH}_2\text{CH}_2\text{OCH}_3)_2)_2]$  and 0.05mg Cys-cRGDyK in 0.5 mL were added and incubated at 100°C for 1 h. Radiolabelled peptides were characterized and the labelling yields were determined by HPLC, method 1.

### 2.3.3. In vitro evaluation of radiolabelled peptides

#### 2.3.3.1. Stability

The stability of the radiolabelled peptides in aqueous solution was tested by incubation of the reaction mixture purified by SPE at a concentration of 200–1000 pmol peptide/mL in phosphate buffer as well as in a solution containing 10 000-fold molar excess of cysteine or histidine over the peptide at pH7.4 at 37°C up to 24 h. Stability in fresh human plasma as well as in kidney and liver homogenates was measured in parallel. After incubation, plasma samples were precipitated with acetonitrile and centrifuged (1750g, 5 min). Degradation of the  $^{99m}\text{Tc}$  complexes was assessed by HPLC through method 1.

For incubation in kidney and liver homogenates, kidneys or liver freshly excised from rats were rapidly rinsed and homogenized in 20mM HEPES buffer, pH7.3, with an Ultra-Turrax T25 homogenator for 1 min at room temperature. The radiopeptides were incubated with fresh 30% homogenates at a concentration of 250–500 pmol peptide/mL at 37°C up to 2 h. Samples were precipitated with acetonitrile, centrifuged (1750g, 5 min) and analysed by HPLC, method 1.

#### 2.3.3.2. Protein binding

For protein binding assessment the SPE purified complexes were incubated at a concentration of 20–100 pmol peptide/mL in fresh human plasma at 37°C and analysed up to 6 h by size exclusion chromatography (MicroSpin G-50 Columns, Sephadex G-50). Protein binding of the  $^{99m}\text{Tc}$  complex was determined by measuring activity in the column and eluate with a gamma counter.

### 2.3.3.3. *Log P values*

0.5 mL of  $^{99m}\text{Tc}$  labelled RGD conjugate in PBS was added to 0.5 mL octanol in an Eppendorf tube. The tube was vigorously vortexed over a period of 15 min and an aliquot of aqueous and octanol layers was collected, counted in the gamma counter and log  $P$  values were calculated.

### 2.3.4. **Internalization and binding studies in $\alpha_v\beta_3$ positive and $\alpha_v\beta_3$ negative cells**

$\alpha_v\beta_3$  positive M21 and negative M21L cells were grown in culture until a sufficient number of cells were available. For internalization experiments, cells were counted up to a concentration of  $2 \times 10^6$  cells/mL in RPMI1640 containing 1% glutamine and 1% PBS. Each 1 mL volume was pipetted into an Eppendorf tube. After addition of the selected  $^{99m}\text{Tc}$  labelled peptide ( $>100\,000$  cpm,  $<1\text{nM}$ ), cells were incubated at  $37^\circ\text{C}$  for 90 min in triplicate with either PBS/0.5% BSA buffer alone (150  $\mu\text{L}$ , total series) or with 10  $\mu\text{M}$  cRGDyK in PBS/0.5% BSA buffer (150  $\mu\text{L}$ , non-specific series). Incubation was interrupted by centrifugation, followed by removal of the medium and rapid rinsing twice with ice cold TRIS buffered saline. Thereafter, the cells were incubated twice in an acid wash buffer (50mM acetate buffer, pH4.2) for 15 min at  $37^\circ\text{C}$ , a period sufficient to remove membrane bound radioligand. The supernatant was collected (membrane bound radioligand fraction) and the cells were washed with acid wash buffer. Cells were lysed by treatment with 1N NaOH and the cell radioactivity was finally collected (internalized radioligand fraction). The internalized and non-internalized fractions were determined by measuring radioactivity in the internalized fraction, and expressed as % (bound activity/total activity).

### 2.3.5. **In vivo evaluation of radiolabelled peptides**

All animal experiments were conducted in compliance with the Austrian animal protection laws and with the approval of the Austrian Ministry of Science. Tumour uptake studies were performed in nu/nu mice (Charles River). For the induction of tumour xenografts, M21 and M21L cells were subcutaneously injected at a concentration of  $5 \times 10^6$  cells/mouse and allowed to grow until tumours of 0.3–0.6 mm were visible. On the day of experiment, each of six mice with M21 and three with M21L tumour were injected intravenously into the tail vein with the selected  $^{99m}\text{Tc}$  labelled peptide (1 MBq/mouse, corresponding to 1  $\mu\text{g}$  peptide). Animals were sacrificed by cervical dislocation at 1 h (M21 and M21L) and 4 h post-injection (M21).

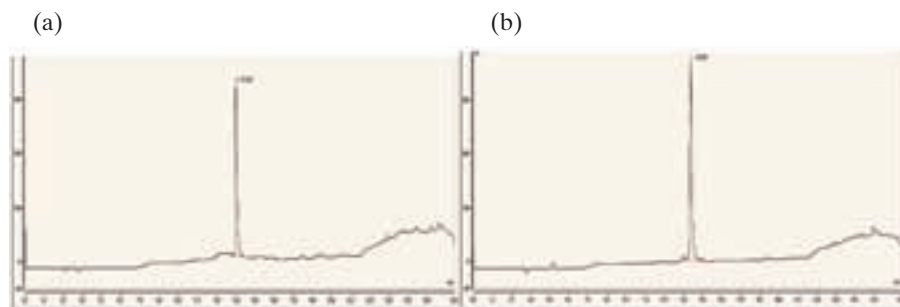


FIG. 2.4. HPLC chromatograms of unmodified cRGDyK (a) and DTPA-cRGDyK (b) (10  $\mu$ g each) using HPLC and method 1.

Tumours and other tissues (blood, lung, heart, stomach, spleen, liver, pancreas, kidneys, muscle and intestine) were removed. The amount of radioactivity was determined with a gamma counter. The results were expressed as percentage of injected dose per gram of tissue (% ID/g), and tumour to organ, stomach to organ, pancreas to organ and kidney to organ ratios were calculated.

## 2.4. RESULTS

### 2.4.1. Characterization of cold peptides

HPLC analysis showed that the unlabelled peptides were produced in high purity and with a good stability for radiolabelling experiments. HPLC retention times varied considerably, especially when applying HPLC method 2. Lipophilicity was in the order unmodified cRGDyK < DTPA-cRGDyK < Cys-cRGDyK < HYNIC-cRGDyK < PZ1-cRGDyK. Two representative chromatograms are shown in Fig. 2.4 and the corresponding retention times are given in Table 2.3.

### 2.4.2. Labelling experiments

The results from labelling experiments are summarized in Table 2.4. All peptide ligands could be labelled at reasonably high specific activities with  $^{99m}\text{Tc}$ . Radiolabelling yields exceeding 90% could be achieved with HYNIC, carbonyl and nitrido approaches. Significant differences were observed in the lipophilicity of the resulting radiolabelled species. Using HPLC method 1, retention times between 14.5 and 22.1 min for the main peak were determined.

## CHAPTER 2

TABLE 2.3. HPLC RETENTION TIMES (MIN) OF UNLABELLED RGD PEPTIDES

Compound	Method 1	Method 2
cRGDyK	13.7	16.6
DTPA-cRGDyK	14.2	17.6
HYNIC-cRGDyK	15.2	19.1
PZ1-cRGDyK	15.7	20.0
Cys-cRGDyK	14.4	18.2

TABLE 2.4. RESULTS FROM LABELLING EXPERIMENTS WITH cRGDyK DERIVATIVES

Compound	Labelling approach	Retention time (min) main peak	Labelling yield (mean, $N = 3$ )	Number of peptide related peaks
DTPA-cRGDyK	Tc(CO) <sub>3</sub>	15.80	98.5	>3
HYNIC-cRGDyK	EDDA	15.1	91.6	2
HYNIC-cRGDyK	Tricine	14.5	98.4	2
HYNIC-cRGDyK	Tc(CO) <sub>3</sub>	19.2	99.5	>5
PZ1-cRGDyK	Tc(CO) <sub>3</sub>	23.0	98.4	1
Cys-cRGDyK	Tc(CO) <sub>3</sub>	21.6	99.5	3
HIS-cRGDyK	Tc(CO) <sub>3</sub>	22.4	91.5	3
TertCys-cRGDyK	Tc(CO) <sub>3</sub>	22.8	95.0	>5
L1-NS <sub>3</sub> -cRGDyK	4 + 1; NS <sub>3</sub>	24.1	84.8	>3
L2-NS <sub>3</sub> -cRGDyK	4 + 1; NS <sub>3</sub>	23.5	96.8	3
L1-NS <sub>3</sub> -COOH-cRGDyK	4 + 1; NS <sub>3</sub> -COOH	23.6	93.3	>3
L2-NS <sub>3</sub> -COOH-cRGDyK	4 + 1; NS <sub>3</sub> -COOH	23.1	88.3	>3
Cys-cRGDyK	Tc-nitrido-PNP	23.8	99.9	1 (2, optimized gradient)

Figure 2.5 shows representative examples of HPLC profiles of the various radiolabelling solutions. Whereas for HYNIC-cRGDyK, using both tricine and EDDA as coligands, and for PZ1-cRGDyK one major peak is related to a single radiolabelled peptide, other cRGDyK derivatives showed a variety of radiolabelled peptide species. Interestingly, HYNIC-RGDyK labelled using

the carbonyl approach resulted in multiple labelled species all possessing a considerable higher lipophilicity as compared with HYNIC-cRGDyK labelled using specific coligands (EDDA and tricine). Hydrophilic properties were observed for  $^{99m}\text{Tc}$ -EDDA- and  $^{99m}\text{Tc}$ -tricine-HYNIC-cRGDyK complexes, while a higher lipophilicity was found for  $^{99m}\text{Tc}(\text{CO}_3)$ -PZ1-cRGDyK and  $^{99m}\text{Tc}$ -L2-cRGDyK complexes. Cys-cRGDyK labelled via the  $\text{Tc}(\text{CO})_3$  approach showed formation of multiple species. Conversely, labelling of Cys-cRGDyK using the Tc-nitrido core and PNP as a coligand afforded a well defined isomeric pair of peptidic complexes with high retention times (23.8 min).

#### 2.4.3. Stability experiments, log *P* and protein binding

All radiolabelled cRGDyK conjugates showed good stability in solution, in human plasma and in kidney and liver homogenates, indicating good stability of the radiolabel as well as of the peptide sequence. Considerable differences were found in the protein binding behaviour. Measured values varied from the lowest protein binding value for  $^{99m}\text{Tc}$ -EDDA-HYNIC-cRGDyK followed by  $^{99m}\text{Tc}(\text{CO})_3$ -DTPA-cRGDyK,  $^{99m}\text{Tc}(\text{CO})_3$ -PZ1-cRGDyK and  $^{99m}\text{Tc}$ -tricine-HYNIC-DTPA-cRGDyK. The data are summarized in Fig. 2.5.  $^{99m}\text{Tc}(\text{CO})_3$ -HYNIC-cRGDyK showed an increase over time in its protein binding values, whereas for other conjugates these values did not vary considerably between 30 min and 2 h.

Log *P* values are shown in Fig 2.6. Again, considerable differences in lipophilicity, partly correlating with HPLC retention times, were observed. The highest lipophilicity, with a log *P* value of 0.92, was found for  $^{99m}\text{Tc}$ -PZ1-cRGDyK, whereas  $^{99m}\text{Tc}$ -EDDA/HYNIC-cRGDyK and  $^{99m}\text{Tc}$ -NS3-L2-cRGDyK showed the highest hydrophilic character, with log *P* of -3.57 and -3.37, respectively. A clear correlation in log *P* values was observed with the 4 + 1 approach by increasing substitution of hydrophilic coligands, log *P* values being lower for the compound containing L2 and the highly hydrophilic  $\text{NS}_3$ -COOH coligand. Consequently,  $^{99m}\text{Tc}$ -NS<sub>3</sub>-COOH-L2-cRGDyK was selected for further evaluation in vivo.

#### 2.4.4. Internalization studies

To evaluate the biological potential of the radiolabelled cRGDyK conjugates, the internalization behaviour was studied in M21 cells with parallel blocking experiments. The results are summarized in Fig. 2.7. The highest uptake values were found for  $^{99m}\text{Tc}$ -nitrido-PNP/Cys-cRGDyK, with more

CHAPTER 2

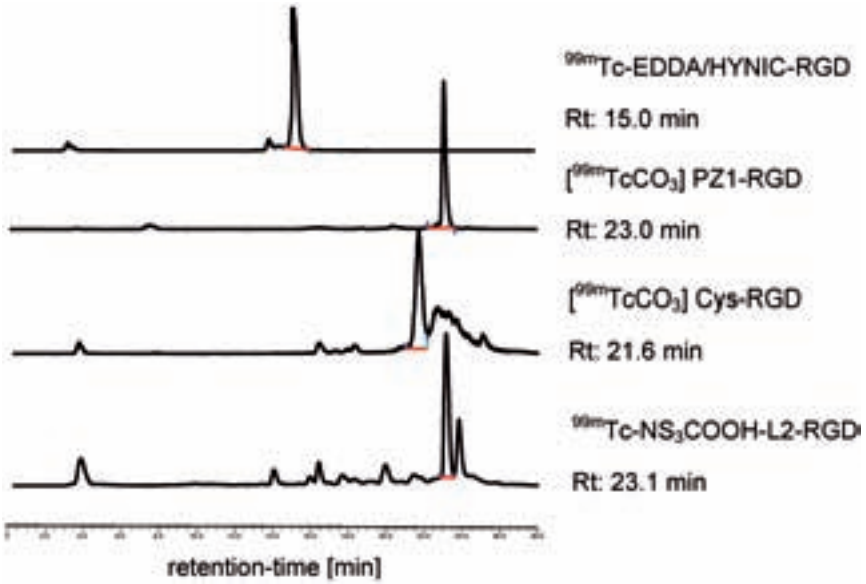


FIG. 2.5. Representative examples of radio-HPLC traces from labelling experiments of some  $^{99m}\text{Tc}$  labelled cRGDyK conjugates reported in this study.

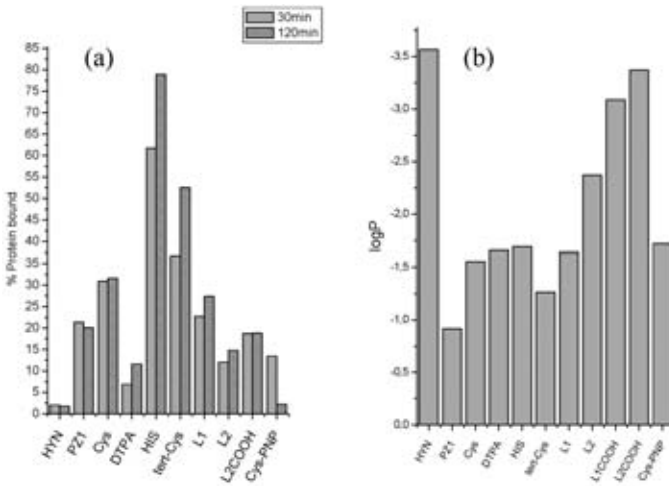


FIG. 2.6. Protein binding (a) and log P values (b) for radiolabelled cRGDyK conjugates reported in this study.

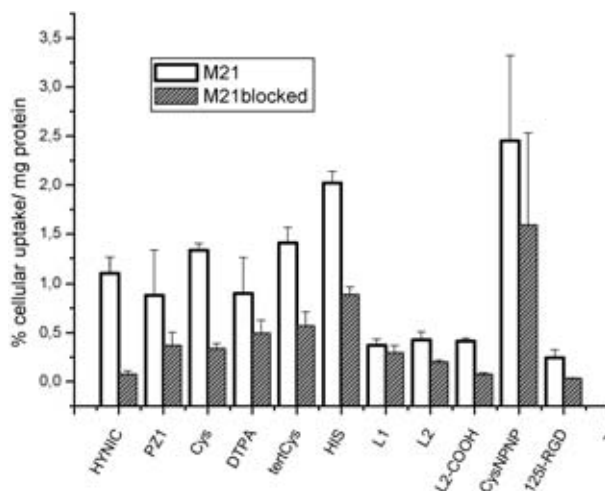


FIG. 2.7. Cell uptake in  $\alpha_v\beta_3$  receptor positive M21 human melanoma cells.

than 2% uptake/mg protein. The lowest values were observed for L1 and L2 labelled via the Tc-(4 + 1) approach. All uptake values were higher compared with  $^{125}\text{I}$ -RGD and were reduced by co-incubation with  $10\mu\text{M}$  excess cRGDyK, although reduction was less significant for  $^{99\text{m}}\text{Tc}$ -L1-cRGDyK and  $^{99\text{m}}\text{Tc}$ -Nitrido-PNP/Cys-cRGDyK.

#### 2.4.5. In vivo tumour model

The results of biodistributions of all tested  $^{99\text{m}}\text{Tc}$  labelled RGD derivatives in a M21 melanoma cell nude mouse tumour model at 1 h post-injection are summarized in Fig. 2.8. Remarkable variations in distribution, excretion pattern and tumour uptake were observed. A low retention in most organs with predominant and rapid renal excretion was observed for  $^{99\text{m}}\text{Tc}$ -EDDA/HYNIC-RGD. Higher uptakes in liver and intestine were found for  $^{99\text{m}}\text{Tc}(\text{CO})_3$ -PZ1-cRGDyK, with 8.9% and 10.8% ID/g, respectively.  $^{99\text{m}}\text{Tc}$ -NS3-L2-cRGDyK revealed predominant hepatobiliary excretion, with intestinal uptake of 32% ID/g at 1 h. Injection of  $^{99\text{m}}\text{Tc}(\text{CO})_3$ -Cys-cRGDyK resulted in the highest radioactivity retention in most tissues, especially liver, blood and kidneys. Tumour uptake was comparable for most organs in  $\alpha_v\beta_3$  positive tumours, with values in the range 2.22–2.72% ID/g, except for  $^{99\text{m}}\text{Tc}$ -NS<sub>3</sub>-L2-cRGDyK, with only 0.2% ID/g accumulation (0.22% ID/g in receptor negative tumour). For all other compounds, uptake in receptor negative tumours was significantly lower and was about 0.71–1.37% ID/g. At

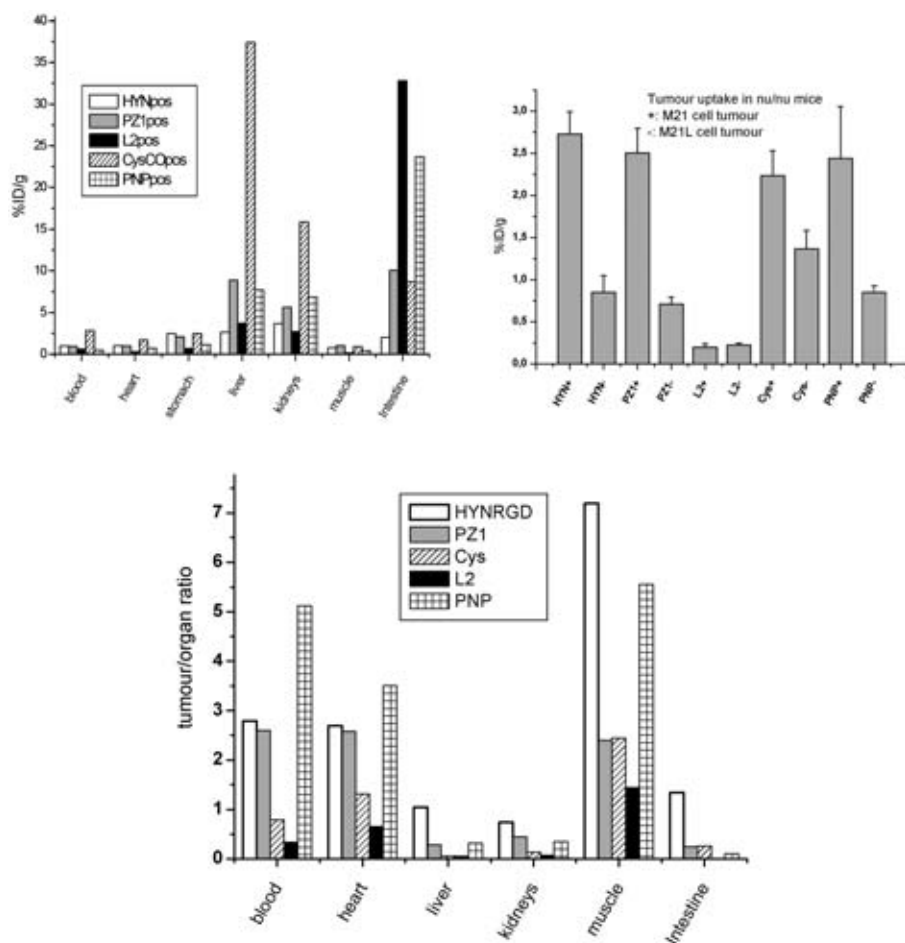


FIG. 2.8. Comparison of in vivo behaviour of  $^{99m}\text{Tc}$ -RGD derivatives in an  $\alpha_v\beta_3$  receptor positive (M21) and negative (M21L) human melanoma nude mouse tumour model. Uptakes in normal organs (top left), in  $\alpha_v\beta_3$  positive and negative tumours (top right) and tumour/organ ratios (bottom) are shown.

4 h post-injection, tumour values decrease by less than 30%, whereas elimination from normal tissues was considerably faster. The highest tumour/organ ratios were found for  $^{99m}\text{Tc}$ -EDDA/HYNIC-RGD,  $^{99m}\text{Tc}(\text{CO})_3$ -PZ1-RGDy and  $^{99m}\text{Tc}$ -Nitrido-PNP/Cys-cRGDyK, with some advantage for  $^{99m}\text{Tc}$ -EDDA/HYNIC-RGD in muscle, liver and intestines. For this compound, values comparable to  $^{18}\text{F}$ -galacto-RGD, the current gold standard, were found.

## 2.5. DISCUSSION AND OUTLOOK

A number of different conjugates of cRGDyK binding to the  $\alpha_v\beta_3$  integrin receptor were prepared and distributed to all interested coordinated research project members. All conjugates were characterized and radiolabelled at our reference laboratory. Radiolabelling using novel technetium cores, including HYNIC, Tc(CO)<sub>3</sub>, Tc-(4 + 1) and Tc-nitrido, could be performed at high specific activities with good in vitro stability. HPLC analysis and protein binding assays revealed significant differences between the various peptide conjugates. All <sup>99m</sup>Tc-RGDs showed specific uptake in receptor positive cells in vitro. However, in a specific tumour model, different pharmacokinetic behaviours and tumour uptakes were observed, with the highest values for [<sup>99m</sup>TcCO<sub>3</sub>]-PZ1-RGD, <sup>99m</sup>Tc-nitrido-PNP/Cys-cRGDyK and <sup>99m</sup>Tc-EDDA/HYNIC-RGD. In conclusion, our studies show that strategies for labelling peptides with <sup>99m</sup>Tc have to be properly selected and optimized. Different in vitro assays are necessary to predict targeting properties in vivo. For radiolabelled peptides to be used as radiopharmaceuticals, properties such as high stability and hydrophilicity conjoined with low plasma protein binding and retention of biological activity usually result in the most promising candidates for sensitive in vivo detection of receptors in oncology, and potentially in other diseases. For central nervous diseases requiring brain uptake, different characteristics might be sought to develop successful imaging agents.

## REFERENCES

- [2.1] HAUBNER, R., et al., Radiolabeled  $\alpha_v\beta_3$  integrin antagonists: A new class of tracers for tumor targeting, *J. Nucl. Med.* **40** (1999) 1061–1071.
- [2.2] BURGESS, K., LIM, D., MOUSA, S.A., Synthesis and solution conformation of cyclo[RGDRGD]: A cyclic peptide with selectivity for the alpha V beta 3 receptor, *J. Med. Chem.* **39** (1996) 4520–4526.
- [2.3] HAUBNER, R., WESTER, H.J., Radiolabeled tracers for imaging of tumor angiogenesis and evaluation of anti-angiogenic therapies, *Curr. Pharm. Design* **10** (2004) 1439–1455.
- [2.4] SUTCLIFFE-GOULDEN, J.L., et al., Rapid solid phase synthesis and biodistribution of 18F-labelled linear peptides, *Eur. J. Nucl. Med. Mol. Imaging* **29** (2002) 754–759.
- [2.5] JANSSEN, M., et al., Comparison of a monomeric and dimeric radiolabeled RGD-peptide for tumor targeting, *Cancer Biother. Radiopharm.* **17** (2002) 641–646.

## CHAPTER 2

- [2.6] HAUBNER, R., et al., Noninvasive imaging of alpha(v)beta3 integrin expression using <sup>18</sup>F-labeled RGD-containing glycopeptide and positron emission tomography, *Cancer Res.* **61** (2001) 1781–1785.
- [2.7] HAUBNER, R., et al., Glycosylated RGD-containing peptides: Tracer for tumor targeting and angiogenesis imaging with improved biokinetics, *J. Nucl. Med.* **42** (2001) 326–336.
- [2.8] JANSSEN, M.L., et al., Tumor targeting with radiolabeled alpha(v)beta(3) integrin binding peptides in a nude mouse model, *Cancer Res.* **62** (2002) 6146–6151.
- [2.9] SIVOLAPENKO, G.B., et al., Imaging of metastatic melanoma utilizing a technetium-99m labelled RGD-containing synthetic peptide, *Eur. J. Nucl. Med.* **25** (1998) 1383–1389.
- [2.10] SU, Z.F., et al., In vitro and in vivo evaluation of a technetium-99m-labeled cyclic RGD peptide as a specific marker of alpha(V)beta(3) integrin for tumor imaging, *Bioconj. Chem.* **13** (2002) 561–570.
- [2.11] VAN HAGEN, P.M., et al., Evaluation of a radiolabelled cyclic DTPA-RGD analogue for tumour imaging and radionuclide therapy, *Int. J. Cancer* **90** (2000) 186–198.
- [2.12] CHEN, X., et al., MicroPET imaging of brain tumor angiogenesis with <sup>18</sup>F-labeled PEGylated RGD peptide, *Eur. J. Nucl. Med. Mol. Imaging* **31** (2004) 1081–1089.
- [2.13] CHEN, X., PARK, R., SHAHINIAN, A.H., BADING, J.R., CONTI, P.S., Pharmacokinetics and tumor retention of <sup>125</sup>I-labeled RGD peptide are improved by PEGylation, *Nucl. Med. Biol.* **31** (2004) 11–19.



## Chapter 3

### **RADIOLABELLING ANGIOGENIC AND APOPTOTIC AGENT WITH DIFFERENT TECHNETIUM-99m TECHNIQUES**

B. LINKOWSKI FAINTUCH\*, R.L.S. RIBEIRO SANTOS\*,  
R. TEODORO\*, E. MURAMOTO\*, L. MORGANTI\*\*,  
I.V. DA SILVA NUNES\*, M.R.Y. OKAMOTO<sup>+</sup>

\* Radiopharmacy Center, Nuclear and Energy Research Institute,  
São Paulo

\*\* Molecular Biology Center, Nuclear and Energy Research Institute,  
São Paulo

<sup>+</sup> Institute of Radiology, University of São Paulo, São Paulo

Brazil

#### **Abstract**

Five cyclic RGD peptide analogue X-RGDyK (cyclo[Arg-Gly-Asp-D-Tyr-Lys]) derivatives, where X = HYNIC, Cys, His, Ter-Cys and PZ1, were synthesized. Three annexin analogues with 13 amino acids [H<sub>2</sub>N-Ala-Glu-Val-Leu-Arg-Gly-Thr-Val-Thr-Asp-Phe-Pro-Gly-OH] (HYNIC-Anx, Cys-Anx and His-Anx) were also synthesized for labelling with <sup>99m</sup>Tc-HYNIC, <sup>99m</sup>Tc-nitrido and <sup>99m</sup>Tc-tricarbonyl techniques. Optimization of the labellings, radiochemical stability and biological studies in healthy animals and in tumour bearing animals were performed and evaluated. The techniques used for labelling RGD and annexin derivatives with <sup>99m</sup>Tc, namely HYNIC (EDDA/tricine), nitrido and carbonyl, showed that the fastest and easiest to perform is with HYNIC. The highest radiochemical yield was achieved by HYNIC followed by the nitrido method. Lung cancer carcinoma was a good model to evaluate RGD derivatives. For annexin derivatives an animal model must be better developed to evaluate their uptake in the apoptosis process. Good uptake by the tumour was obtained with the <sup>99m</sup>Tc-HYNIC-RGD and with <sup>99m</sup>Tc(CO)<sub>3</sub>-Ter-Cys-RGD.

### 3.1. INTRODUCTION

#### 3.1.1. Angiogenesis markers

In the absence of a mechanism for inducing angiogenesis, solid tumors are incapable of growing beyond submillimeter size. Inhibitors of angiogenesis are among the most promising new chemotherapeutic agents under investigation. Dozens of natural proangiogenic and antiangiogenic factors have been identified [3.1]. Cyclic peptides containing RGD sequences have high affinity and selectivity for  $\alpha_v\beta_3$  integrin.  $\alpha_v\beta_3$  integrin, a member of the family of adhesion molecules, plays an important role in endothelial cell migration and survival during angiogenesis [3.2]. This integrin binds to matrix proteins with an exposed RGD (arginine-glycine-aspartate) sequence [3.3]. Several studies have approached angiogenesis imaging using cyclic RGD peptides labelled with  $^{18}\text{F}$  [3.4, 3.5],  $^{99\text{m}}\text{Tc}$  [3.6],  $^{111}\text{In}$  [3.7] and  $^{64}\text{Cu}$  [3.4]. Should the clinical trials be successful, these agents could be useful for pretreatment confirmation of  $\alpha_v\beta_3$  expression as well as for monitoring the response to therapy with  $\alpha_v\beta_3$  antagonists.

#### 3.1.2. Investigation of apoptosis

Apoptosis, or programmed cell death, is an active, energy dependent mechanism for the elimination of cells that have been injured, infected or immunologically recognized as harmful or superfluous [3.8]. While a great number of stimuli can initiate apoptosis, all ultimately lead to a common pathway, in which activation of a cascade of cysteine-aspartic acid proteases (caspases) leads to irreversible changes that include cytoskeletal disruption, chromatin clumping, internucleosomal DNA cleavage and, ultimately, disintegration of the cell into small membrane bound remnants targeted for rapid removal by macrophages [3.9].

Apoptosis has been demonstrated in a wide variety of physiologic processes, including foetal morphogenesis, post-natal brain remodelling, development of immune tolerance, etc. Apoptosis can be seen in a wide variety of malignant tumours, particularly in hypoxic zones adjoining areas of necrosis, and it is the endpoint of most forms of anticancer therapy [3.10]. As part of the apoptotic mechanism, phosphatidylserine, a phospholipid normally sequestered on the inner leaflet of the cell membrane, is abruptly translocated to the external leaflet. Annexin V, a 35 kDa endogenous human protein, binds to exposed phosphatidylserine with an affinity in the nanomolar range, and can be labelled with radioisotopes such as  $^{99\text{m}}\text{Tc}$  and  $^{18}\text{F}$  [3.4, 3.6]. While the degree of uptake of annexin V correlates well with the extent of cell death, uptake is

not completely specific for apoptosis, as it can also be seen in cellular necrosis and in severe metabolic stress [3.11].

### 3.1.3. Labelling procedures

Three different technetium approaches have been the most used in the past to label biomolecules. One of these is the preparation of  $^{99m}\text{Tc}$  compounds based on the incorporation of the nitrogen donor in the metal coordination sphere for labelling small biomolecules, leading to the synthesis of complexes containing nitrido cores. The molecular structure of the five coordinate nitrido  $^{99m}\text{Tc}$  complexes can fall in an asymmetrical form. Asymmetrical complexes possess a distorted trigonal bipyramidal structure in which two different bidentate ligands are bound to the same  $[\text{}^{99m}\text{Tc}\equiv\text{N}]^{+2}$  core [3.12].

Another approach is based on HYNIC conjugates using coligands for the labelling. Technetium-99m binds to the hydrazino moiety forming a  $^{99m}\text{Tc}-\text{N}=\text{N}$  bond. As HYNIC alone cannot satisfy the coordination requirements of a  $\text{Tc}^{+5}$  ion (HYNIC can only occupy one or two coordination sites around the radio-metal), coligands are necessary to complete the coordination sphere of the metallic centre [3.13].

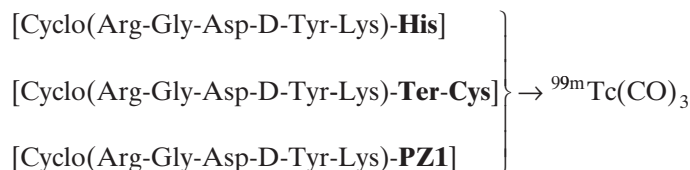
The use of  $[\text{}^{99m}\text{Tc}(\text{CO})_3(\text{H}_2\text{O})_3]^+$  as a radiopharmaceutical precursor opens new routes in the labelling of biomolecules. The  $^{99m}\text{Tc}$ -tricarbonyl core allows the labelling of even the smallest biomolecules with high specific activity and without damaging the biological activity and specificity. This precursor is not only readily water soluble but reveals good stability in aqueous solutions over a broad pH range for several hours. The three labile water molecules coordinated to the highly inert  $[\text{}^{99m}\text{Tc}(\text{CO})_3]^+$  core are readily substituted by a variety of functional groups. Alberto et al. in 1998 [3.14] developed a fully aqueous based kit preparation of the organometallic technetium precursor under mild reaction conditions in the presence of gaseous carbon monoxide and sodium borohydrate, which is investigated here.

In this study five cyclic RGD peptide analogue X-RGDyK (cyclo[Arg-Gly-Asp-D-Tyr-Lys] derivatives, where X = PZ1, HYNIC, Cys, DTPA, His, Ter-Cys, were synthesized. RGD derivatives were distributed from Biosynthan, with funding from the IAEA and under the supervision of C. Decristoforo, Universitätsklinik für Nuklearmedizin, Innsbruck.

Annexin V is a large protein consisting of 320 amino acids. The phosphatidylserine specific sequence might be attributed to an N-terminal chain consisting of 13 amino acids. From this point of view the synthesis of this hypothetically active fragment (Anx13)  $[\text{H}_2\text{N}-\text{Ala}-\text{Glu}-\text{Val}-\text{Leu}-\text{Arg}-\text{Gly}-\text{Thr}-\text{Val}-\text{Thr}-\text{Asp}-\text{Phe}-\text{Pro}-\text{Gly}-\text{OH}]$  and its derivatization with a suitable chelating group for labelling with  $^{99m}\text{Tc}$ -nitrido,  $^{99m}\text{Tc}$ -tricarbonyl and  $^{99m}\text{Tc}$ -HYNIC

technologies was developed. These peptides were provided by Izotop, Hungary.

The peptide derivatives studied with the different  $^{99m}\text{Tc}$  based techniques are given below:



### 3.2. MATERIALS

Nitrido kit was purchased from CIS Biointernational. PNP type diphosphine ligands, which constitute a fundamental ingredient of the  $^{99m}\text{Tc}$ -nitrido asymmetrical approach, were synthesized and provided by A. Duatti, University of Ferrara, Italy. The Carbonyl-Isolink kit was obtained as a gift from Mallinckrodt.

Peptide RGD derivatives: The synthesis of peptides containing an RGD bioactive sequence was carried out by Byosinthan, coordinated by C. Decristforo. Cyclic peptide  $c(\text{Arg-Gly-Asp-D-Tyr-Lys})$  [cyclo RGD(dY)K] having terminal cysteine, HYNIC, Ter-cysteine, histidine and PZ1 for coordination to  $^{99m}\text{Tc}$ -nitrido,  $^{99m}\text{Tc}$ -HYNIC and  $^{99m}\text{Tc}$ -carbonyl cores were provided.

Peptide annexin 13 derivatives: Synthesis of the Anx13 fragment was performed in the Biological Research Centre of the Hungarian Academy of Sciences by using the solid phase peptide synthesis method on Merrifield resin, with BOC chemistry and HF cleavage.

Lung carcinoma cells were A549 (ATCC Number CCL-185). Animals for imaging and biodistribution studies: Swiss mice and nude mice are provided by the animal facility of the Nuclear and Energy Research Institute, Brazil.

Carbon monoxide gas was from White Martins Gases Industriais. Tricine, EDDA, stannous chloride, sodium borohydride, Na/K tartrate and cyclophosphamide were from Sigma-Aldrich.

### 3.3. METHODS

#### **3.3.1. Labelling of HYNIC-RGD and HYNIC-annexin with technetium-99m using EDDA/tricine as exchange products**

To a sealed reaction vial containing 20 mg of tricine and 5 mg of EDDA, 0.5 mL of a 0.1M phosphate buffer solution, previously saturated with a nitrogen stream, was added for favouring dissolution of the salts. Then, 10  $\mu\text{g}$  of {c[Arg-Gly-Asp-D-Tyr-(HYNIC)-Lys]}, 5  $\mu\text{L}$  of a 8.9mM  $\text{SnCl}_2 \cdot \text{H}_2\text{O}$  solution in 0.1N HCl (nitrogen purged) and 500  $\mu\text{L}$  of  $\text{Na}^{99\text{m}}\text{TcO}_4^-$  were added to the solution. The solution was heated for 15 min in a water bath at 100°C and then cooled at room temperature. The pH of the reaction was pH7. For HYNIC-annexin labelling, studies with different parameters were also carried out, to achieve better labelling yields.

#### **3.3.2. Preparation of $^{99\text{m}}\text{Tc}$ -nitrido precursor**

To a readily available lyophilized kit (CIS Biointernational) containing succinic acid dihydrazide (SDH) as nitrido donor ligand and stannous chloride as reducing agent, 0.5 mL of aqueous  $\text{Na}^{99\text{m}}\text{TcO}_4$  and 0.5 mL of absolute ethanol were added. The reaction vial was left standing at room temperature for 30 min to complete the process.

#### **3.3.3. Labelling of Cys-RGD and Cys-annexin using the $^{99\text{m}}\text{Tc}$ -nitrido precursor**

$^{99\text{m}}\text{TcN}(\text{PNP6})\text{-Cys-RGD}$  was prepared by addition of 50  $\mu\text{L}$  of a 0.9mM aqueous solution of Cys-RGD and 3  $\mu\text{g}$  of diphosphine (PNP6), dissolved in 200  $\mu\text{L}$  of ethanol, to the precursor vial. This reaction was carried out for 1 h at 100°C. The same procedure was carried out using Cys-annexin.

### 3.3.4. Radiochemical stability, transchelation towards cysteine and partition coefficient

$^{99m}\text{Tc}\equiv\text{N}(\text{PNP6})\text{-Cys-RGD}$  and  $^{99m}\text{Tc}\equiv\text{N}(\text{PNP6})\text{-Cys-annexin}$  radiochemical stability were monitored for 6 h along with transchelation by cysteine (carried out with 0.1–100mM cysteine solutions), which was checked for 4 h. Partition coefficient was also evaluated in octanol/water. The partition ratios of the labels were calculated by dividing the counts in the organic phase with those in the aqueous phase per volume unit.

### 3.3.5. Synthesis of $^{99m}\text{Tc}$ -carbonyl

The organometallic precursor was prepared according to the procedure published by Alberto et al. [3.14], with minor modifications. Briefly, 4.4 mg  $\text{Na}_2\text{CO}_3$ , 20 mg Na/K tartrate· $\text{H}_2\text{O}$  and 5.5 mg  $\text{NaBH}_4$  were purged for 1 h with carbon monoxide gas. Then, 1 mL of  $\text{Na}^{99m}\text{TcO}_4$  (3700–5550 MBq) was added to the vial containing the mixture of salts purged with carbon monoxide gas. The vial was heated at 75–80°C for 35 min. The reaction was stopped in an ice bath, and the pH was adjusted to pH7 using 0.2 mL of 1M HCl/0.1M phosphate buffer solution (2:1). For the animal experiments, the Isolink kit from Mallinckrodt was used for the preparation of the tracer in accordance with the manufacturer's instructions.

### 3.3.6. Labelling of Ter-Cys-RGD, PZ1-RGD, His-RGD and His-annexin with the precursor $^{99m}\text{Tc}(\text{CO})_3$

The labelling procedure with  $^{99m}\text{Tc}$ -carbonyl for these species was as reported above. In the vial containing 1.1mM (50  $\mu\text{g}$ ) of the peptide, 100–250  $\mu\text{L}$  of  $^{99m}\text{Tc}(\text{CO})_3$  solution was first added. The vial was heated at 75°C for 60 min. The reaction was stopped in an ice bath.

### 3.3.7. Quality control

#### 3.3.7.1. $^{99m}\text{Tc}$ -HYNIC peptide complexes

Radiochemical analysis of  $^{99m}\text{Tc}$ -HYNIC peptides was performed by instant thin layer chromatography (TLC) on silica gel strips (ITLC-SG, Gelman Sciences) with a two-solvent system. Methyleneethylketone (MEK) was used to determine the amount of  $^{99m}\text{TcO}_4^-$  (retention factor ( $R_f$ ) = 1), and 50% acetonitrile solution was used to determine  $^{99m}\text{Tc}$ -colloid ( $R_f$  = 0).

### 3.3.7.2. $^{99m}\text{Tc}(\text{CO})_3$ peptide complexes

Quality control was performed using paper and TLC on Whatman No. 1 strips and aluminium supported TLC plates, respectively, and a mixture of methanol/HCl 6M (99.5:0.5) as mobile phase.

### 3.3.7.3. $^{99m}\text{TcN}(\text{PNP6})$ peptide complexes

Radiochemical evaluation of the Tc-nitrido kit was performed using ITLC-SG. The mixture ethanol:chloroform:toluene:0.5M ammonium acetate (5:3:3:0.5) was employed as mobile phase to detect free  $^{99m}\text{TcO}_4^-$ , and ethyl acetate was used to detect unbound Tc-N. The mixture ethanol/water (1:1) was used to reveal colloidal  $^{99m}\text{TcO}_2$ .

Some of the radiolabelled peptides cited above were also characterized by reverse phase high performance liquid chromatography (HPLC) using  $\text{H}_2\text{O}$ /TFA 0.1% and  $\text{CH}_3\text{CN}$ /TFA 0.1% as gradient solvents.

## 3.3.8. Purification

The purification of the peptides was carried out with a C18 Sep-Pak Mini cartridge (Waters). The column was activated with 5 mL of ethanol and 5 mL of water. The impurities were eluted with 2 mL of water and the radiolabelled peptide with 2 mL of ethanol. For biological studies and other evaluations, the ethanol solvent was slowly evaporated under a nitrogen atmosphere. The residue was taken up with physiological saline solution.

## 3.3.9. Biodistribution studies in healthy animals

All animal studies were approved by the local animal welfare committee. After purification,  $^{99m}\text{Tc}$  labelled preparations (0.1 mL) were intravenously administered via the tail vein in Swiss male mice (body mass 20–25 g) in a radioactive concentration of 185–370 MBq/mL. Mice were sacrificed at 1 and 4 h post-injection. Organs and tissues (blood, heart, lung, spleen, kidneys, liver, pancreas, stomach, large and small intestines, muscle and bone) were excised, weighed and the radioactivity was determined by gamma counting. The results were expressed as a percentage of injected dose per gram (% ID/g) of tissue.

## 3.3.10. Animal model with tumour cells

A549 cells, a human non-small-cell lung carcinoma cell line, were grown in RPMI growth medium, enriched with penicillin (50 IU/mL), streptomycin

(50 µg/mL), amphotericin-B (1.25 µg/mL), L-glutamine 2mM and foetal bovine serum (FBS; 10% (v/v)). The cells were grown to confluency and then harvested by trypsinization. After centrifugation for 5 min at 100g, cells were resuspended in PBS. Cells were counted without staining and further centrifuged and resuspended again in PBS (70 µL) for inoculation in animals.

Athymic male nude mice (18–22 g) were injected subcutaneously on the right higher back with a suspension of  $6.5 \times 10^6$  cells. Tumour bearing mice were used for biodistribution and imaging studies.

### **3.3.11. Animal model for annexin studies**

Nude mice bearing A549 lung tumour cells were injected with cyclophosphamide (150 mg/kg, intraperitoneally) 24 h before the administration of  $^{99m}\text{Tc}(\text{CO})_3\text{-His-annexin}$  injected intravenously in the tail vein. The animals were sacrificed 4 h post-injection. For comparison, other animals without the previous administration of cyclophosphamide were evaluated.

### **3.3.12. Imaging of tumour**

Planar gamma camera imaging was performed in nu/nu athymic mice bearing A549 cell tumour. The scintigraphic imaging was performed using a mobile scintillation camera (LEM-Siemens) equipped with a 4.0 mm pinhole collimator. A syringe with a known amount of radioactivity was scanned along with the mice to allow semiquantification of the results using region of interest (ROI) analysis. All animals were injected intravenously with 0.1 mL (37 MBq) of  $^{99m}\text{Tc-HYNIC-RGD}$ ,  $^{99m}\text{Tc}(\text{CO})_3\text{-Ter-Cys-RGD}$ ,  $^{99m}\text{Tc}(\text{CO})_3\text{-His-RGD}$  and  $^{99m}\text{Tc}(\text{CO})_3\text{-PZ1-RGD}$  in 0.9% saline via the lateral tail vein. Four hours post-injection the animals were anaesthetized by intraperitoneal injection with urethane solution. A total of 500 kcounts was obtained per projection, under a  $64 \times 64$  matrix size. Static images were acquired, after which ROIs were drawn using a magnetic resonance imaging maximum intensity projection.

## **3.4. RESULTS AND DISCUSSION**

### **3.4.1. Labelling of HYNIC-RGD and HYNIC-annexin with technetium-99m using EDDA/tricine as exchange products**

Radiochemical analysis of the  $^{99m}\text{Tc-HYNIC}$  peptides was performed by instant thin layer chromatography (ITLC) on silica strips with MEK and 50% acetonitrile aqueous solution. Radiochemical purity was  $99.45 \pm 0.12\%$ . ITLC

findings were confirmed by HPLC with a retention time for the product of 12.86 min. Only traces (<0.6%) of  $^{99m}\text{TcO}_4^-$  could be detected, with a retention time of 5.33 min. Specific activity was 142.3 MBq/nmol.

The labelling procedure for HYNIC-annexin was the same as used with HYNIC-RGD. Different masses of the ligand (10, 20 and 50  $\mu\text{g}$ ), different heating of reaction (15–60 min) and different masses (10–250  $\mu\text{g}$ ) of the reducing agent ( $\text{SnCl}_2 \cdot 2\text{H}_2\text{O}$ ) were employed to achieve better results.

Increasing the amount of HYNIC-annexin, reaction time and concentration of the coligands tricine/EDDA did not permit any improvement of the radiochemical purity of the complex, which was found to be very low (23.5%). Stannous chloride used varied from 10 to 30  $\mu\text{g}$  in the labelling experiments. It appears, therefore, that factors such as reaction time and concentration of ligand did not affect the radiolabelling results. Using 50  $\mu\text{g}$  of stannous chloride the radiochemical yield increased to 50.25% and with 100  $\mu\text{g}$  to 78.53%. This amount was increased up to 250  $\mu\text{g}$ , but no better results were achieved. The  $^{99m}\text{Tc}$  activity used for labelling varied from 110 to 1850 MBq.

### 3.4.2. Preparation of $^{99m}\text{Tc}$ -nitrido and labelling of Cys-RGD and Cys-annexin

The first reaction that occurs in the conditions of this protocol is reduction of  $^{99m}\text{TcO}_4^-$  by  $\text{SnCl}_2$  in the presence of succinic dihydrazide [ $\text{H}_2\text{N}-\text{NH}-\text{C}(=\text{O})-(\text{CH}_2)_2-(\text{O}=\text{N})\text{NH}-\text{NH}_2 = \text{SDH}$ ], which behaves as a source of nitrido nitrogen groups ( $\text{N}^3$ ) to form the  $\text{Tc}\equiv\text{N}$  bond.

In the second step, the  $\text{Tc}\equiv\text{N}$  core becomes surrounded by two different bidentate ligands, namely a diphosphine ligand (PNP6) (Fig. 3.1) and a Cys peptide ligand, forming a final complex with an asymmetrical structure [3.15].

The asymmetrical alternative has the advantage that it can be prepared by simply mixing in the same vial the ligands PNP and Cys peptide with the

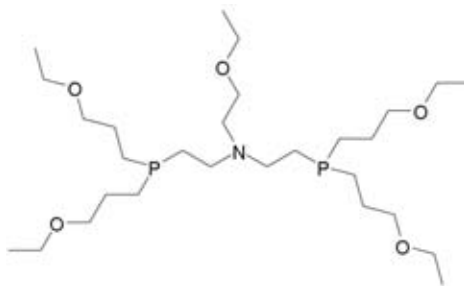


FIG. 3.1. PNP6 molecule.

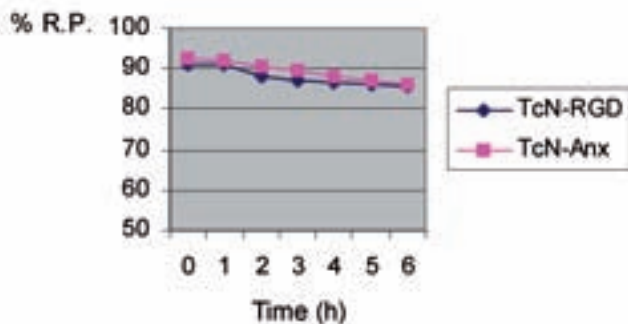


FIG. 3.2. Radiochemical stability of  $^{99m}\text{TcN}(\text{PNP6})\text{-RGD}$  and  $^{99m}\text{TcN}(\text{PNP6})\text{-Anx13}$ .

starting mixture of nitrido precursor. Since a terminal cysteine residue is able to coordinate the fragment  $^{99m}\text{TcN}$ -diphosphine, when this amino acid is conjugated to a small peptide such as an RGD analogue and annexin 13 it allows the peptide sequence to remain stably incorporated into the structure of the final complex.

Radiochemical purity of both  $^{99m}\text{Tc}(\text{PNP6})$  conjugates gave similar results. For  $^{99m}\text{Tc}(\text{PNP6})\text{-Anx13}$  it was  $92.46 \pm 1.24\%$  and for  $^{99m}\text{Tc}(\text{PNP6})\text{-RGD}$  it was  $91.27 \pm 1.83\%$ .

### 3.4.3. Radiochemical stability, transchelation towards cysteine and partition coefficient

The radiochemical stability at different times after preparation is shown in Fig. 3.2. Both radiolabelled  $^{99m}\text{Tc-N}$  peptides are stable for 6 h at room temperature with a loss of radiochemical purity of only 6%.

They were also challenged with cysteine excess to determine their stability against ligand exchange and/or decomposition. The samples were analysed by means of ITLC at 1, 2 and 4 h. The obtained results are presented in Table 3.1, showing that the radiolabelled peptides are quite inert to transchelation when challenged with cysteine. Only  $^{99m}\text{TcN}(\text{PNP6})\text{-RGD}$  was relatively more susceptible to cysteine challenge than  $^{99m}\text{TcN}(\text{PNP6})\text{-Anx13}$ , with a reduction of 4.7%, but the percentage observed is similar to that observed after incubation of the labelled compounds at room temperature in stability studies.

Lipophilicity of a molecule is determined by its structure and can be reflected by its partition ratio between *n*-octanol and water. Partition coefficients of the radiolabelled  $^{99m}\text{Tc-N}$  peptides were evaluated by measuring their partition between *n*-octanol and water. The partition coefficients of

TABLE 3.1. RESULTS OF THE TRANSCHELATION STUDIES OF THE COMPLEXES TOWARDS CYSTEINE

Cysteine	<sup>99m</sup> TcN(PNP6)-annexin (% RP <sup>a</sup> )			<sup>99m</sup> TcN(PNP6)-RGD (% RP)		
	Time					
	1 h	2 h	4 h	1 h	2 h	4 h
Blank	91.48	90.66	90.07	90.79	90.21	89.73
0.1mM	91.07	90.00	89.98	89.94	89.57	89.21
1mM	90.53	89.79	89.11	89.46	88.87	88.32
10mM	88.95	87.96	86.97	88.89	87.66	87.24
50mM	87.47	87.31	87.02	88.21	87.76	87.11
100mM	85.54	86.17	87.62	87.68	87.27	86.04

<sup>a</sup> RP = radiochemical purity.

<sup>99m</sup>TcN(PNP6)-RGD and <sup>99m</sup>TcN(PNP6)-Anx were 0.27 and 0.45, respectively, indicating a significant hydrophilic character for these species.

#### 3.4.4. Synthesis of <sup>99m</sup>Tc-carbonyl and labelling of Ter-Cys-RGD, PZ1-RGD, His-RGD and His-annexin

The precursor [<sup>99m</sup>Tc(H<sub>2</sub>O)(CO<sub>3</sub>)]<sup>+</sup> was formed quantitatively (94.8 ± 2.6%) using either the commercial Isolink kit or carbon monoxide gas. We observed that the purity of the carbon monoxide gas can sometimes affect the yield of this reaction.

The labelling procedure applied to the labelling of the three ligands with <sup>99m</sup>Tc(CO)<sub>3</sub> was almost identical, and yields for these compounds varied from 82.6% to 91.3%. The specific activity was 6.7 MBq/nmol. Initially, we used a volume of 200–250 μL of <sup>99m</sup>Tc(CO)<sub>3</sub>, affording very low labelling yields. When the reaction volume was diminished to 100 μL, the percentage of radiochemical purity increased, thus indicating that the volume is an important factor affecting the radiolabelling yield with carbonyl precursor, unlike the labelling with HYNIC, where a higher volume did not affect the success of the labelling. For <sup>99m</sup>Tc(CO)<sub>3</sub>-Ter-Cys-RGD, no improvement in the labelling yield was achieved by increasing the mass of the ligand up to 100 μg.

Chromatographic evaluation of the carbonyl product could not be performed using the same TLC and paper chromatographic systems employed for the other compounds, as broad radioactive spots were observed for some radiochemical species. Thus characterization was mainly done using separation

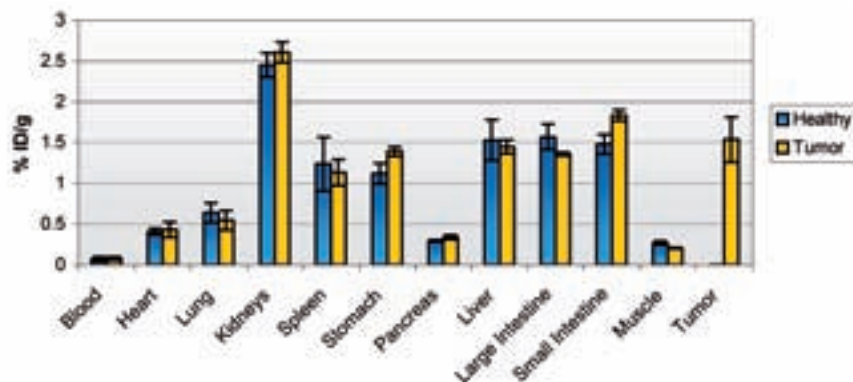


FIG. 3.3. Biodistribution of  $^{99m}\text{Tc}$ -HYNIC-RGD.

by Sep-Pak C18 cartridge. Another observation was that high activity remained in the Sep-Pak filter (approximately 14%), showing that, presumably, colloidal  $^{99m}\text{TcO}_2$  was formed. The results for  $^{99m}\text{Tc}$ -(CO) $_3$ -His-RGD and  $^{99m}\text{Tc}$ -(CO) $_3$ -PZ1-RGD were similar and radiochemical control was carried out by different methods.

#### 3.4.5. Biodistribution studies in normal and tumour bearing animals

Biodistribution studies were carried out in Swiss male mice at 1 and 4 h after administration of the radiolabelled compound. Studies with animals bearing tumours were performed in nude mice only at 4 h post-injection. Each group was composed of three to five animals. The only compound that was not further studied biologically was  $^{99m}\text{Tc}$ -HYNIC-Anx, due to the poor radiochemical profile.

#### 3.4.6. Animal model with tumour cells

A549 cells, a human non-small-cell lung carcinoma cell line, were easy and fast to cultivate compared with other tumour cell lines studied at the molecular biology centre. Usually, after 10 days post-inoculation in the animals, significant tumour growth was achieved and radioactive studies could be carried out.

The biodistribution patterns of  $^{99m}\text{Tc}$ -HYNIC-RGD in normal animals and in tumour bearing animals at 4 h post-injection are illustrated in Fig. 3.3. The conjugate cleared the bloodstream fast and radioactivity in liver and kidney reflect both urinary and hepatic elimination of the tracer. Tumour uptake was  $1.54 \pm 0.28\%$ .

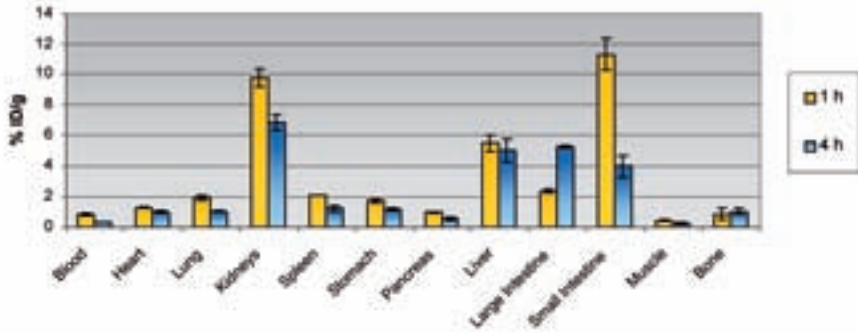


FIG. 3.4. Biodistribution results of  $^{99m}\text{TcN}(\text{PNP6})\text{-RGD}$ .

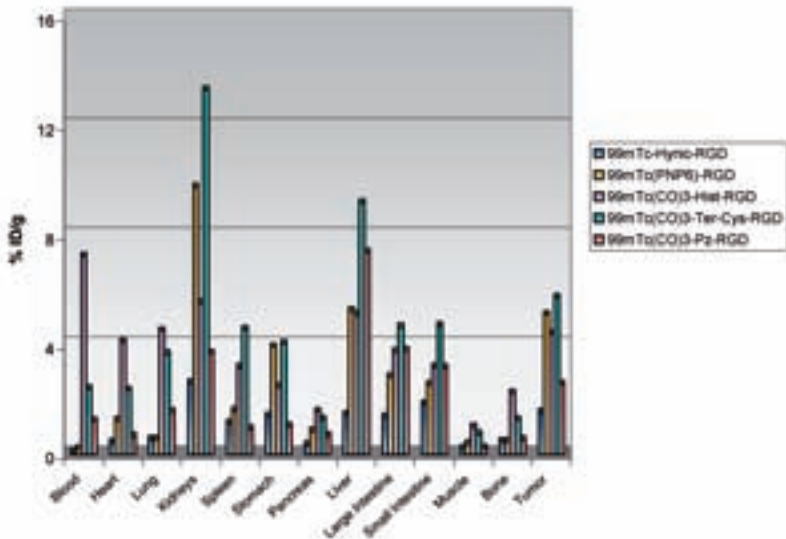


FIG. 3.5. Biodistribution studies of  $^{99m}\text{Tc-RGD}$  derivatives in animals bearing lung tumour.

$^{99m}\text{Tc-N}(\text{PNP6})\text{-RGD}$  was evaluated by biodistribution in healthy animals 1 and 4 h post-injection (Fig. 3.4). High uptake in kidneys, liver and intestines was observed following the pattern of RGD complexes. Biodistribution in animals bearing tumour can be observed in Fig. 3.5. The uptake by the tumour was 5.12%.

TABLE 3.2. RESULTS OF BIODISTRIBUTION STUDIES OF  $^{99m}\text{Tc}(\text{CO})_3\text{-His-RGD}$ ,  $^{99m}\text{Tc}(\text{CO})_3\text{-Ter-Cys-RGD}$  AND  $^{99m}\text{Tc}(\text{CO})_3\text{-PZ1-RGD}$  (% ID/g)

	$^{99m}\text{Tc}(\text{CO})_3\text{-His-RGD}$		$^{99m}\text{Tc}(\text{CO})_3\text{-PZ1-RGD}$		$^{99m}\text{Tc}(\text{CO})_3\text{-Ter-Cys-RGD}$	
	1 h	4 h	1 h	4 h	1 h	4 h
Blood	13.2 ± 0.3	9.5 ± 0.6	0.8 ± 0.0	0.3 ± 0.0	2.6 ± 0.1	1.3 ± 0.0
Heart	3.8 ± 0.6	2.5 ± 0.1	1.2 ± 0.2	1.1 ± 0.1	2.6 ± 0.0	1.6 ± 0.2
Lung	8.2 ± 1.1	5.7 ± 0.8	2.1 ± 0.2	1.2 ± 0.2	5.2 ± 0.3	3.5 ± 0.8
Kidneys	12.9 ± 1.8	8.4 ± 1.9	8.6 ± 0.4	4.8 ± 0.7	14.5 ± 0.4	12.1 ± 0.7
Spleen	2.8 ± 0.3	2.6 ± 0.5	1.7 ± 0.2	1.4 ± 0.2	2.9 ± 0.1	2.8 ± 0.0
Stomach	2.2 ± 0.5	2.3 ± 0.4	2.4 ± 0.4	2.6 ± 0.5	3.3 ± 0.2	1.6 ± 0.1
Pancreas	1.9 ± 0.1	1.7 ± 0.5	0.8 ± 0.1	0.5 ± 0.1	1.2 ± 0.5	0.9 ± 0.2
Liver	8.5 ± 0.7	7.1 ± 0.7	4.5 ± 1.1	2.9 ± 0.2	12.2 ± 0.2	11.8 ± 0.8
Large intestine	2.6 ± 0.4	2.8 ± 0.4	2.4 ± 0.4	4.0 ± 0.3	3.2 ± 0.1	3.6 ± 0.4
Small intestine	4.5 ± 0.5	2.9 ± 0.4	7.1 ± 0.3	2.9 ± 0.2	9.7 ± 1.5	5.4 ± 1.1
Muscle	0.9 ± 0.0	0.6 ± 0.1	0.7 ± 0.1	0.4 ± 0.0	0.8 ± 0.2	0.7 ± 0.2
Bone	2.3 ± 0.2	1.5 ± 0.3	1.1 ± 0.3	1.5 ± 0.3	2.6 ± 0.5	2.1 ± 0.1
Total blood	24	20.4	1.4	0.4	5.1	2.2
Total muscle	9.3	6.4	6.6	4.4	9.1	6.8
Total bone	8.2	3.6	2.7	4.0	8.5	5.4

Table 3.2 shows biodistribution results of  $^{99m}\text{Tc}(\text{CO})_3\text{-His-RGD}$ ,  $^{99m}\text{Tc}(\text{CO})_3\text{-Ter-Cys-RGD}$  and  $^{99m}\text{Tc}(\text{CO})_3\text{-PZ1-RGD}$  in normal mice at 1 and 4 h post-injection. A interesting finding was the very high accumulation of  $^{99m}\text{Tc}(\text{CO})_3\text{-His-RGD}$  in the bloodstream. It has been shown that the blood level of a peptide can be markedly affected by the type of metal chelator. Biodistribution patterns of other RGD complexes were also determined as cited above, showing highest uptake in kidneys, liver and intestines. A similar behaviour was found for  $^{99m}\text{Tc}(\text{CO})_3\text{-Ter-Cys-RGD}$ . Figure 3.5 shows the biodistribution of five RGD metallic derivatives in animals bearing lung tumour cells A549, at 4 h post-injection. The uptake ranged between 1.54 ( $^{99m}\text{Tc-HYNIC-RGD}$ ) and 5.73% ID/g for  $^{99m}\text{Tc}(\text{CO})_3\text{-Ter-Cys-RGD}$ .

Tumour/blood and tumour/muscle ratios are reported in Fig. 3.6. The highest ratios were achieved by  $^{99m}\text{Tc-HYNIC-RGD}$  and  $^{99m}\text{Tc-N(PNP6)-RGD}$ . RGD peptides can be retained in tumour tissue because of the interaction with  $\alpha_v\beta_3$  integrin expressed on the neovasculature, on the tumour

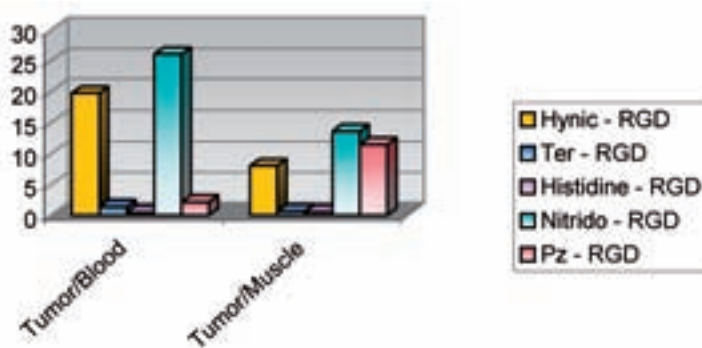


FIG. 3.6. Tumour/blood and tumour/muscle ratio for <sup>99m</sup>Tc-RGD derivatives.

cells, or in a combination of both cell types. In this respect, it remains unclear whether RGD peptides actually target angiogenesis in growing tumours or  $\alpha_v\beta_3$  expression of tumour cells.

#### 3.4.7. Animal model for annexin studies

Apoptosis is a dynamic cellular process that does not affect all tumour cells after cytostatic drug treatment. The onset of this phenomenon is an individual cellular process and apoptotic cells are rapidly eliminated in vivo, which makes it difficult to evaluate the potency of a new apoptotic imaging agent in tumour tissue [3.11, 3.16].

Biodistribution of <sup>99m</sup>TcN(PNP6)-Cys-Anx was investigated in healthy animals at 1 and 4 h post-injection (Fig. 3.7). It was found that excretion was mainly through the hepatobiliary system, with relatively little kidney elimination.

<sup>99m</sup>Tc(CO)<sub>3</sub>-His-Anx was studied in healthy animals and also in tumour bearing animals (Table 3.3). Comparing the biodistribution of nitrido-Anx with carbonyl-Anx in healthy animals at 4 h post-injection it was observed that in the latter excretion was mainly through the kidneys. Nevertheless, the hepatobiliary route was also substantially activated, so that renal and hepatointestinal elimination of the drug had similar importance.

#### 3.4.8. Imaging of tumour uptake

Scintigraphic statics were collected in nude mice bearing A549 lung cancer cells in the right upper back at 4 h post-injection of the compounds <sup>99m</sup>Tc-HYNIC-RGD, <sup>99m</sup>Tc(CO)<sub>3</sub>-Ter-Cys-RGD, <sup>99m</sup>Tc(CO)<sub>3</sub>-His-RGD and

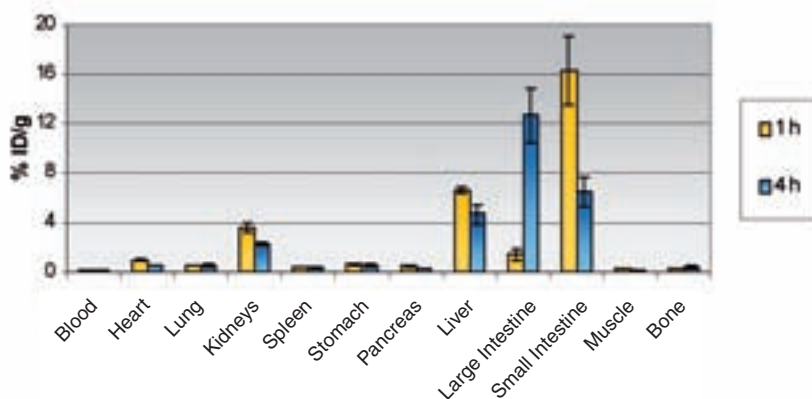


FIG. 3.7. Biodistribution of  $^{99m}\text{TcN}(\text{PNP6})\text{-Cys-Anx}$ .

$^{99m}\text{Tc}(\text{CO})_3\text{-PZ1-RGD}$ . No uptake by the tumour could be observed for the last two compounds. Images of animals injected with  $^{99m}\text{Tc-HYNIC-RGD}$  and  $^{99m}\text{Tc}(\text{CO})_3\text{-Ter-Cys-RGD}$  are shown in Fig. 3.8. Quantification data described by ROI gave 4.92% for  $^{99m}\text{Tc-HYNIC-RGD}$  and 0.81% for  $^{99m}\text{Tc}(\text{CO})_3\text{-Ter-Cys-RGD}$ .

Imaging with  $^{99m}\text{Tc-HYNIC-RGD}$  at 30 min after blockade with  $100\ \mu\text{g}$  of RGD was also attempted, with 0.88% of ROI, suggesting reasonable specificity of the marker for the selected tumour tissue.

Comparing the tumour uptake of these two compounds, as measured in biodistribution studies and by scintigraphic imaging, different results were obtained. Specifically, in biodistribution studies a much higher tumour uptake was found for the complex  $^{99m}\text{Tc}(\text{CO})_3\text{-Ter-Cys-RGD}$ . Conflicting results were obtained in biodistribution studies of the complex  $^{99m}\text{Tc}(\text{CO})_3\text{-Ter-Cys-RGD}$ . The explanation could be that ROI considers uptake in the tumour on the basis of 100% of uptake by the body. Biodistribution was not calculated using the entire body, because some organs, such as the thyroid, carcass, skin, bladder and bone, were not analysed. This methodological detail might justify the discrepancies. We gave the result in % ID/g. The animals used for biodistribution was not the same as those used in scintigraphic imaging.

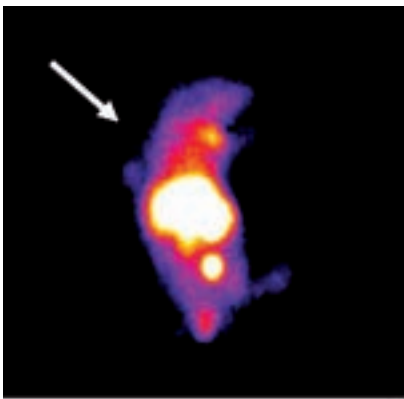
### 3.5. CONCLUSIONS

The techniques used for labelling RGD and annexin derivatives with  $^{99m}\text{Tc}$ , namely HYNIC (EDDA/tricine), nitrido and carbonyl, showed that the

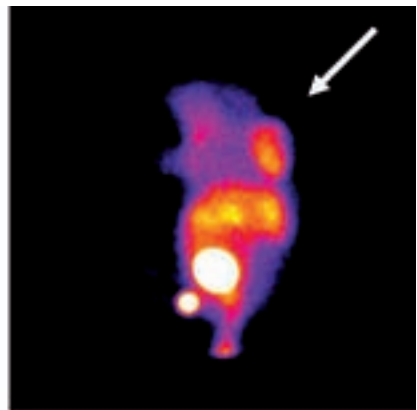
CHAPTER 3

TABLE 3.3. BIODISTRIBUTION STUDIES OF  $^{99m}\text{Tc}(\text{CO})_3\text{-His-ANNEXIN}$  (% ID/g)

	Healthy	Tumour
Blood	0.97	2.37
Heart	0.25	0.74
Lung	0.70	1.69
Kidneys	13.90	10.84
Spleen	0.71	0.60
Stomach	1.90	7.92
Pancreas	0.34	1.01
Liver	15.12	9.50
Large intestine	7.88	8.07
Small intestine	7.62	6.22
Muscle	0.11	0.7
Bone	0.24	2.09
Tumour	—	1.31
Tumour/blood	—	0.44
Tumour/muscle	—	0.24



(a)



(b)

FIG. 3.8. Images of (a)  $^{99m}\text{Tc}(\text{CO})_3\text{-Ter-Cys-RGD}$  and (b)  $^{99m}\text{Tc-HYNIC-RGD}$ .

fastest and easiest alternative to perform is with HYNIC. The highest radiochemical yield was achieved by HYNIC, followed by the nitrido method. Lung cancer carcinoma was a good model to evaluate RGD derivatives. Good uptake by the tumour was obtained with  $^{99m}\text{Tc}$ -HYNIC-RGD and with  $^{99m}\text{Tc}(\text{CO})_3$ -Ter-Cys-RGD. For annexin derivatives, the apoptosis method should be further developed to evaluate their uptake.

### ACKNOWLEDGEMENTS

We are grateful to other participants of this coordinated project, namely J. Smith, A. Duatti, J. Környei and C. Decristoforo, for suggestions and assistance on many occasions.

### REFERENCES

- [3.1] BRACK, S.S., DINKELBORG, L.M., NERI, D., Molecular targeting of angiogenesis for imaging and therapy, *Eur. J. Nucl. Mol. Imaging* **31** (2004) 1327–1341.
- [3.2] STUPACK, D.G., CHERESH, D.A., Integrins and angiogenesis, *Curr. Top. Dev. Biol.* **64** (2004) 207–238.
- [3.3] RUOSLAHI, E., The RGD story: A personal account, *Matrix Biol.* **22** (2003) 459–465.
- [3.4] CHEN, X., et al., MicroPET and autoradiographic imaging of breast cancer  $\alpha_v$ -integrin expression using  $^{18}\text{F}$  and  $^{64}\text{Cu}$ -labeled RGD peptide, *Bioconj. Chem.* **15** (2004) 41–49.
- [3.5] POETHKO, T., et al., Two-step methodology for high-yield routine radiohalogenation of peptides:  $^{18}\text{F}$ -labeled RGD and octreotide analogs, *J. Nucl. Med.* **45** (2004) 892–902.
- [3.6] PSIMADAS, D., et al., Study of the labeling of two novel RGD-peptidic derivatives with the precursor  $^{99m}\text{Tc}(\text{H}_2\text{O})_3(\text{CO})_3^+$  and evaluation for early angiogenesis detection in cancer, *Appl. Radiat. Isot.* **64** (2006) 151–159.
- [3.7] VAN HAGEN, P.M., et al., Evaluation of radiolabeled cyclic DTPA-RGD analogue for tumour imaging and radionuclide therapy, *Int. J. Cancer* **90** (2000) 186–198.
- [3.8] ZORNIG, M., BAUM, W., HUEBBER, A.-O., EVAN, G., “Programmed cell death and senescence”, *The Molecular Basis of Cancer*, 2nd edn (MENDEL-SOHN, J., HOWLEY, P.M., ISRAEL, M.A., LIOTTA, L.A., Eds), WB Saunders, Philadelphia, PA (2001) 19–40.
- [3.9] LAHORTE, C.M.M., et al., Apoptosis-detecting radioligands: Current state of the art and future perspectives, *Eur. J. Nucl. Med. Mol. Imaging* **31** (2004) 887–919.

### CHAPTER 3

- [3.10] GERKE, V., MOSS, S.E., Annexins: From structure to function, *Physiol. Ver.* **82** (2002) 331–371.
- [3.11] BLANKENBERG, F.G., et al., Imaging of apoptosis (programmed cell death) with  $^{99m}\text{Tc}$  annexin V, *J. Nucl. Med.* **40** (1999) 184–191.
- [3.12] BOLZATI, C., et al., The  $^{99m}\text{Tc}(\text{N})(\text{PNP})^{+2}$  metal fragment: A technetium-nitrido synthon for use with biologically active molecules. The N-(2-methoxyphenyl)piperazil-cysteine analogues as examples, *Bioconj. Chem.* **14** (2003) 1231.
- [3.13] BABICH, J.W., FISCHMAN, A.J., Effect of “co-ligand” on the biodistribution of  $^{99m}\text{Tc}$ -labeled hydrazino nicotinic acid derivatized chemotactic peptides, *Nucl. Med. Biol.* **22** (1995) 25–30.
- [3.14] ALBERTO, R., SCHIBLI, R., EGLI, A., SCHUBIGER, A.P., A novel organometallic aqua complex of technetium for the labeling of biomolecules: Synthesis of  $^{99m}\text{Tc}(\text{OH}_2)_3(\text{CO})_3^+$  from  $^{99m}\text{TcO}_4^-$  in aqueous solution and its reaction with a bifunctional ligand, *J. Am. Chem. Soc.* **120** (1998) 7987.
- [3.15] BOLZATI, C., et al., Chemistry of the strong electrophilic metal fragment  $^{99m}\text{Tc}(\text{N})(\text{PXP})^{+2}$  (PXP = diphosphine ligand): A novel tool for the selective labeling of small molecules, *J. Am. Chem. Soc.* **124** (2002) 11468–11479.
- [3.16] BAUER, C., BAUDER-WUEST, U.B., MIER, W., HABERKORN, U., EISENHUT, M.,  $^{131}\text{I}$ -labeled peptides as caspase substrates for apoptosis imaging, *J. Nucl. Med.* **46** (2005) 1066–1074.



## Chapter 4

### RADIOLABELLING OF RGD PEPTIDES USING NOVEL TECHNETIUM-99m CORES

JI HU, BAOJUN CHEN, JIXIN LIANG, LIANZHE LUO,  
HONGYU LI, YANG CHEN, LANGTAO SHEN, ZHIFU LUO  
Isotope Department, China Institute of Atomic Energy, Beijing, China

#### Abstract

Radiolabelled RGD peptides could be potential imaging agents for  $\alpha_v\beta_3$  expressing tumours. In this work, four different peptide conjugates based on the RGDyK sequence (i.e. HYNIC-, His-, Cys- and Cys(X)-RGD) were radiolabelled with different  $^{99m}\text{Tc}$  cores. The radiolabelling yields were in the range 90–98% under optimized preparation conditions. In vitro stability studies indicated that  $[\text{}^{99m}\text{Tc}(\text{H}_2\text{O})_3(\text{CO})_3]^+$  labelled peptides were less stable in the reaction solution as well as in half serum solution compared with their counterparts labelled with  $[\text{}^{99m}\text{Tc}(\text{N})]^{2+}$  and  $^{99m}\text{Tc}$ -HYNIC cores. Biodistribution studies were performed in BALB/c nude mice bearing FWK-1 pancreatic tumour xenografts to explore the in vivo behaviour of  $^{99m}\text{Tc}(\text{N})(\text{PNP6})(\text{Cys-RGD})$  and  $^{99m}\text{Tc-EDDA-HYNIC-RGD}$ . The radiolabelled peptides were all rapidly excreted through kidneys. Uptakes in non-target organs such as liver and intestine were high. Tumour uptake was  $1.34 \pm 0.08\%$  injected dose (ID)/g ( $^{99m}\text{Tc-EDDA-HYNIC-RGD}$ ) or  $2.92 \pm 0.71\%$  ID/g [ $^{99m}\text{Tc}(\text{N})(\text{PNP6})(\text{Cys-RGD})$ ] at 1 h post-injection, and tumour/blood ratios were 6.8 and 11.0 at 4 h post-injection, respectively. Planar gamma imaging allowed well contrasted visualization of  $\alpha_v\beta_3$  expressing tumours at 1 h post-injection. The results showed that the stability and pharmacokinetics of radiolabelled RGD peptides have to be improved for potential clinical application.

#### 4.1. INTRODUCTION

Integrins are a family of transmembrane glycoproteins consisting of an  $\alpha$  and a  $\beta$  subunit and are involved in cell–cell and cell–matrix interactions [4.1]. One of the most important members of this receptor class is the  $\alpha_v\beta_3$  integrin, which is expressed in many kinds of tumour cell and in neovasculature. It plays an important role in the invasion, metastasis, proliferation and apoptosis of tumours [4.2, 4.3]. The high binding specificity to  $\alpha_v\beta_3$  integrin of peptides

TABLE 4.1. SEQUENCE OF RGD PEPTIDES USED IN THIS STUDY

Sequence of RGD peptides	Abbreviation
C(Arg-Gly-Asp-D-Tyr-Lys)	RGD
C(Arg-Gly-Asp-D-Tyr-Lys)-His	His-RGD
C(Arg-Gly-Asp-D-Tyr-Lys)-Cys(X)	Cys(X)-RGD
C(Arg-Gly-Asp-D-Tyr-Lys)-HYNIC	HYNIC-RGD
C(Arg-Gly-Asp-D-Tyr-Lys)-Cys	Cys-RGD

containing Arg-Gly-Asp (RGD) residues suggests that radiolabelled RGD peptides may be useful as tumour specific imaging agents.

Recently, several studies reported the development of radiolabelled RGD peptides with different radionuclides for non-invasive imaging of integrin expression level as well as for integrin targeted radionuclide therapy [4.4–4.8]. Technetium-99m has been the radionuclide of choice for nuclear medicine procedures because of its excellent nuclear properties and wide availability. Therefore, RGD peptide radiolabelled with  $^{99m}\text{Tc}$  is an attractive candidate for imaging of  $\alpha_v\beta_3$  integrin expressed tumours.

In this coordinated research project project, RGD peptides modified with bifunctional chelates and thus radiolabelled by different  $^{99m}\text{Tc}$  approaches are proposed to explore their potential as new radiopharmaceuticals [4.9–4.11]. Here we describe the radiolabelling of cyclic RGD derivatives (Table 4.1 and Fig. 4.1) using novel  $^{99m}\text{Tc}$  cores and their preliminary results on biological distribution in nude mice bearing FWK-1 pancreatic tumour xenograft.

## 4.2. MATERIALS AND METHODS

All chemicals were purchased from the Beijing Chemical Reagents Company. The chemicals and solvents were of reagent grade and unless otherwise stated used without further purification. PNP6 [bis(diethoxypropylphosphinoethyl)ethoxy ethylamine] was obtained from A. Duatti, University of Ferrara, Italy. Freeze dried kits for the preparation of Tc-nitrido intermediate were obtained from CIS Biointernational. RGD peptide derivatives, namely RGD, HYNIC-RGD, His-RGD, Cys-RGD and Cys(X)-RGD, were synthesized by C. Decristoforo at the Universitätsklinik für Nuklearmedizin, Innsbruck.

CHAPTER 4

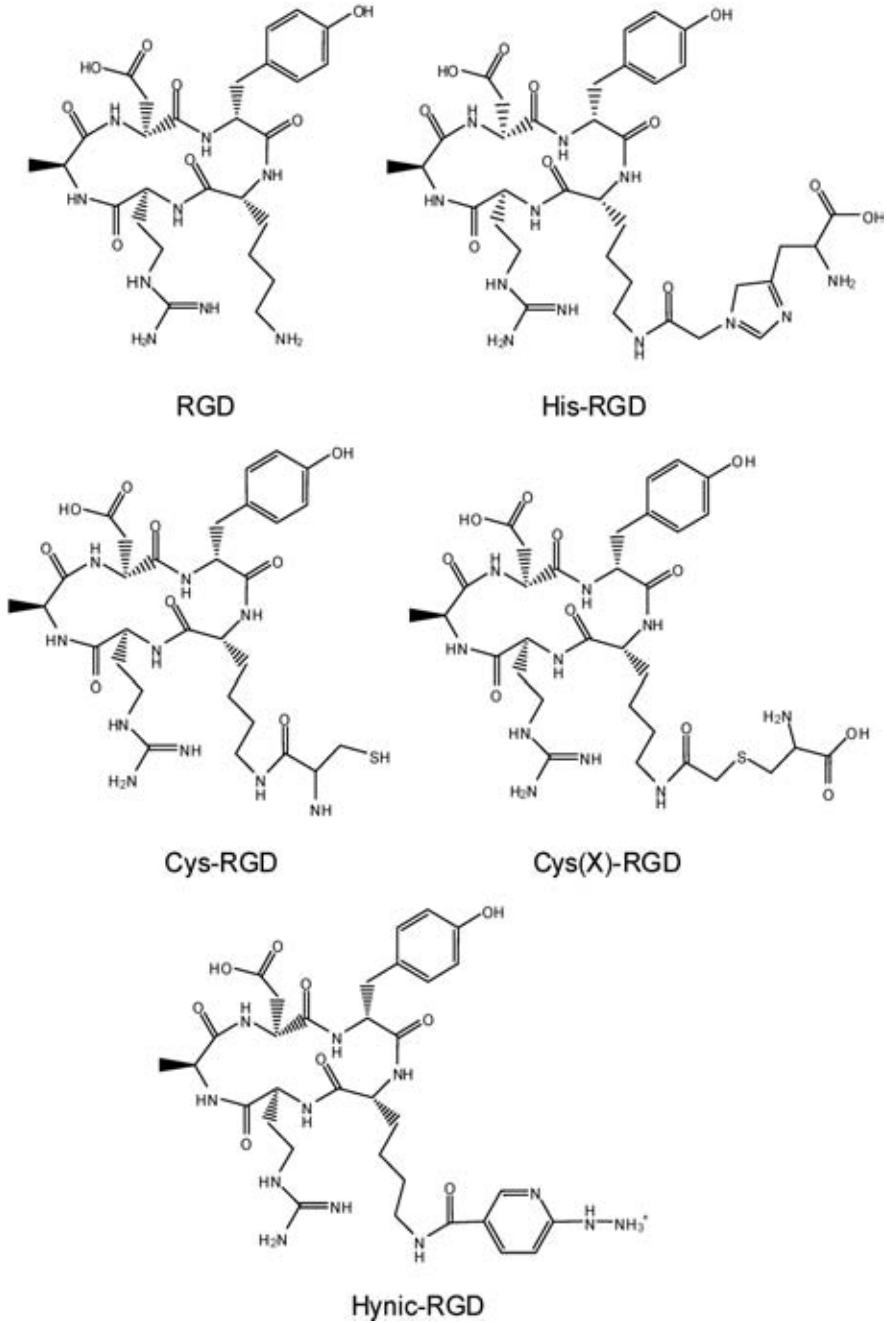


FIG. 4.1. Structure of RGD peptides used in this study.

High performance liquid chromatography (HPLC) analyses were performed on a Varian ProStar system equipped with an ultraviolet (UV) detector and a GABI radiometric detector (Raytest). A Hypersil C18 reverse phase column (4.6 × 250 mm), with flow rates of 1 mL/min and UV detection at 220 nm, were employed with the following gradients:

- (a) Method 1: 0.1% TFA in H<sub>2</sub>O (solvent A) and MeCN (solvent B): 0–2 min 0% B, 2–20 min 0–80% B, 20–26 min 80% B, 26–30 min 80–0% B.
- (b) Method 2: 0.1% TFA in H<sub>2</sub>O (solvent A) and MeCN (solvent B): 0–5 min 30% B, 5–25 min 30–50% B, 25–27 min 50–80% B, 27–35 min 80% B, 35–37 min 80–30% B.
- (c) Method 3: 0.1% TFA in H<sub>2</sub>O (solvent A) and MeOH (solvent B): 0–2 min 0% B, 2–20 min 0–80% B, 20–26 min 80% B, 26–30 min 80–0% B.

#### 4.2.1. Radiolabelling

##### 4.2.1.1. Radiolabelling of Cys-RGD with the [<sup>99m</sup>Tc(N)]<sup>2+</sup> core

[<sup>99m</sup>Tc≡N]<sup>2+</sup> precursor was prepared from a commercial kit containing succinic dihydrazide (SDH, 5.0 mg), SnCl<sub>2</sub>·2H<sub>2</sub>O (100 μg), 1,2 diamino-propane-*N,N,N',N'*-tetra acetic acid (PDTA, 5.0 mg), NaH<sub>2</sub>PO<sub>4</sub> (0.5 mg) and Na<sub>2</sub>HPO<sub>4</sub> (5.8 mg), in accordance with the package insert instructions. To a 10 mL glass vial purged with nitrogen, 10 μL of Cys-RGD solution (1 mg/mL) and 8 μL of PNP6 (in ethanol solution, 1.0 mg/mL) were added, followed by 1.0 mL of freshly prepared [Tc≡N]<sup>2+</sup> precursor (185–1850 MBq), and then reacted at 100°C for 1 h. After cooling to room temperature, the labelling yield of [<sup>99m</sup>Tc(N)(PNP6)(Cys-RGD)] was determined by HPLC (method 2).

##### 4.2.1.2. Radiolabelling of HYNIC-RGD with <sup>99m</sup>Tc

To a 10 mL glass vial containing 1.0 mL of a mixture of tricine/EDDA (20 mg tricine and 10 mg EDDA), 20 μL of SnCl<sub>2</sub>·2H<sub>2</sub>O (1.0 mg/mL in 0.1 mol/L N<sub>2</sub> purged HCl) and 10 μL of HYNIC-RGD (1.0 mg/mL), 0.5 mL of a Na<sup>99m</sup>TcO<sub>4</sub> solution (185 MBq–1.85 GBq) was added and reacted at 100°C for 15 min. The labelling yield was determined by HPLC (method 1).

##### 4.2.1.3. Radiolabelling of His-RGD and Cys(X)-RGD with [<sup>99m</sup>Tc(H<sub>2</sub>O)<sub>3</sub>(CO)<sub>3</sub>]<sup>+</sup>

[<sup>99m</sup>Tc(CO)<sub>3</sub>(H<sub>2</sub>O)<sub>3</sub>]<sup>+</sup> was prepared in accordance with the literature [4.11]. Briefly, Na/K tartrate (15 mg), Na<sub>2</sub>CO<sub>3</sub> (4 mg) and NaBH<sub>4</sub> (5.5 mg) were

placed in a 10 mL glass vial. The vial was sealed and flushed with carbon monoxide for 15 min. 1 mL of  $\text{Na}^{99\text{m}}\text{TcO}_4$  (185 MBq–1.85 GBq) was added and the vial was incubated at 75°C for 30 min. After cooling to room temperature, the pH was adjusted to approximately pH7.0 with 1.0M hydrochloric acid. The labelling yield of  $[\text{}^{99\text{m}}\text{Tc}(\text{CO})_3(\text{H}_2\text{O})_3]^+$  was determined by HPLC (method 3).

In a 10 mL glass vial, 10  $\mu\text{L}$  of His-RGD solution (1.0 mg/mL) or 20  $\mu\text{L}$  of Cys(X)-RGD solution (1.0 mg/mL) was added. The vial was sealed and flushed with  $\text{N}_2$  for 30 min. Then 0.1 mL of freshly prepared  $[\text{}^{99\text{m}}\text{Tc}(\text{H}_2\text{O})_3(\text{CO})_3]^+$  was added and incubated at 80°C for 30 min. After cooling to room temperature, the radiolabelled peptide was analysed by HPLC.

The influence of radiolabelling conditions such as pH, ligand concentration and heating time on the yield of  $^{99\text{m}}\text{Tc}$  radiolabelled RGD peptides was investigated.

#### 4.2.1.4. Purification of radiolabelled RGD peptides

The radiolabelled RGD peptides were purified from  $^{99\text{m}}\text{TcO}_4^-$  and other radioactive impurities by solid phase extraction (SPE). Typically, the C18-Sep-Pak-Light cartridge (Waters) was preactivated with 5 mL ethanol, followed by 5 mL of water and 5 mL of air. The radiolabelled RGD peptides were passed through the cartridge and washed with 5 mL of water, 1.0 mL of 20% ethanol/ $\text{H}_2\text{O}$  and 1.0 mL of ethanol. The ethanol elution was dried in a nitrogen stream and reconstituted in saline.

#### 4.2.1.5. In vitro stability

After preparation, the radiolabelled RGD peptides were left at room temperature and the radiolabelling yields were checked at several time points. Stability in serum was estimated as follows. The radiolabelled RGD peptides were purified by the SPE method as described above. 0.1 mL of the eluate was incubated with 0.9 mL of calf serum at 37°C. After incubation, serum samples were precipitated with acetonitrile and centrifuged (4000g, 5 min). The stability of the radiolabelled RGD in serum was checked by radio-HPLC analysis of the supernatant at 0.5, 1, 2 and 4 h.

### 4.2.2. In vivo animal experiment

#### 4.2.2.1. Tumour xenograft

A cell suspension of FWK-1 pancreatic tumour cells was prepared ( $10^8$  cells/mL). A total of 0.1 mL of the cell suspension was injected subcutane-

ously on the left forelimb of 4–5-week-old female BALB/c nude mice. Two weeks after inoculation, when the tumour grew to a volume of 0.5–1.0 cm<sup>3</sup>, the mice were used for biodistribution studies and gamma camera imaging.

#### 4.2.2.2. Biodistribution studies

Nude mice bearing FWK-1 pancreatic tumour xenografts received an intravenous injection of 1.85–2.78 MBq of <sup>99m</sup>Tc labelled RGD peptide via the tail vein. At 1 h and 4 h after administration, the animals were sacrificed by decapitation. Samples of tumour, blood, liver, kidney, muscle, spleen, lung, stomach, intestine and heart were removed and weighed. The radioactivity in the tissue were measured using an NaI (TI) gamma scintillation counter. The results were expressed as a percentage of injected dose per gram (% ID/g) of tissue after decay correction. Each value represents the mean and standard deviation (SD) for three animals.

#### 4.2.2.3. Blocking studies

Blocking studies were carried out by intravenous injection of 100 µg of cyclo(Arg-Gly-Asp-D-Tyr-Lys) peptide (in 0.05 mL PBS, pH7.4) in tumour bearing nude mice 10 min before injection of 1.85–2.78 MBq of <sup>99m</sup>Tc labelled peptide. The animals were sacrificed by decapitation 4 h after tracer injection. The organs of interest and tumours were removed and data were calculated as described above.

#### 4.2.2.4. Gamma camera imaging

A SPECT camera (Siemens E.CAM duet) was used to record the radio-nuclide distribution in a nude mice model. Data were recorded at 1 h and 4 h after intravenous injection of 1.85–2.78 MBq of <sup>99m</sup>Tc labelled complex. Each image acquired 100 kcounts in a 256 × 256 matrix with an energy window set at the 140 keV photopeak of technetium.

### 4.3. RESULTS AND DISCUSSION

#### 4.3.1. Radiolabelling of RGD peptides

The [<sup>99m</sup>Tc(CO)<sub>3</sub>(H<sub>2</sub>O)<sub>3</sub>]<sup>+</sup> and [<sup>99m</sup>TcN]<sup>2+</sup> precursors were prepared reproducibly with yields of more than 97% as determined by radio-HPLC analysis. The <sup>99m</sup>Tc radiolabelling results are summarized in Table 4.2. The

TABLE 4.2. SUMMARY OF RESULTS OF TECHNETIUM-99m RADIO-LABELLING OF RGD PEPTIDES

Compound	Labelling method	Analysis method	Labelling yield (%)
HYNIC-RGD	HYNIC/tricine/EDDA	Method 1	97.2 ± 1.85
Cys-RGD	Tc-nitrido	Method 2	92.1 ± 2.91
Cys(X)-RGD	Tc-carbonyl	Method 3	90.1 ± 2.23
His-RGD	Tc-carbonyl	Method 3	91.5 ± 1.95

labelling yields of RGD peptides were in the range 90–98% under optimized preparation conditions.

Hydrazinonicotinamide (HYNIC) has been used as chelating agent for labelling peptides and proteins for several years [4.9]. Usually a coligand, such as tricine or ethylenediamine diacetic acid (EDDA), is included in the  $^{99m}\text{Tc}$  labelling of HYNIC conjugates for improving stability, lipophilicity and pharmacokinetics. As reported by Decristoforo and others, replacement of tricine as a coligand by EDDA usually results in a more stable complex (Fig. 4.2a). The radiolabelling of HYNIC-RGD with >98% yield was carried out by a tricine/EDDA exchange method for 15 min at 100°C.

$^{99m}\text{Tc}(\text{N})(\text{PNP6})(\text{Cys-RGD})$  was initially prepared by reacting  $[\text{Cys-RGD-Tc}(\text{N})]^{2+}$  with PNP6 ligand followed by transchelation with Cys-RGD (three-step procedure). Alternatively, the radiolabelling was also performed via the simultaneous addition of both PNP6 ligand and Cys-RGD to  $[\text{Cys-RGD-Tc}(\text{N})]^{2+}$  intermediate (two-step procedure), which resulted in a complex with the same HPLC retention time (Fig. 4.2b). HPLC showed that the preparation gave rise to the formation of two isomeric forms (anti/syn isomer), depending on the orientation of the N-substituted cysteine pendant group with respect to the terminal  $\text{Tc}=\text{N}$  group [4.10]. More than 90% yield could be achieved by employing a PNP6/Cys-RGD ligand ratio higher than 1.5 (data not presented).

The radiolabelling of His-RGD and Cys(X)-RGD was completed by heating at 80°C for 30 min. HPLC analysis of the preparations showed the presence of at least two isomers besides a small amount of residual  $^{99m}\text{TcO}_4^-$  (retention time, 4.6 min) and  $[\text{Cys(X)-RGD-Tc}(\text{CO})_3(\text{H}_2\text{O})_3]^+$  (retention time, 6.3 min) (Figs 4.2c and 4.2d). As a consequence of the instability of radiolabelled compounds (see Section 4.3.2), labelling yields were lower than 90%.

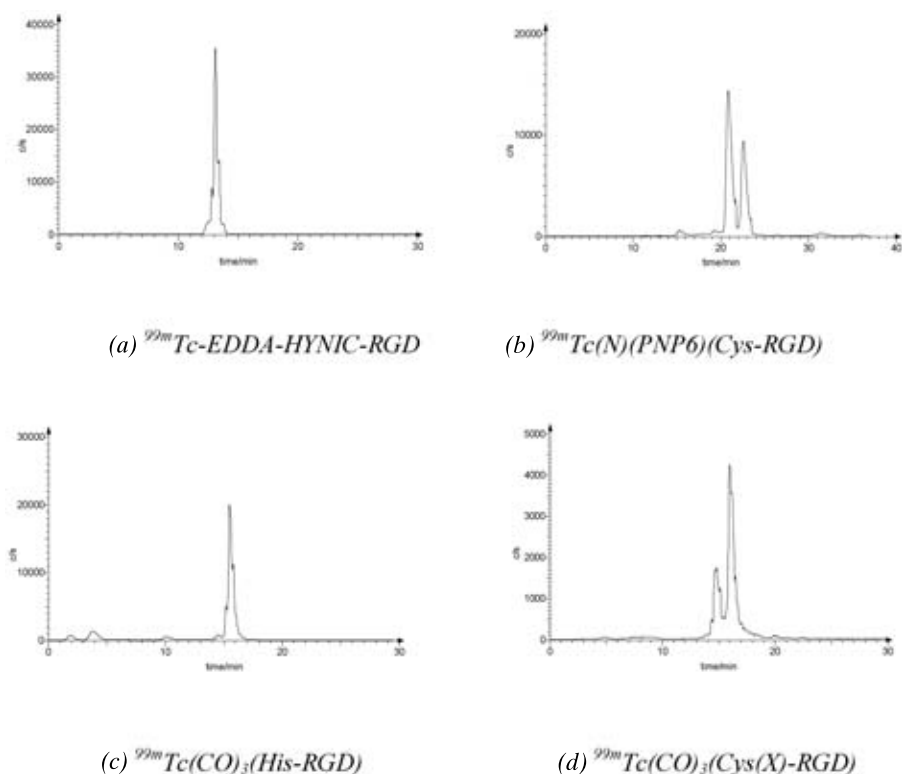


FIG. 4.2. HPLC chromatograms of  $^{99m}\text{Tc}$  labelled RGD peptide.

#### 4.3.1.1. *In vitro* stability

*In vitro* stability studies revealed that  $^{99m}\text{Tc(N)(PNP6)(Cys-RGD)}$  and  $^{99m}\text{Tc-EDDA-HYNIC-RGD}$  had good stability either in solution, at room temperature or in calf serum (Figs 4.3 and 4.4). After incubation in calf serum at  $37^\circ\text{C}$  for at least 4 h, there was no significant change of labelling yield for purified  $^{99m}\text{Tc(N)(PNP6)(Cys-RGD)}$  or  $^{99m}\text{Tc-EDDA-HYNIC-RGD}$  monitored by radio-HPLC. In contrast,  $^{99m}\text{Tc(CO)}_3(\text{Cys(X)-RGD})$  and  $^{99m}\text{Tc(CO)}_3(\text{His-RGD})$  showed a more rapid dissociation after purification by the SPE method. The labelling yield decreased from 96.1% to 89.5% at 3 h for  $^{99m}\text{Tc(CO)}_3(\text{Cys(X)-RGD})$  and from 92.0% to 86.4% at 2 h for  $^{99m}\text{Tc(CO)}_3(\text{His-RGD})$  when reconstituted in saline at room temperature (Fig. 4.3). Therefore,  $^{99m}\text{Tc(CO)}_3(\text{Cys(X)-RGD})$  and  $^{99m}\text{Tc(CO)}_3(\text{His-RGD})$  were not used for further biological evaluation.

## CHAPTER 4

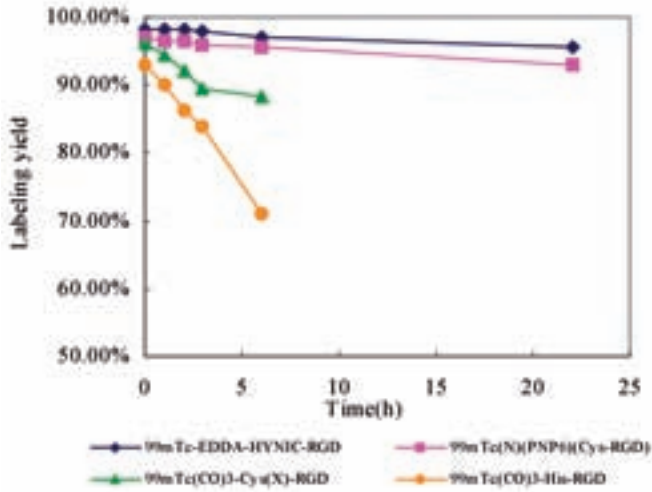


FIG. 4.3. Stability of  $^{99m}\text{Tc}$  labelled RGD peptides purified and reconstituted in saline.

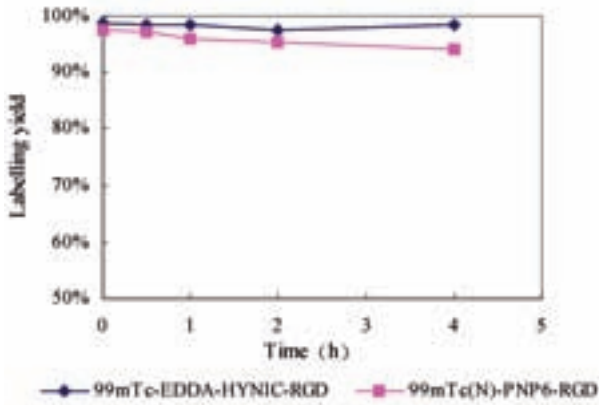


FIG. 4.4. Stability of  $^{99m}\text{Tc}$  labelled RGD peptides in calf serum.

### 4.3.2. Biodistribution studies

Biodistribution studies were performed to explore the in vivo behaviour of  $^{99m}\text{Tc(N)(PNP6)(Cys-RGD)}$  and  $^{99m}\text{Tc-EDDA-HYNIC-RGD}$  in nude BALB/c mice bearing FWK-1 pancreatic tumour xenografts. The biodistribution data are summarized in Tables 4.3 and 4.4. In general, both radiotracers

TABLE 4.3. BIODISTRIBUTION DATA FOR  $^{99m}\text{Tc}$ -EDDA-HYNIC-RGD IN NUDE MICE BEARING TUMOUR XENOGRAPHS (MEAN  $\pm$  SD,  $N = 3$ )

	% ID/g	
	1 h	4 h
Heart	0.51 $\pm$ 0.07	0.56 $\pm$ 0.15
Liver	1.46 $\pm$ 0.01	1.92 $\pm$ 0.28
Spleen	1.27 $\pm$ 0.23	1.65 $\pm$ 0.53
Lung	1.2 $\pm$ 0.48	0.95 $\pm$ 0.33
Kidney	2.92 $\pm$ 0.51	3.11 $\pm$ 0.67
Blood	0.35 $\pm$ 0.01	0.17 $\pm$ 0.03
Stomach	1.86 $\pm$ 0.13	2.21 $\pm$ 0.66
Intestine	1.69 $\pm$ 0.48	2.36 $\pm$ 0.90
Muscle	0.48 $\pm$ 0.07	0.62 $\pm$ 0.17
Tumour	1.34 $\pm$ 0.08	1.06 $\pm$ 0.12
Tumour/blood ratio	3.70 $\pm$ 0.1	6.80 $\pm$ 0.1

TABLE 4.4. BIODISTRIBUTION DATA FOR  $^{99m}\text{Tc}$ (N)(PNP6)(Cys-RGD) IN NUDE MICE BEARING TUMOUR XENOGRAPHS (MEAN  $\pm$  SD,  $N = 3$ )

	% ID/g	
	1 h	4 h
Heart	1.35 $\pm$ 0.42	0.53 $\pm$ 0.07
Liver	3.51 $\pm$ 1.21	3.24 $\pm$ 0.39
Spleen	2.24 $\pm$ 0.53	1.33 $\pm$ 0.29
Lung	2.97 $\pm$ 0.83	1.03 $\pm$ 0.12
Kidney	7.97 $\pm$ 1.43	4.96 $\pm$ 0.51
Blood	2.09 $\pm$ 0.84	0.09 $\pm$ 0.01
Stomach	3.23 $\pm$ 0.14	1.64 $\pm$ 0.34
Intestine	3.41 $\pm$ 0.49	3.06 $\pm$ 1.06
Muscle	0.65 $\pm$ 0.30	0.37 $\pm$ 0.13
Tumour	2.92 $\pm$ 0.71	1.08 $\pm$ 0.15
Tumour/blood ratio	1.50 $\pm$ 0.1	11.0 $\pm$ 0.6

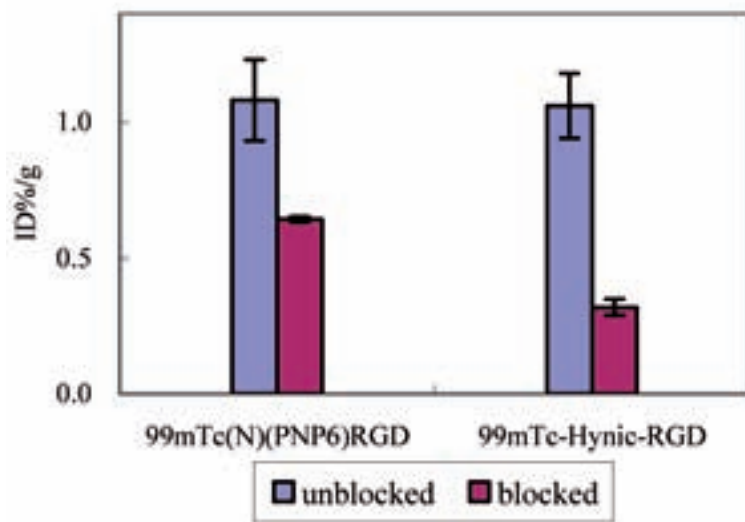


FIG. 4.5. Comparison of the tumour uptake (% ID/g) for  $^{99m}\text{Tc}\text{-EDDA-HYNIC-RGD}$  and  $^{99m}\text{Tc}(\text{N})(\text{PNP6})(\text{Cys-RGD})$  at 24 min post-injection in the absence/presence of excess cyclic RGDfK.

displayed a rapid clearance via the renal route. Uptakes in non-target organs such as liver and intestine were considerable. Tumour uptake was 1.06% ID/g ( $^{99m}\text{Tc}\text{-EDDA-HYNIC-RGD}$ ) or 1.08% ID/g [ $^{99m}\text{Tc}(\text{N})(\text{PNP6})(\text{Cys-RGD})$ ] at 1 h post-injection, and the tumour/blood ratio was 6.8 and 11.0 at 4 h post-injection, respectively. In blocking experiments, activity accumulation in the tumours was substantially reduced to about one half of that found in non-blocking experiments (Fig. 4.5). This suggests that uptakes were tumour specific. Planar gamma imaging allowed well contrasted visualization of  $\alpha_v\beta_3$  expressing tumours at 1 h post-injection (Fig. 4.6).

#### 4.4. CONCLUSION

Several RGD peptide conjugates were successfully radiolabelled with different  $^{99m}\text{Tc}$  cores. Unfortunately, Cys(X)-RGD and His-RGD labelled with  $^{99m}\text{Tc}(\text{CO})_3$  were not satisfactory in terms of their in vitro stability. Biodistribution studies showed that accumulation of  $^{99m}\text{Tc}(\text{CO})_3(\text{Cys(X)-RGD})$  and  $^{99m}\text{Tc}(\text{CO})_3(\text{His-RGD})$  in a nude mice model was in tumours and could be blocked by excess of RGDfK peptide. Planar gamma imaging allowed contrasting visualization of  $\alpha_v\beta_3$  expressed tumours at 1 h post-injection. The

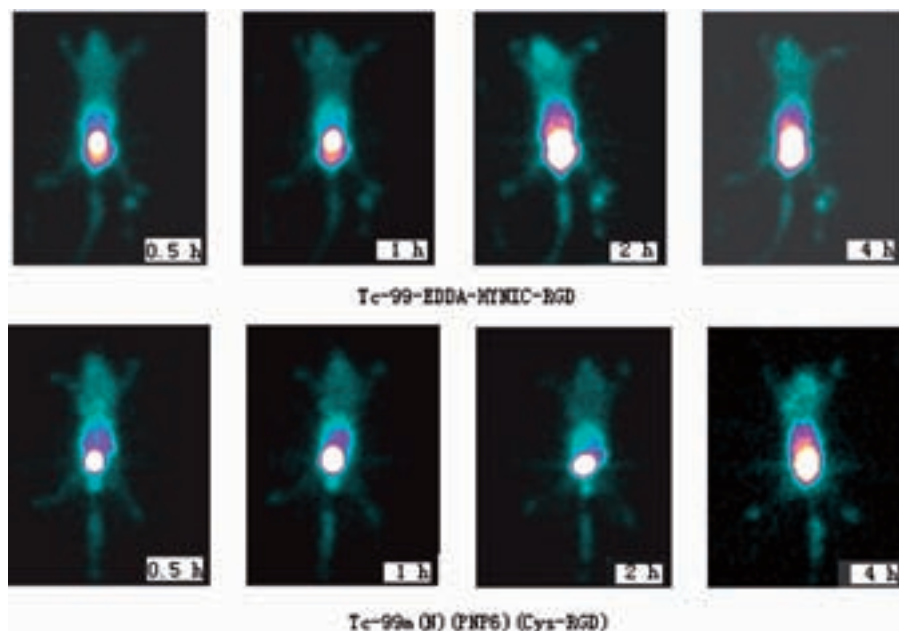


FIG. 4.6. Scintigraphic images of  $^{99m}\text{Tc-EDDA-HYNIC-RGD}$  (top) and  $^{99m}\text{Tc(N)(PNP6)(Cys-RGD)}$  (bottom).

results showed that both the stability and pharmacokinetic behaviour of radiolabelled RGD peptides have to be improved for potential clinical application.

## REFERENCES

- [4.1] RUOSLAHTI, E., PIERSCHBACHER, M.D., New perspectives in cell adhesion: RGD and integrins, *Science* (Washington, D.C.) **238** (1987) 491–497.
- [4.2] BROOKS, P.C., et al., Integrin  $\alpha_v\beta_3$  antagonists promote tumor regression by inducing apoptosis of angiogenic blood vessels, *Cell* **79** (1994) 1157–1164.
- [4.3] ALLMAN, R., COWBURN, P., MASON, M., In vitro and in vivo effects of a cyclic peptide with affinity for the  $\alpha_v\beta_3$  integrin in human melanoma cells, *Eur. J. Cancer* **36** (2000) 410–422.
- [4.4] HAUBNER, R., et al., Glycosylated RGD-containing peptides: Tracer for tumor targeting and angiogenesis imaging with improved biokinetics, *J. Nucl. Med.* **42** (2001) 326–336.
- [4.5] HAUBNER, R., et al., Synthesis and biological evaluation of  $^{99m}\text{Tc}$ -labelled cyclic RGD peptide for imaging the  $\alpha_v\beta_3$  expression, *Nuklearmedizin* **43** (2004) 26–32.

## CHAPTER 4

- [4.6] VAN HAGEN, P.M., et al., Evaluation of a radiolabelled cyclic DTPA-RGD analogue for tumour imaging and radionuclide therapy, *Int. J. Cancer* **90** (2000) 186–198.
- [4.7] SIVOLAPENKO, G.B., et al., Imaging of metastatic melanoma utilising a technetium-99m labelled RGD containing synthetic peptide, *Eur. J. Nucl. Med.* **25** (1998) 1383–1389.
- [4.8] HAUBNER, R., et al., Radiolabeled  $\alpha_v\beta_3$  integrin antagonists: A new class of tracers for tumor targeting, *J. Nucl. Med.* **40** (1999) 1061–1071.
- [4.9] DECRISTOFORO, C., MATHER, S.J., Preparation,  $^{99m}\text{Tc}$ -labelling, and in vitro characterization of HYNIC and  $\text{N}_3\text{S}$  modified RC-160 and  $[\text{Tyr}^3]\text{octreotide}$ , *Bioconj. Chem.* **10** (1999) 431–438.
- [4.10] BOLZATI, C., et al., Chemistry of the strong electrophilic metal fragment  $[\text{}^{99}\text{Tc}(\text{N})(\text{PXP})]^{2+}$  (PXP = diphosphine ligand): A novel tool for the selective labelling of small molecules, *J. Am. Chem. Soc.* **124** (2002) 11468–11479.
- [4.11] ALBERTO, R., et al., A novel organometallic aqua complex of technetium for the labelling of biomolecules: Synthesis of  $[\text{}^{99m}\text{Tc}(\text{OH}_2)_3(\text{CO})_3]^+$  from  $[\text{}^{99m}\text{TcO}_4]^-$  in aqueous solution and its reaction with a bifunctional ligand, *J. Am. Chem. Soc.* **120** (1998) 7987–7988.



## Chapter 5

### **$^{99m}\text{Tc}$ -HYNIC-Anx13: PREPARATION, STABILITY, BIODISTRIBUTION AND IMAGING OF APOPTOSIS**

HONGYU LI, JI HU, JIXIN LIANG, BAOJUN CHEN, JA LU,  
LIANZHE LUO, YANG CHEN, ZHIFU LUO  
Isotope Department, China Institute of Atomic Energy, Beijing, China

#### **Abstract**

The paper describes an annexin V fragment modified with HYNIC (HYNIC-Anx13) and radiolabelled with  $^{99m}\text{Tc}$  using tricine, EDDA or EDDA/tricine as coligands. The effects of various factors on  $^{99m}\text{Tc}$  labelling were investigated. Chromatographic analysis, stability and biodistribution studies in mice and rats, and imaging of apoptosis in rats induced by cyclophosphamide, were performed. The labelled conjugates were stable in aqueous solution and in serum solution *in vitro*, but they were not stable in cysteine solution and *in vivo*. The imaging results were not satisfactory, indicating that HYNIC-Anx13 might not be a promising agent for apoptotic imaging.

#### 5.1. INTRODUCTION

Apoptosis, also known as programmed cell death, is an indispensable component of normal human growth and development, immunoregulation and homeostasis. Apoptosis is nature's primary opponent of cell proliferation and growth. Strict coordination of these two phenomena is essential not only in normal physiology and regulation but also in the prevention of disease [5.1, 5.2].

Programmed cell death causes susceptible cells to undergo a series of stereotypical enzymatic and morphologic changes governed by ubiquitous endogenous biologic machinery encoded by the human genome. In the course of apoptosis, phosphatidylserine (PS) is rapidly exposed on the cell's outer surface. Annexin V, an endogenous human protein, has a high affinity for membrane bound PS. *In vitro* cell binding studies have demonstrated a 20-fold increase in annexin concentration in cells undergoing apoptosis compared with control cells. Annexin V, therefore, is a sensitive marker of the early to intermediate phases of apoptosis. Recently, radiolabelled annexin V has received increasing interest for detecting apoptosis *in vivo* [5.1–5.3]. Particularly,  $^{99m}\text{Tc}$

labelled annexin V has been developed and successfully utilized in clinical trials [5.4].

HYNIC-Anx13 is an annexin V fragment that has been modified with HYNIC. The sequence of this peptide is as follows:

HYNIC-Ala-Gln-Val-Leu-Arg-Gly-Th-Val-Th-Asp-Phe-Pro-Gly (OH)

In this work we report the  $^{99m}\text{Tc}$  labelling of HYNIC-Anx13 with different coligands to stabilize the radio complex and preliminary biological evaluation in animals as a potential agent for apoptotic imaging.

## 5.2. MATERIALS AND METHODS

HYNIC-Anx13 was obtained from J. Környei, Institute of Isotopes Co. Ltd, Budapest. Other chemicals obtained from commercial sources were reagent grade and were used without further purification.

### 5.2.1. Radiolabelling of technetium-99m

#### 5.2.1.1. *Tricine as a coligand*

In a rubber sealed vial, 10  $\mu\text{L}$  of HYNIC-Anx13 solution (1 mg/mL in acetate buffer, pH4.6) was incubated with 150  $\mu\text{L}$  of tricine solution (100 mg/mL in 25mM succinate buffer, pH5.0), 5–10  $\mu\text{L}$  of  $\text{SnCl}_2 \cdot 2\text{H}_2\text{O}$  solution (5–12 mg/mL in 0.1N HCl purged with  $\text{N}_2$ ), 1 mL of 0.07M, pH7.2, PBS and 0.1–0.5 mL of  $^{99m}\text{TcO}_4^-$  (74–740 MBq/mL) for 30 min at room temperature.

#### 5.2.1.2. *EDDA as a coligand*

In a rubber sealed vial, 10  $\mu\text{L}$  of HYNIC-Anx13 solution (1 mg/mL in acetate buffer, pH4.6) was incubated with 0.5 mL of EDDA solution (10 mg/mL in 0.07M phosphate buffer, pH7.0), 5–10  $\mu\text{L}$  of  $\text{SnCl}_2 \cdot 2\text{H}_2\text{O}$  solution (0.5–4 mg/mL in 0.1N HCl) and 0.1–0.5 mL of  $^{99m}\text{TcO}_4^-$  (74–740 MBq/mL) for 60 min at room temperature.

#### 5.2.1.3. *Tricine/EDDA as coligands*

In a rubber sealed vial, 10  $\mu\text{L}$  of HYNIC-Anx13 solution (1 mg/mL in acetate buffer, pH4.6) was incubated with 150  $\mu\text{L}$  of tricine solution (100 mg/mL in 25mM succinate buffer, pH5.0), 0.75 mL of EDDA solution (10 mg/mL in

0.07M PBS, pH7.0), 5–10  $\mu\text{L}$  of  $\text{SnCl}_2 \cdot 2\text{H}_2\text{O}$  solution (0.5–4 mg/mL in 0.1N HCl), 0.5 mL of 0.07M PBS (pH7.2) and 0.1–0.5 mL of  $^{99\text{m}}\text{TcO}_4^-$  (74–740 MBq/mL) for 60 min at room temperature.

## 5.2.2. Quality control

### 5.2.2.1. Thin layer chromatography

Instant thin layer chromatography on silica gel (ITLC-SG, Gelman Sciences) was performed using different mobile phases. Methyl ethyl ketone (MEK) was used to determine the amount of  $^{99\text{m}}\text{TcO}_4^-$  (retention factor ( $R_f$ ) = 1.0), while 50% acetonitrile (MeCN) was used to determine  $^{99\text{m}}\text{Tc}$  colloid ( $R_f$  = 0.0).

### 5.2.2.2. HPLC

A Varian solvent module and Raytest radiodetector were used for reverse phase high performance liquid chromatography (HPLC) analysis. A C18 analytical column (Hypersil,  $4.6 \times 250$  mm) with a flow rate of 1 mL/min and ultraviolet (UV) detection at 254 nm were employed together with the following solvent systems:

- (a) Method 1: MeCN/0.1% TFA/water. Gradient: 0–25 min, 0–100% MeCN; 25–28 min, 100% MeCN; 28–32 min, 100–0% MeCN.
- (b) Method 2: MeCN/0.1% TFA/water. Gradient: 0–3 min, 0–0% MeCN; 3–23 min, 0–80% MeCN; 23–24 min, 80% MeCN; 24–28 min, 80–0% MeCN.
- (c) Method 3: MeCN/0.01M phosphate buffer, pH6. Gradient: 0–3 min, 0% MeCN; 3–23 min, 0–80% MeCN; 23–24 min, 80% MeCN; 24–28 min, 80–0% MeCN.

### 5.2.2.3. Sep-Pak purification procedure

A C18 Sep-Pak Mini cartridge (Waters) was activated using 5 mL of ethanol, followed by 5 mL of water and 5 mL of air. The radiolabelled mixture was passed through the cartridge, which was then washed with 5 mL of water. The radiolabelled peptide was eluted with MeCN and the organic solvent evaporated under a flow of nitrogen.

### 5.2.3. Stability of radiolabelled peptides

The stability of the radiolabelled peptides in aqueous solution was tested by incubation of the Sep-Pak purified peptide in 0.07M phosphate buffer at 37°C up to 4 h. Stability in cysteine solution was measured by incubation of 0.1 mL of the purified peptide solution with 0.2 mL of 0.01mM, 0.1mM and 1mM cysteine solution, respectively, at 37°C up to 4 h. Stability in calf serum was also measured by incubation of 0.1 mL of the purified peptide solution with 1 mL of serum solution (calf serum: 0.07M PBS (v/v) = 1:100) at 37°C for up to 4 h followed by precipitation of serum protein with MeCN. Degradation of the  $^{99m}\text{Tc}$  complex was assessed by ITLC and HPLC.

In vivo stability was determined after administration of the radiolabelled peptides to mice by collecting urine samples, which were subsequently analysed by HPLC.

### 5.2.4. Biodistribution in normal mice

Biodistribution was evaluated after intravenous injection of 740 kBq/0.1 mL of  $^{99m}\text{Tc}$  labelled peptide into normal female Kunming mice. The mice were sacrificed at 10 min, 1 h, 2 h and 4 h post-injection and samples of different organs were dissected and counted. The uptake of the radiolabelled peptide in terms of % injected dose (ID)/g was calculated by reference to standards.

### 5.2.5. Imaging and biodistribution in apoptotic model animals

Young female Sprague–Dawley rats (with an average weight of 166 g) were treated with one dose of 150 mg/kg cyclophosphamide reconstituted in 1 mL of physiologic phosphate buffered saline injected intraperitoneally. Control animals were treated with 1 mL of saline.

Animals were injected in the tail vein with 7.4 MBq/0.2 mL of  $^{99m}\text{Tc}$ -tricine-HYNIC-Anx13 at 1 h (corresponding to 26 h after treatment with cyclophosphamide) and 3.5 h (28 h after treatment), respectively, before imaging and sacrifice. At the time of 15 min before imaging, rats were sedated with ketamine hydrochloride (40 mg/kg) and injected intramuscularly. Data were recorded into a 256 × 256 matrix of a dedicated computer system for digital display and analysis. Zoom in multiple was equal to 1 and collected counts were 200 000 per rat.

Immediately after imaging, the animals were killed for biodistribution assay, and samples of different organs were dissected and counted. The uptake of radiolabelled peptide, in terms of % ID/g, was calculated.

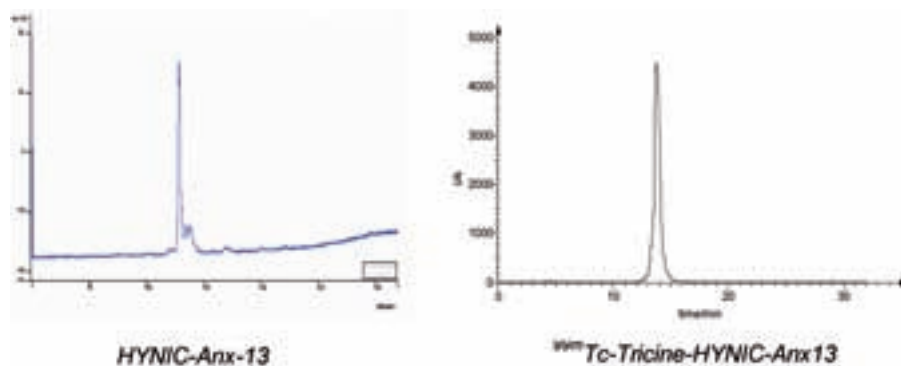


FIG. 5.1. Radiolabelling of HYNIC-Anx13 using tricine as a coligand.

### 5.3. RESULTS AND DISCUSSION

#### 5.3.1. Preparation of $^{99m}\text{Tc}$ -tricine-HYNIC-Anx13 using tricine as a coligand

The labelling yield of the tricine compound was >90% when preparation was carried out at both pH6.1 and pH7.2, but there was a significant increase of  $^{99m}\text{TcO}_4^-$  formation when the pH was pH5.0.

Using method 1, retention times of HYNIC-Anx13 and  $^{99m}\text{Tc}$ -tricine-HYNIC-Anx13 were 12.9 min and 13.8 min, respectively (Fig. 5.1). Using method 2, retention times of HYNIC-Anx13 and  $^{99m}\text{Tc}$ -tricine-HYNIC-Anx13 were 16.0 min and 16.7 min, respectively.

#### 5.3.2. Preparation of $^{99m}\text{Tc}$ -EDDA-HYNIC-Anx13 using EDDA as a coligand

Using EDDA as a coligand, the labelling yield could be improved by heating the reaction mixture in boiling water [5.5]. Considering that higher temperatures may influence the stability of the peptide (data not presented here), the condition of reaction carried out for 1 h at room temperature was preferred. The effect of pH was investigated, and the labelling yield was higher at pH7.0 than at pH6.1.

When EDDA was used as a coligand, the labelling yield was mainly influenced by the concentration of stannous chloride in the labelling solution. The effect of reducing agent on the labelling yield was investigated with various concentrations of stannous chloride, while the amount of EDDA, Anx13 and  $^{99m}\text{TcO}_4^-$  was kept constant. The results are summarized in Table 5.1. Our results of radiolabelling were basically in accordance with the findings of

TABLE 5.1. LABELLING YIELDS OF  $^{99m}\text{Tc}$ -EDDA-HYNIC-Anx13 (EDDA AS A COLIGAND) USING DIFFERENT AMOUNTS OF STANNOUS CHLORIDE

$\text{SnCl}_2 \cdot 2\text{H}_2\text{O}$ ( $\mu\text{g}$ )	5–20	25	60	200
Labelling yield (%)	72.0	57.4	20.9	10.8

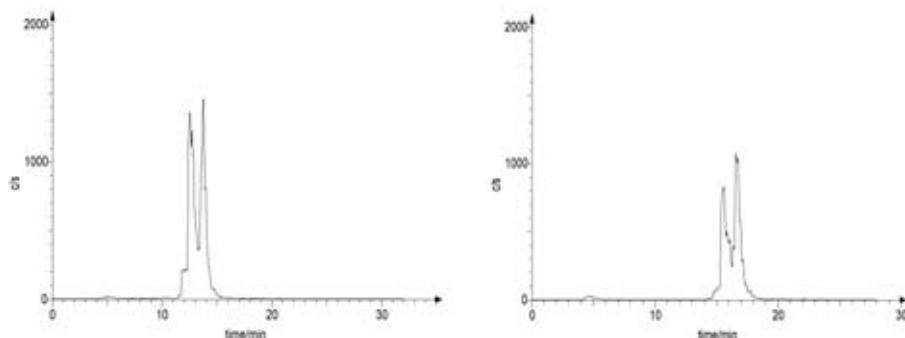


FIG. 5.2.  $^{99m}\text{Tc}$ -EDDA-HYNIC-Anx13 (left: method 1; right: method 2).

Shuang [5.8] and Decristoforo [5.5]. ITLC analysis showed that with an increase in stannous chloride from 5  $\mu\text{g}$  to 200  $\mu\text{g}$  the presence of  $^{99m}\text{TcO}_4^-$  decreased, while  $^{99m}\text{Tc}$  colloid only slightly increased. On the other hand, HPLC analysis showed a rapid decline in labelling yield when increasing the amount of stannous ions. This result suggested that the increase in stannous chloride only accelerated the formation of  $^{99m}\text{Tc}$ -EDDA, which actually hindered the formation of  $^{99m}\text{Tc}$ -EDDA-HYNIC-Anx13.

An average yield of 72% was obtained when the amount of stannous chloride was 5–20  $\mu\text{g}$ . Since EDDA gave consistently lower labelling yields, Sep-Pak purification was performed after each preparation. Retention times of  $^{99m}\text{Tc}$ -EDDA-HYNIC-Anx13 were 12.6 min and 13.7 min using a gradient as detailed in method 1, and 15.7 min and 16.7 min using a gradient as detailed in method 2 (Fig. 5.2).

### 5.3.3. Technetium-99m labelling of HYNIC-Anx13 using EDDA/tricine as coligands

When EDDA/tricine were used as coligands, the labelling yields were still mainly influenced by the concentration of stannous chloride in the labelling

TABLE 5.2. LABELLING YIELDS OF HYNIC-Anx13 (EDDA/TRICINE AS A COLIGAND) USING DIFFERENT AMOUNTS OF STANNOUS CHLORIDE

SnCl <sub>2</sub> ·2H <sub>2</sub> O (μg)	10	20	120	400
Labelling yield (%)	98.4	94.7	60.6	35.2

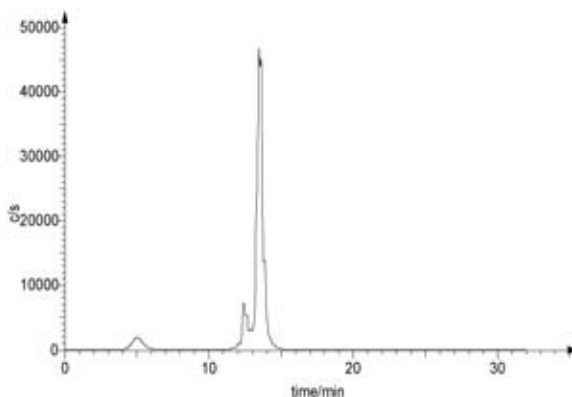


FIG. 5.3. Technetium-99m labelling of HYNIC-Anx13 using EDDA/tricine as coligands (method 1).

solution. With an increase in stannous chloride from 10 μg to 400 μg, the labelling yield declined rapidly from 98% to 35%. The retention time of the product peak was 13.8 min (Fig. 5.3, method 1). The results are summarized in Table 5.2.

HPLC elution profiles were dependent on the pH of the mobile phase employed. As described by Shuang [5.8] and Decristoforo [5.5], labelled HYNIC conjugates with various coligands could be better distinguished by HPLC using a phosphate buffer gradient than using TFA.

In previous experiments, retention times were similar for all <sup>99m</sup>Tc labelled HYNIC-Anx13 conjugates using TFA gradient. In order to achieve a better distinction between different labelled peptide conjugates, samples of labelled conjugates were analysed by HPLC using a phosphate buffer gradient.

When using a phosphate buffer gradient (method 3), the HPLC profile of HYNIC-Anx13 was quite different from that using TFA gradient. <sup>99m</sup>Tc-tricine-HYNIC-Anx13 has a cluster of peaks with retention times of ~15.2 min, and two main peaks with retention times of ~14.2 min were observed for the

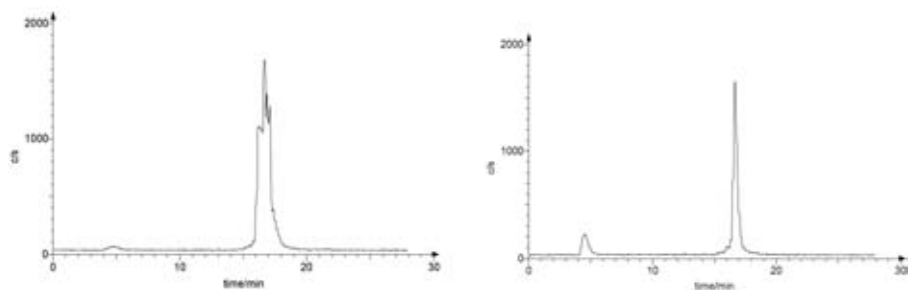


FIG. 5.4. Stability in PBS (0.07M, pH7.2) at 37°C for 5 h (left:  $^{99m}\text{Tc}$ -tricine-HYNIC-Anx13, right:  $^{99m}\text{Tc}$ -EDDA-HYNIC-Anx13).

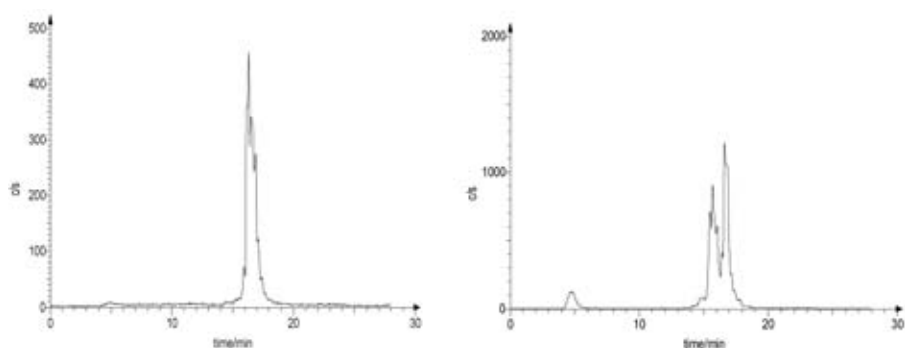


FIG. 5.5. Stability in calf serum at 37°C for 4 h (left:  $^{99m}\text{Tc}$ -tricine-HYNIC-Anx13, right:  $^{99m}\text{Tc}$ -EDDA-HYNIC-Anx13).

labelled conjugate using EDDA as a coligand, which is identical to that using EDDA/tricine as coligands.

### 5.3.4. Stability in vivo and in vitro

$^{99m}\text{Tc}$ -tricine-HYNIC-Anx13 remained stable in aqueous solution and in PBS (0.07M, pH7.2) at 37°C up to 5 h. In contrast, after incubation of purified  $^{99m}\text{Tc}$ -EDDA-HYNIC-Anx13 in PBS (0.07M, pH7.2) up to 5 h, the radiochemical purity declined from 95.6% to 83.1% (Fig. 5.4, method 2).

HPLC analysis of the MeCN fraction of  $^{99m}\text{Tc}$ -tricine-HYNIC-Anx13 after 4 h of incubation in calf serum showed no degradation, while with  $^{99m}\text{Tc}$ -EDDA-HYNIC-Anx13 approximately 6.8% of radioactivity was dissociated as compared with the original complex (Fig. 5.5, method 2).

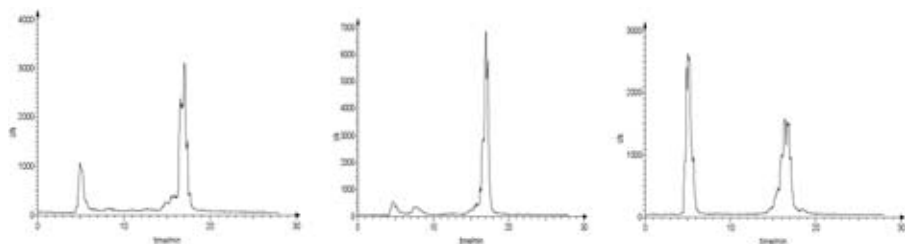


FIG. 5.6. Stability in experiments of challenge with cysteine (from left to right:  $^{99m}\text{Tc}$ -tricine-HYNIC-Anx13 in 0.01mM, 0.1mM, 1mM cysteine solution at 37°C for 4 h).

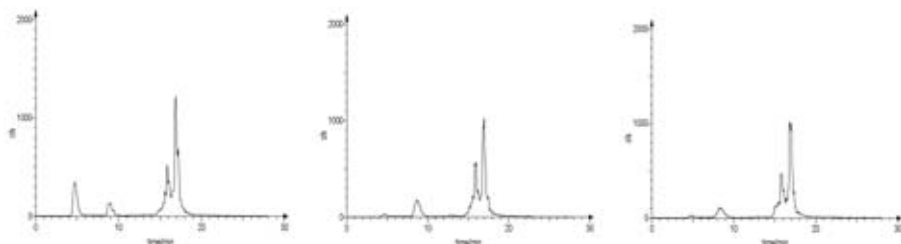


FIG. 5.7. Stability in experiments of challenge with cysteine (from left to right:  $^{99m}\text{Tc}$ -EDDA-HYNIC-Anx13 in 0.01mM, 0.1mM, 1mM cysteine solution at 37°C for 4 h).

Challenge experiments, with 0.01mM, 0.1mM and 1mM cysteine solution at 37°C up to 4 h, showed 20–50% of transchelation for  $^{99m}\text{Tc}$ -tricine-HYNIC-Anx13 (Fig. 5.6) and 10–13% of transchelation for  $^{99m}\text{Tc}$ -EDDA-HYNIC-Anx13, respectively (Fig. 5.7).

Analysis of mouse urine by HPLC at 1 h after injection showed one major species excreted in the urine for both  $^{99m}\text{Tc}$ -tricine-HYNIC-Anx13 and purified  $^{99m}\text{Tc}$ -EDDA-HYNIC-Anx13. The retention times were significantly lower than those of the original injected conjugates (Fig. 5.8). This indicated that these  $^{99m}\text{Tc}$  labelled conjugates were not stable enough in vivo, and some metabolism may occur with conversion of these conjugates to more hydrophilic metabolites.

### 5.3.5. Biodistribution in normal mice

The results of the biodistribution study of  $^{99m}\text{Tc}$ -tricine-HYNIC-Anx13 in normal mice are summarized in Table 5.3.  $^{99m}\text{Tc}$ -tricine-HYNIC-Anx13 was rapidly cleared from the blood. Excretion via the urinary system was also observed.

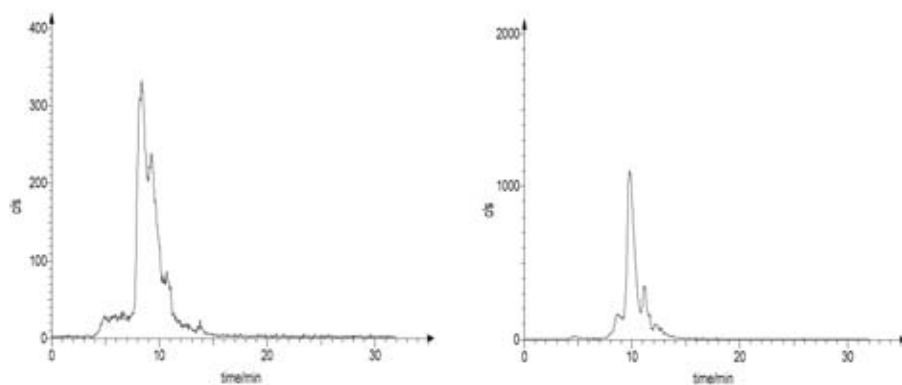


FIG. 5.8. Metabolite analysis in urine collected at 1 h post-injection in normal mice (left:  $^{99m}\text{Tc}$ -tricine-HYNIC-Anx13, right:  $^{99m}\text{Tc}$ -EDDA-HYNIC-Anx13).

TABLE 5.3. BIODISTRIBUTION STUDY OF  $^{99m}\text{Tc}$ -TRICINE-HYNIC-Anx13 IN NORMAL MICE (% ID/g  $\pm$  SD;  $N = 3$ )

	Time after injection (min)			
	10	60	120	240
Heart	$3.08 \pm 0.31$	$0.62 \pm 0.04$	$0.44 \pm 0.04$	$0.28 \pm 0.04$
Liver	$3.78 \pm 0.26$	$1.67 \pm 0.20$	$1.38 \pm 0.05$	$0.81 \pm 0.07$
Spleen	$1.82 \pm 0.37$	$0.45 \pm 0.05$	$0.35 \pm 0.04$	$0.32 \pm 0.06$
Lung	$5.24 \pm 0.67$	$1.04 \pm 0.16$	$0.69 \pm 0.09$	$0.43 \pm 0.05$
Kidney	$19.71 \pm 1.2$	$5.87 \pm 1.01$	$5.07 \pm 0.09$	$2.52 \pm 0.06$
Blood	$8.22 \pm 1.00$	$1.13 \pm 0.10$	$0.73 \pm 0.06$	$0.40 \pm 0.04$
Stomach	$2.84 \pm 0.07$	$0.83 \pm 0.09$	$0.67 \pm 0.12$	$0.40 \pm 0.08$
Small intestine	$2.94 \pm 0.49$	$0.75 \pm 0.06$	$0.51 \pm 0.06$	$0.40 \pm 0.08$
Muscle	$2.10 \pm 0.15$	$0.35 \pm 0.04$	$0.30 \pm 0.02$	$0.16 \pm 0.02$

### 5.3.6. Biodistribution and radionuclide imaging in model animals

A single dose of cyclophosphamide can induce intramedullary apoptosis mainly in rodent bone marrow and spleen. Splenic weights usually decrease after the treatment. It has been reported that apoptosis can be detected in young adult rats as early as 8 h after cyclophosphamide administration, peaks and reaches a plateau at 24 h, and falls slightly at 72 h [5.3].

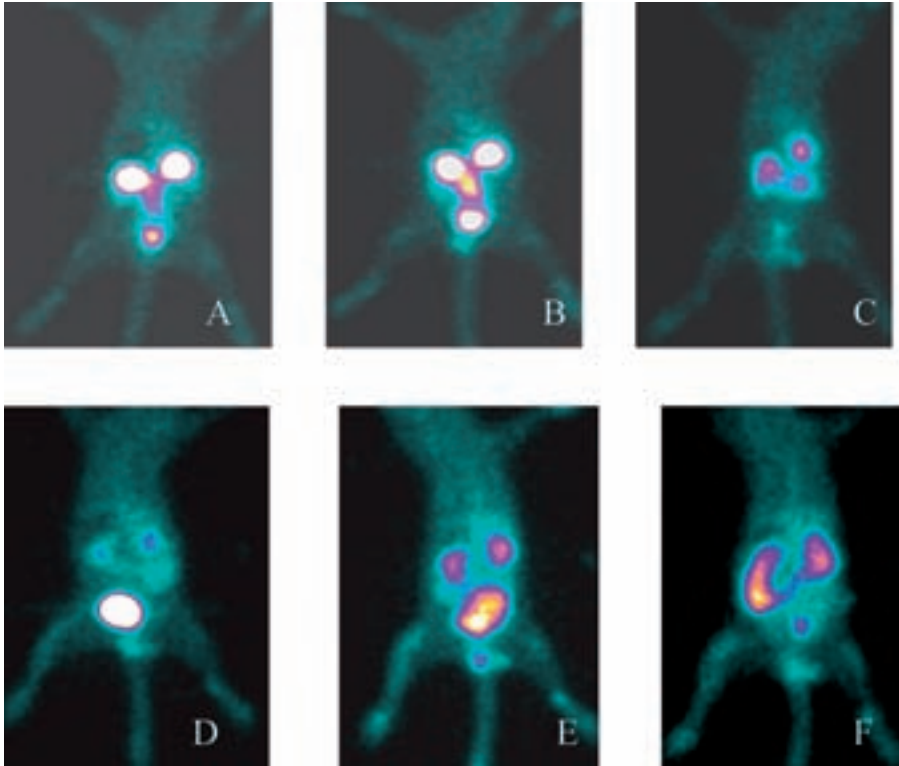


FIG. 5.9. Scintigraphic images of  $^{99m}\text{Tc}$ -tricine-HYNIC-Anx13 in rats (treated, A: 0.5 h post-injection, B: 1.5 h post-injection, C: 3 h post-injection; control, D: 0.5 h post-injection, E: 1.5 h post-injection, F: 3 h post-injection).

Radionuclide images of treated rats and control rats at 1 h (corresponding to 26 h after treatment with cyclophosphamide) and at 3.5 h (28 h after treatment with cyclophosphamide) after injection of  $^{99m}\text{Tc}$ -tricine-HYNIC-Anx13 are shown in Fig. 5.9.

The images show that the uptake of activity was primarily concentrated in the kidneys and bladder, which suggested that radioactivity was mainly cleared through the kidneys. This result was in accordance with that of biodistribution studies in normal mice. Since the rat spleen was superimposed over the left kidney on radionuclide imaging, the uptake of activity of the spleen was obtained solely from counting of the radioactivity in a well counter. Another common primary target tissue, the femur, did not show any specific uptake. There were no significant differences in femur uptake between model rats and control rats.

TABLE 5.4. COMPARISON OF SPLENIC WEIGHTS

	Splenic weight (mg)			
	1 h (model rat)	1 h (control rat)	3.5 h (model rat)	3.5 h (control rat)
1	239.8	444.7	212.3	357.0
2	249.0	464.7	199.2	360.1
3	248.8	418.6	205.5	362.2
Average	245.9	442.7	205.7	359.8

TABLE 5.5. BIODISTRIBUTION OF  $^{99m}\text{Tc}$ -TRICINE-HYNIC-Anx13 IN MODEL RATS (% ID/g  $\pm$  SD;  $N = 3$ )

	Time after injection (h)			
	1 h (model rat)	1 h (control rat)	3.5 h (model rat)	3.5 h (control rat)
Heart	0.09 $\pm$ 0.02	0.06 $\pm$ 0.01	0.06 $\pm$ 0.02	0.05 $\pm$ 0.00
Liver	0.21 $\pm$ 0.04	0.14 $\pm$ 0.00	0.19 $\pm$ 0.04	0.11 $\pm$ 0.00
Spleen	0.15 $\pm$ 0.03	0.07 $\pm$ 0.01	0.16 $\pm$ 0.01	0.07 $\pm$ 0.01
Lung	0.21 $\pm$ 0.06	0.13 $\pm$ 0.03	0.13 $\pm$ 0.02	0.10 $\pm$ 0.00
Kidney	3.81 $\pm$ 0.21	1.13 $\pm$ 0.10	2.09 $\pm$ 0.60	1.35 $\pm$ 0.23
Blood	0.23 $\pm$ 0.05	0.17 $\pm$ 0.02	0.15 $\pm$ 0.01	0.11 $\pm$ 0.01
Stomach	0.26 $\pm$ 0.11	0.10 $\pm$ 0.01	0.13 $\pm$ 0.03	0.08 $\pm$ 0.02
Small intestine	0.52 $\pm$ 0.28	0.12 $\pm$ 0.01	0.11 $\pm$ 0.02	0.09 $\pm$ 0.02
Skeletal muscle	0.06 $\pm$ 0.00	0.05 $\pm$ 0.01	0.07 $\pm$ 0.01	0.04 $\pm$ 0.01
Femur	0.17 $\pm$ 0.01	0.11 $\pm$ 0.01	0.16 $\pm$ 0.00	0.08 $\pm$ 0.01

The comparison of splenic weights between model rats and control rats at 1 h (corresponding to 26 h after treatment with cyclophosphamide) and at 3.5 h (corresponding to 28 h after treatment with cyclophosphamide) after injection of  $^{99m}\text{Tc}$ -tricine-HYNIC-Anx13 is shown in Table 5.4. The results of the biodistribution study at 1 h and 3.5 h after injection of  $^{99m}\text{Tc}$ -tricine-HYNIC-Anx13 are summarized in Table 5.5.

Although higher radioactive uptakes of spleen and femur in model rats than in control rats were observed, this advantage was not predominant as compared with background uptake. Tumour/non-tumour, for example spleen/blood and femur/muscle, was relatively low.

## 5.4. CONCLUSION

Annexin V fragment Anx-13 was modified with HYNIC and labelled with  $^{99m}\text{Tc}$  using tricine and EDDA as coligands. The stability studies suggested that  $^{99m}\text{Tc}$ -tricine-HYNIC-Anx13 and purified  $^{99m}\text{Tc}$ -EDDA-HYNIC-Anx13 were stable in aqueous solution and also in serum solution, although they were not stable in cysteine solution or in vivo. The results of radionuclide imaging and biodistribution in model rats indicated that  $^{99m}\text{Tc}$ -tricine-HYNIC-Anx13 may not be an ideal imaging agent for imaging apoptosis.

## REFERENCES

- [5.1] FRANCIS, G.B., JONATHAN, F.T., WILLIAM STRAUSS, H., Apoptotic cell death: Its implication for imaging in the next millennium, *Eur. J. Nucl. Med.* **27** (2000) 359–367.
- [5.2] FRANCIS, G.B., et al., Imaging of apoptosis (programmed cell death) with  $^{99m}\text{Tc}$  annexin V, *J. Nucl. Med.* **40** (1999) 184–191.
- [5.3] FRANCIS, G.B., et al., Imaging cyclophosphamide-induced intramedullary apoptosis in rats using  $^{99m}\text{Tc}$ -radiolabelled annexin V, *J. Nucl. Med.* **42** (2001) 309–316.
- [5.4] BERRIT, J.K., et al., Safety, biodistribution, and dosimetry of  $^{99m}\text{Tc}$ - HYNIC-Annexin V, a novel human recombinant annexin V for human application, *J. Nucl. Med.* **44** (2003) 947–952.
- [5.5] DECRISTOFORO, C., STEPHEN, J.M., Preparation,  $^{99m}\text{Tc}$ -labelling, and in vitro characterization of HYNIC and  $\text{N}_3\text{S}$  modified RC-160 and  $[\text{Tyr}^3]$ octreotide, *Bioconj. Chem.* **10** (1999) 431–438.
- [5.6] DECRISTOFORO, C., STEPHEN, J.M.,  $^{99m}\text{Tc}$ -labelled peptide-HYNIC conjugates: Effects of lipophilicity and stability on biodistribution, *Nucl. Med. Biol.* **26** (1999) 389–396.
- [5.7] DECRISTOFORO, C., STEPHEN, J.M., Technetium-99m somatostatin analogues: Effect of labelling methods and peptide sequence, *Eur. J. Nucl. Med.* **26** (1999) 869–876.
- [5.8] SHUANG, L., et al., Labelling a hydrazine nicotinamide-modified cyclic IIb/IIIa receptor antagonist with  $^{99m}\text{Tc}$  using aminocarboxylates as coligands, *Bioconj. Chem.* **7** (1996) 63–71.



## Chapter 6

### PREPARATION AND COMPARATIVE EVALUATION OF TECHNETIUM-99m LABELLED FATTY ACIDS

JI HU, JIXIN LIANG, BAOJUN CHEN, LIANZHE LUO,  
HONGYU LI, LANGTAO SHEN, ZHIFU LUO  
Isotope Department, China Institute of Atomic Energy, Beijing, China

#### Abstract

The aim of the present work was to develop a radiolabelling method of modified fatty acids based on  $^{99m}\text{Tc}$  carbonyl chemistry. Undecanoic acids functionalized with iminodiacetic acid and cysteine were radiolabelled with  $[\text{}^{99m}\text{Tc}(\text{CO})_3(\text{H}_2\text{O})_3]^+$  intermediates, and the radiolabelling conditions were carefully studied. Biodistribution of  $^{99m}\text{Tc}(\text{CO})_3\text{-CYST FAC11}$  and  $^{99m}\text{Tc}(\text{CO})_3\text{-IDA FAC11}$  were performed in normal mice. The two  $^{99m}\text{Tc}$  labelled compounds had similar profile in terms of high initial radioactivity uptake and rapid washout of radiotracers in the heart.  $^{99m}\text{Tc}(\text{CO})_3\text{-IDA FAC11}$  was mainly excreted via the hepatobiliary system, in contrast to  $^{99m}\text{Tc}(\text{CO})_3\text{-CYST FAC11}$ , which was from the urinary system. This may be due to the higher lipophilicity of  $^{99m}\text{Tc}(\text{CO})_3\text{-IDA FAC11}$  than that of  $^{99m}\text{Tc}(\text{CO})_3\text{-CYST FAC11}$ .

#### 6.1. INTRODUCTION

Long chain free fatty acids are the major energy source of the normal myocardium. Approximately 60–80% of adenosine triphosphate (ATP) produced in aerobic myocardium is derived from fatty acid  $\beta$  oxidation [6.1]. The measurement of regional difference in the uptakes and retention of radiolabelled fatty acids using nuclear medicine techniques could provide significant information on myocardium energy metabolism in vivo, and thus could be a valuable approach in diagnoses of several heart diseases [6.2]. A variety of fatty acid analogues radiolabelled with  $^{11}\text{C}$  and  $^{123}\text{I}$  have recently been investigated as useful radiopharmaceuticals for the estimation of myocardial fatty acid metabolism [6.3]. A key example of a diagnostic agent is  $^{123}\text{I}$  labelled 15-(p-iodophenyl)-3-R,S-methylpentadecanoic acid (BMIPP), which has been successfully used in clinics for the early detection of myocardial ischaemia and assessment of the severity of ischaemic heart disease. Considering the excellent

nuclide properties and wide availability of  $^{99m}\text{Tc}$ , development of  $^{99m}\text{Tc}$  labelled long chain fatty acid derivatives has also been pursued in this field [6.4, 6.5].

Recently, a convenient method for preparation of *fac*- $[\text{}^{99m}\text{Tc}(\text{CO})_3(\text{H}_2\text{O})_3]^+$  under normal pressure was developed by Alberto et al. [6.6].  $[\text{}^{99m}\text{Tc}(\text{CO})_3(\text{H}_2\text{O})_3]^+$ , a versatile organometallic precursor, could react with various chelating systems and has been widely used for radiolabelling with  $^{99m}\text{Tc}$  of protein, peptides and small biomolecules [6.7, 6.8]. The successful preparation and excellent biological properties of  $[\text{}^{99m}\text{Tc}(\text{MIBI})_3(\text{CO})_3]^+$  attracted increasing interest in the search for new optimal pharmaceuticals for myocardial metabolic imaging agents [6.9]. In this work, undecanoic acid functionalized with iminodiacetic acid and cysteine were radiolabelled with  $[\text{}^{99m}\text{Tc}(\text{CO})_3(\text{H}_2\text{O})_3]^+$  precursor to test its radiobiological properties in vivo when used as a fatty acid analogue.

## 6.2. MATERIALS

CYST FAC11 (S-cysteine undecanoic acid) and IDA FAC11 [(N, N-di(carboxymethyl) amino undecanoic acid)] were provided by I. Pirmettis, Institute of Radioisotopes and Radiodiagnostic Products, Demokritos National Centre of Scientific Research, Greece. The Isolink kits were from Malinkrodt. Other chemicals obtained from commercial sources were reagent grade and used without further purification.

## 6.3. METHODS

### 6.3.1. Preparation of $[\text{}^{99m}\text{Tc}(\text{CO})_3(\text{H}_2\text{O})_3]^+$ intermediate

$[\text{}^{99m}\text{Tc}(\text{CO})_3(\text{H}_2\text{O})_3]^+$  intermediate was prepared as described by Alberto et al. [6.6]. Typically, a 1.0 mL saline solution containing  $^{99m}\text{TcO}_4^-$  (20–50 mCi, 0.74–1.85 GBq) was added to a 10 mL serum vial containing 4.0 mg  $\text{Na}_2\text{CO}_3$ , 5.5 mg  $\text{NaBH}_4$ , 20 mg Na/K tartrate and 1 atm. carbon monoxide (headspace volume). The mixture was heated for 20 min at 95°C while being shaken periodically and then cooled to room temperature and pH adjusted to pH7.0 with 1.0 mol/L hydrochloric acid.  $[\text{}^{99m}\text{Tc}(\text{CO})_3(\text{H}_2\text{O})_3]^+$  was also prepared from a commercial Isolink kit in accordance with the package insert instructions. The solution was analysed by reverse phase high performance liquid chromatography (HPLC) using a C18 analytical column (Hypersil, 4.6 × 250 mm) with a 0.1% TFA/acetonitrile gradient. The applied gradient was (A: 0.1% TFA in water, B: 0.1% TFA in acetonitrile): 0–5 min, 0% B; 5–15 min, 0–80% B; 15–

30 min, 80% B; 30–32 min, 80–0% B; 32–38 min, 0% B. Chromatography was carried out at a flow rate of 1.0 mL/min. In each HPLC analysis, recovery of the radioactivity was determined by comparing the total activities of all fractions with a standard prepared from the injected solution to verify that no activity remained on the HPLC column.

### 6.3.2. Labelling of CYST FAC11 and IDA FAC11

To a 10 mL serum vial purged with N<sub>2</sub>, 0.1 mL of IDA FAC11 (1.0 mg/mL in aqueous 0.1M phosphate buffer solution) was added followed by 0.2 mL of aliquot of the [<sup>99m</sup>Tc(CO)<sub>3</sub>(H<sub>2</sub>O)<sub>3</sub>]<sup>+</sup> intermediate solution and the mixture was heated at 95°C for 30 min. After cooling to room temperature, the radiotracer was analysed by HPLC using conditions identical to those described above for [<sup>99m</sup>Tc(CO)<sub>3</sub>(H<sub>2</sub>O)<sub>3</sub>]<sup>+</sup> analysis. For improving the radiolabelling yield, the reaction time, temperature, concentrations and pH value of the radiolabelling reactions were optimized. Labelling of CYST FAC11 with [<sup>99m</sup>Tc(CO)<sub>3</sub>(H<sub>2</sub>O)<sub>3</sub>]<sup>+</sup> was carried out using the procedure described above.

### 6.3.3. Purification of radiolabelled products by the SPE method

To facilitate biological assays, the products were purified from <sup>99m</sup>TcO<sub>4</sub><sup>-</sup> [<sup>99m</sup>Tc(CO)<sub>3</sub>(H<sub>2</sub>O)<sub>3</sub>]<sup>+</sup> and other radioactive impurities by solid phase extraction. In short, preparations containing labelled compounds were loaded onto a C18 Sep-Pak Light (Waters) solid phase extraction cartridge, pre-flushed with 10 mL of 1.0 mol/L HCl. After rinsing with another 10 mL of 1.0M HCl until no detectable amount of radioactivity was released from the column, the labelled compounds were eluted in 2.0 mL of methanol, dried with an N<sub>2</sub> stream, reconstituted in saline and filtered through a sterile 0.22 μm Millipore filter. The purity of the products was checked by radio-HPLC analysis.

### 6.3.4. In vitro stability

The in vitro stability of <sup>99m</sup>Tc(CO)<sub>3</sub>-CYST FAC11 and <sup>99m</sup>Tc(CO)<sub>3</sub>-IDA FAC11 was assessed by challenging with cysteine and histidine. 0.1 mL of the complex was placed into 0.2 mL of 10 mmol/L cysteine or histidine in 0.1M phosphate buffer solution, respectively, and then incubated for 30 min, 1 h, 2 h and 3 h at 37°C. After incubation, the percentage dissociation of each complex was determined by radio-HPLC analysis and compared with the sample in saline used as a control.

### 6.3.5. Biodistribution studies in normal mice

The specific pathogen free female Kunming mice (weighing 18–22 g) used for the biodistribution studies were housed with free access to food and water and fasted for 12 h before experiments.  $^{99m}\text{Tc}(\text{CO})_3\text{-CYST FAC11}$  and  $^{99m}\text{Tc}(\text{CO})_3\text{-IDA FAC11}$  in saline solution (0.74–1.10 MBq in 0.1 mL) were administered via the tail vein. At appropriate time points after the administration, the animals were sacrificed by decapitation. Samples of blood and organs of interest were excised and weighed and counted in an NaI (TI) gamma scintillation counter. The results were expressed as % ID/g of blood or organs after decay correction.

## 6.4. RESULTS AND DISCUSSION

### 6.4.1. Radiolabelling

The  $[\text{}^{99m}\text{Tc}(\text{CO})_3(\text{H}_2\text{O})_3]^+$  precursor was prepared reproducibly either using commercial kits or carbon monoxide gas with yields of more than 97% as determined by radio-HPLC analysis.  $^{99m}\text{Tc}(\text{CO})_3\text{-CYST FAC11}$  and  $^{99m}\text{Tc}(\text{CO})_3\text{-IDA FAC11}$  could be formed with yields better than 95% under the described specific conditions. HPLC analysis showed that  $[\text{}^{99m}\text{Tc}(\text{CO})_3(\text{H}_2\text{O})_3]^+$  had been quantitatively transformed into the desired product (Figs 6.1 and 6.2). In the reaction solution, there were mostly the main products (retention times of  $^{99m}\text{Tc}(\text{CO})_3\text{-CYST FAC11}$  and  $^{99m}\text{Tc}(\text{CO})_3\text{-IDA FAC11}$ , 20.3 min and 25.1 min, respectively) apart from a small amount of  $^{99m}\text{TcO}_4^-$  (retention time, 4.6 min) and a negligible amount of  $[\text{}^{99m}\text{Tc}(\text{CO})_3(\text{H}_2\text{O})_3]^+$  (retention time, 7.4 min). Recovery of the radioactivity in HPLC analysis was performed and the results indicated that more than 95% of the activity injected was eluted from the column.

Radiolabelling of two fatty acids was investigated under different conditions, namely pH, ligand concentration and heating time. The experimental results showed that radiolabelling yields were not significantly affected by pH values within the range pH6.8–11 (Fig. 6.3), remaining practically unaltered from pH7.8 to pH9.0. The two radio-complexes could be synthesized with high yields using approximately 50  $\mu\text{g}$  of ligand in each preparation (a lower amount of ligand was not investigated) at 95°C and at pH7.8 (Fig. 6.4). Studies on the influence of temperature on reaction kinetics demonstrated that  $[\text{}^{99m}\text{Tc}(\text{CO})_3(\text{H}_2\text{O})_3]^+$  reacted rapidly with 100  $\mu\text{g}$  of each fatty acid derivative at pH7.8 (Fig. 6.5). After heating at 95°C for 10 min, yields higher than 95% could be attained.

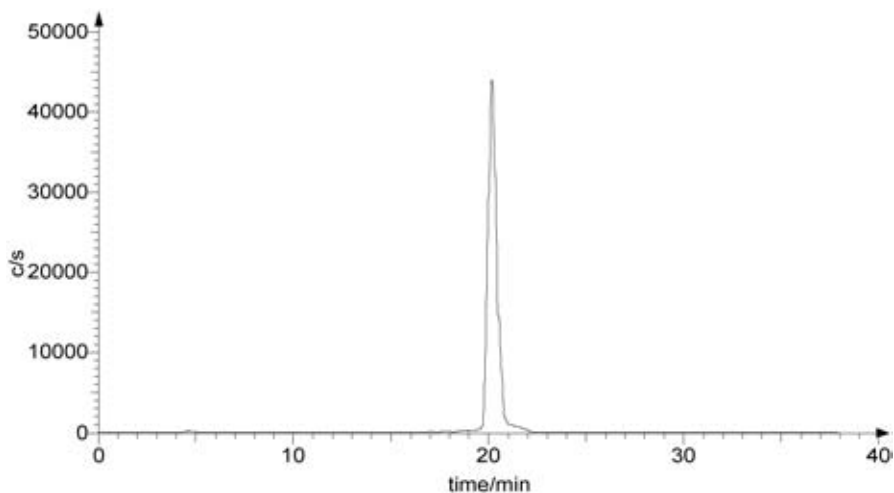


FIG. 6.1. Radio-HPLC chromatograms of  $^{99m}\text{Tc}(\text{CO})_3\text{-CYST FAC11}$ .

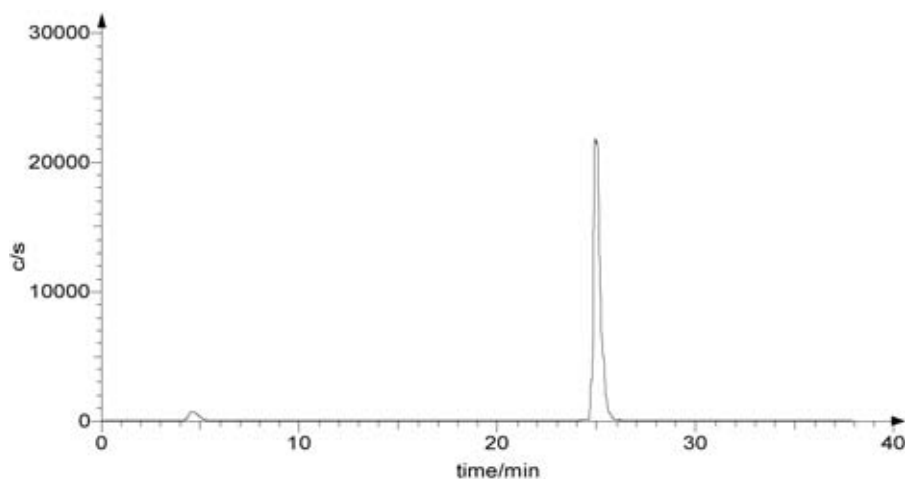


FIG. 6.2. Radio-HPLC chromatograms of  $^{99m}\text{Tc}(\text{CO})_3\text{-IDA FAC11}$ .

#### 6.4.2. In vitro stability

In vitro stability studies revealed that  $^{99m}\text{Tc}(\text{CO})_3\text{-IDA FAC11}$  was more stable than  $^{99m}\text{Tc}(\text{CO})_3\text{-CYST FAC11}$  (Figs 6.6 and 6.7).  $^{99m}\text{Tc}(\text{CO})_3\text{-IDA FAC11}$  remained stable in saline, and no significant degradation was observed up to 3 h when challenged with large excess of histidine and cysteine at  $37^\circ\text{C}$ . In the case of  $^{99m}\text{Tc}(\text{CO})_3\text{-CYST FAC11}$ , the complex showed moderate stability either in saline or in challenging studies.

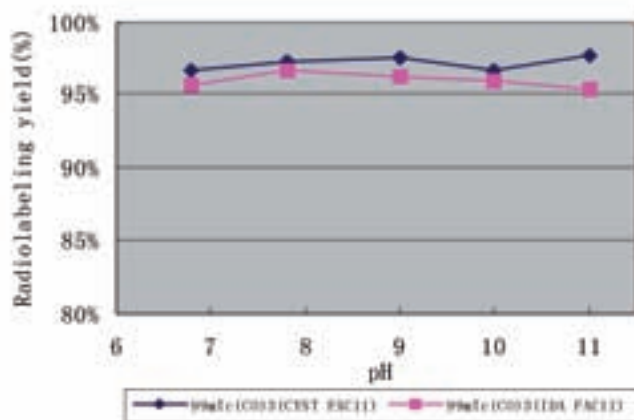


FIG. 6.3. Influence of pH value on the radiolabelling yields of  $^{99m}\text{Tc}(\text{CO})_3\text{-CYST FAC11}$  and  $^{99m}\text{Tc}(\text{CO})_3\text{-IDA FAC11}$  at  $95^\circ\text{C}$ .

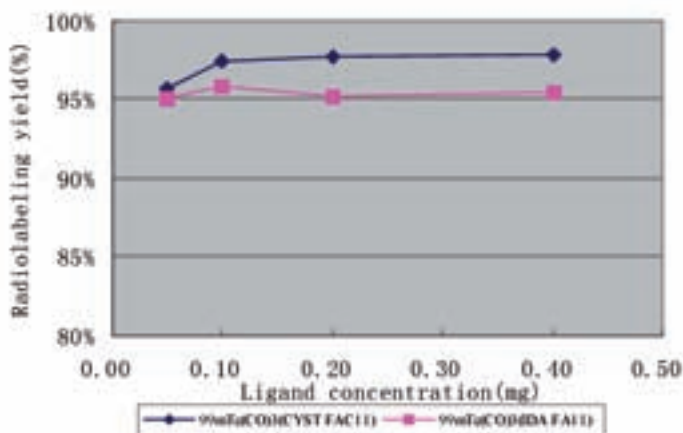


FIG. 6.4. Influence of concentration of ligand on the radiolabelling yields of  $^{99m}\text{Tc}(\text{CO})_3\text{-CYST FAC11}$  and  $^{99m}\text{Tc}(\text{CO})_3\text{-IDA FAC11}$  at  $95^\circ\text{C}$ , pH7.8.

### 6.4.3. Biodistribution

The radiolabelled products used for animal tests were of adequate radiochemical purity. Wherever needed, the product was purified by the SPE method to give only one single species with a radiochemical purity of at least 98% as revealed by radio-HPLC. Biodistribution of  $^{99m}\text{Tc}(\text{CO})_3\text{-CYST FAC11}$

CHAPTER 6

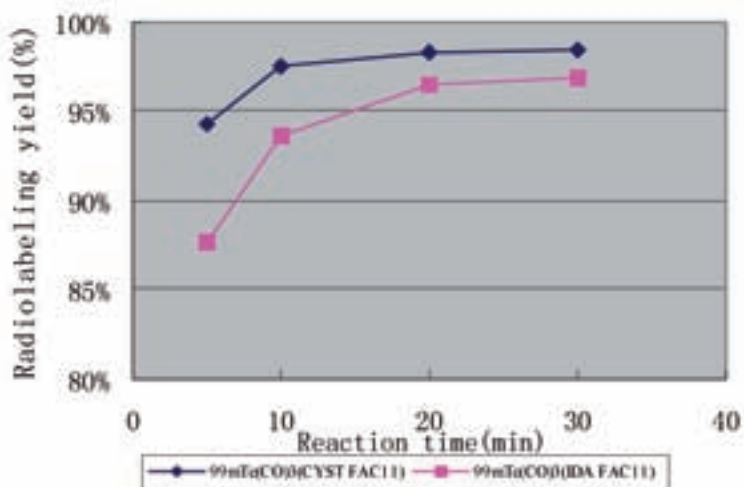


FIG. 6.5. Influence of heating time on the radiolabelling yields of  $^{99m}\text{Tc}(\text{CO})_3\text{-CYST FAC11}$  and  $^{99m}\text{Tc}(\text{CO})_3\text{-IDA FAC11}$  at  $95^\circ\text{C}$ ,  $\text{pH}7.8$ .

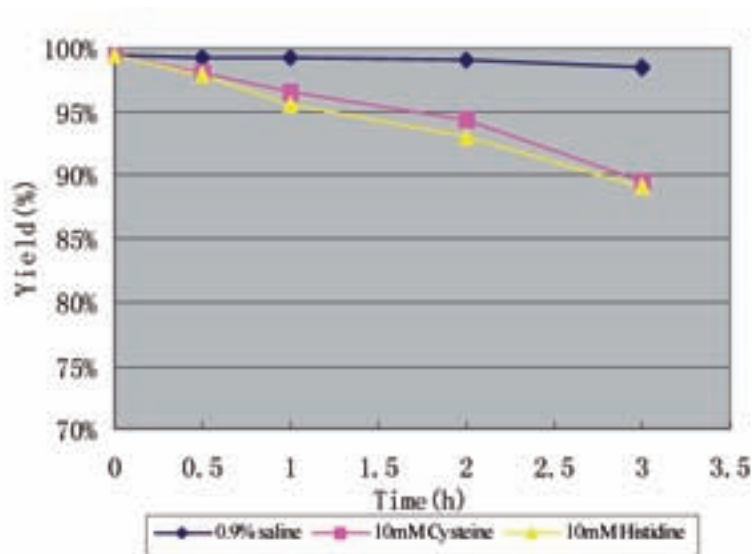


FIG. 6.6. Stability of  $^{99m}\text{Tc}(\text{CO})_3\text{-IDA FAC11}$  in saline, cysteine and histidine solution.

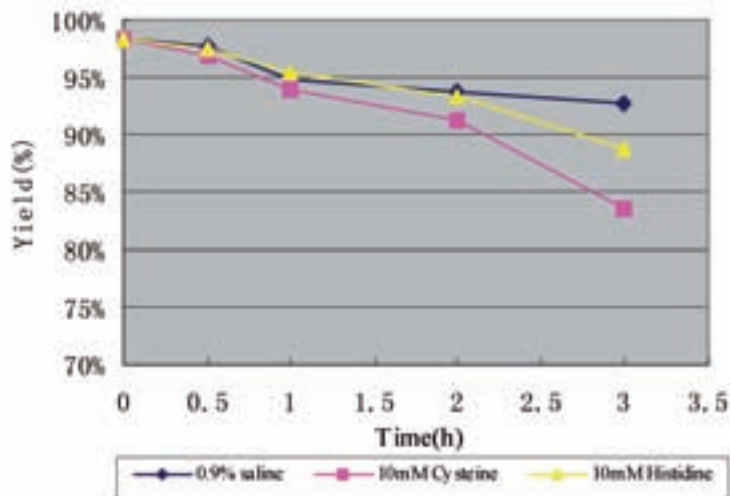


FIG. 6.7. Stability of  $^{99m}\text{Tc}(\text{CO})_3\text{-CYST FAC11}$  in saline, cysteine and histidine solution.

and  $^{99m}\text{Tc}(\text{CO})_3\text{-IDA FAC11}$  was performed in normal mice. Based on the experimental data (Tables 6.1 and 6.2), the two radiolabelled compounds exhibited a similar profile in terms of high radioactivity initial cardiac uptake and rapid washout of these radiotracers from the heart. The uptakes of  $^{99m}\text{Tc}(\text{CO})_3\text{-CYST FAC11}$  and  $^{99m}\text{Tc}(\text{CO})_3\text{-IDA FAC11}$  were 3.11% and 3.44% injected dose (ID)/g at 5 min, dropping to 0.80% and 0.86% ID/g after 30 min, respectively. Meanwhile, the radioactivity in the blood was also cleared rapidly. However, a significant difference could be found in the in vivo elimination of the two radiolabelled compounds. Notably,  $^{99m}\text{Tc}(\text{CO})_3\text{-IDA FAC11}$  was mainly excreted via the hepatobiliary system, whereas  $^{99m}\text{Tc}(\text{CO})_3\text{-CYST FAC11}$  was eliminated mainly through the urinary system. This behaviour could be attributed in part to the higher lipophilicity of  $^{99m}\text{Tc}(\text{CO})_3\text{-IDA FAC11}$  as compared with that of  $^{99m}\text{Tc}(\text{CO})_3\text{-CYST FAC11}$ , and also to the structural difference in the coordination moieties between the two  $^{99m}\text{Tc}$  complexes. The overall results revealed that the two  $^{99m}\text{Tc}$  labelled compounds were not the optimal candidates for myocardial metabolic imaging.

## 6.5. CONCLUSIONS

Radiolabelling of CYST FAC11 and IDA FAC11 could be carried out with high yields using the  $[\text{}^{99m}\text{Tc}(\text{CO})_3(\text{H}_2\text{O})_3]^+$  intermediate under optimized

CHAPTER 6

TABLE 6.1. BIODISTRIBUTION STUDIES OF  $^{99m}\text{Tc}(\text{CO})_3\text{-CYST FAC11}$  IN NORMAL MICE

	Time after intravenous administration (min)			
	5	30	60	120
Blood	7.11 ± 0.15	1.26 ± 0.10	0.80 ± 0.02	0.54 ± 0.05
Heart	3.11 ± 0.44	0.80 ± 0.05	0.50 ± 0.03	0.45 ± 0.09
Liver	30.81 ± 10.4	14.70 ± 2.62	12.53 ± 5.57	6.65 ± 1.81
Spleen	1.96 ± 0.18	0.76 ± 0.07	0.42 ± 0.03	0.37 ± 0.07
Lung	6.13 ± 0.68	2.37 ± 0.22	1.76 ± 0.29	1.37 ± 0.31
Kidney	121.3 ± 11.0	48.00 ± 2.86	17.05 ± 5.13	14.24 ± 4.91
Stomach	1.81 ± 0.11	0.67 ± 0.15	0.63 ± 0.02	0.46 ± 0.06
Intestine	6.23 ± 1.77	2.84 ± 0.35	2.68 ± 1.15	0.58 ± 0.35
Muscle	1.56 ± 0.21	0.49 ± 0.11	0.66 ± 0.18	0.41 ± 0.06

TABLE 6.2. BIODISTRIBUTION STUDIES OF  $^{99m}\text{Tc}(\text{CO})_3\text{-IDA FAC11}$  IN NORMAL MICE

	Time after intravenous administration (min)			
	5	30	60	120
Blood	13.86 ± 1.11	2.15 ± 0.09	1.16 ± 0.15	0.91 ± 0.14
Heart	3.44 ± 0.60	0.86 ± 0.15	0.55 ± 0.07	0.37 ± 0.02
Liver	91.71 ± 7.51	22.00 ± 3.10	10.21 ± 1.38	6.50 ± 1.51
Spleen	3.80 ± 0.23	1.43 ± 0.15	0.95 ± 0.10	1.26 ± 0.12
Lung	6.19 ± 1.92	1.99 ± 0.28	1.23 ± 0.40	0.83 ± 0.06
Kidney	23.32 ± 2.66	7.92 ± 2.73	2.52 ± 0.57	1.21 ± 0.04
Stomach	3.34 ± 1.15	1.92 ± 0.10	2.36 ± 0.75	1.64 ± 0.45
Intestine	10.53 ± 0.97	2.39 ± 0.27	2.37 ± 0.38	1.80 ± 0.96
Muscle	1.10 ± 0.07	0.61 ± 0.11	0.34 ± 0.02	0.47 ± 0.13

conditions. After intravenous administration to normal mice, the experimental results showed that  $^{99m}\text{Tc}(\text{CO})_3\text{-CYST FAC11}$  and  $^{99m}\text{Tc}(\text{CO})_3\text{-IDA FAC11}$  were mainly washed out through the hepatobiliary and urinary systems. Unfortunately, the relative rapid washout of radioactivity from the heart excluded them from use as potential imaging agents for fatty acid metabolisms.

## REFERENCES

- [6.1] LIEDKE, A.J., Alterations of carbohydrate and lipid metabolism in the acutely ischemic heart, *Prog. Cardiovasc. Dis.* **23** (1981) 321–336.
- [6.2] TAMAKI, N., MORITA, K., KUGE, Y., TSUKAMOTO, E., The role of fatty acids in cardiac imaging, *J. Nucl. Med.* **41** (2000) 1525–1534.
- [6.3] KNAPP, F.F., Jr., KROPP, J., Iodine-123-labelled fatty acids for myocardial single-photon emission tomography: Current status and future perspectives, *Eur. J. Nucl. Med.* **22** (1995) 361–381.
- [6.4] JONES, G.S., Jr., ELMALEH, D.R., STRAUSS, H.W., FISCHMAN, A.J., Synthesis and biodistribution of a new <sup>99m</sup>Tc fatty acid, *Nucl. Med. Biol.* **21** (1994) 117–123.
- [6.5] MAGATA, Y., et al., A Tc-99m-labelled long chain fatty acid derivative for myocardial imaging, *Bioconj. Chem.* **15** (2004) 389–393.
- [6.6] ALBERTO, R., ORTNER, K., WHEATLEY, N., SCHIBLI, R., SCHUBIGER, A.P., Synthesis and properties of boranocarbonate: A convenient in situ CO source for the aqueous preparation of [<sup>99m</sup>Tc(OH)<sub>2</sub>]<sub>3</sub>(CO)<sub>3</sub>]<sup>+</sup>, *J. Am. Chem. Soc.* **123** (2001) 3135–3136.
- [6.7] SCHIBLI, R., et al., Influence of the denticity of ligand systems on the in vitro and in vivo behavior of (99m)Tc(I)-tricarbonyl complexes: A hint for the future functionalization of biomolecules, *Bioconj. Chem.* **11** (2000) 345–351.
- [6.8] SCHIBLI, R., SCHUBIGER, P.A., Current use and future potential of organometallic radiopharmaceuticals, *Eur. J. Nucl. Med.* **29** (2002) 1529.
- [6.9] JIANG, Y., LIU, B., A new <sup>99m</sup>Tc labelling complex used for myocardial imaging: [<sup>99m</sup>Tc(CO)<sub>3</sub>(MIBI)<sub>3</sub>]<sup>+</sup>, *Chinese Sci. Bull.* **46** (2001) 727–730 (in Chinese).

## Chapter 7

### TECHNETIUM-99m LABELLING OF AN ANNEXIN FRAGMENT USING THE 4 + 1 MIXED LIGAND CHELATE SYSTEM

J.-U. KÜNSTLER\*, B. PAWELKE\*, A. DUATTI\*\*, J. KÖRNYEI<sup>†</sup>,  
H.-J. PIETZSCH\*

\* Institute of Radiopharmacy,  
Forschungszentrum Dresden–Rossendorf, Germany

\*\* Laboratory of Nuclear Medicine, Department of Clinical  
and Experimental Medicine, University of Ferrara, Italy

<sup>†</sup> Institute of Isotopes Co. Ltd, Budapest, Hungary

#### Abstract

The tridecapeptide AQVLRGTVTDFPG — an annexin fragment — was labelled with <sup>99m</sup>Tc using the 4 + 1 mixed ligand system, in which Tc(III) is coordinated by a monodentate isocyanide and the tetradentate tripodal ligand tris(2-mercaptoethyl)-amine (NS<sub>3</sub>). The tridecapeptide was N-terminally functionalized with the isocyanides 4-isocyanomethylbenzoic acid (L1) and 4-isocyanobutyric acid (L2). Technetium-99m labelling was performed in a two-step procedure using <sup>99m</sup>Tc-EDTA/mannitol as the starting complex, followed by a ligand exchange reaction with a mixture of the isocyanide and the coligand NS<sub>3</sub>. The identity of the <sup>99m</sup>Tc labelled annexin fragments was confirmed by comparison with the high performance liquid chromatography profiles of the analogous rhenium compounds. Stability studies in rats exhibited a rapid metabolism of the labelled annexin fragment. Technetium-99m labelled annexin fragments do not exhibit affinity for apoptotic cells.

#### 7.1. INTRODUCTION

Radiolabelled annexin V has been widely investigated for detection of apoptosis [7.1]. Radiolabelled compounds based on annexin derived peptides have not yet been studied. In this paper we describe the <sup>99m</sup>Tc labelling of the annexin fragment AQVLRGTVTDFPG — a tridecapeptide — using the 4 + 1 mixed ligand system. In vivo stability and cell binding studies were performed.

## 7.2. MATERIALS AND METHODS

### 7.2.1. General

AQVLRGTVTDFPG $\times$ 2TFA (annexin fragment, AF) was obtained from J.K. Környei (Institute of Isotopes Co. Ltd. Hungary). L1-BFCA and Re(NS<sub>3</sub>)(L1-BFCA) were prepared in accordance with Ref. [7.2]. Tris(2-mercaptoethyl)-amine (NS<sub>3</sub>) was synthesized as described in Ref. [7.3]. L2-BFCA was prepared by formylation of 4-amino butyric acid, esterification with 2,3,5,6-tetrafluorphenol and conversion of the formylamino group into the isocyanido group. Re(NS<sub>3</sub>)(L2-BFCA) was obtained by reaction of L2-BFCA with Re(NS<sub>3</sub>)(PMe<sub>2</sub>Ph), which was prepared in accordance with Ref. [7.4].

High performance liquid chromatography (HPLC):

- (a) System 1: Hamilton PRP-1 (10  $\mu$ m, 7  $\times$  305 mm), 2 mL/min; solvent A: acetonitrile with 0.01M NH<sub>3</sub>, solvent B: water with 0.01M NH<sub>3</sub>, gradient elution: 0–20 min, 10–70% A.
- (b) System 2: Phenomenex Jupiter Proteo (4  $\mu$ m, 90 Å, 250  $\times$  10 mm), 3 mL/min; solvent A: water with 0.1% TFA, solvent B: acetonitrile with 0.1% TFA, gradient elution: 0–20 min, 20–80% solvent B.
- (c) System 3: Phenomenex Jupiter Proteo (4  $\mu$ m, 90 Å, 250  $\times$  4.6 mm), 1 mL/min; solvent A: water with 0.1% TFA, solvent B: acetonitrile with 0.1% TFA, gradient elution: 0–20 min, 20–80% solvent B.
- (d) System 4: Agilent Zorbax 300SB-C18 (5  $\mu$ m, 250  $\times$  9.4 mm), 40°C, 2 mL/min, solvent A: water with 0.04% TFA, solvent B: acetonitrile with 0.05% TFA, gradient elution: 0–18 min, 20–80% solvent B.

### 7.2.2. L1-AF, L2-AF, Re(NS<sub>3</sub>)(L1-AF) and Re(NS<sub>3</sub>)(L2-AF)

AQVLRGTVTDFPG $\times$ 2TFA (1  $\mu$ mol) was dissolved in 300  $\mu$ L DMF. 3  $\mu$ mol triethylamine and 1  $\mu$ mol L1-BFCA were added. Similarly, reaction mixtures were prepared using L2-BFCA, Re(NS<sub>3</sub>)(L1-BFCA) and Re(NS<sub>3</sub>)(L2-BFCA) instead of L1-BFCA. After standing the solutions for 6 h at room temperature, the solvent was removed. The residues were purified by semipreparative HPLC. The isocyanide conjugated annexin fragments were purified using system 1 and the rhenium complex bearing peptides using system 2. The yield was 30–50%. The analytical data for the ligands and complexes are given in Table 7.1.

TABLE 7.1. ANALYTICAL DATA OF THE LIGANDS AND RHENIUM COMPLEXES

	Formula of the neutral complex	Calculated mass of the neutral complex	MS <sup>a</sup> , m/z (M <sup>+</sup> )	HPLC, R <sub>t</sub>
L1-AF	C <sub>69</sub> H <sub>102</sub> N <sub>18</sub> O <sub>20</sub>	1502.8	1503.8	9.8 min, system 1
L2-AF	C <sub>65</sub> H <sub>102</sub> N <sub>18</sub> O <sub>20</sub>	1454.8	1455.5	8.9 min, system 1
Re(NS <sub>3</sub> )(L1-AF)	C <sub>75</sub> H <sub>114</sub> N <sub>19</sub> O <sub>20</sub> ReS <sub>3</sub>	1881.8, 1883.8	1882.7, 1884.7 <sup>b</sup>	13.1 min, system 3
Re(NS <sub>3</sub> )(L2-AF)	C <sub>71</sub> H <sub>114</sub> N <sub>19</sub> O <sub>20</sub> ReS <sub>3</sub>	1833.8, 1835.8	1834.8, 1836.8 <sup>b</sup>	11.5 min, system 3

<sup>a</sup> ESI/MS or MALDI/MS.

<sup>b</sup> Two peaks corresponding to <sup>185</sup>Re and <sup>187</sup>Re.

### 7.2.3. <sup>99m</sup>Tc(NS<sub>3</sub>)(L1-AF) and <sup>99m</sup>Tc(NS<sub>3</sub>)(L2-AF)

To prepare <sup>99m</sup>Tc-EDTA/mannitol, 500–1000 MBq eluate of a <sup>99</sup>Mo/<sup>99m</sup>Tc generator was added to a kit formulation as described in Ref. [7.2] containing 1 mg Na<sub>2</sub>EDTA, 5 mg mannitol and 0.1 mg SnCl<sub>2</sub> in freeze dried form. The solution was allowed to stand for 15 min. The radiochemical purity was >95% as determined by thin layer chromatography (TLC) (silica gel strips, Kieselgel 60W, Merck, acetone and water as mobile phases).

The <sup>99m</sup>Tc-EDTA/mannitol solution was added to 0.5–0.1 mg isocyanide modified AF and 0.3 mg NS<sub>3</sub>. Methanol or acetonitrile was added so that it constituted 1/3 of the volume of the labelling mixture. The reaction mixture was heated at 50°C for 2 h. Due to some precipitation, the reaction mixtures were centrifuged before purification by semipreparative HPLC using system 2. For in vivo stability and cell binding studies, the organic solvent was removed and the <sup>99m</sup>Tc compounds were redissolved in saline. The radiochemical purity was >95% (HPLC). HPLC (system 3): retention time (R<sub>t</sub>) = 13.1 min for <sup>99m</sup>Tc(NS<sub>3</sub>)(L1-AF), R<sub>t</sub> = 11.5 min for <sup>99m</sup>Tc(NS<sub>3</sub>)(L2-AF). The <sup>99m</sup>Tc compounds were coeluted with rhenium analogues.

### 7.2.4. In vivo stability

The in vivo stability of <sup>99m</sup>Tc(NS<sub>3</sub>)(L1-AF) was checked using rat arterial blood samples at 3 and 10 min after injection of 20 MBq of the <sup>99m</sup>Tc labelled

AF. The blood samples were centrifuged to precipitate cells. After addition of ethanol to the supernatants, the samples were cooled to  $-60^{\circ}\text{C}$  for 5 min, centrifuged and the supernatants were analysed by HPLC (system 4).

### 7.2.5. Cell binding assay

Immortalized, human THP-1 cells were suspended in an RPMI 1640 medium containing 5% FCS, streptomycin and penicillin. The cells were transferred to a sterile tube and centrifuged at 900 rpm for 8 min to eliminate collapsed cells and the old medium. Finally, the cells were suspended in a freshly prepared medium and counted. After 30 min, the culture cells were treated with staurosporin for 4.0 or 8.0 h to stimulate apoptosis and exposure of phosphatidylserine at the external membrane.

#### 7.2.5.1. Binding studies

Apoptotic cells (treated for both 4.0 and 8.0 h with staurosporin) were centrifuged at 900 rpm for 8 min and suspended in standard saline (composition: NaCl, 125mM; KCl, 5.0mM;  $\text{MgSO}_4$ , 1.0mM;  $\text{NaH}_2\text{PO}_4$ , 1.0mM; hepes, 20.0mM; glucose, 5.5mM;  $\text{NaHCO}_3$ , 5.0mM) containing  $\text{CaCl}_2$  (2.5mM).

The following samples were tested for binding to phosphatidylserine:

- (1)  $2 \times 10^5$  apoptotic cells incubated with free annexin ( $10 \mu\text{L}$  annexin-Alexa488) in ice for 20 min and stored in the dark.
- (2)  $2 \times 10^5$  apoptotic cells incubated with free ligand CN-L2-AF ( $10 \mu\text{L}$ , 1.0mM) in ice for 20 min and stored in the dark.
- (3)  $1.8 \times 10^6$  cells incubated with  $^{99\text{m}}\text{Tc}(\text{NS}_3)(\text{CN-L2-AF})$  in ice for 20 min and stored in the dark.

After incubation, 2.5 mL of standard saline solution containing 2.5mM  $\text{CaCl}_2$  was added to samples (1) and (2). These were then analysed with FACS. Conversely, sample (3) was filtered off on GF/F and washed twice with 2.0 mL p5000. Finally, the resulting cells were counted in order to determine the membrane bound activity.

## 7.3. RESULTS AND DISCUSSION

The annexin fragment AQVLRGTVTDFPG (AF) — a tridecapeptide — was N-terminally modified by an isocyanide group using the bifunctional

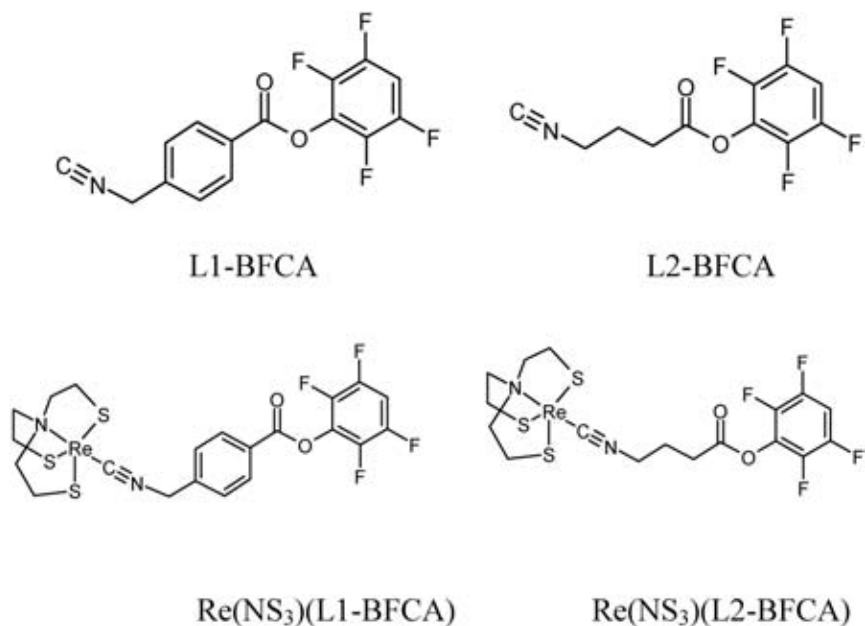


FIG. 7.1. BFCA for isocyanide modification of peptides and rhenium complex containing active esters to prepare rhenium bearing peptides.

coupling agents L1-BFCA and L2-BFCA (Fig. 7.1) to obtain the monodentate ligand for  $^{99m}\text{Tc}$ -(4 + 1) complexation.

For  $^{99m}\text{Tc}$  labelling a two-step procedure was performed as described in Ref. [7.2]. At first,  $^{99m}\text{Tc}$ -EDTA/mannitol was formed, which reacts in a second step with the isocyanide functionalized annexin fragment and the tetradentate tripodal ligand NS<sub>3</sub> (Fig. 7.2). The prepared  $^{99m}\text{Tc}$  labelled annexin fragments are depicted in Fig. 7.3. The procedure enables  $^{99m}\text{Tc}$  labelling of 0.1–0.2 mg annexin fragment with up to 1 GBq and a radiochemical yield of approximately 60%. Purification by semipreparative HPLC resulted in >95% radiochemical purity (Fig. 7.4). To verify the identity of the  $^{99m}\text{Tc}$  labelled annexin fragments, analogous Re-(4 + 1) complex conjugated peptides were prepared (Fig. 7.3) using rhenium 4 + 1 complexes containing active ester (Fig. 7.1). Coelution of the technetium and rhenium analogues is shown in HPLC traces in Fig. 7.4.

The stability of  $^{99m}\text{Tc}(\text{NS}_3)(\text{L1-AF})$  or  $^{99m}\text{Tc}(\text{NS}_3)(\text{L2-AF})$  in the HPLC eluate or in PBS was higher than 90% after 24 h. In vivo stability of  $^{99m}\text{Tc}(\text{NS}_3)(\text{L1-AF})$  was studied in rats. The compound was quickly degraded in at least five metabolites (Table 7.2). Previous studies confirmed the in vivo stability of the 4 + 1 complex unit [7.2], so that the detected metabolites can be primarily explained by the proteolytic cleavage of the tridecapeptide.

1st step:



2nd step:

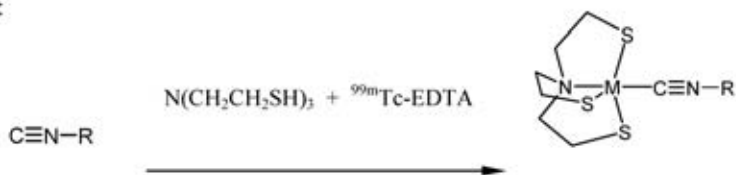


FIG. 7.2. Technetium-99m labelling of the isocyanide functionalized AF.

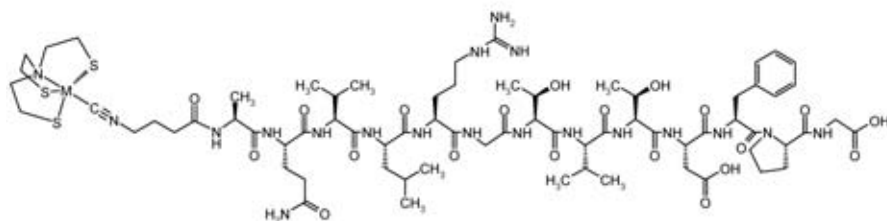
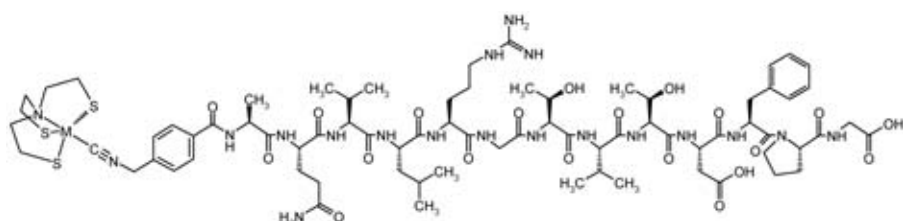


FIG. 7.3. Prepared 4 + 1 complexes bearing annexin fragments.

Binding of L2-AF and  ${}^{99m}\text{Tc}(\text{NS}_3)(\text{L2-AF})$  to apoptotic cells was studied. Neither compound exhibited affinity for apoptotic cells.

Annexin V is a calcium dependent membrane binding protein consisting of four domains. Membrane binding with high affinity depends on calcium binding sites in all four domains [7.5]. Tait et al. concluded that radiolabelled molecules containing only one or two annexin domains are unlikely to be suitable for imaging of apoptosis [7.6].

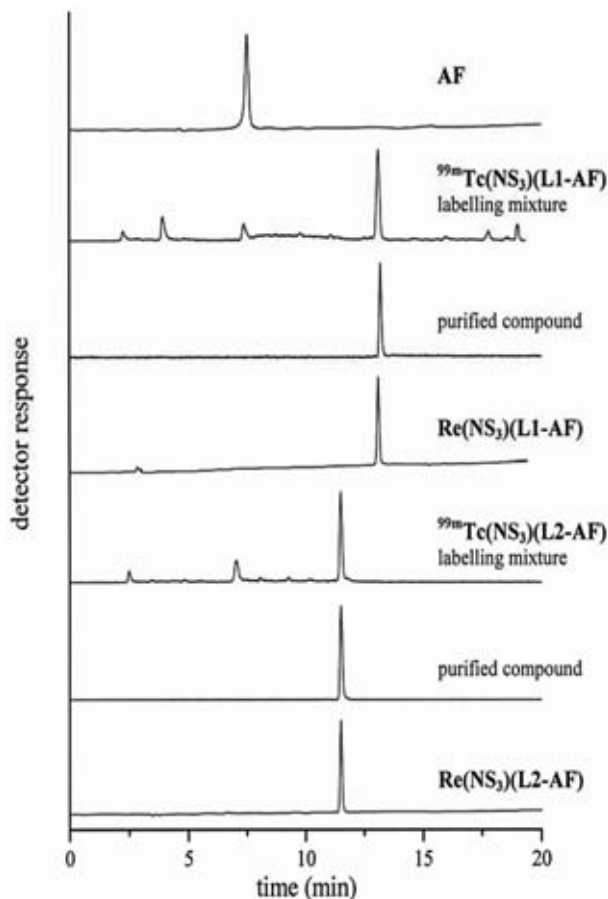


FIG. 7.4. Chromatograms of  $^{99m}\text{Tc}(\text{NS}_3)(\text{L1-AF})$ ,  $^{99m}\text{Tc}(\text{NS}_3)(\text{L2-AF})$ ,  $^{99m}\text{Tc}(\text{NS}_3)(\text{L1-AF})$ ,  $^{99m}\text{Tc}(\text{NS}_3)(\text{L2-AF})$ , gamma detection; AF,  $\text{Re}(\text{NS}_3)(\text{L1-AF})$ ,  $\text{Re}(\text{NS}_3)(\text{L2-AF})$ , detection at 220 nm; HPLC: Phenomenex Jupiter Proteo ( $4\ \mu\text{m}$ ,  $90\ \text{\AA}$ ,  $250 \times 4.6\ \text{mm}$ ),  $1\ \text{mL}/\text{min}$ ; solvent A: water with 0.1% TFA, solvent B: acetonitrile with 0.1% TFA, gradient elution: 0–20 min, 20–80% solvent B.

#### 7.4. CONCLUSIONS

The labelling method described allows the preparation of an annexin derived peptide that bears  $^{99m}\text{Tc}/\text{Re}-(4 + 1)$  mixed ligand complexes. However, the used tridecapeptide annexin sequence has been shown to be unsuitable as a targeting vehicle for apoptosis imaging due to its fast metabolism in vivo and

TABLE 7.2. METABOLISM OF  $^{99m}\text{Tc}(\text{NS}_3)(\text{L1-AF})$  IN RATS  
(peak areas (per cent of total peak area in radiochromatogram) of detected  $^{99m}\text{Tc}$  species in the protein free plasma sample after 3 and 10 min post-injection)

Technetium-99m species	$R_t$ (min)	3 min	10 min
Metabolite 1	13.8	19%	37%
Metabolite 2	14.9	13%	12%
Metabolite 3	15.1	13%	10%
$^{99m}\text{Tc}(\text{NS}_3)(\text{CN-L1-AF})$	15.6	40%	23%
Metabolite 4	15.8	10%	9%
Metabolite 5	16.3	6%	9%

lack of binding to apoptotic cells. The results are consistent with recently published articles that have indicated that all four annexin V domains are essential for high membrane binding affinity [7.5, 7.6].

## REFERENCES

- [7.1] LAHORTE, C.M.M., et al., Apoptosis-detecting radioligands: Current state of the art and future perspectives, *Eur. J. Nucl. Med.* **31** (2004) 887–919.
- [7.2] SEIFERT, S., et al., Novel procedures for preparing  $^{99m}\text{Tc}(\text{III})$  complexes with tetradentate/monodentate coordination of varying lipophilicity and adaptation to  $^{188}\text{Re}$  analogues, *Bioconj. Chem.* **15** (2004) 856–863.
- [7.3] SPIES, H., GLASER, M., PIETZSCH, H.-J., HAHN, F.E., LÜGGER, T., Synthesis and reactions of trigonal-bipyramidal rhenium and technetium complexes with tripodal, tetradentate  $\text{NS}_3$  ligand, *Inorg. Chim. Acta* **240** (1995) 465–478.
- [7.4] PIETZSCH, H.-J., GUPTA, A., SYHRE, R., LEIBNITZ, P., SPIES, H., Mixed-ligand technetium(III) complexes with tetradentate/monodentate  $\text{NS}_3$ /isocyanide coordination: A new nonpolar technetium chelate system for the design of neutral and lipophilic complexes stable in vivo, *Bioconj. Chem.* **12** (2001) 538–544.
- [7.5] JIN, M., SMITH, C., HSIEH, H.-Y., GIBSON, D.F., TAIT, J.F., Essential role of B-helix calcium binding sites in annexin V-membrane binding, *J. Biol. Med.* **279** (2004) 40351–40357.
- [7.6] TAIT, J.F., SMITH, C., BLANKENBERG, F.G., Structural requirements for in vivo detection of cell death with  $^{99m}\text{Tc}$ -annexin V, *J. Nucl. Med.* **46** (2005) 807–815.

## Chapter 8

### TECHNETIUM-99m LABELLING OF A QUINAZOLINE DERIVATIVE USING THE 4 + 1 MIXED LIGAND CHELATE SYSTEM

J.-U. KÜNSTLER\*, I. SANTOS\*\*, I. PIRMETTIS<sup>†</sup>, H.-J. PIETZSCH\*

\* Institute of Radiopharmacy, Forschungszentrum Dresden–Rossendorf,  
Germany

\*\* Department of Chemistry, Institute of Nuclear Technology, Portugal

<sup>†</sup> Institute of Radioisotopes and Radiodiagnostic Products, Demokritos  
National Centre of Scientific Research, Athens, Greece

#### Abstract

The quinazoline derivative (3-chloro-4-fluorophenyl)-quinazoline-4,6-diamine was labelled with <sup>99m</sup>Tc using the 4 + 1 mixed ligand system in which Tc(III) is coordinated by a monodentate isocyanide and the tetradentate tripodal ligand tris(2-mercaptoethyl)-amine (NS<sub>3</sub>). The quinazoline was N-terminally functionalized with the isocyano group via a C<sub>3</sub> alkyl amide linker. Technetium-99m labelling was performed in a two-step procedure using <sup>99m</sup>Tc-EDTA/mannitol as a starting complex, followed by a ligand exchange reaction with a mixture of the isocyanide and 2,2',2''-nitrilotris(ethanethiol) (NS<sub>3</sub>). The identity of the <sup>99m</sup>Tc labelled quinazoline was confirmed by comparison with the high performance liquid chromatography profiles of the analogous rhenium compound. Inhibition of cell proliferation was evaluated by MTT assay (IC<sub>50</sub> = 3.18 μM (after 48 h) and IC<sub>50</sub> = 4.95 μM (after 72 h)).

#### 8.1. INTRODUCTION

Epidermal growth factor receptor (EGFR) is often overexpressed in cancer [8.1]. A suitable radiotracer that binds EGFR would allow, through a nuclear medicine imaging technique, the mapping of this receptor kinase. Radioactively labelled small molecules with high affinity and selectivity for the tyrosine kinase (TK) domain of EGFR might offer a specific and sensitive tool to be used for diagnosis of tumours expressing EGFR, as this is the activation pathway for the receptor [8.2–8.4]. Quinazolines are 1,3 benzodiamines with

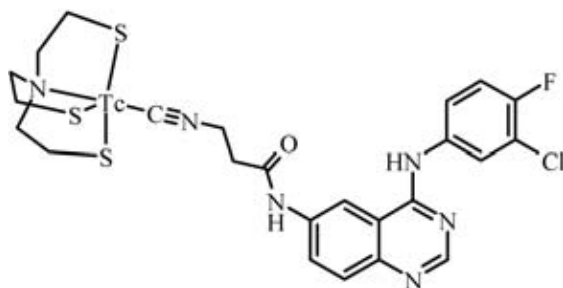


FIG. 8.1. Tc-(4 + 1) complex bearing the (3-chloro-4-fluorophenyl)-quinazoline-4,6-diamine subunit derived from ML03.

the same structure as pyrimidic bases in nucleic acids. Quinazoline derived molecules are among the most active tyrosine kinase (TK) inhibitors with the highest selectivity for EGFR.

## 8.2. RESULTS AND DISCUSSION

Previous studies have shown that Tc(III) mixed ligand complexes with tetradentate/monodentate  $\text{NS}_3$ /isonitrile coordination  $[\text{Tc}(\text{NS}_3)(\text{CN-R})]$  are lipophilic and stable against exchange reactions in vivo [8.5]. This type of organometallic 4 + 1 technetium complex appears suitable for wrapping the metal well in a molecule with receptor binding functionality.

The compound introduced here contains the (3-chloro-4-fluorophenyl)-quinazoline-4,6-diamine moiety derived from ML03, a novel PET biomarker targeting the EGFR-TK, linked to the neutral and oxo free technetium chelate unit via a  $\text{C}_3$  alkyl amide (Fig. 8.1).

The synthesis of the monodentate isocyanide involves coupling of N-formyl- $\beta$ -alanin to (3-chloro-4-fluorophenyl)-quinazoline-4,6-diamine followed by the formation of the isonitrile (Fig. 8.2).

In this study rhenium complex (5) was used as a reference compound for complete chemical characterization, identification of the  $^{99\text{m}}\text{Tc}$  complex and in vitro receptor binding assay. After preparing the precursor complex  $[\text{Re}(\text{NS}_3)\text{PMe}_2\text{Ph}]$ , the desired 4 + 1 complex was formed by addition of the appropriate isocyanide ligand (Fig. 8.3).

The 4 + 1  $^{99\text{m}}\text{Tc}$  mixed ligand complexes were obtained in a two-step reaction. In the first step,  $^{99\text{m}}\text{Tc}(\text{III})$ -EDTA was formed by reduction of  $^{99\text{m}}\text{TcO}_4^-$  (generator eluate) in  $\text{Na}_2\text{EDTA}$  solution. EDTA was substituted in the second reaction step by the tripodal ligand 2,2',2''-nitrilotris(ethanethiol)

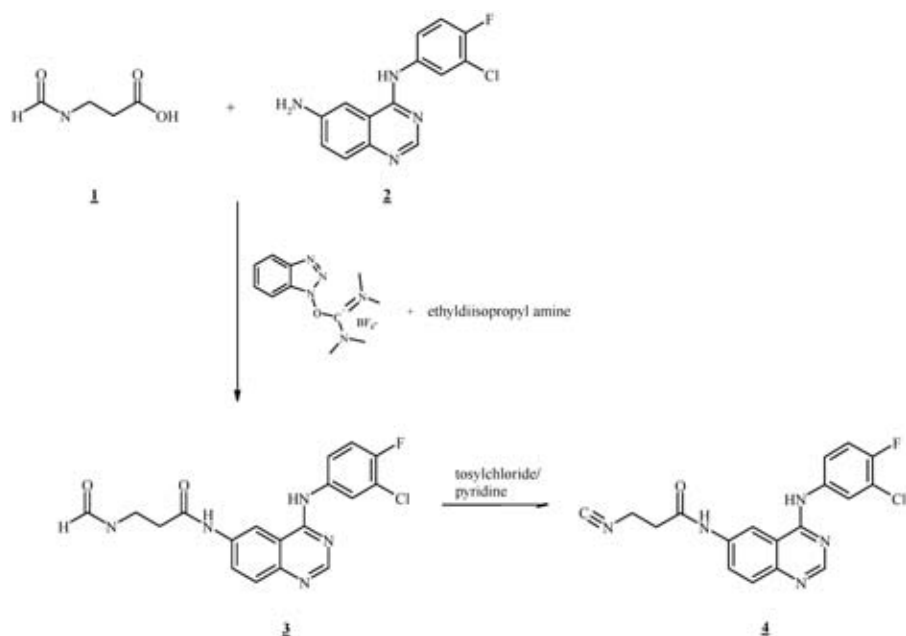


FIG. 8.2. Synthesis of the isocyano-modified quinazoline derivative (4).

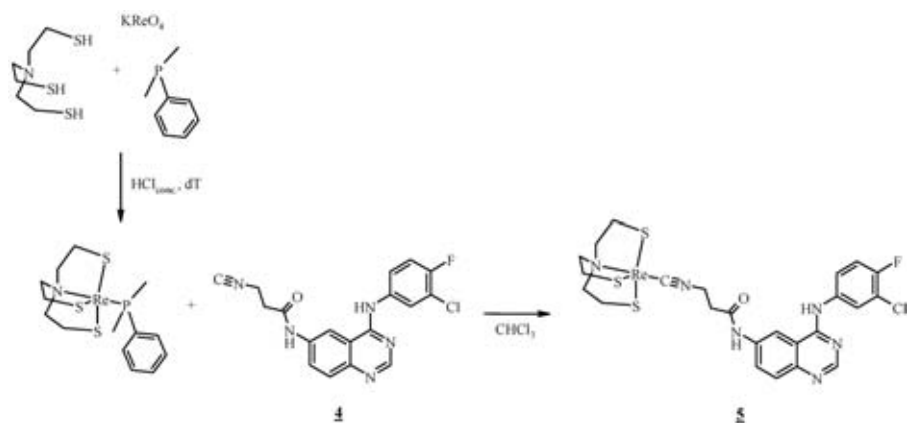


FIG. 8.3. Synthesis of the quinazoline-bearing rhenium derivative (5).

and the monodentate isocyanide ( $C\equiv N-R$ ) that results in the formation of the desired 4 + 1 complex. The yields obtained by this procedure were between 50% and 70%. The  $^{99m}Tc$  complexes and the analogous rhenium complexes exhibited identical retention times in reverse phase high performance liquid chromatography (HPLC) investigations (Fig. 8.4).

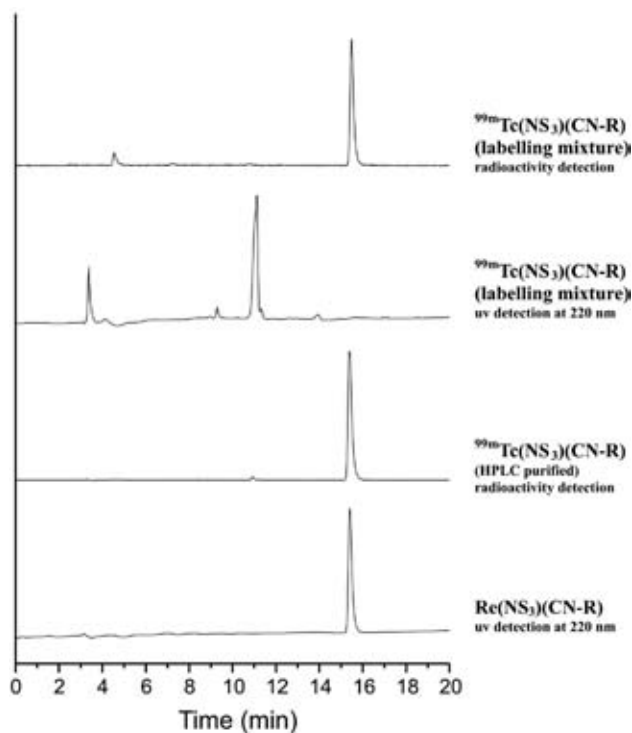


FIG. 8.4. Chromatograms of  $^{99m}\text{Tc}(\text{NS}_3)(\text{CN-R})$  and  $\text{Re}(\text{NS}_3)(\text{CN-R})$ , HPLC: Jupiter Proteo, 4  $\mu\text{m}$ , 90  $\text{\AA}$ , 250  $\times$  4.6 mm, Phenomenex; 1 mL/min; solvent A: water with 0.1% TFA (v/v), solvent B: acetonitrile with 0.1% TFA (v/v), gradient elution: 0–20 min 20–80% solvent B. For the chromatogram of  $\text{Re}(\text{NS}_3)(\text{CN-R})$ , 5  $\mu\text{L}$  of a solution of 0.1 mg  $\text{Re}(\text{NS}_3)(\text{CN-R})$  in 0.1 mL acetonitrile was used.

## 8.2.1. In vitro evaluation

### 8.2.1.1. Inhibition of cell proliferation

Quinazoline is a relatively small biomolecule and hence requires conjugation to a metal fragment without affecting its affinity for the EGFR associated tyrosine kinase (EGFR-TK), and the labelled quinazoline still must compete with ATP (adenosine triphosphate) for binding to the intracellular tyrosine kinase region. To evaluate if the labelling of the quinazoline would affect these properties, cell growth inhibition and phosphorylation studies were performed using A431 cells and the different quinazoline compounds (4) and (5).

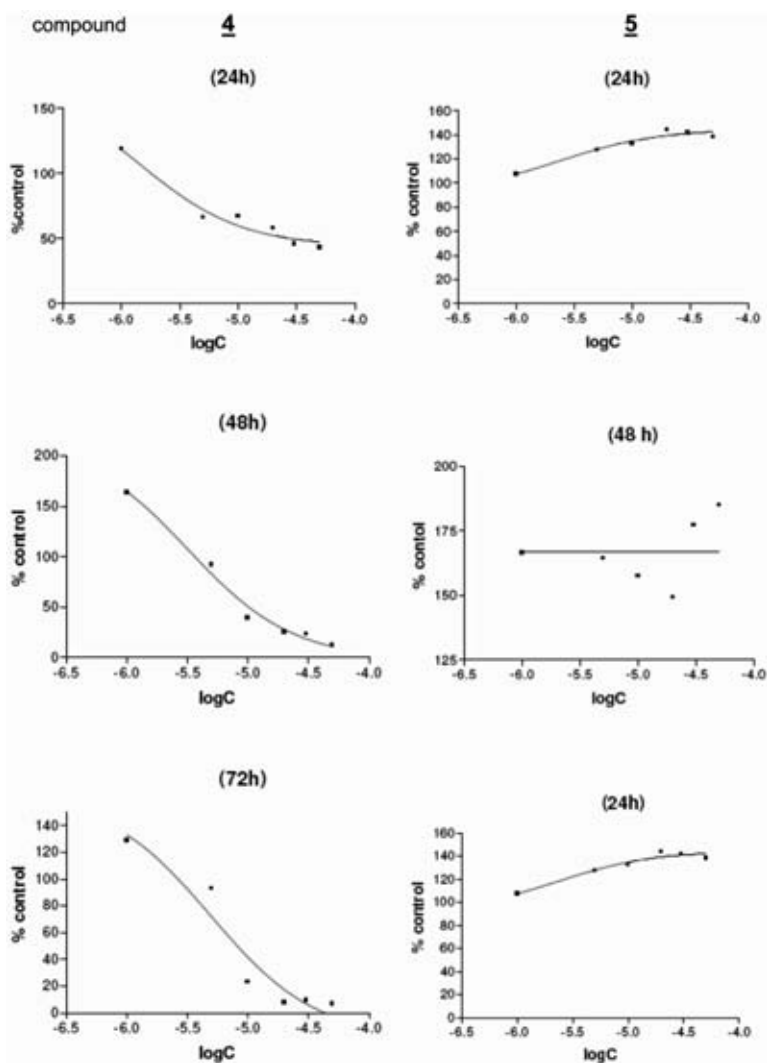


FIG. 8.5. Inhibition of cell proliferation in MTT assay for compounds (4) and (5).

These studies allowed evaluation of the effect of introducing in the quinazoline backbone different functional groups, including a metal fragment. For each compound, cell growth inhibition was calculated after 24, 48 and 72 h of incubation, and four replicates were run for each experimental condition. The average of four experiments at different times for the studied compounds is shown in Fig. 8.5. While the non-coordinated isonitrile ligand exhibited certain inhibition of cell proliferation after 24 h and 72 h —  $IC_{50} = 3.18\mu M$  (48 h),  $IC_{50} = 4.95\mu M$  (72 h) — the appropriate rhenium complex is not active.

### 8.2.1.2. Inhibition of EGFR-TK

The phosphorylation inhibition was also calculated using A431 cells. These cells were incubated for 24 h in the presence of fresh medium without foetal bovine serum. The day after, the cells were incubated in the presence of the different compounds (final concentration, 1  $\mu$ M) for 2 h, after which EGF was added (20 ng/mL) for 5 min. The medium was then removed, the cells were washed with PBS and cell lysis buffer (50mM Tris-HCl, pH7.4, 150mM NaCl, 1% Triton X-100, 1mM PMSF, 50  $\mu$ g/mL aprotinin, 2mM sodium orthovanadate, 50  $\mu$ g/mL leupeptine and 5mM EDTA) was added. Controls consisted of wells without drugs and with or without EGF. The total amount of protein was estimated by a BCA assay in ELISA plates, using a BSA standard curve. A volume of lysis mixture, corresponding to 30 mg of total protein, was loaded on to polyacrilamide gel (8%); proteins were separated by electrophoresis and transferred to PVDF membrane. For visualization of molecular weight bands, the membrane was immersed in Ponceau reagent (0.5% Ponceau in 1% acetic acid) for 5 min. The membrane was washed in H<sub>2</sub>O, blocked overnight in TTN with 5% milk (1% fat) and incubated for 2 h in antiphosphotyrosine antibody diluted 1/2000 (PY20, Santa Cruz Biotechnology). The membrane was then washed three times in TTN and incubated in a horseradish peroxidase conjugated secondary antimouse antibody diluted 1/3000 (Sigma) for 2 h and finally washed three times in TTN. Detection was performed using the chemiluminescent detection system in accordance with the manufacturer's instructions (ECL kit, Amersham). Based on these data and assuming the controls, we can say that all the compounds inhibit phosphorylation to a certain extent (Fig. 8.6). A better quantification of this effect is under way.

## 8.3. CONCLUSIONS

The labelling method enables the <sup>99m</sup>Tc labelling of 3-chloro-4-(4-fluorophenyl)-quinazoline-4,6-diamine via 4 + 1 mixed ligand complexes. While the non-coordinated isonitrile ligand exhibited certain inhibition of cell proliferation, the appropriate rhenium complex is not active. The compounds inhibit phosphorylation to a certain extent. A better quantification of this effect is under way.



FIG. 8.6. Inhibition of phosphorylation of the receptor. Controls were run in the same experimental conditions with EGF (+) and without EGF (-)

## REFERENCES

- [8.1] ARTEAGA, C., Targeting HER/EGFR: A molecular approach to cancer therapy, *Semin. Oncol.* **30** Suppl. 7 (2003) 3–14.
- [8.2] CAPALA, J., et al., Radiolabeling of epidermal growth factor with  $^{99m}\text{Tc}$  and in vivo localization following intracerebral injection into normal and glioma-bearing rats, *Bioconj. Chem.* **8** (1997) 289–295.
- [8.3] BONASERA, T.A., et al., Potential  $^{18}\text{F}$ -labeled biomarkers for epidermal growth factor receptor tyrosine kinase, *Nucl. Med. Biol.* **28** (2001) 359–374.
- [8.4] BEN-DAVID, I., ROZEN, Y., ORTU, G., MISHANI, E., Radiosynthesis of ML03, a novel positron emission tomography biomarker for targeting epidermal growth factor receptor via the labeling synthon:  $^{11}\text{C}$ acryloyl chloride, *Appl. Radiat. Isot.* **58** (2003) 209–217.
- [8.5] SEIFERT, S., et al., Novel procedures for preparing  $^{99m}\text{Tc}$ (III) complexes with tetradentate/monodentate coordination of varying lipophilicity and adaptation to  $^{188}\text{Re}$  analogues, *Bioconj. Chem.* **15** (2004) 856–863.



## Chapter 9

### TECHNETIUM-99m LABELLING OF THE RGD PEPTIDE c(RGDyK) USING THE 4 + 1 MIXED LIGAND APPROACH

J.-U. KÜNSTLER\*, P. ANSORGE\*, R. BERGMANN\*,  
E. GNIAZDOWSKA\*\*, C. DECRISTOFORO<sup>+</sup>, A. REY<sup>++</sup>,  
H. STEPHAN\*, H.-J. PIETZSCH\*

\* Institute of Radiopharmacy,  
Forschungszentrum Dresden–Rossendorf, Germany

\*\* Institute of Nuclear Chemistry and Technology, Warsaw, Poland

<sup>+</sup> Universitätsklinik für Nuklearmedizin, Innsbruck, Austria

<sup>++</sup> Radiochemistry Department, Faculty of Chemistry,  
Universidad de la República, Montevideo, Uruguay

#### Abstract

The RGD peptide c(RGDyK) was labelled with <sup>99m</sup>Tc using the 4 + 1 mixed ligand system consisting of Tc(III), which is coordinated by a monodentate ligand and a tetradentate tripodal chelator. 4-Isocyanomethylbenzoic acid (L1) and 4-isocyanobutyric acid (L2) were used as monodentate ligands conjugated to c(RGDyK). Tris(2-mercaptoethyl)-amine (NS<sub>3</sub>) and its derivatives containing one (NS<sub>3</sub>COOH) and three non-coordinating carboxyl groups (NS<sub>3</sub>(COOH)<sub>3</sub>) were used to vary the tetradentate coligands in terms of lower lipophilicity. The <sup>99m</sup>Tc-(4 + 1) complex bearing c(RGDyK) derivatives were compared for their octanol/PBS distribution ratios. The identity of the <sup>99m</sup>Tc labelled compounds was confirmed by comparison with the high performance liquid chromatography profile of analogous Re-(4 + 1) complex bearing peptides. Biodistribution studies exhibited a low tumour uptake. NS<sub>3</sub> and NS<sub>3</sub>COOH as coligands resulted in a high liver uptake and hepatobiliary elimination, whereas substitution by NS<sub>3</sub>(COOH)<sub>3</sub> showed a predominant urinary excretion.

## 9.1. INTRODUCTION

Radiolabelled RGD derived compounds with a diversity of both the labelling system and the RGD motive have already been described and studied *in vivo* as well as in humans [9.1, 9.2]. However, the high pharmacological influence of the radiometal complex conjugated to a small peptide and the limitations of various labelling concepts require new radiometal labelling systems. The 4 + 1 complex system with its high *in vivo* stability allows an efficient labelling of peptides, but has so far not been widely applied for peptide labelling [9.3, 9.4].

## 9.2. MATERIALS AND METHODS

### 9.2.1. General

c(RGDyK)×2TFA was purchased from Biosyntan. The synthesis of NS<sub>3</sub> was as described in Ref. [9.5] and of NS<sub>3</sub>COOH, L1-BFCA and Re(NS<sub>3</sub>)(L1-BFCA) as described in Ref. [9.4].

High performance liquid chromatography (HPLC):

- (a) System 1: Hamilton PRP-1 (10 μm, 7 × 305 mm), 2 mL/min; solvent A: acetonitrile with 0.01M NH<sub>3</sub>, solvent B: water with 0.01M NH<sub>3</sub>, gradient elution: 0–40 min, 5–65% solvent A.
- (b) System 2: Phenomenex Jupiter Proteo (4 μm, 90 Å, 250 × 10 mm), 3 mL/min; solvent A: water with 0.1% TFA, solvent B: acetonitrile with 0.1% TFA, gradient elution: 0–20 min, 20–80% solvent B.
- (c) System 3: Phenomenex Jupiter Proteo (4 μm, 90 Å, 250 × 4.6 mm), 1 mL/min; solvent A: water with 0.1% TFA, solvent B: acetonitrile with 0.1% TFA, gradient elution: 0–20 min, 20–80% solvent B.

The carboxyl groups bearing ligand NS<sub>3</sub>(COOH)<sub>3</sub> were synthesized by conjugation (via DCC) of the dendritically functionalized amine H<sub>2</sub>N-C(-CH<sub>2</sub>-O-CH<sub>2</sub>-CH<sub>2</sub>-COO-Me)<sub>3</sub> [9.6] to the S-benzyl protected NS<sub>3</sub>COOH [9.4], followed by deprotection. L2-BFCA was prepared by formylation of 4-aminobutyric acid, esterification with 2,3,5,6-tetrafluorophenol and conversion of the formylamino group into the isocyanido group. Re(NS<sub>3</sub>)(L2-BFCA) was obtained by reaction of L2-BFCA with Re(NS<sub>3</sub>)(PMe<sub>2</sub>Ph), which was prepared in accordance with Ref. [9.3]. Re(NS<sub>3</sub>(COOMe)<sub>3</sub>)(CN-BFCA) was prepared starting from NS<sub>3</sub>(COOH)<sub>3</sub>, [Re(tu)<sub>6</sub>]Cl<sub>3</sub> [9.7] and PMe<sub>2</sub>Ph, followed by ligand exchange with L2-BFCA.

TABLE 9.1. ANALYTICAL DATA

	Formula of the neutral complex	Calculated mass of the neutral complex	ESI/MS, m/z (M <sup>+</sup> )	HPLC, R <sub>t</sub>
L1-c(RGDyK)	C <sub>32</sub> H <sub>46</sub> N <sub>10</sub> O <sub>9</sub>	714.4	715.2	12.3 min, system 1
L2-c(RGDyK)	C <sub>36</sub> H <sub>46</sub> N <sub>10</sub> O <sub>9</sub>	762.4	763.4	16.5 min, system 1
Re(NS <sub>3</sub> )(L1-c(RGDyK))	C <sub>42</sub> H <sub>58</sub> N <sub>11</sub> O <sub>9</sub> S <sub>3</sub> Re	1141.3, 1143.3	1142.3, 1144.3 <sup>a</sup>	11.3 min, system 3
Re(NS <sub>3</sub> )(L2-c(RGDyK))	C <sub>38</sub> H <sub>58</sub> N <sub>11</sub> O <sub>9</sub> S <sub>3</sub> Re	1093.3, 1095.3	1094.3, 1096.4 <sup>a</sup>	10.6 min, system 3

<sup>a</sup> Two peaks corresponding to <sup>185</sup>Re and <sup>187</sup>Re.

### 9.2.2. L1-c(RGDyK), L2-c(RGDyK), Re(NS<sub>3</sub>)(L1-c(RGDyK)) and Re(NS<sub>3</sub>)(L2-c(RGDyK))

c(RGDyK)×2TFA (2.5 μmol) was dissolved in 500 μL DMF. 7.5 μmol triethylamine and 2.5 μmol L1-BFCA were added. Accordingly, reaction mixtures were prepared using L2-BFCA, Re(NS<sub>3</sub>)(L1-BFCA) and Re(NS<sub>3</sub>)(L2-BFCA) instead of L1-BFCA. After standing the solutions for 6 h at room temperature, the solvent was removed. The residues were purified by semipreparative HPLC. The free isonitrile containing compounds L1-c(RGDyK) and L2-c(RGDyK) were purified using system 1, the rhenium compounds were purified using system 2. The product fractions were lyophilized. The yield was 30–50%. The analytical data are presented in Table 9.1.

### 9.2.3. Re(NS<sub>3</sub>(COOH)<sub>3</sub>)(L2-c(RGDyK))

c(RGDyK)×2TFA (3 μmol) was dissolved in 1000 μL DMF. 9 μmol triethylamine and 3 μmol Re(NS<sub>3</sub>(COOMe)<sub>3</sub>)(L2-BFCA) were added. After standing the solutions for 6 h at room temperature, the solvent was removed. The residue was dissolved in 1 mL (H<sub>2</sub>O/MeCN, 1/1), and 100 μL 1M NaOH was added. The reaction mixture was put in an ultrasound bath for 30 min. The compound was purified using HPLC system 2 and then lyophilized. The yield was 30%. The analytical data are presented in Table 9.2.

TABLE 9.2. ANALYTICAL DATA

	Formula of the neutral complex	Calculated mass of the neutral complex	ESI/MS, m/z		HPLC, R <sub>t</sub>
			Cation	Anion	
Re(NS <sub>3</sub> (COOH) <sub>3</sub> ) (L2-c(RGDyK))	C <sub>52</sub> H <sub>79</sub> N <sub>12</sub> O <sub>19</sub> S <sub>3</sub> Re	1456.4, 1458.4	1457.8, 1459.8 <sup>a</sup>	1455.5, 1457.5 <sup>a</sup>	9.6 min, system 3

<sup>a</sup> Two peaks corresponding to <sup>185</sup>Re and <sup>187</sup>Re.

#### 9.2.4. Technetium-99m labelling

To prepare <sup>99m</sup>Tc-EDTA/mannitol, 500–1000 MBq eluate of a <sup>99</sup>Mo/<sup>99m</sup>Tc generator was added to a kit formulation as described in Ref. [9.4] containing 1 mg Na<sub>2</sub>EDTA, 5 mg mannitol and 0.1 mg SnCl<sub>2</sub> in a freeze dried form. The solution was allowed to stand for 15 min. The radiochemical purity was >95% as determined by thin layer chromatography (TLC) (silica gel strips, Kieselgel 60W, Merck, acetone and water as mobile phases).

The <sup>99m</sup>Tc-EDTA/mannitol solution was added to isocyanide modified c(RGDyK) (0.1–0.5 mg) and 0.3 mg NS<sub>3</sub>, NS<sub>3</sub>COOH<sub>3</sub> or NS<sub>3</sub>(COOH)<sub>3</sub>. Methanol or acetonitrile was added so that it constituted 1/3 of the volume of the labelling mixture. The reaction mixture was heated at 50°C for 2 h. Due to some precipitation, the reaction mixtures were centrifuged before purification by semipreparative HPLC using system 2. For biodistribution studies the organic solvent was removed and the <sup>99m</sup>Tc compounds were redissolved in saline. The radiochemical purity was >95% (HPLC).

#### 9.2.5. Analytical data

HPLC (system 3): retention time (R<sub>t</sub>) = 11.3 min for <sup>99m</sup>Tc(NS<sub>3</sub>)(L1-c(RGDyK)), R<sub>t</sub> = 10.6 min for <sup>99m</sup>Tc(NS<sub>3</sub>)(L2-c(RGDyK)), R<sub>t</sub> = 11.0 min for <sup>99m</sup>Tc(NS<sub>3</sub>COOH)(L1-c(RGDyK)), R<sub>t</sub> = 9.7 min for <sup>99m</sup>Tc(NS<sub>3</sub>COOH)(L2-c(RGDyK)), R<sub>t</sub> = 9.5 min for <sup>99m</sup>Tc(NS<sub>3</sub>(COOH)<sub>3</sub>)(L2-c(RGDyK)). The <sup>99m</sup>Tc compounds were coeluted with rhenium analogues.

#### 9.2.6. Distribution ratio (log D, octanol/PBS, pH7.4)

Approximately 5 MBq of the <sup>99m</sup>Tc labelled compounds was dissolved in 3 mL PBS, pH7.4. 0.5 mL of this solution was added to 0.5 mL n-octanol (N = 5). The mixture was shaken at room temperature for 15 min and then centrifuged for 3 min at 5000 rpm. 50 μL of the buffer layer and of the octanol

layer was counted. The determination was repeated three times for each compound. The distribution ratio was expressed as the ratio of counts per minute (cpm) in the octanol phase to the cpm in the PBS phase (both corrected for background cpm).

### 9.2.7. Biodistribution studies

For studying the biodistribution of  $^{99m}\text{Tc}(\text{NS}_3\text{COOH})(\text{L2-c(RGDyK)})$ , mice with human melanoma M21 xenografts and, as a negative control, M21L xenografts (incapable of binding the RGD motive) were used. The biodistribution of  $^{99m}\text{Tc}(\text{NS}_3(\text{COOH})_3)(\text{L1-c(RGDyK)})$  and  $^{99m}\text{Tc}(\text{NS}_3(\text{COOH})_3)(\text{L2-c(RGDyK)})$  was studied using normal CD1 mice (female, 20–30 g) and C57B16 mice bearing induced B16F1 murine melanoma. The  $^{99m}\text{Tc}$  compounds were injected via the tail vein. At different intervals after injection the animals were sacrificed by neck dislocation. Selected organs and tissues were removed, weighed and gamma counted. Total urine volume was collected during the biodistribution period and also removed from the bladder after sacrifice.

## 9.3. RESULTS AND DISCUSSION

All metallated RGD peptides used in this study are depicted in Fig. 9.1.

The cyclic RGD peptide c(RGDyK) was modified with 4-isocyanomethylbenzoic acid (L1) and 4-isocyanobutyric acid (L2) using the bifunctional coupling agent L1-BFCA and L2-BFCA (Fig. 9.2). Due to the known lability of the isocyanides in an acidic medium, purification had to be performed under basic conditions using polymer reverse phase columns.

For  $^{99m}\text{Tc}$  labelling a two-step procedure was performed as described in Ref. [9.3]. At first  $^{99m}\text{Tc-EDTA/mannitol}$  was formed, which reacts in a second step with the isocyanide functionalized RGD peptide and the tetradentate tripodal ligands  $\text{NS}_3$ ,  $\text{NS}_3\text{COOH}$  or  $\text{NS}_3(\text{COOH})_3$ . The procedure enables  $^{99m}\text{Tc}$  labelling of 0.1–0.5 mg RGD peptide with up to 1 GBq and a radiochemical yield of 60%. Purification by semipreparative HPLC resulted in >95% radiochemical purity. The stability of the  $^{99m}\text{Tc}$  labelled RGD peptides in the HPLC eluate or in PBS was higher than 90% after 24 h.

To verify the identity of the  $^{99m}\text{Tc}$  labelled c(RGDyK) derivatives, rhenium analogues were synthesized. For a convenient synthesis, Re-(4 + 1) complexes bearing the activated ester were prepared (Fig. 9.3). The rhenium modified peptides are shown in Fig. 9.1.  $\text{Re}(\text{NS}_3(\text{COOMe})_3)(\text{L2-BFCA})$  was synthetically obtained with methyl ester groups, which required hydrolysis of the ester after peptide coupling.

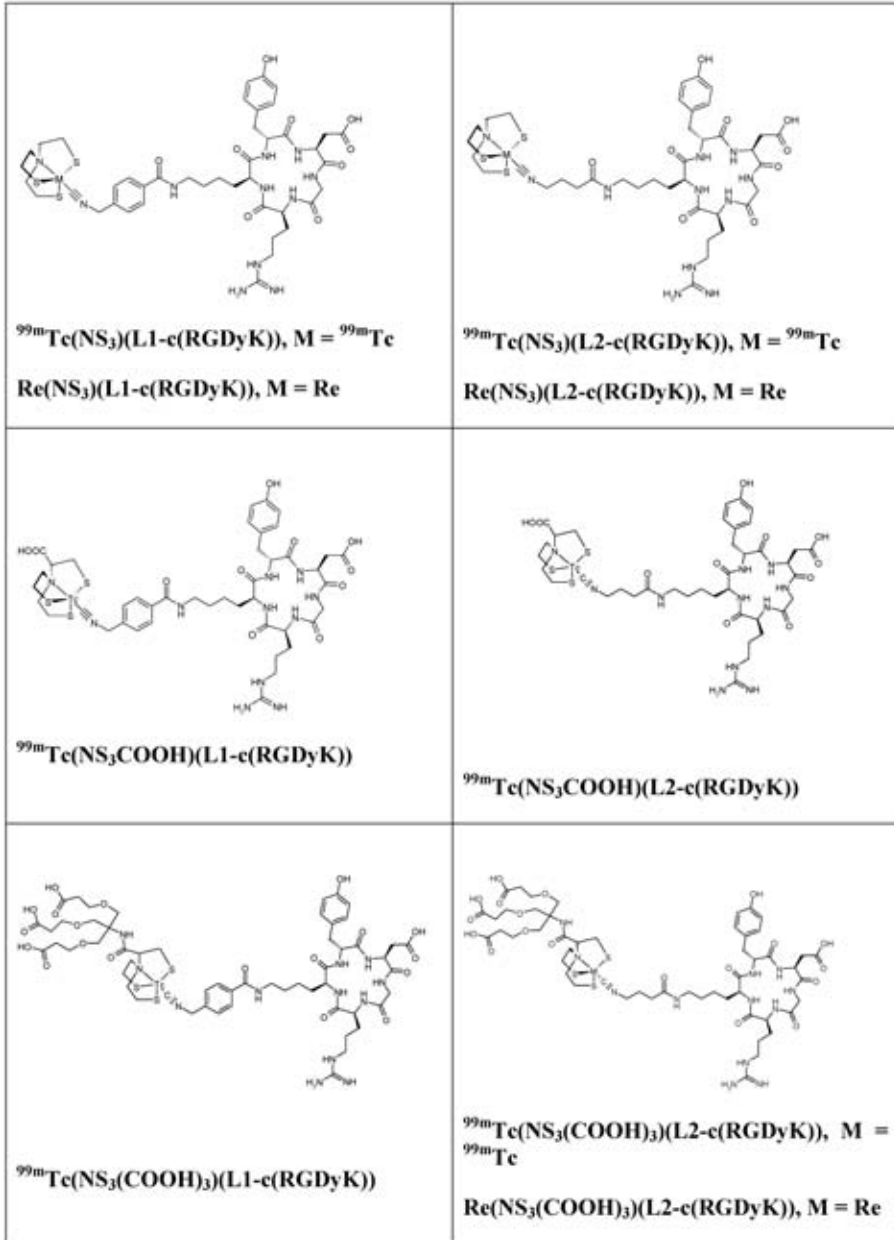


FIG. 9.1. Technetium and rhenium 4 + 1 complexes used in this study.

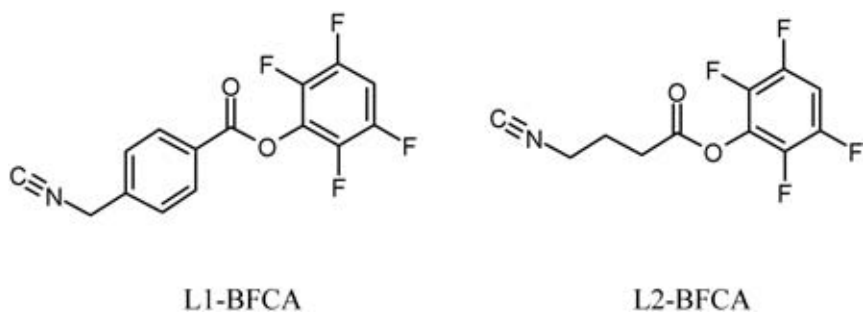


FIG. 9.2. Bifunctional chelating agents (BFCA) for isocyanide modification of peptides.

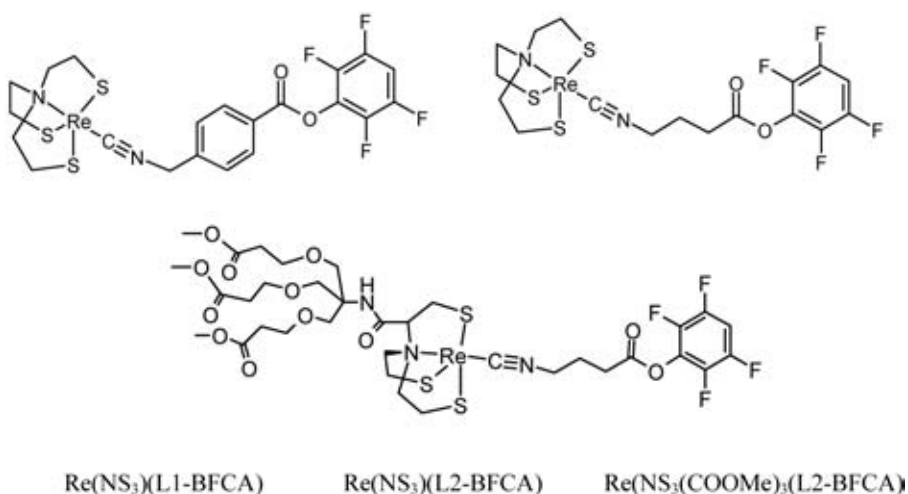


FIG. 9.3. Rhenium complexes containing activated esters for the preparation of non-radioactive reference peptides.

The determined  $\log P$  values at physiological pH (Table 9.3) show the dependence of the lipophilicity on the isocyanide linker and the tetradentate coligand. The complexes formed by  $\text{NS}_3$  are considerably lipophilic, whereas  $\text{NS}_3\text{COOH}$  and  $\text{NS}_3(\text{COOH})_3$  as coligands gave  $\log D$  values in a range often observed for  $^{99\text{m}}\text{Tc}$  labelled peptides. The results of the octanol/PBS distribution assay are also reflected in the retention times of the HPLC analyses, showing shorter retention times for complexes with lower  $\log P$ .

Cell uptake of  $^{99\text{m}}\text{Tc}(\text{NS}_3)(\text{L1-c(RGDyK)})$  and  $^{99\text{m}}\text{Tc}(\text{NS}_3\text{COOH})(\text{L2-c(RGDyK)})$  as well as protein binding of  $^{99\text{m}}\text{Tc}(\text{NS}_3\text{COOH})(\text{L2-c(RGDyK)})$  is discussed in Chapter 2.

TABLE 9.3. DISTRIBUTION RATIO (LOG *P*, OCTANOL/PBS, pH7.4)

	log <i>P</i> ± SD, <i>N</i> = 3
<sup>99m</sup> Tc(NS <sub>3</sub> )(L1-c(RGDyK))	-0.6 ± 0.1
<sup>99m</sup> Tc(NS <sub>3</sub> )(L2-c(RGDyK))	-1.3 ± 0.1
<sup>99m</sup> Tc(NS <sub>3</sub> COOH)(L1-c(RGDyK))	-2.0 ± 0.1
<sup>99m</sup> Tc(NS <sub>3</sub> COOH)(L2-c(RGDyK))	-2.3 ± 0.2
<sup>99m</sup> Tc(NS <sub>3</sub> (COOH) <sub>3</sub> )(L2-c(RGDyK))	-3.3 ± 0.3

### 9.3.1. Biodistribution studies in mice

The biodistribution of <sup>99m</sup>Tc(NS<sub>3</sub>)(L1-c(RGDyK)) and the less lipophilic compounds <sup>99m</sup>Tc(NS<sub>3</sub>COOH)(L2-c(RGDyK)), <sup>99m</sup>Tc(NS<sub>3</sub>(COOH)<sub>3</sub>)(L1-c(RGDyK)) and <sup>99m</sup>Tc(NS<sub>3</sub>(COOH)<sub>3</sub>)(L2-c(RGDyK)) were studied (Tables 9.4–9.9). The biodistribution results of <sup>99m</sup>Tc(NS<sub>3</sub>)(L1-c(RGDyK)) are similar to the data of <sup>99m</sup>Tc(NS<sub>3</sub>COOH)(L2-c(RGDyK)) (Tables 9.4 and 9.5). No specific tumour uptake was observed. This might be due to the high accumulation of the compounds in the liver and fast hepatobiliary elimination. Substitution of the tetradentate ligand NS<sub>3</sub> or NS<sub>3</sub>COOH by the ligand NS<sub>3</sub>(COOH)<sub>3</sub>, which bears three carboxyl groups, resulted in a decrease of the hepatobiliary elimination and a predominant urinary excretion (Tables 9.4 and 9.6). Tumour uptake was also low (Tables 9.8 and 9.9).

## 9.4. CONCLUSIONS

The method described enables the <sup>99m</sup>Tc labelling of c(RGDyK) via 4 + 1 mixed ligand complexes. Structural variations in the tetradentate coligand resulted in a shift from predominant hepatobiliary elimination (NS<sub>3</sub> or NS<sub>3</sub>COOH as a coligand) to urinary excretion (NS<sub>3</sub>(COOH)<sub>3</sub> as a coligand). Further structural modification of the peptide conjugated 4 + 1 complexes in combination with receptor binding studies should be performed to elucidate the influence of the coupled complex in receptor binding. NS<sub>3</sub>(COOH)<sub>3</sub> is a prototype of a dendritically modified tetradentate ligand.

**CHAPTER 9**

**TABLE 9.4. TISSUE DISTRIBUTION (% ID/g TISSUE  $\pm$  SD;  $N = 3$ ) OF ACTIVITY AFTER INJECTION OF  $^{99m}\text{Tc}(\text{NS}_3)(\text{L1-c(RGDyK)})$  IN WISTAR RATS AND NUDE MICE BEARING MDA-MB-468 TUMOUR**

	Rat, 1 h	Mouse, 1 h
Blood	0.32 $\pm$ 0.04	0.56 $\pm$ 0.28
Brown fat	0.17 $\pm$ 0.04	0.22 $\pm$ 0.07
Skin and hair	0.40 $\pm$ 0.16	0.35 $\pm$ 0.09
Brain	0.02 $\pm$ 0.00	0.04 $\pm$ 0.01
Ovaries		0.47 $\pm$ 0.08
Uterus		0.42 $\pm$ 0.12
Pancreas	0.18 $\pm$ 0.03	0.18 $\pm$ 0.13
Spleen	1.41 $\pm$ 0.30	0.74 $\pm$ 0.16
Adrenals	0.33 $\pm$ 0.10	0.99 $\pm$ 0.17
Kidneys	2.78 $\pm$ 0.39	1.19 $\pm$ 0.10
Fat	0.12 $\pm$ 0.04	0.24 $\pm$ 0.09
Muscle	0.12 $\pm$ 0.04	0.13 $\pm$ 0.03
Heart	0.19 $\pm$ 0.05	0.37 $\pm$ 0.05
Lungs	0.54 $\pm$ 0.09	1.62 $\pm$ 0.44
Thymus	0.19 $\pm$ 0.04	
Harderian glands	0.20 $\pm$ 0.04	
Liver	3.49 $\pm$ 0.29	3.84 $\pm$ 0.38
Femur	0.23 $\pm$ 0.04	0.19 $\pm$ 0.04
Testes	0.06 $\pm$ 0.00	
Tumour		0.22 $\pm$ 0.03
Tumour/blood		0.40
Tumour/muscle		1.74

TABLE 9.5. TISSUE DISTRIBUTION (% ID/g TISSUE  $\pm$  SD,  $N = 3$ ) OF ACTIVITY AFTER INJECTION OF  $^{99m}\text{Tc}(\text{NS}_3\text{COOH})(\text{L2-c(RGDyK)})$  IN MICE BEARING M21 XENOGRAFTS AND AS CONTROL M21-L XENOGRAFTS

	M21		M21-L
	1 h	4 h	1 h
Blood	$0.59 \pm 0.03$	$0.42 \pm 0.05$	$0.70 \pm 0.12$
Liver	$3.70 \pm 0.65$	$1.97 \pm 1.25$	$7.79 \pm 2.47$
Lungs	$0.63 \pm 0.07$	$0.53 \pm 0.06$	$4.05 \pm 2.46$
Heart	$0.30 \pm 0.02$	$0.16 \pm 0.01$	$0.42 \pm 0.18$
Stomach	$0.69 \pm 0.26$	$0.24 \pm 0.03$	$2.42 \pm 2.32$
Spleen	$1.21 \pm 0.17$	$1.02 \pm 0.92$	$1.15 \pm 0.14$
Pancreas	$0.23 \pm 0.02$	$0.10 \pm 0.02$	$0.28 \pm 0.08$
Kidneys	$2.69 \pm 0.21$	$2.45 \pm 0.35$	$3.38 \pm 0.49$
Muscle	$0.14 \pm 0.02$	$0.09 \pm 0.03$	$0.14 \pm 0.04$
Intestine	$32.8 \pm 2.3$	$6.41 \pm 0.87$	$35.2 \pm 6.1$
Femur	$0.25 \pm 0.10$	$0.16 \pm 0.09$	$0.33 \pm 0.02$
Tumour	$0.20 \pm 0.04$	$0.10 \pm 0.05$	$0.23 \pm 0.02$

TABLE 9.6. TISSUE DISTRIBUTION (% ID/ORGAN  $\pm$  SD,  $N = 3$ ) OF ACTIVITY AFTER INJECTION OF  $^{99m}\text{Tc}(\text{NS}_3(\text{COOH})_3)(\text{L1-c(RGDyK)})$  IN NORMAL CD1 MICE

	Per cent dose/g			
	0.5 h	1 h	2 h	4 h
Blood	$6.1 \pm 1.5$	$3.7 \pm 0.9$	$2.8 \pm 0.6$	$1.2 \pm 0.3$
Liver	$3.8 \pm 0.6$	$2.5 \pm 0.4$	$1.3 \pm 0.2$	$0.8 \pm 0.2$
Lungs	$5.3 \pm 0.06$	$4.4 \pm 0.8$	$2.4 \pm 0.3$	$1.5 \pm 0.4$
Spleen	$2.2 \pm 0.3$	$1.0 \pm 0.4$	$0.6 \pm 0.1$	$0.5 \pm 0.1$
Kidneys	$10.8 \pm 1.7$	$8.5 \pm 0.1$	$8.0 \pm 1.8$	$5.4 \pm 0.4$
Muscle	$1.1 \pm 0.4$	$1.0 \pm 0.3$	$1.0 \pm 0.1$	$0.7 \pm 0.2$

CHAPTER 9

TABLE 9.7. TISSUE DISTRIBUTION (% ID/g TISSUE  $\pm$  SD,  $N = 3$ ) OF ACTIVITY AFTER INJECTION OF  $^{99m}\text{Tc}(\text{NS}_3(\text{COOH})_3)(\text{L1-c}(\text{RGDyK}))$  IN C57B16 MICE BEARING B16F1 MURINE MELANOMA

	0.5 h	1 h	2 h	4 h
Blood	7.1 $\pm$ 0.07	4.1 $\pm$ 0.1	2.4 $\pm$ 0.6	0.98 $\pm$ 0.07
Muscle	1.2 $\pm$ 0.3	1.2 $\pm$ 0.2	1.2 $\pm$ 0.4	0.61 $\pm$ 0.07
Tumour	3.7 $\pm$ 1.0	2.8 $\pm$ 0.6	2.1 $\pm$ 0.7	1.1 $\pm$ 0.3
Tumour/muscle	2.34 $\pm$ 0.06	2.28 $\pm$ 0.23	1.87 $\pm$ 0.7	1.81 $\pm$ 0.2
Tumour/blood	0.52 $\pm$ 0.15	0.68 $\pm$ 0.14	0.91 $\pm$ 0.34	1.2 $\pm$ 0.4

TABLE 9.8. TISSUE DISTRIBUTION (% ID/ORGAN  $\pm$  SD,  $N = 3$ ) OF ACTIVITY AFTER INJECTION OF  $^{99m}\text{Tc}(\text{NS}_3(\text{COOH})_3)(\text{L2-c}(\text{RGDyK}))$  IN NORMAL CD1 MICE

	Per cent dose/g			
	0.5 h	1 h	2 h	4 h
Blood	1.9 $\pm$ 0.5	1.1 $\pm$ 0.3	0.5 $\pm$ 0.1	0.3 $\pm$ 0.1
Liver	2.5 $\pm$ 0.3	2.2 $\pm$ 0.3	1.1 $\pm$ 0.5	0.6 $\pm$ 0.1
Lungs	2.5 $\pm$ 0.9	1.7 $\pm$ 0.03	1.1 $\pm$ 0.1	0.7 $\pm$ 0.2
Spleen	0.7 $\pm$ 0.1	0.7 $\pm$ 0.1	0.5 $\pm$ 0.1	0.3 $\pm$ 0.1
Kidneys	12.4 $\pm$ 2.0	12.3 $\pm$ 2.0	5.2 $\pm$ 0.14	2.5 $\pm$ 0.3
Muscle	0.9 $\pm$ 0.1	0.56 $\pm$ 0.06	0.56 $\pm$ 0.1	0.5 $\pm$ 0.1

TABLE 9.9. TISSUE DISTRIBUTION (% ID/g TISSUE  $\pm$  SD,  $N = 3$ ) OF ACTIVITY AFTER INJECTION OF  $^{99m}\text{Tc}(\text{NS}_3(\text{COOH})_3)(\text{L2-c}(\text{RGDyK}))$  IN C57B16 MICE BEARING B16F1 MURINE MELANOMA

	0.5 h	1 h	2 h	4 h
Blood	3.5 $\pm$ 0.6	2.1 $\pm$ 0.2	0.93 $\pm$ 0.35	0.61 $\pm$ 0.08
Muscle	1.3 $\pm$ 0.2	0.96 $\pm$ 0.13	0.55 $\pm$ 0.11	0.49 $\pm$ 0.18
Tumour	2.4 $\pm$ 0.4	1.7 $\pm$ 0.5	0.55 $\pm$ 0.11	0.51 $\pm$ 0.05
Tumour/muscle	2.0 $\pm$ 0.5	1.7 $\pm$ 0.3	1.0 $\pm$ 0.07	1.03 $\pm$ 0.09
Tumour/blood	0.78 $\pm$ 0.16	0.79 $\pm$ 0.20	0.62 $\pm$ 0.13	0.8 $\pm$ 0.18

## REFERENCES

- [9.1] HAUBNER, R., WESTER, H.-J., Radiolabeled tracers for imaging of tumor angiogenesis and evaluation of anti-angiogenic therapies, *Curr. Pharm. Design* **10** (2004) 1439–1455.
- [9.2] BEER, A.J., et al., Biodistribution and pharmacokinetics of the  $\alpha_v\beta_3$ -selective tracer  $^{18}\text{F}$ -galacto-RGD in cancer patients, *J. Nucl. Med.* **46** (2005) 1333–1341.
- [9.3] PIETZSCH, H.-J., GUPTA, A., SYHRE, R., LEIBNITZ, P., SPIES, H., Mixed-ligand technetium(III) complexes with tetradentate/monodentate  $\text{NS}_3$ /isocyanide coordination: A new nonpolar technetium chelate system for the design of neutral and lipophilic complexes stable in vivo, *Bioconj. Chem.* **12** (2001) 538–544.
- [9.4] SEIFERT, S., et al., Novel procedures for preparing  $^{99\text{m}}\text{Tc(III)}$  complexes with tetradentate/monodentate coordination of varying lipophilicity and adaptation to  $^{188}\text{Re}$  analogues, *Bioconj. Chem.* **15** (2004) 856–863.
- [9.5] SPIES, H., GLASER, M., PIETZSCH, H.-J., HAHN, F.E., LÜGGER, T., Synthesis and reactions of trigonal-bipyramidal rhenium and technetium complexes with tripodal, tetradentate  $\text{NS}_3$  ligand, *Inorg. Chim. Acta* **240** (1995) 465–478.
- [9.6] NEWKOME, G.R., LIN, X., YOUNG, J.K., Syntheses of amine building blocks for dendritic macromolecule construction, *Synlett* **1** (1992) 53–54.
- [9.7] GAMBINO, D., OTERO, L., KREMER, E., PIRO, O.E., CASTELLANO, E.E., Synthesis, characterization and crystal structure of hexakis-(thiourea-S) rhenium(III) trichloride tetrahydrate: A potential precursor to low-valent rhenium complexes, *Polyhedron* **16** (1997) 2263–2270.

## Chapter 10

### **DEVELOPMENT OF TECHNETIUM-99m LABELLED ANNEXIN V FRAGMENTS USING THE Tc-TRICARBONYL CORE**

D. PSIMADAS, C. ZIKOS, M. FANI, E. LIVANIOU,  
M. PAPADOPOULOS, I. PIRMETTIS  
Institute of Radioisotopes and Radiodiagnostic Products,  
Demokritos National Centre of Scientific Research, Athens, Greece

#### **Abstract**

The paper presents results on the labelling with  $^{99m}\text{Tc}$  of new N-terminal annexin V fragments. Two N-terminal annexin V fragments were successfully labelled, with a high yield, with  $^{99m}\text{Tc}$  using the  $^{99m}\text{Tc}$ -tricarbonyl precursor. The complexes formed were found to be stable against histidine and cysteine challenge. The biodistribution studies of the  $^{99m}\text{Tc}$  labelled peptides in mice showed fast blood and soft tissue clearance.

#### 10.1. INTRODUCTION

Annexin V, a protein consisting of 320 amino acids, is considered a promising target biomolecule for the development of a  $^{99m}\text{Tc}$  tracer for imaging apoptosis, but it has several disadvantages from the pharmaceutical preparation point of view (i.e. kit formulation). In the framework of the coordinated research project, the synthesis, labelling with  $^{99m}\text{Tc}$  and evaluation of new N-terminal annexin peptides were undertaken. In this work we report on labelling with  $^{99m}\text{Tc}$ -tricarbonyls and the evaluation of two theoretically active fragments.

#### 10.2. MATERIALS AND METHODS

##### **10.2.1. General**

Annexin fragments HAQVLRGTVTDFPG $\times$ 2TFA (His-AF13) and CAQVLRGTVTDFPG $\times$ 2TFA (Cys-AF13) were obtained from J. Környei (Izotop, Hungary). High performance liquid chromatography (HPLC) analysis

was performed on a Waters 600E chromatography system coupled to both a Waters 991 photodiode array detector (ultraviolet (UV) trace for rhenium and ligands) and a GABI gamma detector from Raytest (gamma trace for  $^{99m}\text{Tc}$ ). Separations were achieved on a Macherey-Nagel Nucleosil-100-10-C18 (10  $\mu\text{m}$ , 250  $\times$  4.6 mm) column eluted with a binary gradient system at a 1.0 mL/min flow rate. Mobile phase A was 0.1% TFA in methanol, while mobile phase B was 0.1% TFA in water. The elution profile was 0–1 min, 0% A, followed by a linear gradient up to 70% A in 10 min. This composition was held for another 15 min. After a column wash with 95% A for 5 min the column was re-equilibrated by applying the initial conditions (0% A) for 15 min prior to the next injection.

### 10.2.2. Derivatization of CAQVLRGTVTDFPG $\times$ 2TFA with vinyl pyridine

Vinyl pyridine (1  $\mu\text{mol}$ , in 20  $\mu\text{L}$  acetonitrile) was added to an aqueous solution of CAQVLRGTVTDFPG $\times$ 2TFA (1  $\mu\text{mol}$  in 300  $\mu\text{L}$  of distilled water) and the mixture was left at room temperature for 2 h. The sample was purified by semipreparative HPLC and the fraction containing the product was lyophilized. The yield was 90%.

### 10.2.3. Preparation of the precursor [ $^{99m}\text{Tc}(\text{H}_2\text{O})_3(\text{CO})$ ] $^+$

A sealed vial containing 4 mg  $\text{Na}_2\text{CO}_3$ , 5.5 mg  $\text{NaBH}_4$  and 20 mg sodium tartrate (0.07 mmol) was flushed with carbon monoxide for 20 min. Then 2 mL of  $^{99m}\text{Tc}$  pertechnetate (5–30 mCi) was added to the vial and this was heated at 75°C for 15 min. The vial was then cooled in a water bath and the reaction solution was neutralized with hydrochloric acid (1M) to pH7.0. The formation of the complex was tested by HPLC. For characterization, a reference sample of  $\text{Na}^{99m}\text{TcO}_4$  was analysed by HPLC under the same gradient. HPLC analysis showed that  $^{99m}\text{TcO}_4^-$  is eluted at 3–3.5 min and the precursor at 5 min.

### 10.2.4. Radiolabelling of peptides

An aqueous solution of [ $^{99m}\text{Tc}(\text{CO})_3(\text{H}_2\text{O})_3$ ] $^+$  (225  $\mu\text{L}$ ) was added to the peptide solution (25  $\mu\text{L}$ ,  $1 \times 10^{-3}$ – $1 \times 10^{-4}\text{M}$ ). The solution was purged with nitrogen and incubated at 75–80°C for 20 min. After cooling, the complex formation was tested by HPLC and the product was purified by HPLC.

### 10.2.5. Cysteine and histidine challenge of technetium-99m labelled peptides

Aliquots of 70  $\mu\text{L}$  of the  $^{99\text{m}}\text{Tc}$  labelled peptide were added to 630  $\mu\text{L}$  of a 0.01M cysteine or 0.01M histidine solution in PBS, pH7.4. The samples were incubated for 1–3 h at 37°C and analysed by HPLC.

### 10.2.6. Biodistribution studies in mice

Three groups of five Swiss albino mice (male, 30–35 g) were injected with the labelled peptide (0.1 mL, 1–2  $\mu\text{Ci}$ ) through the tail vein. The animals of the first group were sacrificed by cardiectomy under slight ether anaesthesia 30 min after injection, while the animals of the second and third group were sacrificed 2 and 24 h post-injection, respectively. The organs of interest were excised, weighed and counted in an automatic gamma counter. The bladder and excreted urine were not weighed. The stomach and intestines were not emptied of food contents prior to radioactivity measurements. The percentage of injected dose per organ (% ID/organ) was calculated by comparison of sample radioactivity to standard solutions containing 10% of the injected dose. The calculations for blood, muscle and bones were based upon measured activity, sample weight and body composition data (considering that blood, muscle and bones comprise 7%, 43% and 10%, respectively, of body weight). The percentage of injected dose per gram (% ID/g) was calculated by dividing the % ID/organ by the weight of the organ or tissue.

## 10.3. RESULTS AND DISCUSSION

The first peptide (His-AF13) has a histidine at the amino terminal position and thus could be used directly for labelling with the  $^{99\text{m}}\text{Tc}$ -tricarboxyls. The second peptide (Cys-AF13) was modified by introducing the pyridine-ethyl group on the sulphur of cysteine, thus resulting in a derivative (PECys-AF13) that can act as a tridentate ligand for the  $^{99\text{m}}\text{Tc}$ -tricarboxyl core (Fig. 10.1). The two peptides were successfully labelled with  $^{99\text{m}}\text{Tc}$ -tricarboxyls using a low concentration of the peptides (Fig. 10.2).

Both labelled peptides were found to be resistant to transchelation when they were incubated with 1:1000 excess of histidine and cysteine (Fig. 10.3).

The biodistribution of the labelled peptides was studied in mice (Tables 10.1 and 10.2). Before injection, both complexes were purified by HPLC to remove the excess of unlabelled peptide. After intravenous injection, the radiolabelled peptides rapidly cleared from the bloodstream and were

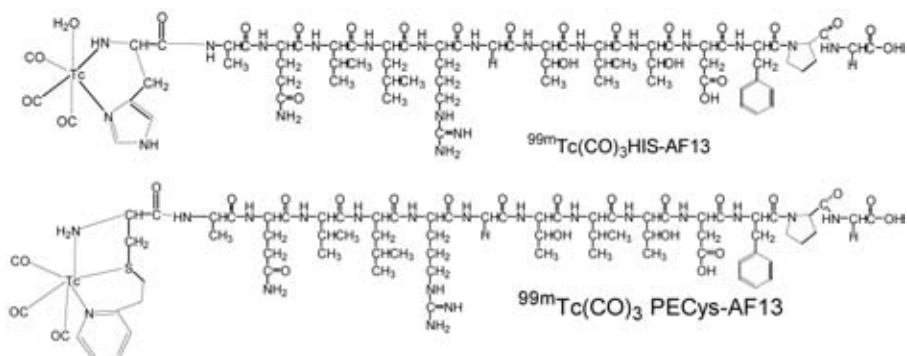


FIG. 10.1. Proposed structure of the labelled peptides.

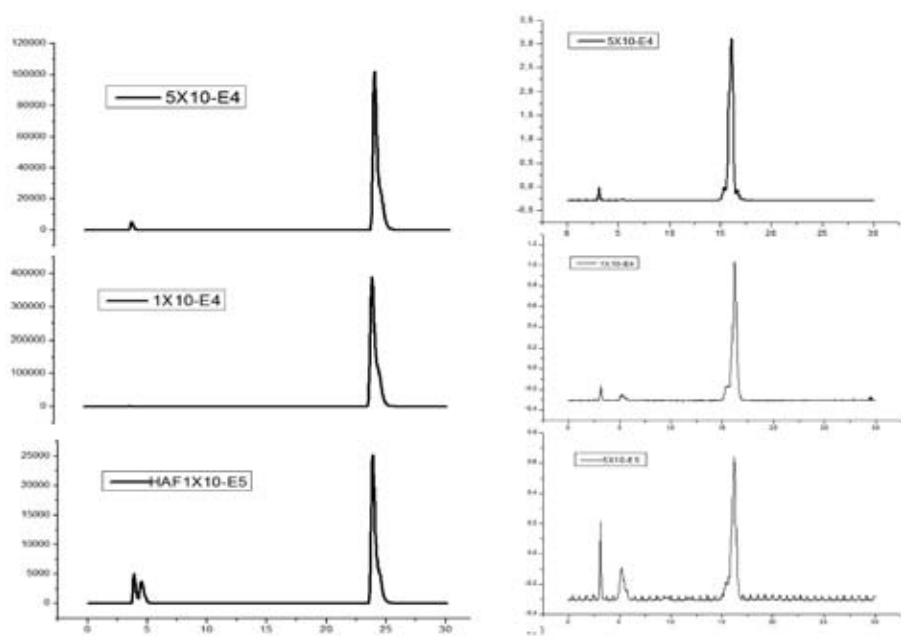


FIG. 10.2. HPLC radiochromatograms showing the effect of ligand concentration on radiochemical purity (left: His-AF13, right: PECyst-AF13).

excreted via both the urinary and the hepatobiliary system.  $^{99m}\text{Tc}(\text{CO})_3\text{-His-AF13}$  was excreted mainly into the urine and to a lesser degree into the intestines. At 24 h most of the activity was cleared out from the body, apart

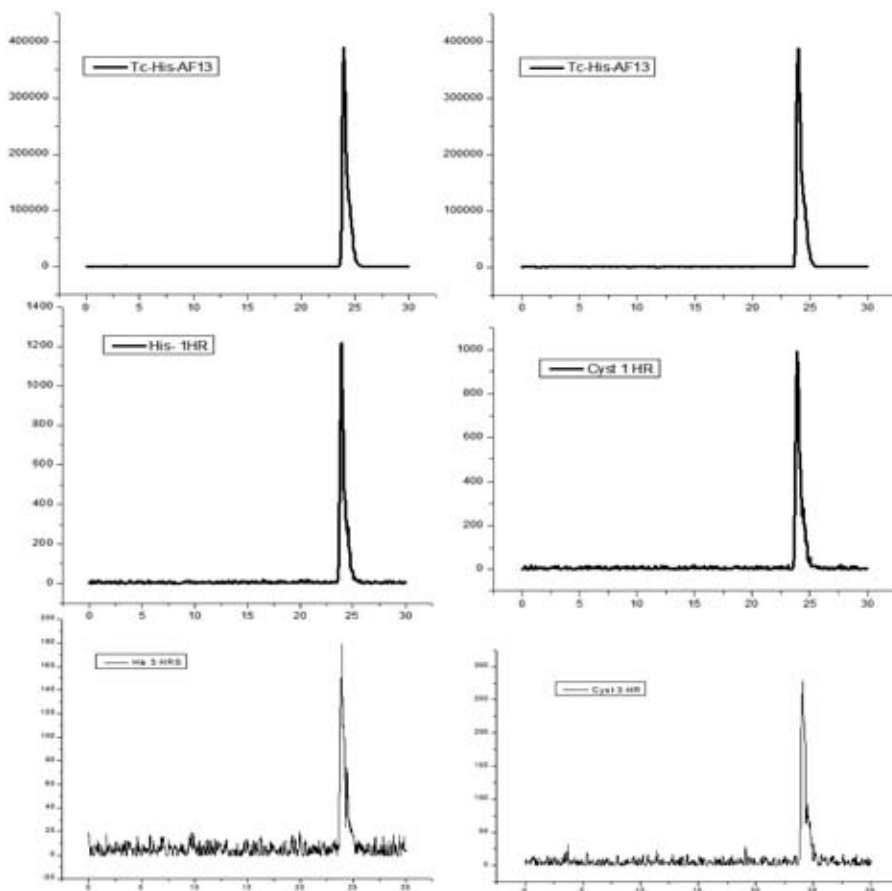


FIG. 10.3. Radiochromatograms of  $^{99m}\text{Tc}(\text{CO})_3\text{-His-AF13}$  immediately after incubation with 1:1000 excess histidine (top left) and cysteine (top right), and after 1 h (middle) and 3 h (bottom).

from a low retention of the activity in the liver and kidneys that was found for  $^{99m}\text{Tc}(\text{CO})_3\text{-His-AF13}$ .

#### 10.4. CONCLUSION

Annexin V fragments can be easily and efficiently labelled with  $^{99m}\text{Tc}$ -tricarbonyls. The chelating moiety was found to play an important role in the distribution of radioactivity in the animals' bodies.

TABLE 10.1. TISSUE DISTRIBUTION OF RADIOACTIVITY AFTER INJECTION OF  $^{99m}\text{Tc}(\text{CO})_3\text{-His-AF13}$  IN MICE (%ID/g)

	30 min	2 h	24 h
Blood	$1.57 \pm 0.17$	$0.61 \pm 0.12$	$0.10 \pm 0.02$
Liver	$6.88 \pm 2.58$	$6.70 \pm 0.83$	$4.04 \pm 1.74$
Heart	$0.87 \pm 0.11$	$0.30 \pm 0.07$	$0.06 \pm 0.01$
Kidneys	$4.83 \pm 0.97$	$2.32 \pm 0.48$	$0.73 \pm 0.21$
Stomach	$1.09 \pm 0.68$	$1.28 \pm 0.35$	$0.07 \pm 0.05$
Intestines	$1.17 \pm 0.39$	$3.70 \pm 0.60$	$0.18 \pm 0.09$
Spleen	$0.52 \pm 0.12$	$0.18 \pm 0.05$	$0.03 \pm 0.02$
Muscle	$0.34 \pm 0.04$	$0.13 \pm 0.06$	$0.02 \pm 0.01$
Lungs	$1.43 \pm 0.36$	$0.48 \pm 0.07$	$0.10 \pm 0.02$
Urine	$39.58 \pm 5.73$	$48.87 \pm 6.57$	—

TABLE 10.2. TISSUE DISTRIBUTION OF RADIOACTIVITY AFTER INJECTION OF  $^{99m}\text{Tc}(\text{CO})_3\text{-PECys-AF13}$  IN MICE (% ID/g)

	30 min	2 h	24 h
Blood	$2.66 \pm 0.39$	$1.00 \pm 0.08$	$0.01 \pm 0.00$
Liver	$7.59 \pm 1.45$	$6.14 \pm 1.89$	$0.42 \pm 0.21$
Heart	$0.98 \pm 0.24$	$0.45 \pm 0.01$	$0.01 \pm 0.01$
Kidneys	$4.15 \pm 0.41$	$1.99 \pm 0.42$	$0.18 \pm 0.08$
Stomach	$1.51 \pm 0.42$	$1.32 \pm 0.31$	$0.02 \pm 0.01$
Intestines	$3.63 \pm 0.63$	$7.20 \pm 0.56$	$0.04 \pm 0.01$
Spleen	$0.57 \pm 0.24$	$0.46 \pm 0.11$	$0.01 \pm 0.01$
Muscle	$0.30 \pm 0.05$	$0.17 \pm 0.03$	$0.01 \pm 0.00$
Lungs	$2.21 \pm 0.18$	$0.85 \pm 0.10$	$0.03 \pm 0.02$
Urine	$25.12 \pm 2.62$	$29.27 \pm 2.26$	—

## Chapter 11

### DEVELOPMENT OF TECHNETIUM-99m LABELLED BIOMARKERS FOR HEART METABOLISM USING THE Tc-TRICARBONYL CORE

A. PAPADOPOULOS\*, C. TSOUKALAS\*,  
A. PANAGIOTOPOULOU\*\*, M. PELECANOU\*\*,  
M. PAPADOPOULOS\*, I. PIRMETTIS\*

\* Institute of Radioisotopes and Radiodiagnostic Products

\*\* Institute of Biology

Demokritos National Centre of Scientific Research, Athens, Greece

#### Abstract

Synthesis and evaluation of a new fatty acid derivative labelled with  $^{99m}\text{Tc}$  was undertaken. Four derivatives of undecanoic acid and two derivatives of hexadecanoic acid were synthesized and their coordination chemistry with  $^{99m}\text{Tc}$ - and Re-tricarbonyl cores was investigated. The Re(I) complex was prepared with a good yield by refluxing the ligand with  $[\text{NEt}_4]_2[\text{ReBr}_3(\text{CO})_3]$  in methanol and was characterized by spectroscopic methods. Four of the derivatives were provided to groups in China, India and the Russian Federation, and in these laboratories high performance liquid chromatography (HPLC) analysis demonstrated that the reaction produces a single complex with a high yield. The  $^{99m}\text{Tc}$  complexes were characterized by comparative HPLC studies using a sample of a well characterized Re(I) complex as reference.

#### 11.1. INTRODUCTION

Long chain fatty acids are the major source of energy for heart muscle and are rapidly metabolized by beta oxidation under normal conditions. Regional alterations in myocardial fatty acid oxidation may indicate ischaemic heart disease and cardiomyopathy at an early stage and therefore possess a remarkable diagnostic potential. Many fatty acids or their analogues have been labelled with positron and gamma emitting radionuclides in order to non-invasively assess changes in fatty acid metabolism [11.1]. Over the past 30 years,

various research groups have explored the possibility of incorporating  $^{99m}\text{Tc}$  into fatty acid carrier molecules using a variety of ligands. Even though neutral lipophilic  $^{99m}\text{Tc}$  complexes were formed, the myocardial profiles of the agents were not adequate [11.2–11.4]. In the framework of the coordinated research project, synthesis and evaluation of new fatty acid derivatives labelled with  $^{99m}\text{Tc}$  was undertaken.

## 11.2. MATERIALS AND METHODS

### 11.2.1. General

Infrared (IR) spectra were recorded as KBr pellets in the range 4000–500  $\text{cm}^{-1}$  on a Perkin-Elmer 1600 FT-IR spectrophotometer. The nuclear magnetic resonance (NMR) spectra were recorded on a Bruker AC 250E spectrometer with TMS as an internal standard. Elemental analysis was performed on a Perkin-Elmer 2400/II automated analyser. All laboratory chemicals were reagent grade. The precursor  $[\text{Et}_4\text{N}]_2[\text{ReBr}_3(\text{CO})_3]$  was synthesized in accordance with literature methods [11.5].

High performance liquid chromatography (HPLC) analysis was performed on a Waters 600E chromatography system coupled to both a Waters 991 photodiode array detector (ultraviolet (UV) trace for rhenium and ligands) and a GABI gamma detector from Raytest (gamma trace for  $^{99m}\text{Tc}$ ). Separations were achieved on a Macherey-Nagel Nucleosil-100-10-C18 (10  $\mu\text{m}$ , 250  $\times$  4.6 mm) column eluted with a binary gradient system at a 1.0 mL/min flow rate. Mobile phase A was methanol, while mobile phase B was water, both containing 0.1% TFA. Three elution profiles were used: 0–1 min 0% A, followed by a linear gradient to 80% A in 10 min. This composition was held for another 15 min.

### 11.2.2. Synthesis of ligands

#### 11.2.2.1. Synthesis of 11-[bis(carboxymethyl)amino] undecanoic acid (IDA-FA11)

11-bromo-undecanoic acid (21.23 g, 0.08 mol) was dissolved in ethanol (100 mL) in a 500 mL two-necked round bottomed flask equipped with a reflux condenser. Then an aqueous solution of iminodiacetic acid (50 mL, 10.64 g, 0.08 mol) that was made alkaline (pH12) with sodium hydroxide was added and the mixture was refluxed for 5 h. The pH was maintained at pH12 by addition of 10% NaOH solution. Whenever a precipitate was formed, more

ethanol was added. At the end of reflux, the ethanol was evaporated. After cooling, the unreacted 11-bromo-undecanoic acid was precipitated and filtered off. The pH of the aqueous solution was adjusted to pH2 with 5N HCl. The white precipitate, 11-[bis (carboxymethyl) amino] undecanoic acid (1), was collected by filtration then washed with water and dried. The product was recrystallized four times with ethanol. The overall yield was 37%. Melting point (MP): 147–149°C.  $^1\text{H NMR}$  ( $\text{D}_2\text{O}$ ): 1.12, 1.25–1.55 (16H, 3-10- $\text{CH}_2$ ), 2.03 (2H, 2- $\text{CH}_2$ ), 2.33 (2H, 11- $\text{CH}_2$ ), 3.01 (4H,  $\text{NCH}_2\text{CO}$ ). IR (KBr): 2810–2950 (m), 1610 (m), 1680 (m). Thin layer chromatography (TLC) (ethyl acetate:MeOH: $\text{NH}_3$ , 10:1:0.3), retention factor ( $R_f$ ) = 0.6. Elemental analysis of  $\text{C}_{15}\text{H}_{27}\text{NO}_6 \cdot 1/2\text{H}_2\text{O} \cdot \text{HCl}$ : calculated, C 49.65, H 8.06, N 3.86; found, C 50.21%; H 8.05%, N 3.75%.

#### 11.2.2.2. Synthesis of 11-(S-cysteine)undecanoic acid Cyst-FA11

Cysteine hydrochloride (1.57 g, 13 mmol) was dissolved in 30 mL 2N NaOH and then 11-bromoundecanoic acid (3.44 g, 13 mmol) was added. The mixture was stirred at room temperature until the acid was completely dissolved (24 h). The pH of the solution was adjusted to pH5 by the addition of glacial acetic acid. The precipitate obtained was worked up with hot methanol/water (80/20), filtrated and washed with cold methanol. The yield was 3.63 g (91.9%). MP: 181–196°C. TLC (MeOH),  $R_f$  = 0.64. IR (KBr): 2918, 1705, 1622, 1582.  $^1\text{H NMR}$  (500 MHz,  $\text{D}_2\text{O}$ )  $\delta$ : 3.19 (1H, t), 2.63 (1H, dd), 2.56 (1H, dd), 2.64 (2H, t), 1.93 (2H, t), 1.32 (4H, m), 1.10 (12H, m). Elemental analysis of  $\text{C}_{14}\text{H}_{27}\text{NO}_4\text{S}$ : calculated, C 55.05, H 8.41, N 4.59; found C 55.04%, H 8.91%, N 4.38%.

#### 11.2.2.3. Synthesis of 16-(S-cysteine)hexadecanoic acid Cyst-FA16

Cysteine hydrochloride (600 mg, 4.95 mmol), 16-bromohexadecanoic acid (500 mg, 1.62 mmol), 1 mL of DMSO and 10 mL of MeONa (5.4M) were added in 170 mL of methanol. The mixture became a homogenous solution by heating at 40°C and the solution was stirred for 3 h at room temperature. The solvents were then removed and 10 mL of water was added to the residue. The pH of the solution was adjusted to pH4.5 by the addition of glacial acetic acid. The precipitate was collected and worked up with 80 mL hot ethanol/water (5:1). The remaining solid was collected by filtration and dried. The yield was 500 mg (89.3%). MP: 204–220°C. TLC (MeOH:c $\text{NH}_4\text{OH}$ , 10:0.4),  $R_f$  = 0.7. IR (KBr): 3043, 2919, 2852, 1703, 1539.  $^1\text{H NMR}$  (not recorded due to low solubility of the product).

*11.2.2.4. Synthesis of 16-(S-cysteine)hexadecanoic acid dimethylester, Cyst-FA16 dimethylester*

16-(S-cysteine)hexadecanoic acid (100 mg, 0.26 mmol) was added in 30 mL of methanol containing 1 mL of concentrated HCl. After cooling to  $-7^{\circ}\text{C}$ , 2 mL  $\text{SOCl}_2$  was added dropwise and the mixture was stirred for 48 h at room temperature. The solvents were removed by rotary evaporator and saturated  $\text{NaHCO}_3$  solution was added to the residue, and the product was extracted in ethylacetate. The organic layer was washed with water, dried by  $\text{Na}_2\text{SO}_4$ , filtrated and finally evaporated to dryness to give the dimethylester. The yield was 100 mg (93%). MP:  $98\text{--}105^{\circ}\text{C}$ . TLC (ethylacetate),  $R_f = 0.5$ . IR (KBr): 3451, 2921, 2851, 1739, 1471, 1438, 1249, 1173, 1095, 1050, 802, 720.  $^1\text{H}$  NMR (500 MHz,  $\text{CDCl}_3$ )  $\delta$ : 4.1 (1H, br), 3.75 (3H, s), 3.6 (3H, s), 3.1 (1H, dd), 2.98 (1H, dd), 2.52 (2H, t), 2.22 (2H, t), 1.52 (4H, m), 1.2 (20H, s).  $^{13}\text{C}$  NMR (250 MHz,  $\text{CDCl}_3$ )  $\delta$ : 174.33 (COO), 170.43 (COO), 53 (CH), 51.4 ( $\text{CH}_2$ ), 34.1, 29.6, 29.5, 29.3, 29.2, 28.7, 28.2, 25.

*11.2.2.5. Synthesis of N-undecanoicdithiocarbamate sodium salt CS2-FA11*

0.96 g (20.4 mmol) of sodium hydroxide was dissolved in 140 mL of water. Under stirring, 2.00 g (9.28 mmol) of 11-aminoundecanoic acid was added. The solution was cooled at  $0^{\circ}\text{C}$  under stirring and, drop by drop, 1.0 mL of carbon disulphide (12.74 mmol) was added. The reaction was stirred overnight (20 h) at  $0^{\circ}\text{C}$ . The solvent was evaporated under reduced pressure and the residue was washed with ethanol, dichloromethane and diethylether. The residue was recrystallized from water/acetone (or dissolved in water and precipitated by the addition of acetone) to form a white solid. The yield was 2.14 g (67%). MP:  $300^{\circ}\text{C}$ . IR (KBr): 2923, 2851, 1640, 1511,  $1395\text{ cm}^{-1}$ .  $^{13}\text{C}$  NMR (250 MHz,  $\text{D}_2\text{O}$ ): 211 ( $\text{CS}_2$ ), 186 (COO), 50 ( $\text{CH}_2(\text{NH})$ ), 40 ( $\text{CH}_2(\text{COO})$ ), 30.6, 30.3, 28.0, 27.8, 27.4.

*11.2.2.6. Synthesis of 16-(N-(pyridine-2-yl-methyl)-N-aminoethyl acetate)hexadecanoic ethylester PAM-FA16*

A solution of 16-bromohexadecanoic ethylester (3.44 g, 9.5 mmol), N-(2-pyridylmethyl)aminoethyl acetate (0.97 g, 5 mmol) and diisopropyl-ethylamine (5 mL) in 60 mL ethanol was refluxed for 24 h and then 1mL diisopropyl-ethylamine and 50 mL n-propanol were added to the solution. The reaction mixture was further refluxed for an additional 72 h and then evaporated under vacuum. The residue was purified by column chromatography to give 0.31 g of the product. The yield was 13%.  $^1\text{H}$  NMR ( $\text{CDCl}_3$ )  $\delta$ : 8.53 (1H, d) 7.67 (1H, m),

7.54 (1H, m), 7.16 (1H, m), 4.14 (4H, m), 3.94 (2H, s), 3.41 (2H, s), 2.65 (2H, t), 2.30 (2H, t), 1.63 (2H, m), 1.49 (2H, m), 1.26 (28H, br).

#### 11.2.2.7. Synthesis of NSC-FA11

A solution of 4-(2-benzimidazolyl)-3-thiabutanoic acid [11.5] (2.40 g, 10 mmol), 11-bromoundecanoic acid (2.65 g, 10 mmol) in 40 mL 1N NaOH was refluxed for 48 h. After cooling, the pH was adjusted to pH5 with hydrochloric acid. The precipitate was collected by filtration and was washed with cold water/methanol. The yield was 20%. HPLC (A) showed one peak at 16.75 min. IR (KBr pellet): 2927(s), 2852(s), 1717(s), 1634(w), 1584(w), 1471(m), 794(m)  $\text{cm}^{-1}$ .  $^1\text{H}$  NMR (DMSO- $d_6$ )  $\delta$ : 7.56 (2H, dd), 7.20 (2H, dt), 4.23 (2H, t), 4.10 (2H, s), 3.40 (2H, t), 3.32 (2H, s), 1.75 (2H, t), 1.50 (2H, br), 1.25 (12H, br).

### 11.2.3. Synthesis of rhenium complexes

#### 11.2.3.1. Synthesis of $\text{Re}(\text{CO})_3(\text{IDA-FA11})$

To a solution of  $[\text{Et}_4\text{N}]_2[\text{ReBr}_3(\text{CO})_3]$  (77 mg, 0.1 mmol) in 5 mL of methanol, 11-[bis (carboxymethyl)amino] undecanoic acid (31.7 mg, 0.1 mmol) and a solution of NaOH 1N (200  $\mu\text{L}$ , 2 mmol) were added under stirring. The solution was refluxed for 2 h and allowed to cool. Then 2 mL of distilled water was added. A white solid precipitate formed after slow evaporation. The solid was recrystallized with methanol/water. The yield was 70 mg (84.2%). HPLC (A) showed one peak at 17.00 min. IR (KBr): 446(m), 2990(m), 2931(m), 2856(m), 2021(s), 1910(s), 1874(s), 1711(m), 1631(s), 1602(w), 1488(w), 1471(w), 1398(m), 1374(w), 1174(w), 1003(w), 915(w), 788(w), 645(w), 537(w).

#### 11.2.3.2. Synthesis of the complex $\text{Re}(\text{CO})_3(\text{Cyst-FA11})$

To a solution of  $[\text{Et}_4\text{N}]_2[\text{ReBr}_3(\text{CO})_3]$  (154 mg, 0.2 mmol) in 5 mL acetonitrile, Cyst-FA11 (61 mg, 0.2 mmol) and a solution of NaOH 1N (400  $\mu\text{L}$ , 4 mmol) were added under stirring. The solution was refluxed for 5 h and allowed to cool. Then 2 mL of distilled water was added. A white solid precipitated after slow evaporation. The yield was 40%. HPLC showed one peak at 21.20 min (profile A). IR (KBr): 2993, 2922, 2853, 2024(s), 1891(s), 1638, 1561, 1488, 1445, 1396, 1174, 1003, 787.  $^1\text{H}$  NMR (DMSO- $d_6$ )  $\delta$ : 3.45 (2H, t), 3.20 (8H, q), 2.45 (1H, m), 1.95 (2H, m), 1.65 (2H, m), 1.41 (2H, m), 1.30 (2H, m), 1.22 (12H, br), 1.16 (12H, t).

### 11.2.3.3. Synthesis of the complex $Re(CO)_3(NSC-FA11)$

To a solution of  $[Et_4N]_2[ReBr_3(CO)_3]$  (154 mg, 0.2 mmol) in 5 mL acetonitrile, NSC-FA11 (0.2 mmol) and a solution of 1N NaOH (400  $\mu$ L, 4 mmol) were added under stirring. The solution was refluxed for 24 h and allowed to cool. Then 2 mL of distilled water was added. A white solid precipitated that was collected by filtration. The yield was 50%. HPLC (B) showed one peak at 18.87 min. IR (KBr): 2928(m), 2853(m), 2029(s), 1896(s), 1632(m), 1541(w), 1456(m), 744(m).  $^1H$  NMR (DMSO- $d_6$ )  $\delta$ : 7.85 (2H, t), 7.50 (2H, m), 4.90 (2H, dd), 4.35 (2H, t), 3.65 (2H, dd), 1.78 (2H, t), 1.50 (4H, m), 1.30 (12H, br).

### 11.2.3.4. Synthesis of the complex $Re(CO)_3PAM-FA16$

To a solution of  $[Et_4N]_2[ReBr_3(CO)_3]$  (77 mg, 0.1 mmol) in 5 mL methanol, PAM FA16 (0.1 mmol) and a solution of 1N NaOH (200  $\mu$ L, 2 mmol) were added under stirring. The solution was refluxed for 2 h and allowed to cool. Then 2 mL of distilled water was added. A white solid precipitated after slow evaporation. The solid was recrystallized with methanol/water. Crystals suitable for X ray analysis were obtained by recrystallization from acetonitrile. The yield was 65%. HPLC showed one peak at 9.3 min (profile C). IR (KBr): 2922(m), 2850(m), 2018(s), 1923(s), 1889(s), 1740(m), 1658(s), 1610(w), 1353(w), 1322(w), 1173(m), 1033(w), 780(m).  $^1H$  NMR (DMSO- $d_6$ )  $\delta$ : 8.78 (1H, d), 8.15 (1H, t), 7.70 (1H, d), 7.57 (1H, t), 4.75 (1H, d), 4.53 (1H, d), 4.05 (2H, q), 3.80 (1H, d), 3.40 (1H, d), 3.19 (2H, t), 2.26 (2H, t), 1.73 (2H, m), 1.5 (2H, m), 1.25 (22H, br), 1.15 (3H, t).

## 11.2.4. Labelling with technetium-99m

### 11.2.4.1. Preparation of the precursor $[^{99m}Tc(H_2O)_3(CO)]^+$

A sealed vial containing 4 mg  $Na_2CO_3$ , 5.5 mg  $NaBH_4$  and 20 mg sodium tartrate (0.07 mmol) was flushed with carbon monoxide for 20 min. Then 2 mL of  $^{99m}Tc$ -pertechnetate (5–30 mCi) was added to the vial, which was heated at 75°C for 15 min. The vial was then cooled in a water bath and the reaction solution was neutralized with hydrochloric acid (1M) to pH7.0 [11.7]. The formation of the complex was tested by HPLC (gradient). For characterization, a reference sample of  $Na^{99m}TcO_4$  was analysed by HPLC under the same gradient. HPLC analysis showed that  $^{99m}TcO_4^-$  was found at 3.0–3.5 min and the precursor at 4.5–5.0 min.

#### 11.2.4.2. General method for the preparation of the technetium-99m labelled fatty acids with $[^{99m}\text{Tc}(\text{CO})_3]^+$

A solution of the ligand (2–100  $\mu\text{L}$ ,  $1 \times 10^{-3}$ – $1 \times 10^{-4}\text{M}$  in DMSO) was added to an aqueous solution of  $[^{99m}\text{Tc}(\text{CO})_3(\text{H}_2\text{O})_3]^+$  (400–900  $\mu\text{L}$ ). The solution was purged with nitrogen and incubated at 75–80°C for 20 min, unless otherwise noted. After cooling, the complex formation was tested by HPLC. The product was purified by HPLC.

#### 11.2.4.3. Synthesis of the technetium-99m complex with 11-[bis(carboxymethyl)amino]undecanoic acid

In a vial containing 500  $\mu\text{g}$  of 11-[bis(carboxymethyl)amino]undecanoic acid, 1 mL of the precursor  $[^{99m}\text{Tc}(\text{H}_2\text{O})_3(\text{CO})]^+$  was added (pH7) and the solution was incubated for 20 min at 70°C. After cooling, the complex formation was tested by HPLC. A second labelling procedure was also performed, where the pH of the solution was adjusted to pH9 by adding NaOH solution, and the final solution was then incubated for 20 min at 70°C. After cooling, the complex formation was tested by HPLC. The yield was 93.3%.

#### 11.2.4.4. Synthesis of the complex $^{99m}\text{Tc}(\text{CO})_3(\text{Cyst-FA11})$

Labelling conditions: 0.16 mg ligand in 0.2 mL DMSO mixed with 0.3 mL precursor at pH7.0 for 30 min at 80°C. The yield was 96%. Retention time ( $R_t$ ), 18.79. (Cys-FA11,  $R_t$ , 18.37).

#### 11.2.4.5. Synthesis of the complex $^{99m}\text{Tc}(\text{CO})_3(\text{NSC-FA11})$

Labelling conditions: 50  $\mu\text{g}$  ligand in 50  $\mu\text{L}$  DMSO mixed with 0.5 mL precursor at pH7.5 for 10 min at 80°C. The yield was 95%.  $R_t$ , 19.20. (NSC-FA11,  $R_t$ , 18.90).

### 11.3. RESULTS AND DISCUSSION

The fatty acid derivatives were synthesized by employing a multistep procedure. The reaction scheme for the preparation of ligand NSC-FA11 is shown in Fig. 11.1.

The ligands were characterized by IR, NMR and elementary analysis. The rhenium complexes (Fig. 11.2) were synthesized as surrogates for the analogous  $^{99m}\text{Tc}$  complex prepared at the no carrier added level and their structures were

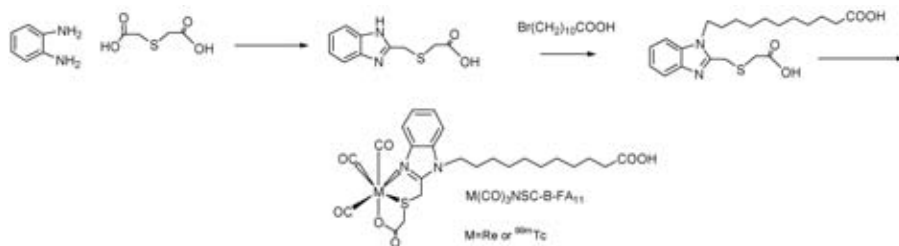


FIG. 11.1. Synthesis of fatty acid derivative attached to NSC chelator.

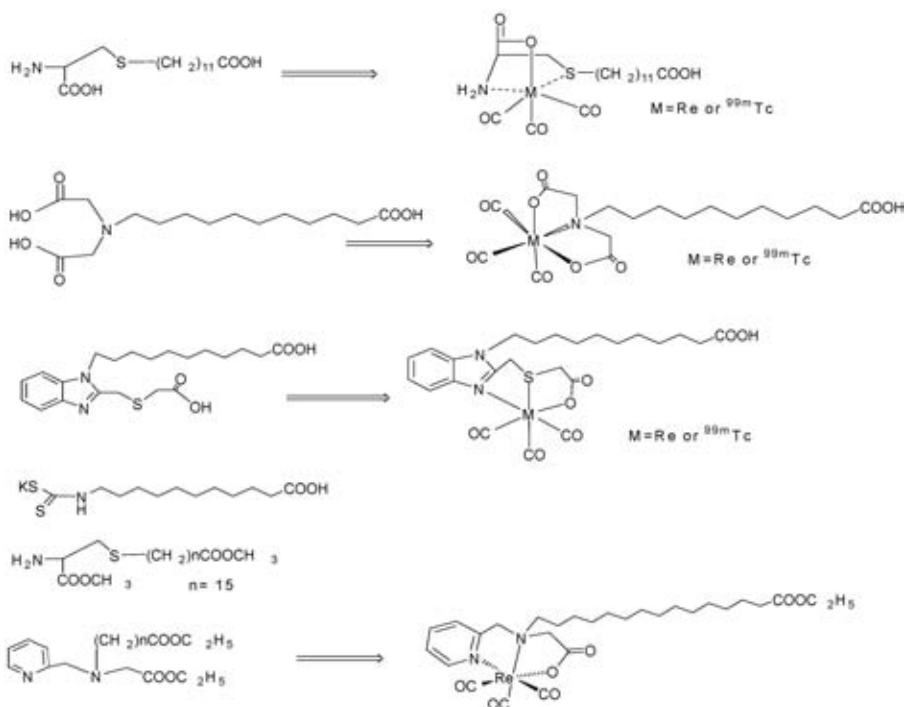


FIG. 11.2. Fatty acid derivatives and their rhenium-tricarbonyl complexes.

fully characterized. Co-injections of pairs of rhenium and  $^{99m}\text{Tc}$  compounds into HPLC under various elution conditions should confirm the structural similarity of both substances. The rhenium complexes were prepared with a good yield by refluxing equimolar amounts of the ligand with  $[\text{Et}_4\text{N}]_2[\text{Re}(\text{CO})_3\text{Br}_3]$  in methanol. Slow cooling of the concentrated reaction mixture, and in some situations addition of water, precipitated the complex as a white solid. HPLC analysis of the complex showed one major peak. The IR

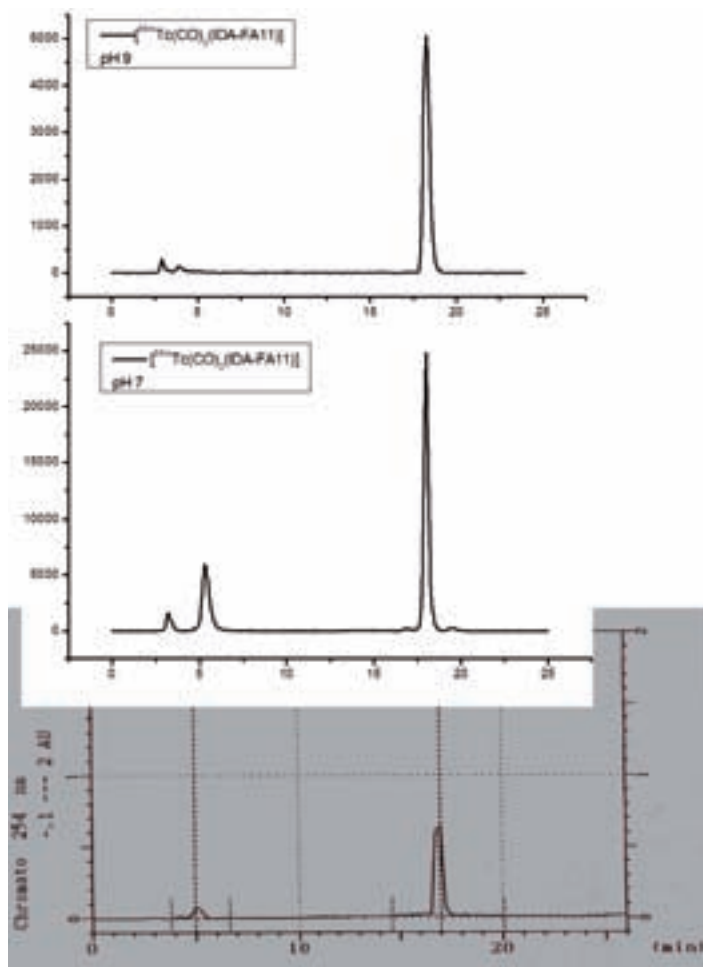


FIG. 11.3. Chromatograms of IDA-FA11 derivatives. Rhenium complex (bottom), labelling with  $^{99m}\text{Tc}$  at pH7 (middle) and at pH9 (top).

spectra of the complex showed the expected strong bands in the region of  $1873\text{--}2025\text{ cm}^{-1}$ , indicating the presence of the *fac*- $\{\text{Re}(\text{CO})_3\}^+$  core.

Labelling with  $^{99m}\text{Tc}$  was carried out by reacting the ligand with  $^{99m}\text{Tc}$ -tricarbonyl precursor at  $50\text{--}80^\circ\text{C}$  for 10–30 min. The pH of the reaction was found to influence the radiolabelling yield (Fig. 11.3). The characterization of the  $^{99m}\text{Tc}$  complexes was performed by comparative HPLC analysis. When rhenium and  $^{99m}\text{Tc}$  complexes were co-injected, both radioactivity (for tracer) and UV (for carrier) detectors exhibited identical chromatographic profiles,

demonstrating that the same chemical species were formed at both the carrier (rhenium) and tracer levels ( $^{99m}\text{Tc}$ ) (Fig. 11.3).

#### 11.4. CONCLUSIONS

The aim of the study was to synthesize and label new biomolecules with  $^{99m}\text{Tc}$  for in vivo targeting of heart metabolism. Undecanoic acid was used as a model for fatty acids. This molecule was conjugated with iminodiacetate, a chelating moiety that selectively coordinates with the Tc-carbonyl core. This derivative was characterized and labelled starting from the  $[\text{}^{99m}\text{Tc}(\text{CO})_3]^+$  synthon. After this first attempt, amounts of this bifunctional ligand were sent to various laboratories involved in this coordinated research project for further evaluation.

#### REFERENCES

- [11.1] TAMAKI, A., MORITA, K., KUGE, Y., TSUKAMOTO, E., The role of fatty acids in cardiac imaging, *J. Nucl. Med.* **41** (2000) 1525.
- [11.2] MAGATA, Y., et al., A Tc-99m-labeled long chain fatty acid derivative for myocardial imaging, *Bioconj. Chem.* **15** (2004) 389.
- [11.3] JONES, G.S., ELMALEH, D., STRAUSS, H.W., FISHERMAN, A.J., Synthesis and biodistribution of a new  $^{99m}\text{technetium}$  fatty acid, *Nucl. Med. Biol.* **21** (1994) 117.
- [11.4] MACH, R.H., KUNG, H.F., JUNGWIWATTANAPORN, P., GUO, Y.-Z., Synthesis and biodistribution of a new class of  $^{99m}\text{Tc}$ -labeled fatty acid analogs for myocardial imaging, *Nucl. Med. Biol.* **18** (1991) 215.
- [11.5] ALBERTO, R., et al., Synthesis and reactivity of  $[\text{NEt}_4]_2[\text{ReBr}_3(\text{CO})_3]$ . Formation and structural characterization of the clusters  $[\text{NEt}_4][\text{Re}_3(\mu_3\text{-OH})(\mu\text{-OH})_3(\text{CO})_9]$  and  $[\text{NEt}_4][\text{Re}_2(\mu\text{-OH})_3(\text{CO})_6]$  by alkaline titration, *J. Chem. Soc. Dalton Trans.* **19** (1994) 2815.
- [11.6] MATTHEWS, C.J., et al., Route to bis(benzimidazole) ligands with built-in asymmetry: Potential models of protein binding sites having histidines of different basicity, *Inorg. Chem.* **35** (1996) 7563.
- [11.7] ALBERTO, R., et al., A novel organometallic aqua complex of technetium for the labeling of biomolecules: Synthesis of  $[\text{}^{99m}\text{Tc}(\text{OH}_2)_3(\text{CO})_3]^+$  from  $[\text{}^{99m}\text{TcO}_4]^-$  in aqueous solution and its reaction with a bifunctional ligand, *J. Am. Chem. Soc.* **120** (1998) 7987.

## Chapter 12

### **DEVELOPMENT OF TECHNETIUM-99m LABELLED BIOMARKERS FOR EGFR-TK USING THE Tc-TRICARBONYL CORE**

N. MARGARITIS\*, N. BOURKOULA\*, M. PARAVATOU\*,  
E. LIVANIOU\*, A. PAPADOPOULOS\*, A. PANAGIOTOPOULOU\*\*,  
C. TSOUKALAS\*, M. PELECANOU\*\*, M. PAPADOPOULOS\*,  
I. PIRMETTIS\*

\* Institute of Radioisotopes and Radiodiagnostic Products

\*\* Institute of Biology

Demokritos National Centre of Scientific Research, Athens, Greece

#### **Abstract**

The aim of the study was to synthesize and label new biomarkers such as EGFR-TK inhibitors using the Tc-tricarbonyl core. 6-amino-4-[(3-bromophenyl)amino]-quinazoline, a compound that is a potent EGFR-TK inhibitor, was selected as one of the lead molecules. This compound was synthesized and distributed to other members, in order to perform coupling with the bifunctional agents. Furthermore, it was derivatized with various chelating moieties and their Re-tricarbonyl complexes were prepared and characterized by infrared spectroscopy and nuclear magnetic resonance spectroscopy. Analogous <sup>99m</sup>Tc-tricarbonyl complexes were also prepared. In vitro studies of the ligands as well as of the Re-tricarbonyl complexes with A431 cells demonstrated their ability to inhibit cell growth as well as to inhibit phosphorylation in the presence of at least 1 μM of the compounds studied.

#### 12.1. INTRODUCTION

EGFR is involved in the proliferation of normal and malignant cells and is overexpressed in many human tumours, such as breast cancer, glioma, laryngeal cancer, carcinoma of the head and neck, and prostate cancer. The EGFR reversible inhibitor Iressa was recently approved by the US Food and Drug Administration for treatment of non-small cell lung cancer and prostate

cancer, and several other anti-EGFR targeted molecules, such as Tarceva, are presently undergoing clinical phase III trials. Consequently, there has been a growing interest in the use of EGFR-TK inhibitors as radiotracers for molecular imaging of EGFR overexpressing tumours by nuclear medicine modalities [12.1–12.4]. Recently, several reversible and irreversible inhibitors, such as ML01, ML03 and ML06–ML08, were labelled with  $^{18}\text{F}$ ,  $^{11}\text{C}$  and  $^{124}\text{I}$ , respectively, and their potential as positron emission tomography biomarkers was investigated both in vitro and in vivo [12.5–12.8].

## 12.2. MATERIALS AND METHODS

### 12.2.1. General

Infrared (IR) spectra were recorded as KBr pellets in the range 4000–500  $\text{cm}^{-1}$  on a Perkin-Elmer 1600 FT-IR spectrophotometer. Nuclear magnetic resonance (NMR) spectra were recorded on a Bruker AC 250E spectrometer with TMS as the internal standard. Elemental analysis was performed on a Perkin-Elmer 2400/II automated analyser. All laboratory chemicals were reagent grade. The precursor  $[\text{Et}_4\text{N}]_2[\text{ReBr}_3(\text{CO})_3]$  was synthesized in accordance with literature methods [12.9].

High performance liquid chromatography (HPLC) analysis was performed on a Waters 600E chromatography system coupled to both a Waters 991 photodiode array detector (ultraviolet (UV) trace for rhenium and ligands) and a GABI gamma detector from Raytest (gamma trace for  $^{99\text{m}}\text{Tc}$ ). Separations were achieved on a Macherey-Nagel Nucleosil-100-10-C18 (10  $\mu\text{m}$ , 250  $\times$  4.6 mm) column eluted with a binary gradient system at a 1.0 mL/min flow rate. Mobile phase A was 0.1% TFA in methanol, while mobile phase B was 0.1% TFA in water. The elution profile was 0–1 min 0% A followed by a linear gradient to 70% A in 9 min; this composition was held for another 15 min. After a column wash with 95% A for 5 min the column was re-equilibrated by applying the initial conditions (0% A) for 15 min prior to the next injection. Alternatively, the column was eluted with an isocratic system of 75% MeOH, 25% water, both containing 0.1% TFA.

### 12.2.2. Synthesis

#### 12.2.2.1. 6-nitroquinazoline (1)

4-hydroxyquinazoline (20 g) was added in portions to a warm (92°C) mixture of nitric acid (20 mL) and concentrated sulphuric acid (20 mL). The

solution was heated (92°C) for a further 45 min, poured into 1 L of cold water and placed overnight in a refrigerator to complete the precipitation. 17.4 g (yield 66.5%) of 6-nitroquinazoline was collected in two crops. The melting point (MP) was 280°C (reference 275–277°C) [12.14]. <sup>1</sup>H NMR (DMSO-d<sub>6</sub>) δ: 8.75 (1H, d), 8.55 (1H, dd), 8.30 (1H, s), 7.85 (1H, d). Analysis: calculated, C, 50.27; H, 2.64; N, 21.98; found, C, 50.52; H, 2.75; N, 22.21.

#### 12.2.2.2. 4-chloro-6-nitroquinazoline (2)

6-nitro-4-hydroxyquinazoline (1.71 g, 8.18 mmol) and SOCl<sub>2</sub> (20 mL) were placed in a two-necked flask and DMF (20 μL) was added. The mixture was refluxed for 1 h and then additional quantities of SOCl<sub>2</sub> (10 mL) and DMF (20 μL) were added. After a 3 h reflux the thionyl chloride was distilled out and the residue was worked up with CH<sub>2</sub>Cl<sub>2</sub> and Na<sub>2</sub>CO<sub>3</sub>. The insoluble material was removed by filtration; the filtrate was dried over MgSO<sub>4</sub> for 20 min and evaporated to dryness. The product was pure enough and used for the next step without any further purification. MP = 130°C (reference 130–131°C) [12.14]. Analysis: calculated, C, 45.84; H, 1.92; N, 20.05; found, C, 45.17; H, 2.01; N, 19.29.

#### 12.2.2.3. 4-[(3-bromophenyl)amino]-6-nitro-quinazoline (3)

3-bromo-aniline (1.72 g, 10 mmol), dissolved in i-PrOH (40 mL) was added to 4-chloro-6-nitroquinazoline (2) (1.05 g, 5 mmol) that was dissolved in a minimal amount of CH<sub>2</sub>Cl<sub>2</sub>. 3-bromo-aniline hydrochloride (50 mg) was added to initiate the reaction, and the solution was stirred at 25°C for 10 min. After removal of CH<sub>2</sub>Cl<sub>2</sub>, the mixture was refluxed for 30 min, cooled and made alkaline by adding NH<sub>4</sub>OH. The formed solid was filtered and rinsed with i-PrOH. The yield was 1.55 g (89.5%). MP = 267–270°C (reference 269.5–273°C) [12.15]. <sup>1</sup>H NMR (DMSO-d<sub>6</sub>) δ: 10.55 (1H, s, NH), 9.65 (1H, d, H-5), 8.75 (1H, s, H-2), 8.55 (1H, dd, H-7), 8.17 (1H, s, H-2'), 7.95 (2H, m, H-6', H-8), 7.40 (2H, m, H-4', H-5'). Analysis: calculated, C, 48.72; H, 2.63; N, 16.23; found, C, 48.52; H, 2.91; N, 16.01.

#### 12.2.2.4. 6-amino-4-[(3-bromophenyl)amino]-quinazoline (4)

A refluxing, stirred solution of 4-[(3-bromophenyl)amino]-6-nitro-quinazoline (3) (500 mg, 1.453 mmol) in aqueous ethanol (1:2, 125 mL) containing acetic acid (1.25 mL) was treated with iron powder (160 mg, 2.9 mmol) in portions. The mixture was heated under reflux for a further 1 h and concentrated ammonia solution (5 mL) was added to precipitate the iron

salts. The resulting mixture was filtered through celite and the filtrate was concentrated under reduced pressure to give 6-amino-4-[(3-bromophenyl)amino]-quinazoline (4) as a yellow solid. The yield was 76.7% (350 mg). MP = 204°C (reference 201.5–203.5°C) [12.15]. <sup>1</sup>H NMR (DMSO-*d*<sub>6</sub>) δ: 9.45 (1H, s, NH), 8.35 (1H, s, H-2), 8.25 (1H, s, H-2'), 7.90 (1H, d, H-6'), 7.55 (1H, d, H-8), 7.35–7.20 (4H, m, H-5, 7, 4', 5'), 5.60 (2H, sbr, NH<sub>2</sub>).

#### 12.2.2.5. 6-(*pyridine-2-methylimin*)-4-[(3-bromophenyl)amino]-quinazoline (5)

6-amino-4-[(3-bromophenyl)amino]-quinazoline (4) (200 mg, 3 mmol) was transferred in a Dean-Stark apparatus containing 70 mL of benzene. The mixture was boiled for 2 h and the benzene was removed. The yellow residue was washed with hot MeOH and dried under vacuum. The yield was 46.9% (120 mg). MP = 233–234°C. The compound decomposed on thin layer chromatography (TLC) (silica gel, aluminum oxide). <sup>1</sup>H NMR (DMSO-*d*<sub>6</sub>) δ: 10.0 (1H, s), 8.35 (1H, d, CH=N), 8.28 (1H, d, H-6p), 8.65 (1H, s, H-5), 8.52 (1H, s, H-2), 8.27 (1H, d, H-3p), 8.22 (1H, s, H-2'), 8.05 (1H, t, H-4p), 7.95 (2H, d, H-7, H-4'), 7.87 (1H, d, H-8), 7.60 (1H, t, H-5p), 7.35 (1H, t, H-6'), 7.22 (1H, d, H-5').

#### 12.2.2.6. *N*-{4-[(3-bromophenyl)amino]-quinazoline-6-yl}-2-chloroacetamide (6)

6-amino-4-[(3-bromophenyl)amino]-quinazoline (4) (150 mg, 0.476 mmol) was dissolved in dry THF (20 mL) and cooled to 0°C. Triethylamine (97.5 μL, 72 mg, 0.704 mmol, 1.5 equiv.) was added and the mixture was kept at 0°C for an additional 15 min. Chloroacetyl chloride (90 μL, 1.117 mmol) was added and the mixture was stirred at 0°C for 30 min. The temperature was then raised to room temperature and a solution of saturated NaHCO<sub>3</sub> (30 mL) was added. THF was evaporated and the residue was extracted with ethyl acetate (3 × 30 mL). The organic layer was dried with Na<sub>2</sub>SO<sub>4</sub> and evaporated. The crude product was purified by silica gel flash chromatography with CH<sub>2</sub>Cl<sub>2</sub>:MeOH, 25:0.2 as eluent. The yield was 46.9% (70 mg). MP > 280°C. <sup>1</sup>H NMR (DMSO-*d*<sub>6</sub>) δ: 10.60 (1H, s, NH), 8.72 (1H, s), 8.60 (1H, s), 8.15 (1H, s), 7.85 (2H, m), 7.30 (2H, m), 5.75 (1H, s, CO=NH), 4.40 (2H, s, Cl-CH<sub>2</sub>).

### 12.2.3. Synthesis of rhenium complexes, general method

To a solution of [Et<sub>4</sub>N]<sub>2</sub>[ReBr<sub>3</sub>(CO)<sub>3</sub>] (0.1–0.2 mmol) in 5 mL acetonitrile, the ligand (0.1–0.2 mmol) was added under stirring. The solution was refluxed for 1–24 h and at the end 2 mL of distilled water was added and the mixture was refluxed for an additional 30 min. After standing overnight at room temperature the complexes were precipitated with good yields. The complexes

were characterized by spectroscopic methods and used as references for the characterization of the analogous  $^{99m}\text{Tc}$  complexes.

### 12.2.4. Labelling with technetium-99m

#### 12.2.4.1. Preparation of the precursor $[^{99m}\text{Tc}(\text{H}_2\text{O})_3(\text{CO})]^+$

A sealed vial containing 4 mg  $\text{Na}_2\text{CO}_3$ , 5.5 mg  $\text{NaBH}_4$  and 20 mg sodium tartrate was flushed with carbon monoxide for 20 min. Then 2 mL of the  $^{99m}\text{Tc}$  pertechnetate (5–30 mCi) was added to the vial, which was heated at  $75^\circ\text{C}$  for 15 min. The vial was then cooled in a water bath and the contained solution was neutralized with hydrochloric acid (solution 1M) to pH7.0 [12.10]. The formation of the complex was tested by HPLC (gradient). For characterization, a reference sample of  $\text{Na}^{99m}\text{TcO}_4$  was analysed by HPLC under the same gradient. HPLC analysis showed that  $^{99m}\text{TcO}_4^-$  eluated at 3–3.5 min and the precursor at 5 min.

#### 12.2.4.2. General method for the preparation of the $^{99m}\text{Tc}$ labelled quinazolines $[^{99m}\text{Tc}(\text{CO})_3]^+$

A solution of the ligand (2–100  $\mu\text{L}$ ,  $1 \times 10^{-3}$ – $1 \times 10^{-4}\text{M}$  in DMSO) was added to the aqueous solution of  $[^{99m}\text{Tc}(\text{CO})_3(\text{H}_2\text{O})_3]^+$  (400–900  $\mu\text{L}$ ). The solution was purged with nitrogen and incubated at  $75$ – $80^\circ\text{C}$  for 20 min, unless otherwise noted. After cooling, the complex formation was tested by HPLC. The product was purified by HPLC.

#### 12.2.4.3. In vitro evaluation of quinazoline analogues

*Cell line and culture conditions.* The human epidermoid carcinoma A431 cell line was kindly provided by E. Mishani (Hadassah Hebrew University, Israel). Cells were maintained in D-MEM (high glucose) supplemented with 10% foetal calf serum and penicillin/streptomycin 100 UI/100  $\mu\text{g}$  per mL in a 5%  $\text{CO}_2$  incubator at  $37^\circ\text{C}$ .

*Cell growth inhibition assay (MTT).* Inhibition of cell proliferation was evaluated by MTT assay. A431 cells were seeded in a 96 well plate at a density of 3000 cells per 100  $\mu\text{L}$  per well and incubated for 24 h for attachment. The day after seeding, exponentially growing cells were incubated with various concentrations of quinazoline analogues (ranging from 0.1 to 500  $\mu\text{M}$  for E1, E2, S, P-Q, P-Q-Re, PD-Q, PD-Q-Re and from 0.1 to 50  $\mu\text{M}$  for ISA1, ISA2, ISA3, ISA4, ISA5, P663, P664 in four replicates) for 24, 48 and 72 h. Controls consisted of wells without drugs. The medium was removed and the cells were

incubated for 4 h in the presence of 1 mg/mL MTT in RPMI without phenol red at 37°C. The MTT solution was removed and 100 mL/well of isopropanol was added. After thorough mixing, absorbance of the wells was read in an ELISA reader at test and reference wavelengths of 540 and 620 nm, respectively. The mean of the optical density (OD) of different replicates of the same sample and the percentage of each value was calculated (mean of the OD of various replicates/OD of the control). The percentage of the OD against drug concentration was plotted on a semilog chart and the IC<sub>50</sub> was determined from the dose–response curve.

*Inhibition of phosphorylation of the receptor.* A431 cells ( $5 \times 10^5$ ) were seeded in a 6 well plate and grown to 70% confluence. Cells were then incubated for 24 h in the presence of fresh medium without foetal bovine serum. The day after, cells were incubated in the presence of drugs at a final concentration of 1  $\mu$ M for 2 h, after which EGF was added (20 ng/mL) for 5 min. The medium was then removed, the cells were washed with PBS and cell lysis buffer (50mM Tris-HCl, pH7.4, 150mM NaCl, 1% Triton X-100, 1mM PMSF, 50  $\mu$ g/mL aprotinin, 2mM sodium orthovanadate, 50  $\mu$ g/mL leupeptine and 5mM EDTA) was added. Controls consisted of wells without drugs and with or without EGF. The total amount of protein was estimated by a BCA assay on ELISA plates, using a BSA standard curve. A volume of lysis mixture, corresponding to 30 mg of total protein, was loaded on to polyacrilamide gel (8%), and proteins were separated by electrophoresis and transferred to PVDF membrane. For visualization of molecular weight bands, the membrane was immersed in Ponceau reagent (0.5% Ponceau in 1% acetic acid) for 5 min. The membrane was washed in H<sub>2</sub>O, blocked overnight in TTN with 5% milk (1% fat) and incubated for 2 h in antiphosphotyrosine antibody diluted 1/2000 (PY20, Santa Cruz Biotechnology). The membrane was then washed three times in TTN and incubated in a horseradish peroxidase conjugated secondary antimouse antibody diluted 1/3000 (Sigma) for 2 h and finally washed three times in TTN. Detection was performed using a chemiluminescent detection system in accordance with the manufacturer's instructions (ECL kit, Amersham).

### 12.3. RESULTS AND DISCUSSION

The quinazoline derivatives (Fig. 12.1) were synthesized in accordance with literature methods. The procedures were not always reproducible and thus several modifications were made. The Re-tricarbonyl complexes were prepared by reacting ligand with the precursor [Et<sub>4</sub>N]<sub>2</sub>[ReBr<sub>3</sub>(CO)<sub>3</sub>], and they were characterized by IR and NMR spectroscopies. Three derivatives (P-Q,

## CHAPTER 12

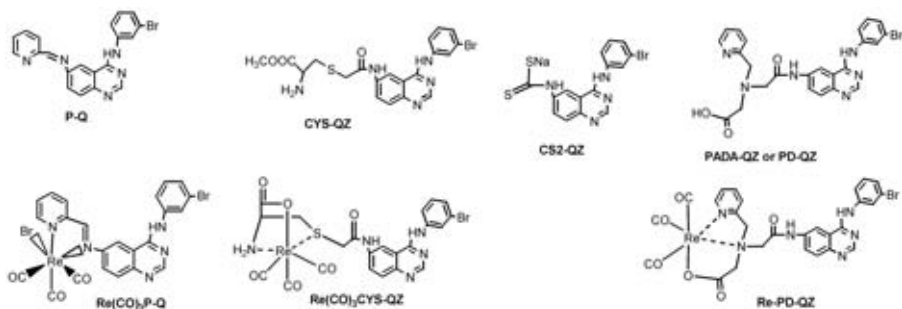


*FIG. 12.1. Structure of the ligands and complexes studied.*

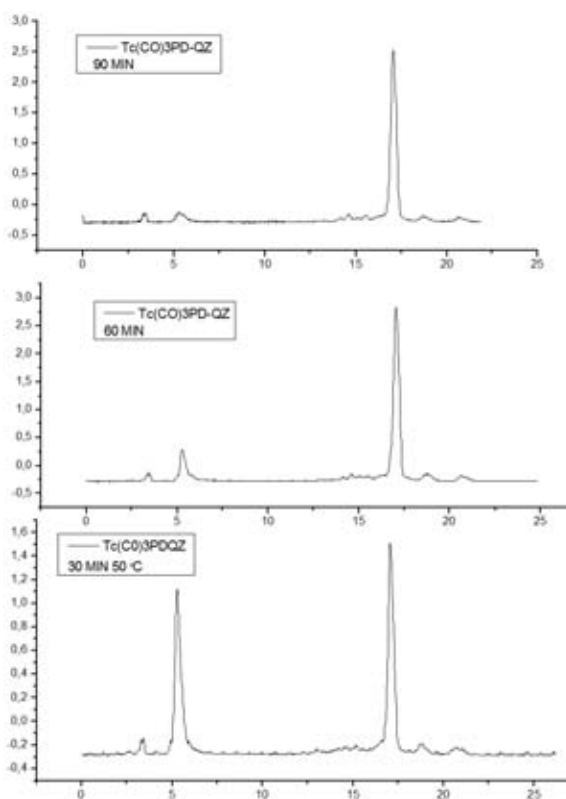


*FIG. 12.2. Radiochromatograms from the labelling of PADA-QZ.*

Cyst-QZ, PADA-QZ) were successfully labelled with a high yield with <sup>99m</sup>Tc-tricarbonyls using a low concentration (Fig. 12.2).

All the ligands as well as their rhenium complexes were evaluated in vitro for their ability to inhibit cell growth and phosphorylation. Initial experiments have shown that the IC<sub>50</sub> of these compounds is in the range of low  $\mu\text{M}$ . Furthermore, they were able to inhibit phosphorylation almost completely in a concentration of  $1\mu\text{M}$ .

#### 12.4. CONCLUSIONS

The quinazoline derivatives were successfully labelled with  $^{99\text{m}}\text{Tc}$  using the tricarbonyl core. The rhenium complexes were also synthesized and characterized. The in vitro studies demonstrating the ability of compounds to inhibit cell growth and phosphorylation in A431 cells are encouraging. Further evaluation in tumour bearing animals is required.

#### REFERENCES

- [12.1] ARTEAGA, C.L., The epidermal growth factor receptor: From mutant oncogene in nonhuman cancers to therapeutic target in human neoplasia, *J. Clin. Oncol.* **19** Suppl. 18 (2001) 32s.
- [12.2] RITTER, C., ARTEAGA, C.L., The epidermal growth factor receptor-tyrosine kinase: A promising therapeutic target in solid tumors, *Semin. Oncol.* **30** (2003) 3.
- [12.3] RAYMOND, E., FAIVRE, S., ARMAND, J.P., Epidermal growth factor receptor tyrosine kinase as a target for anticancer therapy, *Drugs* **60** (2000) 15.
- [12.4] SALOMON, D.S., BRANDT, R., CIARDIELLO, F., NORMANNO, N., Epidermal growth factor-related peptides and their receptors in human malignancies, *Crit. Rev. Oncol. Hematol.* **19** (1995) 183.
- [12.5] BONASERA, T.A., et al., Potential (18)F-labeled biomarkers for epidermal growth factor receptor tyrosine kinase, *Nucl. Med. Biol.* **28** (2001) 359.
- [12.6] ORTU, G., et al., Labeled EGFR TK irreversible inhibitor (ML03). In vitro and in vivo properties, potential as PET biomarker for cancer and feasibility as anticancer drug, *Int. J. Cancer* **101** (2002) 360.
- [12.7] BEN-DAVID, I., ROZEN, Y., ORTU, G., MISHANI, E., Radiosynthesis of ML03, a novel positron emission tomography biomarker for targeting epidermal growth factor receptor via the labeling synthon: [C-11]acryloyl chloride, *Appl. Radiat. Isot.* **58** (2003) 209.
- [12.8] SHAUL, M., et al., Novel iodine-124 labeled EGFR inhibitors as potential PET agents for molecular imaging in cancer, *Bioorg. Med. Chem.* **12** (2004) 3421.

## CHAPTER 12

- [12.9] ALBERTO, R., et al., Synthesis and reactivity of  $[\text{NEt}_4]_2[\text{ReBr}_3(\text{CO})_3]$ . Formation and structural characterization of the clusters  $[\text{NEt}_4][\text{Re}_3(\mu_3\text{-OH})(\mu\text{-OH})_3(\text{CO})_9]$  and  $[\text{NEt}_4][\text{Re}_2(\mu\text{-OH})_3(\text{CO})_6]$  by alkaline titration, *J. Chem. Soc. Dalton Trans.* **19** (1994) 2815.
- [12.10] MORLEY, J.S., SIMPSON, J.C.E., The chemistry of simple heterocyclic systems. Part 1. Reactions of 6- and 7-nitro-4-hydroxyquinazoline and their derivatives, *J. Chem. Soc.* (1948) 360–366.
- [12.11] REWCASTLE, G.W., et al., Tyrosine kinase inhibitors. 5. Synthesis and structure-activity relationships for 4-[(phenylmethyl)amino]- and 4-(phenylamino)quinazolines as potent adenosine 5'-triphosphate binding site inhibitors of the tyrosine kinase domain of epidermal growth factor receptor, *J. Med. Chem.* **38** (1995) 3482.
- [12.12] ALBERTO, R., et al., A novel organometallic aqua complex of technetium for the labeling of biomolecules: Synthesis of  $[\text{}^{99\text{m}}\text{Tc}(\text{OH})_2)_3(\text{CO})_3]^+$  from  $[\text{}^{99\text{m}}\text{TcO}_4]^-$  in aqueous solution and its reaction with a bifunctional ligand, *J. Am. Chem. Soc.* **120** (1998) 7987.



## Chapter 13

### DEVELOPMENT OF ANNEXIN V FRAGMENTS FOR LABELLING WITH TECHNETIUM-99m

J. KÖRNYEI

Institute of Isotopes Co. Ltd, Budapest, Hungary

F. TÓTH, E. SZEMENYEI

Biological Center of the Hungarian Academy of Sciences,  
Szeged, Hungary

A. DUATTI

Laboratory of Nuclear Medicine and Molecular Imaging,  
Department of Radiological Sciences, University of Ferrara, Italy

#### Abstract

Imaging of programmed cell death (i.e. apoptosis) is one of the most important areas of radiopharmaceutical chemistry, and is of high interest in oncology, cardiology and the study of atherosclerosis. It is known that phosphatidylserine is expressed on the surface of apoptotic cells. Thus, development of phosphatidylserine specific  $^{99m}\text{Tc}$  labelled tracers can be of interest to target apoptosis. Since the annexin type proteins generally possess their biospecific sequences on the N-terminal, the phosphatidylserine specific sequence might be attributed to a chain of 13 amino acids on the N-terminal of annexin. The scope of these investigations is the synthesis of the Anx13 fragment and the derivatization of that peptide for novel  $^{99m}\text{Tc}$  labelling approaches.

#### 13.1. INTRODUCTION

Apoptosis (i.e. programmed cell death) is a natural physiological phenomenon of homeostasis. Cells that become deficient in their apoptosis response are susceptible to disease, hence imaging apoptosis has been proven to be significant in clinical diagnosis and management in oncology, cardiology and atherosclerosis [13.1–13.3]. Cell damage is usually sensed by various cellular mechanisms and leads to the disruption at system that causes expression of phosphatidylserine. This phospholipid is normally maintained on the inner surface of the cell membrane in a healthy cell, but in programmed cell

death it appears on the outer surface of the cell membrane, giving the earliest signs of apoptosis [13.1, 13.4, 13.5].

Annexin V, a 36 kDa protein consisting of 320 amino acids, binds specifically to phosphatidylserine with high affinity [13.1, 13.3, 13.6]. Technetium-99m labelled annexin V is considered a useful tool for apoptosis detection, but it has many disadvantages from the point of view of radiopharmaceutical kit formulation, and agents with faster urinary excretion are required for routine clinical applications. Hence, under the current coordinated research project (CRP), focus was on the development of phosphatidylserine specific small  $^{99m}\text{Tc}$  labelled molecules for apoptosis imaging. Annexin type proteins generally possess their biospecific sequences on the N-terminal [13.1, 13.7], and in the case of annexin V the phosphatidylserine specific sequence might be attributed to a chain on the N-terminal consisting of 13 amino acids. Based on this concept, a peptide containing a particular sequence of these 13 amino acids (Anx13) was designed and chosen for novel  $^{99m}\text{Tc}$  labelling using nitrido, tricarbonyl, HYNIC and isonitrile 4 + 1 methods.

## 13.2. MATERIALS AND METHODS

### 13.2.1. Synthesis of annexin V fragments

Synthesis of Anx13 fragment and its derivatives was performed using a solid phase peptide synthesis method on Merrifield resin, with Boc chemistry and HF cleavage. The crude peptides were purified by reverse phase high performance liquid chromatography (HPLC) using a Vydac 218TP1010 (C18) semipreparative column. Identification of the pure peptides was by analytical reverse phase HPLC (Vydac 218TP54 column) using gradient elution (15–40% ACN/25 min, flow rate: 1 mL/min). At the same time, mass spectrum analysis was performed (MALDI-TOF).

### 13.2.2. Stability studies

Long run stability studies of solid, non-radiolabelled peptides were carried out by storing them at  $-18^{\circ}\text{C}$  and at  $+5 \pm 3^{\circ}\text{C}$ . For short time heat tolerance investigations, 25  $\mu\text{g}/\text{mL}$  aqueous/saline solutions of the peptides were used by immersing them in boiling water for 20 and 60 min. The  $^{99m}\text{Tc}$  labelled peptide solutions were stored at ambient temperature up to 24 h for determination of their radiochemical stability.

### 13.2.3. $^{99m}\text{Tc}$ -nitrido labelling

Nitrido intermediate was prepared at room temperature by using 1–5 mg succinic acid dihydrazide (SDH), 50–100  $\mu\text{g}$   $\text{SnCl}_2$  in 0.1 mL saline and 0.9 mL pertechnetate (1–5 mCi, 37–185 MBq). For asymmetric labelling, 25  $\mu\text{g}$  peptide in 0.4 mL saline and 125  $\mu\text{g}$  bis(dimethoxypropylphosphinoethyl)methoxyethylamine (PNP3) in 0.1 mL ethanol was reacted with the previously prepared nitrido intermediate at 100°C for 1 h. Symmetric nitrido labelling was carried out by adding 25–100  $\mu\text{g}$  peptide in 1 mL saline to the intermediate, followed by dilution up to 5 mL and heating at 100°C for 20 and 60 min.

### 13.2.4. Determination of the radiochemical purity

The radiochemical purity of the nitrido labelled peptides was determined by HPLC and thin layer chromatography (TLC) methods. For HPLC, Zorbax 300 SB C18 columns with both radioactivity and ultraviolet (UV) detectors were used. Solutions A and B were prepared for gradient elution containing 0.1% TFA in water and acetonitrile, respectively. Gradient elution was performed for the asymmetric labelled peptide as follows. Up to 25 min, B was set at 5%, between 25 and 35 min, B was increased from 5% to 45%, between 35 and 100 min, B was up to 50%, while between 100 and 125 min, B was increased to 55%. For testing the peptide obtained in symmetric labelling, a different gradient programme was used as follows. Up to 25 min, B was increased from 20% to 40%, between 25 and 30 min, B was up to 100%, between 35 and 100 min, B was 100%, while between 100 and 125 min, B was decreased down to 40%. The flow rate was 1 mL/min in each run.

TLC was carried out by using Kieselgel 60 plates and ethanol/water (1:1 v/v) as mobile phase. For determination of free pertechnetate content, Whatman ET-31 paper and acetone as eluent were used.

## 13.3. RESULTS AND DISCUSSION

### 13.3.1. Peptide synthesis and stability

A peptide containing 13 amino acids corresponding to the N-terminal sequence of the annexin V protein was synthesized. The chemical composition of this Anx13 fragment is shown in Fig. 13.1.

Long term stability studies proved that Anx13 is stable at least for one year when stored in a refrigerator. Chromatograms indicating the stability of



TABLE 13.1. HPLC DATA OF Anx13 13 MONTHS AFTER PREPARATION

Peak	Retention time (min)	Peak's area	Peak's height	Area (%)	Remark
I	22.53	38 543	2221	96.34	Anx13
II	24.50	298	12	0.74	Impurity
III	41.27	1 165	42	2.91	Impurity

TABLE 13.2. DERIVATIVES OF Anx13

	Labelling method
Cys-Anx13	Nitrido
Cys2-Anx13	Nitrido
His-Anx13	Tricarbonyl
HYNIC-Anx13	HYNIC
C≡N-X-Anx13 <sup>a</sup>	Isonitrile 4 + 1 <sup>a</sup>

<sup>a</sup> For isonitrile 4 + 1 labelling, the pure Anx13 was provided for derivatization to H.J. Pietzsch.

The results of stability studies of derivatized Anx13 compounds are given in Table 13.3. It can be observed that, while histidine and cysteine derivatization does not affect the stability of the peptides after three months, the Cys2 and HYNIC derivatization resulted in a lower stability. The reason for the decreasing chemical purity of the Cys2 derivative can be tentatively explained by the possibility of a disulphide bridge formation between the two different -SH groups. In spite of this, partial oxidation of -SH groups seems to reach an equilibrium, as suggested by the fact that during the first month the amount of this impurity grew to approximately 20%, but subsequently no further increase in impurities was observed.

Since some novel technetium labelling methods, for example nitrido labelling, require elevated temperature, short time heat tolerance studies were performed with the cysteine derivatives of Anx13. In the case of the Cys2-Anx13 solution, approximately 90% of the peptide remained unchanged during the 60 min it was immersed in boiling water. At the same time, no change was observed for Cys-Anx13 during the heat tolerance study.

TABLE 13.3. STABILITY OF DERIVATIZED ANNEXIN V FRAGMENTS

	Purity after three months (%)
Cys-Anx13	94.08
Cys2-Anx13	80.80
Hys-Anx13	98.13
HYNIC-Anx13	85.13

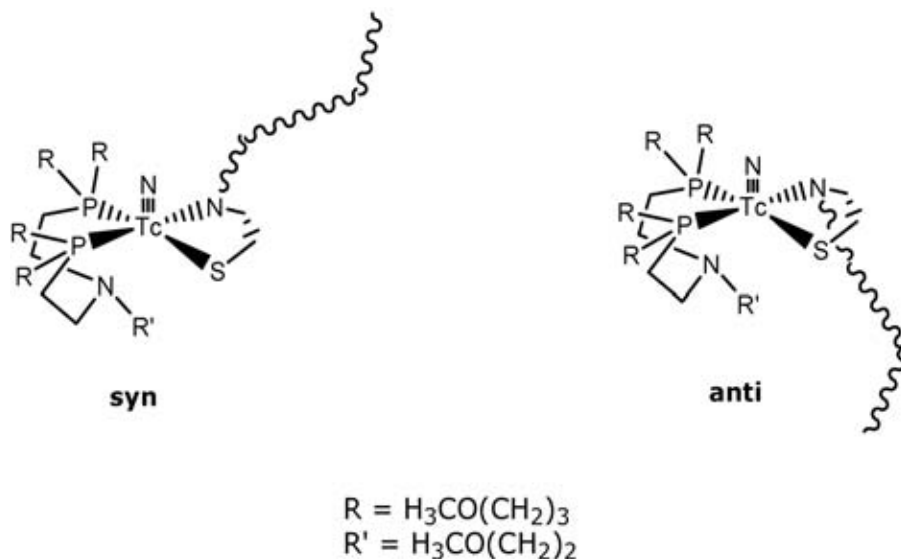


FIG. 13.3. Chemical structure of *syn* and *anti* stereoisomers obtained in asymmetrical nitrido labelling of Cys2-Anx13.

### 13.3.2. $^{99\text{m}}\text{Tc}$ -nitrido labelling

Both asymmetric and symmetric nitrido labelling of Cys2-Anx13 was carried out. In the case of the asymmetric approach, PNP3 phosphine coligand was used and the  $^{99\text{m}}\text{Tc}$  labelled compound was obtained with high radiochemical purity. Two main HPLC peaks were observed at 35.21 and 36.10 min, indicating the presence of *syn* and *anti* stereoisomers. The chemical structure and the chromatogram are shown in Figs 13.3 and 13.4, respectively.

The radiochemical purity of the  $[\text{}^{99\text{m}}\text{Tc}\equiv\text{N}]\text{Cys2-Anx13}(\text{PNP3})$  asymmetric complex was decreased to 73% 2 h after labelling. However, the

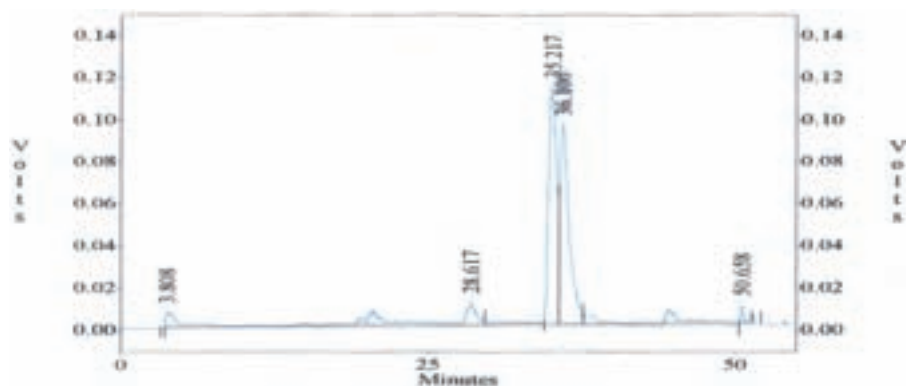


FIG. 13.4. HPLC chromatogram obtained in asymmetric nitrido labelling of Cys2-Anx13.

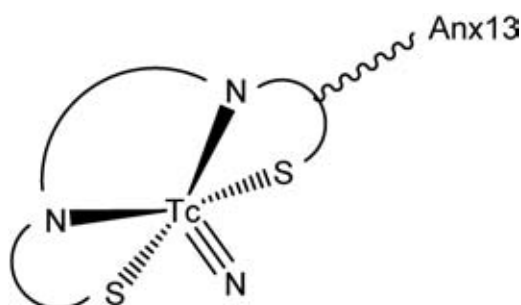


FIG. 13.5. Expected structure of Cys2-Anx13 labelled through the symmetrical approach.

radiochemical purity of the other asymmetric  $[^{99m}\text{Tc}\equiv\text{N}]\text{Cys-Anx13(PNP3)}$  remained over 90% several hours after preparation. The lower stability of the asymmetrically labelled Cys2-Anx13 might be tentatively explained by competition between the different complexing sites offered by the second cysteine and the PNP3 coligand, resulting in the formation of undefined species.

Symmetric labelling (i.e the reaction between Cys2-Anx13 and the  $[^{99m}\text{Tc}\equiv\text{N}]$  intermediate) was completed during 20 min heating. The labelled compound was obtained under two stereoisomeric forms, as revealed by the presence of two peaks in the HPLC chromatogram at retention times of 13.2 min (yield, 74.3%) and 16.9 min (yield, 25.7%). No radiochemical decomposition occurred during 2 h post-labelling. The short retention time suggested that the probability of formation of a monocomplex is higher than that of a real symmetric bis complex. The expected structure of this monocomplex is shown in Fig. 13.5, while TLC chromatograms are shown in Fig. 13.6.

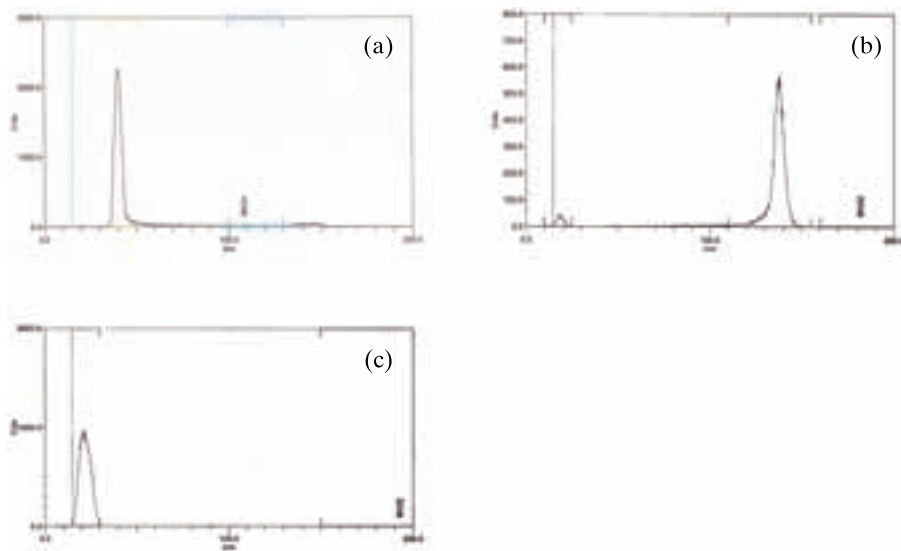


FIG. 13.6. TLC chromatograms. (a)  $^{99m}\text{Tc}$ -nitrido intermediate in K60/EtOH (water) 1:1 system, (b)  $^{99m}\text{TcN}$ -Cys2-Anx13 in K60/EtOH (water) 1:1 system, (c)  $^{99m}\text{TcN}$ -Cys2-Anx13 in Whatman ET-31 paper, acetone system.

Based on these chromatograms, it can be concluded that, in these reactions, the  $^{99m}\text{Tc}$ -nitrido intermediate (Fig. 13.6a) reacted quantitatively with Cys2-Anx13 forming a single complex (Fig. 13.6b) and no residual free pertechnetate was present (Fig. 13.6c).

### 13.3.3. Other studies with derivatized Anx13 fragments

Derivatized Anx13 fragments provided opportunity for further application of nitrido, tricarbonyl, HYNIC and isonitrile 4 + 1 labelling approaches as well as for preliminary biological evaluations. The different activities performed in the various laboratories of participants of this CRP are reported in the individual country reports. A brief comparison between different experimental outcomes and conclusions is given below.

Nitrido labelling of Cys-Anx13 and Cys2-Anx13, as well as tricarbonyl labelling of His-Anx13, always led to good yields and high in vitro radiochemical stability. These compounds also showed considerable resistance to transchelation in studies performed with cysteine and/or histidine challenging solutions. However, for HYNIC-Anx13, the use of tricine as a coligand gave significantly better radiochemical yields than those obtained with EDDA or with a mixture of EDDA + tricine. Isonitrile 4 + 1 labelling showed a radiochemical yield of

approximately 60%, followed by purification resulting in a radiochemical purity of 95%. Rather poor results were obtained in the preliminary biological evaluations, as only [ $^{99m}\text{Tc}\equiv\text{N}$ ]Cys2-Anx13 showed specific binding to apoptotic cells in vitro, while the asymmetric [ $^{99m}\text{Tc}\equiv\text{N}$ ]Cys-Anx13(PNP6) was biologically inactive. The isonitrile 4 + 1 labelled compound was found to undergo in vivo decomposition with formation of five different radioactive metabolites.

#### 13.4. CONCLUSIONS

The Anx13 fragment and its derivatives were synthesized and showed rather good stability when stored in a refrigerator. The novel technetium labelling approaches usually gave high radiochemical yields, indicating the presence of the appropriate complexing centres in the molecules. However, biological evaluations showed a poor behaviour of the resulting labelled compounds, except for the [ $^{99m}\text{Tc}\equiv\text{N}$ ]Cys2-Anx13 complex, obtained through symmetric nitrido labelling, which binds specifically to apoptotic cells in cultures. Further investigations of this compound may reveal the reason for this specific uptake, providing an opportunity for the development of a new radiopharmaceutical targeting apoptosis.

#### REFERENCES

- [13.1] RAYNAL, P., POLLARD, H.B., Annexins: The problem of assessing the biological role for a gene family of multifunctional calcium- and phospholipid-binding proteins, *Biochim. Biophys. Acta* **1197** (1994) 63–93.
- [13.2] TAKEI, T., et al., Time course of apoptotic tumor response after a single dose of chemotherapy: Comparison with  $^{99m}\text{Tc}$ -annexin V uptake and histologic findings in an experimental model, *J. Nucl. Med.* **45** (2004) 2083.
- [13.3] TAKI, J., et al., Detection of cardiomyocyte death in a rat model of ischemia and reperfusion using  $^{99m}\text{Tc}$ -labeled annexin V, *J. Nucl. Med.* **45** (2004) 1536.
- [13.4] TAKEI, T., et al., Enhanced apoptotic reaction correlates with suppressed tumor glucose utilization after cytotoxic chemotherapy: Use of  $^{99m}\text{Tc}$ -annexin V,  $^{18}\text{F}$ -FDG, and histologic evaluation, *J. Nucl. Med.* **46** (2005) 794.
- [13.5] KARTACHOVA, M., et al., In vivo imaging of apoptosis by  $^{99m}\text{Tc}$ -annexin V scintigraphy: Visual analysis in relation to treatment response, *Radiother. Oncol.* **72** (2004) 333.
- [13.6] TAIT, J.F., SMITH, C., BLANKENBERG, F.G., Structural requirements for in vivo detection of cell death with  $^{99m}\text{Tc}$ -annexin V, *J. Nucl. Med.* **46** (2005) 807.
- [13.7] TAIT, J.F., SMITH, C., GIBSON, D.F., Development of annexin v mutants suitable for labeling with tc(i)-carbonyl complex, *Bioconj. Chem.* **13** (2002) 1119.



## Chapter 14

### **DEVELOPMENT OF TECHNETIUM-99m BASED SMALL BIOMOLECLES USING NOVEL TECHNETIUM-99m CORES: <sup>99m</sup>Tc-TRICARBONYL, <sup>99m</sup>Tc-HYNIC AND <sup>99m</sup>Tc-NITRIDO CHEMICAL APPROACHES**

K. KOTHARI\*, A. MUKHERJEE\*, D. SATPATI\*, A. KORDE\*,  
S. JOSHI\*, H.D. SARMA\*\*, A. MATHUR\*, M. MALLIA\*,  
S. BANERJEE\*, M. VENKATESH\*

\* Radiopharmaceuticals Division

\*\* Radiation Biology and Health Sciences Division

Bhabha Atomic Research Centre, Trombay, Mumbai, India

#### **Abstract**

Radiolabelling and characterization of biomolecules such as analogues of cyclic RGD, annexin and cysteine functionalized fatty acid derivatives are described in the paper. Different analogues of cyclic RGD peptide were labelled with <sup>99m</sup>Tc-carbonyl, <sup>99m</sup>Tc-nitrido and HYNIC approaches for targeting tumours. The complexes were characterized by high performance liquid chromatography and their pharmacokinetics was studied in normal Swiss mice. <sup>99m</sup>Tc(CO)<sub>3</sub>-pyrazolyl (PZ1)-RGD, <sup>99m</sup>Tc(N)-cysteine (Cys)-RGD and <sup>99m</sup>Tc-HYNIC-RGD complexes could be prepared with high yields and good stability. In vitro cell uptake studies in the HT29 cell line did not reveal specific uptake of <sup>99m</sup>Tc-HYNIC-RGD. A synthetic peptide containing 13 amino acids of N-terminal annexin V, Anx13, was studied for <sup>99m</sup>Tc labelling and evaluated for apoptosis imaging. Anx13 derivatized with cysteine (C-Anx13) and dicysteine (C2-Anx13) were labelled with <sup>99m</sup>Tc-nitrido core, whereas derivatized with histidine (H-Anx13) was labelled with <sup>99m</sup>Tc(CO)<sub>3</sub> synthon. Stable complexation of <sup>99m</sup>Tc(N)-C2-Anx13 was achieved with high yields. A significant amount of tracer (13%) was specifically taken up in apoptotic human lymphoma cells (HL-60), as revealed by cell studies. Biodistribution studies of <sup>99m</sup>Tc(N)-C2-Anx13 in fibrosarcoma tumour bearing Swiss mice showed tumour uptake of 0.52 (0.17)% injected dose (ID)/g with tumour to blood and tumour to muscle ratio of 1.7 and 3.3, respectively, at 1 h post-injection. Liver apoptosis was induced in rats by cyclohexamide injection, and biodistribution studies in these animals showed increased uptake of <sup>99m</sup>Tc(N)-C2-Anx13 in apoptotic liver tissue as compared with normal liver. Long chain fatty acid derivatives (CYSFA11 and CYSFA16) were also

labelled with  $^{99m}\text{Tc}$  using a tricarbonyl approach and studied for pharmacokinetics and heart uptake in Swiss mice.  $^{99m}\text{Tc}(\text{CO})_3\text{-CYSFA11}$  could be prepared with high yields (>95%) with good stability. The results of the biodistribution studies in Swiss mice did not show any advantage over existing radiopharmaceuticals for myocardial imaging.

#### 14.1. INTRODUCTION

Current functional and metabolic imaging is based on in vivo biochemistry. The future of novel  $^{99m}\text{Tc}$  radiopharmaceuticals will depend upon the success of labelling of lead organic biomolecules such as peptides, steroids and receptor specific drugs without altering their in vivo specificity. Commonly used technetium complexes based on the  $^{99m}\text{Tc}(\text{V})$  oxo core suffer from low specific activity due to the high concentration of chelating agents required for stabilization of the +V oxidation state. Low ligand concentration is the most essential requirement for molecular targeted radiopharmaceuticals. The recent advent of the new, low valent  $[\text{Tc}(\text{CO})_3]^+$  metal core and of the  $[\text{Tc}(\text{N})]^{2+}$  intermediate has introduced new avenues for  $^{99m}\text{Tc}$  labelling of biologically active compounds with high specific activity [14.1–14.4]. The tricarbonyl core  $[\text{Tc}(\text{CO})_3(\text{H}_2\text{O})_3]^+$  is less susceptible to oxidation and possesses a low spin  $d^6$  Tc(I) centre that is kinetically inert and hence offers more flexibility towards choosing ligands for designing complexes of a desirable size, charge and lipophilicity suitable for the specific study. The three substitutionally labile aqua ligands facilitate the formation of stable complexes with a tridentate ligand. The N-containing ligands such as histidine, histamine, imidazole, iminodiacetic acid and diethylene triamine, which form stable complexes with the tricarbonyl precursor, have been functionalized for the development of site specific radiopharmaceuticals using biologically avid molecules. Another novel core is nitrido  $[\text{Tc}(\text{CO})_2\text{N}]^{2+}$ , which is isoelectronic with the  $[\text{Tc}(\text{CO})_3\text{O}]^{3+}$  core and exhibits a very high stability over a wide range of experimental conditions. It shows high affinity towards chelating ligands containing sulphur and phosphorus atoms.

A few bioactive small molecules were identified as lead molecules for development of radiopharmaceuticals. These were suitably modified for  $^{99m}\text{Tc}$  labelling with novel approaches without altering the pharmacophore of the molecule. We focused on three types of bioactive molecules: RGD analogues, annexin 13 fragments and fatty acid derivatives. These were labelled with  $^{99m}\text{Tc}$  using novel chemical approaches and further investigated for potential application as radiopharmaceuticals.

Peptides containing RGD sequences (arginine-glycine-aspartate) are known to target tumours and metastatic lesions via  $\alpha_v\beta_3$  integrin receptors.

Radiolabelled RGD peptides have already shown promising results for tumour imaging and therapy [14.5]. Our earlier work on  $^{99m}\text{Tc}(\text{HYNIC})\text{-RGD}$  showed good labelling yields, stability and pharmacokinetics but non-specific uptake in animal tumour models. Hence newer RGD analogues functionalized with cysteine, histidine and pyrazolylolyl were labelled with  $^{99m}\text{Tc}$  via  $^{99m}\text{Tc}(\text{CO})_3$  synthon and  $^{99m}\text{Tc}(\text{N})$  intermediates. Cysteine derivatives are expected to interact with  $^{99m}\text{Tc}$ -nitrido intermediate to form a symmetric complex with two molecules. Introduction of two biologically active bidentate fragments in a symmetrical manner on a  $^{99m}\text{Tc}$ -nitrido core is not desirable as this could lead to poor bioavailability. A complex with two different bidentate ligands is preferred in order to avoid contemporary insertion of two biofragments on the same core. Hence, asymmetric complexes  $^{99m}\text{Tc}(\text{N})(\text{PNP})^{+2}$  cysteine derivatives were also prepared using PNP, a biphosphine ligand to improve specific activity. All these radiolabelled complexes were characterized and studied in animal models for tumour uptake.

Apoptosis (i.e. programmed cell death) is a natural physiological phenomenon of homeostasis. Cells that become deficient in their apoptosis response are susceptible to disease, hence imaging apoptosis has been proven to be significant in clinical diagnosis and management in oncology, cardiology and atherosclerosis [14.6–14.10]. Cell damage is usually sensed by various cellular mechanisms and causes disruption at system that causes an efflux of phosphatidylserine, a phospholipid on the outer surface of the cell membrane that is normally maintained on the inner surface of the cell membrane in a healthy cell. Hence, expression of phosphatidylserine on the cell surface is taken as one of the earliest signs of apoptosis. Annexin V is a 36 kDa protein consisting of 320 amino acid that binds specifically to phosphatidylserine with high affinity [14.11]. Technetium-99m labelled annexin V is hence considered a useful tool for the detection of apoptosis. Annexin type proteins contain specific sequences on the N-terminal that are responsible for interaction and binding with different molecules. In annexin V, the phosphatidylserine specific sequence is attributed to a chain on the N-terminal consisting of 13 amino acids. Hence dicysteine annexin (C2-Anx13) and histidine annexin (H-Anx13), the synthesized derivatives of annexin 13 fragments, were labelled with  $^{99m}\text{Tc}(\text{N})$  intermediate and  $^{99m}\text{Tc}$ -tricarbonyl precursor, respectively. The labelled complexes were evaluated for their biological activity by carrying out in vitro tests in apoptotic human lymphoma cells HL-60 and with in vivo studies in tumour bearing Swiss mice as well as in rats with drug induced liver apoptosis.

Long chain fatty acids are the primary energy source of the normal myocardium. Technetium-99m labelled fatty acid would enable easy visualization of myocardial energy metabolism [14.12]. We previously performed preliminary studies on labelling IDA-undeconic acid via  $^{99m}\text{Tc}(\text{CO})_3$  synthon.

In continuation of this, we carried out work on labelling cysteine functionalized undecanoic (CYSFA11) and hexa deconoic (CYSFA16) acids and evaluated them in normal animals.

## 14.2. MATERIALS

Sodium borohydride, Na/K tartrate and N-butyl-N-methylamine were purchased from Aldrich. The IAEA facilitated the supply of the materials required from the various sources. The kit for synthesis of  $^{99m}\text{Tc}$ -carbonyl precursor was obtained from Mallinckrodt and the kit for the preparation of Tc-nitrido intermediate was obtained from CIS Biointernational. As per the coordinated research project (CRP) workplan, derivatized biomolecules were synthesized at different laboratories, and these were procured as gift samples through the IAEA. HYNIC, cysteine, histidine and pyrazolylolyl derivatives of cyclic RGD peptide were procured from the Universitätsklinik für Nuklearmedizin, Innsbruck, and cysteine and DTC derivatives of undecanoic acid (Cys-FA11 and DTC-FA11) and cysteine derivative of hexadeconoic acid (Cys-FA16) were obtained from the Demokritos National Centre of Scientific Research, Greece. Biphosphine ligand PNP5 was procured from Ferrara, Italy. Annexin derivatives were synthesized at the Biological Research Centre of the Hungarian Academy of Sciences and at the Institute of Isotopes Co. Ltd, Budapest.

All chemicals and solvents were of reagent grade and used without further purification. Carbon monoxide in 0.5 L refillable canisters was obtained from Alchemie Gases and Chemicals. Aluminium sheet backed  $20 \times 20$  cm silica gel 60 F used for thin layer chromatography (TLC) was from Merck. Whatman 3 MM chromatography paper was used for paper chromatography and paper electrophoresis. All radioactivity measurements were made using an NaI (Tl) scintillation counter after adjusting the baseline at 100 keV and keeping a window of 100 keV for  $^{99m}\text{Tc}$ .

High performance liquid chromatography (HPLC) analysis of  $^{99m}\text{Tc}$  complexes was performed on a Jasco PU 1580 system with a Jasco low pressure gradient valve (LV-1580-03), Jasco mixing module (HG-980-30) and Jasco 1575 tunable absorption detector along with an indigenously developed radiometric detector system. For radiochemical purity (RCP) analysis, a C18 reverse phase HiQ Sil ( $5 \mu\text{m}$ ,  $4 \times 250$  mm) column supplied by KYA TECH was used.

Cell lines used for in vitro specificity evaluation were procured from the National Centre of Cell Sciences, Pune, India. Culture media and supplements were obtained from Sigma, and all other chemicals and solvents used for assay were of analytical reagent grade and procured from manufacturers in India.

Nude mice used for xenograft were maintained at the nude mice housing facility of the Advanced Centre for Treatment, Research and Education in Cancer, Navi-Mumbai, India. Animal tumour models were raised by subcutaneous injection of  $\sim 10^6$  cells/animal. Scintigraphic studies were carried out using a Wipro-GE gamma camera. A Carl Zeiss Axioplan 2 microscope was used for histopathology studies. All animal experiments were carried out in compliance with the national law governing animal experiments after obtaining permission from the Local Animal Ethics Committee.

### 14.3. METHODS

#### 14.3.1. Synthesis and characterization of $^{99m}\text{Tc}(\text{CO})_3\text{-RGD}$ , $^{99m}\text{Tc}(\text{N})\text{-RGD}$ and $^{99m}\text{Tc}\text{-HYNIC-RGD}$ complexes for tumour targeting

Five different cyclic RGD analogues were studied for radiolabelling with  $^{99m}\text{Tc}$ . Table 14.1 gives the structure of cyclic RGD derivatives synthesized at the Universitätsklinik für Nuklearmedizin, Innsbruck, which were labelled with a suitable  $^{99m}\text{Tc}$  core as described below.

##### 14.3.1.1. Synthesis of $^{99m}\text{Tc}$ -tricarbonyl complexes of RGD

*Synthesis of  $^{99m}\text{Tc}$ -tricarbonyl synthon  $[\text{}^{99m}\text{Tc}(\text{CO})_3(\text{H}_2\text{O})_3]^+$ .* The procedure for the synthesis of  $^{99m}\text{Tc}$ -tricarbonyl precursor involves dissolution of  $\text{NaBH}_4$  (5.5 mg),  $\text{Na}_2\text{CO}_3$  (4 mg) and Na/K tartrate (15 mg) in 0.5 mL of double distilled water in a glass serum vial. The vial was sealed and carbon monoxide was purged through the solution for 5 min. 1 mL of the generator elute containing 37–74 MBq of  $^{99m}\text{TcO}_4^-$  in saline was added and the vial was heated at  $80^\circ\text{C}$  for 15 min. After cooling the vial for 10 min and re-equilibration to atmospheric pressure, the pH of the reaction mixture was adjusted to pH7 with 300  $\mu\text{L}$  of 1:3 mixture of 0.5M phosphate buffer (pH7.5):1M HCl. The

TABLE 14.1. STRUCTURE OF CYCLIC RGD DERIVATIVES

$\text{C}(\text{Arg-Gly-Asp-D-Tyr-Lys})\text{-HYNIC} \rightarrow \text{HYNIC-RGD}$
$\text{C}(\text{Arg-Gly-Asp-D-tyr-Lys})\text{-Cys} \rightarrow \text{Cys-RGD}$
$\text{C}(\text{Arg-Gly-Asp-D-tyr-Lys})\text{-tert Cys} \rightarrow \text{tert Cys-RGD}$
$\text{C}(\text{Arg-Gly-Asp-D-tyr-Lys})\text{-His} \rightarrow \text{His-RGD}$
$\text{C}(\text{Arg-Gly-Asp-D-tyr-Lys})\text{-PZ1} \rightarrow \text{PZ1-RGD}$

precursor was characterized by HPLC as described in Section 14.3.1.4 and further used for the preparation of tricarbonyl complexes.

*Preparation of  $^{99m}\text{Tc}(\text{CO})_3$  RGD derivatives.* Three suitable RGD derivatives were used for complexation with  $^{99m}\text{Tc}$ -tricarbonyl precursor. In a typical protocol, PZ1-RGD, tert Cys-RGD and His-RGD derivatives were reacted with 0.5 mL of  $[\text{}^{99m}\text{Tc}(\text{CO})_3(\text{H}_2\text{O})_3]^+$  synthon (3.7–37 MBq/0.5 mL) at 70–80°C for 1 h. The pH of the reaction was maintained in the range pH5–8. The radiolabelling was studied at peptide concentrations ranging between 100 and 500  $\mu\text{g}/\text{mL}$ .

#### 14.3.1.2. Preparation of $^{99m}\text{Tc}$ -nitrido complexes of RGD

*Synthesis of  $^{99m}\text{Tc}(\text{N})$  intermediate.*  $^{99m}\text{Tc}(\text{N})$  intermediate was prepared using a kit from CIS Biointernational that contained succinic dihydrazide (5.0 mg), stannous chloride dihydrate (100  $\mu\text{g}$ ), 1,2 diaminopropane-N,N,N'N'-tetra acetic acid (5 mg), sodium dihydrogen phosphate (0.5 mg) and disodium hydrogen phosphate (5.8 mg) in freeze dried form. The kit vial stored at 4°C was allowed to attain ambient temperature, following which 1 mL of freshly eluted  $^{99m}\text{TcO}_4^-$  (1 mCi/37 MBq) was added, vortexed for 1 min and allowed to stand at room temperature for 20 min. The precursor was characterized by HPLC as described in Section 14.3.1.4 and further used for the preparation of nitrido complexes.

*Preparation of  $^{99m}\text{Tc}$ -nitrido RGD complexes.* Cysteine functionalized RGD derivative (Cys-RGD) was used for preparation of both symmetric and asymmetric complexes using  $^{99m}\text{Tc}(\text{N})$  intermediate.

Synthesis of symmetric complexes of  $^{99m}\text{Tc}(\text{N})$ -Cys RGD: Symmetric complex containing two molecules of Cys-RGD was prepared by reacting 20  $\mu\text{L}$  Cys-RGD (60  $\mu\text{g}$ ) with 1 mL of  $^{99m}\text{Tc}$ -nitrido intermediate at 100°C for 1 h. Synthesis of  $^{99m}\text{Tc}(\text{N})(\text{PNP})^{+2}$ -RGD (asymmetric complex): For asymmetric complex preparation, PNP5, a biphosphine ligand, was reacted with 1 mL of nitrido intermediate and 60  $\mu\text{g}/20 \mu\text{L}$  of Cys-RGD at 100°C for 1 h. PNP5 (10 mg) was diluted to 1 mL with ethanol under inert atmosphere, and 0.1 mL of this ethanolic solution, equivalent to 1 mg PNP5, was used for labelling studies.

#### 14.3.1.3. Synthesis of $^{99m}\text{Tc}$ -HYNIC-RGD

In a standardized labelling protocol, HYNIC derivative of RGD (20  $\mu\text{g}$ ) was reacted with 1 mL EDDA/tricine solution and 1 mL pertechnate in the presence of 20  $\mu\text{L}$  of stannous chloride (1 mg/mL in 0.1N HCl). The reaction mixture was heated in a boiling water bath for 10 min. The EDDA/tricine

solution used for complexation was prepared by dissolving 30 mg EDDA in 1.5 mL of 0.1N NaOH (3 min ultrasound) and mixing with 1.5 mL of tricine containing 60 mg of tricine in 0.2M phosphate buffer at pH6.2.

#### 14.3.1.4. Quality control

Technetium-99m RGD complexes were characterized by reverse phase HPLC analysis. Details of the HPLC system are mentioned in Section 14.2. A dual pump HPLC unit with a C18 reverse phase column (25 cm × 0.46 cm) was used for characterization of labelled complexes. The elution was monitored both by ultraviolet signals at 270 nm as well as by radioactivity signals. The flow rate was maintained at 1 mL/min. Water (A) and acetonitrile (B) mixtures with 0.1% TFA were used as the mobile phase. The column was eluted with a different gradient system for different complexes as described in subsequent sections. The sample volume was usually maintained at 25  $\mu$ L. Recovery of the activity from the column was ascertained by summing the counts in the eluted fractions and comparing it with the total injected activity.

*Characterization of  $[^{99m}\text{Tc}(\text{CO})_3(\text{H}_2\text{O})_3]^+$  synthon,  $^{99m}\text{Tc}(\text{CO})_3$ -PZI-RGD and  $^{99m}\text{Tc}$ -HYNIC-RGD complexes.*  $[^{99m}\text{Tc}(\text{CO})_3(\text{H}_2\text{O})_3]^+$  synthon and RGD complexes such as  $^{99m}\text{Tc}(\text{CO})_3$ -PZI-RGD prepared using  $^{99m}\text{Tc}$ -carbonyl were analysed by HPLC using a binary gradient system of 0–1.5 min 0% B, 1.5–18 min 0–30% B, 18–21 min 30–60% B, 21–24 min 60% B.  $^{99m}\text{Tc}$ -HYNIC-RGD complexes were also eluted with the same mobile phase using the same gradient.

*Characterization of tricarbonyl complexes of tert Cys-RGD, His-RGD and nitrido complexes of Cys-RGD.* The gradient system for HPLC analysis of these complexes started with 90% A/10% B, which gradually changed to 10% A/90% B in 28 min by linear gradient. The composition remained constant at 10% A/90% B during 28–30 min.

#### 14.3.1.5. In vitro studies

*Stability studies.* Stability of the complexes was studied in 0.05M phosphate buffer containing 1% saline at room temperature for 24 h. After incubation, the purity of the  $^{99m}\text{Tc}$ -RGD complexes was estimated by HPLC analysis. The complexes were tested for instability towards exchange with cysteine and histidine. 0.1 mL of tracer was reacted with 10  $\mu$ L of cysteine/histidine solution corresponding to a final concentration of 0.1M, in aqueous medium, and incubated for 1 h at 37°C. After incubation, the percentage dissociation of  $^{99m}\text{Tc}$  was measured by HPLC analysis. Approximately 50  $\mu$ g (50  $\mu$ L) of complexes was incubated with 0.5 mL of serum at 37°C for 30 min. The

serum proteins were precipitated out by reacting with 0.5 mL of acetonitrile. The percentage of serum protein bound activity was estimated by counting the activity associated with the precipitate. The acetonitrile fraction was characterized by HPLC.

*Cell uptake studies.* Human colon carcinoma cells HT29 were isolated from confluent cultures and washed with plain medium followed by washing twice with assay buffer (50mM Tris HCl, pH7.5, 5mM MgCl<sub>2</sub>, 0.1M NaCl with 0.5% BSA). Cells were stabilized for 30 min at 37°C in the same buffer. Cells were concentrated by centrifugation (2500 rpm for 5 min) and the cell suspension was prepared with a final concentration of  $1 \times 10^6$  cells/mL. 40  $\mu$ L (100 fmol) of <sup>99m</sup>Tc-HYNIC-RGD tracer in PBS/0.5% BSA buffer was added per 0.5 mL of cell suspension per tube. Blank or non-specific binding was studied by incubating 100 times in excess of unlabelled RGD (10 $\mu$ M) in addition to tracer. All experiments were carried out in triplicate for each time point. The cells were incubated at 37°C for 1 h and harvested by centrifugation at 2500 rpm for 5 min. The cell pellet was washed with PBS, counted on an NaI (Tl) scintillation counter and the percentage of cell associated activity was estimated.

#### 14.3.1.6. *In vivo studies*

The radiolabelled RGD complexes, namely <sup>99m</sup>Tc(CO)<sub>3</sub>-PZ1-RGD and <sup>99m</sup>Tc(N)Cys-RGD, were tested for their *in vivo* biological behaviour in normal Swiss mice weighing 20–25 g. ~3–4 MBq of the radiolabelled complex was administered via the tail vein and the animals were sacrificed by cervical dislocation at 1 h, 3 h and 24 h post-injection. Three animals were used for each time point. All major organs were isolated, weighed and counted in a flat type NaI (Tl) scintillation counter. The accumulated per cent of injected dose per gram was estimated after applying decay correction for the time lapsed. For estimation of percentage injected dose accumulation per organ, 7%, 40% and 10% of the animal weight was taken as the total weight of blood, muscle and bone, respectively.

#### 14.3.2. **Synthesis and evaluation of <sup>99m</sup>Tc(N)-Anx13 and <sup>99m</sup>Tc(CO)<sub>3</sub>-Anx13 as apoptosis marker**

Three different derivatized annexin 13 fragments (Anx13) were studied for radiolabelling with a suitable <sup>99m</sup>Tc core. The structure of Anx13 derivatives is given below:

*C-Anx13* Cys-Ala-Gln-Val-Leu-Arg-Gly-Thr-Val-Thr-Asp-Phe-Pro-Gly-OH  
*C2-Anx13* LYS Cys-Ala-Gln-Val-Leu-Arg-Gly-Thr-Val-Thr-Asp-Phe-Pro-Gly-OH  
*H-Anx13* His Cys-Ala-Gln-Val-Leu-Arg-Gly-Thr-Val-Thr-Asp-Phe-Pro-Gly-OH

#### 14.3.2.1. Preparation and characterization of technetium-99m Anx13

*Technetium-99m(N)-C-Anx13.* Cysteine functionalized Anx13 was used for preparation of both symmetric and asymmetric complexes using  $^{99m}\text{Tc}$ -nitrido intermediate.  $^{99m}\text{Tc}(\text{N})$  intermediate was prepared as described in Section 14.3.1.2. For preparation of symmetric complex of [ $^{99m}\text{Tc}(\text{N})$  C-Anx13], 100  $\mu\text{g}$  of C-Anx13 in 0.1 mL of water was added to 0.9 mL of  $^{99m}\text{Tc}$ -nitrido intermediate. The reaction mixture was heated in a boiling water bath for 1 h. For the synthesis of asymmetric complex,  $^{99m}\text{Tc}(\text{N})$  (PNP) $^{+2}$ -C-Anx13 preparation, PNP ligand (1 mg) was added to 1 mL of  $^{99m}\text{Tc}(\text{N})$  intermediate along with 0.1 mg (50  $\mu\text{L}$ ) of C-Anx13 and the reaction mixture was heated at 100°C for 1 h under inert atmospheric conditions. PNP solution was prepared as described in Section 14.3.1.2. In both cases, the precursor and the complex were characterized by HPLC using the same gradient as described in Section 14.3.1.4.

*Technetium-99m(N)-C2-Anx13.* Technetium-99m(N) intermediate was prepared by the method described in Section 14.3.1.2.  $^{99m}\text{Tc}(\text{N})$ -C2-Anx13 was prepared in a similar way as described above for  $^{99m}\text{Tc}(\text{N})$ C-Anx13. In short, 100  $\mu\text{g}$  C2-Anx13 in 0.1 mL of water was added to 0.9 mL of  $^{99m}\text{Tc}$ -nitrido intermediate. The reaction mixture was heated in a boiling water bath for 1 h. The precursor and the complex were characterized by HPLC as described in Section 14.3.1.4.

*Technetium-99m(CO)<sub>3</sub>-H-Anx13.*  $^{99m}\text{Tc}$ -tricarbonyl precursor was prepared by the method described in Section 14.3.1.1. 20  $\mu\text{g}$  (10  $\mu\text{L}$ ) of H-Anx13 was added to 0.5 mL of carbonyl precursor at pH6. The reaction was carried out at 80°C for 30 min. The complex was characterized by HPLC as described in Section 14.3.1.4.

#### 14.3.2.2. In vitro studies

*In vitro stability studies.* The  $^{99m}\text{Tc}$  labelled annexin fragments  $^{99m}\text{Tc}(\text{N})$ -Anx13 and  $^{99m}\text{Tc}(\text{CO})_3$ -H-Anx13 were tested for stability in storage, stability against challenge studies with cysteine or histidine and stability in serum. The procedures followed were as described in Section 14.3.1.5.

*In vitro cell uptake studies.* The biological activity of  $^{99m}\text{Tc}(\text{N})$ -C2-Anx13 and  $^{99m}\text{Tc}(\text{CO})_3$ -H-Anx13 was evaluated on exponentially growing HL-60 human leukaemia cells. HL-60 cells were cultured in RPMI growth medium

supplemented with 10% FBS. To induce apoptosis, cells in culture medium were treated with Camptothecin dissolved in DMSO to a final concentration of  $5\mu\text{M}$  and incubated in a 5%  $\text{CO}_2$  incubator at  $37^\circ\text{C}$  for 6 h. Control cells were incubated with DMSO under similar conditions. For binding studies, apoptotic cells were harvested, washed twice with PBS and resuspended in annexin V binding buffer (Pharmingen, 10mM HEPES, pH7.4, 140mM NaCl, 2.5mM  $\text{CaCl}_2$ ) at a concentration of  $2 \times 10^6$  apoptotic cells/mL/tube.  $^{99\text{m}}\text{Tc}(\text{N})\text{-C2-Anx13}$  and  $^{99\text{m}}\text{Tc}(\text{CO})_3\text{-H-Anx13}$  were added individually at a final concentration of  $0.6\mu\text{g/mL}$  to the cell suspension and incubated at room temperature for 30 min. At the end of incubation the cells were centrifuged at 3000 rpm for 5 min and washed with PBS. The radioactivity associated with the pellet was determined using a scintillation counter. To investigate the specificity of binding, apoptotic control HL-60 cells were also incubated with 100 times excess of unlabelled Anx13 fragments prior to the addition of  $^{99\text{m}}\text{Tc}(\text{N})\text{-C2-Anx13}$  and  $^{99\text{m}}\text{Tc}(\text{CO})_3\text{-H-Anx13}$  to block any specific binding. Apoptosis induction in HL-60 cells by Camptothecin was confirmed by flow cytometric analysis.

#### 14.3.2.3. *In vivo studies*

*Biodistribution studies in animal tumour model.*  $^{99\text{m}}\text{Tc}(\text{N})\text{-C2-Anx13}$  was diluted 1:10 in saline and 0.1 mL ( $1\mu\text{g}$ ) was injected into the tail vein of Swiss mice bearing fibrosarcoma tumour. The animals were sacrificed at 30 min, 1 h and 3 h post-injection. Organs were excised and counted in a flat geometry NaI (Tl) scintillation counter. Three animals were used for each time point. The per cent activity retained in different organs was calculated as described in Section 14.3.1.6.

*Biodistribution studies in animal model of apoptosis.* Cyclohexamide (CHX) has been shown to induce apoptosis in rat liver in several *in vivo* studies [14.13]. CHX was selected as the chemical agent to induce apoptosis. Male Wister rats of approximately 200 g were used in control and treated groups to eliminate size dependent differences in tracer uptake. A single dose of CHX at 5 mg/kg was administered intraperitoneally. In control animals the same volume of saline was injected by the intraperitoneal route. After 3 h, rats were injected with  $^{99\text{m}}\text{Tc}(\text{N})\text{-C2-Anx13}$  (3–4 MBq/ $\mu\text{g}$ ) via the tail vein.  $^{99\text{m}}\text{Tc}(\text{N})\text{-C2-Anx13}$  was injected both in control and CHX treated animals and the biodistribution in various organs was estimated at 30 min post-injection in terms of per cent uptake of  $^{99\text{m}}\text{Tc}(\text{N})\text{-C2-Anx13/g}$  tissue.

*Ex vivo histology.* CHX induced liver apoptosis was confirmed by morphology study. Haematoxylin and eosin stained liver sections of control and CHX treated animals were viewed by light microscopy using a Carl Zeiss Axioplan 2 microscope at  $40\times$  magnification.

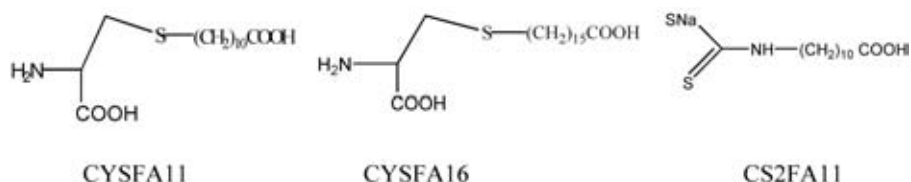


FIG. 14.1. Fatty acid analogues studied.

*Gamma scintigraphic studies in rat liver apoptosis model.*  $^{99m}\text{Tc}(\text{N})\text{-C2-Anx13}$  (3–4 MBq/ $\mu\text{g}$ ) was injected via the tail vein in control as well as CHX injected rats as described in Section 14.3.2.3. For scintigraphic studies, the animal was anaesthetized and scintigraphic images were recorded using a Single Head Digital SPECT Gamma Camera (GE Wipro) with a parallel hole LEHR collimator. Static images were acquired using a  $256 \times 256$  matrix with 300 kcounts at 30 min post-injection.

### 14.3.3. Synthesis and characterization of technetium-99m fatty acid analogues for myocardial imaging

#### 14.3.3.1. Radiolabelling studies

Two cysteine functionalized analogues of undecanoic acid and hexadecanoic acid, namely CYSFA11 and CYSFA16, were radiolabelled using the  $^{99m}\text{Tc}(\text{CO})_3$  approach, whereas the dithiocarbamate derivative of undecanoic acid, CS2-FA11, was labelled via  $^{99m}\text{Tc}(\text{N})$  intermediate. The structures of these derivatives are given in Fig. 14.1.

*Preparation of  $^{99m}\text{Tc}(\text{CO})_3\text{-CYSFA 11}$ .* CYSFA 11 (2 mg) was dissolved in 1.5 mL 0.01M NaOH and 0.5 mL of double distilled water. The resultant pH was around pH8.5. CYSFA11 0.2 mL (200  $\mu\text{g}$ ) was mixed with 0.4 mL of  $^{99m}\text{Tc}$ -carbonyl precursor at pH8, and the reaction mixture was heated at 75°C for 30 min.

*Preparation of  $^{99m}\text{Tc}(\text{CO})_3\text{-CYSFA16}$ .* CYSFA16 (1 mg) was added to 0.5 mL methanol and 0.55 mL of TFA. It was observed that CYSFA16 did not dissolve completely. 0.5 mL of  $^{99m}\text{Tc}$ -carbonyl and 0.16 mL of CYSFA16 in a methanol/water system were mixed together, to which phosphate buffer was added to adjust the pH to pH3, and the reaction was carried out at 75°C for 30 min. Complexation was also tried with CYSFA16 (1 mg) dissolved in 0.25 mL of TFA and with a reaction at pH8 adjusted with 1M NaOH.

*Preparation of  $^{99m}\text{Tc}(\text{N})\text{ CS2-FA11}$ .*  $^{99m}\text{Tc}(\text{N})$  intermediate was prepared as described in Section 14.3.1.2. CS2-FA11 derivative (1.3 mg) was dissolved in 930  $\mu\text{L}$  of NaOH (0.01M) and 70  $\mu\text{L}$  of distilled water. 0.3 mL (390  $\mu\text{g}$ ) of the

above solution of CS2-FA11 was added to 0.4 mL of  $^{99m}\text{Tc}(\text{N})$  intermediate and heated at 80°C for 45 min.

#### 14.3.3.2. Quality control

*Characterization of  $^{99m}\text{Tc}(\text{CO})_3\text{-CYSFA11}$ .* C18 reverse phase HPLC analysis of  $^{99m}\text{Tc}(\text{CO})_3\text{-CYSFA11}$  complex was carried out using water (solvent A) and methanol (solvent B) with 0.1% TFA. The elution gradient consisted of 0–1 min 0% B, 1–9 min 0–75% B, 9–24 min 75% B, 24–25 min 75–95% B, 25–30 min 95% B, 30–35 min 95–100% B.

*Characterization of  $^{99m}\text{Tc}(\text{CO})_3\text{-CYSFA16}$ .* The solvent composition mentioned in Section 14.3.3.2 was used for HPLC analysis of  $^{99m}\text{Tc}(\text{CO})_3\text{-CYSFA16}$  with an isocratic system of 75% methanol and 25% water.

*Characterization of  $^{99m}\text{Tc}(\text{N})\text{-CS2FA11}$ .* For HPLC analysis of  $^{99m}\text{Tc}(\text{N})\text{-CS2FA11}$  complex, water (A) and acetonitrile (B) containing 0.1% TFA was used as the mobile phase. The elution began with 90% A/10% B with a linear gradient to 10% A/90% B from 0 to 28 min and continued without any change until 30 min.

#### 14.3.3.3. In vitro studies

Stability studies were carried out with  $^{99m}\text{Tc}(\text{CO})_3\text{-CYSFA11}$ , as mentioned in Section 14.3.1.5.

#### 14.3.3.4. In vivo studies

$^{99m}\text{Tc}(\text{CO})_3\text{-CYSFA11}$  (3–4 MBq/100  $\mu\text{L}$ ) was administered by tail vein injection in normal Swiss mice. The animals were sacrificed at 1 min, 5 min and 1 h post-injection by cervical dislocation. Tissues of organs of interest were isolated and counted. The accumulated per cent of injected dose per organ as well as per gram in all major tissues was calculated as described in Section 14.3.1.6.

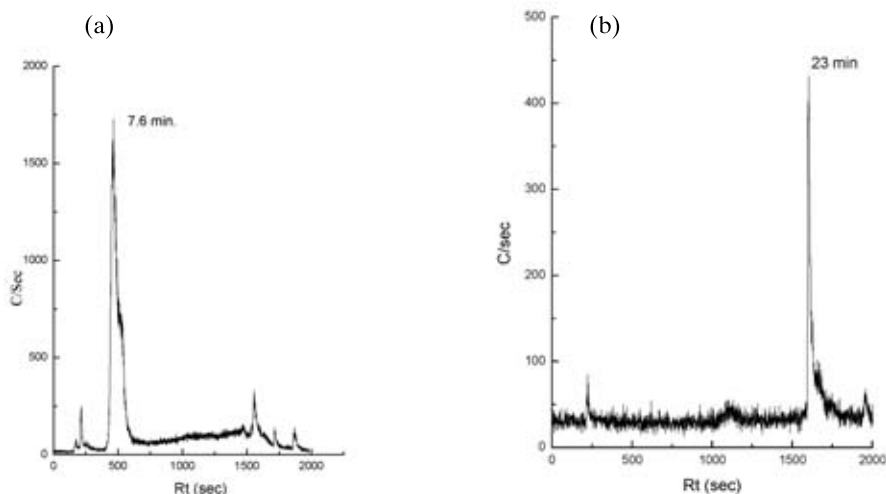


FIG. 14.2. HPLC patterns of (a)  $^{99m}\text{Tc}$ -tricarbonyl precursor, (b)  $^{99m}\text{Tc}(\text{CO})_3\text{-PZI-RGD}$ .

## 14.4. RESULTS

### 14.4.1. Synthesis and characterization of $^{99m}\text{Tc}(\text{CO})_3\text{-RGD}$ and $^{99m}\text{Tc}(\text{N})\text{-RGD}$ for tumour targeting

#### 14.4.1.1. $^{99m}\text{Tc}$ -tricarbonyl complexes of RGD

$^{99m}\text{Tc}(\text{CO})_3\text{-PZI-RGD}$  was formed with high (>95%) yields at an optimum peptide concentration of 400  $\mu\text{g}/\text{mL}$  and reaction pH5. The yield decreased at lower concentration of peptide and higher reaction pH. The HPLC pattern of the complex is depicted in Fig. 14.2. The complex was formed in single species with a retention time of 23 min (Fig. 14.2b). The retention time of the precursor was 7.6 min (Fig. 14.2a). However, His-RGD and tert Cys-RGD showed no complexation with  $^{99m}\text{Tc}[(\text{CO})_3(\text{H}_2\text{O})_3]^+$  synthon.

#### 14.4.1.2. $^{99m}\text{Tc}(\text{N})\text{Cys-RGD}$ (symmetric complexes)

The symmetric complex of  $^{99m}\text{Tc}(\text{N})\text{RGD}$  was formed with 98% yields. The complex was eluted out in HPLC with a retention time of 9.2 min with a shoulder at the base, as seen in Fig. 14.3a.

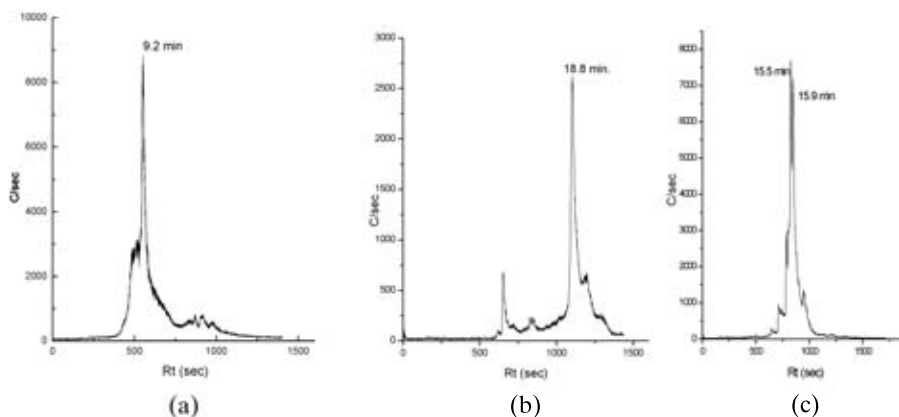


FIG. 14.3. HPLC patterns of (a)  $^{99m}\text{Tc}(\text{N})\text{-Cys-RGD}$ , (b)  $^{99m}\text{Tc}(\text{N})(\text{PNP})^{+2}$ , (c)  $^{99m}\text{Tc}(\text{N})(\text{PNP})\text{-Cys-RGD}$ .

#### 14.4.1.3. $^{99m}\text{Tc}(\text{N})(\text{PNP})\text{-Cys-RGD}$ (asymmetric complex)

The  $^{99m}\text{Tc}(\text{N})(\text{PNP})^{+2}$  precursor was synthesized with >95% yield. The HPLC pattern revealed single species with a retention time of 18.3 min (Fig. 14.3b). However, HPLC analysis of the complex showed formation of two close species with retention times of 15.5 and 15.9 min (Fig. 14.3c).

#### 14.4.1.4. Preparation of $^{99m}\text{Tc}\text{-HYNIC-RGD}$

Based on the earlier results of the participating laboratories, a standard protocol was set up for the preparation of  $^{99m}\text{Tc}\text{-HYNIC-RGD}$ . The complex could be synthesized using the standard protocol with high yields. The complex when characterized by HPLC analysis referred to in the standard protocol (Section 14.3.1.4) was eluted out with a retention time of 15.5 min, close to the referred time of 15.1 min.

#### 14.4.1.5. *In vitro* studies

*Stability studies.*  $^{99m}\text{Tc}$ -tricarbonyl and nitrido complexes of RGD analogues were found to be stable for at least 24 h at ambient temperature.  $^{99m}\text{Tc}(\text{CO})_3\text{-PZ1-RGD}$  and  $^{99m}\text{Tc}(\text{N})(\text{PNP})^{+2}\text{-Cys-RGD}$  were stable to ligand exchange. The complexes showed no dissociation or exchange with cysteine and histidine. However, stability of  $^{99m}\text{Tc}(\text{N})\text{-Cys-RGD}$  to ligand exchange was poor. Complete exchange was observed with cysteine, while 20% dissociation was observed with histidine.

TABLE 14.2. PER CENT TOTAL ACTIVITY BOUND TO SERUM

	Per cent binding with serum
$^{99m}\text{Tc}(\text{CO})_3\text{-PZ1-RGD}$	12
$^{99m}\text{Tc}(\text{N})\text{-Cys-RGD}$	30
$^{99m}\text{Tc}(\text{N})(\text{PNP})\text{-Cys-RGD}$	7

*Serum binding and stability in serum.* The results of serum binding studies for the complexes are given in Table 14.2. Out of the three different complexes evaluated for serum protein binding,  $^{99m}\text{Tc}(\text{N})\text{-Cys-RGD}$  showed maximum binding, while  $^{99m}\text{Tc}(\text{N})(\text{PNP})\text{-Cys-RGD}$  showed the minimum. HPLC of serum supernatant after separation of serum proteins showed no degradation of  $^{99m}\text{Tc}(\text{CO})_3\text{-PZ1-RGD}$  and  $^{99m}\text{Tc}(\text{N})(\text{PNP})\text{-Cys-RGD}$ .

*In vitro cell uptake studies.* In vitro cell uptake studies of  $^{99m}\text{Tc}\text{-HYNIC-RGD}$  were carried out with the HT29 cell line.  $^{99m}\text{Tc}\text{-HYNIC-RGD}$  did not show any uptake in HT29 cells, and only  $1.6 \pm 0.5\%$  of tracer uptake was observed in all the tubes, including non-specific binding.

#### 14.4.1.6. In vitro studies

The results of the biodistribution of  $^{99m}\text{Tc}(\text{CO})_3\text{-PZ1-RGD}$  and  $^{99m}\text{Tc}(\text{N})\text{-Cys-RGD}$  in Swiss mice are given in Tables 14.3 and 14.4, respectively.  $^{99m}\text{Tc}(\text{N})\text{-Cys-RGD}$  showed better pharmacokinetics than  $^{99m}\text{Tc}(\text{CO})_3\text{-PZ1-RGD}$  in Swiss mice. Although both the complexes were excreted via the renal route, the  $^{99m}\text{Tc}(\text{N})\text{-Cys-RGD}$  complex showed faster clearance from blood and lower soft tissue retention.

### 14.4.2. Synthesis and evaluation of $^{99m}\text{Tc}(\text{N})\text{-Anx13}$ and $^{99m}\text{Tc}(\text{CO})_3\text{-Anx13}$ as an apoptosis marker

#### 14.4.2.1. Radiolabelling of Anx13 analogues

$^{99m}\text{Tc}(\text{N})\text{-C-Anx13}$ . C-Anx13 reacted with nitrido intermediate with >95% yields. However, HPLC analysis of  $^{99m}\text{Tc}(\text{N})\text{-C-Anx13}$  revealed formation of two species with retention times of  $13.0 \pm 0.2$  min and  $14.3 \pm 0.2$  min (Fig. 14.4a). When attempts were made to prepare an asymmetric complex via a  $^{99m}\text{Tc}(\text{N})(\text{PNP})^{+2}$  fragment using diphosphine ligand, the complex  $^{99m}\text{Tc}(\text{N})\text{PNP-C-Anx13}$  could be formed with >95% yields, but in this

TABLE 14.3. BIODISTRIBUTION OF  $^{99m}\text{Tc}(\text{CO})_3\text{-PZ1-RGD}$  IN SWISS MICE

	1 h		3 h		24 h	
	% ID	% ID/g	% ID	% ID/g	% ID	% ID/g
Blood	5.9 (1)	3.1 (0.5)	1.0 (0.2)	0.5 (0.1)	UD <sup>a</sup>	UD
Heart	0.5 (0.1)	3.1 (0.6)	0.2 (0.1)	1.2 (0.5)	UD	UD
Liver	9.0 (0.1)	7.1 (0.8)	6.4 (0.8)	4.9 (1.6)	5.1 (1.0)	4.3 (1.7)
Lungs	0.7 (0.1)	3.9 (0.6)	0.8 (0.4)	3.5 (0.6)	0.05 (0.02)	0.8 (0.2)
Kidneys	3.6 (0.4)	7.2 (0.8)	1.6 (0.3)	4.1 (0.4)	0.5 (0.07)	1.5 (1.4)
Stomach	3.4 (0.4)	6.8 (0.3)	4.0 (1.1)	5.1 (2)	0.5 (0.2)	1.2 (0.7)
Intestines	12.9 (2)	3.1 (0.5)	11.3 (1.4)	4.4 (0.2)	4.3 (0.9)	1.6 (0.6)
Brain	0.2 (0.05)	0.5 (0.1)	0.05 (0.02)	0.2 (0.1)	UD	UD
Muscle	11.6 (2.0)	1.0 (0.2)	5.7 (1.4)	0.5 (1.0)	UD	UD
Urine and bladder	58 (5)	—	59 (9)	—	88.7 (10)	—

$N = 3$ ; SD values are given in parentheses.

<sup>a</sup> UD: undetectable.

case HPLC analysis of the complex also revealed formation of two species with retention times of  $18.0 \pm 0.2$  min and  $24 \pm 0.2$  (Fig. 14.4b). Since complexes with multiple species are generally not preferred as these are likely to show differences and variations in their in vivo behaviour, neither of these complexes,  $^{99m}\text{Tc}(\text{N})\text{-C-Anx13}$  and  $^{99m}\text{Tc}(\text{N})(\text{PNP})^{+2}\text{-C-Anx13}$ , were evaluated further for their biological behaviour.

$^{99m}\text{Tc}(\text{N})\text{-C2-Anx13}$ . The complex was formed with high (>95%) yields. The HPLC pattern revealed formation of single species, as depicted in Fig. 14.5a. The probable structure of the nitrido complex with CC-Anx13 is given in Fig. 14.5b.

$^{99m}\text{Tc}(\text{CO})_3\text{-H-Anx13}$ .  $^{99m}\text{Tc}$ -tricarbonyl precursor was formed with >95% yields and eluted out in HPLC with a retention time of 8.3 min. H-Anx13 reacted with the precursor with complexation yields of 95%. The complex eluted out in HPLC with a retention time of 24 min.

#### 14.4.2.2. In vitro studies

*Stability studies.* Both  $^{99m}\text{Tc}(\text{N})\text{-C2-Anx13}$  and  $^{99m}\text{Tc}(\text{CO})_3\text{-H-Anx13}$  were found to be stable at room temperature for 24 h. Both the complexes when tested for instability towards transchelation by challenging with cysteine

TABLE 14.4. BIODISTRIBUTION OF  $^{99m}\text{Tc}$ -(N)-RGD IN SWISS MICE

	1 h		3 h		24 h	
	% ID	% D/g	% ID	% ID/g	% ID	% ID/g
Blood	1.5 (0.1)	0.8 (0.03)	0.05 (0.03)	0.03 (0.02)	0.1 (0.03)	0.04 (0.01)
Heart	0.1 (0.1)	0.6 (0.4)	0.1 (0.07)	0.4 (0.5)	0.03 (0.02)	0.1 (0.06)
Liver	5.1 (0.9)	3.8 (0.3)	3.9 (1.1)	2.4 (2.1)	2.8 (0.2)	2.2 (1.7)
Lungs	0.5 (0.1)	2.4 (0.4)	0.4 (0.1)	0.8 (0.7)	0.3 (0.1)	0.7 (0.1)
Kidneys	3.2 (0.4)	5.4 (2.6)	1.4 (0.3)	4.8 (4.3)	0.7 (0.1)	1.5 (0.4)
Intestines	7.6 (0.6)	1.9 (0.2)	7.6 (2.0)	2.4 (2.2)	3.4 (0.2)	1.2 (0.5)
Brain	0.04 (0.06)	0.1 (0.2)	0.02 (0.01)	0.05 (0.04)	0.01 (0.01)	0.02 (0.01)
Muscle	5.2 (0.8)	0.5 (0.1)	5.2 (0.5)	0.4 (0.3)	3.9 (2.2)	0.4 (0.1)
Excretion	76	—	80	—	90	—

$N = 3$ ; SD values are given in parentheses.

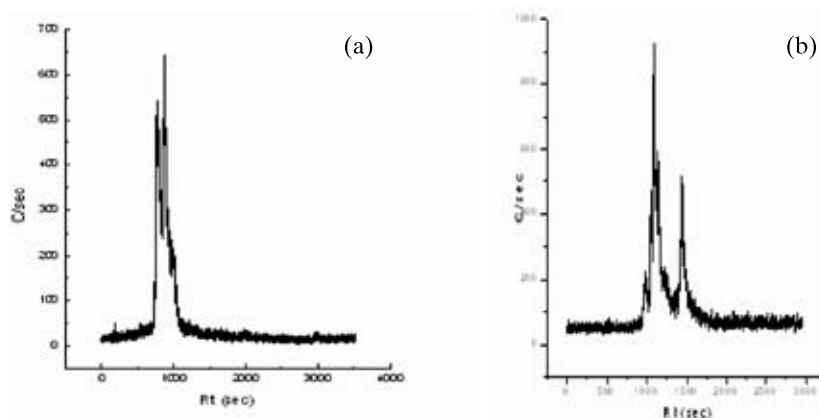


FIG. 14.4. HPLC patterns of  $^{99m}\text{Tc}$ -C-Anx13. (a)  $^{99m}\text{Tc}$ (N)-C-Anx13, (b)  $^{99m}\text{Tc}$ (N)(PNP) $^{+2}$ -C-Anx13.

(0.1M) and histidine (0.1M) showed no dissociation or exchange with cysteine or histidine.

*Cell uptake studies.* Apoptosis induction by Camptothecin in HL-60 cells was confirmed by flow cytometry. In the case of  $^{99m}\text{Tc}$ (N)-C2-Anx13, 6.5% binding was observed in apoptotic cells when incubated for 30 min, whereas the binding was just 1.3% in control (non-apoptotic) cells. When apoptotic cells were incubated with 100-fold cold CC-Anx13 along with  $^{99m}\text{Tc}$ (N)-C2-Anx13,

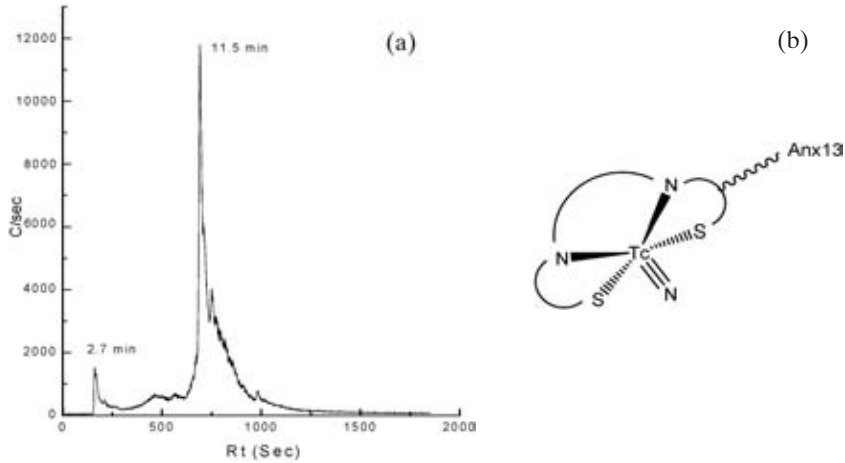


FIG. 14.5. (a) HPLC pattern of  $^{99m}\text{Tc}(\text{N})\text{-CC-Anx13}$ , (b) probable structure of  $^{99m}\text{Tc}(\text{N})\text{-C2-Anx13}$ .

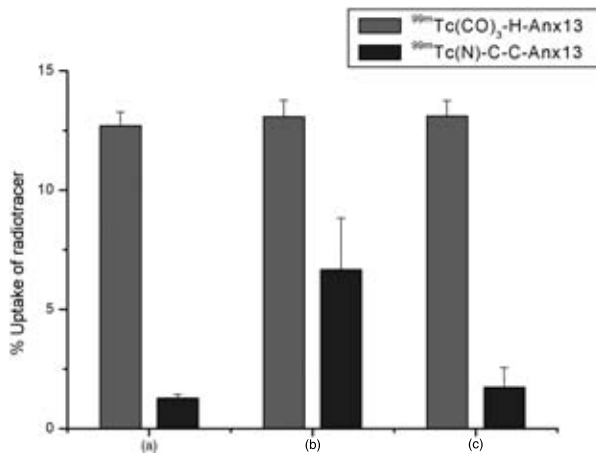


FIG. 14.6. Uptake of  $^{99m}\text{Tc}(\text{N})\text{-C2-Anx13}$  and  $^{99m}\text{Tc}(\text{CO})_3\text{-H-Anx13}$  by (a) HL-60 cells, (b) Camptothecin treated HL-60 cells and (c) Camptothecin treated HL-60 cells in the presence of 100-fold cold CC-Anx13.

the binding decreased to 1.8%, indicating specific uptake of tracer in apoptotic cells. However,  $^{99m}\text{Tc}(\text{CO})_3\text{-H-Anx13}$  exhibited non-specific uptake of ~13% in all studies with control (non-apoptotic) and apoptotic cells in the presence as well as in the absence of cold peptide (Fig. 14.6).

TABLE 14.5. BIODISTRIBUTION STUDIES OF  $^{99m}\text{Tc}(\text{N})\text{-C2-Anx13}$  IN TUMOUR BEARING SWISS MICE

	30 min		1 h		3 h	
	% ID	% ID/g	% ID	% ID/g	% ID	% ID/g
Liver	2.70 (0.66)	2.81 (0.54)	1.38 (0.88)	1.11 (0.65)	1.88 (0.19)	1.49 (0.15)
Intestines and gall bladder	4.10 (0.11)	1.89 (0.09)	3.32 (0.83)	1.32 (0.315)	3.74 (0.35)	1.54 (0.23)
Stomach	0.24 (0.12)	0.70 (0.39)	0.31 (0.11)	0.41 (0.22)	0.38 (0.29)	1.53 (1.23)
Kidney	8.92 (1.02)	32.4 (5.16)	6.23 (0.75)	23.04 (2.30)	9.27 (1.50)	35.2 (6.42)
Heart	0.048 (0.01)	0.40 (0.10)	0.05 (0.02)	0.42 (0.04)	0.01 (0.01)	0.3 (0.01)
Lungs	0.409 (0.12)	2.1 (0.6)	0.42 (0.29)	2.45 (1.70)	0.17 (0.04)	1.44 (0.27)
Spleen	0.03 (0.01)	0.21 (0.09)	0.08 (0.01)	0.19 (0.01)	0.027 (0.014)	0.25 (0.10)
Tumour	0.37 (0.15)	1.08 (0.19)	0.24 (0.03)	0.52 (0.17)	0.14 (0.02)	0.26 (0.09)
Muscles	2.15 (1.03)	0.23 (0.11)	2.34 (2.03)	0.24 (0.21)	1.38 (0.84)	0.15 (0.11)
Blood	2.07 (1.08)	1.37 (0.681)	0.07 (0.06)	0.15 (0.05)	0.26 (0.18)	0.15 (0.11)
Tibia	0.91 (0.5)	0.40 (0.23)	0.015 (0.015)	0.15 (0.1)	0.809 (0.21)	0.32 (0.2)
Tumour/ blood	0.8		3.3		1.7	
Tumour/ muscle	4.7		2.2		1.7	

$N = 3$ ; SD values are given in parentheses.

#### 14.4.2.3. *In vivo* studies

*Biodistribution studies in animal tumour model.* The results of biodistribution studies of  $^{99m}\text{Tc}(\text{N})\text{-C2-Anx13}$  in tumour bearing Swiss mice are shown in Table 14.5. It can be seen that the radioactivity rapidly cleared from blood. Uptake of  $^{99m}\text{Tc}(\text{N})\text{-C2-Anx13}$  in tumour was 1.3 ( $\pm 0.2$ )/%g at 30 min post-injection, which decreased to 0.39 (0.02)/%g at 3 h post-injection. Optimum tumour uptake was 0.63 (0.15)/%g, with a tumour to blood and tumour to muscle ratio of 1.8 and 3.1, respectively, at 1 h post-injection.

*Biodistribution studies in animal model of apoptosis.* Gamma scintigraphy images acquired at 30 min post-injection of  $^{99m}\text{Tc}(\text{N})\text{-C2-Anx13}$  in a control and animal model of liver apoptosis are shown in Fig. 14.7. In the control animal, accumulation of activity was observed mainly in kidneys and urinary bladder. In case of CHX treated animals, accumulation of activity in liver along with uptake in kidneys was observed. The results of biodistribution studies are

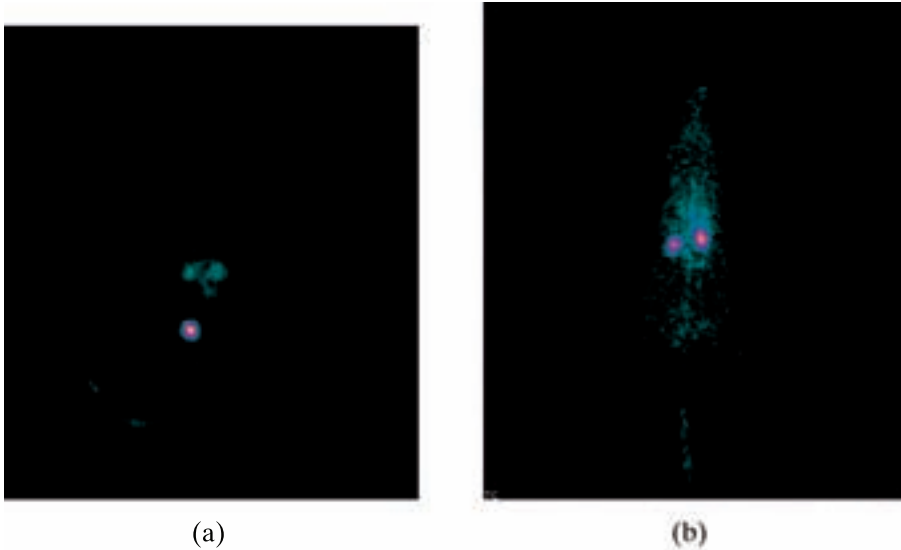


FIG. 14.7. Gamma scintigraphic images of a rat injected with  $^{99m}\text{Tc}(\text{N})\text{CC-Anx13}$ . At 30 min post-injection: (a) control rat, (b) CHX treated rat.

TABLE 14.6. BIODISTRIBUTION OF  $^{99m}\text{Tc}(\text{N})\text{-C2-Anx13}$  IN CONTROL AND CHX TREATED RATS AT 30 MIN POST-INJECTION

	Control (% ID/g)	CHX treated (% ID/g)
Liver	0.420 (0.162)	0.693 (0.11)
Intestines and gall bladder	0.408 (0.08)	0.81 (0.04)
Stomach	0.11 (0.02)	0.09 (0.04)
Kidney	5.82 (1.24)	8.96 (0.58)
Heart	0.26 (0.19)	0.34 (0.16)
Lungs	0.23 (0.15)	0.37 (0.22)
Spleen	0.51 (0.29)	0.62 (0.3)
Muscles	0.33 (0.23)	0.36 (0.3)
Blood	0.44 (0.25)	0.49 (0.23)
Tibia	0.45 (0.34)	0.232 (0.26)

$N = 3$ ; SD values are given in parenthesis.

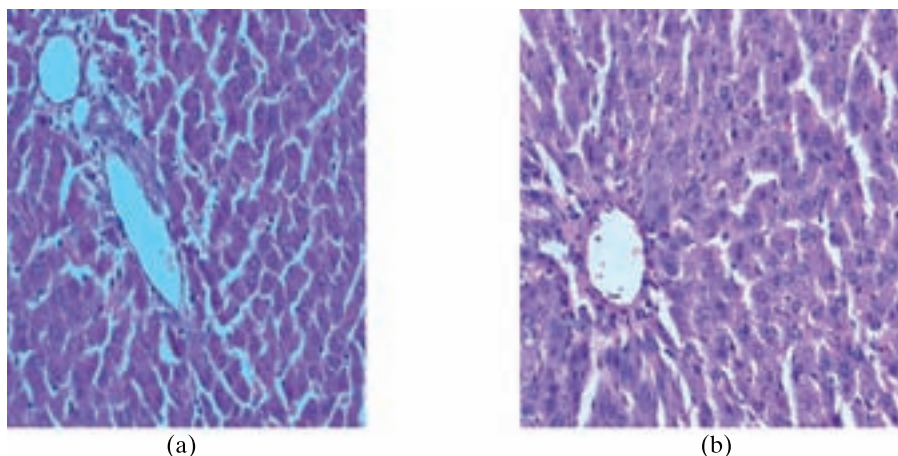


FIG. 14.8. Histology sections of liver stained with hematoxylin and eosin (magnification  $\times 40$ ) in (a) untreated and (b) CHX treated rats.

shown in Table 14.6. Liver tissue in control and apoptosis induced rats showed  $0.4 \pm 0.2\%$  and  $0.7 \pm 0.1\%$  uptake per g, respectively.

*Ex vivo histology.* Histology studies of CHX treated liver indicated development of apoptosis. Histological sections of liver from untreated and CHX treated rats stained with hematoxylin and eosin are depicted in Fig. 14.8. Even though the liver sections from treated animals show a distinct difference from normal liver cells, the number of cells exhibiting apoptotic bodies in liver sections of CHX treated animals is not very high and exact correlation between the apoptosis density in liver determined by histology and the per cent uptake of  $^{99m}\text{Tc}(\text{N})\text{-C2-Anx13/g}$  of liver tissue was not studied.

#### 14.4.3. Synthesis and characterization of $^{99m}\text{Tc}(\text{CO})_3$ undeconic acid for myocardial imaging

##### 14.4.3.1. $^{99m}\text{Tc}(\text{CO})_3\text{-CYSFA11}$

CYSFA11 reacted with tricarbonyl precursor to form a complex with  $>95\%$  yield. The HPLC pattern of  $^{99m}\text{Tc}(\text{CO})_3\text{-CYSFA11}$  revealed single species with a retention time of 14 min (Fig. 14.9).

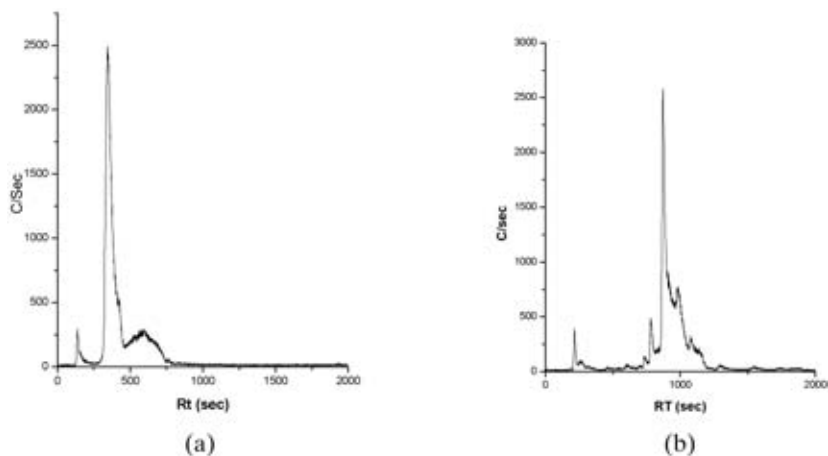


FIG. 14.9. HPLC pattern of (a)  $^{99m}\text{Tc}$ -tricarbonyl precursor and (b)  $^{99m}\text{Tc}(\text{CO})_3\text{-CYSFA11}$ .

#### 14.4.3.2. $^{99m}\text{Tc}(\text{CO})_3\text{-CYSFA16}$

In the case of CYSFA16, dissolution of fatty acid derivative to obtain an aqueous solution was difficult due to its high lipophilicity. The ligand CYSFA16 did not show any complexation with  $^{99m}\text{Tc}$ .

#### 14.4.3.3. $^{99m}\text{Tc}(\text{N})\text{-CS2FA11}$

CS2FA11 formed complexation with  $^{99m}\text{Tc}(\text{N})$  intermediate with >88% yield. The HPLC pattern of  $^{99m}\text{Tc}(\text{N})\text{-CS2FA11}$  revealed a single species with a retention time of 19.7 min (Fig. 14.10).

*In vitro studies.* The  $^{99m}\text{Tc}$ -tricarbonyl complex of CYSFA11 was found to be stable for at least 24 h at room temperature when stored in a phosphate buffer.  $^{99m}\text{Tc}(\text{CO})_3\text{-CYSFA11}$  showed stability towards cysteine exchange, whereas 10% exchange was observed with histidine.  $^{99m}\text{Tc}(\text{CO})_3\text{-CYSFA11}$  showed 60% binding to serum proteins when incubated with human serum at 37°C for 1 h.

*In vivo studies.* The results of biodistribution studies of  $^{99m}\text{Tc}(\text{CO})_3\text{-CYSFA11}$  are shown in Table 14.7. The product showed high retention in blood ( $16 \pm 5\%/g$  at 5 min post-injection) with low heart uptake ( $0.45 \pm 0.1\%/g$  at 5 min post-injection) and poor heart to muscle ratio.

CHAPTER 14

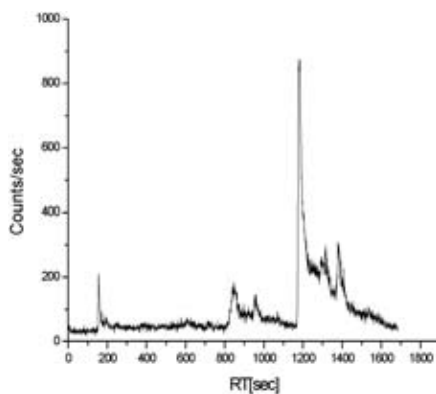


FIG. 14.10. HPLC pattern of  $^{99m}\text{Tc}(\text{N})\text{-CS2FA11}$ .

TABLE 14.7. BIODISTRIBUTION STUDIES OF  $^{99m}\text{Tc}(\text{CO})_3\text{-CYSFA11}$  (% INJECTED DOSE/ORGAN)

	1 min	5 min	1 h
Blood	21.6 (1.4)	15.98 (5.07)	4.86 (3.3)
Liver	33.9 (3.1)	47.3 (3.71)	22.58 (1.28)
Intestines and gall bladder	2.9 (0.2)	11.37 (2.47)	42.9 (13.9)
Kidney	2.9 (0.2)	7.96 (1.35)	2.25 (0.15)
Stomach	0.52 (0.2)	1.04 (0.23)	5.1 (6.13)
Heart	0.6 (0.1)	0.45 (0.11)	0.25 (0.09)
Lungs	1.7 (0.1)	1.48 (0.32)	0.85 (0.56)
Femurs	13.6 (2.1)	2.89 (0.15)	11.75 (9.4)
Muscles	10.7 (2.0)	18.2 (5.58)	5.27 (3.25)
Spleen	0.2 (0.02)	0.20 (0.18)	0.43 (0.39)
Carcass	53.3 (5.0)	28.1 (2.96)	25.2 (9.14)
Excreta	1.7 (0.2)	6.3 (1.9)	11.3 (7.5)

SD values are given in parenthesis.

## 14.5. CONCLUSION

$^{99m}\text{Tc}(\text{CO})_3\text{-PZ1-RGD}$ ,  $^{99m}\text{Tc}(\text{N})\text{-Cys-RGD}$  and  $^{99m}\text{Tc}(\text{HYNIC})\text{-RGD}$  complexes were formed with high yields as single species. In vitro stability of  $^{99m}\text{Tc}(\text{CO})_3\text{-PZ1-RGD}$  was found to be better than that of  $^{99m}\text{Tc}(\text{N})\text{-Cys-RGD}$ . Biodistribution studies of  $^{99m}\text{Tc}(\text{CO})_3\text{-PZ1-RGD}$  revealed fast blood clearance with low soft tissue retention and renal clearance. Further work on evaluation of  $^{99m}\text{Tc}(\text{CO})_3\text{-PZ1-RGD}$  and  $^{99m}\text{Tc}(\text{HYNIC})\text{-RGD}$  with RGD specific tumour cell lines is warranted for the development of a tumour imaging agent.

Dicysteine annexin 13 fragment (C2-Anx13) could be labelled with  $^{99m}\text{Tc}$  via nitrido intermediate with >95% yield. The complex was formed in a single species. In vitro studies showed specific uptake of  $^{99m}\text{Tc}(\text{N})\text{-C2-Anx13}$  in apoptotic HL-60 cells. In vivo studies of  $^{99m}\text{Tc}(\text{N})\text{-C2-Anx13}$  in an animal model of liver apoptosis showed an increase in liver uptake over that of the normal liver tissues, indicating a potential of  $^{99m}\text{Tc}(\text{N})\text{-C2-Anx13}$  tracer for further studies towards an apoptosis imaging agent.

Cysteine functionalized fatty acid derivatives (CYSFA11 and CYSFA16) were labelled with  $^{99m}\text{Tc}$  via carbonyl synthon. Tricarbonyl complexes could be prepared with high yields with CYSFA11. Dithiocarbamate derivative CS2FA11 could be labelled with nitride intermediate with 88% yield. However, the pharmacokinetics of  $^{99m}\text{Tc}(\text{CO})_3\text{-CYSFA11}$  showed high retention in blood with low heart uptake and poor heart to muscle ratio. Studies with CYSFA16 showed poor labelling yields. Further work on synthesis of long chain fatty acid derivatives with good solubility in an aqueous medium and labelling studies with novel cores are warranted for the development of a myocardial imaging agent.

## ACKNOWLEDGEMENTS

The authors are thankful to V. Venugopal, Director, Radiochemistry and Isotope Group, Bhabha Atomic Research Centre, for his support. The sample kits and derivatized biomolecules received as gifts from various CRP member countries are gratefully acknowledged.

## CHAPTER 14

### REFERENCES

- [14.1] ALBERTO, R., et al., A novel organometallic aqua complex of technetium for the labeling of biomolecules: Synthesis of  $[\text{}^{99\text{m}}\text{Tc}(\text{OH}_2)_3(\text{CO})_3]^+$  from  $[\text{}^{99\text{m}}\text{TcO}_4]^-$  in aqueous solution and its reaction with a bifunctional ligand, *J. Am. Chem. Soc.* **120** (1998) 7987.
- [14.2] SCHIBLI, R., et al., Influence of the denticity of ligand systems on the in vitro and in vivo behavior of  $^{99\text{m}}\text{Tc}$  (I) tricarbonyl complexes: A hint for the future functionalization of biomolecules, *Bioconj. Chem.* **11** (2000) 345.
- [14.3] PASQUALINI, R.A., et al., New efficient method for the preparation of  $^{99\text{m}}\text{Tc}$  radiopharmaceuticals containing the T≡N multiple bond, *Appl. Radiat. Isot.* **43** (1992) 1329.
- [14.4] ABRAMS, M.J., et al., Technetium  $^{99\text{m}}$  human polyclonal IgG radiolabeled via the hydrazine nicotinamide derivative for imaging focal sites of infection in rats, *J. Nucl. Med.* **31** (1990) 2022.
- [14.5] HAUBNER, R., et al., Glycosylated RGD containing peptides: Tracer for tumor targeting and angiogenesis imaging with improved biokinetics, *J. Nucl. Med.* **42** (2001) 326.
- [14.6] HOSTRA, L., et al., In vivo detection of apoptointra cardiac tumor, *J. Am. Med. Assoc.* **285** (2001) 1841.
- [14.7] WEN, X., et al., Improved radiolabeling of PEGylated protein: PEGlyted annexin V for non invasive imaging of tumor apoptosis, *Cancer Biother. Radiopharm.* **18** (2003) 819.
- [14.8] THIMISTER, P.W., et al., In vivo detection of cell death in the area at risk in acute myocardial infarction, *J. Nucl. Med.* **44** (2003) 391.
- [14.9] KIETSELEAR, B.L., et al., Non invasive detection of plaque instability with use of radiolabeled annexin A5 in patients with carotid-artery atherosclerosis, *New Engl. J. Med.* **350** (2004) 1472.
- [14.10] BOERSMA, H.H., et al., Past, present and future of annexin A5: From protein discovery to clinical application, *J. Nucl. Med.* **46** (2005) 2035.
- [14.11] MAURER-FOGY, I., et al., Cloning and expression of cDNA for human vascular anticoagulant, a  $\text{Ca}^{2+}$ -dependent phospholipid-binding protein, *Eur. J. Biochem.* **174** (1988) 585.
- [14.12] SUBBARAYAN, M., et al., Simplified method for preparation of  $^{99\text{m}}\text{Tc}$ -annexin V and its biologic evaluation for in vivo imaging of apoptosis after photodynamic therapy, *J. Nucl. Med.* **44** (2003) 650.
- [14.13] LEDDA-COLUMBANO, G.M., CONI, P., FAA, G., MANENTI, G., COLUMBANO, A., Rapid induction of apoptosis in rat liver by cycloheximide, *Am. J. Pathol.* **140** (1992) 545.



## Chapter 15

### LABELLING OF SMALL MOLECULES WITH THE $^{99m}\text{Tc-NITRIDO}$ CORE

M. PASQUALI, L. UCCELLI, A. BOSCHI, A. DUATTI

Laboratory of Nuclear Medicine, Department of Radiological Sciences,  
University of Ferrara, Italy

#### Abstract

In the framework of the project focused on the study of labelling methods of small biomolecules with novel  $^{99m}\text{Tc}$  cores, a number of labelling procedures based on the  $[\text{}^{99m}\text{Tc}\equiv\text{N}]^{2+}$  core have been proposed. It was found that the most useful class of  $^{99m}\text{Tc}$  complexes for incorporating small bioactive molecules was that of bis substituted complexes with bidentate chelating ligands. This class includes both symmetrically and asymmetrically bis substituted complexes. In symmetrical complexes, two identical bidentate ligands are coordinated to the same  $\text{Tc}\equiv\text{N}$  group. Conversely, two different bidentate ligands bind to the same metal centre in asymmetrical nitrido complexes. In the paper, a summary of results obtained within the coordinated research project through the application of the chemistry of  $^{99m}\text{Tc}$ -nitrido complexes is reported.

#### 15.1. INTRODUCTION

The combination of a nitride ion ( $\text{N}^{3-}$ ) with a  $\text{Tc}^{+5}$  ion gives rise to a highly stable molecular fragment, in which the two atoms are tightly bound together through the formation of a terminal  $\text{Tc}\equiv\text{N}$  triple bond. This basic structural motif behaves as a true inorganic functional group exhibiting peculiar chemical properties that can be conveniently exploited to develop efficient methods for labelling small biomolecules. In radiopharmaceutical preparations, the  $[\text{}^{99m}\text{Tc}\equiv\text{N}]^{2+}$  core is efficiently obtained through the reaction of  $[\text{}^{99m}\text{TcO}_4]^-$  with a reducing agent (usually  $\text{SnCl}_2$ ) and a donor of nitride nitrogen atoms (usually a compound containing the hydrazine-like moiety  $-\text{HN}-\text{NH}-$ ). After formation, this core reacts easily with soft  $\pi$  donors and  $\pi$  acceptor ligands to afford five coordinated complexes, which may exhibit structural characteristics ranging between the two limits of square pyramidal and trigonal bipyramidal geometries [15.1, 15.2].

The most extensively studied class of  $^{99\text{m}}\text{Tc}$ -nitrido compounds was that of five coordinated complexes containing two bidentate ligands bound to the same  $[\text{}^{99\text{m}}\text{Tc}\equiv\text{N}]^{2+}$  core. These species fall, essentially, within two different categories, namely symmetrical and asymmetrical complexes. Symmetrical complexes are formed by two identical bidentate ligands coordinated to the same  $\text{Tc}\equiv\text{N}$  group in a five coordinated arrangement. Conversely, asymmetrical complexes include two different bidentate ligands attached to the same  $\text{Tc}\equiv\text{N}$  group. In this work, both types of  $^{99\text{m}}\text{Tc}$ -nitrido bis substituted complexes were used for labelling small molecules and short peptide sequences, which were previously selected for targeting different biological substrates.

## 15.2. LABELLING METHODS

### 15.2.1. Symmetrical complexes

The type of bis substituted symmetrical  $^{99\text{m}}\text{Tc}$  complexes employed in this work for labelling small bioactive molecules is illustrated in Fig. 15.1a. These compounds possess a square pyramidal geometry with an apical  $\text{Tc}\equiv\text{N}$  group and two dithiocarbamate ligands (DTC) spanning the four positions on the basal plane. The lateral functional groups (R and R') on the dithiocarbamate ligand can be conveniently utilized for appending a bioactive moiety to the  $[\text{}^{99\text{m}}\text{Tc}\equiv\text{N}]^{2+}$  core. As a consequence, the resulting bis substituted conjugate complex always incorporates two symmetrically positioned bioactive molecules (Fig. 15.1b) [15.3–15.5].

### 15.2.2. Asymmetrical complexes

Asymmetrical nitrido  $^{99\text{m}}\text{Tc}$  complexes always form when two different bidentate ligands containing  $\pi$  donor and  $\pi$  acceptor coordinating atoms are simultaneously reacted with a  $\text{Tc}\equiv\text{N}$  group. Actually, neutral amino-bis-phosphino (PNP) and monoanionic dithiocarbamate (DTC) ligands provide a representative combination of  $\pi$  acceptor and  $\pi$  donor bidentate chelating ligands for producing asymmetrical complexes, as reported in Fig. 15.2 [15.6–15.10]. The final complex possesses a monopositive charge.

The molecular structure of these compounds lies between the two ideal limits of square pyramidal and trigonal bipyramidal geometries. Usually, the bidentate  $\pi$  donor ligand offers the most convenient site of attachment of a biomolecule. Thus the formation of the asymmetrical conjugate complex could be viewed as resulting from the selective combination of the strong

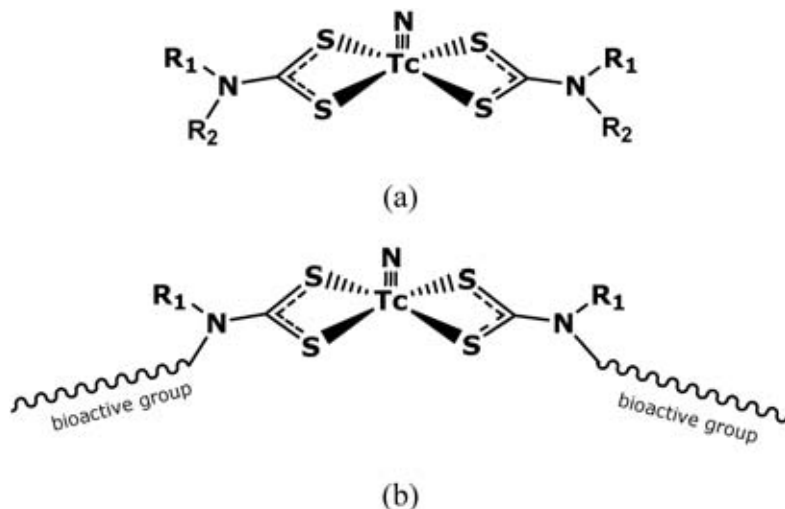


FIG. 15.1. General structure of (a) a symmetrical bis-dithiocarbamate nitrido  $^{99m}\text{Tc}$  complex and (b) of the resulting bis substituted conjugate complex.

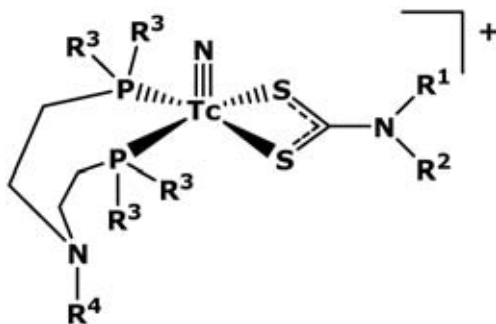


FIG. 15.2. General structure of monocationic asymmetrical amino-bis-phosphino dithiocarbamate nitrido  $^{99m}\text{Tc}$  complexes.

electrophilic metallic fragment  $[\text{}^{99m}\text{Tc}(\text{N})(\text{PNP})]^{2+}$ , with the bidentate  $\pi$  donor ligand bearing the bioactive group (Fig. 15.3).

Recently, a novel class of asymmetrical nitrido  $^{99m}\text{Tc}$  complexes has been introduced. These species are composed of a  $\text{Tc}=\text{N}$  group bound to a phosphino-thiol ligand (PS) and a dithiocarbamate ligand (DTC), as shown in Fig. 15.4 [15.12–15.14]. The procedure for preparing these new complexes is based on the chemical properties of the intermediate compound  $[\text{}^{99m}\text{Tc}(\text{N})(\text{PS})(\text{PPh}_3)\text{Cl}]$  composed of a  $\text{Tc}=\text{N}$  group bound to a bidentate

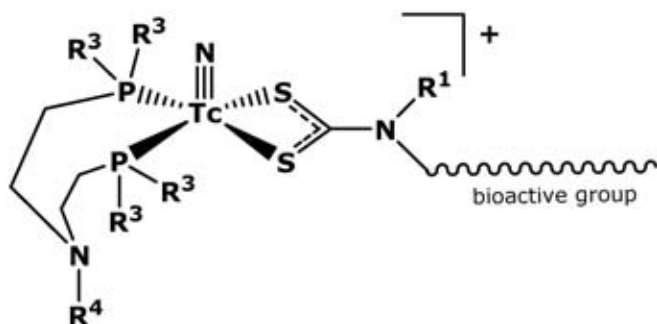


FIG. 15.3. General structure of an asymmetrical conjugate nitrido  $^{99m}\text{Tc}$  complex.

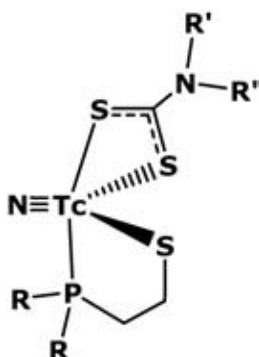


FIG. 15.4. General structure of asymmetrical phosphino-thiol dithiocarbamate nitrido  $^{99m}\text{Tc}$  complexes.

phosphino-thiol ligand, a triphenylphosphine ( $\text{PPh}_3$ ) and a chloride ion, as illustrated in Fig. 15.5. This intermediate readily reacts with bidentate mono-negative dithiocarbamate ligands containing soft  $\pi$  donor coordinating atoms to afford neutral five coordinated asymmetrical nitrido  $^{99m}\text{Tc}$  complexes of the type  $[\text{}^{99m}\text{Tc}(\text{N})(\text{PS})(\text{DTC})]$ .

### 15.3. RESULTS AND DISCUSSION

#### 15.3.1. Development of $^{99m}\text{Tc}$ glucose analogues

Attempts at preparing  $^{99m}\text{Tc}$ -nitrido analogues of glucose were carried out following both the symmetrical and asymmetrical approaches outlined above. A ligand suitable for these applications was designed as illustrated in

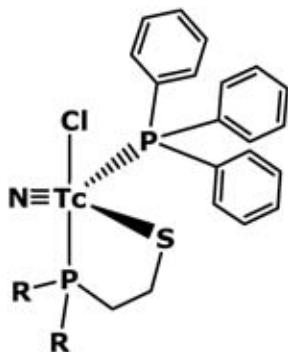


FIG. 15.5. Structure of the intermediate complex  $[^{99m}\text{Tc}(\text{N})(\text{PS})(\text{PPh}_3)\text{Cl}]$ .

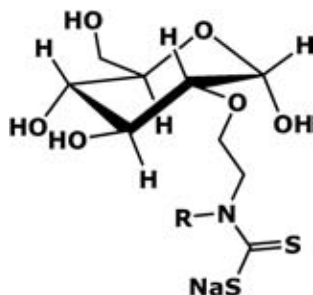


FIG. 15.6. A glucose derived dithiocarbamate bifunctional ligand.

Fig. 15.6. It is composed of a glucose moiety linked to a dithiocarbamate chelating system that is appended at the hydroxylic oxygen in 2 position of the glucose carbon ring through an ethyl bridge.

The above bifunctional ligand could potentially be employed for the preparation of symmetrical (Fig. 15.7a) and asymmetrical (Fig. 15.7b)  $^{99m}\text{Tc}$ -nitrido conjugated complexes. Unfortunately, various efforts to obtain some amount of this mixed glucose-dithiocarbamate bifunctional ligand have so far failed to give satisfactory results.

### 15.3.2. Labelling of bioactive peptides

Only the asymmetrical approach, based on the reactivity of the  $[^{99m}\text{Tc}(\text{N})(\text{PNP})]^{2+}$  metal fragment, has been utilized in this work for labelling short bioactive peptide chains for targeting expression of different receptors [15.11]. Briefly, this labelling method requires a simple derivatization of the selected bioactive peptide sequence by prolonging the length of the amino acid

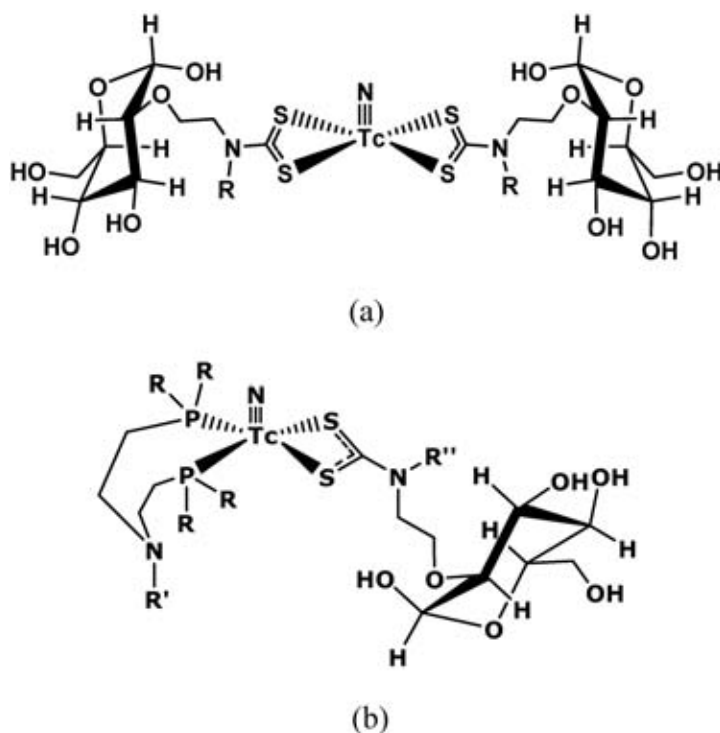


FIG. 15.7. Potential (a) symmetrical and (b) asymmetrical  $^{99m}\text{Tc}$ -nitrido complexes incorporating a glucose-dithiocarbamate bifunctional ligand.

chain through the addition of a terminal cysteine group. This amino acid exhibits a selective affinity for the metallic fragment  $[\text{}^{99m}\text{Tc}(\text{N})(\text{PNP})]^{2+}$ , resulting in the formation of asymmetrical complexes in which cysteine may coordinate to the metal centre either through the terminal negative sulphur and neutral amino nitrogen atom pairs or through the negative sulphur and negative carboxylic oxygen atom pairs, as shown in Fig. 15.8.

Thus peptide sequences having a terminal cysteine residue can be efficiently incorporated into an asymmetrical  $^{99m}\text{Tc}$ -nitrido complex by coordination to the  $[\text{}^{99m}\text{Tc}(\text{N})(\text{PNP})]^{2+}$  fragment, as illustrated in Fig. 15.9.

### 15.3.2.1. RGD peptides

Integrin receptors are selectively targeted by peptides containing a characteristic RGD amino acid sequence. The cyclic RGD peptide (Cys-RGD) shown in Fig. 15.10 has been functionalized by appending a terminal cysteine

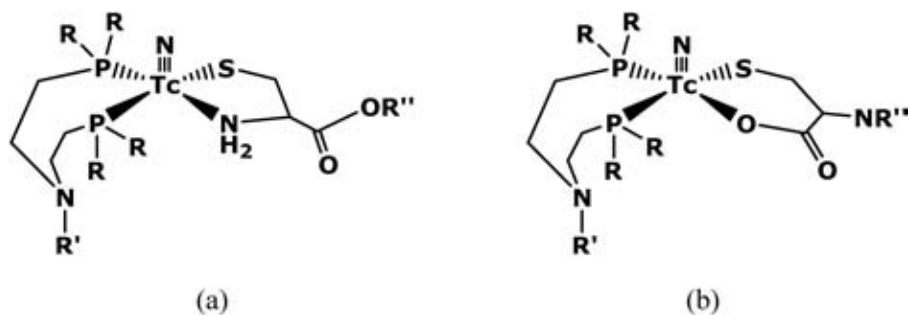


FIG. 15.8. Possible coordination modes of a terminal cysteine to the  $[^{99m}\text{Tc}(\text{N})(\text{PNP})]^{2+}$  metallic fragment.

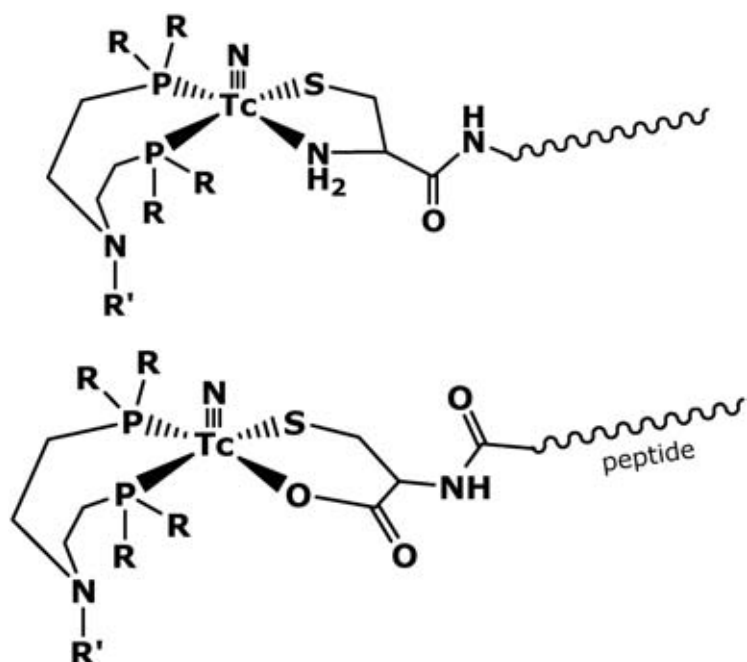


FIG. 15.9. Conjugate asymmetrical  $^{99m}\text{Tc}$ -nitrido complexes incorporating a peptide sequence.

group to the peptide ring. The preparation of this derivative was accomplished at the Universitätsklinik für Nuklearmedizin, Innsbruck.

Reaction of the ligand Cys-RGD with the metal fragment  $[^{99m}\text{Tc}(\text{N})(\text{PNP})]^{2+}$  (PNP = bis(dimethoxypropylphosphinoethyl)methoxyethylamine) led to the formation of the asymmetrical conjugate complex

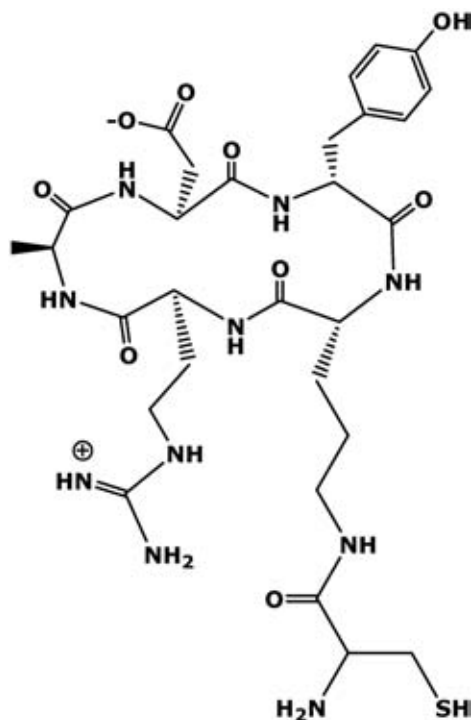


FIG. 15.10. Structure of an RGD peptide with a terminal cysteine group.

[ $^{99m}\text{Tc}(\text{N})(\text{PNP})(\text{Cys-RGD})$ ], where the peptidic ligand binds the metal atom through the deprotonated thiol sulphur atom and the neutral amino nitrogen atom of the terminal cysteine group (Fig. 15.11). The charge of the resulting conjugate complex is monopositive.

The biological properties of this complex have been evaluated in isolated tumour cells expressing integrin receptors and in tumour bearing animal models at the Universitätsklinik für Nuklearmedizin, Innsbruck. This tracer showed a specific uptake in tumour tissues characterized by expression of integrin receptors.

#### 15.3.2.2. Annexin V

The search for a short peptidic sequence mimicking the biological behaviour and receptor affinity for apoptotic cells of the large protein annexin V was carried out at the Biological Research Centre of the Hungarian Academy of Sciences, Budapest. This attempt led to the production of a small peptide composed of 13 amino acids (Fig. 15.12a) that were thought to be

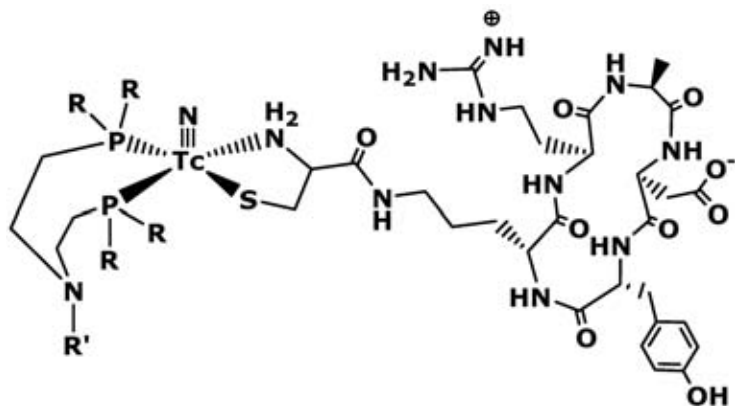


FIG. 15.11. Structure of the complex  $[^{99m}\text{Tc}(\text{N})(\text{PNP})(\text{Cys-RGD})]^+$ .

essential for preserving the receptor affinity for apoptotic cells of the native annexin V protein. This peptide was further modified through the addition of a terminal cysteine residue to allow application of the asymmetrical labelling method with the  $[^{99m}\text{Tc}(\text{N})(\text{PNP})]^{2+}$  (PNP = bis(dimethoxypropylphosphinoethyl)methoxyethylamine) metallic fragment.

Labelling with  $[^{99m}\text{Tc}(\text{N})(\text{PNP})]^{2+}$  yielded the complex reported in Fig. 15.13, where the peptide is tethered to the  $[^{99m}\text{Tc}=\text{N}]^{2+}$  core through the terminal cysteine  $[\text{NH}, \text{S}^-]$  chelating pair of donor atoms. As expected, the complex formed two isomers depending on the *syn* and *anti* positions of the amino acid chain with respect to the  $\text{Tc}=\text{N}$  multiple bond.

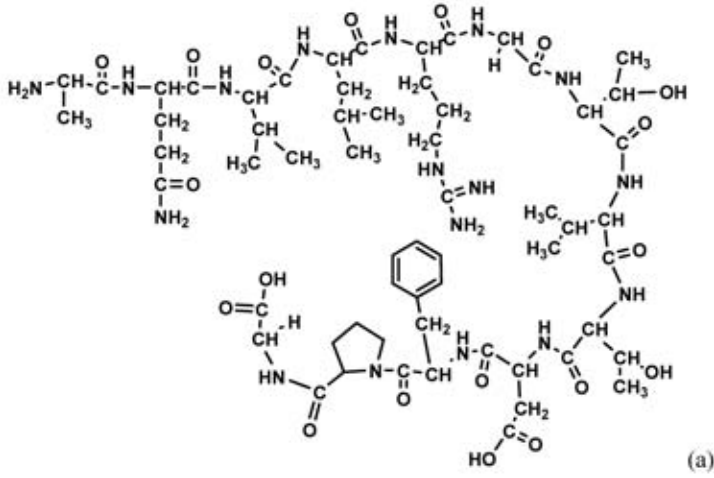
Biological evaluation of this complex was carried out in cultured apoptotic cells. Data revealed that the complex does not exhibit any affinity for phosphatidylserine expressed on the surface of apoptotic cells.

### 15.3.2.3. Quinazoline ligands

Quinazoline derived molecules are among the most active tyrosine kinase (TK) inhibitors with the highest selectivity for epidermal growth factor receptor (EGFR). A quinazoline derivative suitable for attachment of a terminal dithiocarbamate group was prepared by C. Fernandez at the Institute of Nuclear Technology in Portugal. The structure of this ligand is illustrated in Fig. 15.14a.

This compound was successively reacted with carbon disulphide to afford the quinazoline-dithiocarbamate derivative (Qz-DTC) shown in Fig. 15.14b. The presence of the  $-\text{C}(=\text{S})\text{S}^-$  chelating moiety allowed the application of both symmetrical and asymmetrical labelling methods for obtaining conjugate

## Ala-Gln-Val-Leu-Arg-Gly-Thr-Val-Thr-Asp-Phe-Pro-Gly-OH



## Cys-Ala-Gln-Val-Leu-Arg-Gly-Thr-Val-Thr-Asp-Phe-Pro-Gly-OH

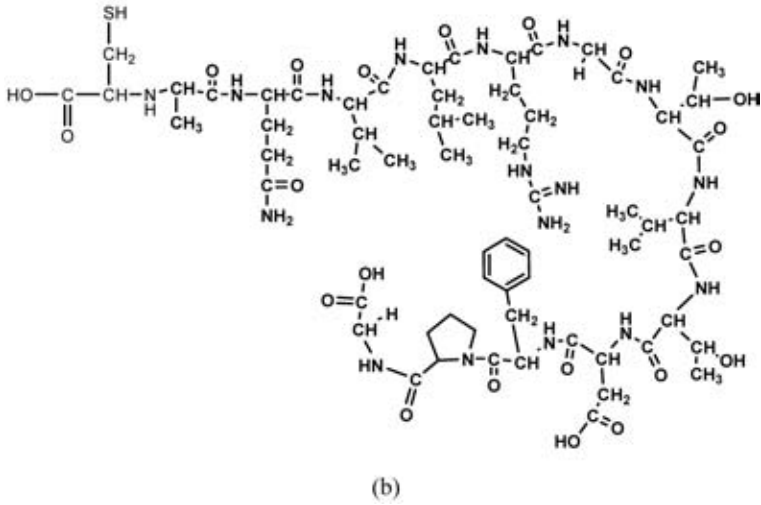


FIG. 15.12. (a) The 13 amino acid annexin V analogue peptide and (b) its cysteine derivative.

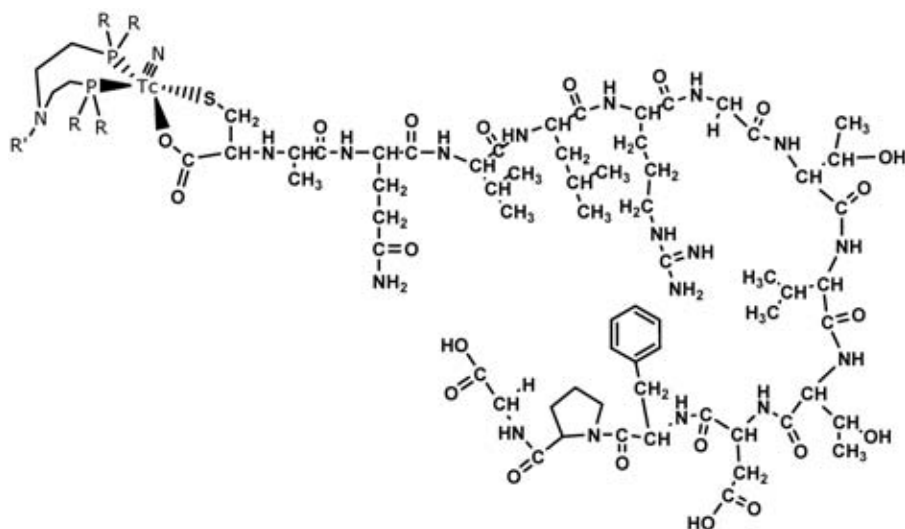


FIG. 15.13. Structure of the conjugate complex containing the annexin V analogue peptide.

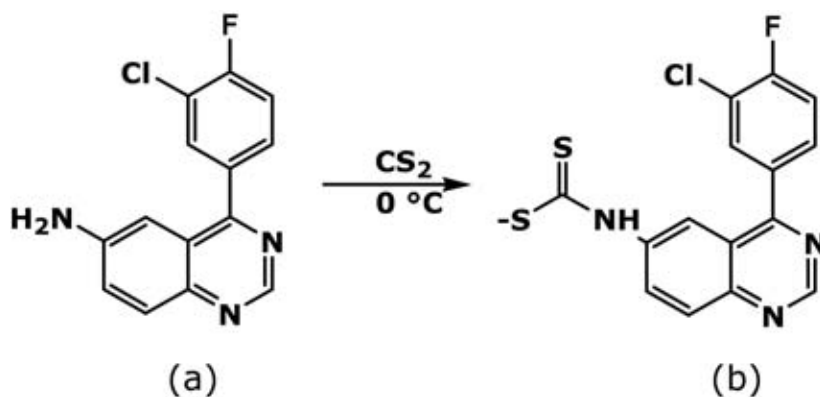


FIG. 15.14. Structures of (a) amino and (b) dithiocarbamate derivatives of quinazoline.

$^{99m}\text{Tc}$ -nitrido complexes with this quinazoline derived ligand. In particular, reaction with the  $[\text{}^{99m}\text{Tc}=\text{N}]^{2+}$  core yielded the bis substituted complex shown in Fig. 15.15, in which two quinazoline-dithiocarbamate ligands are bound to the metal centre. When the same ligand was utilized in the reaction with the metal fragment  $[\text{}^{99m}\text{Tc}(\text{N})(\text{PNP})]^{2+}$  (PNP = bis(dimethoxypropylphosphinoethyl)methoxyethylamine) or with the intermediate complex  $[\text{}^{99m}\text{Tc}(\text{N})(\text{PS})(\text{PPh}_3)\text{Cl}]$  (PS = 2-(isopropylphosphino)ethanethiol), two asymmetrical nitrido complexes were obtained (Fig. 15.15b).

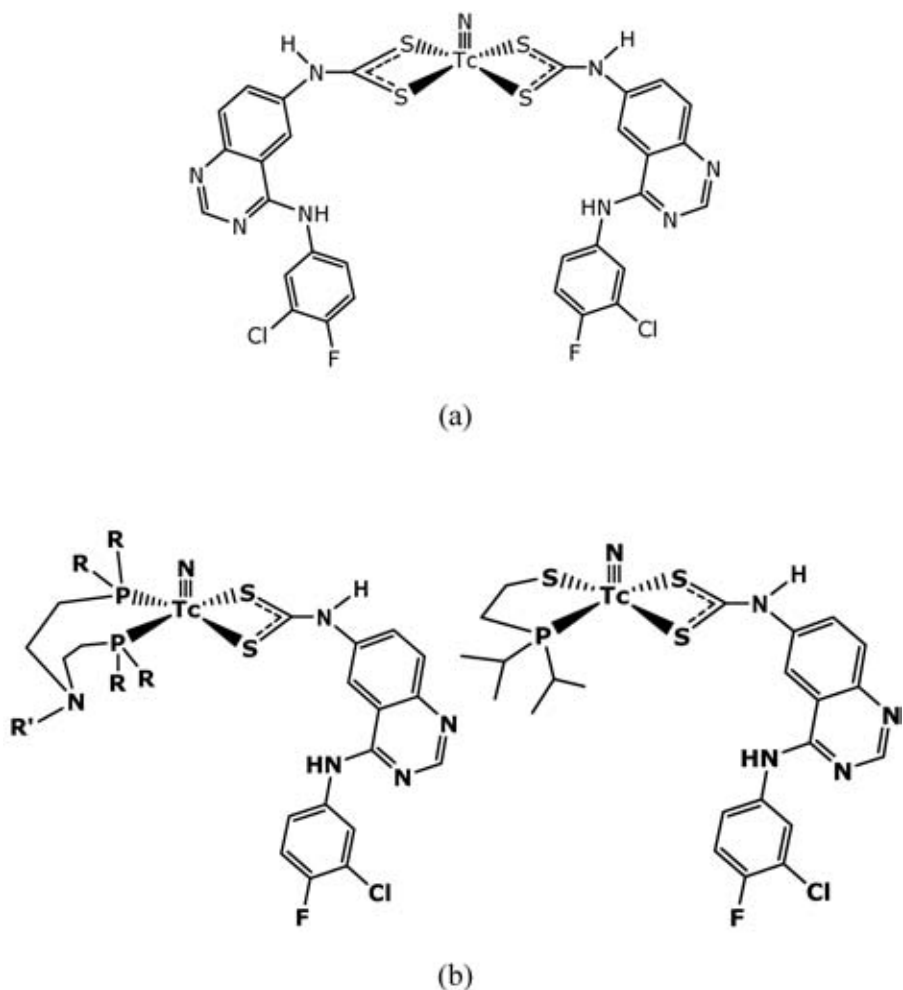


FIG. 15.15. (a) Symmetrical and (b) asymmetrical conjugate  $^{99m}\text{Tc}$ -nitrido complexes containing a dithiocarbamate-quinazoline ligand.

Biodistribution studies of these complexes were conducted in normal mice using a YAP-(S)PET small animal scanner. The most interesting result was obtained with the asymmetrical complex  $[\text{}^{99m}\text{Tc}(\text{N})(\text{PS})(\text{Qz-DTC})]$ , which was found to penetrate the intact blood–brain barrier, as clearly demonstrated by the significant brain accumulation observed at 1 h post-injection in the YAP-(S)PET image shown in Fig. 15.16.



FIG. 15.16. Image of a normal mouse obtained with a YAP-(S)PET small animal scanner after injection of the complex  $[^{99m}\text{Tc}(\text{N})(\text{PS})(\text{Qz-DTC})]$ .

## 15.4. EXPERIMENTAL PROCEDURES

In this section, general procedures for the preparation of symmetrical and asymmetrical nitrido  $^{99m}\text{Tc}$  complexes are reported.

### 15.4.1. Symmetrical complexes

#### 15.4.1.1. Bis(dithiocarbamate) nitrido $^{99m}\text{Tc}$ complexes

The general reaction scheme for the preparation of symmetrical nitrido  $^{99m}\text{Tc}$  complexes with dithiocarbamate ligands (DTC) is given in Fig. 15.17 [15.4]. The first step involves the reduction of  $[^{99m}\text{TcO}_4]^-$  by  $\text{SnCl}_2$  in the presence of succinic dihydrazide  $[\text{H}_2\text{N-NH-C(=O)}-(\text{CH}_2)_2-(\text{O=})\text{NH-NH}_2 = \text{SDH}]$ , as a source of nitrido nitrogen groups, to yield the  $\text{Tc}\equiv\text{N}$  bond. In the second step, the  $\text{Tc}\equiv\text{N}$  group is left to undergo a substitution reaction with a bidentate dithiocarbamate ligand to form the neutral symmetrical complex  $[^{99m}\text{Tc}(\text{N})(\text{DTC})_2]$ .

### 15.4.2. Asymmetrical complexes

#### 15.4.2.1. Mixed $[^{99m}\text{Tc}(\text{N})(\text{PNP})(\text{XY})]^{0/+}$ (PNP = amino-bis-phosphino ligand; XY = monoanionic or dianionic bidentate ligand) complexes

As found for symmetrical complexes, a two-step procedure has to be carried out to prepare asymmetrical nitrido  $^{99m}\text{Tc}$  complexes of general formula  $[^{99m}\text{Tc}(\text{N})(\text{PNP})(\text{XY})]^{0/+}$  (Fig. 15.18) [15.10, 15.11]. The first step is always the formation of the  $\text{Tc}\equiv\text{N}$  group through the action of SDH on  $[^{99m}\text{TcO}_4]^-$  in the presence of  $\text{SnCl}_2$ . Then, the preparation of the asymmetrical complex is simply accomplished by adding simultaneously the two bidentate

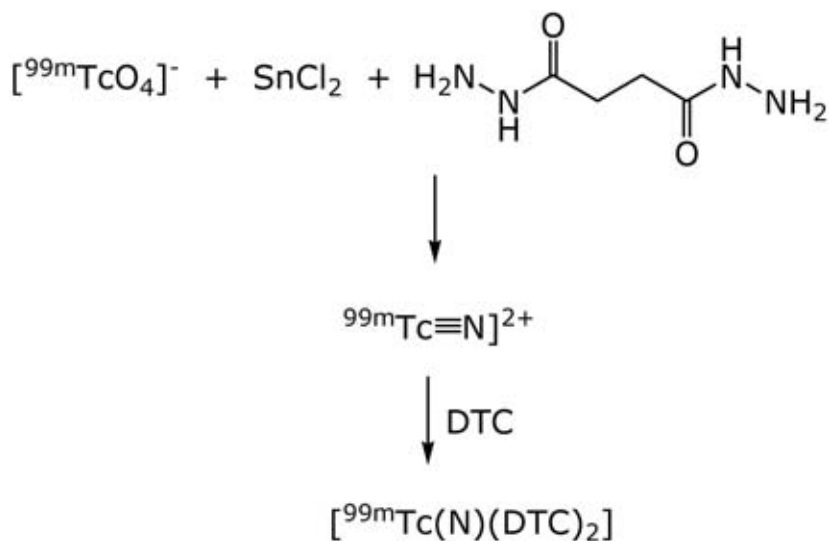


FIG. 15.17. Reaction diagram for the preparation of symmetrical bis(dithiocarbamate) nitrido  $^{99m}\text{Tc}$  complexes.

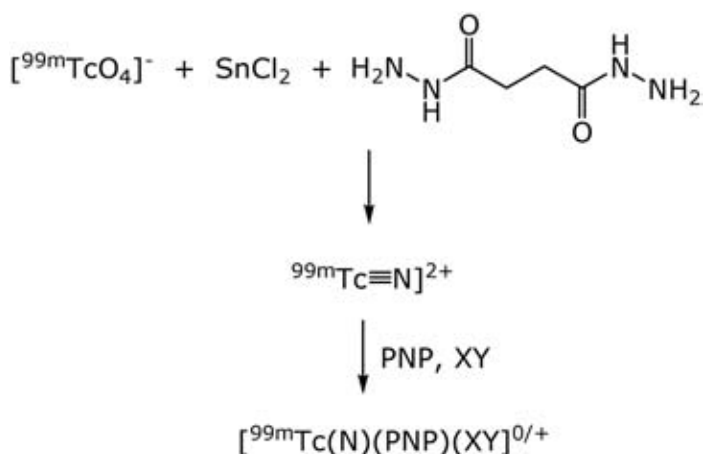


FIG. 15.18. Reaction diagram for the preparation of asymmetrical mixed  $[^{99m}\text{Tc}(\text{N})(\text{PNP})(\text{XY})]^{0/+}$  complexes.

ligands, PNP and XY, to the reaction vial. Radiochemical yields are usually in the range 90–98%, suggesting that the formation of asymmetrical compounds is more favoured than that of the corresponding symmetrical complexes as a consequence of the high electronic stability imparted to the final complex by the special distribution of two  $\pi$  acceptor and two  $\pi$  donor atoms around the  $[^{99m}\text{Tc}\equiv\text{N}]^{2+}$  core.

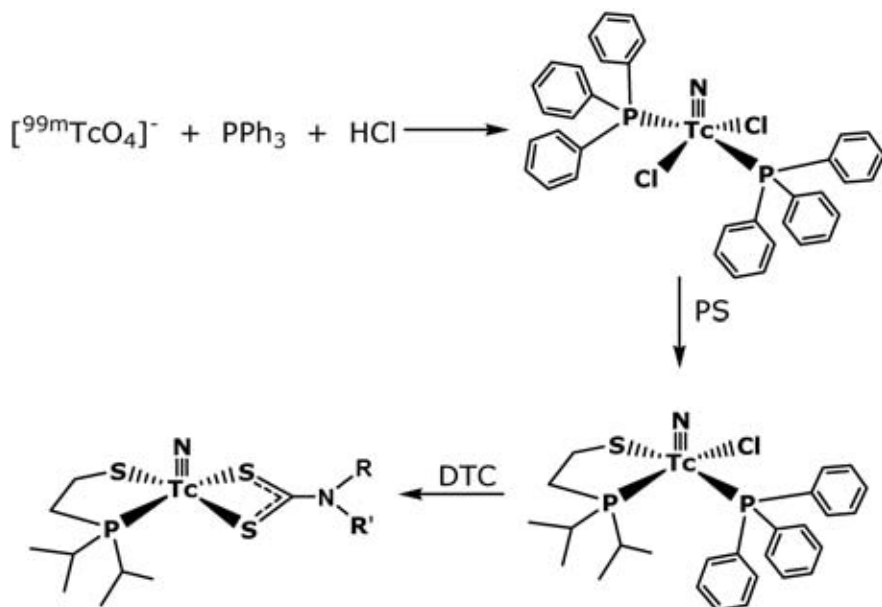


FIG. 15.19. Reaction diagram for the preparation of asymmetrical mixed  $[^{99m}\text{Tc}(\text{N})(\text{PS})(\text{DTC})]$  complexes.

15.4.2.2. Mixed  $[^{99m}\text{Tc}(\text{N})(\text{PS})(\text{DTC})]$  (PS = phosphino-thiol ligand;  
DTC = monoanionic dithiocarbamate ligand) complexes

A three-step procedure involving the formation of different intermediate species is required to obtain neutral mixed  $[^{99m}\text{Tc}(\text{N})(\text{PS})(\text{DTC})]$  complexes [15.14]. The first step is accomplished by reacting  $[^{99m}\text{TcO}_4]^-$  with triphenylphosphine under strong acidic conditions (HCl). This reaction leads to the formation of an intermediate complex that, presumably, corresponds to the mixed halogeno-phosphino complex  $[^{99m}\text{Tc}(\text{N})(\text{PPh}_3)_2\text{Cl}_2]$ . Then, this intermediate compound is mixed with the phosphino-thiol ligand (PS) in the same acidic reaction solution to afford a further reaction intermediate complex  $[^{99m}\text{Tc}(\text{N})(\text{PS})(\text{PPh}_3)\text{Cl}]$ . Finally, addition of a dithiocarbamate ligand to this latter intermediate causes its quantitative conversion to yield the bis substituted asymmetrical complex  $[^{99m}\text{Tc}(\text{N})(\text{PS})(\text{DTC})]$  through the removal of monodentate  $\text{PPh}_3$  and chloride groups (Fig. 15.19).

## REFERENCES

- [15.1] BOSCHI, A., DUATTI, A., UCCELLI, L., Development of technetium-99m and rhenium-188 radiopharmaceuticals containing a terminal metal-nitrido multiple bond for diagnosis and therapy, *Topics Curr. Chem.* **252** (2005) 85–101.
- [15.2] DUATTI, A., UCCELLI, L., Technetium complexes and radiopharmaceuticals containing the Tc≡N multiple bond, *Trends Inorg. Chem.* **4** (1996) 27–41.
- [15.3] PASQUALINI, R., et al., A new efficient method for the preparation of <sup>99m</sup>Tc-radiopharmaceuticals containing the Tc≡N multiple bond, *Appl. Radiat. Isot.* **43** (1992) 1329–1333.
- [15.4] PASQUALINI, R., et al., Bis(dithiocarbamate) nitrido technetium-99m radiopharmaceuticals: A class of neutral myocardial imaging agents, *J. Nucl. Med.* **35** (1994) 334–341.
- [15.5] GIGANTI, M., et al., Advances in radiopharmaceuticals for cardiac imaging: <sup>99m</sup>TcN-NOET, *Q. J. Nucl. Med.* **41** Suppl. (1997) 147–151.
- [15.6] BOLZATI, C., et al., Geometrically controlled selective formation of nitrido technetium(V) asymmetrical heterocomplexes with bidentate ligands, *J. Am. Chem. Soc.* **122** (2000) 4510–4511.
- [15.7] BOLZATI, C., et al., Chemistry of the strong electrophilic metal fragment [<sup>99</sup>Tc(N)(PXP)]<sup>2+</sup> (PXP = diphosphine ligand). A novel tool for the selective labelling of small molecules, *J. Am. Chem. Soc.* **124** (2002) 11468–11479.
- [15.8] REFOSCO, F., et al., Mixed-ligand Tc- and Re-nitrido complexes for radiolabelling bioactive molecules, *Recent Res. Dev. Inorganic Chem.* **2** (2000) 89–98.
- [15.9] BOSCHI, A., et al., Synthesis and biological evaluation of monocationic asymmetric <sup>99m</sup>Tc-nitride heterocomplexes showing high heart uptake and improved imaging properties, *J. Nucl. Med.* **44** (2003) 806–814.
- [15.10] BOLZATI, C., et al., Synthesis, solution-state and solid-state structural characterization of monocationic nitrido heterocomplexes [M(N)(PNP)(DTC)]<sup>+</sup> (M = <sup>99</sup>Tc, Re; DTC = dithiocarbamate; PNP = heterodiphosphane), *Eur. J. Inorg. Chem.* **9** (2004) 1902–1913.
- [15.11] BOSCHI, A., et al., A novel approach to the high-specific-activity labeling of small peptides with the technetium-99m fragment [<sup>99m</sup>Tc(N)(PXP)]<sup>2+</sup> (PXP = diphosphine ligand), *Bioconj. Chem.* **12** (2001) 1035–1042.
- [15.12] BOLZATI, C., et al., Synthesis of a novel class of trigonal bipyramidal nitrido Tc(V) complexes with phosphino-thiol ligands. Crystal structure of [<sup>99g</sup>Tc(N)(L1)<sub>2</sub>] [L1 = 2-(diphenylphosphino)-ethanethiolato] and [<sup>99g</sup>Tc(N)(L5)<sub>2</sub>] (L5 = 2-(ditolylphosphino)propanethiolato), *Inorg. Chem.* **38** (1999) 4473–4479.
- [15.13] BOLZATI, C., et al., Synthesis of a novel class of nitrido <sup>99m</sup>Tc radiopharmaceuticals with phosphino-thiol ligands showing transient heart uptake, *Nucl. Med. Biol.* **27** (2000) 369–374.
- [15.14] BOLZATI, C., et al., From symmetrical to asymmetrical nitrido phosphino-thiol complexes: A new class of neutral mixed-ligand <sup>99m</sup>Tc compounds as potential brain imaging agents, *Bioconj. Chem.* **17** (2006) 419–428.

## Chapter 16

### **LABELLING OF QUINAZOLINE AND RGD PEPTIDES WITH THE [<sup>99m</sup>Tc(CO)<sub>3</sub>]<sup>+</sup> CORE: SYNTHESIS, CHARACTERIZATION AND BIOLOGICAL EVALUATION**

I. SANTOS, C. FERNANDES, S. ALVES, J. GALAMBA, L. GANO  
Department of Chemistry, Institute of Nuclear Technology, Portugal

I. PIRMETTIS  
Institute of Radioisotopes and Radiodiagnostic Products,  
Demokritos National Centre of Scientific Research, Athens, Greece

C. DECRISTOFORO  
Universitätsklinik für Nuklearmedizin, Innsbruck, Austria

C.J. SMITH  
Department of Radiology, University of Missouri-Columbia,  
United States of America

R. ALBERTO  
Institute of Inorganic Chemistry, University of Zurich, Switzerland

#### **Abstract**

This coordinated research project envisaged small biomolecules with affinity for EGFR associated tyrosine kinase and small peptides containing the amino acid sequence RGD to target integrin receptors. We chose 6-amino-4-[(3-chloro-4-fluorophenyl)amino]quinazoline (1) and 6-amino-4-[(3-bromophenyl)amino] to be labelled. Compound (1) was synthesized and derivatized with different functional groups yielding the novel compounds N-[4-[(3-chloro-4-fluorophenyl)amino]quinazolin-6-yl]-chloro-propionylamide (2) and N-[4-[(3-chloro-4-fluorophenyl)amino]quinazolin-6-yl]-bromopropionylamide (3). These quinazoline derivatives were successfully coupled to isonitrile, dithiocarbamate and a novel pyrazolyl containing chelator ligands tailor made for Tc(III), [TcN]<sup>2+</sup> and [Tc(CO)<sub>3</sub>]<sup>+</sup>, respectively. We also synthesized a novel monoanionic pyrazolyl containing chelator (L<sup>1</sup>) which reacts quantitatively with *fac*-[M(OH<sub>2</sub>)<sub>3</sub>(CO)<sub>3</sub>]<sup>+</sup> yielding the complexes *fac*-[M(k<sup>3</sup>-L<sup>1</sup>)(CO)<sub>3</sub>] (M=Re (4), <sup>99m</sup>Tc (4a)). Compound 3 reacts with L<sup>1</sup> yielding the quinazoline-pyrazolyl conjugate L<sup>2</sup>. This bifunctional chelator reacts also quantitatively with Re(I)- and Tc(I)-tricarbonyls yielding the

well defined complexes  $fac-[M(k^3-L^2)(CO)_3]$  ( $M = Re$  (5),  $^{99m}Tc$  (5a)). The results of the biological studies are outlined. Relative to RGD peptides, we provided a neutral and tridentate pyrazolyl ligand (PZ1) for coupling to the lysine group of the peptide cyclo[Arg-Gly-Asp-D-Tyr-Lys]. The final conjugate cyclo[Arg-Gly-Asp-D-Tyr-Lys(PZ1)] reacted almost quantitatively ( $\geq 90\%$ ) with  $fac-[^{99m}Tc(CO)_3(H_2O)_3]^+$  yielding cyclo[Arg-Gly-Asp-D-Tyr-Lys( $k^3$ -PZ1) $^{99m}Tc(CO)_3$ ]. This complex is stable in vitro and in internalization studies, using  $\alpha_v\beta_3$  positive M21 and negative M21L cells, clearly indicated a relatively good and specific internalization in the  $\alpha_v\beta_3$  positive M21 cells (1% of total activity/mg protein). In vivo studies performed in healthy mice and in tumour xenografts have shown stability in vivo, fast blood clearance and elimination mainly through the kidneys. About 2.5% uptake in M21 receptor positive tumours and  $<1\%$  in receptor negative M21L tumours was found in tumour xenografts.

## 16.1. INTRODUCTION

The epidermal growth factor receptor (EGFR) is known to be overexpressed and/or dysregulated in several solid tumour types [16.1]. The EGFR's family consists of four distinct but closely related transmembrane receptors, which normally possess an extracellular ligand binding domain, a transmembrane region and an intracellular cytoplasmic domain with tyrosine kinase activity [16.1]. Several therapeutic agents have been developed for targeting EGFR, namely small molecules such as quinazoline derivatives that exhibit high affinity for the EGFR associated tyrosine kinase (EGFR-TK), competing with ATP (adenosine triphosphate) for binding to the intracellular tyrosine kinase region [16.1–16.3]. A bioprobe to help cancer diagnosis and predict the efficacy of a given class of EGFR-TK inhibitors is needed to optimize the therapeutic potential of EGFR inhibitors [16.2].

Peptides containing the amino acid sequence Arg-Gly-Asp (RGD) have also been used extensively to target integrin receptors upregulated on tumour cells and neovasculature. The RGD consensus sequence appears in several proteins of the extracellular matrix, including vitronectin, fibronectin, fibrinogen, von Willebrand factor, thrombospondin and osteopontin [16.4]. Integrin recognition of the canonical RGD sequence plays a prominent role in many cell–cell and cell–ECM interactions. Integrins are cell surface transmembrane glycoproteins that exist as  $\alpha\beta$  heterodimers. At least 24 different combinations of  $\alpha\beta$  heterodimers are known [16.5]. The integrins of most interest in cancer imaging and therapy contain the  $\alpha_v$  subunit, particularly the  $\alpha_v\beta_3$  and  $\alpha_v\beta_5$  subtypes. The  $\alpha_v\beta_3$  integrin is known to be overexpressed in many tumour types and expressed at lower levels in normal tissues [16.6]. Both  $\alpha_v\beta_3$  and  $\alpha_v\beta_5$  subtypes are expressed in neovasculature during angiogenesis [16.6]. These

expression patterns form the basis of attempts to image angiogenesis and tumour formation in vivo using RGD based peptide targeting vectors. RGD peptides used to target integrin receptors generally fall into one of three categories: linear, disulphide cyclized and head to tail cyclized.

Due to the widespread availability of single photon emission tomography (SPECT) facilities in comparison with positron emission tomography (PET) facilities, the worldwide availability of  $^{99}\text{Mo}/^{99\text{m}}\text{Tc}$  generators and the almost ideal properties of  $^{99\text{m}}\text{Tc}$  for SPECT imaging, there is great interest in  $^{99\text{m}}\text{Tc}$  specific probes for tumour imaging. Within this coordinated research project (CRP), Development of  $^{99\text{m}}\text{Tc}$  Based Small Biomolecules Using Novel  $^{99\text{m}}\text{Tc}$  Cores, quinazoline derivatives for EGFR-TK imaging as well as a cyclic peptide containing the RGD amino acid sequence were chosen to be studied as potential specific probes. The main goal was to develop such probes based on the new  $[\text{TcN}]^{2+}$ ,  $[\text{Tc}(\text{CO})_3]^+$  and  $\text{Tc}(\text{III})$  cores. The effect of these new technologies on the affinity, specificity and biological profile of those biomolecules would be explored and compared [16.7–16.9].

In this paper we present our efforts on synthesis, characterization and labelling with the *fac*- $[\text{Tc}(\text{CO})_3]^+$  moiety and on in vitro and in vivo evaluation of a quinazoline fragment and a cyclic RGD peptide.

## 16.2. RESULTS

### 16.2.1. Synthesis and characterization of quinazoline derivatives to be coupled to different chelators and synthesis of a novel chelator for tricarbonyl

The quinazoline derivatives shown in Fig. 16.1 (1–3) have been synthesized and characterized by  $^1\text{H}$  and  $^{13}\text{C}$  nuclear magnetic resonance (NMR) spectroscopy. The main structure of compounds 1–3 is similar, but they have different terminal groups (1:  $-\text{NH}_2$ , 2:  $\text{Cl}(\text{CH}_2)_2\text{CONH}-$ , 3:  $\text{Br}(\text{CH}_2)_2\text{CONH}-$ ) to further react with the different chelators considered in this CRP for stabilization of the new  $[\text{TcN}]^{2+}$ ,  $\text{Tc}(\text{III})$  and *fac*- $[\text{Tc}(\text{CO})_3]^+$  cores. Of these compounds, compound 1 has been successfully used for coupling the quinazoline to a isonitrile and to dithiocarbamate chelators used for the  $\text{Tc}(\text{III})$  and  $[\text{TcN}]^{2+}$  cores, respectively. Compounds 2 and 3 were synthesized to be conjugated to a tridentate chelator tailor made for the *fac*- $[\text{Tc}(\text{CO})_3]^+$  core.

The novel chelator designed, synthesized and fully characterized for the *fac*- $[\text{Tc}(\text{CO})_3]^+$  core is monoanionic and has an NNO donor atom set (Fig. 16.2).

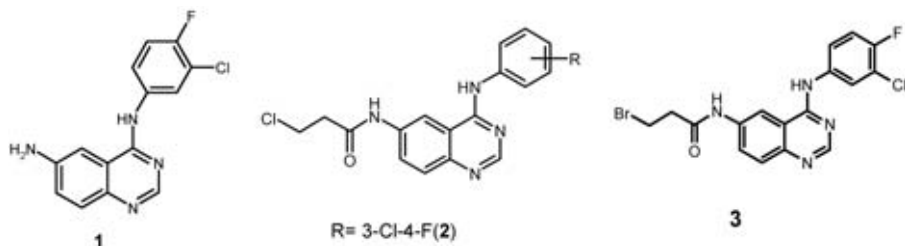


FIG. 16.1. Different quinazoline derivatives to be coupled to tailor made ligandos for Tc(III),  $[TcN]^{2+}$  and  $fac-[Tc(CO)_3]^+$  cores.

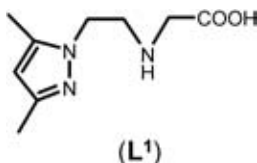


FIG. 16.2. Pyrazolyl-containing chelator with an NNO donor atom set.

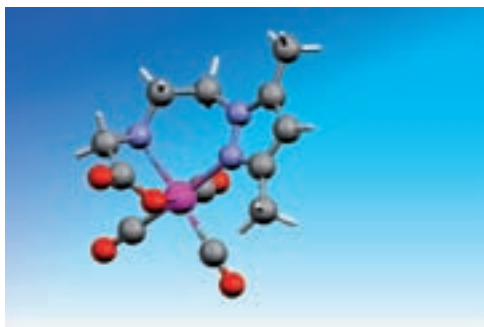


FIG. 16.3. X ray structure of  $fac-[Re(CO)_3(k^3-L^1)]$  (4).

### 16.2.2. Evaluation of L<sup>1</sup> as a new ligand for the $[^{99m}Tc(CO)_3]^+$ core

The suitability of L<sup>1</sup> for the  $fac-[M(CO)_3]^+$  (M = Re,  $^{99m}Tc$ ) moiety was evaluated, and we found that L<sup>1</sup> reacts quite fast with  $fac-[Re(CO)_3(H_2O)_3]^+$  in water, yielding the complex  $fac-[Re(CO)_3(k^3-L^1)]$  (4) with almost quantitative yield (80%). The tridentate coordination mode of L<sup>1</sup> in complex 4 was confirmed in the solid state and in solution by X ray diffraction analysis and <sup>1</sup>H and <sup>13</sup>C NMR spectroscopy, respectively. Figure 16.3 shows the X ray structure of  $fac-[Re(CO)_3(k^3-L^1)]$  (4) and Fig. 16.4 shows the high performance liquid

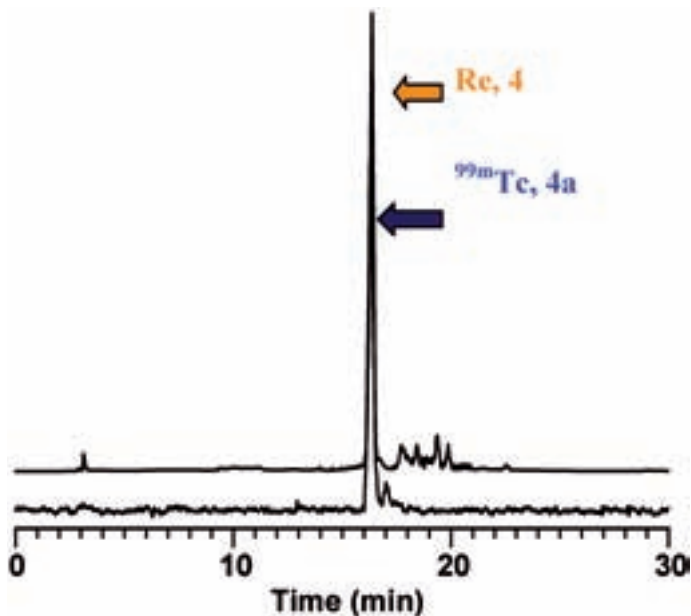


FIG. 16.4. Reverse phase HPLC chromatograms of *fac*-[Re(CO)<sub>3</sub>(k<sup>3</sup>-L<sup>1</sup>)] (4) (*R<sub>t</sub>* = 15.9 min) and *fac*-[<sup>99m</sup>Tc(CO)<sub>3</sub>(k<sup>3</sup>-L<sup>1</sup>)] (4a) (*R<sub>t</sub>* = 16.03 min).

chromatography (HPLC) chromatograms for the pair *fac*-[M(CO)<sub>3</sub>(k<sup>3</sup>-L<sup>1</sup>)] (M = Re (4), <sup>99m</sup>Tc (4a)) [16.10, 16.11].

Complex 4a is obtained with a quantitative yield (>95%) using a low concentration of ligand (<10<sup>-5</sup>M), and is stable in cysteine, histidine and human serum, presenting also a low protein binding (<8%, 15 min–4 h incubation time at 37°C).

### 16.2.3. Conjugation of a quinazoline fragment to L<sup>1</sup> and labelling of the conjugate with the [<sup>99m</sup>Tc(CO)<sub>3</sub>]<sup>+</sup> core

The conjugation of the quinazoline fragment was performed by alkylation of the secondary amine of L<sup>1</sup>; this was only possible using the compound N-[4-[(3-chloro-4-fluorophenyl)amino]quinazolin-6-yl]bromopropionylamide (3). The final conjugate (L<sup>2</sup>) was obtained in a pure form, as indicated by the NMR data (Fig. 16.5).

Further reaction of L<sup>2</sup> with *fac*-[M(CO)<sub>3</sub>(H<sub>2</sub>O)<sub>3</sub>]<sup>+</sup> (M = Re, <sup>99m</sup>Tc) yielded the corresponding *fac*-[M(CO)<sub>3</sub>(k<sup>3</sup>-L<sup>2</sup>)] complexes (M = Re (5), <sup>99m</sup>Tc (5a)). Compound 5a is very stable in serum and also in cysteine and histidine. The in vivo stability of 5a has also been assessed.

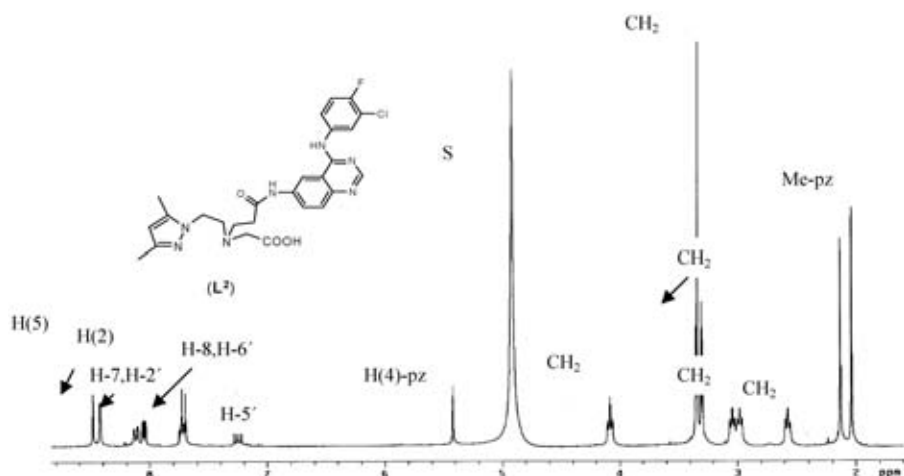


FIG. 16.5.  $^1\text{H}$  NMR spectrum of  $L^2$  and corresponding assignments.

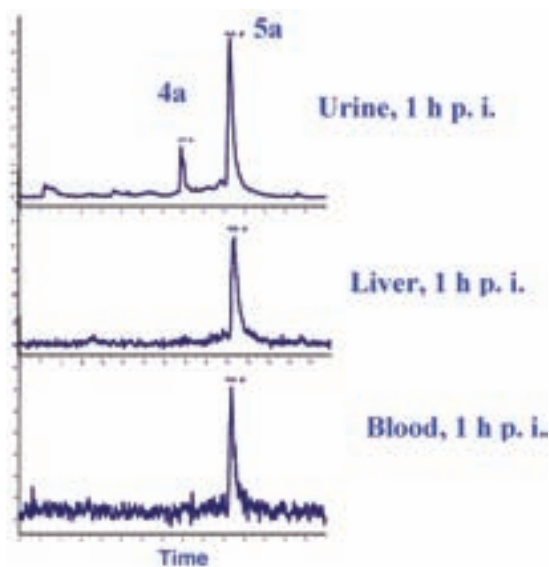


FIG. 16.6. Stability *in vivo* of complex 5a.

As can be seen in Fig. 16.6, complex 5a is the only radiochemical species found in blood and in liver 1 h post-injection. In urine (1 h post-injection) there is a significant amount of 5a (retention time ( $R_t$ ) = 20.5 min), but there is also a small amount of a more hydrophilic metabolite that we have identified as

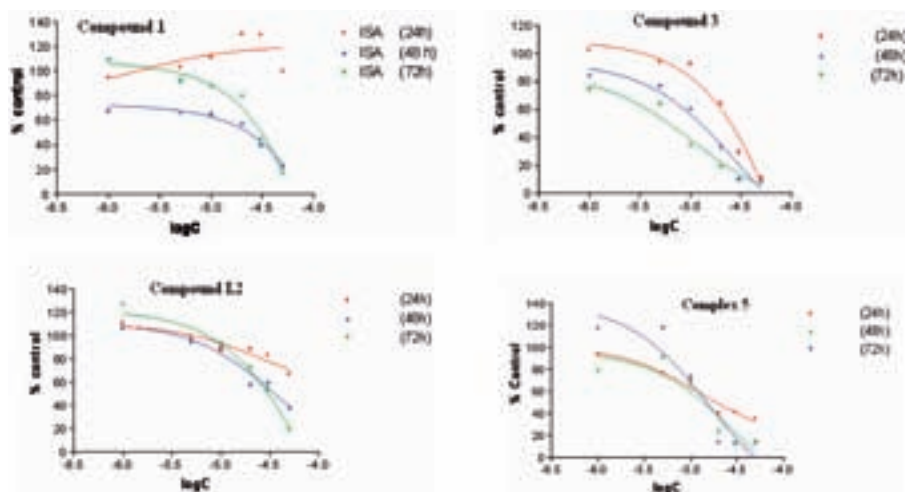


FIG. 16.7. A431 cell growth inhibition promoted by compounds 1, 3,  $L^2$  and complex 5.

complex 4a ( $R_t = 15.9$  min). The regeneration of 4a is certainly due to the hydrolysis of 5a at the secondary amine.

#### 16.2.4. Cell growth and EGFR-TK inhibition

Quinazoline is a relatively small biomolecule, so the conjugation to a metal fragment must be done without affecting its affinity for the EGFR associated tyrosine kinase (EGFR-TK) and the labelled quinazoline still must compete with ATP (adenosine triphosphate) for binding to the intracellular tyrosine kinase region. To evaluate if the labelling of the quinazoline would affect these properties, cell growth inhibition and phosphorylation studies were performed using A431 cells and the different quinazoline compounds synthesized and characterized during this work (i.e. compounds 1, 3,  $L^2$  and complex 5). These studies allowed an evaluation of the effect of introducing in the quinazoline backbone different functional groups, including a metal fragment. For each compound, cell growth inhibition was calculated after 24, 48 and 72 h of incubation, and four replicates were run for each experimental condition. The averages of four experiments at different times for the studied compounds are shown in Fig. 16.7.

Based on these experimental data,  $IC_{50}$  values were calculated for all the compounds 24, 48 and 72 h after incubation. Just for comparison we must refer the values found after 72 h incubation for the most important compounds, namely for N-[4-[(3-chloro-4-fluorophenyl)amino]quinazolin-6-yl]bromopropionylamide (3) ( $IC_{50} = 3.5\mu M$ ), for  $L^2$  ( $IC_{50} = 19.4\mu M$ ) and for complex 5

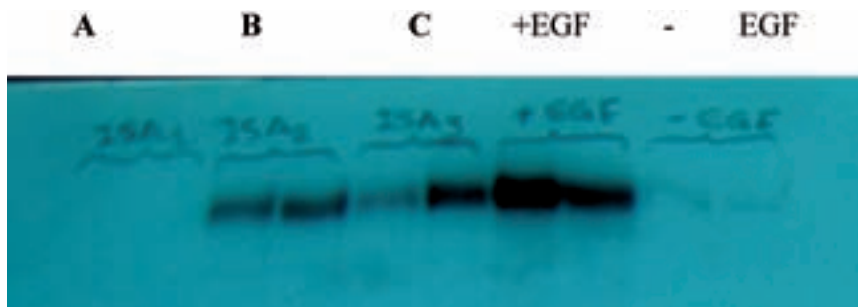


FIG. 16.8. Phosphorilation inhibition of compounds 3 (A),  $L^2$  (B) and complex 5 (C). Controls were run in the same experimental conditions with EGF (+) and without EGF (-).

( $IC_{50} = 6.0\mu M$ ). The  $IC_{50}$  values found are comparable and, apparently, the coordination of the metal fragment  $fac-[M(CO)_3]^+$  to the quinazoline did not affect significantly the inhibition of cell growth. The phosphorilation inhibition was calculated also using A431 cells. These cells were incubated for 24 h in the presence of fresh medium without foetal bovine serum. The day after, cells were incubated in the presence of the different compounds (final concentration,  $1\mu M$ ) for 2 h, after which EGF was added ( $20\text{ ng/mL}$ ) for 5 min. The medium was then removed, the cells were washed with PBS and cell lysis buffer ( $50\text{mM Tris-HCl}$ ,  $pH7.4$ ,  $150\text{mM NaCl}$ ,  $1\%$  Triton X-100,  $1\text{mM PMSF}$ ,  $50\text{ }\mu\text{g/mL}$  aprotonin,  $2\text{mM}$  sodium orthovanadate,  $50\text{ }\mu\text{g/mL}$  leupeptine and  $5\text{mM EDTA}$ ) was added. Controls consisted of wells without drugs and with or without EGF. The total amount of protein was estimated by a BCA assay in ELISA plates, using a BSA standard curve. A volume of lysis mixture, corresponding to  $30\text{ mg}$  of total protein, was loaded on to polyacrilamide gel ( $8\%$ ); proteins were separated by electrophoresis and transferred to PVDF membrane. For visualization of molecular weight bands, the membrane was immersed in Ponceau reagent ( $0.5\%$  Ponceau in  $1\%$  acetic acid) for 5 min. The membrane was washed in  $H_2O$ , blocked overnight in TTN with  $5\%$  milk ( $1\%$  fat) and incubated for 2 h in antiphosphotyrosine antibody diluted  $1/2000$  (PY20, Santa Cruz Biotechnology). Then, the membrane was washed three times in TTN and incubated in a horseradish peroxidase conjugated secondary antimouse antibody diluted  $1/3000$  (Sigma) for 2 h and finally washed three times in TTN. Detection was performed using a chemiluminescent detection system in accordance with the manufacturer's instructions (ECL kit, Amersham) (Fig. 16.8). Based on these data and assuming the controls, we can say that all the compounds inhibit phosphorilation to a certain extend. A better quantification of this effect is under way.





FIG. 16.10. HPLC chromatograms for cyclo[Arg-Gly-Asp-D-Tyr-Lys(PZ1)] ( $R_t = 8.8$  min) (A) (UV-vis detection) and for cyclo[Arg-Gly-Asp-D-Tyr-Lys( $k^3$ -PZ1) $^{99m}\text{Tc}(\text{CO})_3$ ] ( $R_t = 14.2$  min) (B) (gamma detection).

cells. The internalized activity reached 0.88% in M21 versus 0.37% in blocked cells.

### 16.2.7. Biodistribution in healthy and in nu/nu mice

The biodistribution of cyclo[Arg-Gly-Asp-D-Tyr-Lys( $k^3$ -PZ1) $^{99m}\text{Tc}(\text{CO})_3$ ] was studied in healthy CF-1 mice (Table 16.1). The biological profile in normal CF-1 mice has shown that the labelled peptide [ $^{99m}\text{Tc}(\text{CO})_3$ -cyclo[Arg-Gly-Asp-D-Tyr-Lys(PZ1)]] presents a fast blood clearance and a fast overall total excretion (70% of injected dose (ID) excreted at 4 h post-injection), being excreted mainly via the renal-urinary pathway. Some residualization in normal kidney is evident for the cyclo[Arg-Gly-Asp-D-Tyr-Lys( $k^3$ -PZ1) $^{99m}\text{Tc}(\text{CO})_3$ ] conjugate (~4% ID/g, 1 h post-injection), but this radioactivity washes out significantly over time. To demonstrate the effective stability of the new conjugate, urine, serum and liver were analysed at 1 h post-injection. The samples were homogenized and reinjected on to the HPLC to verify product stability. The conjugate showed remarkable *in vivo* stability, as  $\geq 98\%$  of the conjugates were in the form cyclo[Arg-Gly-Asp-D-Tyr-Lys( $k^3$ -PZ1) $^{99m}\text{Tc}(\text{CO})_3$ ].

Tumour uptake studies were performed in nu/nu mice (Charles River). For the induction of tumour xenografts, M21 and M21L cells were subcutaneously injected at a concentration of  $5 \times 10^6$  cells/mouse and allowed to grow until tumours of 0.3–0.6 mL were visible. On the day of experiment, six mice

TABLE 16.1. BIODISTRIBUTION IN NORMAL MICE (% ID/g)

	1 h	4 h
Blood	1.4 ± 0.2	0.74 ± 0.04
Lung	0.7 ± 0.2	0.9 ± 0.2
Heart	0.22 ± 0.02	0.40 ± 0.04
Stomach	0.28 ± 0.08	1.4 ± 0.1
Spleen	0.41 ± 0.05	1.5 ± 0.5
Liver	4.7 ± 0.5	4.6 ± 0.1
Pancreas	0.16 ± 0.01	0.31 ± 0.03
Kidneys	4.1 ± 0.5	2.8 ± 0.5
Muscle	0.13 ± 0.02	0.31 ± 0.05
Intestine	2.2 ± 0.3	5.5 ± 1.3
Femur	2.73 ± 2.91	0.58 ± 0.13
Carcass	12.6 ± 2.6	10.9 ± 1.9
Excretion	69.0 ± 3.5	70.1 ± 4.1

with M21 and three with M21L tumour were injected with cyclo[Arg-Gly-Asp-D-Tyr-Lys( $k^3$ -PZ1) $^{99m}\text{Tc}(\text{CO})_3$ ] (1 MBq/mouse, corresponding to 1  $\mu\text{g}$  peptide) intravenously into the tail vein. They were sacrificed by cervical dislocation 1 h (M21 and M21L) as well as 4 h post-injection (M21). Tumours and other tissues (blood, lung, heart, stomach, spleen, liver, pancreas, kidneys, muscle, intestine) were removed. The amount of radioactivity was determined with a gamma counter. The results were expressed as a percentage of injected dose per gram of tissue (% ID/g) (Table 16.2).

### 16.3. SUMMARY AND CONCLUSIONS

During the CRP we synthesized and characterized different quinazoline derivatives suitable for conjugation to tailor made chelators for the  $[\text{TcN}]^{2+}$ , Tc(III) and  $\text{fac}-[\text{Tc}(\text{CO})_3]^+$  cores. We also synthesized and characterized a novel monoanionic chelator with the donor atom set NNO, which reacts quantitatively with Re(I)- and Tc(I)-tricarbonyl, yielding the neutral complexes  $\text{fac}-[\text{M}(\text{CO})_3(k^3\text{-L}^1)]$  (M = Re, Tc). A quinazoline fragment was conjugated to  $\text{L}^1$  through the secondary amine and conjugate  $\text{L}^2$  reacted with  $\text{fac}-[^{99m}\text{Tc}(\text{CO})_3]^+$  yielding  $\text{fac}-[\text{M}(\text{CO})_3(k^3\text{-L}^2)]$  (M = Re (5),  $^{99m}\text{Tc}$ (5a)).

TABLE 16.2. BIODISTRIBUTION IN M21 AND M21L TUMOUR XENOGRAFTS (% ID/g)

	M21 1 h	M21 4 h	M21L 1 h
Blood	0.96 ± 0.06	0.49 ± 0.11	0.91 ± 0.06
Lung	2.19 ± 0.16	1.07 ± 0.15	2.34 ± 0.39
Heart	0.97 ± 0.12	0.51 ± 0.09	0.89 ± 0.09
Stomach	2.12 ± 1.15	1.05 ± 0.01	1.64 ± 0.58
Spleen	2.08 ± 0.27	1.22 ± 0.14	2.29 ± 0.33
Liver	8.89 ± 0.71	4.58 ± 0.46	10.54 ± 1.32
Pancreas	0.81 ± 0.35	0.34 ± 0.04	0.58 ± 0.02
Kidneys	5.65 ± 0.88	3.12 ± 0.22	5.24 ± 0.42
Muscle	1.04 ± 0.68	0.32 ± 0.08	0.76 ± 0.45
Intestine	10.09 ± 1.30	4.59 ± 0.35	10.15 ± 1.57
Femur	2.73 ± 2.91	0.58 ± 0.13	1.44 ± 0.99
Tumour	2.50 ± 0.29	1.62 ± 0.44	0.71 ± 0.08

Complex 5a is stable in vitro and in vivo and inhibits A431 cell growth significantly, as well as phosphorylation. The in vivo evaluation of 5a as a bioprobe for EGFR-TK is under way.

A pyrazolyl-containing ligand, tridentate and neutral, has been successfully coupled to a cyclo[Arg-Gly-Asp-D-Tyr-Lys] and the metallation of this conjugate with Tc(I)-tricarbonyl quantitatively achieved, yielding complex cyclo[Arg-Gly-Asp-D-Tyr-Lys( $k^3$ -PZ1) $^{99m}$ Tc(CO) $_3$ ]. This compound internalizes specifically in  $\alpha_v\beta_3$  positive M21 cells. This in vitro specific interaction was also confirmed in animal studies, which showed a reasonable tumour uptake 1 h ( $2.50 \pm 0.29\%$  ID/g) and 4 h ( $1.62 \pm 0.44\%$  ID/g) post-injection in M21 tumour xenografts and significantly lower tumour uptake in M21L tumour xenografts 1 h post-injection ( $0.71 \pm 0.08\%$  ID/g). Some modifications can certainly be performed in the RGD sequence and/or in the chelator substituents to improve the tumour uptake and pharmacokinetics.

## REFERENCES

- [16.1] LASKIN, J.J., SANDLER, A.B., Epidermal growth factor receptor: A promising target in solid tumours, *Cancer Treat. Rev.* **30** (2004) 1.

## CHAPTER 16

- [16.2] ARTEAGA, C., Targeting HER1/EGFR: A molecular approach to cancer therapy, *Semin. Oncol.* **30** 7 (2003) 3.
- [16.3] RITTER, C.A., ARTEAGA, A., The epidermal growth factor receptor-tyrosine kinase: A promising therapeutic target in solid tumors, *Semin. Oncol.* **30** 1 (2003) 3.
- [16.4] HEALY, J.M., et al., Peptide ligands for integrin  $\alpha_v\beta_3$  selected from random phage display libraries, *Biochemistry* **34** (1995) 3948.
- [16.5] REINMUTH, N., et al.,  $\alpha_v\beta_3$  integrin antagonist S247 decreases colon cancer metastasis and angiogenesis and improves survival in mice, *Cancer Res.* **63** (2003) 2079.
- [16.6] KERR, J.S., SLEE, A.M., MOUSA, S.A., Small molecule  $\alpha_v$  integrin antagonists: Novel anticancer agents, *Exp. Opin. Invest. Drugs* **9** (2000) 1271.
- [16.7] ALBERTO, R., et al., A simple single-step synthesis of  $[^{99}\text{Tc}_3\text{H}_3(\text{CO})_{12}]$  from  $[^{99}\text{TcO}_4]^-$  and its X-ray crystal structure. Application to the production of no-carrier added  $[^{188}\text{Re}_3\text{H}_3(\text{CO})_{12}]$ , *Chem. Commun.* **11** (1996) 1291.
- [16.8] PIETZSCH, H.-J., GUPTA, A., SYHRE, R., LEIBNITZ, P., SPIES, H., Mixed-ligand technetium(III) complexes with tetradendate/monodendate  $\text{NS}_3$ /isocyanide coordination: A new nonpolar technetium chelate system for the design of neutral and lipophilic complexes stable in vivo, *Bioconj. Chem.* **12** (2001) 538.
- [16.9] BOSCHI, A., DUATTI, A., UCCELLI, L., Development of technetium-99m and rhenium-188 radiopharmaceuticals containing a terminal metal-nitrido multiple bond for diagnosis and therapy, *Top. Curr. Chem.* **252** (2005) 85.
- [16.10] ALVES, S., PAULO, A., CORREIA, J.D.G., DOMINGOS, A., SANTOS, I., Coordination capabilities of pyrazolyl containing ligands towards the *fac*- $[\text{Re}(\text{CO})_3]^+$  moiety, *J. Chem. Soc. Dalton Trans.* **24** (2002) 4714.
- [16.11] SANTOS, I., PAULO, A., CORREIA, J.D.G., Rhenium and technetium complexes anchored by phosphines and scorpionates for radiopharmaceutical applications, *Top. Curr. Chem.* **252** (2005) 45.



## Chapter 17

### LIGANDS OF LOW DENTICITY AS COORDINATION UNITS FOR TETHERING THE $^{99m}\text{Tc}$ -CARBONYL CORE TO BIOMOLECULES

N.I. GORSHKOV, E.M. LEVITSKAYA, A.A. LUMPOV,  
A.E. MIROSLAVOV, G.V. SIDORENKO, D.N. SUGLOBOV  
Khlopin Radium Institute Research and Production Association,  
St. Petersburg, Russian Federation

#### Abstract

The possibility of attaching the  $^{99m}\text{Tc}$ -carbonyl core to biomolecules via ligands of low denticity is examined. Two alternative approaches are considered: the 2 + 1 approach involving a combination of a bidentate ligand with a monodentate ligand and an approach involving the use of higher technetium carbonyls in combination with a bidentate or monodentate ligand. A device and a procedure for preparing higher technetium carbonyls on the non-carrier added level at elevated pressure are developed. Dithiocarbamates and bidentate nitrogen bases are tested as bidentate ligands, and isonitriles, phosphines and imidazole derivatives as monodentate ligands. The stability of complexes in aqueous solutions in the presence of typical bioligands is evaluated. Biodistribution data for certain complexes are obtained.

#### 17.1. INTRODUCTION

In studies aimed at the development of new  $^{99m}\text{Tc}$  radiopharmaceuticals, much attention is given today to the Tc-tricarbonyl core. Its attractive features are low charge of the central atom, Tc(I), high stability in biological media and a smaller number of free coordination sites compared with other technetium species. Tethering of this core to biomolecules involves solution of two problems: construction of the required ligating fragment and linking of this fragment to a biomolecule.

The requirements of the ligating fragment are quite clear. It should provide coordination saturation of technetium (to prevent its interaction with coordination active species in a biological medium) and form a single complex species. Moreover, its concentration ensuring complete binding of  $^{99m}\text{Tc}$  should be as low as possible (the desirable level is about  $10^{-4}\text{M}$ ). Finally, the complex

should be stable in a biological medium and resistant to exchange with biological ligands (e.g. histidine). These requirements are met by various tridentate ligands fitting the facial geometry of the Tc-tricarbonyl core, for example iminodiacetate and triamines.

However, tridentate ligands have some disadvantages as far as the second problem is concerned. First, biomolecules are usually polyfunctional and chemically reactive, and tethering of the chelating unit, also polyfunctional and reactive, involves fine organic synthesis (in particular, protection–deprotection operations), and selective binding is difficult and not always feasible. Second, polar fragments of the chelating units will inevitably affect the native behaviour of a biomolecule by forming additional hydrogen bonds or entering into strong dipole–dipole interactions with fragments of the biomolecule and with the environment.

Therefore, it seems appropriate to examine another possibility provided by the use of simpler bidentate and monodentate ligating groups. In this case, two alternative approaches are possible: using a combination of bidentate and monodentate ligands (the 2 + 1 approach) or using higher Tc-carbonyls with two (for Tc(CO)<sub>4</sub> core) or one (for Tc(CO)<sub>5</sub> core) vacancies to be filled by the ligand. Both these approaches were tested in this study.

## 17.2. EXPERIMENTAL

Technetium-99m was taken in the form of <sup>99m</sup>TcO<sub>4</sub><sup>-</sup> from an extraction (Radium Institute) or adsorption (experiments performed at the Paul Scherrer Institute and Manchester Royal Infirmary) generator in the form of solution in normal saline. Procedures for preparing technetium complexes are described in the text. The infrared (IR) spectra were recorded on a Shimadzu FTIR 8700 spectrometer (Nujol mulls or solutions in appropriate solvents; KBr windows; CaF<sub>2</sub> windows for aqueous and methanolic solutions). The <sup>99</sup>Tc nuclear magnetic resonance (NMR) spectra were recorded on a Bruker CXP-300 or Bruker AM-500 spectrometer.

The high performance liquid chromatography (HPLC) analysis was performed on Separon SG C18 columns, 5 mm, gradient 0.05M triethylammonium phosphate, pH2.25 (A) acetonitrile or methanol (B). With acetonitrile: 0–5 min, 100% A; 5–6 min, from 0 to 25% B; 6–9 min, from 25 to 34% B; 9–20 min, from 34 to 100% B; 20–30 min, 100% B; 30–31 min, from 100% B to 100% A; 31–35 min, 100% A. With methanol: 0–3 min, 100% A; 3–9 min, 25% B; 9–20 min, from 34 to 10% B; 20–22 min, 100% B; then 100% A. The flow rate was 1 mL/min.

The biodistribution experiments were performed on rabbits (injection into the auricular vein, followed by planar scintigraphic examination at 1 s intervals, carried out at the Department of Nuclear Medicine, Central Research Institute of Roentgenology and Radiology, St. Petersburg) and on white rats (injection into the tail vein, sacrifice after 15 min or 1 h, removal and analysis of organs and tissues carried out at the Department of Nuclear Medicine, Manchester Royal Infirmary, Manchester, and Department of Imaging Science, University of Manchester).

### 17.3. 2 + 1 LIGAND SYSTEMS FOR BINDING Tc-TRICARBONYL CORE

Bidentate and monodentate ligands usually form considerably less stable complexes than do tridentate ligands with similar donor fragments. Therefore, only ligands showing very high affinity for technetium should be chosen. Since Tc(I) is a typical soft Lewis acid, soft ligands (in particular, ligands with  $\pi$  acceptor properties) are preferable. The second problem arising in going to 2 + 1 ligand systems is ensuring selective formation of a single complex species when both ligands are in a large excess (even when in low concentrations) relative to  $^{99m}\text{Tc}$  on the non-carrier added level and can, in principle, form other species, for example  $\text{Tc}(\text{CO})_3(\text{monodentate ligand})_3$ .

#### 17.3.1. Complexation with bidentate ligands

We first examined the complexation of  $\text{Tc}(\text{CO})_3$  in aqueous solution with typical anionic bidentate ligands such as dithiocarbamate, xanthate and acetylacetonate. All these ligands contained a carboxymethyl substituent acting as a model of a fatty acid (a typical group of biomolecules) and as a possible functional unit for further derivatization. Experiments were performed both with macroamounts of  $^{99}\text{Tc}$  and with carrier free  $^{99m}\text{Tc}$ . The following results were obtained (for details, see Ref. [17.1]). Acetylacetone and especially its functionalized derivative bind non-carrier added  $^{99m}\text{Tc}(\text{CO})_3$  incompletely, even when added in high concentrations (about  $10^{-1}\text{M}$ ). The xanthate ligand forms a more stable complex and provides complete binding of  $^{99m}\text{Tc}$  at a concentration of  $10^{-3}\text{M}$ .

Better results were obtained with dithiocarbamate (complete binding of  $^{99m}\text{Tc}$  at a ligand concentration of  $10^{-4}\text{M}$ ; approximately 30% content of the initial tricarbonyltriaqua complex at a ligand concentration of  $10^{-5}\text{M}$ ). At the same time, complexation with the second dithiocarbamate ligand (apparently in the monodentate fashion) becomes noticeable only at high concentrations of

the ligand ( $10^{-1}\text{M}$  and more), much exceeding the level admissible for biological studies. This fact favours formation of single complex species in  $2 + 1$  systems with dithiocarbamates and monodentate ligands.

Dithiocarbamate (DTC) is not displaced from the technetium coordination sphere by such a strong biological ligand as histidine (His). Histidine, when added to the system, displaces water from the complex  $\text{Tc}(\text{CO})_3(\text{DTC})(\text{H}_2\text{O})$  and coordinates via imidazole nitrogen atoms (as judged from the  $^{99}\text{Tc}$  NMR spectrum).  $^{99}\text{Tc}$  NMR,  $\delta$ , ppm:  $\text{Tc}(\text{CO})_3(\text{H}_2\text{O})_3^+$   $-868$ ,  $\text{Tc}(\text{CO})_3(\text{DTC})(\text{H}_2\text{O})$   $-1155$ ,  $\text{Tc}(\text{CO})_3(\text{DTC})(\text{His})$   $-1322$ ; cf.  $\text{Tc}(\text{CO})_3(\text{His})$   $-1102$ ,  $\text{Tc}(\text{CO})_3(\text{DTC})(\text{imidazole})$   $-1322$  [17.1].

We also examined on the non-carrier added level the complexation of  $^{99\text{m}}\text{Tc}(\text{CO})_3$  with bidentate nitrogen bases: 4-(2-aminoethyl)imidazole ( $B_1$ ), 2-(aminomethyl)pyridine ( $B_2$ ), 2,2'-bipyridine ( $B_3$ ) and its 4,4'-dimethoxy derivative ( $B_4$ ), and 1,10-phenanthroline ( $B_5$ ). The complexation with a fully aliphatic diamine, ethylenediamine, was weak. Phenanthroline seems particularly attractive in the context of the  $2 + 1$  approach, not only because of strong complexation with technetium, but also because of the rigid structure allowing the bidentate coordination mode only. The latter factor is important from the viewpoint of formation of a single complex species in  $2 + 1$  systems. Phenanthroline and bipyridine ligands ( $B_3$ – $B_5$ ) formed more stable complexes than the diamines, with one aromatic and one aliphatic N atom ( $B_1$ ,  $B_2$ ). However, at ligand concentrations of  $10^{-3}\text{M}$ , the complexation was incomplete, and the HPLC patterns showed the presence of significant (10% and more) amounts of the tricarbonyltriaqua ion.

### 17.3.2. $2 + 1$ systems with dithiocarbamates

As monodentate ligands to be used in combination with dithiocarbamate, we tested mercaptans and their derivatives (butyl mercaptan, its anion, 2-carboxyethyl mercaptan anion and methyl thioether), amines (butylamine, diethylamine), imidazole, phosphine [tris(carboxymethyl)phosphine] and *tert*-butyl isocyanide. All the ligands, as well as the dithiocarbamate, were taken in a concentration of  $10^{-4}\text{M}$  in the experiments with  $^{99\text{m}}\text{Tc}$ . In the experiments at the macro level, the components were taken in a stoichiometric ratio.

A  $^{99}\text{Tc}$  NMR study reliably confirmed the formation of  $2 + 1$  complexes in the systems with mercaptan derivatives, imidazole, phosphine and isonitrile. In the systems with aliphatic amines, no unambiguous conclusion can be made, because the signal position changed insignificantly relative to  $\text{Tc}(\text{CO})_3(\text{DTC})(\text{H}_2\text{O})$ ; only line broadening was observed.

Only the complexes with the phosphine, imidazole and isonitrile appeared to be resistant to exchange with histidine on the macro level, and

these complexes were further tested on the non-carrier added level. An HPLC study showed that the systems with phosphine and imidazole gave, along with the peak of the 2 + 1 complex, also peaks of  $\text{Tc}(\text{CO})_3(\text{DTC})(\text{H}_2\text{O})$  and  $\text{Tc}(\text{CO})_3\text{L}_3$ . In the system with isonitrile, there was a single peak of the 2 + 1 complex in the chromatogram, but the retention times of this complex and other possible species (2 + 1) complex was 21.25 min;  $\text{Tc}(\text{CO})_3(\text{DTC})(\text{H}_2\text{O})$  or  $\text{Tc}(\text{CO})_3(\text{DTC})\text{Cl}$  was 19.48 min;  $\text{Tc}(\text{CO})_3(\text{isonitrile})_3^+$  (20.95 min) was close [17.1]; therefore, it is difficult to detect an impurity of the tris(isonitrile) complex against the background of the 2 + 1 complex.

As already noted, amino acids can be readily converted into dithiocarbamate derivatives. This is a route of linking the 2 + 1 coordination core to biomolecules. Another route is linking via the isonitrile group, starting from commercially available ethyl isocyanacetate. Both these possibilities were tested in a study carried out in cooperation with the Paul Scherrer Institute (for details, see Ref. [17.2]). The ligands and their tricarbonylrhenium complexes were characterized by IR and NMR spectroscopy and by mass spectrometry. It should be noted that in derivatization via dithiocarbamates, the derivatives of primary amines show insufficient stability in the subsequent reactions involved in the peptide synthesis. Therefore, it is necessary to use secondary amino derivatives, in particular proline. On the trace level with  $^{99\text{m}}\text{Tc}$ , however, in both cases (derivatized dithiocarbamate + *tert*-butyl isocyanide, or derivatized isocyanide + diethyldithiocarbamate) two complexes were obtained, according to HPLC: the desired mixed ligand complex and a complex with isonitrile only, or with dithiocarbamate only. Thus if this procedure will be chosen for labelling biomolecules, additional purification will be required.

### 17.3.3. 2 + 1 systems with bidentate nitrogen bases

The above-noted bidentate nitrogen bases were tested in combination with the following compounds: imidazole ( $M_1$ ), 2-nitroimidazole ( $M_2$ ), *tert*-butyl isocyanide ( $M_3$ ), 2,4,4-trimethyl-2-pentyl isocyanide ( $M_4$ ), tributylphosphine ( $M_5$ ) and tris(3-methoxy-3-methylbutyl) phosphite ( $M_6$ ). The phosphites did not ensure formation of single complex species in the 2 + 1 systems; therefore, further experiments were performed with isocyanides and imidazole derivatives, which, according to HPLC, formed single complex species in combination with  $B_1$ – $B_5$ . The complexes with aminoalkyl derivatives appeared to be unstable *in vivo*. Complexes with bipyridine and related compounds in combination with imidazoles and isocyanides are resistant to exchange with histidine (0.1M histidine, 1–1.5 h, room temperature, HPLC monitoring); these complexes were subjected to more detailed tests. It should be noted that although the phenanthroline molecule is rigid, whereas bipyridine is flexible

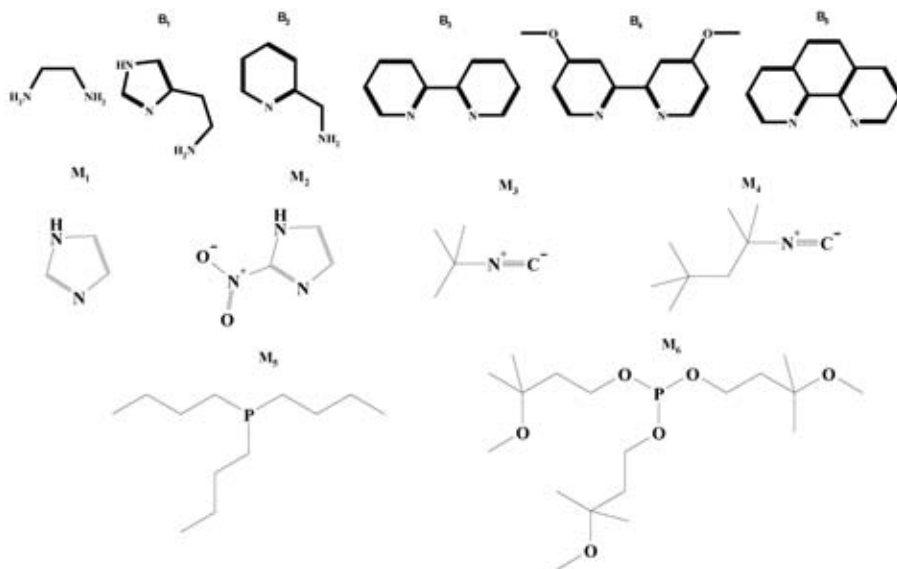


FIG. 17.1. Retention times (min):  $B_1-M_1$ , 18;  $B_1-M_3$ , 20;  $B_2-M_1$ , 21;  $B_2-M_4$ , 22;  $B_3-M_1$ , 21;  $B_3-M_2$ , 23;  $B_3-M_3$ , 22;  $B_3-M_4$ , 23;  $B_4-M_1$ , 21;  $B_4-M_3$ , 23;  $B_4-M_4$ , 23.5.

and can, in principle, coordinate in the monodentate fashion, we found no significant differences in the complexation behaviour of bipyridine and phenanthroline. The retention times (system with methanol, see above) of some of the 2 + 1 complexes are listed in Fig. 17.1.

It should be noted that the retention times of the presumed 2 + 1 complexes and complexes formed in the systems with only one kind of ligand are quite similar. However, none of the ligands taken alone ( $10^{-3}$ M for *tert*-butyl isocyanide,  $2 \times 10^{-4}$ M) ensured complete binding of the Tc-tricarbonyl fragment and formation of a single complex species, whereas in the 2 + 1 system the complexation was complete. Furthermore, complexes with the same bidentate ligand and different monodentate ligands differed in retention times and in biodistribution. These facts indirectly confirm formation of the 2 + 1 complex, with a certain synergistic effect taking place.

#### 17.3.4. Biodistribution studies of 2 + 1 systems with bipyridine and related compounds

The 2 + 1 ligand systems with bipyridine and related compounds as bidentate ligands and imidazoles or isocyanides as monodentate ligands were tested as heart imaging agents. Experiments were performed on rats in

TABLE 17.1. BIODISTRIBUTION OF 2 + 1 COMPLEXES IN RATS (% ID/g) (numerator, heart; denominator, liver; upper figures, 15 min; lower figures, 60 min)

Monodentate ligand	B <sub>1</sub>	B <sub>2</sub>	B <sub>3</sub>	B <sub>4</sub>	B <sub>5</sub>
M <sub>1</sub>	0.13/2.16 0.11/1.84	0.25/1.77 0.15/1.02	— 0.83/0.48	0.99/0.70 1.07/0.56	1.15/0.79 1.12/0.62
M <sub>2</sub>	—	—	—	0.23/1.58 0.18/1.64	—
M <sub>3</sub>	0.11/1.24 0.07/0.77	0.73/0.82 0.75/0.84	1.04/0.94 1.08/2.34	0.97/2.15 1.04/0.94	1.02/0.83 1.02/0.83
M <sub>4</sub>	—	0.44/0.86 0.39/0.65	0.38/2.39 0.31/1.96	1.12/1.39 1.04/0.94	—
M <sub>5</sub>	Weak complexation	Weak complexation	—	—	0.73/0.80 0.79/1.13
M <sub>6</sub>	Weak complexation	Weak complexation	—	—	0.64/1.02 0.64/1.04

Manchester (United Kingdom) in collaboration with B.L. Ellis, M.C. Prescott (both Department of Nuclear Medicine, Manchester Royal Infirmary), R. Braddock, J.C. Adams, A.-M. Smith, H.L. Sharma (all Department of Imaging Science, University of Manchester) and A.N. Yalifimov (Department of Nuclear Medicine, Central Research Institute of Roentgenology and Radiology, St. Petersburg). Table 17.1 gives the heart/liver ratio for some ligand combinations.

Major attention was given to the heart and liver uptake. These parameters showed certain correlation with the lipophilicity (evaluated by the HPLC retention time). The complexes with relatively hydrophilic alkylamino derivatives showed poor heart uptake, whereas too lipophilic complexes with branched isonitriles showed increased liver uptake. The best results were obtained when dimethoxybipyridine or phenanthroline was used in combination with imidazole ( $10^{-3}$ M each). The heart/liver ratio reached 2:1.

The results of these experiments allow us to reach two important conclusions. First, phenanthroline or bipyridine in combination with an imidazole or isonitrile is a suitable ligand system ensuring formation of single complex species with the Tc-tricarbonyl core. Hence, a biomolecule can be linked to the Tc-tricarbonyl core through an imidazole or isonitrile fragment, which in some cases may be considerably simpler than derivatization of a biomolecule with a

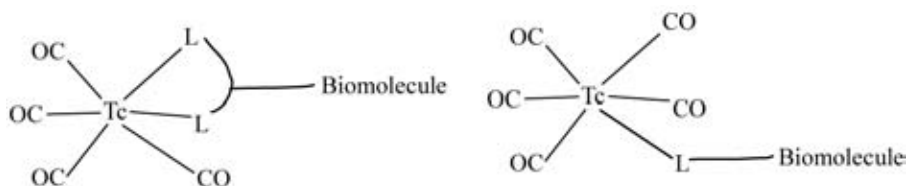


FIG. 17.2. Conceptual drawing of biomolecules linked to bidentate and monodentate ligands and their technetium tetra and penta carbonyl complexes.

tridentate chelating group. Second, the Tc-tricarbonyl-bipyridine or phenanthroline-imidazole core itself, even without a specific biomolecule linked, exhibits appreciable affinity for myocardium. Therefore, this core shows much promise for tethering of biomolecules intended for heart imaging.

#### 17.4. DERIVATIVES OF HIGHER TECHNETIUM-CARBONYLS

An approach alternative to applying 2 + 1 ligand systems is the use of bidentate ligands in combination with the  $\text{Tc}(\text{CO})_4$  core, or of monodentate ligands in combination with the  $\text{Tc}(\text{CO})_5$  core. This approach eliminates problems associated with the possible formation of several complex species in 2 + 1 systems; on the other hand, as compared with tridentate chelating groups, the coordination core in this case is less bulky and less polar, and, as already noted, the derivatization procedure may be simpler (Fig. 17.2).

However, this approach involves two major problems. First, the commercially available kit for preparing Tc-tricarbonyl in aqueous solution at atmospheric pressure allows synthesis of tricarbonyl derivatives only. Preparation of higher carbonyls requires elevated pressures. Second, higher Tc-carbonyls are relatively labile and tend to lose carbon monoxide groups and transform into tricarbonyl species, which severely limits the range of suitable ligands. Our early studies [17.3] showed that the stability of pentacarbonyltechnetium halides increases in the order  $\text{Cl} < \text{Br} < \text{I}$ . This trend is consistent with the results of studying the so called cis-labilization effect [17.4]. All these data indicate that the kinetic stability of higher carbonyls increases in going from harder to softer bases occupying the remaining sites. Therefore, to examine the principal possibility of tethering higher carbonyls to biomolecules, we chose as bidentate ligand dithiocarbamate and as monodentate ligands triphenylphosphine and *tert*-butyl isocyanide.

### 17.4.1. Preparation of higher technetium-carbonyls at the non-carrier added level

Although higher Tc-carbonyls have been extensively studied on the macro level, no procedures have been reported for their preparation on the non-carrier added level. To develop such a procedure, we designed a special mini-autoclave. A vial with the starting  $^{99m}\text{Tc}$  solution (in the form of pertechnetate or in some intermediate form) is placed in a pressure vessel with a threaded lid. Carbon monoxide is either fed from an external source or generated in another pressure vessel by decomposition of formic acid in the presence of sulphuric acid. The device is equipped with a heater and a control panel. The device is compact and easy and safe in operation; it has been certified in the UK as a device for free engineering practice.

In experiments with weighable amounts of  $^{99}\text{Tc}$ , reductive high pressure carbonylation of  $\text{KTcO}_4$  in aqueous solutions in the presence of hydrohalic acids results in the precipitation of the corresponding pentacarbonyl halide. On the non-carrier added level this product cannot form a separate phase and remains in the solution. However, an appreciable fraction of the product (from 10% with chlorine to 30% with iodine) can be transferred in the course of relieving excess carbon monoxide from the warm pressure vessel; it can be trapped by an appropriate solvent (water, alcohol, inert solvent, etc.). This phenomenon is apparently associated with the volatility of technetium pentacarbonyl halides (their vapour pressure at room temperature was estimated in Ref. [17.5] at 0.15 Pa) and with their probable (by analogy with rhenium) capability for steam distillation.

This procedure allows preparation of Tc-carbonyl species free of any foreign components (chloride ion from saline, borate and antioxidants from commercial kits, etc.), which may interfere with further synthesis steps. It also allows the transfer of the Tc-carbonyl precursor into a non-aqueous solvent for subsequent chemical transformations.

Biodistribution experiments revealed very rapid (appreciable uptake is observed within 20 s) and selective accumulation of  $^{99m}\text{Tc}$  in lungs. The results obtained on rabbits in the Russian Federation (Fig. 17.3, data obtained in collaboration with A.N. Yalfimov) and on rats in Manchester (Table 17.2, data obtained in collaboration with B.L. Ellis, R. Braddock, J.C. Adams, A.-M. Smith, M.C. Prescott and H.L. Sharma) were similar. The causes of this phenomenon are unclear; it would be very interesting to determine whether this is a specific feature of iodopentacarbonyltechnetium or a common property of higher Tc-carbonyls.

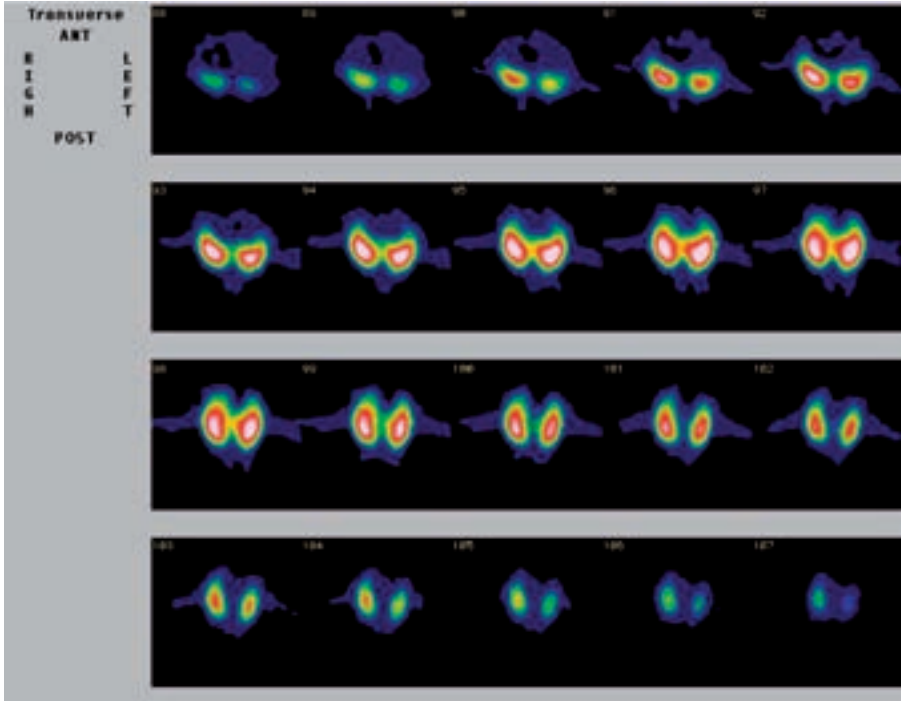


FIG. 17.3. Accumulation of  $^{99m}\text{Tc}(\text{CO})_5\text{I}$  in rabbit lungs (gamma camera patterns of cut layers).

TABLE 17.2. BIODISTRIBUTION OF  $^{99m}\text{Tc}(\text{CO})_5\text{I}$  IN RATS

Time	% ID/organ in Sprague Dawley rats ( $N = 4$ )				
	Lung	Liver	Heart	Kidney	Spleen
15 min	$16.65 \pm 2.30$	$7.47 \pm 1.07$	$0.24 \pm 0.07$	$1.51 \pm 0.46$	$0.15 \pm 0.06$
1 h	$22.47 \pm 2.31$	$10.53 \pm 1.80$	$0.18 \pm 0.01$	$1.20 \pm 0.17$	$0.13 \pm 0.01$

Time	% ID/g in Sprague Dawley rats ( $N = 4$ )					
	Blood	Lung	Liver	Heart	Kidney	Spleen
15 min	$0.26 \pm 0.02$	$8.82 \pm 0.75$	$0.49 \pm 0.05$	$0.20 \pm 0.05$	$0.57 \pm 0.15$	$0.15 \pm 0.03$
1 h	$0.22 \pm 0.02$	$12.8 \pm 2.87$	$0.8 \pm 0.15$	$0.15 \pm 0.01$	$0.47 \pm 0.08$	$0.15 \pm 0.01$

Chloropentacarbonyltechnetium-99m, which is more labile than the iodide form, is obtained by this procedure in a considerably lower and less reproducible yield, which is consistent with the previous observations that  $\text{Tc}(\text{CO})_5\text{Cl}$  is considerably more labile than  $\text{Tc}(\text{CO})_5\text{I}$  [17.3].

#### 17.4.2. Tetracarbonyltechnetium diethyldithiocarbamate

Tetracarbonyltechnetium diethyldithiocarbamate (DTC) was prepared and characterized as far back as 1965 [17.6]. However, no data were available on its stability *in vivo* and *in vitro*, and preparation of the corresponding  $^{99\text{m}}\text{Tc}$  derivative was not reported. In experiments with rhenium and long lived technetium analogues, starting from  $\text{M}(\text{CO})_5\text{I}$ , we obtained the expected tetracarbonyl dithiocarbamate complexes, which were characterized by IR and NMR spectroscopy.  $\text{Re}(\text{CO})_4(\text{DTC})$ . IR ( $\text{CaF}_2$   $\text{CHCl}_3$ ,  $\text{cm}^{-1}$ ): 2100, 2044, 2003, 1980, 1938 (CO), 1510 (CN).  $^1\text{H}$  NMR ( $\text{CDCl}_3$ , ppm): 3.67 q, 1.28 t (Et).  $^{13}\text{C}$  NMR ( $\text{CDCl}_3$ , ppm): 186, 185 (2CO each), 171 (CN), 44, 12 (2Et).  $\text{Tc}(\text{CO})_4(\text{DTC})$ .  $^{99}\text{Tc}$  NMR, ppm: -1712. As shown by  $^{99}\text{Tc}$  NMR monitoring, the technetium complex is stable in polar organic solvents for a long time. It is also resistant to ligand exchange with histidine, which opens prospects for radiopharmaceutical applications of (dithiocarbamate)tetracarbonyltechnetium core taking into account the above mentioned possibility of transforming biomolecules (fatty acids, peptides, etc.) containing a primary or secondary amino group into the corresponding dithiocarbamates. On the trace level, the complex was prepared by transferring  $\text{Tc}(\text{CO})_5\text{I}$  vapour from the pressure vessel to an aqueous ethanol solution of sodium diethyldithiocarbamate. As shown by thin layer chromatography (TLC) monitoring, the conversion was complete at room temperature within 30 min at a ligand concentration of  $10^{-4}\text{M}$ . The retention factor of the complex was identical to that of the reference rhenium analogue. The complex with  $^{99\text{m}}\text{Tc}$  also appeared to be resistant to exchange with histidine.

#### 17.4.3. Pentacarbonyltechnetium phosphine and isonitrile complexes

In direct reactions of pentacarbonyltechnetium halides with neutral ligands, two carbonyl groups are replaced first [17.7]. A similar pattern is observed in the reaction with *tert*-butyl isocyanide: the major product obtained from  $\text{Tc}(\text{CO})_5\text{Cl}$  is  $\text{Tc}(\text{CO})_3\text{Cl}(\text{isocyanide})_2$ . IR ( $\text{CH}_2\text{Cl}_2$ ),  $\nu$ ,  $\text{cm}^{-1}$ : 2048, 1988, 1934 (CO); (MeOH) 2050, 1994, 1946 (CO), 2208, 2187 (NC). This result is obtained both with weighable amounts of  $^{99}\text{Tc}$  and with non-carrier added  $^{99\text{m}}\text{Tc}$ . Therefore, introduction of the neutral ligand should be preceded by replacement of the halide by a more labile anionic ligand.

To prepare complexes  $[\text{}^{99}\text{Tc}(\text{CO})_5\text{L}]^+$  in the form of triflates or perchlorates ( $\text{L} =$  triphenylphosphine, *tert*-butyl isocyanide), a solution of  $\text{Tc}(\text{CO})_5\text{I}$  in methylene chloride was triturated with an excess of solid silver triflate ( $\text{AgOTf}$ ) or perchlorate for 15 min at room temperature. The precipitate of silver salts was separated by centrifugation, and a stoichiometric amount of the neutral ligand was added. The resulting solution was evaporated in a vacuum (in the case of  $\text{PPh}_3$ , the product can be precipitated from methylene chloride with ether). The product was dried in a vacuum. The same reaction performed under homogeneous conditions (solutions of  $\text{Tc}(\text{CO})_5\text{I}$  and silver triflate in ethanol in a stoichiometric ratio) was accompanied by decarbonylation and formation of tricarbonyl species, according to the IR spectra. These species were not further examined.

The products obtained were characterized by IR and  $^{99}\text{Tc}$  NMR spectroscopy.  $[\text{Tc}(\text{CO})_5(\text{PPh}_3)]\text{OTf}$ . IR,  $\nu$ ,  $\text{cm}^{-1}$  ( $\text{CH}_2\text{Cl}_2$ ): 2058 (CO).  $^{99}\text{Tc}$  NMR ( $\text{CH}_2\text{Cl}_2$ ): -1958 ppm (doublet,  $J_{\text{TcP}}$  364 Hz).  $[\text{Tc}(\text{CO})_5(\text{CNC}(\text{CH}_3)_3)]\text{ClO}_4$ . IR,  $\nu$ ,  $\text{cm}^{-1}$  ( $\text{CH}_2\text{Cl}_2$ ): 2073 (CO).  $^{99}\text{Tc}$  NMR ( $\text{CH}_2\text{Cl}_2$ ): -2015 ppm. The triphenylphosphine complex is stable in the solid state for at least a month and in solution (inert solvent) for at least a week, showing no tendency to decarbonylation.

#### 17.4.4. Hexacarbonyltechnetium(I) cation

Hexacarbonyltechnetium(I) cation is of interest from the viewpoint of nuclear medicine as the simplest analogue of a widely used heart imaging agent,  $\text{Tc}(\text{MIBI})_6^+$ . However, certain analogy with another higher carbonyl,  $\text{Tc}(\text{CO})_5\text{I}$ , might be expected. In any case, examination of the biodistribution of this complex would be very interesting. Based on available data for the manganese and rhenium analogues,  $\text{Tc}(\text{CO})_6^+$  is expected to show high kinetic stability compared with pentacarbonyl species. However, no data on the preparation of  $^{99\text{m}}\text{Tc}(\text{CO})_6^+$  at the non-carrier added level have been reported.

Hexacarbonyltechnetium(I) cation was reported for the first time as far back as 1965 [17.6]. The compound was prepared under non-aqueous conditions involving high pressure carbonylation of  $\text{Tc}(\text{CO})_5\text{Cl}$  in the presence of  $\text{AlCl}_3$  (chloride ion acceptor), followed by precipitation of the desired cation in the form of perchlorate. This procedure is apparently unsuitable for carrier free  $^{99\text{m}}\text{Tc}$ .

In a more recent study [17.8], Aebischer et al. examined in detail by NMR the carbonylation of  $^{99}\text{Tc}(\text{CO})_3(\text{H}_2\text{O})_3^+$  in aqueous solution (after removal of chloride ions with  $\text{AgPF}_6$ ). They observed successive formation of tetracarbonyldiaqua, pentacarbonylmonoaqua and hexacarbonyl complexes. The kinetic stability of the hexacarbonyl complex in aqueous solution was high, whereas

the intermediate species decomposed within several hours after relieving the carbon monoxide pressure. The conditions of that study seem to be adaptable to experiments with  $^{99m}\text{Tc}$ ; the only problem is the long reaction time (the conversion to the hexacarbonyl cation was incomplete even in two weeks), whereas the  $^{99m}\text{Tc}$  half-life is about 6 h. To accelerate the reaction and ensure higher yield of the hexacarbonyl cation, the conditions should be made more severe than those used in Ref. [17.8] (310 K, 44 atm. CO).

In our experiments with  $^{99}\text{Tc}(\text{CO})_6^+$ , we started from  $[\text{Tc}(\text{CO})_3\text{OH}]_4$  [17.9, 17.10] and tested several strong acids with a weak coordinating power as reaction media for the carbonylation. The tetrameric hydroxide was dissolved in appropriate acid (100°C, 30 min), and the solution was placed in the pressure vessel. The following results were obtained.

In sulphuric and TFAs (2M, 100–175°C, 100–175 atm. CO, 1–2 h), as judged from the IR spectra of the aqueous solutions obtained upon carbonylation, the hexacarbonyl cation ( $\nu$ , 2096  $\text{cm}^{-1}$ ) was formed with a low yield (the intensity of the above indicated band did not exceed 25% of the total intensity of the Tc-carbonyl bands). The major technetium species were pentacarbonyl and tricarbonyltriaqua complex. In TFA, a precipitate was formed; this precipitate was identified as (trifluoroacetato)pentacarbonyltechnetium by comparison with an authentic sample [17.11]. This fact suggests that even the trifluoroacetate ion is a too strong ligand for pentacarbonyltechnetium, preventing its further carbonylation.

The reaction performed in perchloric acid under the same conditions yielded a solution and a precipitate. In the solution we identified by IR and  $^{99}\text{Tc}$  NMR spectroscopy three technetium species:  $\text{Tc}(\text{CO})_6^+$ ,  $\text{Tc}(\text{CO})_5(\text{H}_2\text{O})^+$  and unchanged  $\text{Tc}(\text{CO})_3(\text{H}_2\text{O})^+$ , in comparable amounts, according to the IR and NMR spectra (the NMR assignments were based on Ref. [17.8]).  $\text{Tc}(\text{CO})_6^+$ :  $\nu$ , 2096  $\text{cm}^{-1}$ ,  $\delta_{\text{Tc}}$ , -1946 ppm.  $\text{Tc}(\text{CO})_5(\text{H}_2\text{O})^+$ :  $\nu$ , 2071, 2023  $\text{cm}^{-1}$ ,  $\delta_{\text{Tc}}$ , -1411 ppm.  $\text{Tc}(\text{CO})_3(\text{H}_2\text{O})_2^+$ :  $\nu$ , 2052, 1935  $\text{cm}^{-1}$ ,  $\delta_{\text{Tc}}$ , -868 ppm. The precipitate contained the major fraction of technetium and consisted of two compounds. The first,  $\text{Tc}(\text{CO})_5\text{Cl}$ , was identified by comparison with an authentic sample; this compound could be separated by washing the precipitate with methylene chloride. The residue was identified by IR and  $^{99}\text{Tc}$  NMR spectroscopy as  $\text{Tc}(\text{CO})_6\text{ClO}_4$  (see above). The amounts of the two solid products were comparable, and their ratio somewhat varied from one experiment to another.

This result indicates that, although perchlorate ion shows no tendency to coordinate with technetium under the reaction conditions, perchloric acid is gradually reduced to hydrochloric acid on heating in the presence of reductants (CO, Tc(I)), and the arising chloride ion captures the pentacarbonyl species, preventing their further carbonylation. Note that the IR band, HPLC band and NMR signal of the pentacarbonylmonoqua complex immediately disappear

on adding chloride ion to concentrations as low as ~0.1M. This fact explains why formation of the hexacarbonyl cation is impossible; for example, in normal saline although the complexation of tricarbonyltriaquatechnetium with the chloride ion is weak [17.12, 17.13], the pentacarbonylmono aqua complex, which is apparently a direct precursor of the hexacarbonyltechnetium cation, takes up chloride ion virtually irreversibly, and the chloride ion (as well as other coordinating anions) prevents further carbonylation. An experiment on carbonylation of  $\text{Tc}(\text{CO})_3(\text{H}_2\text{O})_3^+$  in 2M HCl even under severe conditions (8 h, 250 atm. CO) resulted in the precipitation of  $\text{Tc}(\text{CO})_5\text{Cl}$ , and the aqueous phase, according to  $^{99}\text{Tc}$  NMR, contained only the tricarbonyl species in the form of triaqua, diaquachloro and aquadichloro complexes. No hexacarbonyl was detected.

We also found that formation of the hexacarbonyl cation requires a strongly acidic medium. The yield of the hexacarbonyl cation drastically decreased in going from 2M to 0.1M acid, probably because of higher activity of molecular water as ligand in less acidic solutions. Taking into account these results, we performed the synthesis of  $\text{Tc}(\text{CO})_6^+$  in a still stronger acid,  $\text{HPF}_6$ . The conditions were the same as in the experiments with the other acids. Despite the fact that the acid mostly decomposed in the course of the synthesis, the hexacarbonyltechnetium cation was obtained as the major product (up to 90% and even more). However, this medium is unsuitable for medical applications, and either thorough removal of fluoride ions should be carried out or other superstrong acids should be looked for.

In this respect, trifluoromethanesulfonic acid seems to be a suitable alternative. In this acid, the yield of the hexacarbonyl complex relative to the sum of carbonyl species, estimated from the IR spectrum of the reaction mixture, reached 70% (2M HOTf, 170°C, 150 atm. CO, 1 h).

The hexacarbonyltechnetium cation showed remarkable kinetic stability, which was even higher than that reported in Ref. [17.8]. Although this cation is not formed in the presence of chloride ions, its monitoring for five days revealed no appreciable decomposition in normal saline after neutralization to pH6, even in the presence of histidine.

To perform a similar synthesis with  $^{99\text{m}}\text{Tc}$ , we used a two-step procedure. First, we prepared by high pressure carbonylation  $\text{Tc}(\text{CO})_5\text{Cl}$  and transferred it through the vapour phase into another vial containing water. In so doing, the co-transfer of halide was negligible (if the transfer of hydrogen halide were noticeable, the pH of the trapping solution would decrease, which was not the case). The resulting solution was preheated at 60°C for 15 min to decompose the pentacarbonyl complex to tricarbonyl (without carbon monoxide pressure, no volatilization of Tc-carbonyl is observed in the process). After cooling, the solution was acidified with an aqueous solution of  $\text{HPF}_6$  to a concentration of

2M. The vial with the solution thus obtained was placed in a pressure vessel and carbonylated (175°C, 195 atm. CO, 1 h). The resulting solution was analysed by HPLC. According to HPLC (system with acetonitrile), in this solution about 46% of the technetium activity is in the form of the hexacarbonyl complex (retention time 2.1 min; for the long lived technetium at ultraviolet detection, 1.7 min). The solution contained about 22% tricarbonyltriaqua complex and about 32% unidentified product with a longer retention time.

Thus preparation of  $^{99m}\text{Tc}(\text{CO})_6^+$  is principally possible, the kinetic stability of the cation is sufficiently high for biological applications, but the synthesis procedure requires improvement.

## 17.5. CONCLUSION

Ligands of low denticity can be applied to tethering of the Tc-carbonyl core to biomolecules using two approaches. Within the framework of the first 2 + 1 approach, the use of phenanthroline and related compounds provides blocking of two of three vacant coordination sites in the tricarbonyl core, and the sixth coordination site can be used for linking various molecules via isonitrile or imidazole unit (and probably via other strongly coordinating fragments). The procedure is quite easy, and the technetium precursor can be prepared both by the traditional procedure from the commercial kit and by the high pressure procedure. The use of higher carbonyls is possible with the high pressure procedure only, and the synthesis involves certain additional complications. All these complications will be justified if the final products will be useful as radiopharmaceuticals. Our preliminary results show that the biodistribution of these compounds may be very interesting and deserving of more detailed study.

## ACKNOWLEDGEMENTS

This study was financially supported in part by the ISTC (grant 1723) and by the British Heart Foundation (grant PG/03/011/15027).

## REFERENCES

- [17.1] GORSHKOV, N.I., et al., 2+1 chelating systems for binding organometallic fragment  $\text{Tc}(\text{CO})_3^+$ , *Radiochemistry* **47** (2005) 45.

- [17.2] GORSHKOV, N.I., et al., 2 + 1 dithiocarbamate–isocyanide chelating systems for linking  $M(\text{CO})_3^+$  ( $M = {}^{99m}\text{Tc}$ , Re) fragment to biomolecules, *J. Organomet. Chem.* **689** (2004) 4757.
- [17.3] MIROSLAVOV, A.E., et al., Regular trends in conditions of formation and in properties of lower carbonyltechnetium halides, *Radiokhimiya* **32** 6 (1990) 14 (in Russian).
- [17.4] ATWOOD, J.D., BROWN, T.L., Cis labilization of ligand dissociation. 3. Survey of group 6 and 7 six-coordination carbonyl compounds. The site preference model for ligand labilization effects, *J. Am. Chem. Soc.* **98** (1976) 3160.
- [17.5] BORISOVA, I.V., et al., Tensimetric study of technetium carbonyl compounds, *Radiokhimiya* **33** 6 (1991) 9 (in Russian).
- [17.6] HIEBER, W., et al., Ueber Kohlenoxidverbindungen des Technetiums, *Z. Naturforsch. B* **20** (1965) 1159.
- [17.7] BORISOVA, I.V., et al., Complexes of carbonyltechnetium halides with neutral  $\sigma$ -donor ligands, *Radiokhimiya* **33** 3 (1991) 1 (in Russian).
- [17.8] AEBISCHER, N., et al., Complete carbonylation of *fac*- $[\text{Tc}(\text{H}_2\text{O})_3(\text{CO})_3]^+$  under CO pressure in aqueous media: A single sample story, *Angew. Chem. Int. Ed.* **39** (2000) 254.
- [17.9] MIROSLAVOV, A.E., et al., Tricarbonyltechnetium hydroxide, *Radiokhimiya* **31** 6 (1989) 33 (in Russian).
- [17.10] GORSHKOV, N.I., et al., Synthesis of  $[\text{Tc}(\text{H}_2\text{O})_3(\text{CO})_3]^+$  ion and study of its reaction with hydroxyl ion in aqueous solutions, *Radiochemistry* **42** (2000) 231.
- [17.11] BORISOVA, I.V., et al., Carbonyltechnetium carboxylates, *Radiokhimiya* **33** 6 (1991) 1 (in Russian).
- [17.12] GORSHKOV, N.I., et al., Complexation of tricarbonyltechnetium(I) ion with halide and thiocyanate ions in aqueous solution:  ${}^{99}\text{Tc}$  NMR study, *Radiochemistry* **45** (2003) 127.
- [17.13] GORSHKOV, N.I., et al.,  ${}^{99}\text{Tc}$  NMR study of complexation of  $[\text{Tc}(\text{H}_2\text{O})_3(\text{CO})_3]^+$  with halide and thiocyanate ions in aqueous solution, *Czech. J. Phys. (Suppl. A)* **53** (2003) A745.

## Chapter 18

### SMALL MOLECULE LABELLING WITH [<sup>99m</sup>Tc(OH<sub>2</sub>)<sub>3</sub>(CO)<sub>3</sub>]<sup>+</sup>: LIGANDS, AMINO ACIDS AND INTERCALATORS

R. ALBERTO, Y. LIU, N. AGORASTOS

Institute of Inorganic Chemistry, University of Zurich, Switzerland

I. SANTOS, P. RAPOSINHO

Department of Chemistry, Institute of Nuclear Technology, Portugal

H. KNIGHT

Tyco-Mallinckrodt Health Care, Petten, Netherlands

J. MERTENS, M. BAUWENS

Vrije Universiteit Brussel, Radiopharmaceutical Chemistry,  
Brussels, Belgium

#### Abstract

The labelling of biomolecules with the new cores [TcN]<sup>2+</sup>, [Tc(CO)<sub>3</sub>]<sup>+</sup> and Tc(III) needs tailor made ligands for the particular precursor complex. For all approaches, the ligand needs to be small and of low molecular weight and its physicochemical properties adapted to the particular vector. This coordinated research project (CRP), Development of <sup>99m</sup>Tc Based Small Biomolecules Using Novel <sup>99m</sup>Tc Cores, focused on the labelling of small biomolecules. For the development of the carbonyl approach we developed a number of smallest size ligands based on a tripodal NNO set. To prove the potency of the corresponding complexes, we combined the ligands with amino acids for the targeting of the L type amino acid transporter LAT1. Some of the compounds described in the paper were recognized by LAT1 with relatively high affinity. These [<sup>99m</sup>TcCO<sub>3</sub>]<sup>+</sup> compounds therefore represent the first examples of small molecule technetium conjugates that are actively transported in the intracellular space. Another sort of small molecules are intercalators. Quinazoline as a topic of this CRP was replaced by acridine, since acridine is a more potent nucleus targeting agent than quinazoline. Acridine and derivatives thereof have been derivatized with an isocyanide group. Applying the 2 + 1 mixed ligand principle, complexes were received that go into the intracellular space and highly accumulate in the nucleus. Preliminary cytotoxicity studies show that Auger electrons from <sup>99m</sup>Tc are able to induce lethal damage to cells at a relatively low activity level. Combination with bombesin as a targeting agent shows

high accumulation in the cytoplasm but not in the nucleus. Finally, an improved synthesis for the preparation of  $^{188/186}\text{Re}(\text{OH}_2)_3(\text{CO})_3]^+$  was elaborated. The different literature procedures suffer from harsh reaction conditions or low yields. The two-kit procedure represented here gives a reproducible yield >98% and applies the commercially available Isolink kit.

## 18.1. INTRODUCTION

The precursor complex  $^{99\text{m}}\text{Tc}(\text{OH}_2)_3(\text{CO})_3]^+$  is one of the promising cores for the development of new  $^{99\text{m}}\text{Tc}$  based radiopharmaceuticals [18.1]. Many ligands for the stable binding of the *fac*- $^{99\text{m}}\text{Tc}(\text{CO})_3]^+$  core to biomolecules have been described [18.2]. These ligands are based on the polyamino-polycarboxylate types, aromatic and aliphatic amines as well as cyclopentadienyl ligands and polyamines. Depending on the biomolecule, a particular ligand is selected; for example, tridentate amino acids such as methionine or histidine proved to be particularly useful for peptides, antibodies and other relatively large biomolecules. For small biomolecules as under investigation in this coordinated research project (CRP), it is of utmost importance that the ligands are small and the topology of the complex symmetrical, in order to prevent dominant interactions of the functionalities with receptors in particular, or biomolecules in general. We have developed in the course of this work a new sort of tridentate NNO based ligand that provides a tripod coordination to technetium and with biomolecule conjugation at the tertiary bridgehead carbon. The ligand is highly efficient in coordination to the  $[\text{Tc}(\text{CO})_3]^+$  core and the corresponding complexes are neutral but still highly hydrophilic. These ligands can be used in the context of the biomolecules under investigation in this CRP due to their very good properties but have only been investigated for the labelling of amino acids. The L type amino acid transporter LAT1 is overexpressed on many tumour cell lines [18.3]. The high demand of rapidly proliferating tumour cells for amino acids makes LAT1 an interesting target, probably comparable to GLUT1. If sufficient amounts of labelled amino acid are accumulated in tumours, imaging becomes possible. Due to the difficulties of combining small molecules with bulky technetium complexes, LAT1 has not been investigated in the context of  $^{99\text{m}}\text{Tc}$  labelling but rather in the context of fluorination with  $^{18}\text{F}$  or iodination with  $^{125/131}\text{I}$  [18.4, 18.5].

Another target that has hardly been considered is the cell nucleus [18.6]. This target is difficult since the radiopharmaceutical has to pass two barriers: the cell wall and the wall of the nucleus. Once inside the nucleus, lethal damage can be deposited with Auger or conversion electrons or with normal  $\beta^-$  radiation. Rather extensive studies have been published on  $^{111}\text{In}$  to show the

therapeutic effect of this Auger electron emitter. To prevent unspecific cell uptake, the small molecules have to be combined with a tumour cell targeting agent. An intercalator complex can thus be conjugated via a potentially cleavable linker to the vector. We have shown previously that the Auger cascade from the  $^{99m}\text{Tc}$  decay induces double strand breaks in plasmid DNA and have also shown the cytotoxic effect on cells, especially on mouse melanoma cell lines B16F1 [18.7]. Our conjugates have been rather complicated and we have now simplified the approach by applying the mixed ligand 2 + 1 approach in which the intercalator is bound via a single isocyanide group to the  $[\text{}^{99m}\text{Tc}(\text{CO})_3]^+$  core, whereas a targeting agent is coordinated via a bidentate ligand, typically a picolinic acid derivative [18.8]. These small biomolecules allowed a high accumulation in the nucleus, though without specificity. The additional introduction of bombesin as a targeting agent allowed PC3 cell specific uptake but no internalization into the nucleus, as expected.

Other imaging techniques such as positron emission tomography (PET) are becoming increasingly important and compete with  $^{99m}\text{Tc}$  based single photon emission computed tomography (SPECT). PET nuclides, however, cannot replace SPECT nuclides for therapeutic purposes, and radionuclide based therapy remains one of the most important fields. Rhenium-188/186 is of particular interest owing to its favourable decay properties. The chemistry of rhenium and technetium are, at least in the low valencies, different and one cannot claim a matched pair in this respect. However, the same compounds should have the same biological behaviour regardless if the radionuclide is  $^{99m}\text{Tc}$  or  $^{188/186}\text{Re}$ . The preparation of corresponding precursors is sometimes difficult, as drastically demonstrated by the non-availability of the Re-HYNIC technique. The same is true for the preparation of  $[\text{}^{188}\text{Re}(\text{OH}_2)_3(\text{CO})_3]^+$ . A number of procedures for its preparation have been described, but yields and protocols were not satisfying. In order to access  $[\text{Re}(\text{CO})_3]^+$  based therapy, a reliable and probably kit based synthesis has been developed. This will allow not only the use of this technique for therapeutic purposes, but more basic, comparative studies between technetium and rhenium.

## 18.2. RESULTS

### 18.2.1. New ligands for the $[\text{Tc}(\text{CO})_3]^+$ core

A very small ligand is 2,3-diamino-propionic acid (23dap). It readily forms complexes with  $[\text{}^{99m}\text{Tc}(\text{OH}_2)_3(\text{CO})_3]^+$  at the  $\mu\text{M}$  level. The molecular weight of the complex is low; it is stable for more than 24 h in serum and its retention time is close to that of  $[\text{}^{99m}\text{Tc}(\text{OH}_2)_3(\text{CO})_3]^+$ . This surprisingly short

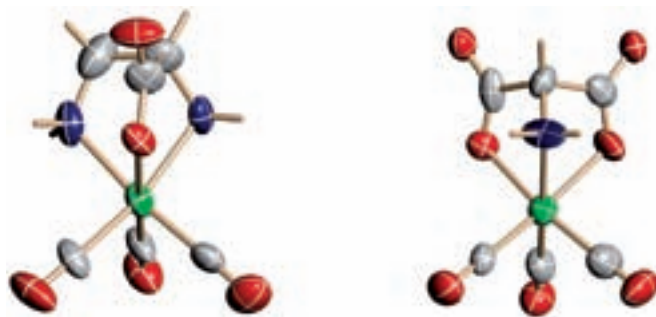


FIG. 18.1. X ray structure of  $[Re(23dap)(CO)_3]$  (left) and  $Re(ama)(CO)_3]$  (right).

retention time is not only due to hydrophilicity but also due to its size. An X ray presentation of the complex  $[Re(23dap)(CO)_3]$  is given in Fig. 18.1.

A similar ligand is represented by amino-malonic acid (ama). This ligand, which provides an NOO donor set, gives negatively charged ligands of very high hydrophilicity. On high performance liquid chromatography (HPLC) it elutes with only 0.5 min delay to  $[TcO_4]^-$ , again a consequence of charge and size. In comparison to polyamino-polycarboxylate type ligands such as IDA or others, this ligand is substantially smaller but the complexes are of comparable if not better stability. Favourable properties such as stability and hydrophilicity of the above complexes make them particularly suitable for peptides, antibodies or other hydrophilic molecules. An ORTEP presentation of  $[Re(ama)(CO)_3]^-$  is also given in Fig. 18.1.

### 18.2.2. Labelling of amino acids

Despite being versatile, the ligands ama and 23dap are difficult to derivatize with functionalities that allow their introduction into biomolecules. Preferentially, the derivatization is performed at the bridgehead carbon but which is a tertiary carbon atom of low reactivity and shielded from the surrounding. We therefore had to do a rather long synthetic procedure in order to conjugate an additional functionality or, more directly, a biomolecule such as an amino acid. The synthetic procedure to receive tripod NNO ligand derivatized amino acids with various spacer lengths is given in Fig. 18.2.

The amino acid functionality is introduced to the cyanide precursor either from terminally halogenated amino acids or by taking malonic acid already comprising the spacer, subsequent ester hydrolysis and decarboxylation. For the first procedure, where feasible, enantiomerically pure complex was received, whereas for the second a *D, L* mixture resulted. In the worst case, the determination of the affinity constant for the transport protein would be half of

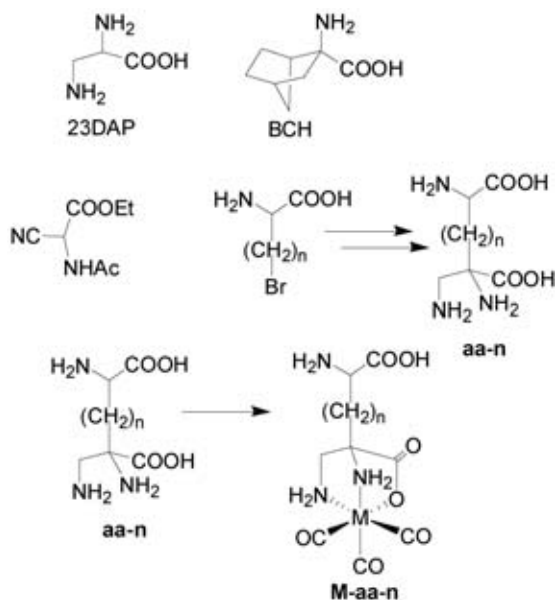


FIG. 18.2. Some model amino acids (BCH) and a concise synthetic approach to derivatized amino acids.

that found for the pure *L* form, which represents 50% of the material, provided that the *D* form is not recognized at all. Thus the numbers given for the derivatized amino acids are on the 'save' side. In contrast to other amino acid derivatives, which did not give any recognition at all, the compounds based on these tripods showed linker length dependent affinity for LAT1. With a C4 linker (derived from lysine) the affinity was about 300  $\mu$ M (vs. 70  $\mu$ M for phenylalanine). The affinity generally increased with increasing length of the spacer, but was still on a well measurable scale. The compounds caused efflux of labelled amino acid from the intracellular space, since LAT1 represents an antiport system. Preliminary animal investigations did not show strong accumulation in the tumour. This is probably not due to too low affinity but due to the rapid washout of the compounds through the kidneys.

It should be emphasized at this point that the compounds presented here are the first small biomolecules labelled with <sup>99m</sup>Tc that are actively transported by a transmembrane protein. Based on the structure affinity relationship available so far, it is well possible to increase the affinity and lipophilicity in order to prevent the observed rapid washout. Despite the long synthetic way to these amino acids, they are small and topologically unpretentious.

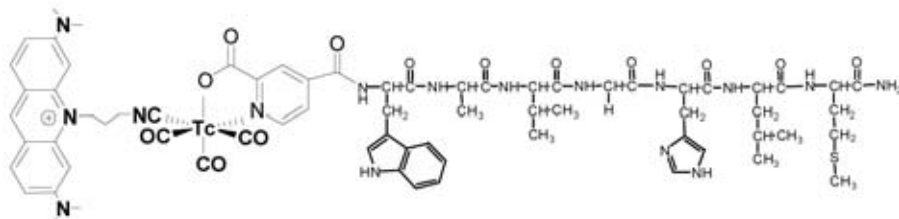


FIG. 18.3. Trifunctional nucleus targeting compound showing the receptor targeting portion (bombesin), the bidentate ligand (dipicolinic acid) and the intercalator bound to the  $[^{99m}\text{Tc}(\text{CO})_3]^+$  core.

From the ligand design, it is clear that the amino acid derivatives can also be introduced as, for example, artificial amino acids in peptides (e.g. as lysine surrogates). However, some ambitious protecting group chemistry is required in order to make this sort of chemistry possible.

### 18.2.3. Targeting the nucleus: intercalators

Small complexes are important for targeting tumours, since penetration of the cell membrane and nucleus membrane does not tolerate large molecules. In addition, charge and lipophilicity are important. Therefore, intercalators represent an interesting proof of principle for the small molecule approach [18.9–18.11]. We have recently shown that the combination of a nuclear localizing peptide sequence (NLS peptides) with a tridentate amine ligand bound to an intercalator leads to accumulation of the radiopharmaceutical in the nucleus, thereby destroying the cell [18.7]. Accumulation was, however, slow and not too high. We switched to a more potent nuclear targeting molecule that is also an intercalator. Many compounds with these characteristics are known from molecular biology, and we have chosen acridine due to its relatively good water solubility and ease of derivatization. The intercalator is bound via an isocyanide to the  $[^{99m}\text{Tc}(\text{CO})_3]^+$  core and the targeting peptide by a bidentate ligand, in most of the cases picolinic acid based. The approach is depicted in Fig. 18.3, and an X ray structure of the complex (without peptide) is shown in Fig. 18.4.

The complex  $[^{99m}\text{Tc}(\text{acr})(\text{pic})(\text{CO})_3]$  can be prepared in one or two steps directly from kit prepared  $[^{99m}\text{Tc}(\text{OH})_2(\text{CO})_3]^+$ . The overall charge of the complex is positive. In vitro tests with mouse melanoma cell lines showed a relatively rapid uptake of the complex into the nucleus within 30–60 min. Isolating the cells revealed about 80–90% of the activity being in the nucleus and about 10–20% still in the cytoplasm. A survival rate of 5% of the cells could be achieved with activities about 20 times lower than with the NLS

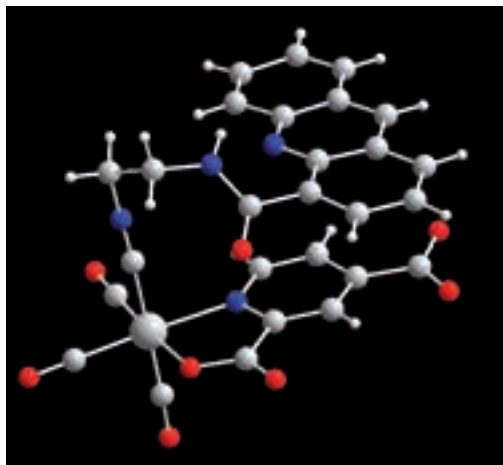


FIG. 18.4. X ray structure of the complex  $[Re(acr)(dipic)(CO)_3]$ .

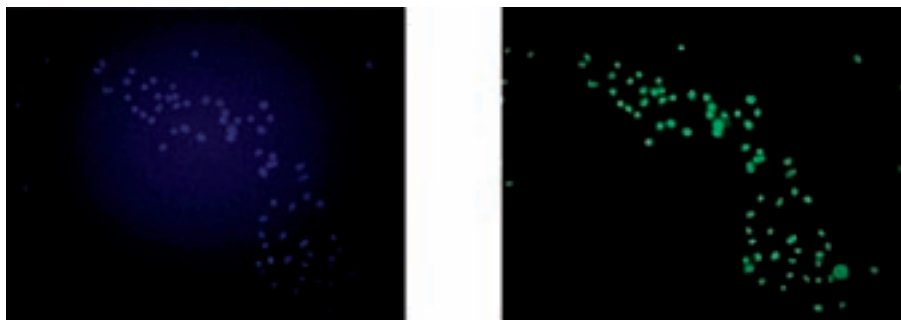


FIG. 18.5. B16F1 cells stained with dapi (left) and with  $[Re(acr)(dipic)(CO)_3]$  (right). Note the spatial agreement between the two pictures.

peptide, showing the superior nucleus targeting properties of acridine in comparison with the NLS peptide.

To follow the uptake not only by measuring activity, we applied fluorescence microscopy with the cold rhenium compounds. Fluorescence microscopy confirmed well the results found with  $^{99m}Tc$ . Figure 18.5 shows the images of mouse melanoma B16F1 cells after 30 min incubation with the acridine compounds. It can be seen very clearly that the pictures are the same for dapi, a known nucleus staining intercalator, and the rhenium-acridine complex.

Despite the relatively large attached metal complex, the compound is still able to penetrate the nucleus. This is only possible due to the overall cationic

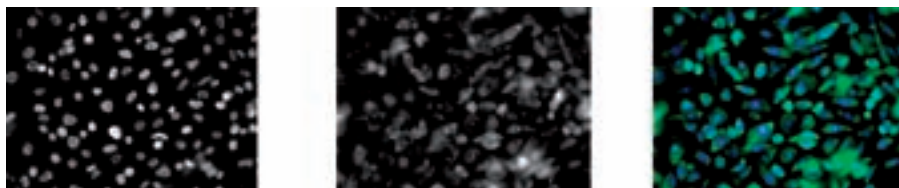


FIG. 18.6. PC3 cells stained with dapi (left), with  $[Re(bomb)(acr)(CO)_3]$  (middle) and superimposition of the two pictures (right). Note that  $[Re(bomb)(acr)(CO)_3]$  remains in the cytoplasm.

nature of the complex, its relatively small size and its innocence in terms of interaction with other functionalities.

The uptake of Re-acridine is, of course, completely unspecific. To overcome this problem, we selected bombesin as a targeting peptide and introduced a bidentate ligand at its N-terminus. ‘Labelling’ with  $[Re(OH_2)_3(CO)_3]^+$  and subsequent reaction with acridine resulted in the complete set of agents, a receptor targeting biomolecule, the radioactive complex and the intercalator. Since the intercalator complex cannot be cleaved from the peptide, it cannot be expected that this bioconjugate will go into the nucleus. This is exactly what has been found.

Figure 18.6 shows a picture of PC3 cells (comprising bombesin receptors) when exposed to Re-acridine. Again, dapi stains the nucleus, but this time the green fluorescence of acridine is not seen in the nucleus but in the cytoplasm only. Accordingly, the bombesin was recognized by its receptor and internalized, but the complex did not cleave from the peptide, hence no penetration into the nucleus took place. As an experiment, the bombesin conjugate was also exposed with B16F1 cells (no bombesin receptors); we observed only very weak fluorescence after a long irradiation time. Again, the nucleus as stained with dapi is clearly visible. These results point clearly to the next logical step, which consists of the introduction of a cleavable linker; first attempts with a hydrazone are due. We aim at investigating the radiotoxic effects imposed by the Auger electrons from  $^{99m}Tc$ . Clearly, if this effect is too weak and the dose deposited in the nuclide too small, one can switch to  $^{188}Re$  or  $^{186}Re$  using the same bioconjugates as for  $^{99m}Tc$ .

#### 18.2.4. Kit preparation of $[^{188/186}Re(OH_2)_3(CO)_3]^+$

The availability of Re-carbonyls is an issue that is considered to be of high importance. Some preparations have been described in the literature, but an Isolink based kit would be desirable [18.12, 18.13]. We have developed a method in which  $[^{186}ReO_4]^-$  is prereduced with  $H_3BNH_3$  in the presence of

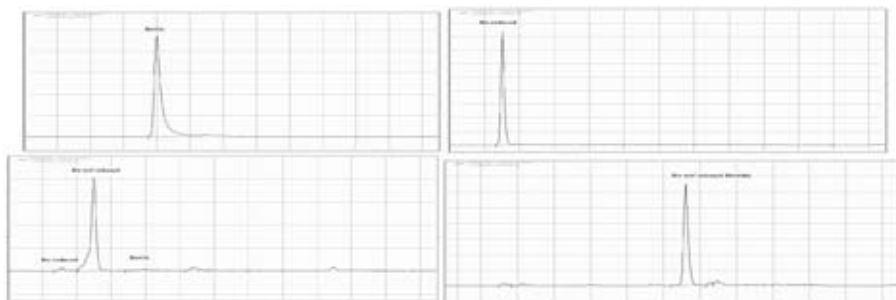


FIG. 18.7. Top left,  $[^{186}\text{ReO}_4]^-$ , top right prereduced  $[^{186}\text{ReO}_4]^-$  after 20 min at room temperature, bottom right  $[^{188/186}\text{Re}(\text{OH}_2)_3(\text{CO})_3]^+$  after 20 min boiling in an Isolink kit, bottom left, conversion of  $[^{188/186}\text{Re}(\text{OH}_2)_3(\text{CO})_3]^+$  to the histidine complex.

$\text{H}_3\text{PO}_4$  in a first vial at room temperature for 20 min and is then transferred to an Isolink kit and boiled at  $100^\circ\text{C}$  for a further 20 min. After this procedure,  $[^{188/186}\text{Re}(\text{OH}_2)_3(\text{CO})_3]^+$  is obtained with a 95–98% yield. We have performed this reaction only with carrier added  $^{186}\text{Re}$  but at a concentration that is similar to high activity  $^{188}\text{Re}$  eluted from the  $^{188}\text{W}/^{188}\text{Re}$  generator. It will be most interesting to see if the procedure is also feasible with high activity  $^{188}\text{Re}$ . Kits are available from Mallinckrodt. Some typical HPLC traces are shown in Fig. 18.7.

### 18.3. SUMMARY AND CONCLUSIONS

We have achieved as part of the CRP some very important results for the development of novel radiopharmaceuticals using the new cores. A small (possibly smallest classical) tripod ligand has been synthesized and attached to amino acids. The amino acid was still recognized by its transporter LAT1. Affinity is not yet as good as natural amino acids, but is very close. This novel radiopharmaceutical can be further developed and the structure varied in order to achieve a perfect surrogate of natural amino acids. We could show with intercalators the possibility of targeting the nucleus. High radiotoxicity was imposed with the Auger electrons from  $^{99\text{m}}\text{Tc}$ . Fluorescence images proved that the complexes attached to intercalators accumulate to a high extent in the nucleus. Finally, a new and very convenient preparation of  $[^{188/186}\text{Re}(\text{OH}_2)_3(\text{CO})_3]^+$  has been established, allowing the exploration of radiopharmaceuticals for therapy and comparison of rhenium with technetium chemistry.

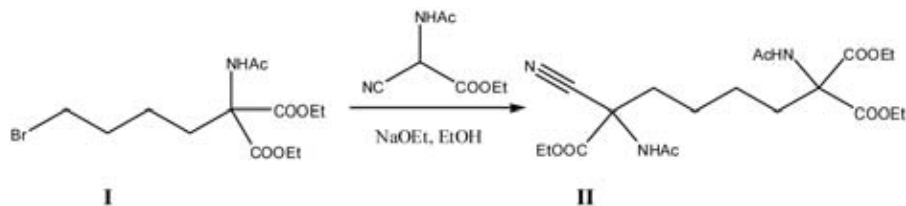


FIG. 18.8. Synthetic scheme for the preparation of triethyl 1,6-diacetamido-6-cyano-hexane-1,1,6-tricarboxylate (II).

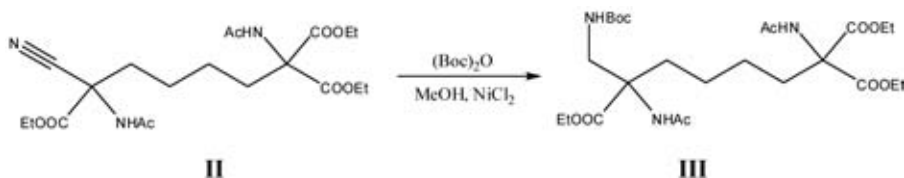


FIG. 18.9. Synthetic scheme for the preparation of triethyl 1,6-diacetamido-7-(tert-butoxycarbonylamino)heptane-1,1,6-tricarboxylate (III).

## 18.4. EXPERIMENTAL

### 18.4.1. Triethyl 1,6-diacetamido-6-cyano-hexane-1,1,6-tricarboxylate (II)

To a flask containing absolute ethanol (20 mL) was added sodium (23 mg, 1 mmol) while being stirred. After complete dissolution of sodium, ethyl acetamidocyanoacetate (170 mg, 1 mmol) was added and warmed up to 60°C for 30 min (Fig. 18.8). After cooling down to room temperature, diethyl 2-acetamido-2-(4-bromobutyl)malonate (352 mg, 1 mmol) was added to the solution in one portion. The reaction mixture was refluxed overnight and then the solvent was removed under reduced pressure. The resulting residue was treated with H<sub>2</sub>O (20 mL) and was extracted with EtOAc (2 × 50 mL). The organic phase was washed with brine and dried over MgSO<sub>4</sub>. After filtration, the organic phase was evaporated to give a colourless oil, which was crystallized from EtOAc/hexane to yield colourless crystals (350 mg, 79%).

*Analysis.* Calculated for C<sub>20</sub>H<sub>31</sub>N<sub>3</sub>O<sub>8</sub>: C, 54.41; H, 7.08; N, 9.52. Found: C, 54.57; H, 7.02; N, 9.44.

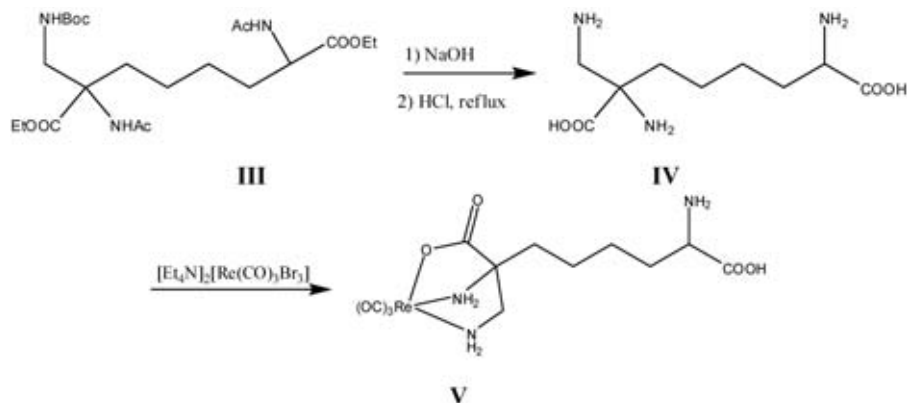


FIG. 18.10. Synthetic scheme for the preparation of  $\text{Re}(\text{CO})_3$ -triethyl 1,6-diacetamido-6-cyanoheptane-1,1,6-tricarboxylate (III).

#### 18.4.2. Triethyl 1,6-diacetamido-7-(tert-butoxycarbonylamino)heptane-1,1,6-tricarboxylate (III)

To the MeOH (10 mL) solution of II (220 mg, 0.5 mmol) cooled in an ice bath was added  $(\text{Boc})_2\text{O}$  (218 mg, 1 mmol) and  $\text{NiCl}_2 \cdot 6\text{H}_2\text{O}$  (12 mg, 0.05 mmol) to give a green solution (Fig. 18.9). To this solution was added  $\text{NaBH}_4$  (152 mg, 4 mmol) in portions with stirring. The purple mixture was stirred overnight and diethylenetriamine (0.06 mL) was added. The reaction was stirred for 1 h before the volatile part of the mixture was removed by vacuum. The residue was partitioned between EtOAc and saturated  $\text{NaHCO}_3$  solution. The organic phase was dried with  $\text{MgSO}_4$ . Removal of organic solvent gave a colourless residue, which was recrystallized with EtOAc/hexane to yield colourless crystals (200 mg, 73%).

#### 18.4.3. Preparation of V

To the solution of NaOH (20 mg in 3 mL  $\text{H}_2\text{O}$ ) was added III (110 mg, 0.2 mmol) (Fig. 18.10). The reaction mixture was stirred at  $70^\circ\text{C}$  overnight, and then 1 mL HCl (32% wt) was added. The reaction mixture was refluxed overnight, cooled down to room temperature and washed with diethyl ether. The aqueous solution was neutralized to pH  $\sim 7$ , and 40 mg  $[\text{Et}_4\text{N}]_2[\text{Re}(\text{CO})_3\text{Br}_3]$  (0.05 mmol) was added. The reaction mixture was refluxed overnight and then water was removed. The residue was washed repeatedly with  $\text{CH}_2\text{Cl}_2$ . Column chromatography purification gave V as a white solid (19 mg, 74% calculated from  $[\text{Et}_4\text{N}]_2[\text{Re}(\text{CO})_3\text{Br}_3]$ ).

## ACKNOWLEDGEMENTS

We thank Mallinckrodt for financial support.

## REFERENCES

- [18.1] BANERJEE, S.R., et al., New directions in the coordination chemistry of Tc-99m: A reflection on technetium core structures and a strategy for new chelate design, *Nucl. Med. Biol.* **32** (2005) 1.
- [18.2] ALBERTO, R., Technetium, *Comprehensive Coordination Chemistry II* (McCLEVERTY, J.A., MEYER, T.J., Eds), Elsevier (2003).
- [18.3] KANAI, Y., et al., Expression cloning and characterization of a transporter for large neutral amino acids activated by the heavy chain of 4F2 antigen (CD98), *J. Biol. Chem.* **273** (1998) 23629.
- [18.4] LAHOUTTE, T., et al., SPECT and PET amino acid tracer influx via system L (h4F2hc-hLAT1) and its transstimulation, *J. Nucl. Med.* **45** (2004) 1591.
- [18.5] MERTENS, J., et al., Synthesis, radiosynthesis, and in vitro characterization of [I-125]-2-iodo-L-phenylalanine in a R1M rhabdomyosarcoma cell model as a new potential tumor tracer for SPECT, *Nucl. Med. Biol.* **31** (2004) 739.
- [18.6] BRANA, M.F., et al., Intercalators as anticancer drugs, *Curr. Pharm. Design* **7** (2001) 1745.
- [18.7] HAEFLIGER, P., et al., Induction of DNA-double-strand breaks by Auger electrons from <sup>99m</sup>Tc complexes with DNA-binding ligands, *Chem. Biochem.* **6** (2005) 414.
- [18.8] MUNDWILER, S., KUNDIG, M., ORTNER, K., ALBERTO, R., A new [2+1] mixed ligand concept based on [<sup>99(m)</sup>Tc(OH<sub>2</sub>)<sub>3</sub>](CO)<sub>3</sub>]<sup>+</sup>: A basic study, *J. Chem. Soc. Dalton Trans.* **9** (2004) 1320.
- [18.9] BEHR, T.M., et al., Therapeutic advantages of Auger electron- over beta-emitting radiometals or radioiodine when conjugated to internalizing antibodies, *Eur. J. Nucl. Med.* **27** (2000) 753.
- [18.10] BEHR, T.M., et al., Therapeutic efficacy and dose-limiting toxicity of Auger-electron vs. beta emitters in radioimmunotherapy with internalizing antibodies: Evaluation of I-125- vs I-131-labeled CO17-1A in a human colorectal cancer model, *Int. J. Cancer* **76** (1998) 738.
- [18.11] GRIFFITHS, G.L., et al., Cytotoxicity with Auger electron-emitting radio-nuclides delivered by antibodies, *Int. J. Cancer* **81** (1999) 985.
- [18.12] HE, J., et al., Radiolabelling morpholinos with Re-188 tricarbonyl provides improved in vitro and in vivo stability to Re-oxidation, *Nucl. Med. Commun.* **25** (2004) 731.
- [18.13] SCHIBLI, R., SCHUBIGER, P.A., Current use and future potential of organo-metallic radiopharmaceuticals, *Eur. J. Nucl. Med. Mol. Imaging* **29** (2002) 1529.

## Chapter 19

### **DESIGN AND EVALUATION OF POTENTIAL <sup>99m</sup>Tc RADIOPHARMACEUTICALS BASED ON THE Tc-CARBONYL, 4 + 1 MIXED LIGAND CHELATE SYSTEM AND Tc-NITRIDO APPROACHES**

J. GIGLIO\*, A. MUSLERA\*, M. INCERTI\*\*, R. FERNÁNDEZ\*\*,  
E. LEÓN\*, A. PAOLINO\*, A. BRUGNINI<sup>†</sup>, E. MANTA\*\*,  
A. CHABALGOITY<sup>†</sup>, A. LEÓN\*, A. REY\*

\* Cátedra de Radioquímica, Facultad de Química

\*\* Cátedra de Química Farmacéutica, Facultad de Química

<sup>†</sup> Laboratorio de Vacunas Recombinantes, Instituto de Higiene, Facultad de Medicina

Universidad de la República, Montevideo, Uruguay

#### **Abstract**

The aim of the work was to explore the possibilities of the novel labelling strategies in the development of <sup>99m</sup>Tc labelled small biomolecules. Different steps required to fulfil this objective were undertaken: organic synthesis of glucose derivatives, optimization of labelling and in vitro and in vivo evaluation of RGD peptides and annexin 13 derivatives using either the HYNIC bifunctional ligand, the Tc-tricarbonyl, the 4 + 1 mixed ligand or the Tc(V)-nitrido approaches. Glucose-O-hexylbromide, glucose-O-butylbromide and glucose-O-butylamine were successfully synthesized, opening the possibility of introducing different chelators according to the desired labelling procedure. c(RGDyK) derivatives bearing different chelators were labelled with <sup>99m</sup>Tc using novel approaches and evaluated both in vitro and in vivo in order to compare the effect of the chelator and labelling method on the physicochemical and biological behaviour. Annexin 13 peptides were also labelled using the HYNIC and Tc(I)-tricarbonyl approaches. A primary evaluation in normal animals and in a model of cardiac apoptosis is also presented. Cooperation with other participants was crucial to develop this work.

## 19.1. INTRODUCTION

Radiopharmaceutical research has taken a new direction in recent years motivated by the needs of modern nuclear medicine for molecular probes of high selectivity and specificity. Increasing emphasis has been directed towards radiopharmaceuticals that interact with physiological processes such as cell surface receptors, enzymes or other metabolic systems. The so called third generation technetium agents are compounds that imitate biochemical ligands *in vivo*. The design of such agents using the non-physiological metal technetium requires sophisticated coordination chemistry [19.1–19.3].

Recently, new  $^{99m}\text{Tc}$  moieties have been introduced as potentially adequate for labelling small biomolecules. Alberto et al. succeeded in low pressure synthesis of Tc-carbonyl complexes, which can be used as precursors to obtain a great diversity of potential radiopharmaceuticals [19.4, 19.5]. The carbon monoxide is tightly bound and stabilizes low oxidation states. In an aqueous medium the well defined aquo ion of technetium  $[\text{Tc}(\text{OH}_2)_3(\text{CO})_3]^+$  is formed. This novel type of complex is at the same time small and very stable, due to the  $d^6$  configuration of the metallic centre, and gives the possibility to substitute the three weakly bound water molecules with a great variety of ligands. Derivatization of these ligands to introduce different pharmacophores can produce a variety of technetium labelled small biomolecules. This approach has been applied recently to the labelling of peptides, CNS receptor ligands, myocardial imaging agents, DNA intercalators, etc. [19.6–19.8]. Further research using other pharmacophores is still necessary for full understanding of the potentiality of this approach.

Another possible system based on an oxo free core with the metal at a lower oxidation state is represented by the 4 + 1 mixed ligand complexes proposed by Pietzsch et al. This new type of Tc(III) chelates formed by combination of the tripodal 2,2',2''-nitrilotris-ethanethiol and a monodentate isocyanide fulfills the requirements for a non-polar building block stable against *in vivo* ligand exchange. This labelling approach has been proven with simple isocyanides, providing  $^{99m}\text{Tc}$  complexes with high *in vitro* stability both in aqueous solution and in plasma [19.9, 19.10].

Another novel approach for the radiolabelling of biologically active compounds is the use of the Tc-nitrido core. Initially developed by Baldas et al. [19.11], symmetric and asymmetric nitrido Tc(V) and Re(V) are good tools for the design of novel radiopharmaceuticals. The co-ordination sphere of these complexes is either built up by two molecules of bidentate  $\sigma$  donor ligands or a combination of 'pseudotridentate'  $\sigma$  donors,  $\pi$  acceptors diphosphinoamines (PNP) and bidentate  $\sigma$  donor ligands (XY) [19.12, 19.13]. Various bidentate  $\sigma$  donor ligands that can be coupled to biologically relevant molecules have

been evaluated and demonstrate the potentiality of this approach [19.14, 19.15]. However, further development is still necessary in this area.

In this framework, the aim of our work was to explore the possibilities of new design approaches in the development of  $^{99m}\text{Tc}$  labelled small biomolecules. In order to fulfil this objective, different steps are required: identification of potential molecular probes, organic synthesis of ligands containing adequate donor groups, development and optimization of labelling techniques and evaluation by *in vitro* and *in vivo* methods. This paper reports the work performed by our group in all of these stages for different potential radiopharmaceuticals, including: synthesis of ligands for the preparation of potential  $^{99m}\text{Tc}$  labelled glucose analogues, optimization of labelling and *in vitro* and *in vivo* evaluation of RGD peptides and annexin 13 derivatives using either the HYNIC bifunctional ligand, the Tc-tricarbonyl, the 4 + 1 mixed ligand or the Tc(V)-nitrido approaches.

## 19.2. MATERIALS

All laboratory chemicals were reagent grade and used without further purification. Solvents for chromatographic analysis were high performance liquid chromatography (HPLC) grade.  $[\text{}^{99m}\text{Tc}]\text{NaTcO}_4$  was obtained from a commercial generator (Tecnonuclear). Isolink carbonyl labelling agent was provided by Mallinckrodt and kits for the preparation of Tc-nitrido intermediates were provided by CIS Biointernational. RGD peptides were purchased from Biosyntan and distributed by the IAEA. Isocyanide derivatives of RGD peptides were provided by H.-J. Pietzsch. Annexin 13 derivatives were prepared by the Biological Research Centre of the Hungarian Academy of Sciences and provided by J. Környei.

## 19.3. METHODS

### 19.3.1. Synthesis of glucose derivatives

#### 19.3.1.1. *N*-(3,4,6-tri-*O*-acetyl- $\beta$ -*D*-glucopyranosyl)piperidine (1)

$\beta$ -*D*-pentaacetyl glucose (20 g, 0.05 mol) was cooled to 20°C and piperidine (23 mL, 0.23 mol) was added slowly. The reaction was kept at 20–25°C for 30 min until the suspended solution became clear, and after 15 min precipitation began. The reaction was cooled to 0°C and diethylether (80 mL) was added. After 4 h stirring the reaction mixture was allowed to reach room

temperature and filtered. The solid was rinsed with diethylether and cold ethanol, and dried in vacuo. The yield was 39%.  $^1\text{H}$  nuclear magnetic resonance (NMR) (400 MHz,  $\text{CDCl}_3$ )  $\delta$ : 5.11 (t, 1H, 4-CH), 4.94 (t, 1H, 3-CH), 4.21 (dd, 1H, 6- $\text{CH}_2$ ), 4.08 (dd, 1H, 6- $\text{CH}_2$ ), 3.87 (d, 1H, 1-CH), 3.69 (t, 1H, 2-CH), 3.62–3.56 (m, 1H, 5-CH), 2.93–2.86 (m, 2H,  $\text{CH}_2\text{-N}$ ), 2.64–2.56 (m, 2H,  $\text{CH}_2\text{-N}$ ), 2.06 (s, 6H,  $\text{CH}_3$ ), 2.01 (s, 3H,  $\text{CH}_3$ ), 1.62–1.44 (m, 6H,  $\text{CH}_2$ ).

19.3.1.2. *N*-[3,4,6-tri-*O*-acetyl-2-*O*-(6-bromohexyl) $\beta$ -*D*-glucopyranosyl]piperidine (2)

Compound 1 (2 g, 5.35 mmol) was dissolved in benzene (50 mL) at room temperature. Dibromohexane (2 g), molecular sieves (5 g),  $\text{Ag}_2\text{CO}_3$  (3.7 g) and  $\text{AgClO}_4$  (1.66 g) were added. The reaction mixture was heated to 50–55°C and allowed to react protected from light for five days. After reaching room temperature the precipitate was filtrated through celite, rinsed with benzene and purified by flash column chromatography (hexane:ethylacetate 30%). The yield was 40%.  $^1\text{H}$  NMR (400 MHz,  $\text{CDCl}_3$ )  $\delta$ : 5.09 (t, 1H, 3-CH), 4.90 (t, 1H, 4-CH), 4.22 (dd, 1H, 6- $\text{CH}_2$ ), 4.08 (dd, 1H, 6- $\text{CH}_2$ ), 3.94–3.85 (m, 2H, 1-CH, 2-CH), 3.54–3.47 (m, 1H, 5-CH), 3.41 (dt, 4H,  $\text{CH}_2\text{O}$  and  $\text{CH}_2\text{Br}$ ), 2.94–2.88 (m, 2H,  $\text{CH}_2\text{N}$ ), 2.68–2.60 (m, 2H,  $\text{CH}_2\text{N}$ ), 2.06 (d, 6H,  $\text{CH}_3$ ), 2.02 (s, 3H,  $\text{CH}_3$ ), 1.94–1.80 (m, 2H,  $\text{CH}_2$ ), 1.70–1.30 (m, 12H,  $\text{CH}_2$ ).

19.3.1.3. *N*-[3,4,6-tri-*O*-acetyl-2-*O*-(6-bromobutyl) $\beta$ -*D*-glucopyranosyl]piperidine (2')

Compound 1 (2 g, 5.35 mmol) was dissolved in benzene (50 mL) at room temperature. Dibromobutane (1.77 g), molecular sieves (5 g),  $\text{Ag}_2\text{CO}_3$  (3.7g) and  $\text{AgClO}_4$  (1.66 g) were added. The reaction mixture was heated to 50–55°C and allowed to react protected from light for five days. After reaching room temperature, the precipitate was filtrated through celite, rinsed with benzene and purified by flash column chromatography (petroleum ether:ethylacetate 2:1). The yield was 40%.  $^1\text{H}$  NMR (400 MHz,  $\text{CDCl}_3$ )  $\delta$ : 5.03 (t, 1H, 3-CH), 4.95 (t, 1H, 4-CH), 4.20 (dd, 1H, 6- $\text{CH}_2$ ), 4.01 (dd, 1H, 6- $\text{CH}_2$ ), 3.94–3.85 (m, 2H, 1-CH, 2-CH), 3.85 (t, 2H,  $\text{CH}_2\text{N}_3$ ), 3.54–3.47 (m, 1H, 5-CH), 3.41 (dt, 2H,  $\text{CH}_2\text{O}$ ), 2.90–2.85 (m, 2H,  $\text{CH}_2\text{N}$ ), 2.68–2.63 (m, 2H,  $\text{CH}_2\text{N}$ ), 2.07 (d, 6H,  $\text{CH}_3$ ), 2.01 (s, 3H,  $\text{CH}_3$ ), 1.92–1.81 (m, 2H,  $\text{CH}_2$ ), 1.70–1.40 (m, 12H,  $\text{CH}_2$ ).

*19.3.1.4. (2R,3S,4R,5R)-2-(acetoxymethyl)-5-(4-azidobutyl)-6-(piperidin-1-yl)-tetrahydro-2H-pyran-3,4-diyl diacetate (3)*

To a stirred solution of 2' (2.0 g, 4.06 mmol) in dry DMF (30 mL), TMSN<sub>3</sub> (805 mg, 7.00 mmol) and NH<sub>4</sub>Cl (400 mg, 7.00 mmol) were added at room temperature, and the suspension was stirred at 115°C under nitrogen for 4 h. The solution was poured on to ice water and extracted with Et<sub>2</sub>O. The organic layer was washed with brine, dried over MgSO<sub>4</sub> and evaporated in vacuo. The residue was chromatographed on silica gel using petroleum ether:ethyl acetate (1:1) as eluent, to yield compound 3. The yield was 65%. <sup>1</sup>H NMR (400 MHz, CDCl<sub>3</sub>) δ: 5.03 (t, 1H, 3-CH), 4.95 (t, 1H, 4-CH), 4.20 (dd, 1H, 6-CH<sub>2</sub>), 4.01 (dd, 1H, 6-CH<sub>2</sub>), 3.94–3.85 (m, 2H, 1-CH, 2-CH), 3.85 (t, 2H, CH<sub>2</sub>N<sub>3</sub>), 3.54–3.47 (m, 1H, 5-CH), 3.41 (dt, 2H, CH<sub>2</sub>O), 2.90–2.85 (m, 2H, CH<sub>2</sub>N), 2.68–2.63 (m, 2H, CH<sub>2</sub>N), 2.07 (d, 6H, CH<sub>3</sub>), 2.01 (s, 3H, CH<sub>3</sub>), 1.92–1.81 (m, 2H, CH<sub>2</sub>), 1.70–1.40 (m, 12H, CH<sub>2</sub>).

*19.3.1.5. (2R,3S,4R,5R)-2-(acetoxymethyl)-5-(4-aminobutyl)-6-(piperidin-1-yl)-tetrahydro-2H-pyran-3,4-diyl diacetate (4)*

A solution of 2 (1.4 g, 3.08 mmol) in EtOH (20 mL), containing 0.18 g of 10% Pd/C was hydrogenated (1.1 atm.) at room temperature over 4 h. The reaction mixture was filtered through a celite pad and the filtrate was concentrated in vacuo. The residue was purified by flash chromatography (silica gel, ethyl acetate) to afford compound 4. The yield was 70%. <sup>1</sup>H NMR (400 MHz, CDCl<sub>3</sub>) δ: 5.10 (t, 1H, 3-CH), 4.99 (t, 1H, 4-CH), 4.20 (dd, 1H, 6-CH<sub>2</sub>), 4.01 (dd, 1H, 6-CH<sub>2</sub>), 3.97–3.80 (m, 2H, 1-CH, 2-CH), 3.54–3.47 (m, 1H, 5-CH), 3.41 (dt, 2H, CH<sub>2</sub>O), 2.65 (t, 2H, CH<sub>2</sub>NH<sub>2</sub>), 2.90–2.85 (m, 2H, CH<sub>2</sub>N), 2.75–2.63 (m, 2H, CH<sub>2</sub>N), 2.01 (d, 6H, CH<sub>3</sub>), 2.00 (s, 3H, CH<sub>3</sub>), 1.92–1.81 (m, 2H, CH<sub>2</sub>), 1.76–1.40 (m, 12H, CH<sub>2</sub>).

*19.3.1.6. 2-(2-aminoethylamino)acetic acid (5)*

To a cold (0°C) solution of ethylene diamine (250 mL, 3.7 mol), chloroacetic acid (37.5 g, 0.4 mol) was added portionwise. The mixture was stirred for 22 h at room temperature, then toluene was added (to form an azeotrope) and the solution was evaporated under reduced pressure. 500 mL of DMSO was added to the residue and the solution was stirred overnight at room temperature. A white precipitate was formed. After filtration, this precipitate was washed with ether. Recrystallization in H<sub>2</sub>O/ethanol gives 31.9 g (68%) of white crystals. <sup>1</sup>H NMR (400 MHz, D<sub>2</sub>O): 3.3 (d, 2H, J = 2.5 Hz), 2.99 (t, 2H, J = 6.0 Hz), 2.89 (t, 2H, J = 6.0 Hz).

### 19.3.2. Preparation and evaluation of technetium-99m labelled RGD peptides

#### 19.3.2.1. Technetium-99m labelling

*HYNIC/EDDA method (method 1).* A kit formulation containing 10 mg EDDA, 20 mg tricine, 50 mg manitol and 15  $\mu\text{g}$   $\text{SnCl}_2$  was reconstituted with a mixture of 0.5 mL  $\text{Na}_2\text{HPO}_4 \cdot 2\text{H}_2\text{O}$  solution (35.6 mg/mL) and 0.5 mL  $^{99\text{m}}\text{Tc}$ -sodium pertechnetate (370–740 MBq). RGDyK-HYNIC (5  $\mu\text{L}$ , 5  $\mu\text{g}$ ) was added and the mixture was incubated at 70°C for 30 min.

Radiochemical purity (RP) was evaluated by HPLC analysis using an LC-10 AS Shimadzu liquid chromatograph coupled to a Parken 2''  $\times$  2'' NaI (TI) crystal scintillation detector and a reverse phase C18 Delta Pack column (5  $\mu\text{m}$ , 300 A, 150  $\times$  3.9 mm, Waters). The elution was obtained by means of a binary gradient system at a 1.0 mL/min flow rate, mobile phase A: 0.1% TFA in water. Mobile phase B: 0.1% TFA in acetonitrile. Elution profile: 0–1.5 min, 100% A; 1.5–18 min, linear gradient to 30% A; 18–21 min, linear gradient to 60% B; this composition was held for another 5 min. Purification was achieved on Sep-Pak C18 light cartridges (Waters) using ethanol as eluent.

*HYNIC/tricine method (method 2).* 0.5 mL of a solution of tricine (140 mg in 2 mL water) was mixed with 5  $\mu\text{L}$  of RGD-yK-HYNIC (1  $\mu\text{g}/\mu\text{L}$ ), followed by 0.5 mL  $^{99\text{m}}\text{Tc}$ -sodium pertechnetate (370–740 MBq) and 20  $\mu\text{L}$  of  $\text{SnCl}_2$  solution (1  $\mu\text{g}/\text{mL}$  in 0.1N HCl). The mixture was allowed to stand at room temperature for 15–45 min. RP was evaluated by HPLC analysis as described in Section 19.3.2.1. Purification was achieved on Sep-Pak C18 light cartridges using ethanol as eluent.

*Tc-tricarbonyl method (method 3).* The precursor *fac*- $[\text{}^{99\text{m}}\text{Tc}(\text{OH}_2)_3(\text{CO})_3]^+$  was prepared using either a kit formulation or  $\text{CO}(\text{g})$ .  $^{99\text{m}}\text{Tc}$ -sodium pertechnetate (185–1850 MBq, 1 mL) was added to an Isolink kit and the mixture was incubated at 75°C for 30 min. The  $^{99\text{m}}\text{Tc}$  precursor was prepared as follows: Na/K tartrate (20 mg),  $\text{Na}_2\text{CO}_3$  (4 mg) and  $\text{NaBH}_4$  (5.5 mg) were placed in a vial. The vial was sealed and flushed with carbon monoxide for 30 min.  $^{99\text{m}}\text{Tc}$ -sodium pertechnetate (185–1850 MBq) was added and the mixture was incubated at 75°C for 30 min.

Complex formation was checked by HPLC analysis using an LC-10 AS Shimadzu liquid chromatograph coupled to a Parken 2''  $\times$  2'' NaI (TI) crystal scintillation detector and a reverse phase Luna (Phenomenex) 5  $\mu\text{m}$  C18 column (4.69  $\times$  150 mm). Elution was performed with a binary gradient system at a 1.0 mL/min flow rate, mobile phase A: phosphate buffer pH2.5 with 2% triethylamine, mobile phase B: methanol; elution profile: 0–3 min, 100% A;

3–6 min, linear gradient to 75% A; 6–9 min, linear gradient to 66% A; 9–20 min, linear gradient to 0% A; this composition was held for another 10 min.

Substitution by RGD bearing the chelator systems DTPA, PZ1 and N- $\epsilon$ -acetyl histidine (Fig. 19.3) was performed as follows: 100  $\mu\text{L}$  of  $\text{fac-}[^{99\text{m}}\text{Tc}(\text{OH}_2)_3(\text{CO})_3]^+$  neutralized by addition of 25  $\mu\text{L}$  of  $\text{NaH}_2\text{PO}_4$  (520 mg/mL) was incubated with peptide solution (20–40  $\mu\text{L}$ , 20–40  $\mu\text{g}$ ) at 70°C for 30 min. RP was evaluated by HPLC analysis as described in Section 19.3.2.1. Purification was achieved on Sep-Pak C18 light cartridges using ethanol as eluent.

*4 + 1 mixed ligand formation method (method 4).* 100  $\mu\text{L}$  EDTA solution (10 mg  $\text{Na}_2\text{EDTA}$  per mL) and 100  $\mu\text{L}$  mannitol solution (50 mg/mL) were transferred into a vial and reacted with  $\text{SnCl}_2$  solution (0.1 mg, 20  $\mu\text{L}$ ), and  $^{99\text{m}}\text{Tc}$ -sodium pertechnetate (300–1500 MBq) was added for 15–20 min at room temperature. The RP was checked by thin layer chromatography (TLC) using Whatman 1 paper/acetone.  $\text{NS}_3(\text{COOH})_3$  (0.3 mg, 100  $\mu\text{L}$ ) was added to  $^{99\text{m}}\text{Tc}$ -EDTA/mannitol and the solution was transferred to a vial containing 0.05–0.15 mg CN-L1-RGD or CN-L2-RGD peptides in methanol. The mixture was incubated at 50°C for 2 h. RP was controlled by HPLC as described in Section 19.3.2.1. Purification was achieved on HPLC using identical conditions.

*Nitrido complex formation method (method 5).*  $\text{Na}[^{99\text{m}}\text{TcO}_4]$  (0.9 mL, 300 MBq) was added to a vial containing 5.0 mg of SDH and 0.05 mg of  $\text{SnCl}_2 \cdot 2\text{H}_2\text{O}$  (suspended in 0.10 mL of saline). The mixture was kept at room temperature for 15 min. To the resulting solution, 0.025–0.1 mg of peptide 7, dissolved in 0.4 mL of saline, and 0.125 mg of PNP5, dissolved in 0.1 mL of ethanol, were simultaneously added. The vial was heated at 100°C for 1 h. RP was controlled by HPLC as described above.

### 19.3.2.2. *In vitro* evaluation

*Stability in labelling medium.* Technetium-99m labelled peptides were incubated at room temperature and the RP was checked by HPLC analysis as described in Section 3.2.1 for up to 4 h after labelling.

*Stability in plasma, liver and kidney homogenates.* Liver and kidney homogenates were prepared as follows: freshly excised rat kidneys and liver were rapidly rinsed and homogenized for 1 min at room temperature in 20mM HEPES buffer pH7.3, in 30% concentration, with an Ultra-Turrax T25 homogenator. The Sep-Pak purified radiolabelled peptides (100  $\mu\text{L}$ ) were incubated either with human plasma or fresh homogenates (1 mL) for up to 120 min. After different incubation times (10, 30, 60 and 120 min), samples were precipitated with ethanol, centrifuged (1750g, 5 min) and analysed by HPLC as described in Section 19.3.2.1.

*Histidine and/or cysteine challenge.* Radiolabelled peptides (40  $\mu\text{L}$ ) were incubated with 100–1000 molar excess of either histidine or cysteine solution (40  $\mu\text{L}$  labelled) at 37°C and analysed by HPLC at 1, 2, 3 and 4 h as described in Section 19.3.2.1.

*Protein binding studies.* Radiolabelled RGD peptides purified by Sep-Pak (25  $\mu\text{L}$ ) were incubated with human plasma (450  $\mu\text{L}$ ) at 37°C for 180 min. At 30, 60, 120 and 180 min, 25  $\mu\text{L}$  samples were added to Microspin G-50 columns (Pharmacia Biotech), which were prespun at 2000g for 1 min. Columns were centrifuged again at 2000g for 2 min and the collected eluate and the column were counted in an NaI scintillation counter. Protein bound peptide was calculated as the percentage eluted from the column.

### 19.3.2.3. *In vivo* evaluation

*Normal biodistribution.* Animal studies were approved by the Ethics Committee of the Faculty of Chemistry. Normal CD1 mice (female, 25–30 g, three animals per group) were injected via a lateral tail vein with  $^{99\text{m}}\text{Tc}$ -RGD peptides (0.1 mL, 0.037–0.37 MBq). At different intervals after injection animals were sacrificed by neck dislocation. Whole organs and samples of blood and muscle were collected, weighed and assayed for radioactivity. Total urine volume was collected during the biodistribution period and was also removed from the bladder after sacrifice. The bladder, urine and intestines were not weighed. Corrections by different sample geometry were applied when necessary. The results were expressed as % dose/organ.

*Biodistribution in mice bearing induced tumours.* A culture of B16F1 murine melanoma cells was expanded and treated with trypsin previous to inoculation. A cell suspension in PBS ( $2.5 \times 10^6$  cells/mL) was prepared and 200  $\mu\text{L}$  was injected subcutaneously in the right limb of C57B16 mice (8–10 weeks old). Ten to 15 days later, the animals developed palpable tumour nodules and were used for biodistribution.

Three animals per group were injected via a lateral tail with  $^{99\text{m}}\text{Tc}$ -RGD peptides (0.1 mL, 0.037–0.37 MBq). At different intervals after injection the animals were sacrificed by neck dislocation. Whole tumour and samples of blood and muscle were collected, weighed and assayed for radioactivity. The results were expressed as % dose/g tissue.

### 19.3.3. Preparation and evaluation of technetium-99m labelled annexin 13 peptides

Technetium-99m labelling, stability studies as well as biodistribution studies were conducted as reported for RGD peptides above.

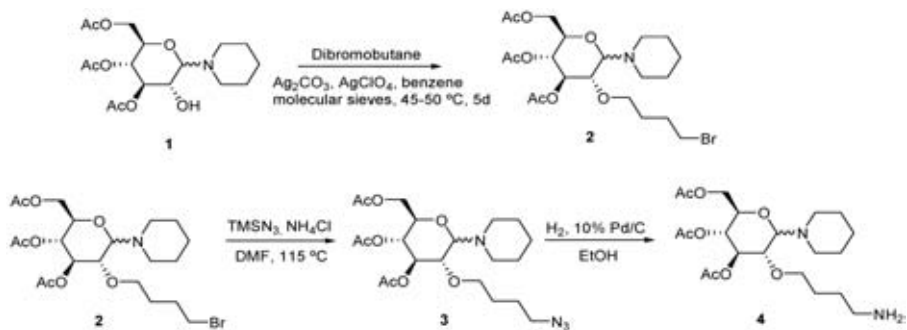


FIG. 19.1. Synthesis of precursor for glucose derivatives.

### 19.3.3.1. Biodistribution in animals treated with doxorubicin

Two groups of adult female Wistar rats (250–300 g, three animals per group) were used. Group 1 was injected intraperitoneally with 5 mg/kg of doxorubicin (Farmaco). Group 2 received an identical volume of saline. After 48 h all animals were injected via a lateral tail vein with  $^{99\text{m}}\text{Tc}$ -annexin 13 peptides (0.1 mL, 0.037–0.37 MBq) and at 1 h post-injection biodistribution was performed as in Section 19.3.2.3. The results were expressed as % dose/g of heart, muscle or blood.

## 19.4. RESULTS AND DISCUSSION

### 19.4.1. Glucose derivatives

Glucose is considered a key molecule in metabolic function and therefore availability of a  $^{99\text{m}}\text{Tc}$  labelled glucose as a single photon emission computed tomography analogue to the well established positron emission tomography tracer [ $^{18}\text{F}$ ]FDG is considered of great interest. As a first step to achieve this goal, synthesis of glucose derivatives containing adequate donor groups for  $^{99\text{m}}\text{Tc}$  labelling using the approaches under investigation was pursued.  $\beta$ -D-pentaacetyl glucose was used as the starting material. The whole process is shown in Fig. 19.1. As a first step a six-carbon linker was introduced by a two-step procedure [19.16, 19.17]. The same synthesis scheme was also used to produce an analogous derivative with a four-carbon linker. The following step consisted of the substitution of the bromine atom by an amino group in order to introduce appropriate chelators for labelling with  $^{99\text{m}}\text{Tc}$  using the

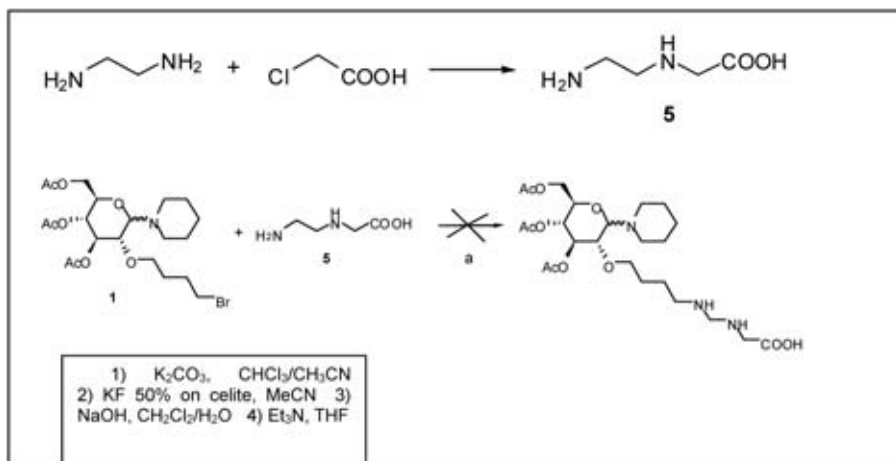


FIG. 19.2. Synthesis of potential glucose derivatives for  $^{99m}Tc$  labelling.

Tc(V)-nitrido and Tc(III) mixed ligand approaches. The procedure was initially performed on the bromobutyl derivative. All intermediate products were obtained with reasonable yield and high purity, as demonstrated by  $^1H$  NMR analysis. The results agreed with bibliographic data. Reaction schemes for inclusion of appropriate chelators and final deprotection of the glucose moiety are being performed.

A potential tridentate chelator for the Tc(I) tricarbonyl core is the 2-(2-aminoethylamino)-acetic acid. Synthesis was easily achieved upon reaction between diamine and chloroacetic acid, as shown in Fig. 19.2, and the expected product was obtained with a reasonable yield and high purity, as demonstrated by  $^1H$  NMR analysis. Different synthesis strategies have been applied to combine this chelator with the bromo derivative of glucose, but there was very little success until this report.

#### 19.4.2. RGD peptides

Peptides targeting the integrin receptor were also chosen as interesting molecules to be labelled with  $^{99m}Tc$  for in vivo tumour targeting. The integrin receptor occurs at very low or undetectable levels in only a subset of epithelial cells in normal adults, but is consistently overexpressed in carcinomas, especially at the invasive edge and in a stage where metastatic processes are initiated. Peptides target the  $\alpha_v\beta_{3/6}$  receptor and contain the RGD sequence (Arg-Gly-Asp) [19.18–19.20]. The ‘model’ peptide selected for the studies was a cyclic RGD peptide (c(RGDyK)) including the amino acid lysine, which was

TABLE 19.1. c(RGDyK) DERIVATIVES USED IN THIS STUDY

Peptide	Chelator	Labelling method
1	HYNIC	EDDA/tricine (1), tricine (2)
2	DTPA	Tc(I)-tricarboxyl (3)
3	PZ1	Tc(I)-tricarboxyl (3)
4	N- $\epsilon$ -acetyl-histidine	Tc(I)-tricarboxyl (3)
5	L1-CN	Tc(III) 4 + 1 mixed ligand (4)
6	L2-CN	Tc(III) 4 + 1 mixed ligand (4)
7	Cysteine	Tc(V)-nitrido (5)

used to introduce a variety of chelators. The HYNIC (hydrazidonicotinamide) derivative was used as a model, since procedures for labelling peptides using this chelator are well established. DTPA, PZ1 and N- $\epsilon$ -acetyl- were the selected moieties for the Tc(I)-tricarboxyl approach, cysteine was used as a chelator for the Tc(V)-nitrido core and two isocyanide derivatives, RGDyK-L1CN and RGDyK-L2CN, were used for the Tc(III) mixed ligand approach. Table 19.1 summarizes the different RGD peptides used in this study, and their structures are shown in Fig. 19.3.

#### 19.4.2.1. Labelling of RGD peptides with HYNIC

All peptides were dissolved in 0.01N HCl in a concentration of 1  $\mu\text{g}/\mu\text{L}$  and analysed by reverse phase HPLC using different acetonitrile/TFA gradients, in order to establish their retention time and corroborate their purity. Detection was accomplished by on flow ultraviolet (UV) detection at 220 and 280 nm. These studies demonstrated that all peptides were in optimal condition, with only minor impurities, and were consequently adequate for labelling. The peptide RGDyK-HYNIC was labelled with  $^{99\text{m}}\text{Tc}$  using either EDDA or tricine as coligands. High specific activity (750–1500 Ci/mmol) was obtained by both methods. RP greater than 91% and stability of at least 6 h were achieved when EDDA was used as a coligand. Sep-Pak purification using C18 light cartridges eluted with ethanol increased the RP to >96%, but only 40–50% of the activity was recovered. Two different species (25% and 75%, respectively) were formed when the coligand was tricine. However, only 0.9% of the activity corresponded to a low retention time species, probably oxidation products. No significant change was achieved by Sep-Pak purification. Instability was significant, with an increase of oxidation products from 0.9%

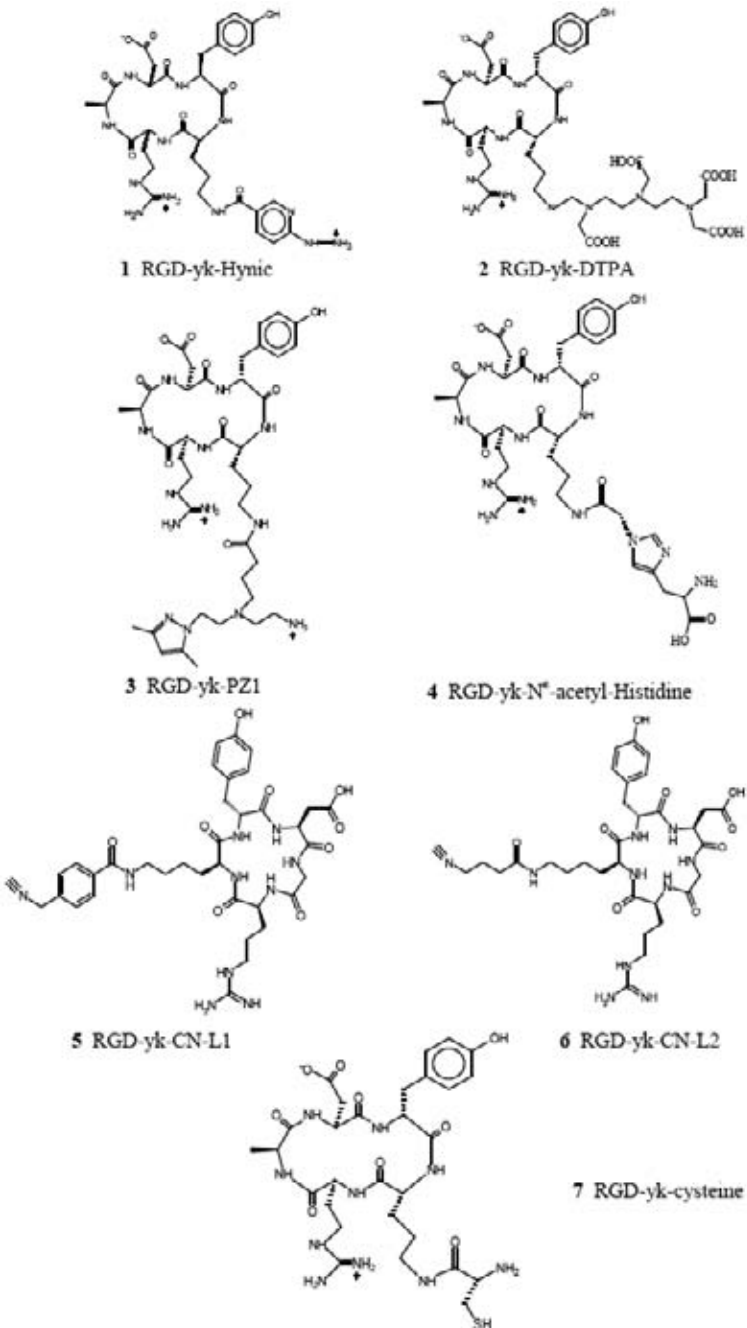


FIG. 19.3. Structure of RGD peptides.

( $t = 0$ ) to 8.6% (2 h) and 13.9% (4 h). In vitro stability in plasma, kidney and liver homogenates was also studied. No evidence of metabolic degradation was observed. Cystein challenge with 1000:1 molar excess of cysteine was performed. No evidence of ligand exchange was observed up to 4 h.

Binding to plasma protein was studied using size exclusion chromatography. A very low protein binding of about 2% was obtained when EDDA was the coligand, indicating low lipophilicity and correlating with a high in vitro stability. Protein binding was not modified significantly by incubation time. A high protein binding of 44% resulted for the peptide having tricine as a coligand. This result might be explained by the high in vitro instability of the labelled compounds formed by method 2.

Biodistribution in normal CD1 mice at 1 h and 4 h post-injection was studied only for the labelled peptide obtained by method 1. Table 19.2 shows biodistribution results as a function of time.

Blood, lung and liver uptake at 1 h post-injection was low ( $1.6 \pm 0.8\%$ ,  $0.34 \pm 0.05\%$  and  $5.5 \pm 0.6\%$ , respectively), as expected from a product with low lipophilicity and protein binding. Clearance from blood and lungs after 4 h was almost complete. Excretion occurs mainly through the urinary tract ( $70 \pm 6\%$  and  $78 \pm 2\%$  at 1 h and 4 h, respectively). Stomach and thyroid values were within acceptable levels ( $0.8 \pm 0.1\%$  and  $0.04 \pm 0.01\%$ , respectively, at 4 h), indicating minimal in vivo reoxidation.

TABLE 19.2. BIODISTRIBUTION RESULTS FOR RGDyK-HYNIC IN NORMAL CD1 MICE

	% dose/organ			
	0.5 h	1 h	2 h	4 h
Blood	$1.9 \pm 0.6$	$1.6 \pm 0.7$	$0.41 \pm 0.05$	$0.28 \pm 0.02$
Liver	$3.7 \pm 0.6$	$5.5 \pm 0.6$	$4.0 \pm 0.1$	$4.8 \pm 0.5$
Lungs	$0.34 \pm 0.06$	$0.34 \pm 0.05$	$0.17 \pm 0.02$	$0.17 \pm 0.02$
Spleen	$0.16 \pm 0.02$	$0.15 \pm 0.06$	$0.12 \pm 0.02$	$0.13 \pm 0.04$
Kidneys	$1.6 \pm 0.4$	$1.2 \pm 0.2$	$0.97 \pm 0.07$	$0.76 \pm 0.09$
Thyroid	$0.04 \pm 0.02$	$0.07 \pm 0.01$	$0.04 \pm 0.02$	$0.04 \pm 0.01$
Muscle	$5.9 \pm 0.6$	$4.5 \pm 1.1$	$3.3 \pm 0.1$	$2.5 \pm 0.2$
Stomach	$0.7 \pm 0.1$	$0.9 \pm 0.1$	$0.47 \pm 0.06$	$0.8 \pm 0.2$
Intestine	$5.6 \pm 0.7$	$6.8 \pm 0.9$	$5.0 \pm 0.5$	$7.0 \pm 0.6$
Bladder and urine	$68.8 \pm 4.3$	$69.5 \pm 6.0$	$79.5 \pm 1.5$	$78.3 \pm 1.6$

TABLE 19.3. BIODISTRIBUTION RESULTS FOR RGD $\gamma$ K-HYNIC IN C57B16 MICE BEARING INDUCED B16F1 MURINE MELANOMA

	% dose/g tissue	
	1 h	4 h
Blood	1.8 $\pm$ 0.5	0.34 $\pm$ 0.06
Muscle	0.92 $\pm$ 0.35	0.84 $\pm$ 0.19
Tumour	1.7 $\pm$ 0.5	1.2 $\pm$ 0.4
Tumour/muscle	2.6 $\pm$ 0.5	1.4 $\pm$ 0.2
Tumour/blood	1.3 $\pm$ 0.2	3.6 $\pm$ 1.6

Tumour uptake was evaluated in an animal model obtained by subcutaneous inoculation of B16F1 murine melanoma cells in C57B16 mice at 1 h and 4 h post-injection (Table 19.3). Tumour uptake at 1 h post-injection was high (2.1  $\pm$  0.7%), but the clearance after 4 h was considerable (0.7  $\pm$  0.3%).

#### 19.4.2.2. Labelling of RGD peptides with tricarbonyl

Labelling using the Tc-tricarbonyl approach was performed for peptides 2–4. Specific activities achieved by this method were significantly lower (15–125 Ci/mmol). Labelling yields were very different, according to the chelator present in each peptide. PZ1 (peptide 3) resulted in the highest RP (>95%) and a stability of at least 4 h.

RP achieved with DTPA (peptide 2) was variable (40–85%), but Sep-Pak purification increased these values to 85–98%. No significant decomposition was observed for at least 4 h. RP of  $^{99m}\text{Tc}$  labelled N- $\epsilon$ -acetyl-histidine derivative (peptide 4) was high (>90%) when the peptide was labelled soon after reconstitution and the labelled peptide was stable in the labelling medium for at least 2 h. However, stability problems of the cold peptide during storage were observed both in frozen and in lyophilized form. RP of the labelled peptide decreased considerably after short periods of reconstitution and made work with this derivative very difficult.

Histidine challenge was performed for peptides labelled by the Tc-tricarbonyl approach by incubation with 1000:1 molar excess of histidine followed by HPLC analysis. Histidine forms very stable complexes with the Tc-tricarbonyl precursor, and consequently *in vitro* and *in vivo* transchelation might be expected. This test assessing *in vitro* stability in the presence of histidine helps in predicting *in vivo* stability. No evidence of transchelation was

CHAPTER 19

TABLE 19.4. BIODISTRIBUTION RESULTS FOR TRICARBONYL LABELLED RGDyK-DTPA, RGDyK-PZ1 AND RGDyK-N- $\epsilon$ -ACETYL-HISTIDINE IN NORMAL CD1 MICE

	RGDyK-DTPA	
	% dose/organ	
	0.5 h	2 h
Blood	6.0 $\pm$ 0.8	1.9 $\pm$ 0.3
Liver	6.8 $\pm$ 1.9	6.2 $\pm$ 0.9
Lungs	0.7 $\pm$ 0.1	0.3 $\pm$ 0.01
Spleen	0.37 $\pm$ 0.12	0.32 $\pm$ 0.07
Kidneys	2.3 $\pm$ 0.4	1.6 $\pm$ 0.1
Thyroid	0.12 $\pm$ 0.05	0.04 $\pm$ 0.01
Muscle	9.4 $\pm$ 2.6	5.3 $\pm$ 0.4
Stomach	0.89 $\pm$ 0.07	0.7 $\pm$ 0.1
Intestine	8.8 $\pm$ 1.3	7.4 $\pm$ 1.3
Bladder and urine	51.7 $\pm$ 5.1	67.3 $\pm$ 2.4

	RGDyK-PZ1			
	% dose/organ			
	0.5 h	1 h	2 h	4 h
Blood	2.0 $\pm$ 0.5	5.3 $\pm$ 0.7	1.4 $\pm$ 0.08	1.1 $\pm$ 0.2
Liver	13.0 $\pm$ 1.7	12.3 $\pm$ 1.2	8.5 $\pm$ 1.4	5.8 $\pm$ 1.4
Lungs	0.5 $\pm$ 0.06	0.51 $\pm$ 0.09	0.28 $\pm$ 0.04	0.18 $\pm$ 0.05
Spleen	0.34 $\pm$ 0.04	0.40 $\pm$ 0.10	0.23 $\pm$ 0.04	0.13 $\pm$ 0.07
Kidneys	2.4 $\pm$ 0.3	2.2 $\pm$ 0.2	1.50 $\pm$ 0.2	1.1 $\pm$ 0.2
Thyroid	0.08 $\pm$ 0.01	0.04 $\pm$ 0.01	0.04 $\pm$ 0.02	0.05 $\pm$ 0.01
Muscle	6.1 $\pm$ 1.2	5.3 $\pm$ 1.6	2.8 $\pm$ 0.5	2.0 $\pm$ 1.0
Stomach	1.0 $\pm$ 0.4	0.8 $\pm$ 0.2	0.6 $\pm$ 0.04	0.6 $\pm$ 0.1
Intestine	12.5 $\pm$ 5.0	19.5 $\pm$ 4.2	15.4 $\pm$ 1.6	20.9 $\pm$ 3.7
Bladder and urine	52.8 $\pm$ 7.4	49.8 $\pm$ 6.3	64.3 $\pm$ 2.1	62.4 $\pm$ 7.0

TABLE 19.4. BIODISTRIBUTION RESULTS FOR TRICARBONYL LABELLED RGDyK-DTPA, RGDyK-PZ1 AND RGDyK-N- $\epsilon$ -ACETYL-HISTIDINE IN NORMAL CD1 MICE (cont.)

	RGDyK-N- $\epsilon$ -acetyl-histidine			
	% dose/organ			
	0.5 h	1 h	2 h	4 h
Blood	13.8 $\pm$ 2.6	11.6 $\pm$ 2.4	9.3 $\pm$ 2.3	8.3 $\pm$ 1.7
Liver	11.1 $\pm$ 2.2	11.6 $\pm$ 2.2	9.3 $\pm$ 2.0	10.7 $\pm$ 0.4
Lungs	1.5 $\pm$ 0.5	0.81 $\pm$ 0.1	0.90 $\pm$ 0.09	0.7 $\pm$ 0.1
Spleen	0.35 $\pm$ 0.14	0.36 $\pm$ 0.02	0.20 $\pm$ 0.02	0.32 $\pm$ 0.10
Kidneys	2.8 $\pm$ 0.3	2.3 $\pm$ 0.3	2.0 $\pm$ 0.2	2.1 $\pm$ 0.2
Thyroid	0.08 $\pm$ 0.03	0.14 $\pm$ 0.09	0.07 $\pm$ 0.01	0.15 $\pm$ 0.01
Muscle	15.5 $\pm$ 3.0	8.7 $\pm$ 1.1	12.5 $\pm$ 1.4	8.5 $\pm$ 1.0
Stomach	1.1 $\pm$ 0.5	1.2 $\pm$ 0.2	0.63 $\pm$ 0.04	0.9 $\pm$ 0.2
Intestine	15.6 $\pm$ 3.4	19.8 $\pm$ 2.8	18.8 $\pm$ 0.7	26.0 $\pm$ 3.1
Bladder and urine	24.4 $\pm$ 6.8	27.8 $\pm$ 5.7	36.4 $\pm$ 6.1	35.9 $\pm$ 4.4

observed for radiolabelled peptides 2 and 3. Peptide 4, however, was unstable and transchelation of 20% at 1 h and 40% at 2 h incubation was observed. In vitro stability of  $^{99m}\text{Tc}$  labelled peptides 2 and 3 in plasma, kidney and liver homogenates was also studied at 30 min, 1 h and 2 h of incubation and no evidence of metabolic degradation was observed.

Binding to plasma protein was also studied by size exclusion chromatography for peptides 2 and 3. Results of 11.8% and 19.7% of binding, respectively, were obtained. Protein binding was not modified significantly by incubation time. Table 19.4 shows biodistribution results as a function of time.

Biodistribution of peptide 2 is characterized by low blood activity (1.9  $\pm$  0.3% at 2 h post-injection), by preferential urinary excretion (dose in urine 67.3  $\pm$  2.4% at 2 h post-injection) and by significant liver uptake (6.2  $\pm$  0.9% at 2 h post-injection) and hepatobiliary excretion (7.4  $\pm$  1.3% at 2 h post-injection). Peptide 3 also presents low blood activity (1.4  $\pm$  0.08% at 2 h post-injection), similar liver uptake (8.5  $\pm$  1.4% at 2 h post-injection) but considerably higher hepatobiliary excretion (20.9  $\pm$  3.7% at 2 h post-injection), probably due to higher lipophilicity. Peptide 3 presents significantly high blood and liver activity (9.3  $\pm$  2.3% and 9.3  $\pm$  2.0%, respectively, at 2 h post-injection) and similar values of hepatobiliary and urinary excretion (26.0  $\pm$  3.1% and 35.9  $\pm$  4.4%,

TABLE 19.5. BIODISTRIBUTION RESULTS FOR RGD $\gamma$ K-PZ1 IN C57B16 MICE BEARING INDUCED B16F1 MURINE MELANOMA

	% dose/g tissue (1 h)
Blood	6.1 $\pm$ 0.3
Muscle	0.62 $\pm$ 0.11
Tumour	1.5 $\pm$ 0.6
Tumour/muscle	2.4 $\pm$ 0.7
Tumour/blood	0.25 $\pm$ 0.10

respectively, at 2 h post-injection). These results are indicative of poor in vivo stability and high protein binding.

Tumour uptake at 1 h post-injection was evaluated in C57B16 mice bearing induced B16F1 murine melanoma (Table 19.5).

#### 19.4.2.3. Labelling of RGD peptides with 4 + 1 chemistry

The 4 + 1 mixed ligand chelate system, based on the simultaneous coordination of a tetradentate NS<sub>3</sub> ligand and a monodentate isocyanide to Tc(III), was applied to the preparation of <sup>99m</sup>Tc-RGD peptides. The lysine  $\epsilon$  amino group of c(RGD $\gamma$ K) was functionalized with an isocyanide using the bifunctional chelating agents 4-isocyanomethyl-benzoic acid (L1) and 4-isocyanobutanoic acid (L2). A tris-(2-mercaptoethyl)-amine (NS<sub>3</sub>) derivative containing three non-coordinating carbonyl groups was used as a tetradentate tripodal ligand. Technetium-99m labelling was performed using <sup>99m</sup>Tc-EDTA as a precursor. This procedure enables labelling of 0.05–0.1 mg of peptide with an RP of 60%. Purification by HPLC resulted in an RP >95% and stability was >90% after 24 h. The identity of the technetium labelled products was corroborated upon coinjection with analogous 4 + 1 rhenium complex conjugated peptide.

Plasma protein binding of 27% for <sup>99m</sup>Tc-(NS<sub>3</sub>)(COOH)<sub>3</sub>L1 (peptide 5) and 15% for <sup>99m</sup>Tc-(NS<sub>3</sub>)(COOH)<sub>3</sub>L2 (peptide 6) was found. Normal biodistribution results in CD1 mice were consistent with lipophilicity and protein binding (Table 19.6). RGD peptide 5 showed higher initial blood, lung and liver uptake as well as slower depuration. Excretion occurs mainly by the urinary system for both compounds (% dose in urine of 55.0% and 75.2% at 2 h post-injection).

Uptake in C57B16 mice bearing induced B16F1 murine melanoma was moderate for both compounds, but higher tumour/muscle ratios were achieved for peptide 5 at all time points ( $1.8 \pm 0.2$  and  $1.0 \pm 0.1$  at 4 h post-injection) (Table 19.7).

TABLE 19.6. BIODISTRIBUTION RESULTS FOR CN-RGDyK DERIVATIVES LABELLED WITH 4 + 1 CHEMISTRY IN NORMAL CD1 MICE

CN-L1-RGDyK				
	% dose/organ			
	0.5 h	1 h	2 h	4 h
Blood	$11.3 \pm 3.2$	$6.8 \pm 1.7$	$5.3 \pm 0.67$	$2.1 \pm 0.7$
Liver	$6.3 \pm 1.0$	$4.2 \pm 0.6$	$2.4 \pm 0.1$	$1.4 \pm 0.4$
Lungs	$1.05 \pm 0.14$	$1.03 \pm 0.4$	$0.49 \pm 0.08$	$0.29 \pm 0.07$
Spleen	$0.37 \pm 0.05$	$0.18 \pm 0.09$	$0.11 \pm 0.02$	$0.09 \pm 0.03$
Kidneys	$4.2 \pm 1.0$	$3.5 \pm 0.12$	$3.4 \pm 0.5$	$2.2 \pm 0.2$
Thyroid	$0.18 \pm 0.04$	$0.16 \pm 0.05$	$0.13 \pm 0.02$	$0.08 \pm 0.05$
Muscle	$12.4 \pm 3.4$	$11.1 \pm 3.4$	$11.6 \pm 0.7$	$7.5 \pm 2.5$
Stomach	$1.4 \pm 0.1$	$0.88 \pm 0.13$	$0.90 \pm 0.26$	$0.81 \pm 0.18$
Intestine	$11.3 \pm 0.3$	$11.3 \pm 1.7$	$12.3 \pm 2.0$	$11.3 \pm 1.7$
Bladder and urine	$27.4 \pm 2.4$	$47.0 \pm 8.4$	$55.0 \pm 7.4$	$68.7 \pm 5.5$

CN-L2-RGDyK				
	% dose/organ			
	0.5 h	1 h	2 h	4 h
Blood	$3.3 \pm 0.8$	$2.1 \pm 0.6$	$0.94 \pm 0.36$	$0.40 \pm 0.15$
Liver	$4.0 \pm 1.4$	$4.0 \pm 1.4$	$1.7 \pm 0.9$	$0.52 \pm 0.03$
Lungs	$0.48 \pm 0.18$	$0.34 \pm 0.09$	$0.20 \pm 0.03$	$0.14 \pm 0.07$
Spleen	$0.18 \pm 0.05$	$0.13 \pm 0.02$	$0.08 \pm 0.03$	$0.05 \pm 0.03$
Kidneys	$4.7 \pm 1.5$	$4.5 \pm 1.6$	$2.8 \pm 1.2$	$1.0 \pm 0.3$
Thyroid	$0.04 \pm 0.02$	$0.03 \pm 0.01$	$0.01 \pm 0.01$	$0.02 \pm 0.01$
Muscle	$10.1 \pm 1.8$	$6.5 \pm 1.1$	$6.0 \pm 0.9$	$5.6 \pm 1.9$
Stomach	$1.0 \pm 0.3$	$0.78 \pm 0.31$	$0.68 \pm 0.32$	$0.32 \pm 0.10$
Intestine	$9.9 \pm 3.8$	$8.8 \pm 2.6$	$9.9 \pm 1.2$	$10.5 \pm 3.0$
Bladder and urine	$59.1 \pm 9.9$	$67.1 \pm 7.1$	$75.2 \pm 8.5$	$75.3 \pm 8.5$

TABLE 19.7. BIODISTRIBUTION RESULTS FOR RGDyK-CNL1 AND RGDyK-CNL2 LABELLED WITH 4 + 1 CHEMISTRY IN C57B16 MICE BEARING INDUCED B16F1 MURINE MELANOMA

RGDyK-CNL1				
	% dose/g tissue			
	0.5 h	1 h	2 h	4 h
Blood	7.1 ± 0.07	4.1 ± 0.1	2.4 ± 0.6	0.98 ± 0.07
Muscle	1.2 ± 0.3	1.2 ± 0.2	1.2 ± 0.4	0.61 ± 0.07
Tumour	3.7 ± 1.0	2.8 ± 0.6	2.1 ± 0.7	1.1 ± 0.3
Tumour/muscle	2.34 ± 0.06	2.28 ± 0.23	1.87 ± 0.7	1.81 ± 0.2
Tumour/blood	0.52 ± 0.15	0.68 ± 0.14	0.91 ± 0.34	1.2 ± 0.4
RGDyK-CNL2				
	% dose/g tissue			
	0.5 h	1 h	2 h	4 h
Blood	3.5 ± 0.6	2.1 ± 0.2	0.93 ± 0.35	0.61 ± 0.08
Muscle	1.3 ± 0.2	0.96 ± 0.13	0.55 ± 0.11	0.49 ± 0.18
Tumour	2.4 ± 0.4	1.7 ± 0.5	0.55 ± 0.11	0.51 ± 0.05
Tumour/muscle	2.0 ± 0.5	1.7 ± 0.3	1.0 ± 0.07	1.03 ± 0.09
Tumour/blood	0.78 ± 0.16	0.79 ± 0.20	0.62 ± 0.13	0.8 ± 0.18

#### 19.4.2.4. Labelling of RGD peptides with nitrido chemistry

Application of nitrido chemistry to the development of potential  $^{99m}\text{Tc}$  bioactive radiopharmaceuticals was another goal of this project. We worked on the labelling of the RGDyK derivative bearing a terminal bidentate cystein by means of an asymmetrical nitrido complex. The bidentate PNP5 phosphine acts as a coligand completing the coordination sphere of the metal. Technetium- $^{99m}$  labelling was performed by a two-step procedure. The Tc-nitrido group is efficiently obtained upon reduction of pertechnetate in the presence of a donor of nitrido nitrogen atoms (SDH). Simultaneous substitution of the peptide and the diphosphine yields the desired radiolabelled product with a specific activity of 185–370 Ci/mmol and an RP above 90%. The radiolabelled product is stable for at least 4 h. A protein binding of 6.9% was determined by size exclusion chromatography.

TABLE 19.8. BIODISTRIBUTION RESULTS FOR  $^{99m}\text{TcN-RGDyK-CYSTEINE}$  IN NORMAL CD1 MICE

	% dose/organ		
	0.5 h	1 h	2 h
Blood	$1.6 \pm 0.2$	$0.7 \pm 0.1$	$0.28 \pm 0.06$
Liver	$7.2 \pm 1.6$	$2.7 \pm 0.3$	$3.0 \pm 0.2$
Lungs	$0.17 \pm 0.07$	$0.11 \pm 0.03$	$0.08 \pm 0.03$
Spleen	$0.07 \pm 0.01$	$0.05 \pm 0.01$	$0.02 \pm 0.01$
Kidneys	$4.3 \pm 0.8$	$4.1 \pm 0.8$	$2.4 \pm 0.6$
Thyroid	$0.04 \pm 0.01$	$0.05 \pm 0.02$	$0.06 \pm 0.01$
Muscle	$15.5 \pm 2.9$	$18.3 \pm 1.1$	$19.3 \pm 0.9$
Stomach	$0.46 \pm 0.08$	$0.7 \pm 0.3$	$0.4 \pm 0.1$
Intestine	$20.1 \pm 3.5$	$23.6 \pm 2.5$	$25.4 \pm 4.1$
Bladder and urine	$41.7 \pm 6.2$	$45.7 \pm 4.0$	$46.4 \pm 5.4$

Normal biodistribution was studied in CD1 mice (Table 19.8). Blood, lung and liver uptake at 1 h post-injection was low ( $0.7 \pm 0.1\%$ ,  $2.7 \pm 0.3\%$  and  $0.11 \pm 0.03\%$ , respectively), as expected from a product with low protein binding. Clearance from blood after 2 h was almost complete. Combined excretion through the urinary and hepatobiliary tract ( $45.7 \pm 4.0\%$  and  $23.6 \pm 2.5\%$ , respectively, at 1 h post-injection) was observed. A remarkable feature was the high muscle uptake at all biodistribution times.

### 19.4.3. Annexin

Development of phosphatidylserine specific  $^{99m}\text{Tc}$  labelled tracers for imaging of programmed cell death was also in the focus of this project. For this purpose, the preparation, labelling and evaluation of a series of peptides containing the 13 amino acid sequence of the N-terminal portion of the protein annexin V (the hypothetically active fragment) [19.21, 19.22] was pursued. The chelators HYNIC and histidine were incorporated, producing the Anx13-HYNIC (1) and Anx13-histidine (2) derivatives.

Once received, the peptides were dissolved in saline in a concentration of  $1 \mu\text{g}/\mu\text{L}$  and analysed by reverse phase HPLC, in order to corroborate their purity. Detection was accomplished by on flow UV detection at 220 and 280 nm. These studies demonstrated that the peptides were in optimal condition.

*19.4.3.1. Labelling of annexin peptides with HYNIC and carbonyl*

Peptide 1 (Anx13-HYNIC) was labelled by a standard procedure using EDDA as a coligand. High specific activity (up to 7000 Ci/mmol) and RP (90–95%) was obtained. The labelled peptide was stable in a labelling medium for at least 4 h, and no signs of degradation were observed in plasma after up to 2 h of incubation. A protein binding of 28% was established by size exclusion chromatography. No transchelation was observed upon incubation with a molar excess of cysteine of 1000:1 for up to 2 h.

Peptide 2 (Anx13-histidine) was labelled using the Tc(I)tricarbonyl approach using the *fac*-[<sup>99m</sup>Tc(OH<sub>2</sub>)<sub>3</sub>(CO)<sub>3</sub>]<sup>+</sup> as precursor. Substitution was quantitative using 20–50 µg of peptide. A high RP (90–95%) and a specific activity of 300–500 Ci/mmol was achieved. In vitro stability of at least 4 h was established. The protein binding of this labelled peptide was very high (46.7%). Besides, significant decomposition was observed upon incubation with plasma. Activity of the main HPLC peak decreased from 90% to 73%, 60%, 28% and 17% in 30 min, 60 min, 120 min and 180 min, respectively. Histidine challenge was also performed by incubation with 1000:1 molar excess of histidine followed by HPLC analysis. No evidence of transchelation was observed for up to 2 h of incubation.

Biodistribution was studied in CD1 mice (Tables 19.9 and 19.10). Blood, lung and liver uptake at 1 h post-injection for peptide 1 was low ( $0.72 \pm 0.07\%$ ,  $0.52 \pm 0.1\%$  and  $0.06 \pm 0.03\%$ , respectively), as expected from a product with low lipophilicity and protein binding. Clearance from blood after 2 h was almost complete. Excretion occurs mainly through the urinary tract ( $87.4 \pm 6.3\%$  and  $93.9 \pm 1.9\%$  at 1 h and 2 h, respectively).

Peptide 2, however, showed higher uptake in liver, slower clearance from blood and combined excretion by urinary and hepatobiliary tract (% dose in urine  $59.7 \pm 2.8\%$  and  $55.6 \pm 3.1\%$  and % dose in intestines  $16.3 \pm 1.6\%$  and  $17.3 \pm 1.2\%$  at 1 and 2 h, respectively). Stomach and thyroid values were within acceptable levels for both peptides, indicating minimal in vivo reoxidation.

Evaluation of the potentiality for imaging in cardiac apoptosis was evaluated in an animal model described in the literature [19.23]. Apoptosis was induced in Wistar rats by intraperitoneal injection of 5 mg/kg of doxorubicin. A second group was injected with the same volume of saline and used as a control. 48 h after this treatment, <sup>99m</sup>Tc labelled peptide 2 was injected into all animals and biodistribution at 1 h post-injection was performed. The results expressed as % dose/g of blood heart and muscle are shown in Table 19.11. Cardiac uptake was very low in both animal groups and no significant difference was observed as a consequence of the apoptosis induction.

TABLE 19.9. BIODISTRIBUTION RESULTS OF ANNEXIN PEPTIDE 1 (HYNIC LABELLING) IN NORMAL CD1 MICE

	% dose/organ		
	0.5 h	1 h	2 h
Blood	3.2 ± 0.9	0.72 ± 0.07	0.23 ± 0.08
Liver	1.7 ± 0.8	0.52 ± 0.13	0.43 ± 0.10
Lungs	0.17 ± 0.06	0.06 ± 0.03	0.03 ± 0.01
Spleen	0.05 ± 0.02	0.02 ± 0.01	0.01 ± 0.01
Kidneys	2.7 ± 0.2	4.8 ± 2.8	2.1 ± 1.0
Thyroid	0.02 ± 0.01	0	0
Muscle	7.6 ± 0.4	2.4 ± 0.4	0.49 ± 0.28
Stomach	0.36 ± 0.15	0.17 ± 0.09	0.11 ± 0.09
Intestine	2.8 ± 1.5	1.2 ± 0.6	1.4 ± 0.2
Bladder and urine	72.9 ± 1.4	87.4 ± 6.3	93.9 ± 1.9

TABLE 19.10. BIODISTRIBUTION RESULTS OF ANNEXIN PEPTIDE 2 (CARBONYL LABELLING) IN NORMAL CD1 MICE

	% dose/organ		
	0.5 h	1 h	2 h
Blood	2.0 ± 0.3	1.5 ± 0.2	0.85 ± 0.03
Liver	13.1 ± 1.0	13.2 ± 3.7	12.0 ± 2.2
Lungs	0.23 ± 0.03	0.19 ± 0.03	0.15 ± 0.04
Spleen	0.10 ± 0.04	0.05 ± 0.02	0.07 ± 0.02
Kidneys	3.0 ± 0.3	2.5 ± 0.5	1.7 ± 0.1
Thyroid	0.04 ± 0.01	0.03 ± 0.02	0.04 ± 0.01
Muscle	2.4 ± 0.2	3.2 ± 2.7	1.2 ± 0.5
Stomach	1.4 ± 0.4	1.5 ± 0.3	3.2 ± 0.8
Intestine	19.0 ± 0.8	16.3 ± 1.6	17.3 ± 1.2
Bladder and urine	55.4 ± 2.2	59.7 ± 2.8	55.6 ± 3.1

TABLE 19.11. BIODISTRIBUTION RESULTS FOR Anx13-HISTIDINE (PEPTIDE 2) IN WISTAR RATS (NORMAL AND TREATED WITH DOXORUBICIN)

	% dose/g tissue	
	Non-treated	Treated with doxorubicin (5 mg/kg)
Blood	0.23 ± 0.03	0.18 ± 0.04
Muscle	0.05 ± 0.02	0.04 ± 0.03
Heart	0.07 ± 0.01	0.09 ± 0.01

## 19.5. CONCLUSIONS

The development of novel  $^{99m}\text{Tc}$  bioactive radiopharmaceuticals is an ambitious goal that requires expertise in different fields and strong collaboration among participants. Our group undertook some of the required steps during this project. Organic synthesis of glucose derivatives was started and various potential precursors were obtained and characterized. The developed chemistry gives a variety of possibilities, in particular variation of linker length and introduction of different chelators. Derivatization is in progress and requires further optimization.

Technetium-99m labelling of RGD peptides using three different approaches was performed. In vitro characterization, including RP, stability under different challenging conditions and protein binding, was performed. In vivo behaviour in normal animals was also evaluated. Comparison among chelators and labelling methods shows clear differences in the labelling yields, RPs, specific activities and overall biodistribution, thus allowing selection of the best candidates for further evaluation. Studies in a tumoural model were performed for some of the compounds, but the results were not very promising. Other biological models will be needed to decide on potentiality for nuclear medicine imaging and therapy.

Technetium-99m labelling of annexin 13 derivatives was performed using two different methods. Comparison between the physicochemical and biological behaviour of both radiolabelled peptides was performed as for the RGD peptides. Preliminary evaluation on a model for cardiac apoptosis failed to show any uptake.

The most important outcome of the project is the experience in the different labelling methodologies and the cooperation established with different participants. Continuation and extension of this cooperation to other

fields, in particular to rhenium chemistry, will be essential for the development of potential diagnostic and therapeutic radiopharmaceuticals in the future.

### ACKNOWLEDGEMENTS

The authors are thankful to R. Alberto, C. Decristoforo, A. Duatti, H. Pietzsch and I. Pirmettis for their active collaboration during the project.

### REFERENCES

- [19.1] JOHANNSEN, B., SPIES, H., "Technetium (V) as relevant to nuclear medicine", Topics in Current Chemistry, Vol. 176, Technetium and Rhenium, Springer (1995) 176.
- [19.2] DIZIO, J., et al., Technetium and rhenium- labelled progestins: Synthesis, receptor binding and in vivo distribution of an 11 $\beta$ -substituted progestin labelled with technetium-99 and rhenium-186, J. Nucl. Med. **33** (1992) 558–569.
- [19.3] JURISSON, S.S., YDON, J.D., Potential small molecule radiopharmaceuticals, Chem. Rev. **99** (1999) 2205–2218.
- [19.4] ALBERTO, R., et al., Potential of the [M(CO)<sub>3</sub>]<sup>+</sup> (M=Re, Tc) moiety for the labelling of biomolecules, Radiochim. Acta **87** (1997) 99–103.
- [19.5] ALBERTO, R., et al., Basic aqueous chemistry of [M(OH)<sub>2</sub>]<sub>3</sub>(CO)<sub>3</sub><sup>+</sup> (M=Re, Tc) directed towards radiopharmaceutical application, Coord. Chem. Rev. **190** (1999) 901–919.
- [19.6] SCHIBLI, R., SHUBIGER, A., Current use and future potential of organometallic radiopharmaceuticals, Eur. J. Nucl. Med. **29** (2002) 1529–1542.
- [19.7] EGLI, A., et al., Organometallic <sup>99m</sup>Tc- aquaion labels peptide to unprecedented high specific activity, J. Nucl. Med. **40** (1999) 1913–1917.
- [19.8] GARCÍA-GARAYOA, E., et al., Preclinical evaluation of a new, stabilized neurotensin (8-13) pseudopeptide radiolabeled with <sup>99m</sup>Tc, J. Nucl. Med. **43** (2002) 374–383.
- [19.9] PIETZSCH, H.-J., et al., Mixed-ligand technetium(III) complexes with tetradentate/monodentate NS<sub>3</sub>/isocyanide coordination: A new nonpolar technetium chelate system for the design of neutral and lipophilic complexes stable in vivo, Bioconj. Chem. **12** (2001) 538–544.
- [19.10] SEIFERT, S., et al., Novel procedures for preparing <sup>99m</sup>Tc(III) complexes with tetradentate/monodentate coordination of varying lipophilicity and adaptation to <sup>188</sup>Re analogues, Bioconj. Chem. **15** (2004) 856–863.
- [19.11] BALDAS, J., BONNYMAN, J., Substitution reactions of <sup>99m</sup>TcNCl<sub>4</sub><sup>-</sup> — A new route to a new class of <sup>99m</sup>Tc-radiopharmaceuticals, Int. J. Appl. Radiat. Isot. **36** (1985) 133.

## CHAPTER 19

- [19.12] PASQUALINI, R., et al., Bis (dithiocarbamate) nitrido technetium-99m radiopharmaceuticals: A class of neutral myocardial imaging agents, *J. Nucl. Med.* **35** (1994) 334–341.
- [19.13] BOLZATI, C., et al., Chemistry of the strong electrophilic metal fragment [99Tc(N)(PXP)]<sup>2+</sup> (PXP) diphosphine ligand). A novel tool for the selective labeling of small molecules, *J. Am. Chem. Soc.* **124** (2002) 11468–11479.
- [19.14] BOSCHI, A., et al., Asymmetrical nitrido Tc-99m heterocomplexes as potential imaging agents for benzodiazepine receptors, *Bioconj. Chem.* **14** (2003) 1279.
- [19.15] BOLZATI, C., et al., Synthesis, characterization and biological evaluation of neutral technetium(V) mixed ligand complexes containing dithiolates and aminodiphosphines. A novel system for linking technetium biomolecules, *Bioconj. Chem.* **15** (2004) 628–637.
- [19.16] POZSGAY, E., et al., Synthesis of kojidextrins and their protein conjugates. Incidence of steric mismatch in oligosaccharide synthesis, *J. Org. Chem.* **62** (1997) 2832–2846.
- [19.17] HODGE, J., et al., N-(3,4,6-triacetyl-D-glucosyl)-piperidine and its use in preparing 2-substituted glucose derivatives, *J. Am. Chem. Soc.* **74** (1952) 1498–1500.
- [19.18] BROOKS, P., Role of integrins in angiogenesis, *Eur. J. Cancer* **32** (1996) 2423–2429.
- [19.19] RUOSLAHTI, E., PIERSCHBACHER, M.D., Arg-Gly-Asp: A versatile cell recognition signal, *Cell* **44** (1986) 517–518.
- [19.20] VAN HAGEN, P.M., et al., Evaluation of a radiolabelled cyclic DTPA-RGD analogue for tumour imaging and radionuclide therapy, *Int. J. Cancer (Radiat. Oncol. Invest.)* **90** (2000) 186–198.
- [19.21] TAIT, J.F., et al., Development of annexin V mutants suitable for labeling with Tc(I)-carbonyl complex, *Bioconj. Chem.* **13** (2002) 1119–1123.
- [19.22] TAIT, J.F., et al., Structural requirements for in vivo detection of cell death with <sup>99m</sup>Tc-annexin V, *J. Nucl. Med.* **46** (2005) 807–815.
- [19.23] AROLA, O.J., et al., Acute doxorubicin cardiotoxicity involves cardiomyocyte apoptosis, *Cancer Res.* **60** (2000) 1789–1792.



## Chapter 20

### **IN VITRO AND IN VIVO EVALUATION OF [<sup>99m</sup>Tc(CO)<sub>3</sub>-CYCLO[Arg-Gly-Asp-D-Tyr-Lys(PZ1)]]**

S. ALVES, J.D.G. CORREIA, I. SANTOS

Department of Chemistry, Institute of Nuclear Technology, Portugal

C. DECRISTOFORO

Universitätsklinik für Nuklearmedizin, Innsbruck, Austria

R. ALBERTO

Institute of Inorganic Chemistry, University of Zurich, Switzerland

C.J. SMITH

Department of Radiology, University of Missouri-Columbia School of  
Medicine, Columbia, Missouri, United States of America

#### **Abstract**

As part of a coordinated research project, Development of <sup>99m</sup>Tc Based Small Biomolecules Using Novel <sup>99m</sup>Tc Cores, with the International Atomic Energy Agency, we report the design and development of a new cyclic RGD analogue cyclo[Arg-Gly-Asp-D-Tyr-Lys(PZ1)] (PZ1 = 3,5Me<sub>2</sub>-PZ(CH<sub>2</sub>)<sub>2</sub>N((CH<sub>2</sub>)<sub>3</sub>COOH)(CH<sub>2</sub>)<sub>2</sub>NH<sub>2</sub>) that can be radiolabelled with the <sup>99m</sup>Tc(CO)<sub>3</sub> metal fragment. Radiochemical evaluation, including synthesis, in vitro uptake analyses and in vivo pharmacokinetics in normal mice, is discussed.

#### 20.1. INTRODUCTION

Peptides containing the amino acid sequence Arg-Gly-Asp (RGD) have been used extensively to target integrin receptors upregulated on tumour cells and neovasculature. The RGD consensus sequence appears in several proteins of the extracellular matrix, including vitronectin, fibronectin, fibrinogen, von

Willebrand factor, thrombospondin and osteopontin [20.1]. Integrin recognition of the canonical RGD sequence plays a prominent role in many cell–cell and cell–ECM interactions. Integrins are cell surface transmembrane glycoproteins that exist as  $\alpha\beta$  heterodimers. At least 24 different combinations of  $\alpha\beta$  heterodimers are known [20.2]. The integrins of most interest in cancer imaging and therapy contain the  $\alpha_v$  subunit, particularly the  $\alpha_v\beta_3$  and  $\alpha_v\beta_5$  subtypes. The structure of the extracellular domain of the  $\alpha_v\beta_3$  integrin has been determined crystallographically to a resolution of 3.1 Å [20.3].

The  $\alpha_v\beta_3$  integrin is known to be overexpressed in many tumour types and expressed at lower levels in normal tissues [20.4]. Both  $\alpha_v\beta_3$  and  $\alpha_v\beta_5$  subtypes are expressed in neovasculature during angiogenesis. These expression patterns form the basis of attempts to image angiogenesis and tumour formation in vivo using RGD based peptide targeting vectors. RGD peptides used to target integrin receptors generally fall into one of three categories: linear, disulphide cyclized and head to tail cyclized.

At least two examples of integrin targeting using linear RGD-containing peptides have been described. In one instance, two RGD peptide sequences from human fibronectin were linked in series and labelled with  $^{99m}\text{Tc}$  [20.5]. A single cysteine residue intervening between the two RGD sequences presumably served to localize  $^{99m}\text{Tc}$  binding at that position within the molecule. This conjugate was studied in 14 melanoma patients. In this group, 11 metastatic lesions were visualized, with high background activity in the lung and abdomen [20.5].

A second study described the N-terminal labelling of an RGD-containing peptide (KPQVTRGDVFTEG-NH<sub>2</sub>) with an [<sup>18</sup>F]fluorobenzoyl moiety by solid phase synthesis [20.6]. RGD dependent tumour uptake of this agent was not observed in a C26/BalbC in vivo model, probably due to both the relatively low affinity of the linear molecule for the integrin receptor (IC<sub>50</sub> = 20 μM) and to the rapid rate of proteolytic breakdown of the construct.

Cyclization of RGD-containing peptides has been shown to increase both the specificity and affinity of peptides for defined integrin subtypes [20.7, 20.8]. In one instance, screening of a phage display library yielded an RGD peptide cyclized via two disulphide bonds, termed RGD-4C [20.9]. An abbreviated version of this cyclic RGD peptide has been used as a substrate for  $^{99m}\text{Tc}$  labelling [20.10]. The affinity of the  $^{99m}\text{Tc}$  labelled peptide for the  $\alpha_v\beta_3$  integrin was estimated to be approximately 70-fold lower than that of RGD-4C, suggesting that some aspect of the tracer synthesis could be responsible for a lack of specific tumour uptake in vivo.

A large number of studies have been carried out utilizing head to tail cyclized RGD peptides, and these represent the most promising class of RGD based imaging agents [20.11]. Early investigations into the effect of head to tail

cyclization on RGD affinity for the  $\alpha_v\beta_3$  integrin led to the identification of cyclo(RGDfV), an  $\alpha_v\beta_3$  antagonist with a low nanomolar IC<sub>50</sub>. Further characterization led to the observation that a bulky hydrophobic residue was required in position 4 for maximum affinity, while position 5 was tolerant of a range of substitutions [20.12].

One result of these observations was that D- or L-tyrosine was inserted into either position 4 or 5 to yield RGD peptide substrates for iodination reactions. The resulting <sup>125</sup>I labelled peptides have been tested in vitro and in vivo to examine the feasibility of using cyclic RGD peptides as in vivo imaging agents [20.12]. These peptides displayed rapid blood clearance through hepatobiliary excretion, and tumour uptake at 1 h post-injection of  $1.30 \pm 0.13\%$  injected dose (ID)/g in M21 melanoma human tumour xenografts. In an attempt to improve the pharmacokinetics of these compounds, a glycosylated analogue was synthesized and tested [20.13]. Substitution of a lysine residue permitted the attachment of a carbohydrate moiety to the  $\alpha$  amino group of lys5. The resulting molecule showed decreased uptake in liver and intestine relative to an analogue lacking carbohydrate, with  $1.22 \pm 0.32\%$  ID/g vs.  $11.23 \pm 1.95\%$  ID/g in the liver at 1 h post-injection. Additionally, the glycosylated species showed increased tumour uptake and residualization, with  $2.05 \pm 0.55\%$  ID/g in M21 melanoma human tumour xenografts. Similar biodistribution results were obtained using an <sup>18</sup>F labelled galacto-RGD analogue [20.14].  $\alpha_v\beta_3$  targeted cyclic pentapeptides commonly include a lysine residue in position 5 for the purpose of appending a diverse array of labelling moieties. Positron emission tomography tracers have been synthesized by appending a PEG-[<sup>18</sup>F]fluorobenzoate domain [20.15]. Metal chelators such as DTPA and DOTA have also been used to coordinate a range of radionuclides useful for imaging and therapy [20.16, 20.17].

Increasing attention is currently focused on the development of dimeric or multimeric cyclic RGD peptide constructs. Multimerization is expected to increase the apparent affinity of targeting vectors for their cognate receptors due to avidity effects. In one instance, a dimeric cyclo(RGDfK) construct was synthesized by bridging two lysine amino groups with a DOTA-glutamic acid moiety [20.18]. This peptide, when labelled with <sup>111</sup>In, showed high receptor mediated tumour uptake of  $7.5\%$  ID/g at 2 h post-injection in an OVCAR-3/nude mouse in vivo model. Receptor mediated uptake in non-target tissues such as spleen, liver and lung was also surprisingly high in this study.

In a second study, cyclo(RGDfE) multimers were formed using variable length PEG spacers linked to a diamino propionic acid/lysine backbone [20.19]. Monomeric, dimeric and tetrameric forms were synthesized and labelled with <sup>18</sup>F. Biodistribution of the dimer compared favourably with that of a <sup>18</sup>F labelled galacto-RGD analogue.

Alberto et al. have well established the organometallic chemistry of Tc(I)- and Re(I)-tricarbonyl complexes containing the *fac*-M(CO)<sub>3</sub> moiety [20.20–20.27]. They have shown that the *fac*-M(CO)<sub>3</sub> moiety can be obtained by direct carbonylation of the permethylate salt, by the action of borohydride under atmospheric carbon monoxide pressure [20.28–20.34]. With the advent of the new kit preparation of the *fac*-<sup>99m</sup>Tc(CO)<sub>3</sub>(H<sub>2</sub>O)<sub>3</sub> synthon (Isolink, available from Mallinckrodt), clearly a new avenue for preparation of <sup>99m</sup>Tc based bioconjugates has been established.

In this paper, as part of a coordinated research project, Development of <sup>99m</sup>Tc Based Small Biomolecules Using Novel <sup>99m</sup>Tc Cores, we report the design and development of a new cyclic RGD analogue cyclo[Arg-Gly-Asp-D-Tyr-Lys(PZ1)] (PZ1 = 3,5Me<sub>2</sub>-PZ(CH<sub>2</sub>)<sub>2</sub>N((CH<sub>2</sub>)<sub>3</sub>COOH)(CH<sub>2</sub>)<sub>2</sub>NH<sub>2</sub>) that can be radiolabelled with the <sup>99m</sup>Tc(CO)<sub>3</sub> metal fragment. Radiochemical evaluation, including synthesis, in vitro uptake analyses and in vivo pharmacokinetics in normal mice, is discussed.

## 20.2. MATERIALS

Cyclo[Arg-Gly-Asp-D-Tyr-Lys(PZ1)] was from Biosynthan. Funding from the IAEA allowed for the purchase of this peptide conjugate. All other reagents were purchased from either Fisher Scientific or Sigma-Aldrich and used without further purification. High performance liquid chromatography (HPLC) analyses of the <sup>99m</sup>Tc complexes were performed on a Shimadzu C-R4A chromatography system equipped with a Berthold LB 505 gamma detector and with a tunable absorption ultraviolet (UV) detector. Separations were achieved on Nucleosil 250-4 100-10 C18 columns or on 250-4 100-5 C18 columns using flows of 1 mL/min or 0.5 mL/min, respectively. UV detection: 254 nm; eluents: A-TFA 0.1%, B-ACN; method: *t* = 0–3 min: 0% ACN; 3–3.1 min: 0–25% ACN; 3.1–9 min: 25% ACN; 9–9.1 min: 25–34% ACN; 9.1–20 min: 34–100% ACN; 20–22 min: 100% ACN; 22–22.1 min: 100–0% ACN; 22.1–30 min: 0% ACN. Technetium-99m, in the form of <sup>99m</sup>TcO<sub>4</sub><sup>-</sup>, was eluted from a <sup>99</sup>Mo/<sup>99m</sup>Tc generator provided by Mallinckrodt.

## 20.3. METHODS

### 20.3.1. Synthesis of PZ1 (3,5Me<sub>2</sub>-PZ(CH<sub>2</sub>)<sub>2</sub>N((CH<sub>2</sub>)<sub>3</sub>COOH)(CH<sub>2</sub>)<sub>2</sub>NH-BOC)

An equimolar amount of BOC-ON in THF was added dropwise to a solution of 3,5Me<sub>2</sub>-PZ(CH<sub>2</sub>)<sub>2</sub>NH(CH<sub>2</sub>)<sub>2</sub>NH<sub>2</sub> (4.0 g, 22.5 mmol) in THF (70 mL)

at 0°C, and the reaction mixture was left at this temperature for 3 h. A saturated aqueous solution of Na<sub>2</sub>CO<sub>3</sub> and CH<sub>2</sub>Cl<sub>2</sub> was added at room temperature, the organic phase was separated, dried over anhydrous MgSO<sub>4</sub> and vacuum dried. The yellow oil obtained, 3,5Me<sub>2</sub>-PZ(CH<sub>2</sub>)<sub>2</sub>NH(CH<sub>2</sub>)<sub>2</sub>NH<sub>2</sub>-BOC (5.7 g, 20 mmol), was dissolved in CH<sub>3</sub>CN (60 mL) and excess of K<sub>2</sub>CO<sub>3</sub>, KI and ethyl 4-bromobutyrate was added. After 11 days at room temperature, the solution was filtered, vacuum dried and the residue purified by column chromatography (ethyl acetate (50–100%)/hexane).

The BOC protected derivative (4 g, 10.2 mmol) was dissolved in THF, excess of NaOH was added and refluxed overnight, for saponification of the ethyl ester. The solution was neutralized with HCl 1N, the solvents were removed and the residue extracted with CH<sub>2</sub>Cl<sub>2</sub>. The crude product obtained corresponding to 3,5Me<sub>2</sub>-PZ(CH<sub>2</sub>)<sub>2</sub>N((CH<sub>2</sub>)<sub>3</sub>COOH)(CH<sub>2</sub>)<sub>2</sub>NH-BOC was purified by column chromatography (MeOH (5–100%)/CHCl<sub>3</sub>), yielding a pale yellow oil (2.2 g, 86%). <sup>1</sup>H nuclear magnetic resonance (NMR) (CDCl<sub>3</sub>) δ: 5.81 (s, pyrazol, 1H), 4.93 (s br, NH, 1H), 4.12 (t br, CH<sub>2</sub>, 2H), 3.04 (q br, CH<sub>2</sub>, 2H), 2.86 (t br, CH<sub>2</sub>, 2H), 2.58–2.64 (m, CH<sub>2</sub>, 4H), 2.42 (t, CH<sub>2</sub>, 2H), 2.24 (s, CH<sub>3</sub>, 3H), 2.19 (s, CH<sub>3</sub>, 3H), 1.79 (m, CH<sub>2</sub>, 2H), 1.40 (s, C(CH<sub>3</sub>)<sub>3</sub>, 9H). KBr: ν(C = O) 1694, 1559, 1442, 1210, 845, 804, 725.

### 20.3.2. Peptide synthesis

Cyclo[Arg-Gly-Asp-D-Tyr-Lys(PZ1-BOC)] was synthesized and purchased from Biosynthan. Upon pre-activation of the 3,5Me<sub>2</sub>-PZ(CH<sub>2</sub>)<sub>2</sub>N((CH<sub>2</sub>)<sub>3</sub>COOH)(CH<sub>2</sub>)<sub>2</sub>NH-BOC with TNTU/DIEA (1:1.2:1.2) in DMF for 1 h, two equivalents of the corresponding ONB-ester solution (HPLC: ~72% active ester formation) were added to one equivalent of the unprotected cyclopeptide side chain cyclo[Arg-Gly-Asp-D-Tyr-Lys] in DMF (pH8 after addition of NMM) with stirring. The reaction time was 48 h.

Briefly, the cyclic peptide was purified by standard solid phase synthetic methods. The peptide was purified using preparative reverse phase HPLC techniques, utilizing a Shimadzu LC-8A system equipped with a SPD-6A tunable absorbance detector calibrated to 220 nm. HPLC solvents consisted of H<sub>2</sub>O containing 0.05% TFA (solvent A) and acetonitrile/water (80:20 containing 0.05% trifluoroacetic acid (solvent B). An UltraSep C18 column (10.0 μm, 100 Å, 20 × 250 mm, Sepserv) was used with a flow rate of 15.0 mL/min. The HPLC gradient system begins with a solvent composition of 95% A and 5% B and follows a linear gradient of 2.5% B per minute. MALDI/MS of the BOC protected cyclo peptide was performed, confirming the final structure of the purified conjugate (calculated: 970.2; experimental: 970.4).

The cyclic RGD analogue cyclo[Arg-Gly-Asp-D-Tyr-Lys(PZ1)] was obtained by reacting cyclo[Arg-Gly-Asp-D-Tyr-Lys(PZ1-BOC)] with TFA/H<sub>2</sub>O (95:2) for 1 h. Purification by preparative HPLC was performed and the final purified analogue was analysed by MALDI/MS (calculated: 870.2; experimental: 870.1).

### **20.3.3. Radiolabelling of PZ1-RGD conjugate cyclo[Arg-Gly-Asp-D-Tyr-Lys(PZ1)]**

To  $5 \times 10^{-5}$  M cyclo[Arg-Gly-Asp-D-Tyr-Lys(PZ1)] in aqueous solution was added 0.25 mL of [<sup>99m</sup>Tc(H<sub>2</sub>O)<sub>3</sub>(CO)<sub>3</sub>]<sup>+</sup> prepared via the Isolink kit (Fig. 20.1). The solutions were allowed to incubate at 75°C for 1 h. Quality control (radiochemical yield and purity determination) of the products was determined by reverse phase HPLC. Product purification and final preparation of the labelled species were performed by collecting the samples off of the chromatographic system, removal of solvent via a nitrogen stream and reconstitution in normal saline. All further analyses were carried out using the HPLC purified products.

### **20.3.4. In vitro serum stability**

To 1 mL of whole human blood, collected in heparinized polypropylene tubes, was added a solution of the <sup>99m</sup>Tc-RGD conjugate (≈10 MBq). The mixture was incubated at 37°C. Samples were taken at 5 min, 45 min and 4 h post-incubation and centrifuged for 15 min at 2000 rpm at 4°C. The plasma was separated and ethanol was added in a 2:1 (v/v) ratio. The samples were centrifuged at 3000 rpm and the supernatant was analysed by HPLC. A reverse phase Hypersil 120 ODS column (250 × 4 mm, 10 μm) was used and the mobile phase was methanol/water at 1.0 mL/min flow rate and with a linear gradient of 70–100% methanol over 10 min followed by 10 min at 100% of methanol.

### **20.3.5. In vitro internalization analysis**

In vitro internalization analysis of [<sup>99m</sup>Tc(CO)<sub>3</sub>-cyclo[Arg-Gly-Asp-D-Tyr-Lys(PZ1)]] was carried out by incubation of  $\sim 3 \times 10^6$  cells (see Section 20.4 for the list of cell lines tested) (in D-MEM/F-12K media containing 0.01M MEM and 2% BSA, pH5.5) in the presence of 20 000 cpm [<sup>99m</sup>Tc(CO)<sub>3</sub>-cyclo[Arg-Gly-Asp-D-Tyr-Lys(PZ1)]] at 37°C for selected timepoints of 30, 60, 90 and 120 min. Upon completion of the incubation, the reaction medium was aspirated and the cells were washed four times with media. Surface bound radioactivity was removed by washing the cells with 0.2N acetic acid/0.5M NaCl

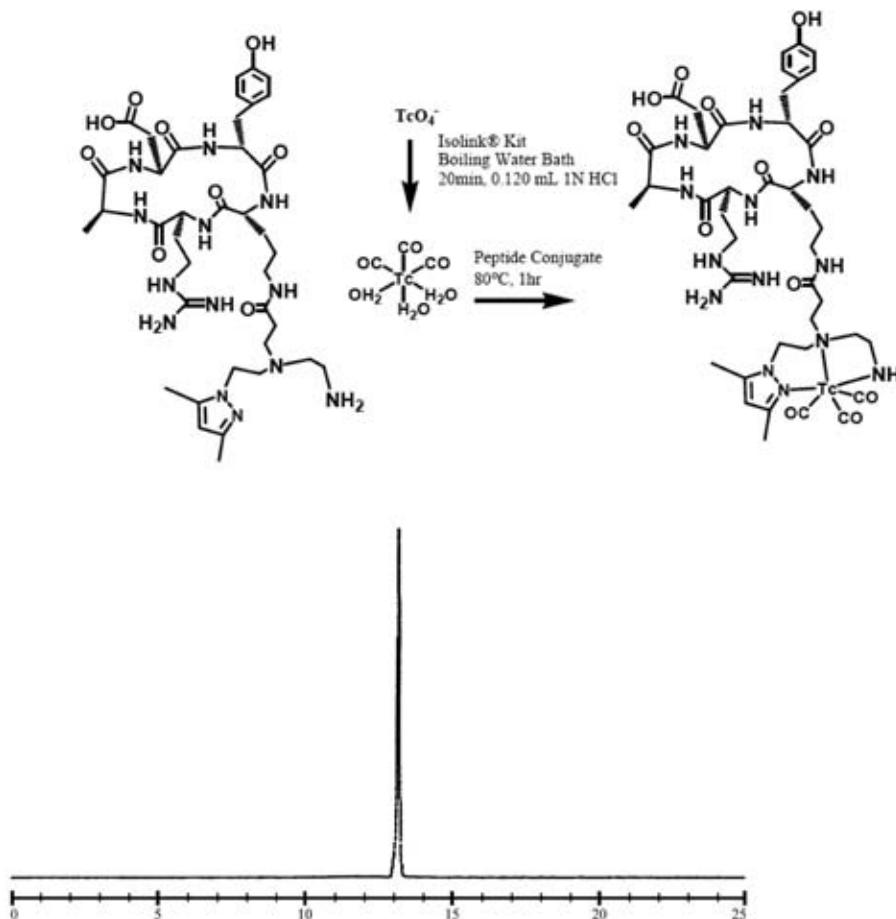


FIG. 20.1. Technetium-99m radiolabelling and purification ( $R_t = 13.2$  min) of the RDG sequence.

(pH2.5). The percentage of internalized, cell associated radioactivity as a function of time was determined by counting in a Packard Riastar gamma counting system.

### 20.3.6. In vivo evaluation of [ $^{99m}\text{Tc}(\text{CO})_3$ -cyclo[Arg-Gly-Asp-D-Tyr-Lys(PZ1)]] in normal mouse models

Biodistribution studies were performed using groups of five female CD1 mice (randomly bred, Charles River) weighing approximately 20–25 g each. Prior to administration, complexes were diluted with PBS, pH7.4. Animals

were intravenously injected with 100  $\mu\text{L}$  (2.5–12.5 MBq) of each preparation via the tail vein and were maintained on a normal diet ad libitum. At 5 min, 30 min, 1 h and 4 h mice were sacrificed by cervical dislocation. The radioactive dosage administered and the radioactivity in the sacrificed animals were measured in a dose calibrator (Aloka, Curiometer IGC-3). The difference between the radioactivity in the injected animal and the sacrificed animal was assumed to be due to excretion, mainly urinary excretion. Blood samples were taken by cardiac puncture at sacrifice. Tissue samples of the main organs were then removed, weighed and counted in a gamma counter (Berthold, LB2111). Accumulation of radioactivity in the tissues was calculated and expressed as a percentage of the injected dose per total organ (% ID/total organ) and/or per gram tissue (% ID/g organ). For blood, bone and muscle, the total activity was calculated assuming that these organs constitute 6%, 10% and 40% of the total weight, respectively. Urine was also collected at sacrifice.

The *in vivo* stability of the complexes was assessed by urine and murine serum HPLC analysis, using the above referred experimental conditions. Urine: the urine was collected at sacrifice and filtered through a Millex GV filter (0.22  $\mu\text{m}$ ) before reverse phase HPLC analysis. Serum: blood collected from mice was immediately centrifuged for 15 min at 3000 rpm at 4°C and the serum was separated. Aliquots of 100  $\mu\text{L}$  of serum were treated with 200  $\mu\text{L}$  of ethanol to precipitate the proteins. Samples were centrifuged at 4000 rpm for 15 min at 4°C. Supernatant was collected and passed through a Millex GV filter (0.22  $\mu\text{m}$ ) prior to reverse phase HPLC analysis. Liver homogenate: after injection, animals were kept for 1 h on a normal diet ad libitum; immediately after sacrifice, the liver was excised and rapidly rinsed and placed in chilled 50mM TRIS/0.2M sucrose buffer, pH7.4, wherein it was homogenized. Aliquots (in duplicate) of the liver homogenate were treated with ethanol in a 2:1 EtOH/aliquot v/v ratio. The samples were then centrifuged at 25 000 rpm for 15 min at 4°C, filtered through Millex GV (0.22  $\mu\text{m}$ ) and analysed by HPLC, following the experimental conditions referred to above.

## 20.4. RESULTS

Synthesis of PZ1-BOC (3,5Me<sub>2</sub>-PZ(CH<sub>2</sub>)<sub>2</sub>N((CH<sub>2</sub>)<sub>3</sub>COOH)(CH<sub>2</sub>)<sub>2</sub>NH-BOC) was as previously reported (Fig. 20.2) [20.35–20.38]. PZ1-BOC was provided to Biosynthan for conjugation to RGD by the working group of I. Santos. The cyclic peptide cyclo[Arg-Gly-Asp-D-Tyr-Lys(PZ1)] (Fig. 20.3) was synthesized by standard solid phase synthetic methods. The peptide was purified using preparative reverse phase HPLC techniques and characterized by MALDI/MS (exact mass, 869, experimental, 870.1; Fig. 20.4).

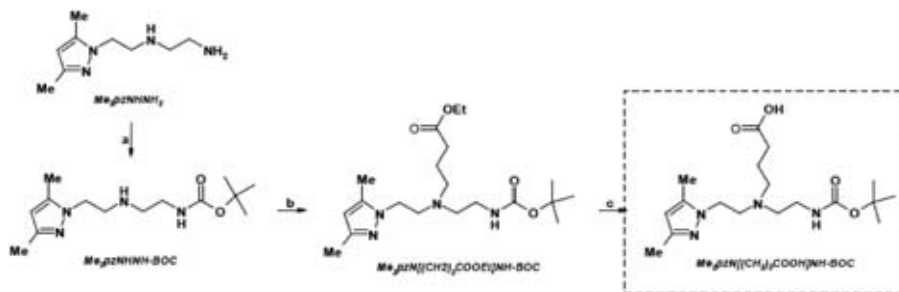


FIG. 20.2. Synthesis of  $\text{Me}_2\text{PZN}[(\text{CH}_2)_3\text{COOH}]\text{NH-Boc}$ : (a) BOC-ON, THF/DMF,  $0^\circ\text{C}$ , 2 h; (b) ethyl 1-bromobutyrate/ $\text{K}_2\text{CO}_3/\text{KI}/\text{CH}_3\text{CN}$ ; (c) NaOH,  $\text{H}_2\text{O}$ , THF, reflux, overnight.

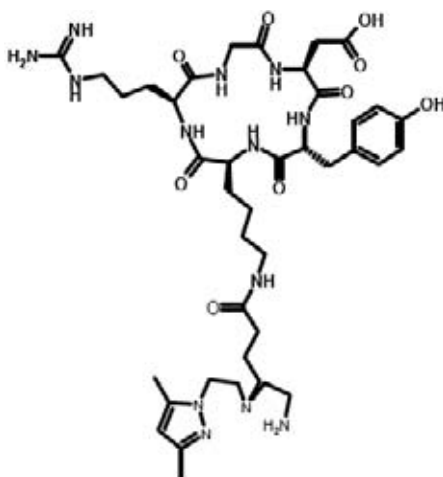


FIG. 20.3. Cyclo[Arg-Gly-Asp-D-Tyr-Lys(PZ1)].

The  $^{99\text{m}}\text{Tc}$  conjugate of the cyclo[Arg-Gly-Asp-D-Tyr-Lys(PZ1)] was produced with a high yield ( $\geq 90\%$ ) upon addition of  $[\text{}^{99\text{m}}\text{Tc}(\text{H}_2\text{O})_3(\text{CO})_3]^+$  to a vial containing  $100\ \mu\text{g}$  ( $\sim 5 \times 10^{-5}\text{M}$ ) of cyclo[Arg-Gly-Asp-D-Tyr-Lys(PZ1)] with heating. Radiochemical yields of the new  $^{99\text{m}}\text{Tc}$  conjugates were monitored by reverse phase HPLC. The HPLC chromatographic profile for the  $^{99\text{m}}\text{Tc}$  conjugate of cyclo[Arg-Gly-Asp-D-Tyr-Lys(PZ1)] is shown in Fig. 20.4. The chromatogram shows a single peak (retention time ( $R_t$ ) = 14.2 min) corresponding to the new radiometallated conjugate. Pertechnetate had a retention time of 3.0 min under identical HPLC conditions. The HPLC chromatographic profile for the non-metallated conjugate cyclo[Arg-Gly-Asp-D-Tyr-Lys(PZ1)] (Fig. 20.5) shows the non-metallated conjugate as a single peak with a retention time of 8.8 min.

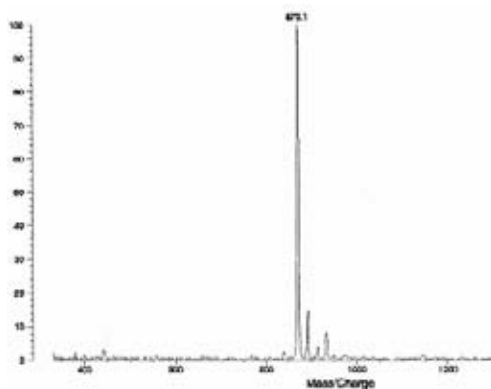


FIG. 20.4. MALDI/MS (exact mass, 869, experimental, 870.1).

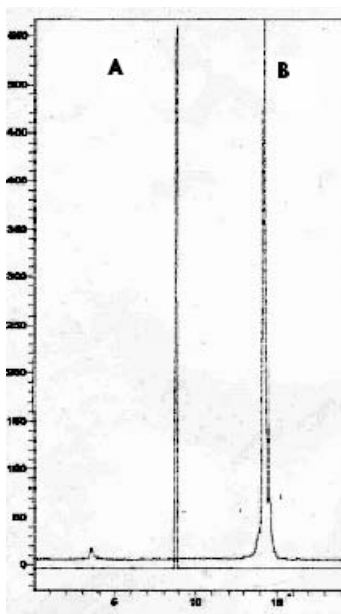


FIG. 20.5. HPLC chromatogram of the RGD analogue *cyclo*[Arg-Gly-Asp-D-Tyr-Lys(PZI)] (A) and of the metallated conjugate *cyclo*[Arg-Gly-Asp-D-Tyr-Lys(PZI)<sup>99m</sup>Tc(CO)<sub>3</sub>] (B).

The stability of the new conjugate was studied *in vitro* as previously described [20.35–20.37]. The conjugate showed remarkable *in vitro* stability in human serum. In fact, the conjugate was  $\geq 8\%$  intact at 4 h post-preparation.

TABLE 20.1. CELL LINES USED IN THIS STUDY

Cell line	Target
T-84	Colon cancer
MDA MB-231	Estrogen independent breast cancer
PC-3	Prostate cancer
CFPAC-1	Pancreatic cancer
T-47D	Estrogen dependent breast cancer
DU145	Prostate cancer
A375	Melanoma cancer
NCI H69	Lung cancer
LnCAP	Prostate cancer
OVCAR	Ovarian cancer

Specific binding of the [ $^{99m}\text{Tc}(\text{CO})_3\text{-cyclo}[\text{Arg-Gly-Asp-D-Tyr-Lys}(\text{PZ1})]$ ] and conjugate to receptors expressed on OVCAR-3 cells, available through the University of Missouri-Columbia Cell Core (Table 20.1), following incubation (40 min) of  $3 \times 10^6$  cells with high specific activity  $^{99m}\text{Tc}$  analogues (i.e. HPLC purified conjugates) is shown in Fig. 20.6. The degree of internalization and efflux for the  $^{99m}\text{Tc}$ -RGD conjugate to this particular cell line was minimal. In fact, less than 1% of the incubated dose was taken up by the OVCAR-3 cells. An  $\text{IC}_{50}$  of  $2.49 \pm 6.65\text{mM}$  was found in the OVCAR-3 cell line using  $^{125}\text{I}$  echistatin as the radiolabelling gold standard.

We further assessed the uptake of the  $^{99m}\text{Tc}$ -RGD conjugate in additional cell lines (Table 20.1). It can be ascertained that no appreciable number of effective receptors was available on these particular cell lines. In accordance with the protocol set by the Subcommittee for Animal Studies at the Harry S. Truman Memorial Veterans Hospital, we could not perform *in vivo* pharmacokinetic evaluation in tumour bearing mouse models, as there was no appreciable tumour uptake in *in vitro* models.

Biodistribution studies in normal CD1 mice showed the [ $^{99m}\text{Tc}(\text{CO})_3\text{-cyclo}[\text{Arg-Gly-Asp-D-Tyr-Lys}(\text{PZ1})]$ ] conjugate to be a hydrophilic species (Figs 20.7 and 20.8). The conjugate effectively cleared the bloodstream 30 min post-injection, and more than 60% of the injected dose was excreted at 4 h post-injection via the renal-urinary pathway for the PZ1 conjugate. Some residualization in normal kidney is evident for the [ $^{99m}\text{Tc}(\text{CO})_3\text{-cyclo}[\text{Arg-Gly-Asp-D-Tyr-Lys}(\text{PZ1})]$ ] conjugate ( $\sim 6\%$  ID/g, 1 h post-injection), but this radioactivity washes out significantly over time. Biodistributions of this conjugate

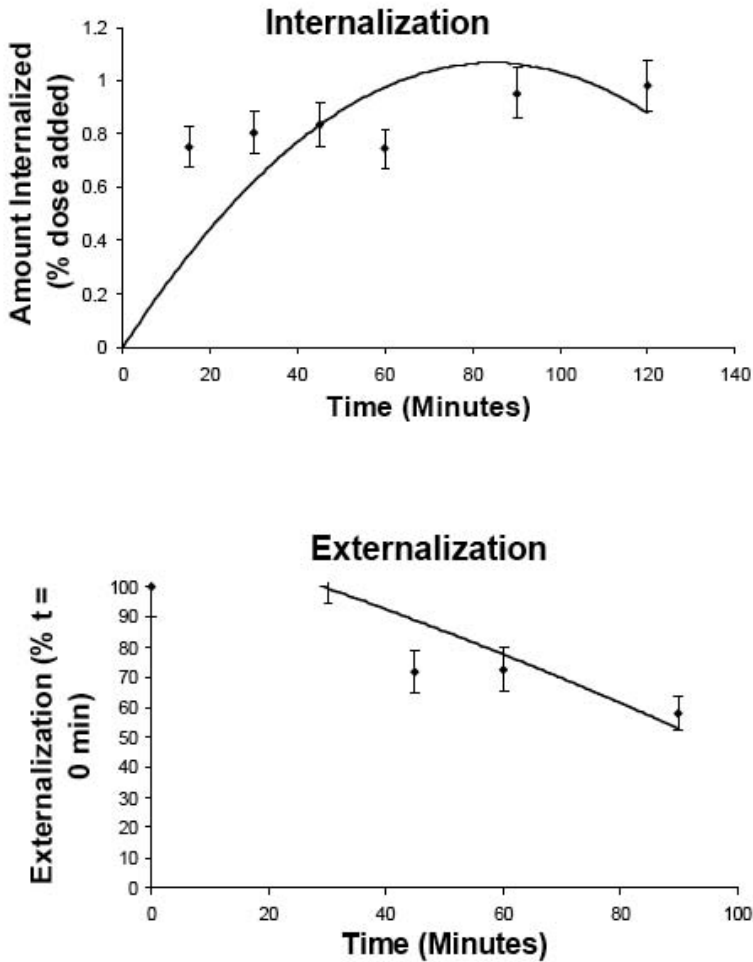


FIG. 20.6. Internalization/externalization of  $^{99m}\text{Tc}$ -RGD conjugate in OVCAR-3 cancerous cells.

were validated at the University of Missouri-Columbia Biomolecular Imaging Core and are comparable with those reported by Santos et al. (Table 20.2).

To demonstrate the effective stability of the new conjugate, urine, serum and liver were analysed at 1 h post-injection. The samples were homogenized and reinjected on to the HPLC to verify product stability. The conjugate showed remarkable in vivo stability as  $\geq 98\%$  of the conjugates were in the form  $[^{99m}\text{Tc}(\text{CO})_3\text{-cyclo}[\text{Arg-Gly-Asp-D-Tyr-Lys}(\text{PZ1})]]$  at 1 h post-injection.

CHAPTER 20

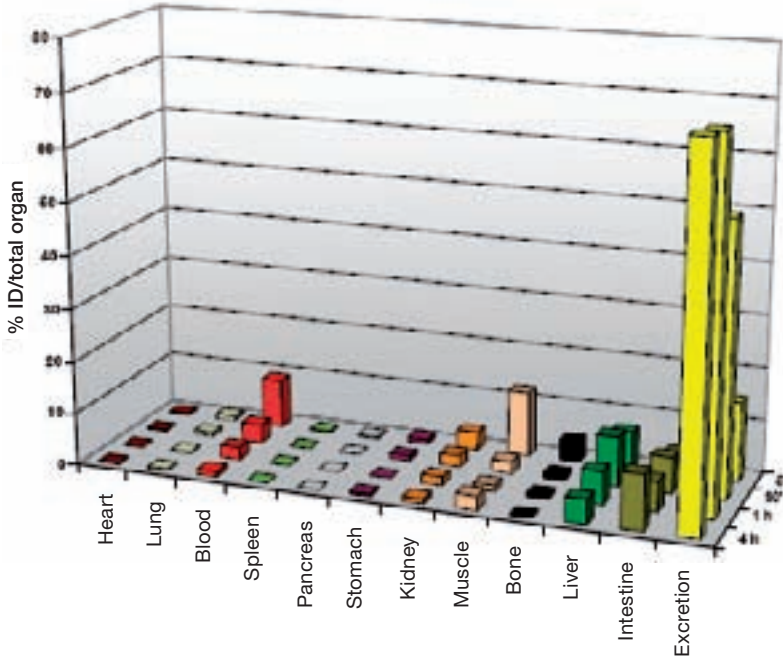


FIG. 20.7. Results of the biodistribution studies of  $[^{99m}\text{Tc}(\text{CO})_3\text{-cyclo}[\text{Arg-Gly-Asp-D-Tyr-Lys}(\text{PZI})]]$  in normal CD1 mice (% ID/organ).

TABLE 20.2. BIODISTRIBUTION RESULTS

	1 h	4 h	24 h
Bladder	2.34 (1.42)	1.06 (0.23)	0.24 (0.33)
Heart	0.56 (0.09)	0.31 (0.11)	0.08 (0.13)
Lungs	1.24 (0.21)	0.59 (0.12)	0.19 (0.09)
Liver	2.03 (0.20)	0.90 (0.21)	0.18 (0.03)
Kidney	3.11 (0.32)	1.75 (0.27)	0.56 (0.10)
Spleen	1.14 (0.31)	0.45 (0.06)	0.42 (0.60)
Stomach	0.71 (0.16)	0.76 (0.27)	0.18 (0.07)
Intestines	4.25 (0.70)	6.80 (1.26)	0.57 (0.18)
Muscle	0.34 (0.05)	0.26 (0.05)	0.12 (0.05)
Bone	1.06 (0.36)	0.66 (0.12)	0.23 (0.07)
Pancreas	0.53 (0.11)	0.33 (0.10)	0.04 (0.01)
Blood	0.23 (0.06)	0.03 (0.01)	0.01 (0.01)

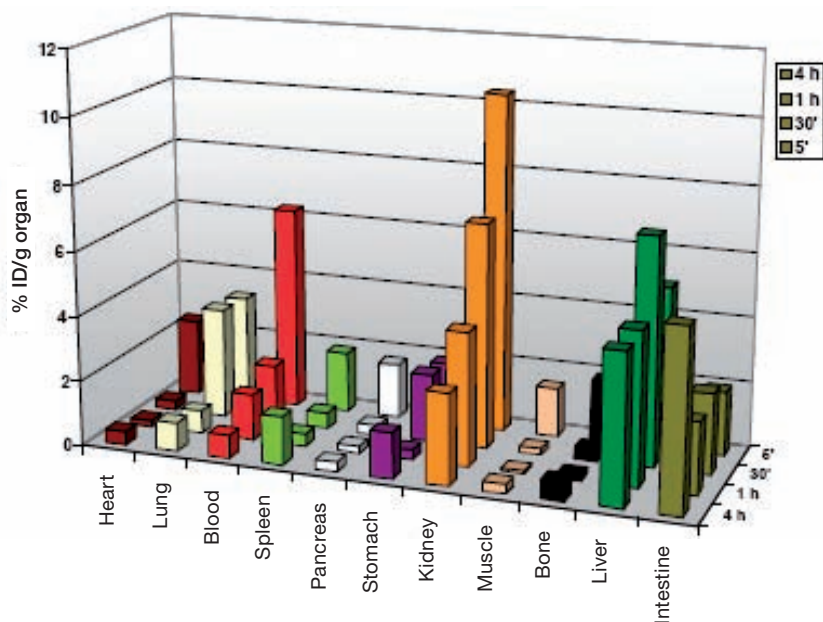


FIG. 20.8. Results of the biodistribution studies of [ $^{99m}\text{Tc}(\text{CO})_3\text{-cyclo}[\text{Arg-Gly-Asp-D-Tyr-Lys}(\text{pz1})]$ ] in normal CD1 mice (% ID/g).

## 20.5. CONCLUSION

Recent reports by Chen et al. have described positive uptake of  $^{18}\text{F}$ -fluorobenzoyl c(RGDyK) peptide in subcutaneous U87MG glioblastoma and PC3 prostate tumour models. Images indicated receptor specific uptake with high tumour to background ratios, although these data were not reported [20.39]. In our hands, we were to effectively show that the new conjugate cyclo[Arg-Gly-Asp-D-Tyr-Lys(PZ1)] could be radiolabelled with a very high yield upon simple heating with *fac*- $^{99m}\text{Tc}(\text{CO})_3(\text{H}_2\text{O})_3$  synthon. The new conjugate was stable in human serum for periods up to 4 h post-incubation. Preliminary in vivo evaluation of the conjugate demonstrated rapid clearance from the bloodstream and excretion primarily via the renal-urinary pathway. Subsequent stability evaluation of the conjugate in human tissue showed that the conjugate was not readily metabolized in vivo, with 98% of the conjugate remaining intact upon in vivo administration. We were not able to effectively demonstrate in vitro cellular uptake for the [ $^{99m}\text{Tc}(\text{CO})_3\text{-cyclo}[\text{Arg-Gly-Asp-D-Tyr-Lys}(\text{PZ1})]$ ] conjugate in the human prostate PC3 tumour cell line. We did make a single effort to image a mouse that had been xenografted with PC3

## CHAPTER 20

tumours on the right and left flanks of the back legs. Planar images were obtained, and specific uptake of the new conjugate was not observed. Subsequent animal studies (tumour bearing mouse models) on this tumour model were not performed, as set by institutional protocol.

## REFERENCES

- [20.1] HEALY, J.M., et al., Peptide ligands for integrin selected from random phage display libraries, *Biochemistry* **34** (1995) 3948–3955.
- [20.2] REINMUTH, N., et al.,  $\alpha_v\beta_3$  integrin antagonist S247 decreases colon cancer metastasis and angiogenesis and improves survival in mice, *Cancer Res.* **63** (2003) 2079–2087.
- [20.3] XIONG, J., et al., Crystal structure of the extracellular segment of integrin  $\alpha_v\beta_3$ , *Science* **294** (2001) 339–345.
- [20.4] KERR, J.S., SLEE, A.M., MOUSA, S.A., Small molecule  $\alpha_v$  integrin antagonists: Novel anticancer agents, *Exp. Opin. Invest. Drugs* **9** (2000) 1271–1279.
- [20.5] SIVOLAPENKO, G.B., et al., Imaging of metastatic melanoma utilizing a technetium-99m labelled RGD-containing synthetic peptide, *Eur. J. Nucl. Med.* **25** (1998) 1383–1389.
- [20.6] SUTCLIFFE-GOULDEN, J.L., et al., Rapid solid phase synthesis and biodistribution of  $^{18}\text{F}$ -labelled linear peptides, *Eur. J. Nucl. Med.* **29** (2002) 754–759.
- [20.7] PIERSCHBACHER, M.D., RUOSLAHTI, E., Influence of stereochemistry of the sequence Arg-Gly-Asp-Xaa on binding specificity in cell adhesion, *J. Biol. Chem.* **262** (1987) 17294–17298.
- [20.8] GOTTSCHALK, K., KESSLER, H., The structures of integrins and integrin-ligand complexes: Implications for drug design and signal transduction, *Angew. Chem. Int. Ed. Engl.* **41** (2002) 3767–3774.
- [20.9] ASSA-MUNT, N., JIA, X., LAAKKONEN, P., RUOSLAHTI, E., Solution structures and integrin binding activities of an RGD peptide with two isomers, *Biochemistry* **40** (2001) 2373–2378.
- [20.10] SU, Z., et al., In vitro and in vivo evaluation of a technetium-99m-labeled cyclic RGD peptide as a specific marker of  $\alpha_v\beta_3$  integrin for tumor imaging, *Bioconj. Chem.* **13** (2002) 561–570.
- [20.11] HAUBNER, R., WESTER, H.J., Radiolabeled tracers for imaging of tumor angiogenesis and evaluation of anti-angiogenic therapies, *Curr. Pharm. Design* **10** (2004) 1439–1455.
- [20.12] HAUBNER, R., et al., Radiolabeled  $\alpha_v\beta_3$  integrin antagonists: A new class of tracers for tumor targeting, *J. Nucl. Med.* **40** (1999) 1061–1071.
- [20.13] HAUBNER, R., et al., Glycosylated RGD-containing peptides: Tracer for tumor targeting and angiogenesis imaging with improved biokinetics, *J. Nucl. Med.* **42** (2001) 326–336.

- [20.14] HAUBNER, R., et al., Noninvasive imaging of  $\alpha_v\beta_3$  integrin expression using  $^{18}\text{F}$ -labeled RGD-containing glycopeptide and positron emission tomography, *Cancer Res.* **61** (2001) 1781–1785.
- [20.15] CHEN, X., et al., MicroPET imaging of brain tumor angiogenesis with  $^{18}\text{F}$ -labeled PEGylated RGD peptide, *Eur. J. Nucl. Med. Mol. Imaging* **31** (2004) 1081–1089.
- [20.16] VAN HAGEN, P.M., et al., Evaluation of a radiolabelled cyclic DTPA-RGD analogue for tumor imaging and radionuclide therapy, *Int. J. Cancer* **90** (2000) 186–198.
- [20.17] CHEN, X., et al., MicroPET and autoradiographic imaging of breast cancer alpha v-integrin expression using  $^{18}\text{F}$ - and  $^{64}\text{Cu}$ -labeled RGD peptide, *Bioconj. Chem.* **15** (2004) 41–49.
- [20.18] JANSSEN, M.L., et al., Tumor targeting with radiolabeled  $\alpha_v\beta_3$  integrin binding peptides in a nude mouse model, *Cancer Res.* **62** (2002) 6146–6151.
- [20.19] POETHKO, T., et al., Two-step methodology for high-yield routine radiohalogenation of peptides:  $^{18}\text{F}$ -labeled RGD and octreotide analogs, *J. Nucl. Med.* **45** (2004) 892–902.
- [20.20] SCHIBLI, R., et al., Steps toward specific activity labeling of biomolecules for therapeutic application: Preparation of precursor  $[\text{}^{188}\text{Re}(\text{H}_2\text{O})_3(\text{CO})_3]^+$  and synthesis of tailor-made bifunctional ligand systems, *Bioconj. Chem.* **13** (2002) 750–756.
- [20.21] ALBERTO, R., et al., Metal carbonyl syntheses XXII. Low pressure carbonylation of  $[\text{MOCl}_4]^-$  and  $[\text{MO}_4]^-$ : The technetium(I) and rhenium(I) complexes  $[\text{NEt}_4]_2[\text{MCl}_3(\text{CO})_3]$ , *J. Organomet. Chem.* **493** (1995) 119–127.
- [20.22] ALBERTO, R., et al., A simple single-step synthesis of  $[\text{}^{99}\text{Tc}_3\text{H}_3(\text{CO})_{12}]$  from  $[\text{}^{99}\text{TcO}_4]^-$  and its X-ray crystal structure. Application to the production of no-carrier added  $[\text{}^{188}\text{Re}_3\text{H}_3(\text{CO})_{12}]$ , *Chem. Commun.* **11** (1996) 1291–1292.
- [20.23] ABRAM, U., ABRAM, S., ALBERTO, R., SCHIBLI, R., Ligand exchange reactions starting from  $[\text{Re}(\text{CO})_3\text{Br}_3]^{2-}$ . Synthesis, characterization, and structures of rhenium(I) tricarbonyl complexes with thiourea and thiourea derivatives, *Inorg. Chim. Acta* **248** (1996) 193–202.
- [20.24] PIETZSCH, H.J., et al., Chemical and biological characterization of technetium (I) and rhenium (I) tricarbonyl complexes with dithioether ligands serving as linkers for coupling the  $\text{Tc}(\text{CO})_3$  and  $\text{Re}(\text{CO})_3$  moieties to biologically active molecules, *Bioconj. Chem.* **11** (2000) 414–424.
- [20.25] SCHIBLI, R., KATTI, K.V., HIGGINBOTHAM, C., VOLKERT, W.A., ALBERTO, R., In vitro and in vivo evaluation of bidentate, water-soluble phosphine ligands as anchor groups for the organometallic *fac*- $[\text{}^{99\text{m}}\text{Tc}(\text{CO})_3]^+$ -core, *Nucl. Med. Biol.* **26** (1999) 711–716.

- [20.26] SCHIBLI, R., KATTI, K.V., VOLKERT, W.A., BARNES, C.L., Novel coordination behavior of *fac*-[ReBr<sub>3</sub>(CO)<sub>3</sub>]<sub>2</sub> with 1,3,5-triaza-7-phosphaadamantane (PTA). Systematic investigation on stepwise replacement of the halides by PTA ligand. Phase transfer studies and X-ray crystal structure of [NEt<sub>4</sub>][ReBr<sub>2</sub>(PTA)(CO)<sub>3</sub>], [ReBr(PTA)<sub>2</sub>(CO)<sub>3</sub>], and [Re(PTA)<sub>3</sub>(CO)<sub>3</sub>]PF<sub>6</sub>, *Inorg. Chem.* **37** (1998) 5306–5312.
- [20.27] PIETZSCH, H.J., et al., “Thioether ligands as anchor groups for coupling the “Tc(CO)<sub>3</sub>” and “Re(CO)<sub>3</sub>” moieties with biologically active molecules”, *Technetium, Rhenium and Other Metals in Chemistry and Nuclear Medicine* (NICOLINI, M., ULDERICO, M., Eds), SGEEditoriali, Padova (1999) 313–316.
- [20.28] EGLI, A., et al., “[<sup>99m</sup>Tc(OH<sub>2</sub>)<sub>3</sub>(CO)<sub>3</sub>]<sup>+</sup> labels peptide to an unprecedented high specific activity. A labelling study with amino acids and neurotensin”, *Technetium, Rhenium and Other Metals in Chemistry and Nuclear Medicine* (NICOLINI, M., ULDERICO, M., Eds), SGEEditoriali, Padova (1999) 507–512.
- [20.29] LA BELLA, R., et al., In vitro and in vivo evaluation of a <sup>99m</sup>Tc(I)-labeled bombesin analogue for imaging of gastrin releasing peptide receptor-positive tumors, *Nucl. Med. Biol.* **29** (2002) 553–560.
- [20.30] ALBERTO, R., et al., Potential of the “[M(CO)<sub>3</sub>]<sup>+</sup>” (M = Re, Tc) moiety for the labeling of biomolecules, *Radiochim. Acta* **79** (1997) 99–103.
- [20.31] SCHIBLI, R., Influence of the denticity of ligand systems on the in vitro and in vivo behavior of <sup>99m</sup>Tc(I)-tricarbonyl complexes: A hint for the future functionalization of biomolecules, *Bioconj. Chem.* **11** (2000) 345–351.
- [20.32] ALBERTO, R., SCHIBLI, R., SCHUBIGER, P.A., First application of *fac*-[<sup>99m</sup>Tc(OH<sub>2</sub>)<sub>3</sub>(CO)<sub>3</sub>]<sup>+</sup> in bioorganometallic chemistry: Design, structure, and in vitro affinity of a 5-HT<sub>1A</sub> receptor ligand labeled with <sup>99m</sup>Tc, *J. Am. Chem. Soc.* **121** (1999) 6076–6077.
- [20.33] ALBERTO, R., SCHIBLI, R., EGLI, A., SCHUBIGER, P.A., A novel organometallic aqua complex of technetium for the labeling of biomolecules: Synthesis of [<sup>99m</sup>Tc(OH<sub>2</sub>)<sub>3</sub>(CO)<sub>3</sub>]<sup>+</sup> from [<sup>99m</sup>TcO<sub>4</sub>]<sup>-</sup> in aqueous solution and its reaction with a bifunctional ligand, *J. Am. Chem. Soc.* **120** (1998) 7987–7988.
- [20.34] ALBERTO, R., et al., “From [TcO<sub>4</sub>]<sup>-</sup> to an organometallic aqua-ion: Synthesis and chemistry of [<sup>99m</sup>Tc(OH<sub>2</sub>)<sub>3</sub>(CO)<sub>3</sub>]<sup>+</sup>”, *Technetium, Rhenium and Other Metals in Chemistry and Nuclear Medicine* (NICOLINI, M., ULDERICO, M., Eds), SGEEditoriali, Padova (1999) 27–34.
- [20.35] ALVES, S., PAULO, A., CORREIA, J.D.G., DOMINGOS, Â., SANTOS, I., Coordination capabilities of pyrazolyl containing ligands towards the *fac*-[Re(CO)<sub>3</sub>]<sup>+</sup> moiety, *J. Chem. Soc. Dalton Trans.* **24** (2002) 4714–4719.
- [20.36] ALVES, S., PAULO, A., CORREIA, J.D.G., GANO, L.Â., SANTOS, I., “New building blocks for labeling peptides with the [<sup>99m</sup>Tc(CO)<sub>3</sub>]<sup>+</sup> core”, *Technetium, Rhenium and Other Metals in Chemistry and Nuclear Medicine 6* (NICOLINI, M., MAZZI, U., Eds), SGEEditoriali, Padova (2002) 139–142.

- [20.37] VITOR, R., ALVES, S., CORREIA, J.D.G., PAULO, A., SANTOS, I., Rhenium(I)- and technetium(I) tricarbonyl complexes anchored by bifunctional pyrazole-diamine and pyrazole-dithioether chelators, *J. Organomet. Chem.* (in press).
- [20.38] ALVES, S., PAULO, A., CORREIA, J.D.G., GANO, L., SANTOS, I., Pyrazolyl derivatives as bifunctional chelators for labelling biomolecules with the *fac*-[M(CO)<sub>3</sub>]<sup>+</sup> moiety (M = <sup>99m</sup>Tc, Re): Synthesis, characterization and biological behaviour, *Bioconj. Chem.* **16** (2005) 438–449.
- [20.39] CHEN, X., PARK, R., SHAHINIAN, A.H., BADING, J.R., CONTI, P.S., Pharmacokinetics and tumor retention of <sup>125</sup>I-labeled RGD peptide are improved by PEGylation, *Nucl. Med. Biol.* **31** (2004) 11–19.

## PAPERS PUBLISHED BY THE PARTICIPANTS RELATED TO THE COORDINATED RESEARCH PROJECT

### Journal papers:

ALVES, S., et al., In vitro and in vivo evaluation of a novel  $^{99m}\text{Tc}(\text{CO})_3$ -pyrazolyl conjugate of cyclo(Arg-Gly-Asp-D-Tyr-Lys), *Bioconj. Chem.* **16** (2005) 438–449.

ALVES, S., et al., Pyrazolyl conjugates of bombesin: A new tridentate ligand framework for stabilization of the *fac*- $\text{M}^{\text{I}}(\text{CO})_3$  moiety, *Nucl. Med. Biol.* **33** (2006) 625–634.

ALVES, S., et al., Pyrazolyl derivatives as bifunctional chelators for labeling tumor-seeking peptides with the *fac*- $[\text{M}(\text{CO})_3]^+$  moiety ( $\text{M} = ^{99m}\text{Tc}, \text{Re}$ ): Synthesis, characterization, and biological behavior, *Bioconj. Chem.* **16** (2005) 438–449.

DECRISTOFORO, C., et al., [ $^{99m}\text{Tc}$ ]HYNIC-RGD for imaging integrin  $\alpha_v\beta_3$  expression, *Nucl. Med. Biol.* **33** (2006) 945–952.

DECRISTOFORO, C., et al.,  $^{99m}\text{Tc}$ -labelling and preclinical characterisation of an RGD peptide for imaging tumour angiogenesis, *Nuklearmedizin* **44** (2006) A192.

DECRISTOFORO, C., et al., Comparison of in vitro and in vivo properties of  $^{99m}\text{Tc}$ -cRGD peptides labelled using different novel Tc-cores, *Q. J. Nucl. Med. Mol. Imaging* **51** (2007) 33.

DECRISTOFORO, C., VON GUGGENBERG, E., RUPPRICH, M., HAUBNER, R., Entwicklung von Metall-markierten RGD Peptiden für die Molekulare Bildgebung von  $\alpha_v\beta_3$  Integrinen, *Sci. Pharm. Suppl.* **1 74 2** (2006) S37.

FAINTUCH, B.L., et al.,  $^{99m}\text{Tc}$ -HYNIC-bombesin (7-14) $\text{NH}_2$ : Radiochemical evaluation with co-ligands EDDA (EDDA = ethylenediamine-N,N'-diacetic acid), tricine, and nicotinic acid, *J. Synth. React. Inorgan. Metal-Organ. Nano-metal Compd* **35** (2005) 43–51.

FERNANDES, C., GANO, L., BOURKOULA, A., PIRMETTIS, I., SANTOS, I., “Novel  $\text{Re}(\text{I})/^{99m}\text{Tc}(\text{I})$  tricarbonyl complexes bearing quinazoline moiety as biomarkers for epidermal growth factor receptor positive tumors”, *Technetium, Rhenium and Other Metals in Chemistry and Nuclear Medicine*, Vol. 7 (MAZZI, U., Ed.), SGEEditoriali, Padova (2006) 487–490.

GIGLIO, A.J., et al., “ $^{99m}\text{Tc}$ -labelled RGD-peptide using the ‘4+1’ mixed-ligand approach”, *Technetium, Rhenium and Other Metals in Chemistry and Nuclear Medicine* (NICOLINI, M., MAZZI, U., Eds), SGEEditoriali, Padova (2006) 331–332.

GIGLIO, J., et al., Complejos  $^{99m}\text{Tc}(\text{I})$ -tricarbonilos en el diseño de potenciales radiofarmacos para diagnostico de hypoxia, *Alasbimn J.* **8** 31 (2006).

GORSHKOV, N.I., et al., “2+1” dithiocarbamato-isocyanide chelating systems for linking  $\text{M}(\text{CO})_3$  ( $\text{M} = ^{99m}\text{Tc}$ , Re) fragment to biomolecules, *J. Organomet. Chem.* **689** (2004) 4757–4763.

GORSHKOV, N.I., et al., “Technetium-99m and rhenium tricarbonyl “2 + 1” complexes as potential myocardial perfusion agents”, *Technetium, Rhenium and Other Metals in Chemistry and Nuclear Medicine* (NICOLINI, M., MAZZI, U., Eds), SGEEditoriali, Padova (in press).

GORSHKOV, N.I., LUMPOV, A.A., MIROSLAVOV, A.E., SUGLOBOV, D.N., 2 + 1 chelating systems for binding organometallic fragment  $\text{Tc}(\text{CO})_3^+$ , *Radiochemistry* **47** (2005) 45–49.

KORDE, A., et al.,  $^{99m}\text{Tc}$ -labeling of colchicine using  $[\text{}^{99m}\text{Tc}(\text{CO})_3(\text{H}_2\text{O})_3]^+$  and  $[\text{}^{99m}\text{TcN}]^{2+}$  cores for the preparation of potential tumor targeting agents, *Bioorg. Med. Chem.* **14** (2006) 793–799.

KUNSTLER, J.-U., VEERENDRA, B., SIECKMAN, G.L., SMITH, C.J., PIETZSCH, H.-J., “Novel approaches for  $^{99m}\text{Tc}$  labeling of peptides: Organometallic  $\text{Tc}(\text{III})$  complexes for bombesin labeling”, *Technetium, Rhenium and Other Metals in Chemistry and Nuclear Medicine* (NICOLINI, M., MAZZI, U., Eds), SGEEditoriali, Padova (2006) 317–318.

MARGARITIS, N., et al., “A new technetium-99m biomarker for EGFR-TK”, *Technetium, Rhenium and Other Metals in Chemistry and Nuclear Medicine*, Vol. 7 (MAZZI, U., Ed.), SGEEditoriali, Padova (2006) 523–524.

MUKHERJEE, A., et al.,  $^{99m}\text{Tc}$  labeled annexin V fragments: A potential SPECT radiopharmaceutical for imaging cell death, *Nucl. Med. Biol.* **33** (2006) 635–643.

REY, A., et al., Nuevos cores de  $^{99m}\text{Tc}$  en la marcación de péptidos con potencialidad para imágenes de neoangiogénesis tumoral, *Alasbimn J.* **8** 31 (2006).

SATPATI, D., BABAT, K., SARMA, H.D., BANERJEE, S., VENKATESH, M., Preparation and biological evaluation of  $^{99m}\text{Tc}$ -carbonyl complex of 5-hydroxy tryptamine derivative, *Appl. Radiat. Isot.* **64** (2006) 888–892.

SMITH, C.J., et al., Technetium(I) pyrazolyl bombesin conjugates: A concise in vitro/in vivo study, *J. Labelled Compd Radiopharm.* **48** (2005) S46.

SUGLOBOV, D.N., et al., "High pressure synthesis of higher technetium-99m carbonyls as potential precursors for development of new radiopharmaceuticals", *Technetium, Rhenium and Other Metals in Chemistry and Nuclear Medicine* (NICOLINI, M., MAZZI, U., Eds), SGEEditoriali, Padova (in press).

SUGLOBOV, D.N., MIROSLAVOV, A.E., SIDORENKO, G.V., GORSHKOV, N.I., LUMPOV, A.A., Complexation of  $Tc(CO)_3^+$  aq with anions of monobasic carboxylic acids in aqueous solutions: A  $^{99m}Tc$  NMR study, *Radiochemistry* **47** (2005) 50–55.

Presentations at national and international meetings:

AYROSA, A.M.I.B., FAINTUCH, B.L., PITOMBO, R.N.M., "Hygroscopic behavior of  $^{99m}Tc$  radiopharmaceutical lyophilized kits", paper presented at Ann. Mtg and Lyophilization Conf., São Paulo, 2005.

DECRISTOFORO, C., et al., "Comparison of in vitro and in vivo properties of  $^{99m}Tc$ -RGD peptides for targeting tumour angiogenesis labeled using different, novel,  $^{99m}Tc$ -cores", paper presented at European Symp. of Radiopharmacy and Radiopharmaceuticals, Lucca, Italy, 2006.

DECRISTOFORO, C., et al., "Comparison of radiometal labeled RGD peptides targeting  $\alpha_v\beta_3$  integrin expression", paper presented at European Association of Nuclear Medicine Congress, Athens, 2006.

ELLIS, B.L., et al., "Pre-clinical evaluation of  $^{99m}TcI(CO)_5$ ", paper presented at 52nd Ann. Mtg of the Society of Nuclear Medicine, Toronto, 2005.

FAINTUCH, B.L., AYROSA, A.M.I.B., SMITH, C.J., CASTANHEIRA, C.E., "Characterization of lyophilized parameters of a new radiopharmaceutical kit for prostate tumor diagnostic", paper presented at Ann. Mtg and Lyophilization Conf., São Paulo, 2005.

FAINTUCH, B.L., et al., " $^{99m}Tc$ -asymmetrical nitrido complex of annexin analog and RGD analog", paper presented at 53rd Ann. Mtg of the Society of Nuclear Medicine, San Diego, CA, 2006.

FAINTUCH, B.L., et al., "Labeling of bombesin analogue by asymmetrical technetium-99m nitrido core", paper presented at Int. Symp. on Trends in Radiopharmaceuticals, Vienna, 2005.

FAINTUCH, B.L., STOIANOV, V., SANTOS, R.L.S.R., DUATTI, A., SMITH, C.J., "Labeling of bombesin analogue by the asymmetrical technetium-99m nitrido core", paper presented at Int. Symp. on Trends in Radiopharmaceuticals, Vienna, 2005.

FAINTUCH, F.L., et al., "Evaluation of  $^{99m}\text{Tc}$ -HYNIC-RGD analog in mice bearing lung cancer cells", paper presented at 53rd Ann. Mtg of the Society of Nuclear Medicine, San Diego, CA, 2006.

FERNANDES, C., et al., "Promising SPECT biomarkers for molecular imaging of EGFR positive tumours", paper presented at 8th European Biological Inorganic Chemistry Conference, Aviero, Portugal, 2006.

FERNANDES, C., SANTOS, I., "Novel nuclear imaging agents for targeting epidermal growth factor receptors (EGFR)", paper presented at XIV Porto Cancer Mtg, Hormonal and TK Receptors in Breast Cancer, Porto, Portugal, 2005.

GIGLIO, A.J., et al., " $^{99m}\text{Tc}$ -labelled RGD-peptide using the '4+1' mixed-ligand approach", paper presented at 7th Int. Symp. on Technetium in Chemistry and Nuclear Medicine, Bressanone, Italy, 2006.

GIGLIO, J., et al., " $^{99m}\text{Tc}$ -labelled RGD-peptides using the '4+1' mixed-ligand approach", paper presented at 7th Int. Symp. on Technetium in Chemistry and Nuclear Medicine, Bressanone, Italy, 2006.

GIGLIO, J., et al., "Complejos  $^{99m}\text{Tc}(\text{I})$ -tricarbonilos en el diseño de potenciales radiofarmacos para diagnostico de hipoxia", paper presented at the XX ALASBIMN Congreso, Punta del Este, Uruguay, 2005.

GORSHKOV, N.I., et al., "Strategy of conjugation of "2+1" dithiocarbamate-isonitrile  $\text{M}(\text{CO})_3^+$  complexes (M = Tc, Re) with amino acid residue", paper presented at 2nd Int. Symp. on Bioorganometallic Chemistry, Zurich, 2004.

GORSHKOV, N.I., et al., "Technetium-99m and rhenium tricarbonyl "2 + 1" complexes as potential myocardial perfusion agents", paper presented at 7th Int. Symp. on Technetium in Chemistry and Nuclear Medicine, Bressanone, Italy, 2006.

GORSHKOV, N.I., LUMPOV, A.A., MIROSLAVOV, A.E., SUGLOBOV, D.N., " $\text{M}(\text{CO})_5\text{I}$  (M = Tc, Re) as potential precursors for labeling of biomolecules", paper presented at 2nd Int. Symp. on Bioorganometallic Chemistry, Zurich, 2004.

GORSHKOV, N.I., LUMPOV, A.A., MIROSLAVOV, A.E., SUGLOBOV, D.N., SHATIK, S.V., "Preparation of  $^{99m}\text{Tc}(\text{CO})_5\text{I}$  and its application as potential precursor for labeling of biomolecules", paper presented at 12th European Symp. on Radiopharmacy and Radiopharmaceuticals, Gdansk, 2004.

GORSHKOV, N.I., SCHIBLI, R., LUMPOV, A.A., MIROSLAVOV, A.E., SUGLOBOV, D.N., "2+1" approach in  $\text{M}(\text{CO})_3^+$  (M = Tc, Re) chemistry: Hint for

labeling biomolecules”, paper presented at Int. Symp. on Technetium — Science and Utilization (IST-2005), Oarai, Japan, 2005.

KODINA, G.E., et al., “Synthesis and in vitro evaluation of  $\text{Tc}(\text{CO})_3^+$  complexes with dithiocarbamate ligands containing morpholine moiety”, paper presented at Int. Symp. on Technetium — Science and Utilization (IST-2005), Oarai, Japan, 2005.

KUNSTLER, J.-U., VEERENDRA, B., SIECKMAN, G.L., SMITH, C.J., PIETZSCH, H.-J., “Novel approaches for  $^{99\text{m}}\text{Tc}$  labeling of peptides: Organometallic  $\text{Tc}(\text{III})$  complexes for bombesin labelling”, paper presented at 7th Int. Symp. on Technetium in Chemistry and Nuclear Medicine, Bressanone, Italy, 2006.

LUMPOV, A.A., et al., “Synthesis of  $^{99\text{m}}\text{Tc}(\text{CO})_5\text{I}$  and its biodistribution in rabbits”, paper presented at 2nd Int. Symp. on Bioorganometallic Chemistry, Zurich, 2004.

MATHUR, A., MALLIA, M.B., KOTHARI, K., BANERJEE, S., VENKATESH, M., “Synthesis and radiolabeling of a fatty acid xanthate with  $^{99\text{m}}\text{Tc}$ -nitrido [ $^{99\text{m}}\text{Tc}=\text{N}]^{+2}$  core for possible use in myocardial imaging”, paper presented at Int. Symp. on Trends in Radiopharmaceuticals, Vienna, 2005.

REY, A., et al., “Nuevos cores de  $^{99\text{m}}\text{Tc}$  en la marcación de péptidos con potencialidad para imágenes de neoangiogénesis tumoral”, paper presented at the XX ALASBIMN Congress, Punta del Este, Uruguay, 2005.

REY, A., LEÓN, E., GIGLIO, J., DECRISTOFORO, C., VON GUGGENBERG, E., “Preparation and characterization of  $^{99\text{m}}\text{Tc}$ -RGDyK-HYNIC peptide as potential radiopharmaceutical for nuclear oncology”, paper presented at Int. Symp. on Trends in Radiopharmaceuticals, Vienna, 2005.

SMITH, C.J., et al., “Technetium-I pyrazolyl bombesin conjugates: A concise in vitro/in vivo study”, paper presented at 16th Int. Symp. on Radiopharmaceutical Chemistry, Iowa City, IA, 2005.

SUGLOBOV, D.N., et al., “High pressure synthesis of higher technetium- $^{99\text{m}}$  carbonyls as potential precursors for development of new radiopharmaceuticals”, paper presented at 7th Int. Symp. on Technetium in Chemistry and Nuclear Medicine, Bressanone, Italy, 2006.



## **PARTICIPANTS IN THE COORDINATED RESEARCH PROJECT**

Alberto, R.	University of Zurich, Switzerland
Decristoforo, C.	Universitätsklinik für Nuklearmedizin, Innsbruck, Austria
Duatti, A.	University of Ferrara, Italy
Hu Ji	China Institute of Atomic Energy, China
Környei, J.	Institute of Isotopes Co. Ltd, Hungary
Kothari, K.	Bhabha Atomic Research Centre, India
Linkowski Faintuch, B.	Nuclear and Energy Research Institute, Brazil
Pietzsch, H.-J.	Forschungszentrum Dresden–Rossendorf, Germany
Pillai, M.R.A.	International Atomic Energy Agency
Pirmettis, I.	Demokritos National Centre of Scientific Research, Greece
Santos, I.R.D.	Institute of Nuclear Technology, Portugal
Rey, R.A.M.	Universidad de la República, Uruguay
Smith, J.	University of Missouri-Columbia, United States of America
Suglobov, D.	Khlopin Radium Institute, Russian Federation
Observers:	
Korde, A.	Bhabha Atomic Research Centre, India
Sidorenko, G.	Khlopin Radium Institute, Russian Federation

**This report presents the results of an IAEA coordinated research project (CRP) on the Development of  $^{99m}\text{Tc}$  Based Small Biomolecules Using Novel  $^{99m}\text{Tc}$  Cores. The CRP, which included participating laboratories in Austria, Brazil, China, Germany, Greece, Hungary, Italy, India, Portugal, the Russian Federation, Switzerland, the USA and Uruguay, had the objective of developing biomolecules with novel  $^{99m}\text{Tc}$  metal cores such as  $^{99m}\text{Tc}$ -carbonyl,  $^{99m}\text{Tc}$ -nitrido,  $^{99m}\text{Tc}$ -(4 + 1) and  $^{99m}\text{Tc}$ -HYNIC. The preparation, quality assessment and biological evaluation of a large number of  $^{99m}\text{Tc}$  complexes were achieved.**